03
05
APRIL

BLED, SLOVENIA

THE PROCEEDINGS OF THE AUSTRIAN – SLOVENIAN POLYMER MEETING 2013

WWW.ASPM.SI

ASPM 2013

AUSTRIAN - SLOVENIAN
POLYMER MEETING

ORGANISERS

Center of Excellence PoliMaT®
Polymer Materials and Technologies

REPUBLIC OF SLOVENIA
MINISTRY OF EDUCATION, SCIENCE, CULTURE AND SPORT

Investing in your future
OPERATION PART FINANCED BY THE EUROPEAN UNION
European Regional Development Fund

PCCL
Polymer Competence Center Leoben

Slovensko kemijsko društvo
Slovenian Chemical Society

Kemijski inštitut
Ljubljana
Slovenija

National
Institute of Chemistry
Slovenia

SPONSORS

Waters
THE SCIENCE OF WHAT'S POSSIBLE.™

TA Instruments

15 YEARS ON A GOOD ROAD
GOODYEAR DUNLOP
SAVA TIRES

NETZSCH

Anton Paar

METTLER TOLEDO

Kračun d.o.o.

ECONYL®
REGENERATION FOR LIFE

FLAME
material_innovation_future

SPIRIT SLOVENIJA
Javna agencija Republike Slovenije za spodbujanje podjetništva, inovativnosti, razvoja, investicij in turizma

I FEEL SLOVENIA

PARTNER PROFESSIONAL ORGANIZATIONS

GCH

EuCheMS

AIM

epf

CENTRAL AND EAST EUROPEAN
CEEPN
POLYMER NETWORK

MEDIA PARTNERS

polymers
an open access journal
by MDPI

IRT3000
inovacije razvoj tehnologije

ventil
REVIJA ZA FLUIDNO TEHNIKO, AVTOMATIZACIJO IN MEHATRONIKO

ASPM 2013
AUSTRIAN - SLOVENIAN POLYMER MEETING
BLED, SLOVENIA, 3-5 APRIL, 2013

The Proceedings of the Austrian – Slovenian Polymer Meeting 2013

Austrian – Slovenian Polymer Meeting – ASPM 2013
3 – 5 April 2013
Bled, Slovenia
www.aspm.si
info@aspm.si

Editors:
Majda Žigon
Teja Rajšp

Cover design:
Alenka Paveo

Publisher:
Centre of Excellence PoliMaT
Tehnološki park 24
1000 Ljubljana
Slovenia
www.polimat.si

CIP - Kataložni zapis o publikaciji
Narodna in univerzitetna knjižnica, Ljubljana

678.7(082)(0.034.2)

AUSTRIAN - Slovenian Polymer Meeting (2013 ; Bled)
The proceedings of the Austrian - Slovenian Polymer Meeting 2013 [Elektronski vir] / Austrian - Slovenian Polymer Meeting - ASPM 2013, 3-5 April 2013, Bled, Slovenia ; editors Majda Žigon, Teja Rajšp. - El. zbornik. - Ljubljana : Centre of Excellence PoliMaT, 2013

ISBN 978-961-269-992-5 (pdf)
1. Gl. stv. nasl. 2. Žigon, Majda
266351872

TABLE OF CONTENTS

PLENARY LECTURES

PL 1
Sustainable biobased materials

Ann-Christine Albertsson*, Ulrica Edlund
Fibre and Polymer Technology, Royal Institute of Technology (KTH), Stockholm, Sweden
*aila@kth.se

Global and major challenges for future material resource sustainability are to secure building block resources other that fossil and to minimize the accumulation of plastic waste. One approach is to develop materials by mimicking commodity plastics while replacing the oil refinery with a bio refinery. It is possible to use monomers, pre-polymers and polymers from nature but limiting factor so far has often been the recovery and purification of biomass derived molecules without using too much solvents and energy. It has also to be done without conflict with food supply.

Instead of building up a new industry based on a bio refinery and virgin biomass we have focused on existing industry and the use of crude biomass released to process water and side streams. We have shown how it is possible to upgrade waste waters in a cheap way and recover hemicellulose rich fractions useful for making microspheres, hydrogels, and barrier films. Making inexpensive, yet functional and competitive materials from biomass require innovative approaches.

References
[1] Saadatmand, S., Edlund, U., Albertsson, A.-C., *Polymer* **2011**, 52, 4648.
[2] Edlund, U., Svensson, M., Albertsson, A.-C., *Eur. Polym. J.* **2012**, 48(2), 372.
[3] Edlund, U., Yu, Y., Ryberg, Y. Z., Krause-Rehberg, R., Albertsson, A.-C., *Anal. Chem*. **2012**, 84(8), 3676.
[4] Ibn Yaich, A., Edlund, U., Albertsson, A.-C. *Biomacromolecule*s **2012**, 13, 466.
[5] Edlund, U., Albertsson, A.-C*., J. Polym. Sci. A Polym. Chem*. **2012**, 50, 2650.
[6] Saadatmand, S., Edlund, U., Albertsson, A.-C., Danielsson, S.; Dahlman, O., *Environ. Sci. Technol.* **2012**, 46(15), 8389.
[7] Ryberg, Y. Z., Edlund, U., Albertsson, A.-C., *Biomacromolecules* **2012**,13(8), 2570.
[8] Edlund, U., Rodriguez-Emmenegger, C., Brynda, E., Albertsson, A.-C., *Polym. Chem*. **2012**, 3(10), 2920.
[9] Ibn Yaich, A., Edlund, U. Albertssson,A.-C., *Carbohydr. Polym*. **2013**, in press.

PL 2
Synthesis and self-assembly of well-defined copolypeptides

Nikos Hadjichristidis
King Abdullah University of Science and Technology (KAUST), Thuwal, Kingdom of Saudi Arabia

Block copolypeptides, which combine the self assembly of block copolymers and the highly ordered 3D structures of proteins, are potential candidates for novel supramolecular structures and biotech applications, such as biosensors, tissue engineering, and selective drug delivery. Attempts to synthesize well-defined polypeptides by the ring-opening polymerization of α-amino acid N-carboxyanhydrides (NAC) with primary amines, have been plagued by unwanted side reactions for more than fifty years. Recently, we have shown that the ring opening polymerization of α-amino acid N-carboxyanhydrides (NCAs) with n-hexylamine using high vacuum (HV) techniques, leads to high molecular weight, well-defined living polypeptides in ~100 % yield with low polydispersity. The method is a general one, leading to molecules with high structural complexity, which will facilitate the design of biologically active molecules. The synthesis of a few block copolypeptides and macromolecular *chimeras*, as well as their self-assembly in bulk and in water will be discussed.

References
Biomacromolecules, 5, 1653 (2004); 6, 2352 (2005); 7, 3379 (2006); 8, 2173 (2007); 9, 1959 (2008); 9, 2072 (2008) ; 12, 2396 (2011). **Chem. Rev.,** 109, 5528 (2009). **Angew.Chem.,** 50, 2516 (2011). **Macromolecules,** 43, 1874 (2010) ; 43, 9071 (2010) ; 45, 2850 (2012).

PL 3

Polyvinylphosphonic acid (PVPA) – the challenge to create a polyelectrolyte for advanced technologies

Gerhard Wegner*
Max-Planck-Institute for Polymer Research
D-55128 Mainz/Germany
*wegner@mpip-mainz.mpg.de

1. Introduction

Poly(acrylic) (PA), Poly(vinylsulfonic acid) (PVS) and poly(vinylphosphonic acid) (PVPA) are a series of analogous polymers of prototype structure and are paradigmatic polyelectrolytes. While literature and applications concerning PA are legion, this is less true for PVS. Astoundingly, PVPA was barely known and only scarce information on its synthesis, properties and structure was available before 2006. Interest in its potential as component of low-temperature fuel cells prompted our attention.

2. Synthesis and Properties

In 2006 Bahar Bingol [1] succeeded in our laboratory [2-4] to develop a synthesis for high molecular weight PVPA and simultaneously gave the mechanistic clue why previous workers had failed in their attempts of synthesis
Bingol explored the direct free radical polymerization of VPA (2) to PVPA (1). Realizing that it is the VPA-anhydride which undergoes cyclopolymerization she was able for the first time to obtain high mol. wt. PVPA. Later it was shown by W. Meyer et al [6] that anionic polymerization of VPA-esters is possible and HMW-PVPA can be obtained via saponification of the poly(phosphonates).

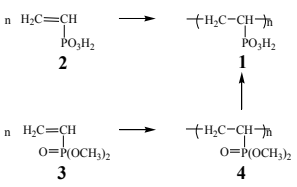

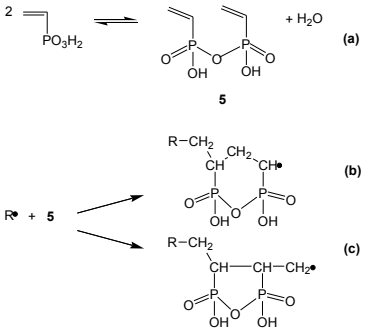

More recently B. Rieger et al. [7] have reported that Diethyl VPA can be polymerized using specific rare-earth metal catalysts via (probably) a GTP-mechanism and saponification of the product yields HMW-PVPA as well. A comprehensive review is available [8].
PVPA acts as a medium-strong monobasic acid, comparable to PA. However, it has considerable interest as a material for the design of fuel cells as it shows good proton conductivity and temperature stability [2], [5].
Further work demonstrated the formation of copolymers and hydrogels [5] pointing into the direction of biocompatible materials.
The presentation summarizes the recent developments under the auspices of material science devoted to advances materials.

References

[1] Synthesis, microstructure, and acidity of poly(vinylphosphonic acid)
Bingol B., Meyer W., Wagner M., Wegner G., Macromol. RC **2006**, 27, 1719-24
[2] High-resolution solid-state NMR studies of poly(vinylphosphonic acid) proton-conducting polymer: Molecular structure and proton dynamics, Lee Y.J, Bingol B., Wegner G. et al., J. Phys. Chem. B **2007**, 111, 9711-21
[3] Copolymers and hydrogels based on vinylphosphonic acid
Bingol B., Strandberg C., Szabo A., Wegner G., Macromolecules **2008**, 41, 2785-2790
[4] Characterization of oligo(vinyl phosphonate)s by high-resolution electrospray ionization mass spectrometry
Bingol B. et al, Macromolecules **2008**, 41, 1634-39
[5] Water sorption of poly(vinylphosphonic acid) and its influence on proton conductivity
Kaltbeizel A., Bingol B., Wegner G. et al, Solid State Ionics **2007**, A 178, 469-474
[6] VPA Homo- and Block Copolymers, Wagner Th., Meyer W., et al., Macromol. Chem. Phys. **2009,** 210, 1893-1914
[7] Rieger B. et al., Angew. Chem. Int. Ed. **2010**, 49, 1489-1491
[8] Macarie L., Ilia G., Progr. Polym. Sci. **2010**, 35, 1078-1092

PL4

Directed assembly of block copolymer thin films for nanotechnology applications

Gurpreet Singh (1), Kevin G. Yager (2), Detlef-M. Smilgies (3), Manish M. Kulkarni (1), David G. Bucknall (4) and Alamgir Karim (1)

(1) Department of Polymer Engineering, University of Akron (UA), Akron, OH 44325, USA
(2) Center for Functional Nanomaterials, Brookhaven National Laboratory, Upton, NY 11973, USA
(3) Cornell High Energy Synchrotron Source (CHESS), Cornell University, Ithaca, New York 14853, USA
(4) Materials Science and Engineering, Georgia Institute of Technology, Atlanta, GA 30332, USA

Fabricating ordered nanodomains of multi-component polymer thin films on diverse substrates *via* continuous processing methods is particularly attractive for nanomanufacturing of next-generation electronics. We report such a method, termed cold-zone annealing (CZA) utilizing a dynamic sharp thermal gradient (~ 45 oC/mm) (i.e. CZA-S). This method applied to block copolymers (BCP) allows for production of etchable and vertically oriented cylindrical domains of poly(styrene-b-methylmethacrylate) in |100-1000| nm thick films on low thermal conductivity rigid (quartz) and flexible (PDMS, Kapton) substrates. Competing substrate wetting interactions dominate BCP orientation in films below 100 nm while broadening of the thermal gradient profile in films thicker than 1000 nm leads to loss of vertical orientation. An optimal dynamic sweep rate (~ 5 icron/s) produces the best vertical order. At too fast a sweep rate (> 10 micron/s) the BCP film ordering is kinetically hindered, while at too slow a sweep rate (< 1 micron/s), polymer relaxation and preferential surface wetting dynamics favor parallel BCP orientation. Equivalently static gradient conditions produces vertically aligned BCP cylinders only at the maximum T. CZA-S mechanism involves propagating this vertically oriented BCP zone across the sample. We also report the discovery of a rapid and continuous dynamic thermal gradient process, termed as Cold Zone Annealing – SoftShear "CZA-SS", to directionally align cylindrical block copolymer (BCP) films on rigid and flexible substrates. In CZA-SS, BCP films are confined under a soft-shear polydimethylsiloxane (PDMS) layer and subsequently zone annealed to obtain defect-free unidirectional horizontal cylinders over large areas (> 50 cm2). AFM and GISAXS analysis reveal ≥ 95% aligned orientational order with an angular spread of ≤ 9 degrees FWHM. This orientational order is preserved even for thick films (> 1 m) on flexible substrates at extremely high processing speeds (~ 0.2 mm/s), essential for scale-up to roll-to-roll manufacturing purposes. Extensions of the method to other multicomponent polymer systems are in progress.

KEYNOTE LECTURES

KNL 1
Non-linear macromolecules of controlled structure and high functionality

Andrzej Dworak*, Wojciech Wałach, Agnieszka Kowalczuk, Barbara Trzebicka
Polish Academy of Sciences, Centre of Polymer and Carbon Materials, 41-812 Zabrze, Poland
*andrzej.dworak@cmpw-pan.edu.pl

1. Introduction

Non-linear macromolecules have aroused considerable interest both from the fundamental point of view and from the point of view of their envisaged applications [1a-c]. They were considered to constitute a polymer chemistry response to the dendrimers, perfectly symmetric and uniform macromolecules of promising properties, but tedious to synthesize.

Non-linear macromolecules differ in their properties from chain-like ones. They are not able to adopt the coil-like conformation, as they do not consist of a single chain and assume a more compact conformation, thus influencing the properties of both bulk and in solution. They have on their outside numerous functional groups, capable of undergoing modification reactions and deciding about the interactions with the surrounding medium (solubility). They may assume a core-corona structure (unimolecular micelles), thus being prospective carriers for active species. Even if no decisive breakthrough has been achieved, they constitute an interesting and living subject of research both in the academia and in the industry.

The subject of this contribution is to discuss the synthesis and properties of highly hydroxyl functional, hydrophilic and amphiphilic star-like and hyperbranched polyethers.

2. Building blocks

Following polyethers have been incorporated into the star and HB macromolecules:

The monomers selected were capable to undergo living anionic polymerizations (substituted oxiranes) or controlled radical, also self-condensing polymerizations (styrene and derivatives). The monomers were bearing functional groups, frequently protected for sake of the polymerization control, to introduce requested hydrophilicity to open modification possibilities necessary to imprint desired functions:

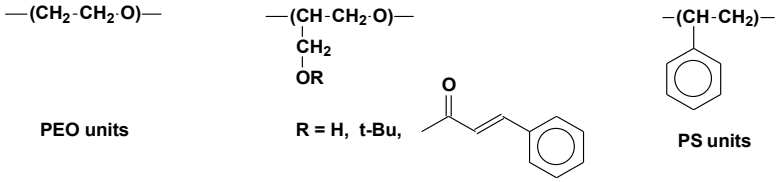

3. Structures obtained

Basing upon this blocks and applying living polymerization of corresponding oxiranes following structures were obtained and their properties in solution studied:

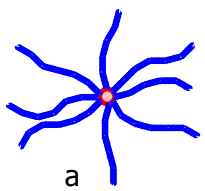

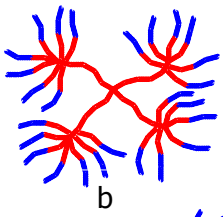

Stars [2a-c] and dendritic stars [2d] of hydrophobic (red on schemes) core and hydrophilic (blue on schemes) shell with up to 1200 OH groups were obtained. Some of them are thermosensitive and the cloud point depends on the structure and hydrophilic/hydrophobic units ratio. Due to their polar character they self-organize in solutions, a process which may be at least partially controlled, and are able to transport hydrophobic species.

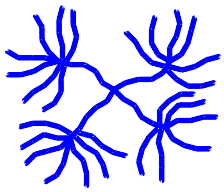

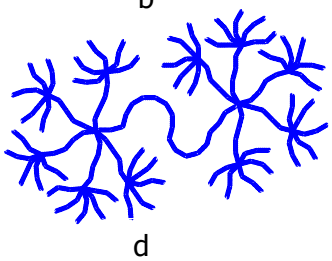

Well defined dendritic block copolymer of poly(ethylene oxide) and highly functional polyglycidol corona were obtained [3]. This strongly hydrophilic copolymer with high content of functional hydroxyl group is soluble also in nonpolar organic solvents.

Pom-pom-like poly(ethylene oxide) with oligoglycidol branching blocks achieve molar mass up to 200 000 and more than 400 OH groups per molecule [4].

1. a) A. Hult *et al.*, Adv. Polym. Sci. 1999, **143**, 1; b) S.-E. Stiriba *et al.*, Angew. Chem. Int. Ed. 2002, **41**, 1329; c) C. Gao, D. Yan, Prog. Polym. Sci. 2004, **29**, 183.
2. a) A. Dworak *et al.*, Polym. Bull. 2002, 49, 9; b) M. Jamroz-Piegza *et al.*,J. Colloid Interface Sci. 2008, **325**, 141; c) M. Libera *et al.*, Polymer 2011, **52**, 250; d) M. Libera *et al.*, Polymer 2011, **52**, 3526.
3. A. Dworak, W. Walach, Polymer 2009, **50**, 3440.
4. W. Walach, B. Trzebicka, J. Justynska, A. Dworak, Polymer 2004, **45**, 1755.

KNL 2
Functional materials from polysaccharides

Volker Ribitsch (1) and Karin Stana-Kleinschek (2)
(1) Institute of Chemistry, Karl-Franzens-University Graz, Heinrichstraße 28/III, AT-8010 Graz, Austria
(2) Laboratory for Characterization and Processing of Polymers, Faculty of Mechanical Engineering, University of Maribor, Smetanova 17, SI-2000 Maribor, Slovenia

Polysaccharides show versatile physicochemical properties and can be used for many applications ranging from packaging to functional coatings. This presentation gives an overview about the different ways to design new material using compounding processes.
Cellulosic materials such as cellulose films or cellulose acetate membranes can be modified on their surface in order to introduce new properties. An aqueous layer by layer coating with positively charged polysaccharides and negatively charged nano-clay platelets for instance, can be used as a barrier coating for water vapour and cellulose acetate membranes can be modified with chitosan and carboxymethyl cellulose, to generate anti-fouling or anti-microbial coatings. Furthermore cellulose itself has several unique properties. Its special chemical and physical structure makes it an ideal candidate for the production of hydrophilic but insoluble nanometric surface coatings on solid substrates. One of the methods to produce such structures is to coat cellulose derivatives on substrates and subsequently regenerate these coatings to pure cellulose. Various thin films of cellulose can be produced and characterized with respect to their surface properties using contact angle measurements and X-ray photoelectron spectroscopy. These films can micro-structured using lithographic processes in combination with enzymatic digestion. Furthermore structure property relationships of cellulosic bulk materials can be elucidated by small or wide angle X-ray scattering (SWAXS) whereas surface characteristics and orientation effects can be studied by gracing incidence small or wide angle X-ray scattering (GI-SWAXS). As another example cellulose acetate nanoparticles with incorporated functional polysaccharides can be manufactured. These particles show an outstanding application potential for targeted drug delivery and antimicrobial or antifouling surface coatings.
The research leading to these results has received funding from the European Union Seventh Framework Programme (FP7/2007-2013) under grant agreement n° 214653.

KNL 3
Regioselective functionalization of polymer constructs with growth factor peptides for regenerative medicine: gels, fibers & scaffolds

Matthew L. Becker
Department of Polymer Science, The University of Akron, USA
Center for Biomaterials in Medicine, Austen Bioinnovation Institute in Akron, USA

Stem cells respond to many cues from their microenvironment, which may include chemical signals, mechanics, and topography. Importantly, these cues may be incorporated into scaffolding to control stem cell differentiation and optimize their ability to produce tissues in regenerative medicine applications. Despite the significant amount of work in this area, the materials have been primarily static and uniform. The number of rationally designed and translationally-relevant materials emerging from research laboratories remains limited. To this end, we have developed a number of technologies that include the ability to attach highly functional and bioactive groups to polymer constructs that include hydrogels, fibers and polymeric scaffolds. All are degradable and designed to be restorative or therapeutic in nature. This presentiaton will highlight our recent efforts in this area.

KNL 4
Alkyd technology

Mark D. Soucek*
Department of Polymer Engineering, University of Akron, Akron, OH 44313, USA
*msoucek@uakron.edu

Research in biomass derived coatings account for ~1/3 of the Soucek group research portfolio. The Soucek group has reported on extensively on the functionalization of seed oils to prepare reactant diluents for coatings. Reactive diluents perform the role of an organic solvent without volatizing into the atmosphere, and unlike organic solvents participate in the crosslinking process during film formation. Using simple Diels-Alder Chemistry, autoxidative, UV-curable, and moisture curable reactive diluents have successfully prepared and integrated into coating systems. Colloidal additives which can react autoxidatively or via thiol-ene chemistry. In addition to reactive diluents, controlled polymerization (RAFT) has been utilized to create acrylic-alkyd hybrids suitable for both waterborne and solventborne media.

KNL 5
Open molecular dynamics simulation of star polymers

Matej Praprotnik*
National Institute of Chemistry, Hajdrihova 19, SI-1001, Ljubljana, Slovenia
*praprot@cmm.ki.si

In this talk, I will present a multiscale method, based on the flux-exchange coupling, which concurrently links atomistic, mesoscopic, and continuum models of liquids [1,2]. Our approach enables the insertion of large molecules into the atomistic domain via a mesoscopic region and it allows for molecular simulations either in the grand-canonical ensemble or under non-equilibrium conditions. The applicability of the method will be demonstrated on an open molecular dynamics simulation of a star polymer melt where we open up the molecular system to exchange mass and momentum with its surroundings.

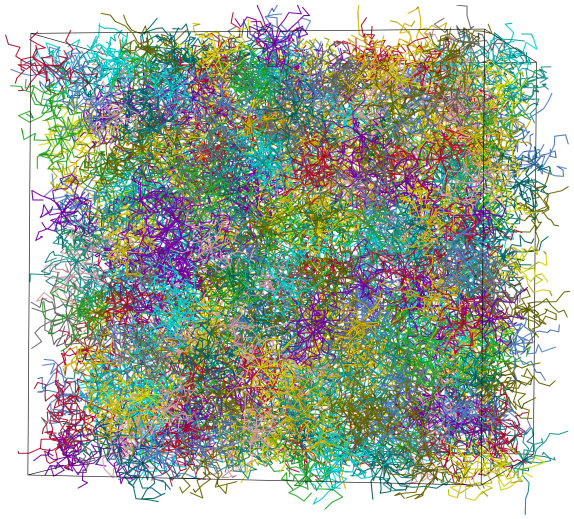

Figure 1. An equilibrated system of star polymer melt [3].

Acknowledgements
Financial support through the Grants J1-4134 and P1-0002 from the Slovenian Research Agency is acknowledged.

References
[1] R. Delgado-Buscalioni, K. Kremer, M. Praprotnik, *J. Chem. Phys.* **2008,** 128, 114110.
[2] R. Delgado-Buscalioni, K. Kremer, M. Praprotnik, *J. Chem. Phys.* **2009,** 131, 244107.
[3] J. Sablić, B.S. Thesis, University of Ljubljana, 2012.

KNL 6

Utility of chromatographic and spectroscopic techniques for a detailed characterization of poly(styrene-b-isoprene) miktoarm star copolymers with complex architecture

Ema Žagar (1,2)*, David Pahovnik (1) and Majda Žigon (1,2)
(1) Laboratory for Polymer Chemistry and Technology, National Institute of Chemistry, Hajdrihova 19, SI-1000 Ljubljana, Slovenia
(2) Centre of Excellence for Polymer Materials and Technologies, Tehnološki park 24, SI-1000 Ljubljana, Slovenia
*ema.zagar@ki.si

This lecture focuses on a detailed characterization of poly(styrene-*b*-isoprene) ($PS(PI)_x$) miktoarm star copolymers which were synthesized by anionic polymerization of polystyrene (PS) and polyisoprene (PI) blocks and selective chlorosilane coupling chemistry. The $PS(PI)_x$ star copolymers consist of one long PS block and different number of shorter PI blocks (x = 2, 3, 5 and 7). $PS(PI)_x$ star copolymers differ also in the length of PI block, which decreases with the number of PI blocks in the star copolymer.
Our aim was to determine the purity of samples and to identify exactly the constituents of individual samples. For this purpose we used a variety of separation techniques (size-exclusion chromatography (SEC), reversed-phase liquid-adsorption chromatography (RP-LAC) and two-dimensional liquid chromatography (2D-LC)), and characterization techniques (UV-MALS-RI multi-detection SEC system, NMR and MALDI-TOF MS). The results of our research work show that detailed characterization of complex polymers requires a comprehensive study, comprising not only the spectroscopic techniques but also efficient chromatographic techniques hypenated with multi-detection systems.

KNL 7

Thiol-ene polymerization of biocompatible monomers in additive manufacturing technology

Robert Liska*
Vienna University of Technology, Institute of Apllied Synthetic Chemistry, Austria
*Robert.liska@tuwien.ac.at

1. Introduction
UV curing of photopolymerizable formulations has been used for more than a half century for protective and decorative coatings of paper, wood, metals or plastics. Advantages can for sure been found in the high curing speed that allows the conversion of typically (meth)acrylate-based monomers within the fraction of a second. Furthermore, a large variety of monomers is commercially available so that the mechanical properties and other polymer characteristics can be easily tuned.
Thiol-Ene polymerization is also known since the 50's of the last century and has gained tremendously increasing interest during the last decade, thanks to the rediscovery by Hoyle [1] and recent efforts by Bowman [2]. Advantages such as low oxygen inhibition and shrinkage, uniform networks with significantly improved mechanical properties are accompanied by up to now unsolved disadvantages such as unpleasant odour and poor storage stability.

2. Results and discussion
This presentation will give an overview on new aspects in thiol-ene polymerization. On the one hand we were able to introduce a new concept in thiol-ene stabilization which gives excellent storage stability with nearly no increase in viscosity with several months up to one year [3].
Very recently we have demonstrated that vinylesters and vinylcarbonates [4] are a promising class of new, low toxic monomers not only for biomedical applications [5] but also for classical coatings. The only limitation of moderate reactivity between those of methacrylates and acrylates has been circumvented by thiol-ene polymerization [6]. Degradation can be easily tuned giving non-toxic low molecular polyvinyl alcohol as degradation product and various non-toxic alcohols such as glycerol or polyethylene glycol. In vivo experiments demonstrated excellent biocompatibility.
If one wants to have arbitrarily shaped 3D cellular structures, additive manufacturing technology (AMT), also called Rapid Prototyping, is the method of choice. Different setups are commercially available that allow the printing of photopolymerizable formulations from a simple CAD model. Laser or DLP (Digital light processing) based systems fabricate polymer parts with a feature resolution of about 10 µm. In recent days not only prototypes are of interest, also small number of individual parts that can be used in the automotive industry or for medical applications are important.
For the 3D printing process, the rather new two photon polymerization technique has also gained increasing interest during the last year. Especially the recently demonstrated significant increase in writing speed [7] will make it nowadays interesting for translation into industrial processes. With newly designed two photon initiators we were also able to show the 3D printing of vinylester-modified gelatine with free thiol-groups of bovine serum albumin, for potential tissue engineering application.

References
1. Hoyle, C. E.; Hensel, R. D.; Grubb, M. B. J Polym Sci, Polym Chem (1984), 22(8), 1865-73
2. Cramer, Neil B.; Bowman, Christopher N. J Polym Sci, Polym Chem (2001), 39(19), 3311-3319.
3. (a) Cherkaoui Z.; Esfandiari P.; Frantz R.; Lagref J.-J.; Liska R. WO2012126695 (A1)
(b) Esfandiari P.; Ligon S. C.; Cherkaoui Z.; Frantz R.; Lagref J.-J.; Liska R. Macromol. Rapid Comm. 2013 submitted.
4. B. Husaar, R. Liska; Chem Soc Rev 2012;41(6):2395-2405
5. C. Heller, M. Schwentenwein, G. Russmüller, T. Koch, D. Moser, C. Schopper, F. Varga, J. Stampfl, R. Liska: J Polym Sci, Polym Chem 49 (2011), 3; 650 - 661.
6. A. Mautner, X. Qin, B. Kapeller, G. Russmueller, T. Koch, J. Stampfl, R. Liska, Macromol. Rapid Comm., 2012, in print DOI: 10.1002/marc.201200502
7. http://www.bbc.co.uk/news/technology-17357374

KNL 8
Enyzmatic catalysis for polycondensation: Potential impact and technological barriers

Alessandro Pellis (1), Livia Corici (2), Valerio Ferrario (1), Cynthia Ebert (1) and Lucia Gardossi (1)*
(1) Dipartimento di Scienze Chimiche e Farmaceutiche, Università degli Studi di Trieste, Piazzale Europa 1, 34127 Trieste, Italy
(2) SPRIN S.p.A., via Flavia 23/1, 34148 Trieste, Italy
*gardossi@units.it

1. Introduction

The extraordinary catalytic potential of enzymes and lipases in particular in polyesters synthesis has been reported in the last two decades.[1] Enzymes are selective bio-catalysts that enable the minimization of protection/deprotection strategies so that monomers with functionalities can be used while avoiding branching. The benefits coming from the use of enzymes in polycondensation reactions are also related to their sustainability and high efficiency at mild conditions: toxic metal catalysts can be avoided and processes can be carried out at temperatures below 80°C. Although the Mn of products attainable by enzymatic polycondensation is in most cases below 10.000, the technology can be used in the production of pre-polymers or in combination with chemical or thermal polymerization. Thanks to the mild reaction conditions, the enzymatic approach to polycondensation is complementary to the chemical synthesis providing a route for the introduction of functional groups inside the polymeric chain with the aim of production of "reactive" polyesters. However, the wide array of enzymatic polyester synthesis described in the scientific literature at laboratory scale are currently not exploited at industrial scale, especially because of low biocatalyst efficiency under process conditions. Recyclability, stability in the viscous conditions of polymerization process and under stirring are the main problems investigated by the "Laboratory of Applied and Computational Biocatalysis" of the University of Trieste. Results achieved in our recent studies will be presented, along with specific enzymatic and synthetic methodologies that can be now used in the enzymatic polycondensation of bio-based polyols and diacids.

2. Results and discussion

The reactions were performed using a robust immobilized enzymes suspended in the monomers, without addition of solvent. A specific immobilization method has been developed for preventing the release of the enzyme during the polycondensation into the polymeric product.[2] Lipase B from *Candida antarctica* (CALB) was used as biocatalyst.

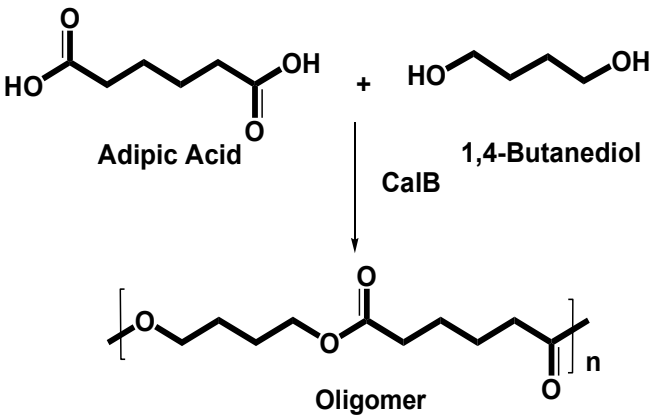

Figure 1: An example of polycondensation catalyzed by Lipase B from *Candida antarctica* (CALB)

Different oligomers were obtained starting from di-acids and corresponding diesters. The synthesis of functionalized polymers has been also evaluated, by using monomers having different active functional groups as side chain. The effect of reaction conditions on enzyme activity and stability was investigated.
In order to control the thermodynamics of the reaction and to improve the kinetics, the polycondensation process was designed in such a way that the reaction mixture forms a thin film. The procedure leads to optimal mass transfer, easy removal of co-products (alcohol or water) and no need of mechanical stirring. The latter factor is of major importance for avoiding damage or grinding of the solid biocatalyst that must be recycled.

3. Conclusions
The study reports an analysis of the potential of biocatalysed synthesis to complement chemical routes for the production of functionalized polymers. New immobilization methods and reaction configurations were developed to overcome the barriers that still hamper the implementation of enzymatic polycondensation at industrial level.

Acknowledgement
Livia Corici gratefully acknowledges European Commission (FP7, People) for a fellowship (REFINE project).

[1] R.A. Gross, M Ganesh, W. Lu, *Trends Biotechnol*, 2010, 28, 436-443.
[2] V. Ferrario, C. Ebert L. Knapic, D. Fattor, A. Basso, P. Spizzo, L. Gardossi. *Adv. Synth. Catal*. 2011, 353, 2466 – 2480

KNL 9
Scanning force microscopy beyond imaging: determine polymer properties on the nm-scale

Sabine Hild*
Johannes Kepler University, Institute of Polymer Science, Altenberger Strasse 69, 4040, Linz, Austria
*sabine.hild@jku.at

1. Introduction
The development of advanced polymers and polymer based composite materials requires detailed information about the physical and chemical properties. Analysis techniques such as differential scanning calorimetry (DSC), thermomechanical analysis (TMA) and dynamical mechanical analysis (DMA) are important and reliable instruments in polymeric research, however, up to now mainly bulk properties are detected. Polymeric materials are often heterogeneous on nanometer scale and composition as well as heterogeneity can vary due to processing. Since polymer microstructure, material properties and processing conditions are linked the thermal or mechanical characterization on a microscopic scale and the visualization of morphology have to be carried out simultaneously. Scanning force microscopy (SFM) has proven to represent a suitable method to fulfill this task.
Dynamic imaging techniques such as Tapping mode and phase imaging have been widely explored as a tool for morphology characterization allowing the in-situ monitoring of deformation or thermal induced changes in polymer microstructure. The high spatial resolution of this technique can also be combined with the characterization capabilities of mechanical and thermal analysis. Thus, it is possible to directly measure the mechanical and thermal responds of a specimen in a localized region rather than on the macroscopic scale. Thereby on inhomogeneous samples the material properties can be mapped and determined for different phases on the sub-µm scale.

2. Nanomechanical characterization
On macroscopic scale nanoindentation provides accurate material properties measurements that can directly be compared to Dynamic Mechanical Analysis (DMA). When the cantilever of a SFM is used as an indenter instead of being scanned laterally across the sample surface nanoindentation experiments can be performed and mechanical properties can determined on the nanometer scale. To use the SFM tip as an instrument for depth sensing the load applied on the tip and the relative motion between tip and sample will be detected recording a force curve, i.e., a plot of penetration depth vs. applied load. Subsequent application of contact mechanics models enables the estimation of mechanical parameters.
Besides the high spatial resolution key benefits on using the SFM as a nanoindenter are on one hand that the indented area can be imaged, and the shape and evolution of the indent imprints can be studied as a function of time. On the other hand, a unique versatility in the load range achieved by changing the cantilever stiffness, which can vary between fractions of nN up to a few tens of µN. Nevertheless, some experimental difficulties and calibrations have to taken into account. First of all, since the load is applied through a bending cantilever the traveling distance of the piezo does not directly reflect the indentation depth. For this reason, the deflection of the cantilever has to be calibrated on a hard material to determine the deflection sensitivity. For each probe the cantilever elastic constant has to be taken from producer data or estimated on the basis of approximate methods. Furthermore, for the calculation of mechanical parameter tip curvature radius, or, in some cases the overall tip geometry has to be known. Ussually, this value has been taken from producer data not considering the production scattering or that the tip shape of conventionally used silicon cantilever can change due to mechanical damage or contamination with soft material. To find a remedy well special indentation cantilevers were used in our experiments with calibrated spring constants and square shaped diamond tips.

Conventional nanoindentation refers to quasi-static indentation testing in the submicrometer range. Additionally, by modulating the force and/or the displacement nanoindentation can be performed in dynanmic (ac) mode. Thus, performing the experiments at variable temperatures quantitative studies of dynamic mechanical properties such as viscoelasticity becomes possible.

3. Nanothermal characterization

Thermal analysis have been important and reliable instruments for polymeric research, however, up to now mainly bulk properties are detected. To understand local mechanisms for temperature-induced phase transitions quantitative measurements of the thermomechanical behavior such as glass transition and melting temperatures as well as temperature dependent elastic modulus and thermal expansion coefficients in nanoscale volumes are required. Local thermal analysis (LTA) combines the basic concept of common thermal analysis and the high resolution of scanning probe microscopy to form a novel technique for polymer characterization. In LTA a heatable tip is broad into contact with a polymeric surface and the cantilever deflection is measured as the tip temperature is increased. A sharp deflection of the tip into the material occurs at a specific 'softening temperature' that is presumably related to either the glass transition temperature (T_G) or the melting temperature (T_M) of the material being tested. In conventional thermomechanical analysis a Wollaston wire based scanning tip have been is used. This system is not suitable for thermal analysis at sub-μm length scales because a 5 μm diameter wire is bent into a tip with 20 μm radius of curvature. The development of highly doped Si AFM tip that is resistively heated allows spatially resolved measurement of thermomechanical properties at nanometer length scales, resulting in nano-LTA measurements.

Previous nano-LTA observations have led to many contradictory observations, because the 'softening' transition in polymer films is related non-trivially to the supporting solid substrate below the film and to the environment above it by thermal and mechanical couplings. For the quantitative data analysis an appropriate temperature calibration method has to be established, which correlates unambiguously the deflection signal of the measurement with the softening temperature of the probe. However, the interpretation of the softening temperature is complicated by a number of factors, such as the film thickness and the thermal and mechanical properties of the substrate on which the film is supported. An appropriate calibration procedure based on polymer softening temperatures and power applied to the tip will be presented to correlate the results of nano-LTA measurements with results obtained from DSC.

4. Outlook of the talk

In the presentation experimental basics of SFM nanoindentation and local thermal analysis (LTA) for polymer characterization on the nanometer scale will be discussed. SFM nanoindentation and local thermal analysis are applied to investiagted the solvent induced changes in the thermal and mechanical properties of polymer coatings and in a close to surface region of bulk materials. The suitability of ac nanoindentation at variable temperatures for the determination of local viscoelasticity will be demonstrated.

KNL 10
New synthetic polymers and nanocomposites: From self-directed assembly to semiconductor superhighways

Todd Emrick*, Emily Pentzer, Jimmy Lawrence, and Zachariah Page
Polymer Science and Engineering Department, University of Massachusetts Amherst, Amherst, MA 01003, United States of America
*tsemrick@mail.pse.umass.edu

This presentation will describe the synthesis of polymers and nanoparticles, and the combination of polymers and particles into well-organized arrays. These arrays, or 'superhighways', give access to nanostructured hybrid materials that align p-type (hole carrying) and n-type (electron carrying) components. Such materials are potentially ideally suited as active layers in devices, such as solar cells. The presentation will also highlight syntheses of conjugated polymers that possess orthogonal solubility to conventional active layers, such as hydrophilic poly(benzothiadiazoles) that alter the work function of metals when present as thin films on metal surfaces.

KNL 11
Rechargeable batteries based on Li-sulfur/poly(acrylonitrile) composite materials: Synthesis and structure-related electrochemistry

Jean Fanous (1), Marcus Wegner (1), Jens Grimminger (1), Malte Rolff (1), Änne Andresen (1), Abhishek N. Mondal (2), Michael R. Buchmeiser (2)
(1) Robert Bosch GmbH, Corporate Sector Research and Advance Engineering, 70049 Stuttgart, Germany
(2) Institute of Polymer Chemistry, University of Stuttgart, 70569 Stuttgart, Germany

Among the most promising element combinations for the next generation of batteries is lithium/sulfur. Starting from elemental sulfur, i.e. from S_8, the electrochemical reduction cascade finally leads to poly(sulfide)s, S_x^{2-}, which are soluble in the chosen electrolyte for at least x≤3. Consequently, diffusion of active cathode material, i.e. of poly(sulfide)s to the anode occurs, resulting in the formation of Li_2S at the lithium surface and a sometimes dramatic loss in capacity. One concept for poly(sulfide) retention is to embed sulfur inside a cyclized poly(acrylonitrile) (PAN) structure by heating PAN and elemental sulfur to >300°C.[1] In course of this procedure, the sulfur dehydrogenates PAN, which forms cyclic structures with a conjugated π-system. In order to clarify how sulfur is embedded into the cyclic PAN-derived network, different PAN/sulfur composites were synthesized. TOF-SIMS, XPS and FT-IR experiments strongly suggest that in all composites the sulfur is exclusively covalently bound to carbon and not to nitrogen. Moreover, N-C-S- fragments, most probably resulting from 2-pyridylthiolates as well as S_x (x≥2) and thioamide fragments, have been identified by TOF-SIMS. A structure for the composite is presented that explains for all analytical data as well as for the entire electrochemistry observed. A sulfur balance carefully established during discharge strongly suggests that the polymer backbone, which most probably consists of a conjugated π-system, significantly contributes to the initially measured capacity. Finally, issued concerning the Li-anode will be addressed.

1. J. Wang; J. Yang; J. Xie; X. Naixin. *Adv. Mater.* **2002** (14) 963.
2. J. Fanous, M. Wegner, J. Grimminger, Ä. Andresen, M.R. Buchmeiser *Chem. Mater.* **2011** (23) 5024.
3. J. Fanous, M. Wegner, J. Grimminger, M. Rolff, M.B.M. Spera, M. Tenzer and M.R. Buchmeiser, *J. Mater. Chem*. **2012**, in press.

KNL 12
New ways for the characterization of appearance properties of plastic products and components close to human vision

Dieter P. Gruber (1)*, Gerald R. Berger (2), Walter Friesenbichler (2)
(1) Polymer Competence Center Leoben GmbH, Leoben, Austria
(2) Montanuniversitaet Leoben, Chair of Injection Molding of Polymers, Leoben, Austria
*dieter.gruber@pccl.at

1. Introduction
The first impression of a product's quality is formed by the appearance of its surface and in most cases, strong conditioning has produced expectations on specific surface attributes that a certain product has to show. In this respect, the human eye-apparatus is still considered to be the most sophisticated evaluation tool. However, evaluation of surface appearance performed exclusively through human observation proves insufficient since the judgment depends on individual factors like the observer's eyesight, experience and mood at the time of the evaluation. Consequently, there is a strong demand for measurement techniques which provide results that are for one unambiguous and reproducible, but also correspond to the visual perception of individual evaluators. Our newly developed surface inspection methods include the quantitative evaluation of a variety of visual surface deficiencies [1-3]. The methods can be translated into practice, e.g. for a better in-depth optimization of injection molding and extrusion processes and for IN-LINE quality inspection of extruded or injection molded parts.

2. Measurement
For our investigations, a multifunctional injection mold was used to manufacture examination samples with controlled defect formation. The polymer part includes ribs with varying thickness. The focus of current studies lies in the quantitative evaluation of the visual perceptibility of sink marks caused by ribs at the sample's back side. The main wall thickness of the test part measures 2.5 mm while ribs are 1.2 mm, 1.6 mm, 2.0 mm and 2.5 mm thick (Figure 1). Sink marks are shrinkage related phenomena that depend on processing parameters like mold and melt temperature and holding pressure. In a test series, the holding pressure was varied within a range of 20 MPa to 80 MPa. Other processing parameters like the barrel and mold temperature, as well as the injection rate were kept constant. The used polymer was black polycarbonate (PC). In order to ensure a stationary process, 10 cycles of each setting were discarded. The machine vision system included CCD-cameras and D6500 standard light sources. The light sources were adjusted that way that surface structure showed maximal contrast. Finally, images are captured which form the raw data for the calculation of the perceptibility of the surface defects.

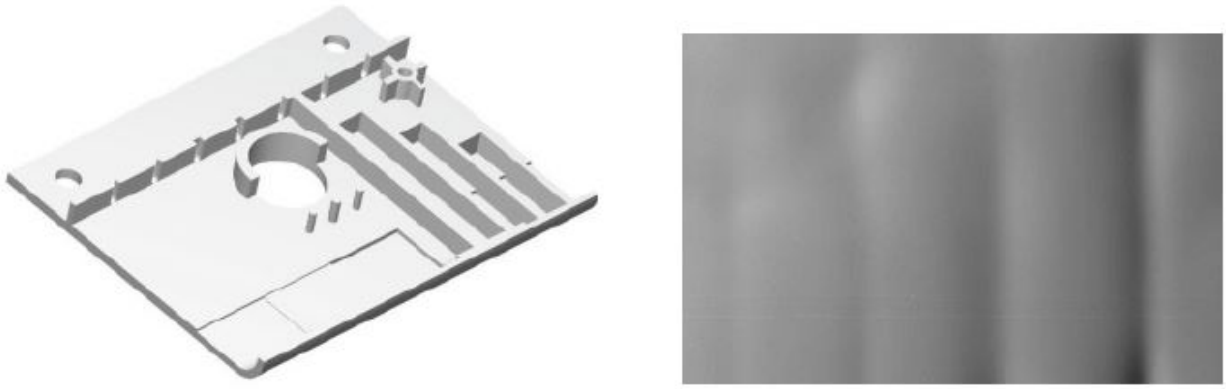

Figure 1: Backside of an injection molded test part (left) and image of sink marks (right) caused by reinforcing rips

3. Results and discussion

Intensity matrices taken from digital images of the regions of interest contain information about shadows, gloss and other visual parameters which form quality deciding aspects. One objective was to derive a model parameter which allows for fast evaluation of the visual perceptibility of any given sink mark. In the first processing step profiles were calculated from the image matrices across the expansion of the sink marks. From these profiles, the second derivative was calculated. For further processing, a polynomial was used to fit the second derivative. The resulting smooth function ensures a fast and robust calculation of higher order derivatives. A high extreme value of the second derivative corresponds to a local low extreme value of the original profile. Hence, the amplitudes of the second derivative tend to form a measure for the magnitude of sink marks. In order to locate the sink marks within the image data, the zero-crossing of the second derivative was determined. It lies necessarily between two zero-crossings of the first derivative. The local extreme values of the second derivative were found between two zero-crossings of the first derivative. These positions do not alter. It became apparent that the amplitude of the second derivative (ASD) is related to a sink mark's visual perceptibility. In order to prove the results of the machine vision system, a panel study was carried out where human evaluators rated the visibility of different sink marks. The assessors were instructed to rate sink marks by using grades between 0 and 10. The highest grade 10 was defined to be mandatory for the visually strongest sink mark in a series. The lowest grade 0 was only to be taken for specimens without a perceptible sink mark. That determination enabled the comparison of the assessments of different evaluators. Figure 2 shows a selection of inspected surface defects.

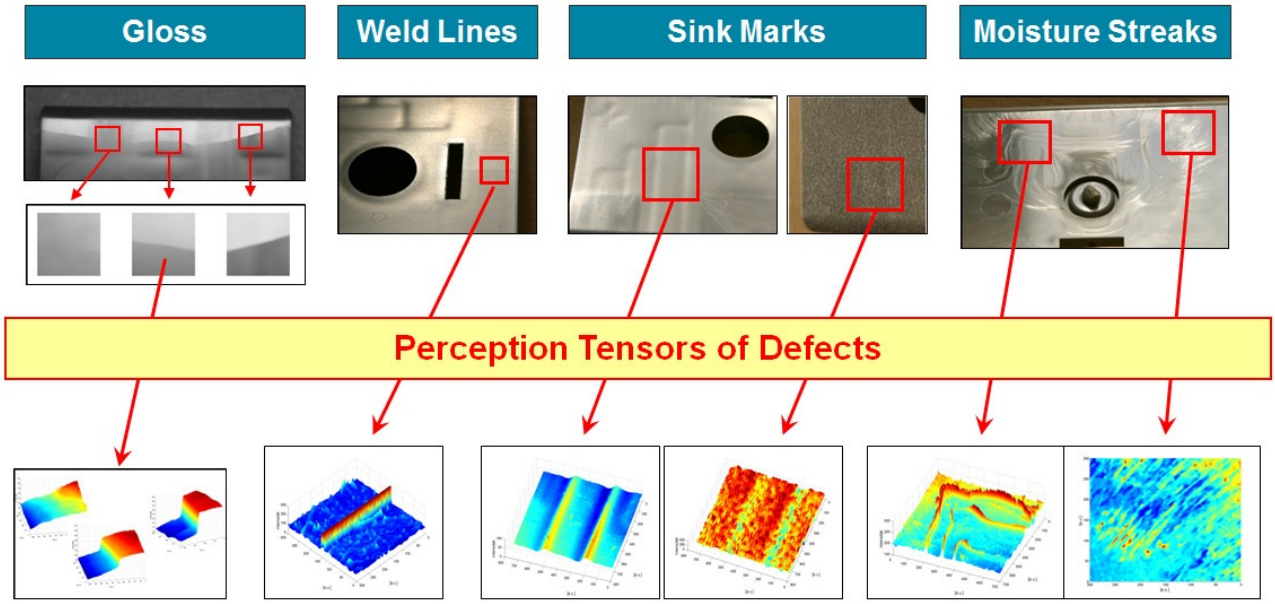

Figure 2: Selection of characterized surface defect types at an injection molded test parts

5. Conclusions

There is a strong industrial demand for automated defect characterization of injection molded polymer parts. For In-Line use, processing has to be fast and the results have to correspond to human vision. A newly developed surface inspection system enables the quantitative evaluation of a variety of different polymer surface defects. In order to quantify the perceptibility of these defects,

a model function was derived. Molded polymer parts, which exhibit sink marks caused by a series of differently pronounced ribs on the back side of the parts, were evaluated. In the processing, profiles of the surfaces were calculated from surface image matrices across the expansion of the sink marks. From these profiles, the second derivative was calculated and fitted to a polynomial. The surface data was captured by the machine vision system and the visual perceptibility of each sink mark was calculated automatically by applying the model function. The results of the machine vision system were compared to results gained in a human assessment study and they turned out to correlate very well to human vision. The method can be translated into practice, e.g. for a better in-depth optimization of injection molding processes and for IN-LINE quality inspection.

Acknowledgements
The research work of this paper was performed at the Polymer Competence Center Leoben GmbH (PCCL, Austria) within the framework of the COMET-program of the Austrian Ministry of Traffic, Innovation and Technology with contributions by the Chair of Injection Molding of Polymers, Montanuniversitaet Leoben. The PCCL is funded by the Austrian Government and the State Governments of Styria and Upper Austria.

References
[1] D.P. Gruber, G. Berger, G. Pacher, W. Friesenbichler, Novel approach to the measurement of the visual perceptibility, Polymer Testing, Polymer Testing 30 651–656 ,2011
[2] D.P. Gruber, Neuartige Methode zur Messung der Glanz-Klarheit des Erscheinungsbildes von Werkstoff- und Produktoberflächen, Patent pending, 2011,
[3] D.P. Gruber, Method for automatically detecting defects on the surface of a molded part, Patent, 2010, 102319A1

KNL 13
Nanoparticle-polymer hybrid solar cells

Gregor Trimmel*
Graz University of Technology, Institute for Chemistry and Technology of Materials & Christian Doppler Laboratory for Nanocomposite Solar Cells, Stremayrgasse 9, 8010, Graz, Austria
*gregor trimmel@tugraz.at

1. Introduction
Organic based solar cells have seen impressive progress during the last 5 years reaching power conversion efficiencies of 10 % [1]. In this presentation, a short introduction of the status quo of polymer based solar cells will be given, focusing then on nanoparticle-polymer hybrid solar cells consisting of both organic semiconductors and inorganic semiconductor nanoparticles. Although the currently obtained power conversion efficiencies are lower (4-5%), this type of material aims at combining the specific advantages of organic semiconductors, like easy processability and high absorption coefficients with the high charge carrier mobilities in inorganic semiconductors [2]. Whereas in classical polymer-fullerene solar cells, the absorption of light is optimized by the absorption properties of the polymer, in hybrid solar cells this can be achieved either by the polymer or the semiconductor nanoparticles. The quantum confinement effects as well as the possibility to use nanoparticles of different shapes (dots, rods, tetrapods, multibranched crystals) lead to unique features of this type of materials. Different synthetic approaches towards nanocomposite solar cells will be discussed in detail. Besides the low thermal stability of conjugated polymers, the main challenge are the different polarity of inorganic nanoparticles and the conjugated polymers requiring synthetic optimisation for both phases and the control of the interface and morphology of the nanocomposite materials.

2. Results and Discussion
In the second part, the influence of several synthesis routes on the obtained morphology and purity of the hybrid layers and consequently on the solar cell parameters will be exemplarily discussed. In particular, the in-situ preparation of copper indium sulfide nanoparticles directly in a matrix of the conjugated polymer via the decomposition of metal xanthates at relatively low termperatures yields solar cells with power conversion efficiencies up to 2.8% [3]. Different conjugated polymers based on poly(thiophenes), poly(fluorenes) and alternating copolymers have been used for the preparation of hybrid solar cells. A critical issue for efficient solar cells is to balance the thermal processing temperatures necessary for the complete decomposition of the metal xanthates with the crystallization of the polymer. A schematic representation of the metal xanthate route is shown in Scheme 1.

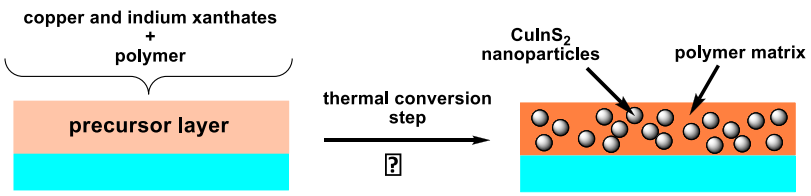

Figure 1. Schematic representation of the metal xanthate route to metal sulfide /polymer hybrid layers

References
[1] G. Li, R. Zhu, Y. Yang, *Nature Photonics* **2012**, 6, 153-161.
[2] A.J. Moulé, L. Chang, C. Thambidurai, R. Vidu, P. Stroeve J. *Mater. Chem.* **2012**, 22, 2351-2368.
[3] T. Rath, M. Edler, W. Haas, A. Fischereder, S. Moscher, A. Schenk, R. Trattnig, M. Sezen, G. Mauthner, A. Pein,D. Meischler, K. Bartl, R. Saf, N. Bansal, S. A. Haque, F. Hofer, E. J.W. List, G. Trimmel, *Adv. Energ. Mater*. **2011**, 1, 1046-1050.

KNL 14
Creating hierarchically porous polymer materials with emulsion templating

Peter Krajnc*
University of Maribor, Faculty of Chemistry and Chemical Engineering, PolyOrgLab, Smetanova 17, SI-2000, Maribor, Slovenia and Centre of Excellence PoliMaT, Tehnološki park 24, SI-1000, Ljubljana, Slovenia
*peter.krajnc@um.si

Emulsions with a high volume fraction of droplet phase can be used to template macro pores within a polymer material if the continuous phase contains monomers and the polymer is obtained by curing the emulsion without compromising the emulsion structure. Secondary pores are created between the macro pores during the curing process and the polymer film itself can contain meso and micro pores, depending on the conditions of preparation, crosslinking degree and the solvent used in the continuous phase. The lecture will present latest developments in the field of emulsion templating, present new chemistries and new results of combining emulsion templating with other methods for the preparation of hierarchically porous materials.
High internal phase emulsions are known as emulsions containing more than 74,05 vol% of internal phase. By polymerizing the continuous phase, a solid polymer with large pores in place of the droplets of internal phase and a series of interconnecting pores is prepared. Relatively large pore sizes yield material with low surface area. In order to enlarge the surface area, a post-polymerisation hypercrosslinking reaction is possible. Additional linkages are created resulting in smaller pores and higher surface area. In this way a hierarchical porous monolithic polymer can be prepared.
A Friedel-Crafts reaction between chloromethyl groups in the polymer matrix can be utilized for post-polymerisation crosslinking approach (Figure 1). The reaction is processed via Friedel-Craft catalyst and the amount of chloromethylated groups reacting can be controlled by kinetics. A number of mesopores are created which has a dramatic effect on the surface area of the polymer. For example, a 2 % crosslinked vinylbenzyl chloride based polyHIPE, subsequently hypercrosslinked was prepared and an increase of surface area from 5.7 to 990.0 m^2/g was found. A substantial amount of chloromethylated groups were left enabling further functionalisation of the polymer.

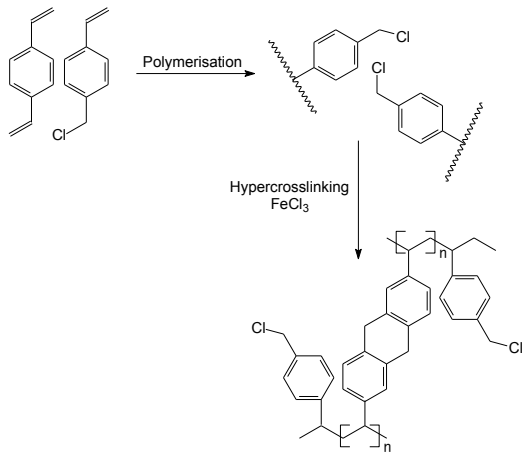

Figure 1. Hypercrosslinking via Friedel-Crafts Reaction

Another approach to hypercrosslinking is to utilize the remaining double bonds in the polymer matrix which can react with multifunctional thiols. For this purpose a series of polyHIPE samples with varied crosslinking degree were prepared. Samples were reacted with both 2,2(ethylenedioxy)-diethanethiol and pentaerythritol tetrakis(3-mercaptopropionate) with radical initiator in order to obtain linkages with double bonds via thiol-ene reactions (Figure 2). By using a mixture of 2,2(ethylenedioxy)-diethanethiol and bifunctional alkene, the reaction resulted in significant enlargement of BET surface area, from 107 to 233 m^2/g.

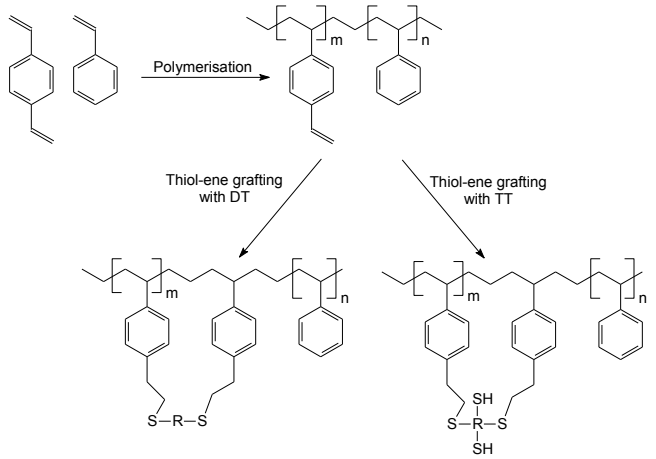

Figure 2. Thiol-ene grafting onto STY/DVB polyHIPEs

References

[1] K. J. Lissant, *Emulsions and Emulsion Technology*, Part 1, Marcel Dekker, New York, **1974**, Chap.1.
[2] I. Pulko, P. Krajnc, *Macromol. Rapid Commun*. **2012**, 33, 1731-1746.
[3] S. D. Kimmins, N. R. Cameron, *Adv. Funct. Mater.* **2011**, 21, 211-225.
[4] N. R. Cameron, P. Krajnc, M. S. Silverstein, *Colloidal Templating*; in M. S. Silverstein, N. R. Cameron, M. A. Hillmyer (Eds.), *Porous Polymers*, John Wiley & Sons, Inc., Hoboken, New Jersey, **2011**.
[5] V. A. Davankov, M. P. Tsyurupa, *React. Polym.* **1990**, 13, 27-42.
[6] K. Aleksieva, J. Xu, L. M. Wang, A. Sassi, Z. Pientka, Z. P. Zhang, K. Jeřabek, *Polymer* **2006**, 47, 6544-6550.
[7] I. Pulko, J. Wall, P. Krajnc, N. R. Cameron, *Chem. Eur. J.* **2010**, 16, 2350-2354.
[8] C. E. Hoyle, C. N. Bowman, *Angew. Chem. Int. Ed*. **2010**, 49, 1540-1573.

KNL 15
Synthesis of functionalized PLA and PLGA

Coleen Pugh*, Abhishek Banerjee, Colin Wright, Xiang Yan, Peiyao Wang, Jialu Yan, William Storms
The University of Akron, Department of Polymer Science, 170 University Ave., Akron, OH, USA
*cpugh@uakron.edu

1. Introduction

Polyesters of lactic acid (PLA), glycolic acid (PGA) and their copolymers (PLGA) are the most commonly used materials for biomedical, and disposable or non-recoverable polymer goods applications because they degrade under biological and environmental conditions; their degradation products occur naturally in the body and the environment; and their monomers are naturally derived. We recently designed and synthesized acrylate inimers that produced the first truly hyperbranched analogs of linear polyacrylates upon *homo*polymerization by atom transfer radical polymerization.[1] The key intermediate of this new class of inimers is a 2-halo-3-hydroxypropionic acid (halo = Cl or Br), which we synthesize regioselectively starting from serine,[2] a natural amino acid that can be isolated from soybean protein. Since 2-halo-3-hydroxypropionic acids are halogenated isomers of lactic acid, yet have a primary alcohol group like glycolic acid, we believe they are ideal comonomers to copolymerize with glycolic acid and/or lactic acid to provide PLA and PLGA with sites for attaching biologically active or other functional molecules.[2] The aim of this research is to establish the synthesis and properties of halogenated PLAs and PLGAs, and their functionalization reactions based on the bromine substituent.

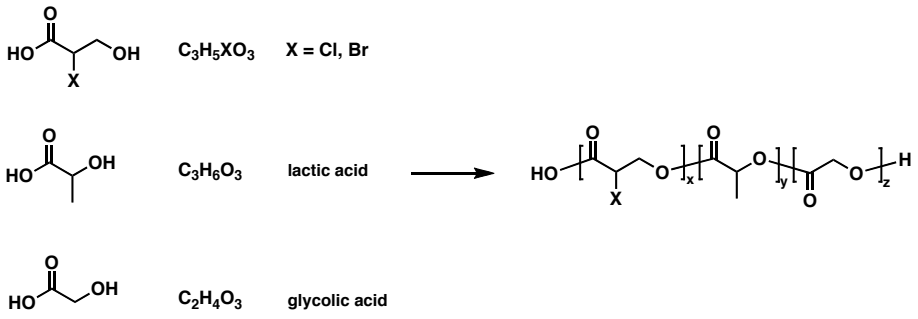

Figure 1. Synthesis of hyperbranched polyacrylates and halogenated polyesters based on 2-halo-3-hydroxypropionic acid

Sample	Feed Ratio LA : GA: BrA	Yield (%)	M_n x 10^{-4}	DP_n	pdi	T_g (^oC)
PLA	100 : 0 : 0	54	3.16	439	1.62	51
PLGBrA502030	50 : 20: 30	70	1.89	203	3.86	39
PLBA5050	50 : 0 : 50	44	2.03	182	1.93	35

Table 1. Acid Catalyzed "Bulk" Copolyesterification of 2-Bromo-3-hydroxypropionic Acid at 95 ^oC in Vacuo for 48 h.

2. Results and discussion

Table 1 presents the *p*-toluenesulfonic acid catalyzed copolyesterification results of 2-bromo-3-hydroxypropionic acid (BrA) with glycolic and/or lactic acid on a 1 g scale. Although both GA and BrA decrease the molecular weight (according to GPC relative to linear polystyrene) of the copolymers relative to homopolymerization of LA, it Is possible to generate brominated polymers in the 20 kDa range. Both GA and BrA also decrease the glass transition temperatures slightly. We will elaborate on these results, as well as present various functionalization reactions.

3. Conclusions

Relatively high molecular weight (M_n ~ 20 kDa) halogenated PLAs and PLGAs can be synthesized by polyesterification. These halogenated polymers can be functionalized through nucleophilic substitution and radical reactions.

Acknowledgements

We gratefully acknowledge partial funding by NSF (DMR-0630301), NIH (ARRA Supplement for GM86895-2), and Omnova Solutions.

References

[1] (a) C. Pugh, A. Singh, A. "Synthesis of Inimers and Hyperbranched Polymers", WO2008045299-A1; EP2079844-A1; IN200902573-P1; CA2665607-A1; CN101553571-A; JP2010506000-W, April 17, 2008. (b) C. Pugh, A. Singh, R. Samuel, K.M. Bernal Ramos, K.M. *Macromolecules* 2010, *43*, 5222-5232.

[2] Pugh, C.; Raveendra, B.; Singh, A.; Samuel, R.; Garcia, G. *SynLett* 2010, 1947-1950.

[3] Pugh, C.; Banerjee, A.; Storms, W; Wright, C.. "Functional Biodegradable Polyesters", UAkron 810, U.S. Patent Application 61/368413, filed on July 28, 2011.

KNL 16
Zwitterionic polymers: kinetics, characterization and biomedical applications

Peter Kasák (1,2), Patrik Sobolčiak (1), Vladislav Semak (1), Marek Stach (1), Zuzana Kroneková (1), Gabriela Kolláriková (1), Igor Krupa (1,2), Dušan Chorvát (3), Igor Lacík (1)

(1) Polymer Institute SAS, Department for Biomaterials Research, Dubravska cesta 9, 845 41 Bratislava, Slovakia
(2) Current address: Center for Advanced Materials, Qatar University, P.O. Box 2713, Doha, Qatar
(3) International Laser Centre, Department of Biophotonics, Ilkovicova 3, 841 04 Bratislava, Slovakia

1. Introduction

Zwitterionic polymers have been intensively studied owing to their suitability for the design of non-biofouling materials and surfaces with unique physical and chemical properties [1,2]. Polyzwitterions are built of electrically neutral monomer units formally containing both positive and negative charges on different atoms in a monomer unit. The monomer units are represented by various chemical structures such as sulfobetaines, carboxybetaines and phosphorylbetaines. This contribution will highlight our recent activities in the areas of synthesis, characterization and application of zwitterionic polymers and hydrogels.

2. Results and discussion

The synthesis of zwitterionic polymers is so far lacking a detailed description of mechanism and kinetics of polymerization. Our experience in this area, specifically related to the free-radical polymerization kinetics and mechanism of water-soluble monomers polymerized in aqueous solutions [3], was recently applied for the kinetic studies of sulfobetaine monomers [4]. By employing the pulsed-laser polymerization in conjunction with the size-exclusion chromatography, the first propagation rate coefficients, k_p, were determined. The Arrhenius parameters characterizing k_p and the solvent effect manifested by the k_p decrease with increased monomer concentration were of similar range than those for partially neutralized methacrylic acid [3]. The increase in k_p values was observed in the presence of simple salt due to the anti-polyelectrolyte effect.

Sulfobetaine hydrogels of various characteristics were prepared by free-radical polymerization in the presence of newly synthesized zwitterionic crosslinkers [5]. These crosslinkers were used in order to suppress the compositional drift during the hydrogel formation. Hydrogels crosslinked using different crosslinking conditions were characterized in terms of mechanical properties, degree of crosslinking, equilibrium water content, sorption degree, diffusion coefficient of water, state of water and attachement of fibroblast cells. Zwitterionic hydrogels were successfully applied as the immobilization matrix for functional entrapment of the glucose-binding protein, which was used for sensing the glucose level in the design of implantable glucose biosensor.

Zwitterionic polymers and hydrogels were tested in several other areas. Electrografting of sulfobetaine polymers to the conductive surface resulted in highly reduced biofouling tested by fibroblast cells [6]. In addition, the photo-induced coating made of sulfo- and carboxybetaines was used to modify the surface of various polymeric substrates. Recently we proposed the novel cationic copolymer that is light-switchable to the zwitterionic carboxybetaine [7]. This principle was demonstrated in the capture and release, upon illumination, of DNA as well as on light-switching from antibacterial to non-toxic surface characteristics (Figure 1). Finally, the preliminary data on application of zwitterionic polymers in the design of microcapsules aimed at immunoprotection of transplanted cells will be shown.

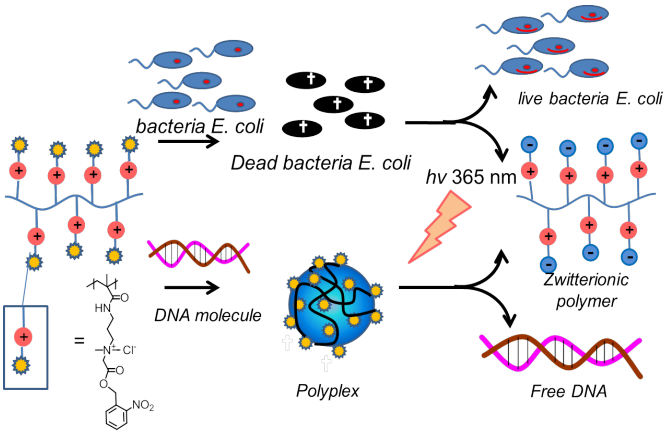

Figure 1. Light-switchable polymer from cationic to carboxybetaine forms for controlling the interactions with DNA and bacterial cells.

3. Conclusions

The group of zwitterionic polymers is a pleasant "play-ground" with numerous opportunities for studies in macromolecular chemistry as well as at the border between macromolecular chemistry and biological sciences. The outcomes from our work represent a new knowledge in the kinetics and mechanism of polymerization, which should continue towards the complete kinetic scheme and modeling of polymerization, and exemplifies a few from a number of possibilities, where zwitterionic polymers are advantageous in controlling the interaction with biological compounds.

Acknowledgements

This work has been financially supported by the Slovak Research and Development Agency under the contracts No. APVV-0486-10, by VEGA Grant Agency under the contract No. 2/0160/12, the EFSD New Horizons grant and the Sixth Framework Program of the EU, IP-031867, P. Cezanne.

References

[1] A. B. Lowe, C. L. McCormick, Polyelectrolytes and polyzwitterions: synthesis, properties, and applications, ACS Books, Washington DC, 2006.
[2] A. J. Keefe, S. Jiang, S. *Nature Chem.* **2012**, 4, 59–63.
[3] I. Lacík, L. Učňová, S. Kukučková, M. Buback, P. Hesse, S. Beuermann, *Macromolecules* **2009**, 42, 7753–7761.
[4] P. Sobolčiak, P. Kasák, M. Stach, D. Chorvát, I. Lacík, prepared for publication.
[5] P. Kasák, Z. Kroneková, I. Krupa, I. Lacík, *Polymer* **2011**, 52, 3011-3020.
[6] M. Stach, Z. Kroneková, P. Kasák, J. Kollár, M. Pentrák, M. Mičušík, D. Chorvát T. S. Nunneyd, I. Lacík, *Appl. Surf. Sci.* **2011**, 257, 10795-10801.
[7] P. Sobolčiak, M. Špírek, J. Katrlík, P. Gemeiner, I. Lacík, P. Kasák, Macromol. Rapid Commun. **2013**, early view DOI: 10.1002/marc.201200823

LECTURES

Session 1: Advances in Polymer Synthesis and Modification

S1-L1
Covalent modification of unsaturated polymers using iEDDA click chemistry

Astrid-Caroline Knall (1)*, Sebastijan Kovačič, Christian Slugovc
(1) Institute for Chemistry and Technology of Materials (ICTM), Graz University of Technology, Stremayrgasse 9/V, A-8010 Graz, Austria
*a.knall@TUGraz.at

1. Introduction

The inverse-electron demand Diels-Alder addition between tetrazines and alkenes (Figure 1) has been recently applied for the conjugation of functional materials, especially in life sciences (due to its bioorthogonal nature) [1]. Tetrazines act here as electron-deficient dienes, whereas the dienophile should be electron-rich. The bicyclic Diels-Alder adduct decomposes upon elimination of nitrogen, and the resulting dihydropyridazine intermediate is then oxidized to the final pyridazine product. Other driving forces are ring strain and a low degree of sterical hindrance [2]. Recently, this new concept for click chemistry has also gained attention in the polymer science community as a facile method for polymer modification and the preparation of block copolymers [3].

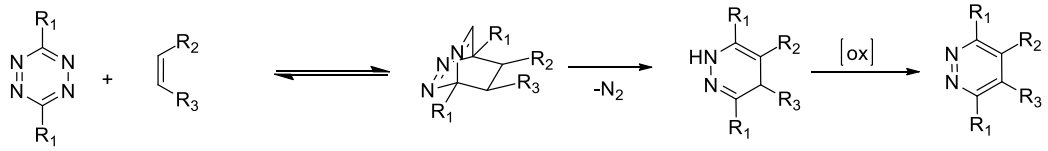

Figure 1. iEDDA click chemistry

2. Experimental

Screening experiments (Table 1): Equimolar amounts of the respective alkene and tetrazine (3,6-diphenyl- and 3,6-di(pyridin-2-yl)-1,2,4,5-tetrazine) were mixed in dichloromethane at room temperature. Reaction progress was monitored visually and by TLC and reactions were stopped after full turnover by evaporating the solvent. The solid residue was taken up in $CDCl_3$ and conversion was determined by ^1H NMR spectroscopy using the tetrazine peaks in the region of 9 to 7.5 ppm (for py-Tz) and the peaks of the formed (dihydro)pyridazine products.

Kinetic measurements of iEDDA reactions in methanol (Figure 2) were performed by monitoring the characteristic tetrazine absorption maximum at 545 nm using different molar (excess) ratios of tetrazines and alkenes under pseudo first-order conditions. A tetrazine starting concentration of 1 mmol/l was used in all experiments whereas 10, 14, 16 and 20 equivalents of the respective alkene were added. All experiments were repeated three times.

3. Results and discussion

In Table 1, results for pre-screening experiments are presented. It is evident that for a successful click reaction, electron-withdrawing groups need to be present at the tetrazine ring. Cyclopentene and DCPD both undergo an iEDDA reaction, treatment of DCPD with two equivalents of tetrazine resulted only in partial labeling of the cyclopentene double bonds, most likely due to sterical hindrance.

Table 1. NMR pre-studies

tetrazine	alkene	Time	Tz Conversion*
ph-Tz	**1**	24h	No reaction
ph-Tz	**2a**	24h	No reaction
py-Tz	**1**	24h	>99%**
py-Tz	**2a**	24h	>99%
py-Tz	**3**	24h	61%
py-Tz	**4**	12h	>99%
py-Tz	**5**	24h	No reaction
py-Tz	**6**	24h	No reaction

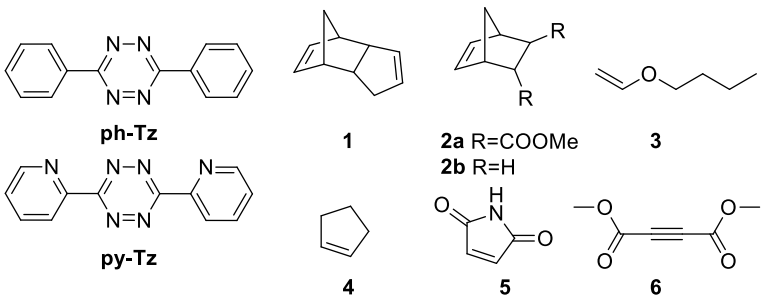

*determined by NMR spectroscopy **the strained norbornene double bond is preferred

While strained, electron-rich double bonds can be converted using iEDDA chemistry, no reaction products were detected when **5** and **6** were reacted with **py-Tz**, which are examples of typical substrates for Michael thiol-ene and copper-free azide-alkyne click chemistry.

Furthermore, reaction constants for different labeling experiments were determined and are shown in Figure 2. The reaction rate for cyclopentene was around one order of magnitude lower than for norbornene reflecting the lower amount of ring strain. The lower reaction rate obtained for DCPD can be explained due to steric crowding of the double bond.

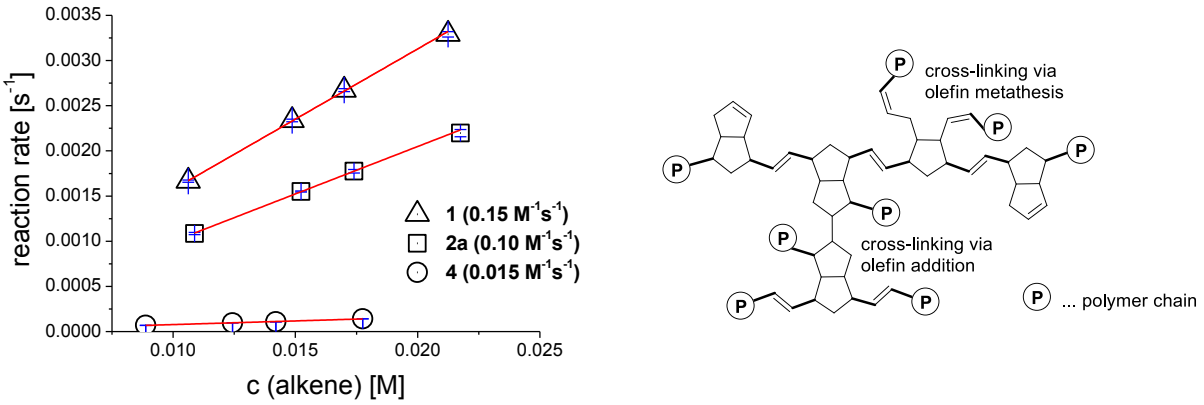

Figure 2. a) Reaction constants of different labeling experiments: norbornene-py-Tz, DCPD-py-Tz, cyclopentene-py-Tz b) structure of poly(dicyclopentadiene)

Bulk ring-opening metathesis polymerization of **1** leads to polyDCPD, a tough, rigid, thermoset polymer exhibiting high impact resistance, high chemical corrosion resistance and high heat deflection temperature [4]. During the polymerization, the less strained cyclopentene double bond of **1** is partially converted which creates crosslinking (Figure 2b). This approach was recently used for the preparation of polymerized high-internal phase emulsions (poly-HIPEs) [5,6]. Also, derivatization of the double bonds of these DCPD polyHIPEs using thiol-ene chemistry was demonstrated [6]. Consequently, the remaining strained cyclopentene double bonds could be utilized for iEDDA derivatization as indicated by our preliminary results.

4. Conclusions

Different strained and electron-rich olefins were screened for their ability to act as dienophiles in inverse-electron demand Diels Alder reactions with 3,6-di(pyridin-2-yl)-1,2,4,5-tetrazine. Currently, investigations are underway to perform iEDDA click chemistry on various polymers with incorporated strained or electron-rich olefins where we focus on orthogonality to other click reactions and materials with inherently reactive double bonds.

Acknowledgements

A-C.K thanks the Austrian Fonds zur Förderung der Wissenschaften (FWF) for a Hertha-Firnberg fellowship (T-578-19). Financial support of the European Community (CP-FP 211468-2 EUMET), the Oesterreichischer Austauschdienst and the Slovenian Research Agency (OEAD, Project SI 22/2011) is gratefully acknowledged. Christoph Schlögl, Julia Wappel, Manuel Hollauf and Alexander Eibel are acknowledged for their skillful work.

References

[1] a) M. L. Blackman, M. Royzen, J. M. Fox, *J. Am. Chem. Soc.* 2008, 130, 13518-13519. b) H. S. Han, N. K. Devaraj, J. Lee, S. A. Hilderbrand, R. Weissleder, M. G. Bawendi, *J. Am. Chem. Soc.* 2010, 132, 7838-7839.

[2] a) F. Thalhammer, U. Wallfahrer, J. Sauer, *Tetrahedron Lett.* 31, 6851-6854. b) A. Meier, J. Sauer, *Tetrahedron Lett.*, 1990, 31, 6855-6858.

[3] a) C. F. Hansell, R. K. O'Reilly, *ACS Macro Lett.* 2012, 1, 896-901. b) I. A. Barker, D. J. Hall, C. F. Hansell, Claire F. Du Prez, R. K. O'Reilly, A. P. Dove, *Macromol. Rapid Commun.* 2011, 32, 1362-1366. c)R. J. Williams, I. A. Barker, R. K. O'Reilly, A. P. Dove, *ACS Macro Lett.* 2012, 1, 1285-1290.

[4] J. C. Mol, *J. Mol. Catal. A: Chem.* 2004, 213, 39-45.

[5] a) S. Kovačič, K. Jeřabek, P. Krajnc, C. Slugovc, C. *Polym. Chem.* 2012, 3, 325-328. b) S. Kovačič, N. B. Matsko, K. Jeřabek, P. Krajnc, C. Slugovc, C. *J. Mater. Chem. A* 2013, in press.

[6] S. Kovačič , P. Krajnc, C. Slugovc, *Chem. Commun.* 2010, 46, 7504–7506.

S1-L2
Preparation and characterization of NIR-absorbing polyolefins

Patrick Knaack*, Meng Xiaoyan, Simone Knaus
Institute of Applied Synthetic Chemistry, Vienna University of Technology, Getreidemarkt 9, 1060 Vienna
*patrick.knaack@ias.tuwien.ac.at

1. Introduction

NIR-absorbing dyes have several broad and rapidly expanding fields of applications. One of these fields in polymer engineering are manufacturing techniques like laser welding and laser cutting. These techniques use IR-Laser (Diode, NdYAG, CO_2 laser) to bring the necessary thermal energy in the material. This works pretty well for polyamides (e.g. PA12) and some others, but, due to the fact that they are rather IR-transparent, not for polyolefins. Therefore, NIR-absorbers, like graphite, nanomaterials or organic dyes, are needed.
Because of their extraordinary non polar character polyolefins are a challenge as substrates for dyes, which are often polar or possibly even ionic substances due to their donor/acceptor architecture.
To avoid separation, agglomeration or migration and therefore possible elution of the NIR-absorber we wade from two sides into the problem. At first, we searched for a NIR-absorbing dye with an as non-polar as possible molecular architecture. On the other hand we modified polyolefins with epoxy-functionalities to realize a covalent bonding of the dye to the polyolefin surface. [1]

2. Results and discussion

The aim of our work was to immobilize a non-polar functional NIR-absorber onto epoxy-functionalized polyolefin surfaces.
We are working with perylenes as chromophore which stands out due to their thermal and bleaching stability and their non polar behavior. If they are fused with anthraquinones, they show a broad and intensive absorption band in the NIR. The slightly modified four step synthesis for the perylene-based dye 1 (Figure 1a) follows the literature [2] and gives an overall yield of 34%. The nucleophilicity of the amino group and, therefore, its accessibility and reactivity towards the epoxy functionality is enhanced by the introduction of an aliphatic spacer.

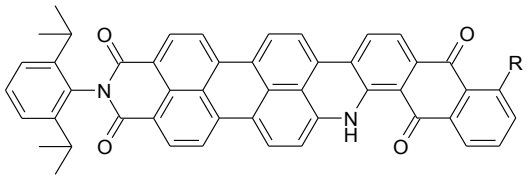

1 R= -NH_2 or -spacer-NH_2

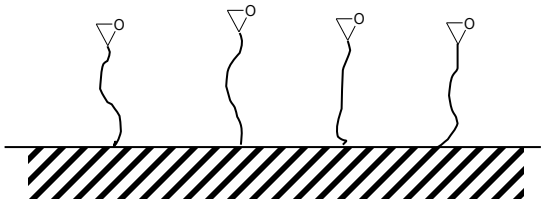

Figure 1. a) anthraquinone fused perylene dye b) epoxy-functionalized PP

Epoxy-functionalization of the polyolefins (Figure 1b) was achieved by melt-grafting in a mini-extruder. As monomers commercially available glycidylmethacrylate or, to hold the mechanical properties of the modified polyolefin at the high level of the virgin material, epoxy-monomeres containing long-chain aliphatic spacers were used [3]. The latter should lead us to materials with good mechanical properties, which have the distinction of being easily processible and achievable for laser manipulation without the drawbacks of common NIR-absorbers.
The epoxy groups on the polyolefin surface were used to immobilize the amino functionalized NIR-absorbers. The reaction of different amino functionalities (more or less sterically hindered aromatic amines, depending where in the dye the amino-functionality is introduced and aliphatic amines for the case of an introduced spacer) and the different epoxy moieties was investigated by several model reactions to ensure a high turnover even if the electronic and/or steric requirements are not at their optimum. Therein chloroform and toluene at 60°C show the best results (complete conversion in 6 hours). Latest results of characterization of the NIR-absorber-functionalized polyolefins will be presented.

References

[1] S. Becker *Dissertation (Monomere und polymere Rylenfarbstoffe als funktionelle Materialien), Johannes Gutenberg-Universität,* Mainz **2000**.
[2] S. Becker *Dissertation (Monomere und polymere Rylenfarbstoffe als funktionelle Materialien), Johannes Gutenberg-Universität,* Mainz **2000**.
[3] K. Schübel *Performance Polymers, EVONIK industiries,* Marl 2008

S1-L3
Sensor dyes for covalent immobilization to polymers, nanoparticles and textiles

Gerhard J. Mohr*
JOANNEUM RESEARCH Forschungsgesellschaft mbH – Materials, Steyrergasse 17, A-8010 Graz, Austria
*gerhard.mohr@joanneum.at

Indicator dyes are widely used for the development of optical chemical sensors. Typically, the indicator dyes are immobilized into polymer materials, similar to well-known pH indicator test strips, and exposed to analyte solutions. Furthermore, sensor devices are built where a polymeric sensor layer is immobilized on top of an optical fiber. The light guided from a light source through the optical fiber to the sensor layer and back to the detector is used to calculate analyte concentrations. Fluorescent nanosensors have recently found increasing interest in medical and biological research because they enable continuous monitoring of analytes in living cells, tissues and microorganisms. Nanosensors are obtained by physical embedding or covalent attachment of fluorescent indicator dyes into organic and inorganic nanoparticles. Polymer nanoparticles have some advantages over conventional marker and indicator dyes in that they are less toxic to biosamples, are less cross-sensitive to proteins and can be tailored to enable ratiometric measurements.
These sensor materials and optical sensor devices then may find application in medical research, process control, biotechnology, environmental monitoring and food quality control. However, often the indicator dyes are only physically embedded in the polymer matrix, which causes leaching of the dye and thus instability in signal and sensor performance, and more importantly, contamination of the sample. In order to overcome such limitations, indicator dyes have to be covalently linked to polymer materials and sensor surfaces. Several approaches to the covalent immobilization of indicator dyes on copolymers, nanoparticles and textiles will be presented. Vinylsulfonyl dyes with pH-sensitivity can be immobilised to cellulosic materials, thus giving sensor wound dressings and sensor textiles [1]. Methacrylate derivatives of indicator dyes with sensitivity to aliphatic amines are copolymerized with methyl and butyl methacrylates to give sensor layers for continuous monitoring of amines [2,3]. Functional indicator dyes sensitive to pH, fructose and ATP are immobilized within silica nanoparticles via trimethoxysilyl functions [3-6]. All of these sensor materials are characterized for their colour and fluorescence changes as well as sensitivity, reversibility and selectivity towards the analytes.

References

[1] S. Trupp, M. Alberti, T. Carofiglio, E. Lubian, H. Lehmann, R. Heuermann, E. Yacoub-George, K. Bock, G. J. Mohr, Development of pH sensitive indicator dyes for the preparation of micropatterned optical sensor layers, *Sensors and Actuators B*, **2010**, 150, 206-210.
[2] G. J. Mohr, N. Tirelli, U. E. Spichiger, Plasticizer-free optode membranes for dissolved amines based on copolymers from alkyl methacrylates and the fluoro reactand ETHT 4014, *Analytical Chemistry*, **1999**, 71 1534-1539.
[3] G. J. Mohr, N. Tirelli, C. Lohse, U. E. Spichiger, Development of chromogenic copolymers for optical detection of amines, *Advanced Materials*, **1998**, 10, 1353-1357.
[4] T. Doussineau, S. Trupp, G. J. Mohr, Ratiometric pH nanosensors based on rhodamine-doped silica nanoparticles functionalized with a naphthalimide derivative, *Journal of Colloid and Interface Science*, **2009**, 339, 266-270.
[5] A. J. Moro, J. Schmidt, T. Doussineau, A. Lapresta-Fernandez, J. Wegener, G. J. Mohr, Surface-functionalized fluorescent silica nanoparticles for the detection of ATP, *Chemical Communications*, **2011**, 47, 6066-6068.
[6] T. Doussineau, A. Schulz, A. Lapresta-Fernandez, A. Moro, S. Koersten, S. Trupp, G. J. Mohr, On the design of fluorescent ratiometric nanosensors, *Chemistry - A European Journal*, **2010**, 16, 10290-10299.

S1-L4
Kinetic study of single particle gas-phase ethylene homo-polymerization with Ziegler-Natta catalyst

Leonhard Mayrhofer (1)*, Ravindra R. Tupe (2), Christian Paulik (3)
(1) Kompetenzzentrum Holz GmbH, Altenberger Strasse 69, 4040 Linz, Austria
(2) Process Development Group, Borealis Polymers Oy, P.O. Box330 Porvoo, Finland
(3) Johannes Kepler University, Institute of Chemical Technology of Organic Materials, Altenbergerstraße 69, 4040 Linz, Austria
*l.mayrhofer@kplus-wood.at

1. Introduction

The main objective of the present study is to understand the kinetic behavior of Ziegler-Natta (ZN) catalyst systems at particle level during gas-phase ethylene homo-polymerization. Video microscopy of growing polymer particles at near industrial conditions was used for studying the kinetic characteristics of the catalyst.

2. Theory

Nearly 50 years after Nobel Prize in chemistry for K. Ziegler and G. Natta for their breakthrough works on transition metal catalyzed polymerizations, these processes are still contributing >70 % [1] to the world production (~235 Mtons in 2011) [2] of plastics. Nowadays the enhancement of polymers (e.g. in reactor blending) plays an important role for advanced polymer solutions [3].
The group of Pater et al. [4] showed that a micro-reactor is a very useful tool to study the kinetics of a growing polymer particle.

3. Experimental

The concept of using a micro-reactor for studying the polymerization of a single particle at near-industrial conditions is demonstrated in the present study. The micro-reactor is equipped with a video microscope for capturing the growth of a catalyst particle and with an infrared camera to sense the surface temperature of the growing catalyst particle during polymerization.
Conditions used during the experiments are reaction temperatures in the range of 40 to 85 °C and maximum ethylene pressures of 20 bar.
A commercial ZN catalyst was used for the gas phase homo-polymerization with ethylene. Triethylaluminium (TEA) was used for scavenging and as co-catalyst. After 30 minutes of pre-contacting, few activated catalyst particles were placed on a polymerization platelet. 5 µL TEA was added next to the polymerization platelet in order to scavenge any present impurities or catalyst poisons.

4. Results and discussion

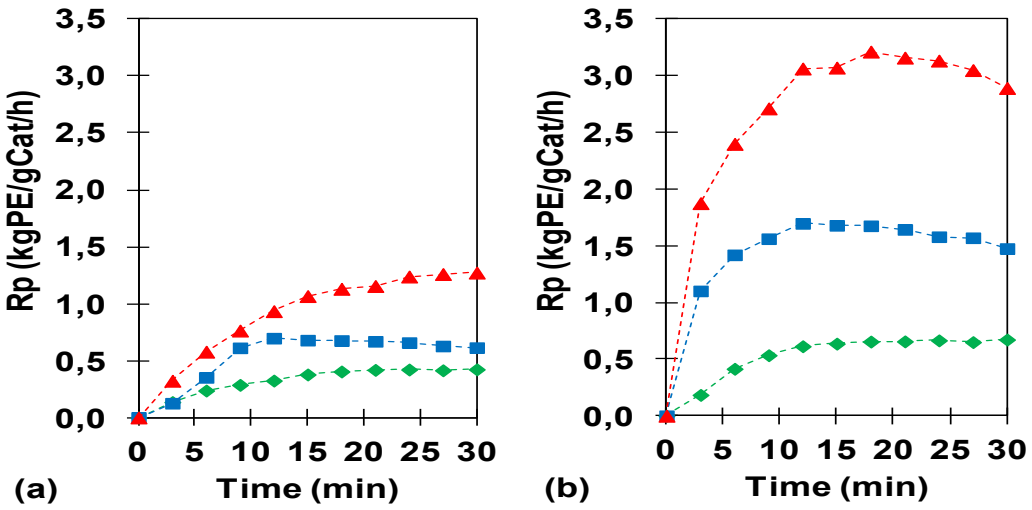

Figure 01: Polymerization rate (Rp) as function of time at following conditions: (a) 40 °C and (b) 70 °C, respectively, with 20 bar(a) of ethylene pressure (▲ Average of fastest growth; ■ Average of medium growth; ♦ Average of slowest growth)

The obtained results show the complexity with respect to the ZN catalyst based olefin polymerization. It appears that at particle-scale, different polymerization rates can be expected for different particles.
This can be associated to a different fragmentation behavior of the individual particles giving access of the necessary monomer to the active sites, which in turn determines the particle growth. Other factors which influence the fragmentation behavior, hence polymerization kinetics, are mass and heat transfer resistances, different active sites as well as the distribution of active sites within the catalyst particle [5]. The importance of particle fragmentation behavior and its influence of the polymerization kinetics are very well summarized by McKenna et al. [1]. Further studies will focus more on evaluating the impact of different process variables on particle fragmentation behavior, and accordingly on polymerization kinetics.

5. Conclusions

The micro-reactor experiments exhibited the influence of reaction parameters on the growth of different catalyst particles. The single particle growth kinetic is obtained by processing the visual images, using video microscope during the entire polymerization time. In addition the growth rate estimated based on the increasing volume of growing particles is evaluated to understand the kinetic behavior of this catalyst system at a particle level for different process parameters.

Acknowledgements

The authors thank Borealis for financial and intellectual support.

References

[1] McKenna T. F. L. et al., Catalytic olefin polymerization at short times: using specially adapted reactors, The Can. Jour. of Chem. Engg., 2012, 9999.
[2] Plastics Europe, www.plasticseurope.org, *Plastics-the facts 2012*, Page 8

[4] Pater, J. T. M., Weickert, G., Swaaij van, W. P. M., Optical and infrared imaging of growing polyolefin particles, AIChE Journal, 2003, 49(2), 450–464
[3] Ruff M., Paulik C., Controlling Polyolefin Properties by In-Reactor Blending, 1-Polymerization Process, Precise Kinetics, and Molecular Properties of UHMW-PE Polymers, Macromolecular Reaction Engineering (2012) 6 (8), pp. 302–317.
[5] Ferrari, D., Videomikroskopische Einzelkornanalyse der Olefinhomo- und Copolymerisation mit heterogenen Katalysatoren, Ph.D. Thesis, 2005

Session 3: Polymers from Renewable Resources

S3-L5
Renewable (waste) material based polyesters as plasticizers for adhesives

Matjaž Kunaver (1,2)*, Edita Jasiukaitytė-Grojzdek (1,2), Dolores Kukanja (1,3), Darko Moderc (1,3)
(1) Center of Excellence PoliMaT, Tehnološki park 24, 1000 Ljubljana, Slovenia
(2) National Institute of Chemistry, Hajdrihova 19, 1000 Ljubljana, Slovenia
(3) Mitol, d.d., Partizanska 78, 6210 Sežana, Slovenia
*matjaz.kunaver@polimat.si

1. Introduction

Liquefaction of the biomass based materials has been considered as an effective method for the utilization of the renewable resources in polymer chemistry. Biomass as a main precursor in the liquefaction reaction can be any kind of lignocellulosic materials; the most common source is different types of wood and wood wastes as well as the lignocellulosic parts of industrial plants and agricultural wastes. The liquefied biomass contains depolymerised products of cellulose, lignin and hemicelluloses. Liquefied biomass has a high reactivity due to a large amount of hydroxylic groups that are present. These functional groups can be used in creation of polyurethanes, polyesters and epoxides after the reaction with epichlorohydrin.

Poly(ethylene terephthalate) (PET) plastic packaging is produced in considerable amounts and represents a significant portion of household waste. Depolymerization with ethylene glycol or higher glycols and converting the depolymerised PET into new products such as unsaturated polyesters, polyester polyols and polyurethanes is the most common industrial process used nowadays. The glycolysis proces involves utilzation of small amounts of glycol and some transesterification catalyst such as zinc acetate.

Poly(vinyl acetate) (PVAc) adhesives are an important type of thermoplastic adhesive, especially in flooring applications, furniture manufacturing and carpentry. They are ready to use, have a short setting time, and give invisible joints. In order to extend its applicability, the flexibility and plastification of the PVAc is achieved by addition of plasticizer. The increasing demand for more environmental friendly materials causes the intensive investigations into new plasticizers and coalescing agents that improve the PVAc adhesive performance. The aim of presented work was the fully replacement of phthalate based plasticizers with environmental friendly materials. Polyesters synthesized from the liquefied wood (PE-LW) and from depolymerized PET (PE-PET) were used as renewable raw materials and tested as substitutes for plasticizers used in PVAc dispersion adhesives for flooring applications. The prepared PVAc adhesives were evaluated with respect to solids content, viscosity, glass transition temperature (Tg), tensile shear strengths and binding strength of the bondline between two wood specimens. As a reference material the PVAc based on 1,2,3-triacetoxypropane (CL) as plasticizer was used.

2. Experimental

2.1 Liquefaction of wood (LW) and synthesis of polyester from LW (PE-LW)

The polyhydroxy alcohol mixture of glycerol (150g) and diethylene glycol (150g), p-toluene sulfonic acid (9g) were placed into the 1000 cm^3 three necked glass reactor, equipped with mechanical stirring. The mixture was heated with constant stirring to 180°C. After the wood (100g) was added to the preheated reaction mixture the liquefaction reaction was carried out for 120 min. Afterwards, adipic acid was added. Dibutyl tin oxide (0.1% w/w) was added as the esterification / transesterification catalyst. After the completion of the reaction, when the acid value was reduced to less than 30 mg KOH/g, the reaction mixture was cooled to ambient temperature. The hydroxyl value of the polyester was 334 mgKOH/g.

2.2 Glycolysis of PET waste and synthesis of polyester from depolymerised PET (PE-PET)

PET waste flakes (10g) together with (31.25g) of polyethylene glycol (PEG) 400 (molar ratio of PET:PEG 400 = 1:1.5) and transesterification catalyst (0.1% w/w) were added into the reactor. The glycolysis of PET waste was carried out at 220°C over 6h. The reaction mixture was cooled to 190°C and adipic acid (4.12g) was added in two portions. After the completion of the reaction, when the acid value was reduced to less than 5 mg KOH/g, the reaction mixture was cooled to ambient temperature. The resulting polyester was identified as PS-PET. The hydroxyl value was 88 mgKOH/g.

2.3 Adhesive preparation

Water based adhesives were prepared from commercially available PVAc dispersion Mekolit H45 (Mitol) used as a binder, calcium carbonate (Calcit) used as a filler and a plasticizer. Commercial plasticizer (CL; 1,2,3-triacetoxypropane), PE-LW and PE-PET were used to prepare adhesives by varying the plasticizer amount from 0 up to 25% (w/w). Thin adhesive films were prepared with

special stencil on silicon-impregnated paper. Prior the testing, adhesive films were dried for 7 days at 23 ± 2°C and 50 ± 5% relative humidity.

2.4 Methods

Thermogravimetrical analysis (TGA) was performed on Metller Toledo TGA/DSC1 apparatus and differential scanning calorimetry (DSC) measurements were performed on a Metller Toledo DSC1 apparatus. Intrinsic viscosity measurements of polyesters were performed using a Brookfield DV-E rotational viscometer according to the International standard (ISO 2555). Tensile strength (N/mm^2) and elongation (%) were determined using Zwick/Roell Z 010. Testing was performed using three specimens with the dimensions of 100 mm (length) and 15mm (width). (Modification of the ASTM 882-95a standard method)

Binding strength (N/mm^2; wood-wood) was measured using Zwick 1435 mechanical testing machine. For this purpose three specimens with adhering surface of 2 cm^2 were kept under the pressure of 7.5 kg/cm^2 for at least 24h. Binding strength was determined after 72h of sample conditioning at room temperature with constant crosshead speed of 50 mm/min. (Modification of the EN 14293:2006 standard method)

4. Results and discussion

The influence of different addition of plasticizers on mechanical properties of PVAc adhesives for flooring applications was studied. The highest thermal stability exhibited samples prepared with PE-PET independently from the amount of the added plasticizer. As a result, with the addition of PE-PET up to 25% (w/w), the 5% weight loss temperature ($T_{dec\text{-}5\%}$) was reduced only by 10°C, while due to the addition of PE-LW and CL, $T_{dec\text{-}5\%}$ was reduced by 90°C and 150°C, respectively. PE-PET and PE-LW are more compatible with the PVAc polymer and they stay with the polymer for a considerably longer time than commercial plasticizer. Increasing amounts of CL and PE-PET in adhesive formulation greatly reduced Tg, while the least affected Tg was determined for the samples prepared with PE-LW. The optimal required viscosity (< 85000 mPas) exhibited adhesives with addition of 5% (w/w) of PE-PET and 20% (w/w) of PE-LW. The dispersion adhesive ductility dependence on the amount of plasticizer in adhesive composition was revealed by examination of the mechanical properties. The increasing amount of the plasticizer in adhesive reduces the tensile strength and accordingly increases elongation. The solid content for all adhesives were measured according to ISO 1625 standard. The weight loss is very intensive in the samples prepared by commercial plasticizer. Both polyesters have higher molar mass and polymer structure and have reduced migration properties.

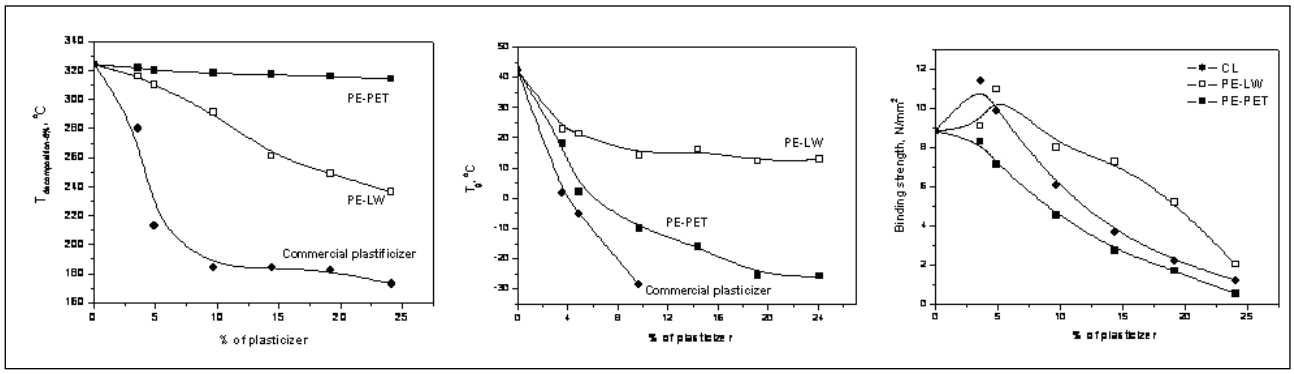

Figure 1: **The 5% weight loss temperature, glass transition (T_g) temperature and binding strength dependence on the percentage of plasticizer,**

5. Conclusions

We replaced the commercial plasticizer in a PVAc adhesive with environmental friendly polyesters synthesized from the liquefied wood and from depolymerized PET.

TGA analysis showed significant differences between thermal stability of added polyesters and commercial plasticizer. Samples prepared with PE-PET exhibit the highest thermal stability even at the addition of 25%. PE-LW was less stable although still better than commercial plasticizer. PE-PET and PE-LW are more compatible with the PVAc polymer, have higher interactions with it and therefore stay in the mixture for a considerably longer time.

The DSC measurements revealed a decrease in glass transition peaks temperature with increasing amounts of CL and PE-PET. The least affected Tg was determined for the samples prepared with PE-LW where the lowest Tg was reached in adhesive with 24.1% of PE-LW addition.

Increased content of plasticizer in dispersion adhesive composition tends to reduce wood-wood binding strength. The increased amount of the plasticizer in adhesive reduces the tensile strength and accordingly increases elongation.

A significant difference is observed in solid content of adhesive when samples were dried at elevated temperature. While the commercial plasticizer slowly evaporates both polyesters remain in the mixture due to polymer structure which are completely stable at that temperature.

The requirements for the parquet adhesives were fulfilled by the compositions containing 5% (w/w) of PE-PET and 20% (w/w) of PE-LW.

Acknowledgements
The authors wish to gratefully acknowledge the support for the presented work received from the Ministry of Higher Education, Science and Technology of the Republic of Slovenia through the contract No. 3211-10-000057 (Center of Excellence for Polymer Materials and Technologies) and for the analysis of products within the Program P2-0145 (National Institute of Chemistry).

S3-L6
Lignin polyols – renewable resin compounds

Kerstin Wallisch*, Dzanana Dautefendic, Simone Knaus
Vienna University of Technology, Institute of Applied Synthetic Chemistry, Getreidemarkt 9, 1060 Vienna, Austria
*kerstin.wallisch@ias.tuwien.ac.at

1. Introduction
Lignin, the second major component of wood and annual plants, is a highly branched and irregular macromolecule, whose structure based on phenylpropanoic units varies with the vegetable species and the method of isolation. Being an abundant and renewable polymer, much effort has been made in the last decades to modify lignin so that it can be incorporated in polymeric material and thus used in applications of higher value. Oxypropylation of lignin is an established method to overcome technical limitations and adverse effects resulting from the polymeric nature of lignin when directly used for synthesis purposes. It increases the reactivity of lignin's functional groups and improves its solubility and uniformity. Such formed low-cost polyols from renewable resources might be able to replace conventional polyols in the polyurethane industry if they possess a certain viscosity and hydroxyl index. Oxypropylation is always accompanied by homopolymerization of propylene oxide, so that the produced polyols are a mixture of oxypropylated lignin and polypropylene oxide homopolymers. Until now only such mixtures, containing a very low amount of lignin, were tested for the manufacture of polyurethanes. The aim of the present work is to investigate which degree of grafting is necessary to convert lignin into a polyol suitable for such applications with respect to viscosity and hydroxyl index. [1,2]

2. Experimental
For synthesis of the polyols two different types of lignin (Alcell lignin and Protobind 2400) were reacted with varying amounts of propylene oxide in a high-pressure reactor at 100°C and purified according to literature (scheme 1) [3].
OH COOH O CH2 CH O H CH3 n CH2 CH CH3 O H n COO O Lignin Lignin KO H autoclave: 100°C/ 15h purification: 1) liquid-liquid extraction (acetonitrile/hexane) removal of homopolymer 2) precipitation in water removal of oligomers

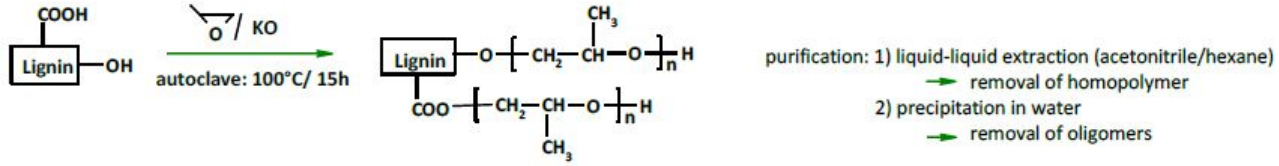

Scheme 1. Oxypropylation of lignin
Oxypropylated lignin was acetylated and 1H-NMR spectra recorded to determine the amount of propylene oxide grafted to lignin and resultant the length of the grafted chains; for calculation of the hydroxyl index the polyols - together with an internal standard - were derivatised with 2-chloro-4,4,5,5-tetramethyl-1,3,2-dioxaphospholane (TMDP) and 31P-NMR spectra were recorded (Scheme 2). Additionally the hydroxyl index was also determined by titration.

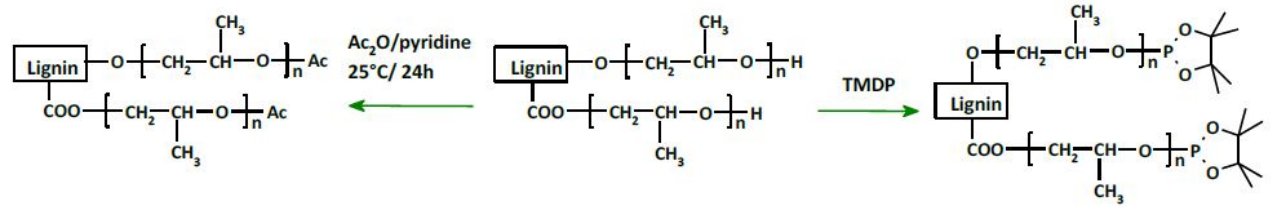

Scheme 2. Acetylation and phosphitylation of oxypropylated lignin for analytical purposes O CH2 CH O H CH3 n CH2 CH CH3 O H n COO O CH2 CH O Ac CH3 n CH2 CH CH3 O Ac n COO O CH2 CH O P CH3 n OO CH2 CH CH3 O P n COO OO Lignin Lignin Lignin Ac2O/pyridine 25°C/ 24h TMDP
Rheological tests were carried out with a plate/plate rheometer. The viscosity was determined not only from the raw polyol mixture, but also from the oxypropylated lignin after removal of the oligomers.

3. Results and discussion

Objective of the present work is to synthesize oxypropylated lignins and evaluate if they are suitable for the manufacture of polyurethanes regarding their viscosity and hydroxyl index in comparison to conventional polyols used for this application.

For the synthesis of polyols with different viscosities the molar ratio of lignin to propylene oxide was varied from 1:5 to 1:20. The content of propylene oxide homopolymers was determined by weighing the hexane-soluble fraction after liquid-liquid extraction of the polyol mixture.

The lignin polyols were acetylated and 1H-NMR spectra from the derivatives recorded. The length of the grafted side chains was found to be in the range of 1.5-8.5.

31P-NMR spectroscopy after derivatisation with TMDP allows distinguishing between hydroxyl groups of oxypropylated side chains and other aliphatic hydroxyls that remained unreacted. Additionally also the amount of phenolic hydroxyls and carboxylic groups can be determined. So it could be shown that it is possible to synthesize lignin polyols where nearly all functional groups are grafted.

The hydroxyl indices were not only determined by titration, a well-established method, but also calculated from results of 31P-NMR spectroscopy, as an alternative technique. Hydroxyl indices obtained from 31P-NMR spectra (100-150) showed a good correlation with results obtained after titration of the hydroxyl groups. Therefore 31P-NMR spectroscopy is an adequate and fast tool for hydroxyl value analysis which, additionally, has the advantage that smaller amounts are needed for the analysis.

According to results of Nadji et al. [4] polyols with hydroxyl indices in the range of 100-200 are suitable for rigid polyurethane foams confirming that our lignin polyols can be used for that application.

Another important parameter is the viscosity of the polyols which should be lower than about 300 Pa*s for the manufacture of polyurethanes [4]. The investigation of oxypropylation reactions of different lignins showed that the properties of the products depend strongly on the nature of the lignin and the applied molar ratio of lignin and propylene oxide. Rheometer measurements showed that a chain length of more than 4 is needed to obtain a viscosity low enough for polyurethane synthesis, otherwise the oxypropylated lignin has to be used in a mixture with the PPO homopolymer.

Acknowledgements

Part of this work was done within the frame of the program “Factory of Tomorrow”, an initiative of the Austrian Federal Ministery of Transport, Innovation and Technology.

References

[1] A. Gandini, Macromolecules 2008, 41(24), 9491-9504.
[2] C. A. Cateto et al, Industrial & Engineering Chemistry Research 2009, 48, 2583-2589
[3] L. C.-F. Wu and W.G. Glasser, Journal of Applied Polymer Science 1984, 29, 1111-11
[4] H. Nadji et al, Macromolecular Materials and Engineering 2005, 290, 1009-1016

S3-L7
Synthesis of novel polymer-bound antioxidants via ADMET polymerization

Stephan Beer*, Oliver Brüggemann
Institute of Polymer Chemistry, Johannes Kepler University Linz, Welser Strasse 42, A-4060 Leonding, Austria
*stephan.beer@jku.at

1. Introduction

The project SolPol-2 [1] targets the development of novel polymeric materials based solar water heating systems including new polymer compounds specifically for solar-thermal applications. The unique conditions in these systems require novel solutions for the stabilization of polymeric materials. A particular problem experienced in the use of polymeric materials for such applications is the leaching of the antioxidant in the high-temperature aqueous environment. Our work focuses on the immobilization of antioxidants in order to develop additives for the long-term stabilization of polyolefins suitable for the construction of solar water heating systems.

Several approaches for the immobilization of antioxidants via melt free-radical grafting to polyolefins have been reported. Thereby reactive antioxidants, like maleimide-bound antioxidants [2] or acrylic monomers [3] are applied in the grafting reaction to obtain polyolefin-bound antioxidants.

In our work we are investigating the ADMET-polymerization of monomer-bound antioxidants, a new approach for the immobilization of antioxidants. Using fatty acid derivatives as monomers leads to polyolefins with functional groups with a well-defined distribution [4]. The presence of these functional groups allows the coupling of antioxidants to the polymer backbone, which can otherwise only be achieved by free-radical reactions under harsh conditions. In our work the applied monomers are based on plant oils, hence renewable resources are employed.

2. Results and discussion

The immobilization of antioxidants was achieved by ADMET-polymerization of different monomer-bound antioxidants. These compounds were produced by the synthesis of α,ω-dienes which were then coupled to phenolic antioxidants yielding monomers ready for ADMET-polymerization. The ADMET-polymerization of the antioxidant-bearing monomers was carried out using a Hoveyda–Grubbs 2nd generation catalyst. The obtained polymers were characterized by NMR- and FTIR-spectroscopy. High-temperature GPC was used for the determination of molecular weights.

The polymer-bound antioxidants were compounded to non-stabilized polypropylene using a lab extruder. For comparison some compounds were stabilized with the commercially used Irganox 1010. In order to achieve comparable results, adjusted amounts of polymer-bound antioxidants and Irganox 1010 were applied leading to equal concentrations of phenol groups in the different compounds. Finally, DSC was employed to measure the oxidation induction time (OIT) of the obtained products. Compared to non-stabilized polypropylene, the OIT can be significantly enhanced by addition of small amounts of polymer-bound antioxidant. The comparison with Irganox 1010 as a stabilizer shows even more interesting results, since the polymer-bound antioxidant surpasses the stabilization achieved by Irganox 1010 (figure 1).

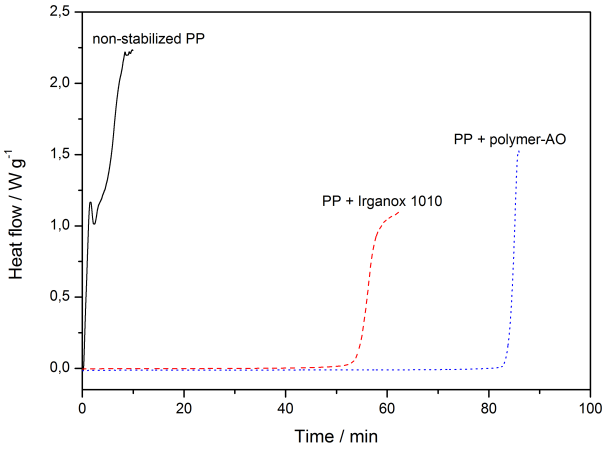

Figure 1. Sample OIT measurements showing how the addition of polymer-bound antioxidant (dotted line) enhances the oxidation induction time of polypropylene (PP) compared to non-stabilized PP (solid line) and compared to PP stabilized with Irganox 1010 (dashed line)

3. Conclusions

A novel route to polymer-bound antioxidants was successfully developed using ADMET-polymerization. The antioxidant activity of the products was confirmed by OIT measurements.

Acknowledgements

This work was financed by the Austrian Research Promotion Agency (FFG) and the "Klima- und Energiefonds" of the Austrian federal government in line with the program "Neue Energien 2020". NMR measurements were carried out at the Austro-Czech RERI-uasb NMR center which was established with financial support from the European Union through the EFRE INTERREG IV ETC-AT-CZ programme (project M00146, "RERI-uasb").

References

[1] R. W. Lang, G. M. Wallner, *Public Service Review: European Science & Technology*; **2012**, 14, 68-69.
[2] T. H. Kim, D, R. Oh, *Polymer Degradation and Stability* **2004**, 84, 499-503.
[3] S. Al-Malaika, N. Suharty, *Polymer Degradation and Stability* **1995**, 49, 77-89.
[4] O. Kreye, T. Tóth, M. A. R. Meier, *European Journal of Lipid Science and Technology* **2011**, *113*, 31-38.

S3-L8
Membranes for water-purification based on nano-cellulose

Andreas Mautner (1)*, Koonyang Lee (1), Kang Li (2), Alexander Bismarck (1,3)
(1) Imperial College London, Polymer and Composite Engineering group, London SW7 2AZ, United Kingdom
(2) Imperial College London, Department of Chemical Engineering, London SW7 2AZ, United Kingdom
(3) University of Vienna, Institute for Materials Chemistry & Research, Währinger Straße 42, 1090 Wien, Austria
*a.mautner@imperial.ac.uk

1. Introduction
Clean water nowadays seems to be commonplace in our part of the world. Nevertheless, the struggle for potable water is an all-day trouble in huge areas of planet earth and with the number of people living on this globe still increasing this problem will become even bigger. By this, the need of, preferably cheap and easy to handle, devices for decentralized industrial and domestic water treatment aiming at the removal of various contaminants is an important task. Moreover, devices such as membranes applied for this purpose should not add to pollution of the environment neither through the production processes of base materials and membranes nor through the disposal of used membranes.

2. Theory
Since the purification of water is gaining more and more significance, membranes from renewable resources like cellulose have come into the viewpoint of research interest since there is an almost unlimited stock of base materials that derive from renewable resources and whose disposal through composting is an environmentally friendly process. Of course, cellulose as membrane material is well established, but until now the utilization as membrane for the removal of certain types of contaminants like pesticides or microbial contamination was not a comprehensive success. Thus, the aim of this study is to create cellulose-based membranes featuring special characteristics deriving from extraordinary structures and/or derivatives that lead to specific properties of the final membranes that are necessary in the domain of water purification and removal of challenging pollutants. One base material that can be utilized for this purpose is so-called nanofibrillated cellulose (NFC). NFC can be produced via two approaches: top-down and bottom-up. Through the top-down approach (first reported by Herrick [1] and Turbak [2]) nanofibres are produced by disintegration of (ligno)cellulose biomass, such as wood fibres. During this process, the wood pulp is fed through a high-pressure homogenizer to decrease the size of the fibres to finally reach the nanoscale. NFC produced via the bottom-up approach utilizes the fermentation of low molecular weight sugars using cellulose-producing bacteria, such as from the acetobacter species.[3]

3. Experimental
To achieve membranes based on NFC, the surface of NFC has been partly modified to achieve more hydrophobic behavior while maintaining the structure composed of nanowhiskers. Thus, organic acids of different length (from acetic acid to dodecanoic acid) have been grafted onto NFC and membranes produced. To characterize the membranes, the degree of surface substitution (DS) of NFC by organic acids was analyzed with a method based on hydrogen/deuterium exchange, the crystallinity by using XRD, the streaming-ζ-potential with an electro kinetic analyzer, the hydrophobicity by performing contact angle measurements, and the thermal stability by means of TGA. To study the MW cut-off, polystyrene standards have been used that were analyzed by GPC before and after passing the membrane.

4. Results and discussion
The DS on the surface was around 1.5 which is sufficient since only partly modification was desired. Accordingly, the contact angles increased with increasing length of the grafted acid-residues. Nevertheless, the resulting films exhibit no loss in crystallinity compared to neat NFC, which illustrates that the substitution reaction was restricted to the surface only. The isoelectric point derived from ζ-potential measurements was shifted to slightly higher values indicating the loss of acidic OH-groups due to the substitution reaction. The degradation temperature slightly decreased with increasing carbon chain length due to the reduced number of effective hydrogen bonds between NFC nanofibres. Finally, the MW cut-off lies in the region of a few kDa, which demonstrates the ability of performing nanofiltration with these type membranes.

5. Conclusions
We have shown that it is possible to produce membranes based on renewable resources without the need of environmentally problematic solvents, which enable the elimination of contaminants in the range of a few kDa.

Acknowledgements
The authors greatly acknowledge the funding provided by the EU FP7 project NanoSelect.

References
[1] F.W. Herrick, R.L. Casebier, J.K. Hamilton, K.R. Sandberg; in Sarko, A., (Ed.); Microfibrillated Cellulose: Morphology and Accessibility, Proceedings of 9th Cellulose Conference, Ed. Wiley: New York, 1983; p. 797.
[2] A.F. Turbak, F.W. Snyder, K.R. Sandberg; *J. Appl. Polym. Sci. Appl. Polym. Symp.* 1983, 37, 459–494.
[3] D. Klemm, B. Heublein, H.P. Fink, A. Bohn; *Angew. Chem., Int. Ed.* 2005, 44 (22), 3358–3393.

S3-L9

Structural rearrangements in amorphous nanometric cellulose model films induced by heat treatment

Stefan Spirk (1)*, Tamilselvan Mohan (1) , Rupert Kargl (2), Ales Doliska (1), Roland Resel (3), Volker Ribitsch (2), Karin Stana-Kleinschek (1)

(1) University of Maribor, Institute for Engineering Materials & Design, Smetanova Ulica 17, 2000 Maribor, Slovenia
(2) University of Graz, Institute of Chemistry, Heinrichstr. 28, 8010 Graz, Austria
(3) University of Technology Graz, Institute of Solid State Physics, Petersgasse 17, 8010 Graz, Austria
*Stefan_spirk@yahoo.de

1. Introduction

Probably, there is hardly any other single material that offers such a wide variety of applications in materials sciences as cellulose, the most abundant polysaccharide on earth. It is used in papers, fibers, textiles, packaging materials, hygienic products and serves as a support material in chromatography and life science applications as well. In addition, nanoscale cellulosic materials such as nanocrystals and nanofibrils have gained more and more attention during the past few years due to their unique mechanical and non-linear optical properties. In addition, cellulose is compatible with many other organic and inorganic materials which facilitates the creation of hybrid materials and nanocomposites exhibiting unique properties such as conductive fibers, papers with printed circuits or flame retardant materials for instance.

Although most of the aforementioned applications are influenced and determined by the supramolecular structure of cellulose (e.g. different reactivities of crystalline and amorphous domains for nanocrystal preparation), the interaction behavior of cellulose especially with water molecules is not fully understood. In this context, Lindman and co-workers initiated a discussion about the importance of hydrophobic and electrostatic interactions in the course of the dissolution process of cellulose. The authors outlined that cellulose is an amphiphilic molecule which is able to interact via hydrogen bonding as well as by dispersive forces and electrostatics with the solvent called 'hornification') and result in a decrease in mechanical strength, a lower water retention value and an increased hydrophobicity to mention just the most important ones. These undesired and irreversible changes originate from a change in the supramolecular structure but a detailed knowledge in this area about the structure property relationship is still missing.

2. Results and discussion

The insolubility of cellulose in water and many other solvents requires another strategyl for the preparation of thin films. The most convenient way to make amorphous films is the use of trimethylsilyl cellulose (TMSC) which is readily soluble in toluene at a high degree of substitution. ThIn TMSC is spin coated onto a substrate and exposed to HCl vapors for a ceratin time which cleave off the silyl groups (=regeneration) resulting in a smooth cellulose film (d~25 nm)

In this contribution, the structural rearrangement of such partly and fully regenerated amorphous cellulose model thin films is investigated by exposing the films to elevated temperature (105 °C) for a prolonged time (6 hours) under ambient atmosphere. This heating procedure is very common in pulp processing and drying of fibers. A structural rearrangement in the films from a featureless to a fibrillar structure is observed upon heating which correlates with the regeneration time and DS_{Si} of the cellulose. (**Fig.1**)

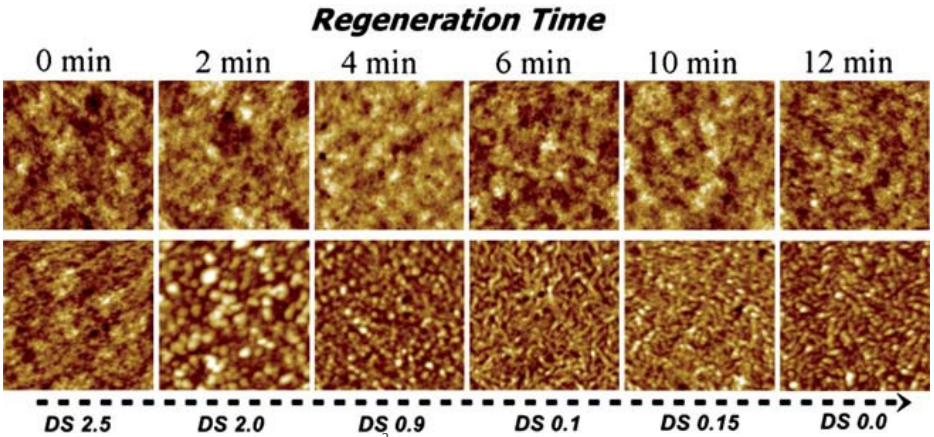

Figure 1. AFM height images (1x1 mm^2; z-scale, 20 nm) of time-dependent regenerated cellulose surfaces before (upper row) and after (lower row) heat treatment. The DS_{Si} is given for each regeneration time.

Results derived from ATR-IR spectroscopy indicate that the hydrogen bonding mode in the films is changed from a mainly O2–H2···O6' (intramolecular) motif to O5···H3-O3' (intramolecular) and O6–H6···O3' (intermolecular) ones upon heat treatment. As proven by grazing incidence X-ray diffraction experiments using synchrotron irradiation, the films retain their amorphous character; probably, small ordered domains are formed which are lacking a long range order. In addition, the heat induced changes enhance

the order of the supramolecular structure which results in a more pronounced amphiphilic behavior of the cellulose molecules and, a hydrophobization of the surfaces can be observed. While SFEs are in a similar range for non-heat treated and heat treated surfaces, the components of the SFE differ completely. In the case of heat treated films, the dispersive character is the main contribution while in non-heat treated films equal disperse and electron donor components are present. The water sorption capacity is reduced as proven by QCM-D. Upon exposure to water for a prolonged time, the heat treated surfaces do not exhibit changes in morphology while untreated ones are prone to swelling and fine fibrils are formed (Figure 2).
A determination of the water content of the nanometric films by QCM-D revealed a decrease from 60 to 31% upon drying. Although there is some evidence for the amphiphilicity of cellulose (e.g. swelling behavior, wettability, SFE), we could not find any proof for hydrophobic interactions in the course of the drying procedure for fully regenerated cellulose films. Probably, these interactions do not play a role in the course of drying at all. In the case of partly regenerated films (RT < 4 minutes), an increase in layer thickness is observed upon heat treatment which indicates a rearrangement due to the minimization of the hydrophilic/ hydrophobic interactions. However, in these cases the hydrophobic silyl groups can be regarded as the driving force for the rearrangement. These results give new insights into the understanding of the interaction of cellulose with water.

Acknowledgements
The research leading to these results has received funding from the European Community's Seventh Framework Programme [FP7/2007-2013] under grant agreement no. 214015. We also would like to thank Dr Christian Schuster (Lenzing AG) and Dr Silvo Hribernik for fruitful discussions. Dr Wolfgang Caliebe (DESY - HASYLAB) is acknowledged for experimental support.

References
For further reading see:
[1] Mohan, T.; Spirk, S.; Kargl, R.; Doliska, A.; Vesel, A.; Salzmann, I.; Resel, R.; Ribistch, V.; Stana-Kleinschek, K. *Soft Matter* **2012**, *8,* 9807.

Session 4: Polymers for Biomedical Applications

S4-L10
Poly(ethylene imine)-derived contact biocides: Fabrication of antimicrobially active surfaces

Frank Wiesbrock (1,2)*, Andrew M. Kelly (1), Verena Kaltenhauser (2) and Inge Mühlbacher (1)
(1) Polymer Competence Center Leoben GmbH, Roseggerstrasse 12, 8700 Leoben, Austria
(2) Graz University of Technology, Institute for Chemistry and Technology of Materials, Stremayrgasse 9, 8010 Graz, Austria
*frank.wiesbrock@pccl.at

Summary. Poly(2-oxazoline)-derived polymers were used as additives in PP compound plates. Antimicrobial activity of these compound plates' surfaces against *S. aureus* was observed only if partially hydrolyzed poly(2-nonyl-2-oxazoline)s were used as additives, while contact biocidal activity against *coli*, *P. aeruginosa* and *C. albicans* depended only on the degree of hydrolysis of the poly(2-oxazoline)s.

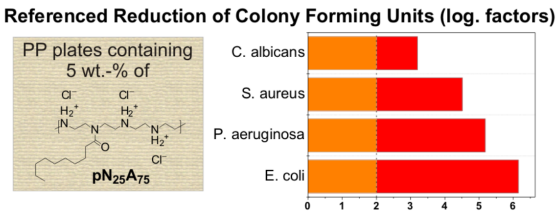

E.

1. Introduction
The equipment of surfaces with antimicrobially active compounds is aimed for in applications where sterile environments are required despite contact with a large number of individuals [1]. In this context, antimicrobial polymers have gained considerable attention [2]: In addition to the advantage of maintenance-free sterile surfaces, small molecule biocides can be eliminated from this strategy. The mechanism of the permanent antimicrobial activity of polymers has not yet been fully understood: Positive charges in the polymers have been verified as key prerequisite for antimicrobial activity; for the induction of phase separation, hydrophobic alkyl chains in the polymers have been attributed synergistic co-effects [3]. In this study, various poly(2-oxazoline)-derived copolymers were prepared and their antimicrobial activity in compounds was determined in order to contribute to the understanding of the action mechanism of contact biocides.

2. Experimental
2-Ethyl-2-oxazoline **E** was purchased from Sigma-Aldrich, 2-nonyl-2-oxazoline **N** was prepared according to a literature recipe [4]. Polypropylene (PP) was provided by Borealis (Linz, Austria). All polymerizations were performed in the microwave reactor Initiator Eight from Biotage. Poly(2-ethyl-2-oxazoline) p$\mathbf{E}_{100}$ and poly(2-nonyl-2-oxazoline) p$\mathbf{N}_{100}$ were prepared according to literature reports from cationic ring-opening polymerizations [5]. Hydrolyses of the polymers at different reaction times provided the

copolymers p$\mathbf{E}_{100\text{-}25n}\mathbf{A}_{25n}$ and p$\mathbf{N}_{100\text{-}25n}\mathbf{A}_{25n}$ (n = 1-4) (**Scheme 1**); yields: 77-95%. Plate pressing was carried out in a Collin P 200 PV Laboratory Platen Press at 25 bar and 200 °C for 15 min. Biocide tests of the PP (compound) plates were performed at HBICON GmbH at Bielefeld, Germany, in compliance with ISO 22196:2007.

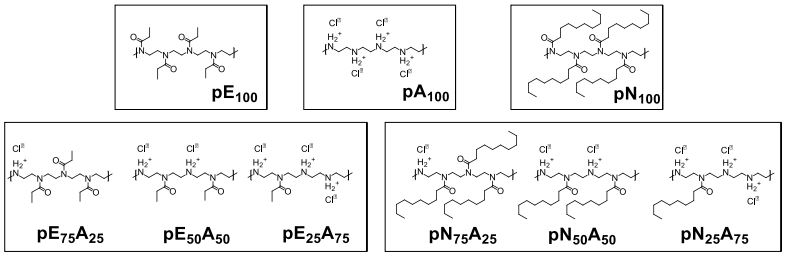

Scheme 1: Overview of the nine poly(2-oxazoline)-derived polymers investigated for antimicrobial activity.

3. Results and discussion

Hydrolysis. Starting from p$\mathbf{E}_{100}$ and p$\mathbf{N}_{100}$, the number of cationic functionalities in the polymers was continuously increased by continued acid-mediated hydrolysis of the amide bonds in an aqueous HCl solution, yielding copolymers of 2-oxazolines **E/N** and aziridinium chloride **A**. Optimized work-up conditions enabled the recovery of the (partially) hydrolyzed polymers from extraction procedures in high purity according to 1H-NMR analyses. The degree of hydrolysis was found to follow first-order kinetics for the hydrolysis of both, p$\mathbf{E}_{100}$ and p$\mathbf{N}_{100}$. The hydrolysis rates of p$\mathbf{E}_{100}$ were significantly higher than that of p$\mathbf{N}_{100}$, which seemingly originated from the steric shielding of the reaction center by the nonyl chains that collapsed around the amide bonds in aqueous environments.

Specimen Preparation. For the production of PP compound plates, samples of p$\mathbf{E}_{100\text{-}25n}\mathbf{A}_{25n}$ and p$\mathbf{N}_{100\text{-}25n}\mathbf{A}_{25n}$ (n = 0-4) were thoroughly ground and mixed with PP (5/95 w-%). Platen pressing was carried out in a preheated oven. The surface energies of the (compound) PP plates were determined from contact angle measurements and found to be in the range of 25-33 $mN \cdot m^{-1}$ [SE(PP) = 28.5 $mN \cdot m^{-1}$], indicative of neither pronouncedly hydrophobic nor hydrophilic character. Hence, the wettability of the compound plates was suitable for the application of the compound materials as substitutes for PP-based devices. “Antifouling” properties, nonetheless, cannot be concluded from these data.

Antimicrobial Activity. Antimicrobial tests were performed as triplicates in full compliance with ISO 22196:2007 against gram-negative *E. coli* and *P. aeruginosa*, gram-positive *S. aureus*, and the fungus *C. albicans*. The logarithmic numbers of colony forming units on the plates after 24 h relative to the beginning of the test were used to evaluate the antimicrobial activity. In general, the antimicrobial activity increased with the degree of hydrolysis. Antimicrobial activity against *E. coli* and *C. albicans* (**Figure 1**) was observed starting from hydrolysis degrees of 50% for p$\mathbf{E}_{100\text{-}25n}\mathbf{A}_{25n}$ and p$\mathbf{N}_{100\text{-}25n}\mathbf{A}_{25n}$ (n = 2-4); antimicrobial activity against *P. aeruginosa* was observed for the same set of polymers with the exception of p$\mathbf{E}_{50}\mathbf{A}_{50}$. Against gram-positive *S. aureus*, however, antimicrobial activity was only observed for polymers that exhibited cationic charges as well as long hydrophobic side-chains, namely p$\mathbf{N}_{100\text{-}25n}\mathbf{A}_{25n}$ (n = 1-3) [6]. The synergism in the interaction of cationic charges and long hydrophobic side-chains was referred to cell perturbation by interactions with membrane components like lipoteichoic acids that are abundant in the outer cell walls of S. aureus.

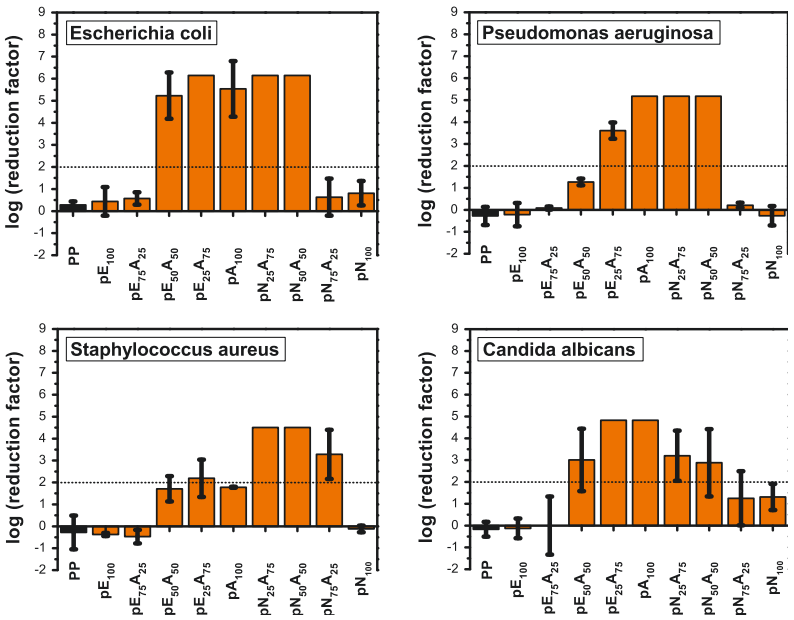

Figure 1. Logarithmic reduction factors of PP compound plates containing 5% of poly(2-oxazoline)-based copolymers and pure PP plates against various microbes. Standard deviations are indicated unless no residual CFUs were detected.

4. Conclusions

p**N**$_{50}$**A**$_{50}$ and p**N**$_{25}$**A**$_{75}$ showed antimicrobial activity against all tested microbes in 5 w.-% dosage in PP plates. Of particular notice is the necessity of two functional groups, cationic charges and hydrophobic side-chains, for antibacterial activity against *S. aureus*. Structural motifs of the cell wall of *S. aureus* provide the explanation for the synergism of cationic charges and hydrophobic moieties in antimicrobial activity against this bacterium.

Acknowledgements

This study was performed at the Institute for Chemistry and Technology of Materials of the Graz University of Technology with funding and contributions from the Polymer Competence Center Leoben GmbH (PCCL, Leoben) and Kekelit Kunststoffwerk GmbH (Linz) within the frameworks of the COMET and FEMTECH programs of the Austrian Ministry of Traffic, Innovation and the Ministry of Economy, Family and Youth. PCCL is funded by the Austrian Government and the State Governments of Styria and Upper Austria.

References

[1] S.B. Lee, R.R. Koepsel, S.W. Morley, K. Matyjaszewski, Y. Sun, A.J. Russell, *Biomacromolecules* 2004, 5, 877-882.
[2] J.C. Tiller, C.-J. Liao, K. Lewis, A.M. Klibanov, *Proc. Natl. Acad. Sci.* 2001, 98, 5981-5985.
[3] N. Pasquier, H. Keul, E. Heine, M. Moeller, *Macromol. Biosci.* 2008, 8, 903-915.
[4] M. Beck, P. Birnbrich, U. Eicken, H. Fischer, W. E. Fristad, B. Hase, H.-J. Krause, *Angew. Makromol. Chem.* 1994, 223, 217-233.
[5] F. Wiesbrock, R. Hoogenboom, M.A.M. Leenen, M. A. R. Meier, U.S. Schubert, *Macromolecules* 2005, 38, 5025-5034.
[6] A.M. Kelly, V. Kaltenhauser, I. Mühlbacher, K. Rametsteiner, H. Kren, C. Slugovc, F. Stelzer, F. Wiesbrock, *Macromol. Biosci.* 2013, in press. DOI: 10.1002/mabi.201200240.

S4-L11

Antimicrobial surfaces from block copolymers based on acrylic acid

Günther Gratzl (1)*, Christian Paulik (1), Silke Maninger (2), Josef Peter Guggenbichler (2), Maximilian Lackner (2)

(1) Johannes Kepler University, Institute for Chemical Technology of Organic Materials, Altenbergerstr. 69, 4040, Linz, Austria
(2) AMiSTec GmbH & Co. KG, Leitweg 23, 6345 Kössen in Tirol, Austria
*guenther.gratzl@jku.at

1. Introduction

For years hospitals and other medical facilities have used antibiotics to kill pathogenic bacteria. As a result multi-resistant bacteria are the reason for more than 380,000 hospital-acquired infections and about 25,000 deaths in the European Union, Norway and Iceland per year [1]. Despite of high hygienic standards in the EU the number of multi-resistant bacteria is still increasing. To change the situation the strategy against microorganisms has to be reformed from devitalizing and reducing the bacterial count to preventive actions with non-viable environments for pathogenic bacteria.
Up to now some antimicrobially active surfaces based on polymeric materials have been published like immobilized quaternary ammonium compounds, polyelectrolyte multilayers or immobilized natural organic substances (guanidinium, chitosan, peptides or enzymes) [2-4]. The mode of action for the antimicrobial activity is not completely established today, but it has already been shown that the pH-value of the surface is a crucial factor [5]. Acting like the acid-mantle of the human skin it was the idea to produce films with acidic surfaces as antimicrobially active substances. Block copolymers of acrylic acid with styrene and methyl methacrylate should provide these acidic surfaces.

2. Experimental

The block copolymers polystyrene-b-polyacrylic acid (PS-*b*-PAA) and polymethyl methacrylate-*b*-polyacrylic acid (PMMA-*b*-PAA) with varying PAA contents have been produced by anionic polymerization of styrene and MMA with *tert*.-butylacrylate initiated by *n*-butyllithium with a slight molar excess of *α*-methylstyrene in the presence of LiCl in a nitrogen-atmosphere at -78 °C. Subsequently an acid catalyzed hydrolysis of the *tert*.-butyl group with *p*-toluenesulfonic acid resulted in the acrylic acid block copolymers as it was verified by ^{1}H NMR (Bruker digital Avance III 300 MHz). Casts of the products from *1,4*-dioxane have been tested for their antimicrobial activity against strains of Escherichia coli (Ec, DSM 1104), Staphylococcus aureus (Sa, DSM 1103) and Pseudomonas aeruginosa (Pa, DSM 50071) by dropping 100 µl of bacteria-suspensions with a bacteria count of 10^7 CFU/ml on the cast surfaces. After 3, 6, 9 and 12 hours 10 µl of the drop have been transferred on a culture medium (Columbia-blood-agar) and bred at 37 °C for 24 h. The cultured bacteria are stored at 8 °C until the test was finished.

3. Results and discussion

The compositions of the block copolymers have been analyzed by ^{1}H NMR spectroscopy in $CDCl_3$ before hydrolysis. For polystyrene-*b*-poly-*tert.*-butylacrylate (PS-*b*-PtBA) the signal-intensity of 5 aromatic-hydrogen-atoms between 6.20 ppm and 7.20 ppm has been related to the signal-intensity of the proton in alpha position of the *tert*.-butyl ester at 2.18 ppm and for polymethyl methacrylate-*b*-poly-*tert.*-butylacrylate (PMMA-*b*-PtBA) the signal-intensity of 3 methyl-ester-hydrogen-atoms at 3.60 ppm has been related to the signal-intensity of the proton in alpha position of the *tert*.-butyl ester at 2.18 ppm to verify the content of each block. Since after hydrolysis the *tert.*-butyl-hydrogen-atoms-signal at 1.39 ppm disappeared, the hydrolysis-reaction can be supposed to be complete [6]. In case of PS-*b*-PtBA a weak signal can still be detected at 1.44 ppm after hydrolysis coming from the *ß*-methylene-protons of styrene, which usually give a multiplet centered at 1.50 ppm. Due to a weak solubility of polymers with higher acrylic acid contents $CDCl_3$-$(CD_3)_2CO$-mixtures have been used as a solvent for ^{1}H NMR spectroscopy. Additional to the acrylic acid copolymers a pure polystyrene-*b*-polymethyl methacrylate (PS-*b*-PMMA) with 50 mol% PS and 50 mol% PMMA has been produced and treated the same way as the PS-*b*-PAA and PMMA-*b*-PAA copolymers.
The results of the antimicrobial tests can be correlated to the acrylic acid-content of the polymer as shown in table 1. A complete elimination is given when no more bacteria can be cultured on the culture medium.

Table 1: Antimicrobial activity depending on the acrylic acid content of the block copolymer. The acrylic acid values were calculated from ^{1}H NMR results. Elimination times in brackets indicate a nearly-elimination at this time.

Polymer name	Acrylic acid content / mol%	Antimicrobial test: Time for elimination of Sa / h	Time for elimination of Ec / h	Time for elimination of Pa / h	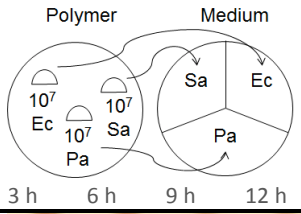
PS1	47.3	9	6	6	
PS2	42.0	-	(12)	-	
PS3	29.6	-	-	-	
PMMA1	46.3	9	6	6	
PMMA2	38.5	(12)	-	12	
PMMA3	28.7	-	-	-	
PS-*b*-PMMA	0	-	-	-	

4. Conclusion

The antimicrobial effect of PS-*b*-PAA and PMMA-*b*-PAA block copolymers with acrylic acid as active substance has been shown in this study. As well, a dependence of the antimicrobial activity from the acrylic acid content had been indicated.

References

[1] ECDC, EMA, The bacterial challenge: time to react, Joint Technical Report from ECDC and EMA, Stockholm, September 2009
[2] A. Munoz-Bonilla, M. Fernández-García, Progress in Polymer Science 2012, 37, 281-339
[3] S. Siedenbiedel, J.C. Tiller, Polymers 2012, 4, 46-71
[4] J.A. Lichter, K.J. van Vliet, M.F. Rubner, Macromolecules 2009, 42, 8573-8586
[5] C. Zollfrank, K. Gutbrod, P. Wechsler, J.P. Guggenbichler, Materials Science and Engineering C 2012, 32, 47-54
[6] J.-P. Hautekeer, S.K. Varshney, R. Fayt, C. Jacobs, R. Jérôme, Ph. Teyssié, Macromolecules 1990, 23, 3893-3898

S4-L12

Shell crosslinked micelles from RAFT generated amphiphilic block copolymers

Maria Schachner (1)*, Stephan Benedikt (1), Claudia Dworak (1), Heinrich Gruber (1), Barbara Kapeller (2), Karin MacFelda (2)

(1) Institute of Applied Synthetic Chemistry, Vienna University of Technology, Austria
(2) Department for Medical Research, Medical University of Vienna, General Hospital, Austria
*maria.schachner@ias.tuwien.ac.at

1. Introduction & Theory

Controlled/Living radical polymerization methods, including Reversible Addition-Fragmentation chain Transfer (RAFT) polymerization, are highly efficient tools to prepare well-defined amphiphilic block copolymers which have the ability to form micelles in aqueous media.[1] Due to their versatile usage, especially in the medical field, this type of block copolymers has received an ever increasing interest in recent years. Furthermore, RAFT polymerization can be used for a variety of monomers which are of interest for drug delivery systems. For this study, focusing on the synthesis and characterization of such amphiphilic block copolymers, laurylmethacrylate was used to form the first, hydrophobic block. For the hydrophilic block we used N-acryloyl

morpholine. To allow crosslinking and/or further modifications with molecules bearing an amino functionality, succinimide moieties were incorporated within the hydrophilic block by copolymerization.[2] Additionally fluorescein moieties were introduced to the hydrophobic block to investigate biological activity of the micelles in further in-vitro studies.

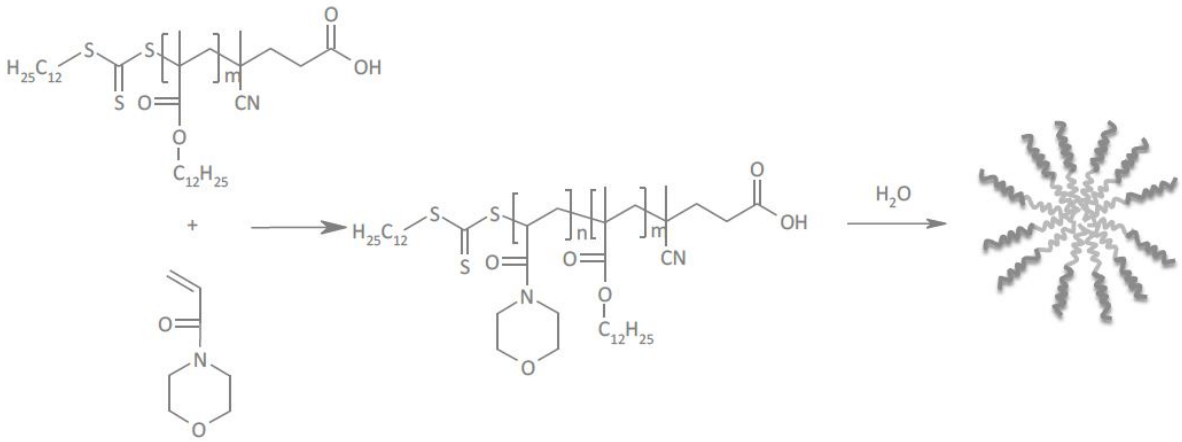

Figure 1. Synthesis of amphiphilic block copolymer p(LMA)-co-p(NAM) and formation of micelles

2. Experimental

The chain transfer agent (CTA) was synthesized according to literature [3] by the reaction of carbon disulfide and dodecanthiol to deliver bis(dodecylsulfanylthiocarbonyl) disulfide. In the next step 4-4´azo(bis(4-cyano pentanoic acid) was left to react with the intermediate product to form the desired CTA. N-methacryloxysuccinimide was synthesized from methacrlylic acid an N-hydroxy succinimide using N,N'-dicyclohexylcarbodiimide as a coupling agent. The general polymerization procedure was as follows: CTA/macro CTA, monomer, AIBN and naphthaline were dissolved in dry dioxane. After bubbling with N2 the solution was put into a preheated oil bath for a specific period of time. After polymerization the polymer was purified by precipitation in methanol. Since the thiol groups of the CTA are considered to be cytotoxic they had to be removed. For this purpose we used an access of 4-4´azo(bis(4-cyano pentanoic acid) to eliminate the mentioned groups by a radical induced process.

3. Results and discussion

We successfully prepared well-defined, functionlaized amphiphilic block copolymers with low polydispersity indices (<1.5) by the means of RAFT polymerization. They comprise of poly(laurylmethacrylate) in the hydrophobic block an poly(N-acryloylmorphonline) in the hydrophilic block. Copolymerization of N-Methacryloxysuccinimde in the hydrophilic block gave the possibility for shell crosslinking of the prepared micelles by a diamine linker. The polydispersity of the generated polymers was determined by size exclusion chromatography. By using naphthaline as an internal standard we were able to use 1H-NMR to calculate the monomer conversion and thereof the molecular weight of the polymers. Additionally we used fluorescence spectroscopy to gain information about the critical micelle concentration. First studies on the uptake of such micelles by living cells were performed by fluorescence microscopy. S S S OH O CN O OC12H25 O NO n m H25C12 S S S m OH O CN O OC12H25 H25C12 O NO + H2O

4. Conclusions

Summing up, we synthesized amphiphilic block copolymers from laurylmethyacrylate and N-acryloylmorpholine which have the ability to form micelles in aqueous media. In addition we copolymerized succinimde functionalities within the hydrophilic part to improve the stability of the micelles by using these activated esters for crosslinking with a diamine linker. Furthermore fluoresceine moieties included in the polymer backbone were used for monitoring the cellular uptake and cytotoxicity of the micelles. The existence of micelles and the CMC were determined by he means of fluorescence spectroscopy and dynamic light scattering.

References

[1] York, A.W. et al., Advances in the synthesis of amphiphilic block copolymers via RAFT polymerization: Stimuli responsive drug and gene delivery. Adv. Drug Delivery Reviews, 2008. 60(9): p. 1018-1036.
[2] Li, Y., et al., *Facile Formation of Uniform Shell-Crosslinked Nanoparticles with Built-in Functionalities from N-Hydroxysuccinimide Activated Amphiphilic Block Copolymers.* Advanced Functional Materials, 2008. **18** (4): p. 551-559
[3] Farnham, W. B., Synthesis of trithiocarbonate RAFT agents and intermediates thereof. 2005. p. 13 pp

S4-L13
Thermoplastic polyurethane elastomers derieved from new building blocks for vascular tissue engineering

Paul Michael Potzmann (1)*, Konstanze Seidler (1), Samuel Clark Ligon (1), Thomas Koch (2), Jürgen Stampfl (2), Babara Messner (3), Christian Grasl (4), Helga Bergmeister (5), Heinrich Schima (4), Robert Liska (1)

(1) University of Technology, Inst. of Applied Synthetic Chemistry, Getreidemarkt 9/163, 1060 Vienna, Austria
(2) University of Technology, Inst. of Material Science and Engineering, Favoritenstraße 9, 1040 Vienna, Austria
(3) Medical University, Department of Surgery, Waehringer Gürtel 18-20, 1090 Vienna, Austria
(4) Medical University, Center for Med. Physics and Biomed. Engineering, Waehringer Guertel 18-20/4L, 1090 Vienna, Austria
(5) Medical University, Institute of Biomedical Research, Währinger Gürtel 18-20 / AKH 1Q, 1090 Vienna Austria
*paul.potzmann@ias.tuwien.ac.at

1. Introduction
Coronary heart disease is the leading cause of mortality not only in Austria but also in all western countries. As autografts are still state-of-the-art, synthetic and tissue-engineered vascular grafts are an auspicious alternative. In particular scaffolds based tissue engineering (TE) show great promise. The aim of our work is to develop biodegradable, biocompatible thermoplastic polyurethanes (TPUs). We accomplished this goal by modifying the thermoplastic urethane elastomer (TPU) Pellethane™ (Dow) and introducing degradability. Further we synthesized potential degradation products to proof their low cytotoxicity and tune the mechanical and biodegradable properties based on the use of aliphatic diisocyanates. The possible application areas for these improved biodegradable TPUs include drug delivery systems, disposable medical tubing, textiles and show great promise in all areas of soft tissue engineering such as vascular grafts.

2. Theory
To achieve mechanical properties comparable to native blood vessels TPUs are a good choice because of their segmented configuration. The use of a macrodiol as a prepolymer leads to the formation of flexible soft-blocks and rigid hard- blocks, which form aggregates to give the desired elastomeric properties.

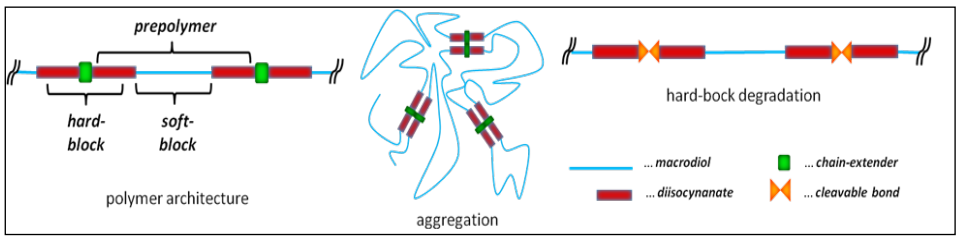

Figure 1. Basic concept of thermoplastic elastomers and introduction of degradability.[1]

Biodegradability is a very important feature of scaffolds for vascular tissue engineering. The degradation rate of the artificial graft must be well balanced with the regrowth of native tissue. This could be achieved by using a chain-extender containing a cleavable bond and by variation the used diisocyantes and diols.
Electrospinning is a suitable method to fabricate small-diameter blood vessels that imitate the architecture of native tissue. It is possible to manufacture seamless, non-woven, fibrous structures with high porosity.

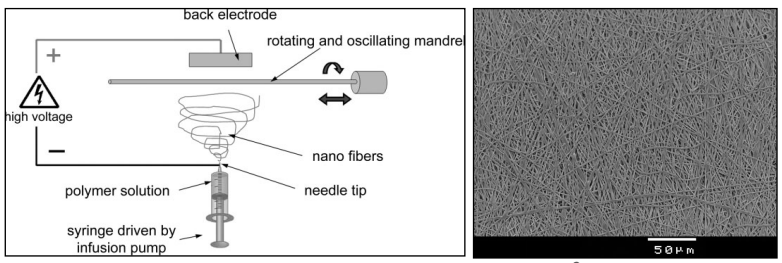

Figure 2. Schematic diagram of the electrospinning device.[2] / SEM image of the luminal side of an electrospun prosthesis[2]

3. Results and discussion
All synthesized thermoplastic urethane elastomeres achieved biodegrability with slow degradation rates that potentially correlate with the regrowth of native tissue. Further most of the tested compositions tend to be within the same scale as the pellethane reference in terms of mechanical properties. The formulation containing the aliphatic diisocyanate (HMDI) has shown the highest

potential to be used as artificial vascular craft due to its low steric hindrance of the urethane groups in the hard- block.
Expected degradation products of all synthesized TPUs showed no cytotoxic response up to concentrations of 1 mM in in-vitro tests with human umbilical vein endothelial cells (HUVECs).
Electrospun grafts were implanted into the infrarenal aorta of 7 rats and retrieved after 6 months and showed no signs of aneurysms or foreign body reaction. Cells populated nearly all areas of the conduit wall.

4. Conclusions

- The synthesis of degradable thermoplastic urethane elastomeres could be realized
- The degradation rate and mechanical properties can be adjusted by variation of the building blocks.
- Potential degradation products were synthesized and showed nearly no cytotoxicity on HUVECs
- In vivo tests of the synthesized TPUs show promising results.

References

[1] I. Yilgor, E. Yilgor, Polym. Rev. (Philadelphia, PA, U. S.) 2007. 47(4): p. 487-510.
[2] C. Grasl, H. Bergmeister, M. Stoiber, H. Schima, G. Weigel, J. of Biomed. Matl. Research Part A 2010 (93A), 716-723.
[3] S. Baudis, C.S. Ligon, K. Seidler, G. Weigel, C. Grasl, H. Bergmeister, H. Schima, R. Liska, J. of Polymer Science, Part A Polymer Chemistry 2012, 50(7), 1272-1280.

S4-L14
Modulation of mediators of inflammation with polystyrene divinylbenzene copolymers suppresses lipopolysaccharide-induced endothelial activation

Viktoria Weber (1)*, Tanja Buchacher (1), Tanja Eichhorn (1), Anita Schildberger (1)
(1) Danube University Krems, Center for Biomedical Technology and Christian Doppler Laboratory for Innovative Therapy Approaches in Sepsis, Krems, Austria
*viktoria.weber@donau-uni.ac.at

1. Introduction

Sepsis is defined as the systemic inflammatory response of the body to an infection. Sepsis and sepsis-associated multiple organ failure are associated with extensive tissue damage due to over-activation of the innate immune system and the excessive release of pro-inflammatory cytokines. Worldwide, sepsis is one of the leading causes of morbidity and mortality, and its incidence continues to increase. The development of targeted therapies for sepsis remains a major challenge due to the extreme heterogeneity of septic patients and due to the complex network of inflammatory mediators involved in the septic process.
Extracorporeal blood purification, such as hemofiltration or apheresis, has been proposed as promising strategy to modulate the inflammatory mediators, such as cytokines, in septic patients.

2. Theory

The endothelium is involved in regulation of blood flow, vascular tone, thrombosis, thrombolysis, adherence of platelets, and extravasation of circulating leukocytes. In infection, endothelial cells are activated either directly by pathogen-associated molecular patterns, such as lipopolysaccharide (LPS) from Gram-negative bacteria, or by host-derived mediators, such as chemokines, cytokines, complement, and serine proteases. The endothelium responds to these mediators by switching to a pro-inflammatory and pro-coagulant state, which is associated with enhanced adhesion of platelets, monocytes, and neutrophils. Thus, endothelial injury and endothelial dysfunction play a crucial role in sepsis and multiple organ failure.
The aim of this study was to monitor the effect of the adsorption of inflammatory mediators on endothelial cell activation using a cell culture model (Figure 1). Two different adsorbents were used, namely a specific adsorbent for the pro-inflammatory cytokine tumor necrosis factor alpha (TNF-α), and a selective adsorbent (albumin-coated polystyrene-divinylbenzene copolymer of defined porosity), which binds a range of cytokines and other inflammatory mediators based on hydrophobic interactions.

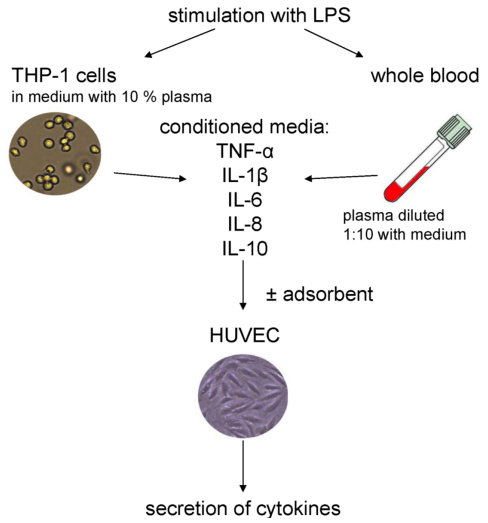

Figure 1: Cell culture model to monitor endothelial activation. Monocytes, monocytic THP-1 cells, or whole blood are stimulated with lipopolysaccharide, the resulting conditioned medium is harvested and transferred to endothelial cells. Endothelial activation is monitored by release of cytokines and expression of surface adhesion molecules.

3. Experimental

Human umbilical vein endothelial cells (HUVEC) were activated with conditioned medium obtained by stimulation of monocytic THP-1 cells or whole blood with lipopolysaccharide. Mediators of inflammation were adsorbed from the conditioned medium prior to its application to the endothelial cells and the effect of mediator adsorption on endothelial cell activation was assessed using different read-out assays. Two different adsorbents were used: a specific adsorbent for the pro-inflammatory cytokine TNF-α was produced by covalent immobilization of an anti-TNF-α antibody on CNBr-activated Sepharose beads. A polystyrene-divinylbenzene copolymer with an average pore size of 15 nm was used for the selective adsorption of cytokines, which bind to the resin by hydrophobic interactions. The adsorbent was coated with human serum albumin to improve its biocompatibility.

4. Results and Discussion

Application of both adsorbents resulted in significantly reduced endothelial activation, as shown by reduced release of IL-6 and IL-8 and reduced expression of adhesion molecules (Figure 2). The effect was statistically significant for both adsorbents, but stronger for the selective cytokine adsorbent, indicating that TNF- α plays a crucial role in endothelial activation, but other factors are involved in addition.

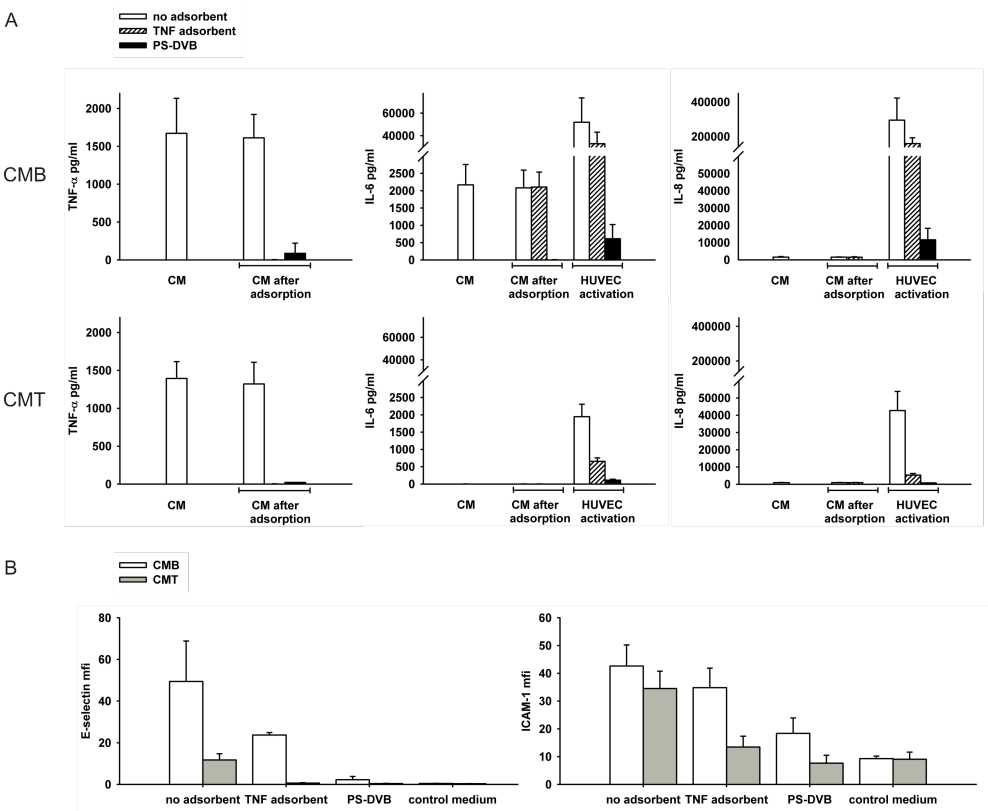

Figure 2: Effect of mediator modulation with a specific TNF- α adsorbent or a selective cytokine adsorbent (PS-DVB) on endothelial activation. Panel A: release of cytokines; Panel B: expression of adhesion molecules.

5. Conclusions

Adsorptive modulation of mediators of inflammation by extracorporeal techniques may be a promising supportive therapy for sepsis, since it reduced endothelial activation in a cell culture model.

6. Acknowledgements

This work was funded by the Christian Doppler Society and Fresenius Medical Care (Christian Doppler Laboratory for Innovative Therapy Approaches in Sepsis).

Session 11: Advances in Polymer Analysis, Characterisation and Testing

S11-L15
Accelerated weathering of multi-layer films – effect of specimen preparation

Gernot Oreski (1)*, Gerald Pinter (2)

(1) Polymer Competence Center Leoben, Roseggerstraße 12, 8700 Leoben, Austria

(2) University of Leoben, Chair of Materials Science and Testing of Polymers, Otto-Glöcklstraße 2, 8700 Leoben, Austria

*oreski@pccl.at

1. Introduction

Multi-layer laminates are widely used as backsheet films for photovoltaic (PV) modules. Backsheet materials primarily have to provide mechanical strength and weathering protection to the PV module. Further requirements are low cost, good processability, low water absorption and permeability, high resistance to UV degradation and thermal oxidation, good adhesion to solar cell encapsulation materials and chemical inertness. To fulfill these requirements usually multi-layer films are used. The outer layer serves mainly as a weathering protection. Therefore mainly fluoropolymers such as polyvinyl fluoride (PVF), polyvinylidene fluoride (PVDF) or ethylene tetrafluoroethylene (ETFE) are used. But over the last years also new materials like polyethylene terephthalate (PET), polyamide (PA) and even modified polyethylene (PE) were introduced. State of the art for the middle layers are polyesters such as polyethylene terephthalate (PET), mainly to provide mechanical strength as well as electrical insulation and high barrier to water vapor and oxygen. Regarding the inner layer a broad variety of materials can be found on the market, which ranges from a

symmetrical build-up using the outer layer material, surface modified polyesters to adhesion promoting layers made from polyethylene copolymers.
Since PV modules service life times of at least 20 years are requested, it is absolutely essential to analyze the durability of new materials under typical outdoor load conditions and to describe the degradation behavior and its impact on performance of a PV module [1]. Mechanical testing, especially tensile tests, proved to a versatile and sensitive characterization method in describing the aging behavior of backsheet films [2].
During previous research projects after accelerated weathering effects of the multi-layer build-up like delamination were observed that influenced the results of the mechanical testing significantly. Also sample preparation and handling seemed to have an influence on the aging test results [3]. Hence, the main objective of this paper is the systematic investigation of the effect of specimen preparation of laminated multi-layer films on the accelerated weathering test results, especially mechanical testing results.

2. Experimental

A three layer laminate consisting of ethylene vinyl acetate (EVA) – PET – fluoropolymer was chosen for the investigations. In order to investigate the aging behavior the specimens were exposed up to 5000h at 85°C and 85 %RH (damp heat test). To investigate the influence of sample preparation, both precut specimen and whole sheets, which have to be cut afterwards, were exposed at damp heat conditions. Furthermore two different specimen geometries (according to ISO 527-3) were investigated: Rectangular strip specimens (type 2) of 100mm in length and 15mm in width and dumb bell specimen (type 5).
Tensile tests were carried out with a screw driven universal test machine (Zwick Z010 Allround-Line, Zwick, Ulm, D) at 23°C according to EN ISO 527-3. The test speed was 50mm/min. From a total of at least five specimens for each test series, average numbers for elastic modulus (E), stress-at-break (σ_b) and strain-at-break (ε_b) were deduced.

3. Results and discussion

Figure 1 shows the cutting edge of specimen that was cut after damp heat exposure. Several cracks with size up to a few millimeters were found after damp heat testing. The crack formation after cutting can be attributed to the strong embrittlement of the PET layer due to hydrolysis. Regarding mechanical testing a significant notch effect of the cracks was found. Therefore it can be concluded that cutting of multi-layer laminate specimen should be done preferably before exposure to accelerated weathering test in order to avoid effects of specimen cutting on the evaluation of the aging behavior.

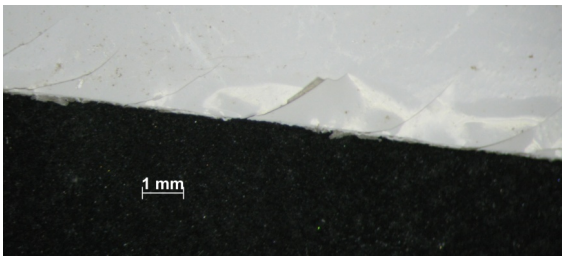

Figure 1. Cutting edge of specimen that was cut after damp heat exposure.

Figure 2 shows the stress-strain curves of unaged and aged multi-layer films for both specimen geometries. As expected for the unaged films a significant difference in the deformation behavior and stress-strain curves was found. The mechanical properties exhibited brittle material behavior and are dominated by the PET layer, which is the stiffest material in the laminate. In case of the dumb bell specimen higher stiffness and nearly no plastic deformation was observed. For the strip specimen instead significant plastic deformations with strain-at-break values around 180% were detected. For both films no delamination effects were observed. After exposure to damp heat conditions significantly different mechanical failure was observed for the two specimen geometries. Already after 250h of damp heat testing for the dumb bell specimen a complex fracture behavior with large-scale delamination and consecutive failure of the single layers was observed. For the strip specimen instead until 2000h no delamination effects were detectable. After 5000h the same complex fracture behavior was observed for the strip specimen. Assumedly the dumb bell specimen geometry promotes strong delamination effects after weathering. A possible explanation would be differences in the stress distribution within the specimen, where the different geometries may cause shear or peel stresses. Another reason may be variations in the state of hydrolysis of the adhesive layer due to different moisture ingress for the two geometries.

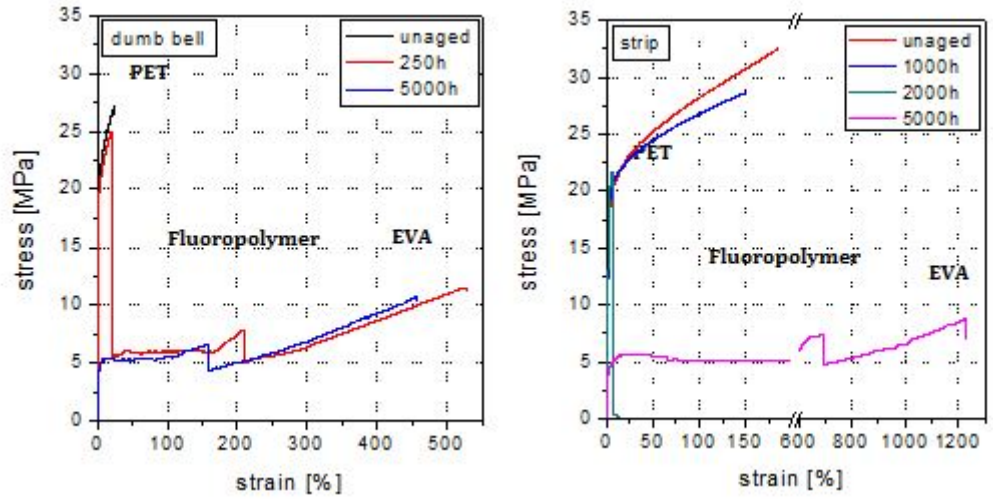

Figure 2. Stress-strain curves of unaged and aged multi-layer films; left: dumb bell specimen; right: strip specimen.

The next step within this project will be the clarification of these effects. To assess the influence of humidity specimen of both geometries are currently exposed to dry heat conditions (85°C, humidity not controlled). Furthermore the stress distribution will be modeled via finite element method in order to identify shear or peel stresses.

4. Conclusion and outlook

Specimen preparation and handling has a significant influence on the outcome of accelerated weathering tests and the evaluation of aging effects of multi-layer films. The point as well as the mode of cutting had significant influence on the mechanical properties after weathering. Also the choice of the sample geometry is important, as dumb bell specimen geometry supposedly promote stronger delamination effects during mechanical testing than strip specimen.
The next step within this project will be the assessment of the influence of humidity and stress distribution on the weathering results of multi-layer films for the different specimen geometries.

Acknowledgements

Thanks to my colleagues Astrid Rauschenbach, Bettina Hirschmann, Marlene Knausz (PCCL) and Prof. Gerald Pinter (University of Leoben) for the support within this project. This research work was performed at the Polymer Competence Center Leoben (PCCL) within the project “PV Polymer” (FFG Nr. 825379, 3. Call “Neue Energien 2020”, Klima- und Energiefonds) in cooperation with the Chair of Materials Science and Testing of Plastics at the University of Leoben. The PCCL is funded by the Austrian Government and the State Governments of Styria and Upper Austria.

References

[1] A. W. Czanderna, F. J. Pern, Sol Energ Mat Sol C. 1995, 43, 101-181.
[2] G. Oreski, G.M. Wallner, R.W. Lang, Biosystems Engineering 2009, 103, 489-496.
[3] G. Oreski, Proceedings of SPIE - The International Society for Optical Engineering 7773, 2010, Article number 77730D.

S11-L16

Implementation and evaluation of accelerated weathering tests for the aging characterisation of polymer composite films used in photovoltaic modules

Bettina Hirschmann*, Gernot Oreski
Polymer Competence Center, Roseggerstraße 12, 8700 Leoben, Austria
*bettina.hirschmann@pccl.at

1. Introduction

In the photovoltaic (PV) industry it is required to ensure a high quality product standard and as a result module lifetimes of at least 25 years are guaranteed [1]. Therefore not only the module but also the components of a PV module have to be tested concerning the quality. Currently the standard testing method for lifetime valuation of backsheets of PV modules is a damp heat (DH) test at 85°C and 85% relative humidity (RH) for up to 2000 hours (h). The test duration of 2000 h equals approximately 3 months, which takes too long for a fast material pre-selection.
Hence the objective of this work was to find an accelerated weathering test to estimate the aging behaviour of polymer backsheet films and to correlate it with the damp heat test for fast qualification of new materials. As accelerated weathering test a pressure cooker test (PCT) was implemented and evaluated.

2. Experimental

A standard composite backsheet film, consisting of polyvinyl fluoride (PVF) and polyethylene terephthalate (PET), was investigated. Samples were artificial weathered under damp heat test conditions up to 3000 h and under pressure cooker test conditions up to 48 h at different temperature levels, which were all above the glass transition of PET (approximately 80°C), shown in Table 1 [2]. The aging behaviour was investigated by differential scanning calorimetry (DSC) and tensile tests according to ISO 527-3 [3].

The DSC tests were performed on the composite film using a Mettler Toledo DSC 1 (Schwerzenbach, CH). Thermograms were recorded under nitrogen environment. The heating rate was 10 K/min. The melting enthalpy of PET which corresponds to the crystallinity degree of the material was evaluated. Tensile tests were carried out by a Zwick-Roell (Ulm, D) Z010 tensile testing machine at 23°C and a crosshead speed of 50 mm/min. Rectangular specimens with a width of 15 mm, a length of 100 mm and a gauge length of 50 mm were used.

Table 1. Test conditions

	Damp heat test	Pressure cooker test			
Temperature	80°C	100°C	110°C	120°C	140°C
Relative humidity	85%	100%			
Duration	500h, 1000h, 2000h, 3000h	12h, 24h, 48h	12h, 24h, 48h	12h, 24h, 48h	12h, 24h

3. Results and discussion

As already shown in the literature, PVF exhibited no significant changes after artificial weathering [4]. This is the reason why only DSC results of PET will be discussed. In Fig. 1 the melting enthalpies of the PET layer are displayed for all unaged and different aged samples. With rising damp heat test duration the melting enthalpy increased from 31.0 J/g ± 0.7 J/g (unaged) up to 44.8 J/g ± 0.8 J/g after 3000 h. The same temperature dependence was found for all specimens after the pressure cooker tests. Pressure cooker tests at 100°C and 110°C for 48 h caused an increase in the melting enthalpy until 12 h of exposure. Then the values after both temperatures stagnated at about 33.6 J/g ± 1.0 J/g and 34.4 J/g ± 2.0 J/g, respectively. Assumedly these temperatures were too low to cause the same amount of physical aging as the damp heat tests within the desired testing time. The samples aged at 120°C for 48 h exhibited a melting enthalpy value of 37.4 J/g ± 1.2 J/g, which correlates with the value of 38.5 J/g ± 1.7 J/g for the damp heat test after 1000 h. By comparison with the damp heat test results also a similar curve progression was found. An aging temperature of 140°C was supposedly too harsh for the material. Already after 24 h strong embrittlement was observed. The melting enthalpy increased from 31.0 J/g ± 0.7 J/g to 47.3 J/g ± 3.6 J/g.

Fig. 2 depicts the influence of aging on the strain at break value, which is a sensitive degradation indicator. For all samples an embrittlement after damp heat testing was observed. The strain at break value decreased significantly with increasing test durations. After 2000 h of damp heat testing the samples were brittle and broke before yield stress was reached at a strain at break value of about 1.6% ± 0.2%. After 3000 h of damp heat testing the material was too brittle to cut tensile test samples. High scattering of the results, especially after 1000 h of damp heat testing, was be observed. The material aged under pressure cooker test conditions exhibited similar behavior – with increasing duration the strain at break value decreased. After 48 h at 100°C the strain at break value decreased from 205.3% ± 5.1% (unaged) to 119.7% ± 5.6%. The samples aged at 110°C for 48 h exhibited a strain at break value of 84.0% ± 8.5%. After 100°C and 110°C the curve progressions were different to the damp heat test result within the desired time. Assumedly the exposure at 100°C and 110°C led to a different amount of chemical degradation. By comparison with the other temperatures the results after 120°C correlated the most with the damp heat test results. After 48 h the strain at break value was 41.3% ± 14.6%. In contrary 140°C were supposedly too rough and led to a fast embrittlement with a strain at break value of 0.5% ± 0.2% after 24 h.

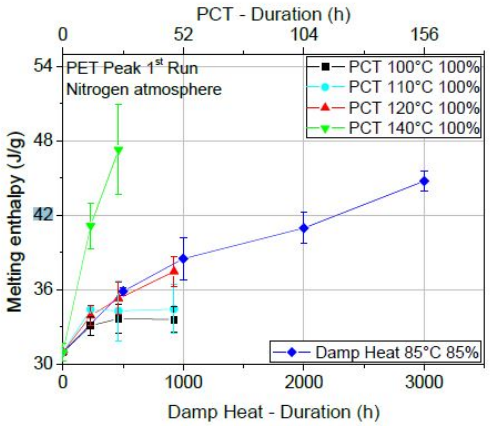

Figure 1. PET Melting enthalpy of different aged and unaged samples

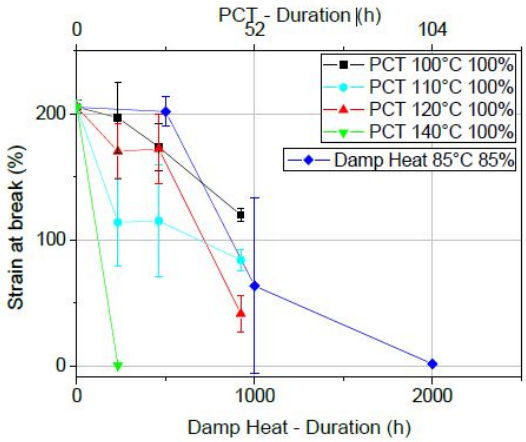

Figure 2. Strain at break values over the test duration for unaged and damp heat and pressure cooker aged samples

4. Conclusions and Outlook

As an accelerated aging test method pressure cooker tests were implemented and evaluated to estimate the aging behaviour of a standard polymer backsheet films used in PV modules. The aim of this work was to correlate the pressure cooker test (different temperature levels, 100% RH) with the established damp heat test (85°C and 85% RH) for time efficiency. The aging behaviour of the laminate material after damp heat and pressure cooker test aging was characterized by DSC and by mechanical tensile tests.
The results of the DSC and the tensile tests exhibited that the pressure cooker test aging at 120°C and 100% RH corresponded the best with the damp heat test. Further investigations of 96 h aged samples under 120°C pressure cooker test conditions will be done for a better verification of the results. In addition infrared spectroscopy analysis of all samples will be conducted to get more information about the degradation behaviour of the polymer laminate under both aging methods.

Acknowledgements

This research work was performed at the Polymer Competence Center Leoben (PCCL) within the contract project “Implementierung und Evaluierung von beschleunigten Bewitterungstests für die Alterungscharakterisierung von Polymerfolienverbunden” in cooperation with AT&S AG and with the Institute of Materials Science and Testing of Plastics at the University of Leoben. The PCCL is funded by the Austrian Government and the State Governments of Styria and Upper Austria.

References

[1] A. W. Czanderna, F. J. Pern, Solar Energy Materials and Solar cells **1996**, 43, 101-181
[2] H. Domininghaus, P. Eyerer, P. Elsner, T. Hirth, (7. Ed.); Die Kunststoffe und ihre Eigenschaften, Springer-Verlag, Berlin Heidelberg, 2004, p. 837.
[3] ISO 527-3, Plastics – Determination of tensile properties – Part 3: Test conditions for films and sheets
[4] G. Oreski, G. Wallner, Solar Energy **2005**,79, 612-617

S11-L17
Investigation in the thermal expansion behavior of PV module encapsulation materials

Marlene Knausz (1)*, Gernot Oreski (1), Peter Guttmann (2)
(1) Polymer Competence Center Leoben GmbH, Roseggerstraße 12, 8700 Leoben, Austria
(2) Chair of Materials Science and Testing of Plastics, Montanuniversity, Otto Glöckel-Straße 2, 8700 Leoben, Austria
*marlene.knausz@pccl.at

1. Introduction

Different materials are used in a PV module like glass, polymers, semiconducters and metals. Hence there are different coefficients of thermal expansion (CTE) for these components. These differences can lead to overstressing or even cracking of components. To compensate the different CTEs the solar cells with interconnectors are encapsulated in a low modulus, elastomeric polymer.
State of the art for solar cell encapsulation is the usage of ethylene vinyl acetate (EVA). During PV module lamination EVA fits together all components (glazing, interconnectors, cells and backsheet) by melting with following chemical crosslinking. The crosslinking is necessary for the thermo-mechanical stability of the EVA as well as the compensation of the different CTEs of the materials.
CTE of EVA is not only important during service life, but also in the lamination process. Inadequate processing and handling of the EVA films can lead to variable CTEs. This can result in troubles during lamination like exorbitant shrinkage, deformation of

backsheets, dislocation of cells, breakage of interconnectors and in special cases also to wrinkles in the module[1]. Therefore the main objective was the investigation in the CTE of three commercial available EVA films.

2. Experimental

Three different ethylene vinyl acetates (EVA), two standard cure and one ultra-fast cure type were investigated, which are listed in Table 1.

Table 1. Investigated EVA films.

Abbreviation	ENCAPSULANTS	**Manufacturer**	**Thickness [µm]**
EVA 1	EVA SC	A	400
EVA 2	EVA SC	B	460
EVA 3	EVA UFC	A	465

Specimen with a length of 10 mm and a width of 6 mm were made out of the above listed materials for CTE measurements. At least three measurements of each direction (along and across extrusion direction) per film were made. The measurements were carried out using a thermomechanical analyser (TMA) of the type Mettler Toledo TMA/SDTA840 (Schwerzenbach, CH). The measurements were all done in air atmosphere and started at 25 °C for 3 min then the sample was heated up with a heating rate of 2 K/min until 70 °C were reached for encapsulants. All tests were done in air atmosphere. The CTE was evaluated then by

$$\alpha_{th} = \frac{1}{l_0} \times \frac{l_2 - l_1}{T_2 - T_1} \quad (1)$$

l_0 is the initial length of sample, before measurements are started; l_2 is the length at end temperature (T_2=60 °C) and l_1 is the length at starting temperature (T_1=30 °C) of evaluation.

4. Results and discussion

Figure 1 shows CTE as a function of temperature in machine and transversal direction for all investigated films.

The first change of the slope of CTE values at 40 °C can be related to the melting of secondary crystals in EVA due to storage at slightly elevated temperatures. The melting temperature of EVA can be found around 60 °C. Above 60 °C the material softens and no reliable results were obtainable.

With increasing temperature all films showed an increase in CTE values. Furthermore, an anisotropic behaviour of the CTE was found for all films. In transversal direction the CTE was higher than in machine direction. These can be attributed to the orientations of the chain molecules out of the extrusion process. Interestingly the films of manufacturer A exhibited a far more significant anisotropy, which can be related to higher orientation. This clearly indicates that the production parameters like drawing off speed of the film from manufacturer A was too fast. Also the CTE values of the films of manufacturer A were higher than the values of manufacturer B. EVA 1 has an over 3,5 times and EVA 3 has an over 6 times higher value of the CTE in machine direction at 60 °C than EVA 2 from the manufacturer B.

To confirm these assumptions and to identify all reversible effects from film production rerun measurements (3 reruns with the same specimen) with an EVA 1 sample in machine and transversal direction was made.

Due to the melting of the films all orientations relaxated and resulted in significant lower CTE values similar to EVA 2. Also the differences between machine and transversal direction were minimized. This confirms the assumption of former induced orientation effects due to extrusion.

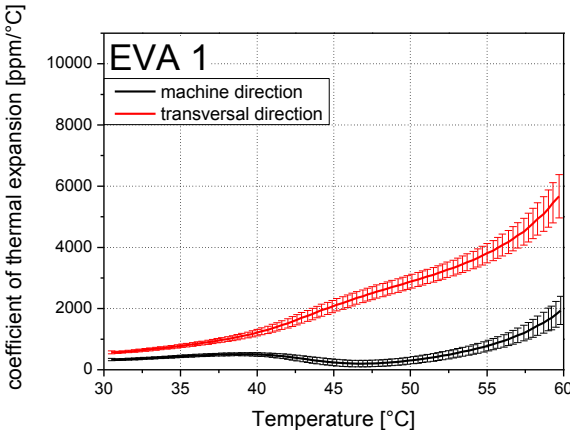

a)

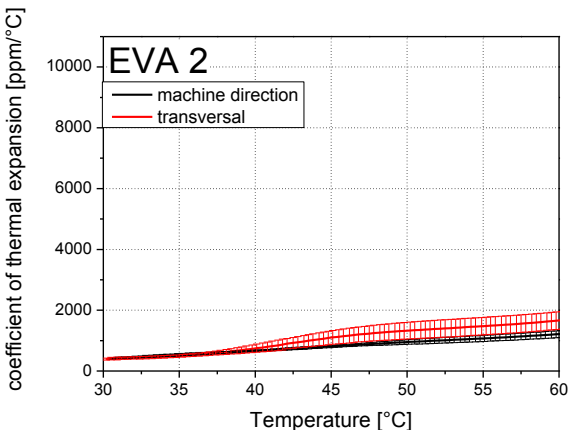

b)

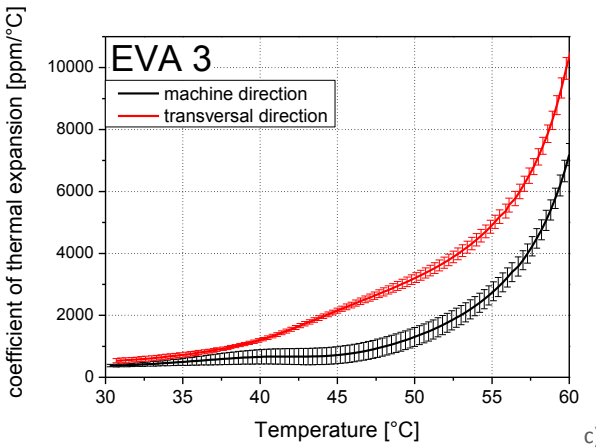

c)

Figure 1. CTE as a function of temperature in machine and transversal direction for **a)** EVA 1 **b)** EVA 2 **c)** EVA 3

5. Conclusions

The results showed a temperature dependency on the CTE of the investigated EVA samples. Furthermore, an anisotropic behaviour of the CTE was found for all films. The differences in machine and transversal direction can be attributed to orientations of the chain molecules due to the extrusion process.

Strong anisotropy can result in troubles during lamination like exorbitant shrinkage, deformation of backsheets, dislocation of cells, breakage of interconnectors and in special cases also to wrinkles in the module. TMA proved to be a suitable method for qualification but also for quality control of different encapsulation films.

Acknowledgements

The research work was performed at the Polymer Competence Center Leoben GmbH (PCCL, Austria) in cooperation with the Institute of Materials Science and Testing of Plastics at the University of Leoben within the framework of the COMET-program of the Austrian Ministry of Traffic, Innovation and the Ministry of Economy, Family and Youth with contributions by academic and commercial partners. The PCCL is funded by the Austrian Government and the State Governments of Styria and Upper Austria.

References

[1] C. Hirschl et al. (2012). In Proc. “EU PVSEC 2012”, (Nowak, S. und Jäger-Waldau, A.), 4BV.3.55, Frankfurt, D.

S11-L18
Characterisation of the damping behavior of thin multilayer films

Gilbert Knapp (1)*, Gernot Oreski (1), Gerald Pinter (2)

(1) Polymer Competence Center Leoben, Roseggerstrasse 12, 8700 Leoben, Austria

(2) University of Leoben, Material Science and Testing of Plastics, Otto Glöckel-Strasse 2, 8700 Leoben, Austria

*gilbert.knapp@pccl.at

1. Introduction

In structures, which are exposed to high frequencies the knowledge of the damping behavior is essential for a successful design. In the present work a method is introduced to study the temperature and frequency dependent damping behavior of thin multilayer polymer films with an overall thickness below 50 µm, based on the concept of dynamic mechanic analysis (DMA).

2. Theory

The damping of the investigated thin multilayer films happens due to the constraint layer effect, i. e. damping occurs due to shear deformation of a soft viscoelastic layer constrained by two stiff outer layers when the sandwich design is bent, as depicted in Figure 1 [1-5]. Therefore to characterize the damping behavior of thin multilayer films without the need to build up the whole structure a test was set-up in DMA-shear mode.

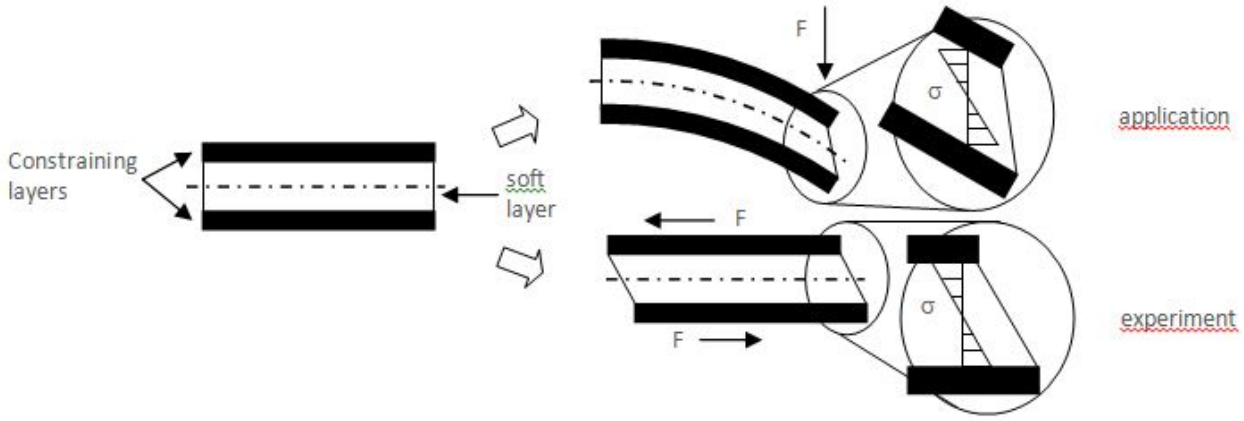

Figure 1. Schematic diagram of the constraint layer concept where damping in a sandwich design occurs due to shear deformation of a soft viscoelastic layer which is constraint by two stiff layers and comparison of the load situation in application and in the experiment [1-5].

3. Experimental

A dynamic mechanic analyzer (DMA) of the type Mettler Toledo DMA/SDTA 861^e with special shear clamps was used to characterize thin multilayer films with thicknesses below 50 µm due to their damping behavior in a temperature range from -40 up to 220 °C and frequencies from 1 to 200 Hz. During a dynamic heating segment of 2 K/min frequencies of 1, 10, 100 and 200 Hz were altered continuously. To prevent the shear brackets from contact quartz plates where attached between the specimens and the brackets. Subsequently the frequency-temperature behavior of the loss factor tan d maximum was described via the Williams-Landel-Ferry concept (WLF) and the temperature for the tan d maximum at application relevant frequencies up to 800 Hz was calculated [6]. This frequency was chosen because in the application the laminates have to damp the whole structure, which they are built in, at the resonance frequency at 800 Hz. In order to obtain an easy to use factor which should be comparable with experiments of the whole structure the frequency dependent integrated average of tan d was calculated in a temperature range relevant for the application from 0 to 60 °C.

4. Results and discussion

In Figure 2 results from DMA experiments with frequencies of 1, 10, 100 and 200 Hz and the succeeding calculation of the integrated average of the loss factor tan d are shown. The tan d curves exhibited a sharp increase starting at -40 °C, followed by a broad maximum, a plateau with a lower damping levels and a decrease starting at 140 °C. Whereas the maximum was related to the softening of the viscoelastic adhesive layer, the decrease starting at 140 °C was related to the glass transition of the stiff outer layers. With increasing frequencies a broadening and a shift to higher temperatures of the loss factor maximum was found. The latter was described via the WLF concept followed by a calculation of tan d curves for frequencies up to 800 Hz by shifting the whole curve from 200 Hz, as depicted in Figure 2(a). The maximum of the loss factor shifted over 23 °C from -18 °C at 1 Hz to 5 °C at 200 Hz and an additional difference of 9 °C was calculated for the maximum at 800 Hz and 14 °C. Finally the integrated average of tan d in the temperature range from 0 to 60 °C, which is relevant for the application, was calculated for frequencies from 1 to 800 Hz. Also for the integrated average of the loss factor tan d frequency dependent damping behavior was found with significant lower loss factors at frequencies below 100 Hz.

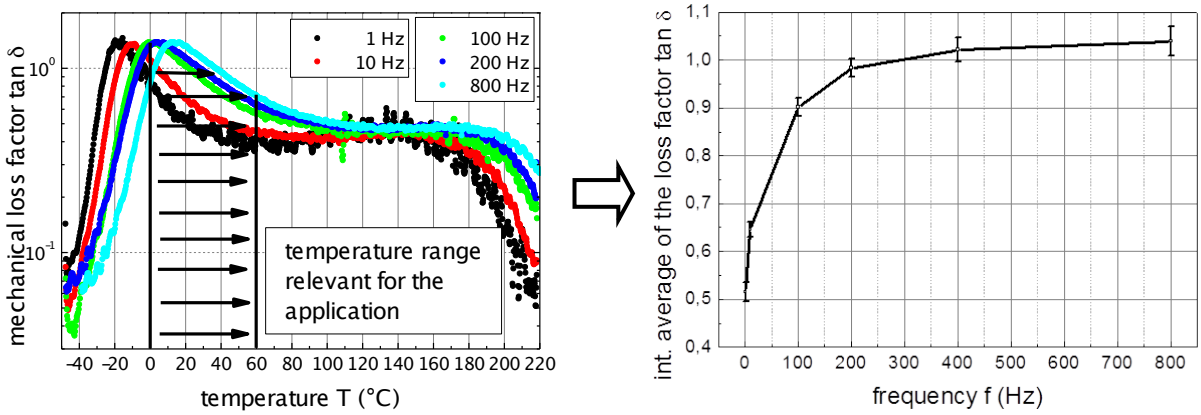

Figure 2. Schematic evaluation of measured damping behavior (a) and calculated integral average of the loss factor tan d (b) in order to ease comparison between different film types.

5. Conclusions

In the present work a method was introduced to study the damping behavior of thin multilayer films with thicknesses below 50 µm. In the constraint layer design of the investigated films the damping occurs due to shear deformation of the soft viscoelastic middle layer and therefore a test was set-up in DMA shear mode. Via the WLF concept and the integrated average of the loss factor tan d the damping behavior of the films was described with an easy to use factor in order to enable a ranking of different film compositions. As a result it was possible to characterize the damping behavior in application relevant temperature and frequency conditions. Additionally the main requirements for thin laminates in order to obtain an optimal damping behavior were found with a high mechanical loss factor at a frequency of 800 Hz over a temperature range from 0 to 60 °C. Therefore further optimization of thin laminates is enabled without the necessity of building the whole structure.

Acknowledgements

The research work of this paper was performed at the Polymer Competence Center Leoben GmbH (PCCL, Austria) within the framework of the COMET-program of the Federal Ministry for Transport, Innovation and Technology and Federal Ministry for Economy, Family and Youth. The PCCL is funded by the Austrian Government and the State Governments of Styria and Upper Austria.

References

[1] E.M. Kerwin, *J. Acoust. Soc. Am.* 1959, 31, 952-962.
[2] L.H. Sperling, in R.D. Corsaro and L.H. Sperling; Sound and Vibration Damping with Polymers, American Chemical Society, Washington DC, 1990, p. 5.
[3] R.N. Capps and L.L. Beumel, in R.D. Corsaro and L.H. Sperling; Sound and Vibration Damping with Polymers, American Chemical Society, Washington DC, 1990, p. 63.
[4] E.E. Ungar, in L.L., Beranik, (Ed.), Noise and Vibration Control, McGraw-Hill, New York, 1971, Ch. 14.
[5] D. Ross et al., in J.E. Ruzicke, (Ed.), Structural Damping, American Society of Mechanical Engineering, New York, 1959, p. 49-87.
[6] M. Williams et al., *J. Am. Chem. Soc.* 1955, 77, 3701-3707.

Session 7: Coatings and Adhesives

S7-L19

Microcellular foaming with UV light – new strategies for the formation of 3D structures in offset printing techniques

Sandra Schlögl (1)*, Martin Reischl (2), Volker Ribitsch (2), Wolfgang Kern (1,3)
(1) Polymer Competence Center Leoben GmbH, Roseggerstraße 12, 8700 Leoben, Austria
(2) Joanneum Research Forschungsgesellschaft mbH, Steyrergasse 17, 8010 Graz, Austria
(3) University of Leoben, Chair of Chemistry of Polymeric Materials, Otto Glöckel-Straße 2, 8700 Leoben, Austria
*Sandra.Schloegl@pccl.at

1. Introduction

The present study aims at the development of new photochemically expandable inks for the formation of firm and raised structures in offset printing techniques. The UV assisted foaming of acrylic offset inks is based on the excitation of a selected photoacid generator by ultraviolet light (UV) to release Brønsted acids. In the presence of calcium carbonate particles, carbon dioxide is generated and employed as blowing agent. Regarding the formation of raised 3D structures, a sufficient amount of blowing agent has to be generated to obtain the required increase of the film thickness [1]. To enhance the proton formation and to increase the concentration of the blowing gas, selected photosensitizers following different sensitizing mechanisms have been added to the ink formulation. To ensure that the gas bubbles are trapped in the cured resin a balance has to be found between the curing speed of the ink and the foaming speed. In the present study crucial process parameters including photoacid generator level, choice of photosensitizer, light intensity and concentration of calcium carbonate particles are determined and their influence on the foam properties including cell morphology and the expansion of the film thickness is discussed.

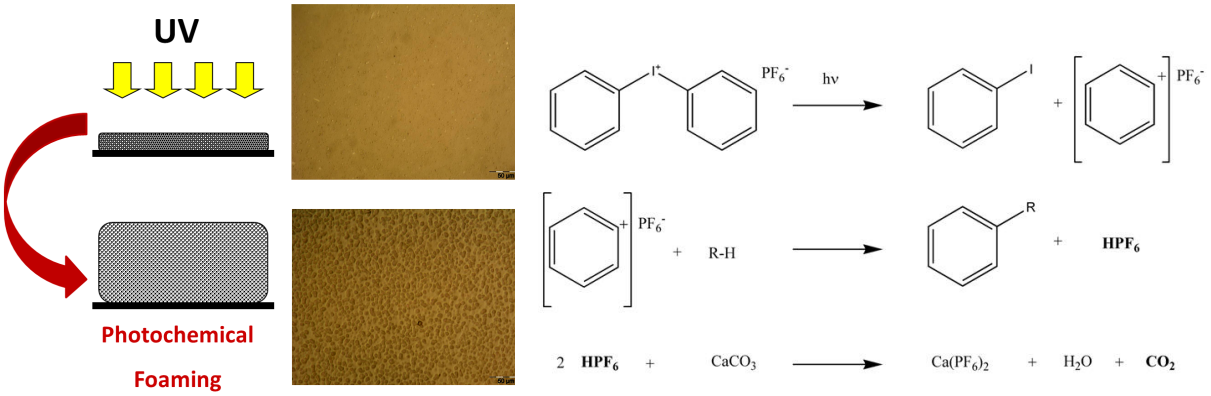

Figure 1. Photochemical foaming of acrylic inks

2. Experimental

The photosensitizer (2-ethyl-9,10-dimethoxyanthracene) was dissolved in ethyl acetate in the first step. The $CaCO_3$ particles were added to the solution and dispersed by means of an ultrasonic bath for 10 min at room temperature. This dispersion containing the calcium carbonate particles and the dissolved sensitizer was mixed with the UV curable offset ink and the photoacid generator (Iodonium-(4-methylphenyl)[4-(2-methylpropyl)phenyl]hexafluorophosphate). The ink formulation was then stirred for 30 min using a magnetic agitator and was degassed in vacuum for 10 min. The ink was spin cast (8000 rpm, 40 s) on a glass substrate and the samples were illuminated with a UV spot curing unit (Efos Novacure high pressure Hg emitter) with a wave length range between 290 and 410 nm. The curing and foaming were carried out with an irradiation intensity between 0.5 and 4.0 J/cm^2.

The morphology of the photochemically foamed acrylate films was studied using an Olympus BX 51 optical microscope, and both cell size and cell size distribution were measured using the image analysis software Analysis® Five. Cross-sections of the foamed and cured films were prepared by slicing and breaking the glass substrate bearing the ink layer under liquid nitrogen. The relative increase of the film thickness was measured with an optical microscope (Olympus BX 51) using the image analysis software Analysis® Five.

3. Results and discussion

With respect to offset inks, the cross-linking of acrylated resins by UV or visible light has become an established technology, due to the short reaction time and ambient temperature of the curing process. In the present study the UV assisted foaming was carried out in a commercially available offset printing ink containing triacrylate oligomers as base resin. The results reveal that at a given particle concentration of 5 wt.-%, high photoacid generator levels (20 wt.-%) are required to generate a sufficient amount of the blowing agent CO_2 and consequently to obtain a significant increase in the film thickness ranging from 30 to 35 % (see **Figure 2a**). Moreover, it is evident that an increase of the illumination dose does not lead to an enhancement of the film thickness. This may be explained by the fact that the cross-linking of the acrylate matrix is accomplished within 10 s UV irradiation dose of 1.0 J/cm^2. The cured and rigid resin prevents the further formation and the growth of gas bubbles. Consequently, the additional increase of the UV irradiation time does not significantly influence the film expansion. However, from the results it can be concluded that the photochemical foaming makes the formation of raised structures feasible by applying only one process step.

To enhance the spectral response of the photoacid generator, anthracene derivatives have been employed to extend the initiating window for the proton formation to the near visible spectrum [2]. **Figure 2b** illustrates the relationship between the concentration of 2-ethyl-9,10-dimethoxyanthracene used as photosensitizer and the relative thickness of the expanded ink layer. Due to the better exploitation of the light source an enhancement of proton generation is obtained resulting in a considerable increase of the film thickness.

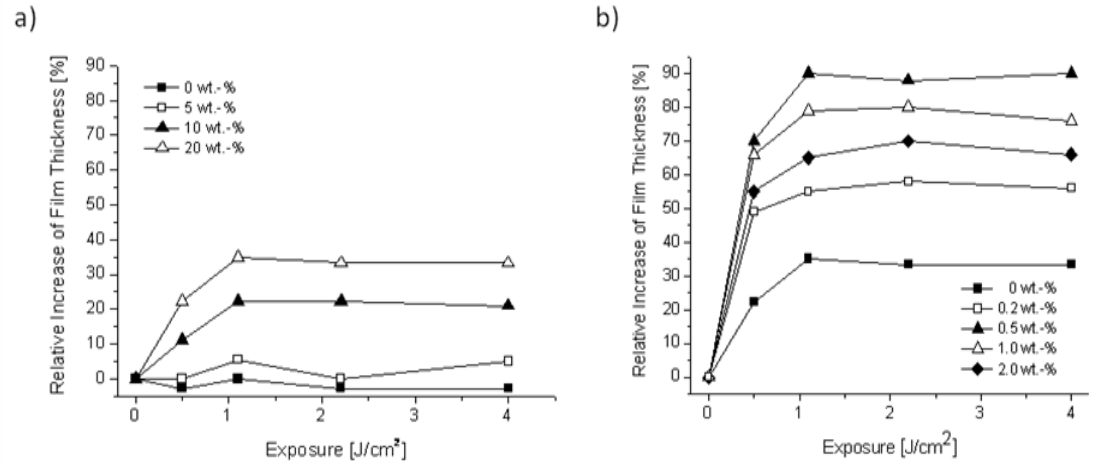

Figure 2. Relative film thickness versus irradiation dose of photochemically foamed ink formulations containing different levels of a) photoacid generator and b) photosensitizer concentration

In particular, the most intensive expansion of the film thickness is observed with 0.5 wt.-% photosensitizer, leading to an almost a doubling of the thickness of the ink layer. The corresponding cell morphology is shown in **Figure 3c** and reveals that dense cells are achieved with diameters ranging from 5 to 14 µm. With respect to foamed inks containing only the photoacid generator, lower cell densities and the cell diameters (1 - 7 µm) are observed (see **Figure 3b**). Both the results of the cell morphology and the film expansion give a good indication that a higher amount of blowing gas can be released compared to the foaming without any photosensitizer.

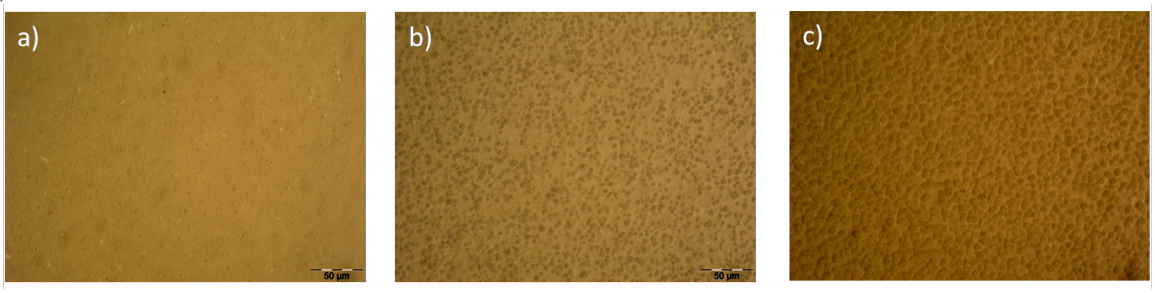

Figure 3. Optical micrographs of foamed ink layers a) prior to and b,c) after UV illumination

4. Conclusions

Due to the photochemical foaming employing a photoacid generator and calcium carbonate particles, 3D structures can be produced in offset printing techniques with one process step. The foaming proceeds at room temperature and can be accomplished within seconds. Additionally, it makes the formation of firm and raised structures feasible by applying only one ink layer.

Acknowledgements

This study was performed at the Polymer Competence Center Leoben GmbH (PCCL, Austria) within the framework of the COMET-program of the Federal Ministry for Transport, Innovation and Technology and the Federal Ministry for Economy, Family and Youth with contributions by the University of Leoben, Graz University of Technology and Joanneum Research Forschungsgesellschaft mbH.

References

[1] S. Schlögl, M. Reischl, V. Ribitsch, W. Kern, *Prog. Organ. Coat.* **2012**, 73, 54-61.
[2] Y. Yağci, I. Reetz, *Prog. Polym. Sci.* **1998**, 23, 1485-1538.

S7-L20
Organic-inorganic hybrid silver nanocomposites as antimicrobial corrosion protective coating materials

Deewan Akram (1,2)*, Eram Sharmina (1), Sharif Ahmada (1)
(1) Materials Research Lab., Dept. of Chemistry, Jamia Millia Islamia, New Delhi-110025, India
(2) Dept. of Chemistry, Faculty of Science, Jazan University, Jazan, P.O. Box 2097, Saudi Arabia
*deewanakram@gmail.com

Abstract
Organic-inorganic hybrid materials have been prepared with the goal of combining properties of inorganic and organic materials. These hybrid materials provide synergistic properties of organic matrix such as environment friendliness, lightweight, flexibility, good impact resistance and good process ability, and inorganic components which improve physical, good chemical resistance, mechanical, and thermal properties, as well as gas barrier and photonic properties.
In this work, attempt has been made for hydroxylation of linseed oil through non-isolable epoxide intermediate forming polyol [Lpol]. Lpol was treated with TEOS resulting in organic-inorganic hybrids (LPOSi), preparation of silver nano-particles in organic-inorganic hybrids (LPOSi) via reduction of silver salt ($AgNO_3$) by employing *N,N*-dimethylformamide (DMF) as reducing agent at room temperature to obtain organic-inorganic hybrid silver nanocomposites (Ag/LPOSi), the latter underwent polyaddition reaction with toluene-2, 4-diisocyanate [TDI] to form their polyurethane (Ag/LPOSiPU). UV–visible and TEM studies substantiate the formation of silver nanoribbons of average length < 500nm, width 10nm and thickness around 4nm, along with silica nanoparticles of diameter 50-80 nm. Thermogravimetric analysis showed improved thermal stability of Ag/LPOSiPU. The physicomechanical and corrosion resistance performances (in various corrosive media) tests of Ag/LPOSiPU coatings were also conducted to evaluate their coating properties. These studies revealed that the incorporation of silver nanoparticles has a significant influence on structural and physico-chemical aspects. The polymer nanocomposites exhibit enhanced antimicrobial efficacy against *S. aureus* and *E. coli*, respectively, and will pave way in plethora of biological and chemical applications as coating materials.

References
[1] D.Akram, S.Ahmad, E.Sharmin, S.Ahmad, Macromol.Chem.Phys. **2010**, 211, 412-419.
[2] A.Kumar, P.K.Vemula, P.M.Ajayan, G.John, Nature Materials, **2008**, 7, 236-241.

S7-L21
Water-developable Poly(2-oxazoline)-based photoresists

Martin Fimberger (1,2)*, Verena Schenk (1,2), Elisabeth Rossegger (1,2) and Frank Wiesbrock (1,2)
(1) Polymer Competence Center Leoben GmbH, Roseggerstrasse 12, 8700 Leoben, Austria.
(2) Graz University of Technology, Institute for Chemistry and Technology of Materials, Stremayrgasse 9, 8010 Graz, Austria.
*martin.fimberger@pccl.at

Summary. Two copolymers, namely **pEtOx$_{80}$Bu$^{=}$Ox$_{20}$** (composed of 2-ethyl- and butenyl-2-oxazoline) and **pPhOx$_{80}$Dc$^{=}$Ox$_{20}$** (composed of 2-phenyl- and 2-9'-decenyl-2-oxazoline), were synthesized in a microwave reactor in less than 100 minutes. Copoly(2-oxazoline)-based photoresist formulations containing the copolymer, a tetrathiol and a photoinitiator were prepared in 1-methoxy-2-propanol. Films of the copolymers were crosslinked via thiol-ene reactions upon irradiation, reproducing patterns preset by the masks. The photoresist **pEtOx$_{80}$Bu$^{=}$Ox$_{20}$** could be developed in water, revealing resolutions of 2 µm.

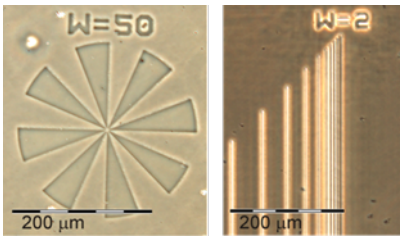

2-3'-

UV

1. Introduction
Photolitography resembles the state-of-the-art technology for manufacturing printed circuit boards and integrated circuits. Thin three-dimensional structures can be patterned to various surfaces [1] either as positive or negative reproduction, depending on the kind of photoresist used. The current work aimed at the preparation of a high-resolution negative photoresist with tailor-made adhesion. 2-Oxazolines comprise a vast number of easily obtainable differently substituted congeners which allows for the synthesis of (co-)polymers with various different characteristics [2-4]. The living cationic ring-opening polymerization of 2-oxazolines is usually supported by microwave radiation which grants narrow molecular weight distributions and reasonably short reaction times [5,6]. For the application of the poly(2-oxazolines) as negative photoresists, olefinic side-chains were chosen as reactive sites for the tetrathiol during crosslinking.

2. Experimental

With the exception of commercially available **EtOx**, all other monomers were synthesized according to literature procedures: **PhOx** was obtained by the procedure of Witte and Seeliger, and **Dc$^{=}$Ox** according to the method described in a Henkel Patent [2,3]. **Bu$^{=}$Ox** was prepared via a three-step synthesis [4]. The copolymerizations (**Scheme 1**) were conducted in a microwave reactor under autoclave conditions, which allowed for reaction times of 100 minutes or less and sufficiently low molecular weight distributions (PDI < 2) [7]. For the formulation of the photoresists, 25 wt.-% of the copolymer were dissolved in 1-methoxy-2-propanol. The amount of crosslinker **4SH** (**Scheme 1**) was calculated for quantitative conversion of the olefinic side-chains (ratio SH:ene = 1:1). As photoinitiator, **PI (Scheme 2)**, Lucirin TPO-L™ was added. The resists were cast onto the substrates and UV-illuminated through a quartz mask.

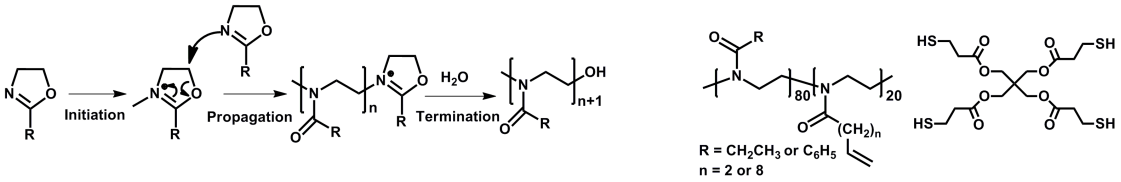

Scheme 1: Reaction scheme of the cationic ring-opening polymerization of 2-oxazolines (left) and structures of the copoly(2-oxazoline)s **pEtOx$_{80}$Bu$^{=}$Ox$_{20}$** and **pPhOx$_{80}$Dc$^{=}$Ox$_{20}$** as well as the thiol crosslinker **4SH** (right).

3. Results and discussion

Two different copoly(2-oxazoline)s, one hydrophilic and one hydrophobic representative, were evaluated. The copolymers contained 20 mol-% of the monomer bearing the olefinic motif (**Bu$^{=}$Ox**, **Dc$^{=}$Ox**) and 80 mol-% of the monomers with the non-functionalized side-chains (**EtOx**, **PhOx**), providing quantitative crosslinking upon UV irradiation (see below). Keeping future scale-up in mind, commercially or synthetically easily available monomers were used whenever possible: **Bu$^{=}$Ox** was chosen as hydrophilic monomer and **Dc$^{=}$Ox**, which can be easily prepared from 10'-undecenoic acid from renewable resources, as hydrophobic monomer. Copolymerizations were conducted in a microwave reactor under autoclave conditions. ^{1}H-NMR analyses confirmed polymerization degrees of 100 and monomer compositions of 80:20 as targeted. 25 wt.-% solutions of the polymers in halogen-free 1-methoxy-2-propanol were prepared, and the crosslinker **4SH** and photoinitiator **PI** were added. The formulations could be stored for three months at ambient temperature without the need of additional stabilizers.

The crosslinking photoreaction was initiated by illumination with UV-light, which homolytically cleaved the photoinitiator and yielded two radicals that started the thiol-ene reactions (**Scheme 2**). The illuminated resists could be developed either in 1-methoxy-2-propanol or, in the case of **pEtOx$_{80}$Bu$^{=}$Ox$_{20}$**, in water. In order to characterize the achievable resolution, **pEtOx$_{80}$Bu$^{=}$Ox$_{20}$** was spincoated onto CaF_2 substrates, illuminated through a mask aligner system and developed. The photoresist pattern was visualized by an optical microscope and exhibited resolutions of 2 µm. Storage of the photoresist formulations for several months had no adverse effect to the attainable resolution.

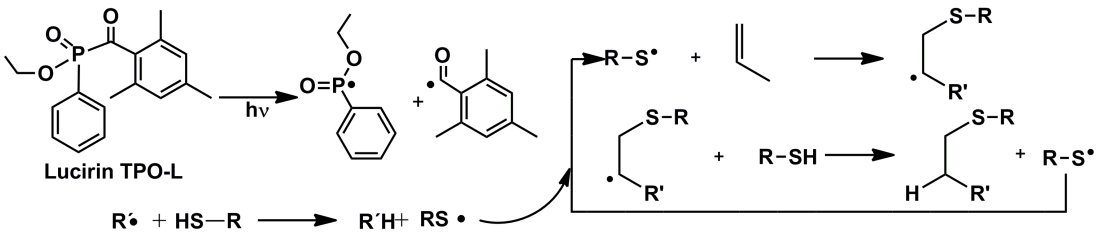

Scheme 2. Photoinitiator decomposition and initiation of the thiol-ene click reaction (left) and thiol-thiyl cycle during the thiol-ene reaction (right). The structure of the photoinitiator **PI** is shown in the left half of this scheme.

4. Conclusions

Copoly(2-oxazolines) with olefinic side-chains can be crosslinked in the film-state employing thiol-ene click reactions with a tetrathiol. Formulations of the copoly(2-oxazoline)s, a tetrathiol, and a photoinitiator revealed stability for several months. Photoresists that were cast onto substrates enabled 2.5-dimensional patterning after UV illumination and subsequent development: Geometric pattern preset by masks were reproduced with resolutions in the 2 mm range.

Acknowledgements

This study was performed at the Institute for Chemistry and Technology of Materials of the Graz University of Technology and the Polymer Competence Center Leoben GmbH (PCCL) within the framework of the Kplus-program of the Austrian Ministry of Traffic, Innovation and Technology. PCCL is funded by the Austrian Government and the State Governments of Styria and Upper Austria.

References
[1] E. Reichmanis, O. Nalamasu, F.M. Houlihan, *Acc. Chem. Res.* 1999, 32, 659-667.
[2] H. Witte, W. Seeliger, *Liebigs Ann. Chem.* 1974 ,996-1009.
[3] M. Beck, P. Birnbrich, U. Eicken, H. Fischer, W.E. Fristad, B. Hase, H.-J. Krause, *Angew. Makromol. Chem.* 1994, 223, 217-233.
[4] A. Gress, A. Völkel, H. Schlaad, *Macromolecules* 2007, 40, 7928-7933.
[5] F. Wiesbrock ,R. Hoogenboom, M.A.M. Leenen, S.F.G.M. van Nispen, M. van der Loop, C.H. Abeln, A.M. van den Berg, U.S. Schubert, *Macromolecules* 2005, 38, 7957-7966.
[6] R. Hoogenboom, F. Wiesbrock, H. Huang, M.A.M. Leenen, H.M.L. Thijs, S.F.G.M. van Nispen, M. van der Loop, C.-A. Fustin, A.M. Jonas, J.-F. Gohy, U.S. Schubert, *Macromolecules* 2006, 39, 4719-4725.
[7] V. Schenk, L. Ellmaier, E. Rossegger, M. Edler, T. Griesser, G. Weidinger, F. Wiesbrock, *Macromol. Rapid Commun.* 2012, 33, 396-400.

S7-L22
Monitoring the copolymerization of vinyl acetate and ethylene in emulsion using a high pressure RC1 reactor: a case study

Ida Poljanšek (1), Klemen Burja (1)*, Ema Fabjan (1), Dolores Kukanja (1,2)
(1) Centre of Excellence PoliMaT, Tehnološki park 24, 1000 Ljubljana, Slovenia
(2) Mitol, Partizanska cesta 78, 6210 Sežana, Slovenia
*klemen.burja@polimat.si

1. Introduction
The free radical polymerization of vinyl acetate in emulsion is commercially conducted either in batch or continuous reactor at atmosphere pressure. In order to improve the properties of poly(vinyl acetate) (PVA) a co-monomer can be added and copolymerized with the vinyl acetate [1].
In this work we present the high pressure synthesis of vinyl acetate and ethylene (VAE) copolymers in emulsion with different contents of ethylene monomer [2]. The polymerization of vinyl acetate (VAc) and ethylene (E) was carried out in a Mettler Toledo RC1 high pressure batch reactor enabling an accurate control of reaction parameters as well as *in-situ* monitoring of the copolymerization reaction and the consumption of monomers.

2. Experimental
The emulsion synthesis of VAE copolymers with different contents of ethylene was carried out in RC1^e – reaction calorimeter equipment (Mettler Toledo) in a 1.8 L HP60 high pressure stainless steel semi-batch reaction vessel, a stainless steel-anchor stirrer, a digital thermometer, a calorimeter probe and FTIR K6 conduit 16 mm Dicomp probe. Ethylene consumption during the polymerization process was measured by gas uptake unit while pressure in the vessel was controlled by external automatic gas valve. HP60 Prominent Micro delta Optodrive pump was used for dosing of vinyl acetate. The temperature, dosing and pressure during the polymerization were accurately controlled by Mettler Toledo iControle software.
Vinyl acetate was introduced into a water solution of the polymer surfactant poly(vinyl alcohol) (mixture of two polyols with different molecular weight in concentration 3.5 wt.%, Mw=160.000, and 7 wt.%, Mw=31.000), 0.1 wt.% ammonium persulfate as initiator and ethylene in a controlled manner (dosing time from 180 to 240 min). The applied pressure of ethylene during the polymerization at 75 °C was controlled by automatic pressure valve either at 20 bar or 30 bar.
The reaction was monitored by *in-situ* Attenuated Total Reflectance Fourier Transform Infrared spectroscopy (ATR-FTIR). Particle size growth and particle size distribution was determined by *in-situ* Focused Beam Reflectance Measurement (FBRM) while the ethylene consumption was measured by a pressure drop in a gas tank. During the VAc dosing process at 75 °C polymerization heat release was measured to monitor the course of the reaction and ethylene incorporation in the VAE dispersions.
The resulting copolymer composition and thermal properties were determined by ^{1}H NMR spectroscopy and Differential Scanning Calorimetry (DSC).

3. Results and discussion
The course of copolymerization between vinyl acetate and ethylene at 75 °C was studied *in-situ* by ATR-FTIR transmission probe immersed directly into the pressure reactor. The concentration profiles for VAc, E and VAE copolymer at 75 °C are presented in Figure 1. The relative ratios of the monomeric units in the copolymer were determined by comparing the intensities (areas) of the characteristic bands of VAc (C-O and C=O stretching at 1138 cm^{-1} and 1738 cm^{-1}, respectively) and ethylene (C-H stretching at 2864 cm^{-1}). After the total addition of VAc its amount in the reaction mixture decreases rapidly during the copolymerization. Moreover, the slower dosage of VAc into the reaction mixture leads to an increase in ethylene units in the copolymer as determined by NMR and gas consumption analysis. Weight percent of incorporated ethylene was calculated using Flory-Fox theory by Tg determination of VAE with DSC method.
Particle size growth was monitored by *in-situ* FBRM method. Since the method does not differ among different particle forms, particle counts represent a sum of emulsified vinyl acetate monomer droplets and emerging dispersed copolymer particles. Particle

size distribution curves for particles under 50 µm showed similar trends as indicated by ATR-FTIR curves for formation of VAE dispersion. After copolymer dispersion was formed (when approx. one third VAc was added), median of measured particle size remained constant with about 3.8 µm and matched the average particle size of 3.4 µm for end VAE dispersion as measured by dynamic light scattering.
Ethylene pressure in the reaction vessel was kept constant during the whole polymerization process by automatic gas valve. Ethylene consumption was measured and calculated by pressure drop in gas dosing tank. The ethylene monomer unit content in VAE copolymer was determined by ^{1}H NMR and calculated from Tg obtained from DSC analysis. The obtained results matched the measured ethylene molar consumption.

Figure 2 shows total heat of polymerization at 75°C, 30 bar of ethylene and 240 min of VAc dosing. During polymerization 324.7 kJ of heat was released and represents sum of released polymerisation heat for 2.9 mol VAc (258.8 kJ) and 65.9 kJ of released heat for ethylene, which is 0.7 mol of ethylene (polymerisation heat for VAc is 89.12 kJ/mol [3] and ethylene 94.5 kJ/mol [4]). The same quantity of moles (0.69 mol) of ethylene was measured with gas consumption method.

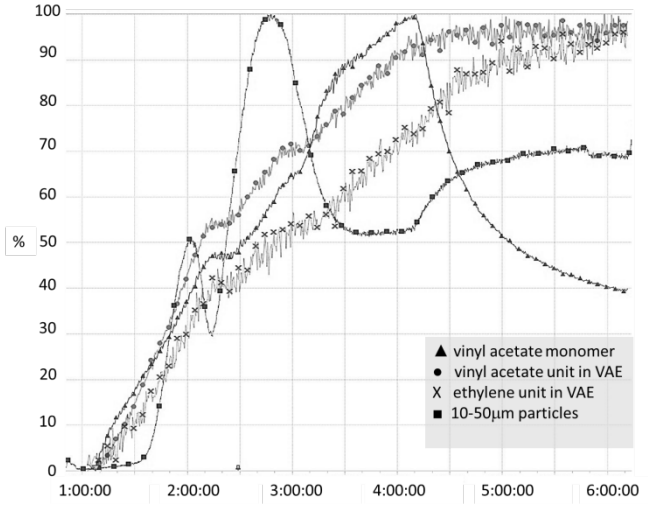

Figure 1. The concentration profiles in weight % for vinyl acetate, ethylene, and reaction product VAE during the copolymer synthesis at 75°C based on *in situ* ATR-FTIR measurements

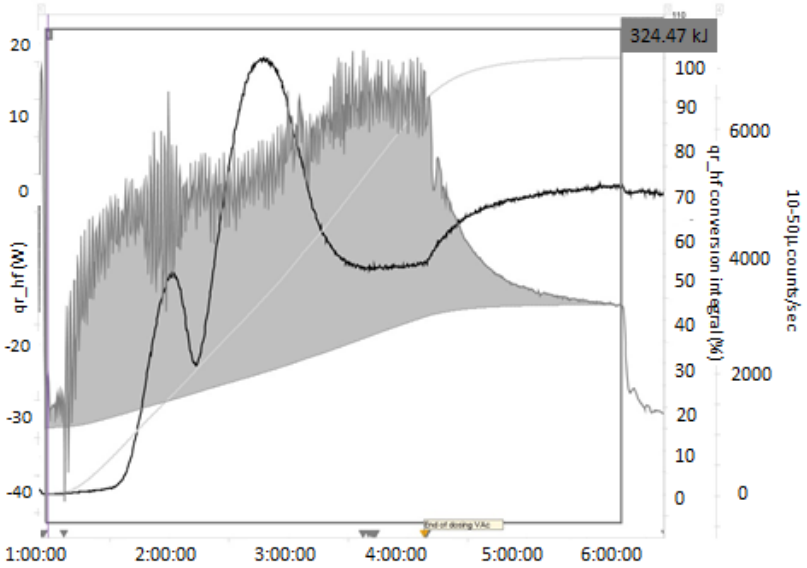

Figure 2. The heat release during the polymerization performed at 75 °C (gray area). The corresponding conversion and particles count curves are marked in gray and black, respectively.

3. Conclusions

RC1 reactor calorimeter was used for the preparation of VAE copolymers as it enables the accurate setting and control of the reaction conditions (temperature, pressure and monomer dosing). *In situ* ATR-FTIR spectroscopy, FBRM, gas consumption and calorimetric measurements were used for monitoring the course of reaction, while DSC evaluation and ^{1}H NMR spectroscopy of the resulting copolymer were applied for the determination of the ethylene monomer unit contents.

Acknowledgements

The authors wish to gratefully acknowledge Mitol, Sežana for providing all chemicals used in this study and for permission to publish this paper. This work was supported by the Ministry of Education, Science, Culture and Sport of the Republic of Slovenia Grant number 3211-10-000057 (Centre of Excellence for Polymer Materials and Technologies).

References

[1] K. Geddes, Handbook of Adhesive Technology, Marcel Dekker, New York, 1994, Chapter 35.
[2] I. Poljanšek, E. Fabjan, K. Burja, D. Kukanja, accepted for publication in *Progress in Organic Coatings*
[3] www.vinylacetate.org/properties.pdf
[4] http://www.journaloftheoretics.com/Articles/2-1/ZP-fp.htm

Session 8: Theory, Modeling and Simulations

S8-L23
Dendritic vs linear polymer brushes in planar and spherical geometries

Tatiana M. Birshtein (1)*, Alexey A. Polotsky (1), Oleg V. Borisov (1,2), Oleg V. Rud (1)
(1) Institute of Macromolecular Compounds, Russian Academy of Sciences, 31 Bolshoy pr., 199004 St.-Petersburg, Russia
(2) Institut Pluridisciplinaire de Recherche sur l'Environnement et les Materiaux, UMR 5254 CNRS/UPPA, Pau, France
*birshtein@imc.macro.ru

1. Introduction

The polymer brush is among the best studied systems in polymer science. Brushes, formed by long polymer chains densely grafted to a solid-liquid or to a liquid-liquid interfaces, received ample attention from both theoretical and experimental perspectives. In the meantime, advanced synthetic approaches now allow the making of macromolecules with a virtually arbitrary complex and well-controlled branched architecture (stars, combs, dendrons). Moreover, the technology to attach these to surfaces becomes available. It is believed that brushes from branched architectures may introduce novel desired features, such as enhanced stimuli responsiveness, outstanding nanomechanical properties, and tuned biointeractivity. From a physical point of view, brushes of branched macromolecules are challenging because the distribution of the elastic tension and the fluctuations of the individual molecules is far from trivial as these properties will differ from the behavior of the same molecules in solution.
In the present work, equilibrium structural properties of planar and spherical polymer brushes formed by dendritic polymer chains (dendrons) are studied by means of Scheutjens-Fleer self-consistent field (SF-SCF) modeling and scaling analysis.

2. Model

We consider a spherical polymer brush formed by dendrons grafted by the terminal (root) segment onto the surface of a spherical core particle of radius R_0 at the density σ (number of dendrons per unit area) and immersed in a good (athermal) solvent. A dendron is characterized by the number of generations g, and a functionality q of each branching point. The functionality is defined as the ratio between the number of spacers in generation g+1 and that in generation g. The number of monomer units per spacer, n, is fixed throughout the dendron. We assume that the spacers in the dendrons are intrinsically flexible.

3. Results and discussion

We demonstrate, that the effect of the branched topology of individual macromolecules forming the brush on the integral structural properties of the brush can be accounted for by using the universal scaling parameter $N/M > 1$, where N is the total number of monomer units in a dendron and M is the number of monomer units in the longest elastic path. In the limit $M = N = 1$ the properties of the brushes formed by end-grafted linear polymers are recovered.
As follows from the results of SF-SCF modeling, in both linear and dendritic spherical brushes a variation of the ratio of the surface curvature radius R_0 to the characteristic brush thickness H affects not only the shape of the monomer density profile, but also the character of fluctuations in extension of individual macromolecules forming the brush: In linear brush the density decreases as a power-law function of a distance from the center and chain ends distribution is peaked near the edge of the brush at small R_0 , whereas at large $R_0$the density decay is weaker and the chain ends are distributed throughout the brush. In contrast, in dendritic brush the density distribution is fairly uniform irrespectively of the ratio R_0/H. This uniform density distributions are assured by fairly uniform distribution of the end segments throughout the brush at $R_0/H << 1$ or by multi-modal distribution of the overall extension of dendrons at $R_0/H >> 1$. The latter means that an increase in the curvature radius of the surface is accompanied by

emerging segregation into two (or more, for larger number of generations) populations of dendrons: the less extended and the more extended ones. The former ones fill the space in the central region of the brush, the latter brings the majority of the monomer units closer to its periphery.

Acknowledgements
This work has been partially supported within Scientific and Technological Cooperation Program Switzerland-Russia, project " Experimental studies and theoretical modelling of amphiphilic di-/triblock and dendritic functional polymers at surfaces: influence of interfacial architecture on biological response", Grant Agreements No. 128308, by the Russian Foundation for Basic Research (grants No. 11-03-00969a and No. 12-03-31243) and by Department of Chemistry and Material Science of the Russian Academy of Sciences.

References
[1] A.A. Polotsky, T. Gillich, O.V. Borisov, F.A.M. Leermakers, M. Textor, T.M. Birshtein, *Macromolecules* 2010, 43, 9555-9566.
[2] A.A. Polotsky, F.A.M. Leermakers, E.B. Zhulina, T.M. Birshtein, *Macromolecules* 2012, 45, 7260-7273.
[3] O.V. Rud, A.A. Polotsky, T. Gillich, O.V. Borisov, F.A.M. Leermakers, M. Textor, T.M. Birshtein, submitted to *Macromolecules* 2012.

S8-L24
Collective ordering of colloids in grafted polymer layers

Tine Curk (1), Francisco J. Martinez-Veracoechea (1), Daan Frenkel (1), and Jure Dobnikar (1, 2)*
(1) Department of Chemistry, University of Cambridge, Lensfield Road, CB2 1EW, Cambridge, UK
(2) Department for theoretical physics, Jožef Stefan Institute, Jamova 39, 1000 Ljubljana, Slovenia
*jd489@cam.ac.uk

A grafted polymer layer can be used to prevent large colloidal particles from reaching a solid surface. However, under the influence of a sufficiently strong external field, the colloids will penetrate and form solid-like structures within the polymer layer. The polymer-mediated colloidal interactions are typically of the order of k_BT (i.e., comparable to the entropic terms). The colloid-polymer mixtures are thus inherently less ordered than molecular systems. Sufficiently strong external forces constrain the translational degrees of freedom of the colloids, and enable the weak polymer-induced interactions to steer the assembly into ordered patterns.
We present Monte Carlo simulations of colloidal particles pulled into grafted polymer layers by constant external force. The insertion free energy of a single colloid into the polymer layer is qualitatively different for surfaces with an ordered and a disordered distribution of grafting points. Moreover, the tendency of colloidal particles to traverse the grafting layer is strongly size dependent.
In dense colloidal suspensions, under the influence of sufficiently strong external force, a collective instability allows the colloids to penetrate and form internally ordered, columnar structures spanning the polymer layer. Depending on the conditions, these colloidal clusters may be isolated or laterally percolating. The morphology of the observed patterns can be controlled by the external fields, which opens up new routes for the design of thin structured films.

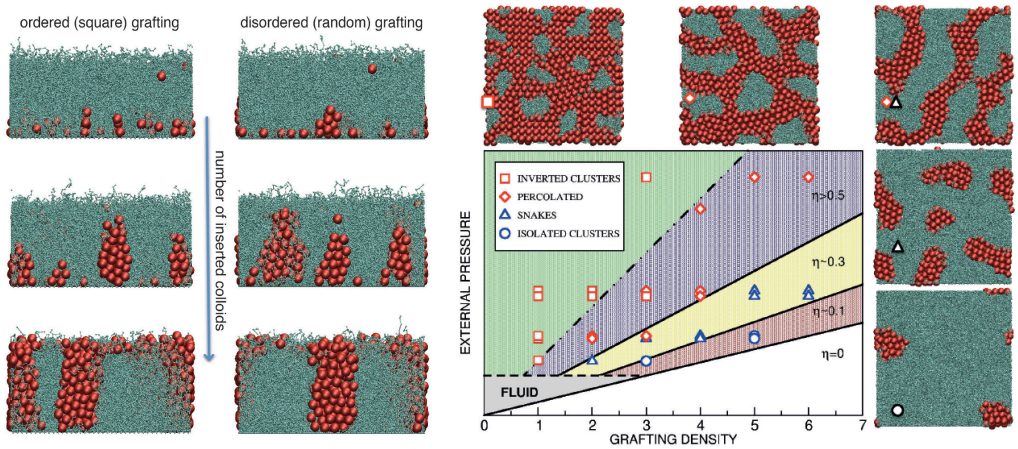

Figure 1. Cluster growth sequence and phase diagram of lateral colloidal structures in grafted polymer layers..

References
[1] T. Curk, F.J. Martinez-Veracoechea, D. Frenkel, and J. Dobnikar, submited (2012)

S8-L25

Effect of polymer-colloid interactions on polymer-mediated forces and selected static and dynamic properties of polymer-nanocolloid sytems

Alexander I. Chervanyov*, Gert Heinrich
Leibniz Institute of Polymer Research Dresden, Hohe 6, 01069, Dresden, Germany
*chervanyov@ipfdd.de

1. Effective interaction between colloids mediated by non-adsorbing and reversibly adsorbing polymers

In order to study the effect of the polymer adsorption on the polymer-mediated (PM) interactions between nano-colloids, we have performed a comparative analysis of these interactions mediated by non-adsorbing and reversibly adsorbing excluded volume polymers by developing and making use of an analytic theory [1,2]. As a first application of this theory, we have calculated the potential of the depletion interactions acting between nano-colloids immersed in the bath of non-adsorbing polymers as a function of the separation H between colloids. Figure 1 shows the comparison of our theoretical findings with the results of Monte Carlo simulations of the depletion potential U in the protein limit where the colloid radius R is much smaller than the polymer gyration radius R_G. As is clearly seen from this Figure, the developed theory adequately describes the Monte Carlo simulation results [3] in the domain of polymer concentrations spanning across the dilute to dense regimes.

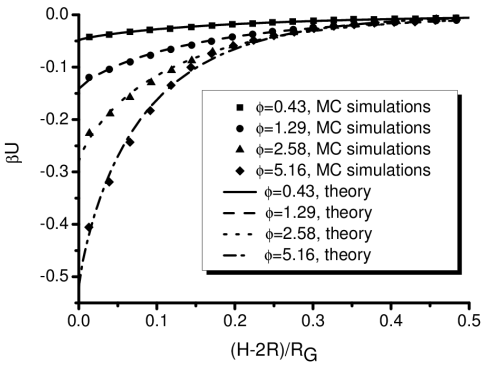

Figure 1. Comparison between theoretical results and Monte Carlo simulations [3] of the PM potential for several values of the polymer volume fraction φ and the colloid radius $R=0.1R_G$.

As a next step, we have calculated the potential of the polymer mediated interactions for the case of reversibly adsorbing polymers as a function of colloid radius R, separation H, polymer correlation length ξ, polymer volume fraction φ and the introduced absorbance α that quantifies the affinity of the colloid surface for polymers. The developed theory describes the limit of the weak adsorption where the correlation length ξ of the excluded volume polymer system is much smaller than the characteristic adsorption length (colloid absorbance) α. Similarly to the case of non-adsorbing polymers, the resulting expression for the PM potential U mediated by adsorbing polymers is shown to factorize into the product of the immersion free energies of the colloids and the correlation function of the uniform polymer system. A typical example of the calculation of U for several values of the reduced colloid radius R/ξ and ξ/α=0.1 is shown in Figure 2.

Note that according to Figure 2, the dependence of the magnitude of the PM potential U on the colloid radius R for the case of adsorbing polymers shows just the opposite trend in comparison with the purely entropic depletion potential that increases with R. This difference stems from different dependencies of the colloids immersion energy W on its radius R for the above cases of non-adsorbing and adsorbing polymers. Specifically, in the case of non-adsorbing polymers W occurs to be proportional to the colloid surface ~R2. The dependence W(R) for the case of adsorbing polymers is much less pronounced, for that the main factor affecting the immersion energy in this case is the strength of the adsorption interactions. The above explained qualitative difference between the dependencies W(R) for adsorbing and non-adsorbing polymers results in the above mentioned quantitative difference in the dependencies U(R) for the above two cases that can be elucidated from Figures 1 and 2.

2. Equation of state of the colloid-polymer-solvent system in the presence of adsorption interactions between polymers and colloids

By making use of the obtained results for the potential of PM interactions mediated by adsorbing and non-adsorbing polymers, we have calculated the equation of state (EOS) of the nanocolloid-polymer-solvent system for the respective cases of polymer adsorption. For the case of non-adsorbing polymers, the equations of state shows non-trivial dependence on the polymer volume fraction that is overlooked by the previous theories. For the case of reversibly adsorbed polymers, the obtained EOS exhibits a complicated interplay between the purely entropic forces and the adsorption interactions that leads to different phase behavior of the colloid-polymer system in dependence on the colloid radius, affinity of the colloid surfaces for polymers, and the volume fractions of colloids and polymers in solution. As a main result of the described studies, we have identified the relative significance

of the entropic interactions, physical adsorption and bridging of colloids by polymers for different domains of the above listed parameters.

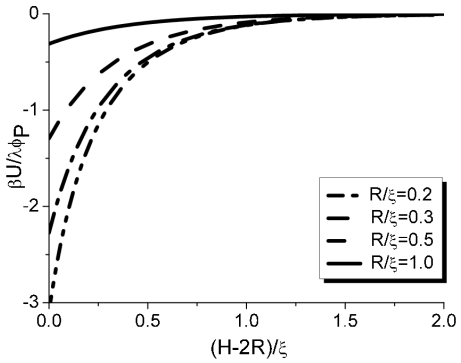

Figure 1. Reduced PM potential for several values of the reduced colloid radius R/ξ and the selected value of the reciprocal adsorption length ξ/α=0.1; λ=ξ/RG.

3. Relaxation times of the colloid aggregation assisted by adsorbing and non-adsorbing polymers.

As a final stage of the reported work, we have calculated the relaxation time τ of the colloid aggregation for the case of dilute solution of colloids in polymer-solvent system. In line with the previous two stages, we have distinguished the cases of non-adsorbing and weakly adsorbing polymers. We have found that τ decreases with increasing the volume fraction of adsorbing polymers and increases with increasing the volume fraction of non-adsorbing polymers at fixed colloid radius R. The above difference in the behavior of τ as a function of the polymer volume fraction is attributed to different dependencies of the PM potential on the colloid radius and polymer volume fraction for the cases of adsorbing and non-adsorbing polymers.

4. Conclusions

In summary, we have comparatively investigated the effect of purely entropic and adsorption interactions between polymers and nano-colloids on the polymer mediated interaction among these colloids. We have used the obtained results in order to derive the equation of state of the colloid-polymer-solvent system for the respective cases of polymer adsorption. In addition, we have derived the characteristic times of the colloid aggregation in dependence of the strength of the polymer adsorption onto the nano-colloids. The obtained results are compared with the available Monte Carlo simulations.

Acknowledgements

This research was supported in part by priority program SPP 1369 of the DFG.

References

[1] A. I. Chervanyov, *Phys. Rev. E* 2011, 83, 061801.
[2] A. I. Chervanyov, G. Heinrich, *J. Chem. Phys.* 2011, 131, 4907.
[3] P. G. Bolhuis, E. J. Meijer, A.A Louis., *Phys. Rev. Lett.* 2003**,** 90, 068304.

S8-L26
Secondary motions in channel flows of glass-fiber-filled polypropylene melts

Thomas Köpplmayr (1)*, Rudolf Haßlacher (2), Bernhard Plank (3), Dietmar Salaberger (3), Jürgen Miethlinger (1)

(1) Institute of Polymer Extrusion and Building Physics, Johannes Kepler University Linz, Altenberger Str. 69, 4040 Linz, Austria
(2) Institute of Polymer Science, Johannes Kepler University Linz, Altenberger Str. 69, 4040 Linz, Austria
(3) University of Applied Sciences Upper Austria – Wels Campus, Stelzhamerstr. 23, 4600 Wels, Austria
*thomas.koepplmayr@jku.at

1. Introduction

In addition to their shear-thinning behavior, polymer melts are characterized by first and second normal stress differences, which are responsible for the occurrence of secondary motions. Viscoelastic flows through straight ducts exhibit secondary motions which cannot be explained solely by the first normal stress difference. Debbaut et al. [1] showed that these secondary motions originate from the combination of second normal stress difference and non-circular geometry.

Thermoplastic materials such as polypropylene random copolymers are often filled with glass fibers to improve properties such as

stiffness, strength, and heat distortion temperature compared to their unfilled counterparts. However, because large aspect ratio fibers are dispersed in a polymer matrix, the rheological properties are complex. It is well known that a thermoplastic polymer filled with glass fibers with initially isotropic orientation exhibits, in the molten state, a viscosity overshoot when sheared in the parallel plate geometry of a rheometer.
In this study, we varied the duration of different levels of pre-shearing in order to achieve an optimal orientation of the fibers parallel to the plates. Storage and loss moduli were measured accordingly. Numerical simulations were performed on the basis of a five-mode Giesekus model and were in good agreement with experimental observations.

2. Theory

Let $\underline{\underline{T}}$ denote the viscoelastic extra-stress tensor. If a discrete spectrum of N relaxation times is considered, $\underline{\underline{T}}$ can be decomposed as follows:

$$\underline{\underline{T}} = \sum_{i=1}^{N} \underline{\underline{T}}_i , \tag{1}$$

where $\underline{\underline{T}}_i$ is the contribution of the i-th relaxation time to the viscoelastic stress tensor. For all individual extra-stress contributions $\underline{\underline{T}}_i$, we select the Giesekus constitutive equation [2] given by

$$\underline{\underline{T}}_i \left[\underline{\underline{I}} + \frac{\alpha_i \lambda_i}{\eta_i} \underline{\underline{T}}_i \right] + \lambda_i \overset{\nabla}{\underline{\underline{T}}}_i = 2\eta_i \underline{\underline{D}} , \tag{2}$$

where l_i and h_i are the relaxation time and the partial viscosity factor, respectively, and the symbol ∇ denotes the upper-convected time derivative operator and represents rates of change with respect to a convected coordinate system that moves and deforms with the fluid. In Eq. (2), a_i are additional material parameters of the model which control the ratio of the second to the first normal stress difference. In particular, for low shear rates, we have $a_1 = -2N_2/N_1$, where a_1 is associated with the highest relaxation time l_1.

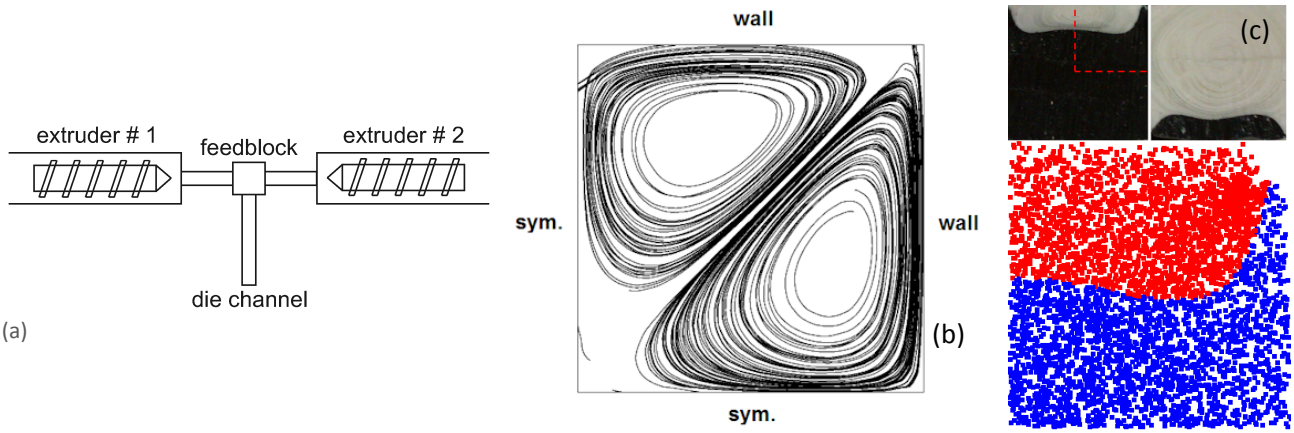

Figure 1. (a) Experimental setup, (b) streamlines of secondary motions obtained by numerical simulation, and (c) comparison of experimental observations (top) with numerical surface tracking (bottom).

3. Experimental

A Borealis RA130E polypropylene random copolymer intended for plumbing and heating applications was used as a base polymer. Three types of compounds were prepared and investigated in this study: compounds with (i) 100% short fibers (max. length 1.5 mm), (ii) 20% long (max. length 4.5 mm) and 80% short fibers, and (iii) 70% long and 30% short fibers.
The rheological properties were measured using a stress- and strain-controlled rheometer equipped with an electrically heated thermostating unit. In order to investigate initial wall effects, we varied the duration of different levels of pre-shearing used to achieve an optimal orientation of the fibers parallel to the plates. The orientation of glass fibers was monitored using x-ray computed tomography (X-CT), and the measured viscosity was compared to results obtained from capillary slit rheometry.
The effect of second normal stress difference was analyzed by observing the coextrusion of two batches of the same viscoelastic fluid, each with a different pigmentation, in a square duct. The development of secondary motions was observed by tracking the motion of the interface between both fluids. It has previously been found that the pigmentation does not affect fluid properties.
The materials were extruded separately but at the same temperature (220°C). After the screws, they were merged in a feedblock at a well-controlled ratio, as shown in Figure 1. The black/white interface is almost horizontal when the material enters the channel and is deformed due to the occurrence of secondary motions towards the channel exit.

4. Results and discussion

As shown in Figure 2, shear viscosity decreases with increasing levels of pre-shearing. In addition to the shear rate, the duration of pre-shearing also plays an important role, although its effect is less pronounced. An initial loading of 0.1 s^{-1} for 60 min turned out to be sufficient to reduce orientation effects to a level at which they can be ignored. Further pre-shearing damages samples, as indicated by a strong decrease in viscosity and results which cannot be reproduced.

We selected a discrete spectrum of five relaxation times l_i ranging from 10^{-3} to 10 s. The corresponding partial viscosities h_i were fitted on the basis of the dynamic properties G' and G'', while the parameters a_i were selected on the basis of the shear viscosity. Using a single polymer melt with different pigmentation made observing the development of secondary motions in square die channels possible. In particular, the ways in which the black and white melt layers deformed under the action of second normal stress differences became visible. The experimental observations and their numerical counterparts were found to be in good accordance.

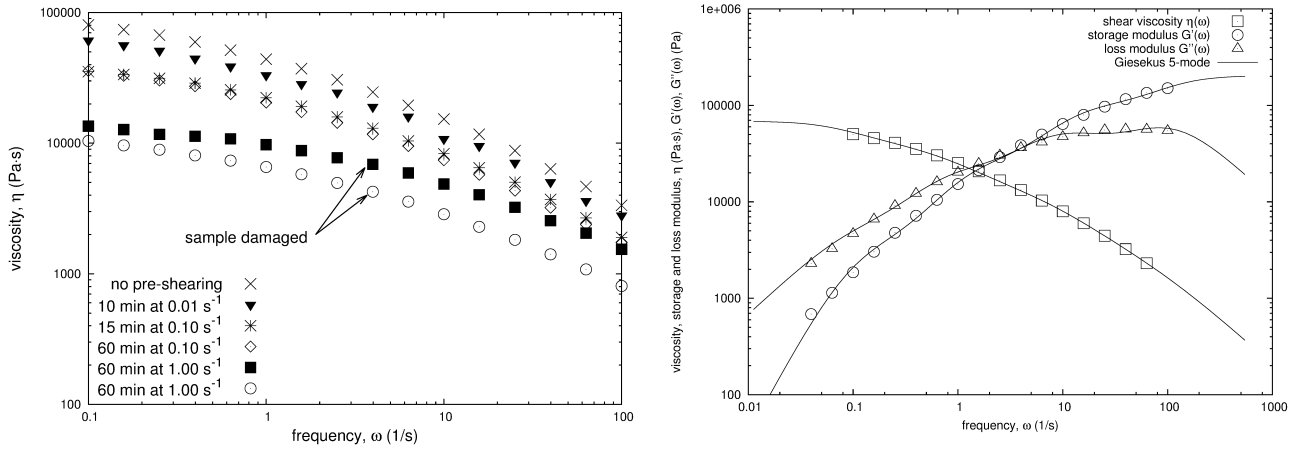

Figure 2. (a) Variation of the degree of pre-shearing and (b) fitting rheological data with a five-mode Giesekus model.

Acknowledgements
Financial support by the Austrian Center of Competence in Mechatronics GmbH (ACCM) is gratefully acknowledged. ACCM is funded by the Austrian Government and the Provincial Government of Upper Austria as part of the COMET program.

References

[1] B. Debbaut, T. Avalosse, J. Dooley, K. Hughes, On the development of secondary motions in straight channels induced by the second normal stress difference: experiments and simulations, *J. Non-Newtonian Fluid Mech.* **1997**, 69, 255 271.
[2] H. Giesekus, A simple constitutive equation for polymer fluids based on the concept of deformation dependent tensorial mobility, *J. Non-Newtonian Fluid Mech.* **1982**, 11, 69-109.

Session 11: Advances in Polymer Analysis, Characterisation and Testing

S11-L27
The impact of time, temperature and media on polymer selection for high demand applications

Peter Guttmann*, Florian Röper, Gerald Pilz
Montanuniversitaet Leoben, Chair of Materials Science and testing of Polymers
*peter.guttmann@unileoben.ac.at

1. Introduction
During the last decades polymeric materials, especially fiber-reinforced types, have been increasingly replacing metallic materials for designing structural components in high demand applications [1]. A number of polymer specific databases and tools (e.g. Cambridge Engineering Selector (CES [2]), UL-IDES [3], CAMPUS [4]…) are available to support engineers in proper materials selection. Because these tools mainly contain data for short term and standard conditions they are merely limited to a preselection of potentially suitable materials. To take account of application relevant conditions such as elevated temperatures and/or media influence appropriate materials testing methods have to be part of the materials selection process. This study focuses on the time and temperature dependent behaviour of technical high performance polymers, using an efficient approach for creep investigations in combination with dynamic mechanical analysis under the influence of ambient media.

2. Methodology and experimental
As an initial step of materials selection for a specific application with high thermo-mechanical requirements combined with media influence, Cambridge Engineering Selector software tool [2] was used for materials preselection. The following selection criteria were exemplarily used (limits in brackets): high level of Young's Modulus (> 12 GPa), tensile strength (> 80 MPa) and fracture

toughness (> 5 MPa*$m^{0,5}$). Additionally a service temperature of 60 °C and general water durability (no degradation in materials performance expected after long term exposure [5]) as well as processability and materials price were considered.
In order to get application relevant material information efficiently, a proper thermo-mechanical testing route was defined, containing water immersion of the test specimens at 60 °C until saturation (wet material state), dynamic mechanical characterization (DMA) and creep tests at elevated temperatures. The DMA experiments were performed in 3-point bending mode at various frequencies from 0.01 up to 100 Hz within a temperature range from -60 to 180 °C.
For the creep investigations a special media cell was developed which allows the performance of creep test in water immersion. The stress level applied was 20 MPa at various temperature levels (T_1=60 °C, T_2=70 °C, T_3=80 °C) using the stepped isothermal method (SIM) [6].

3. Results and discussion

The initial materials preselection process based on the Cambridge Engineering Selector software tool leads to Polyphthalamide with glass fibre reinforcement of 35 % (PPA-GF35), among other fibre-reinforced high performance polymers. In order to get application relevant information about temperature dependent materials performance, dynamic mechanical tests (DMA) were performed, both for dry and wet materials state. The dependency of the dynamic modulus E'(T, f) on temperature for various testing frequencies in the range from 0.1 to 100 Hz is shown in Figure 1, indicating a distinctive shift of the glass-transition temperature from 132 in dry to 57 °C in wet condition. Using the time/temperature superposition principle (TTS), which is based on the reduction of relaxation times at higher temperatures, the frequency dependent modulus data were plotted for various temperatures (measuring range) and shifted along the frequency axis to extend the resulting frequency range (extrapolation range). For this procedure also experimental temperature influences such as hysteretic and heating effects were regarded. The resulting modulus mastercurves for an application relevant temperature of 60 °C and the dry and wet materials state are shown in Figure 1.
The frequency dependency of the dynamic storage modulus leads to a slight and almost linear decrease of the mastercurve for the dry materials state at the low frequency range. Modulus values of around 11 GPa were found for extrapolated test frequencies of 10^{-6} Hz. For the wet materials state the frequency dependency of the modulus mastercurve is distinctly stronger. Starting at modulus values of about 10 GPa the modulus decreases significantly to about 7 GPa for the low frequency range, mainly due to the low glass transition temperature of the wet materials state.
In order to analyse the time dependent material performance for the wet state at a service temperature of 60 °C, creep tests were performed at elevated temperatures in water immersion. For test temperatures of 60, 70 and 80 °C and static tensile loading of 20 MPa the resulting creep curve is shown in Figure 2. After a subsequent calculation of the corresponding creep modulus curves, the curve segments for the higher test temperatures were shifted towards the long term range according to the time/temperature superposition principle. Also in this case the resulting mastercurve (s. Figure 2) shows a significant time dependent modulus decrease for the wet materials state corresponding to the glass-transition lowered to temperatures beneath 60 °C.

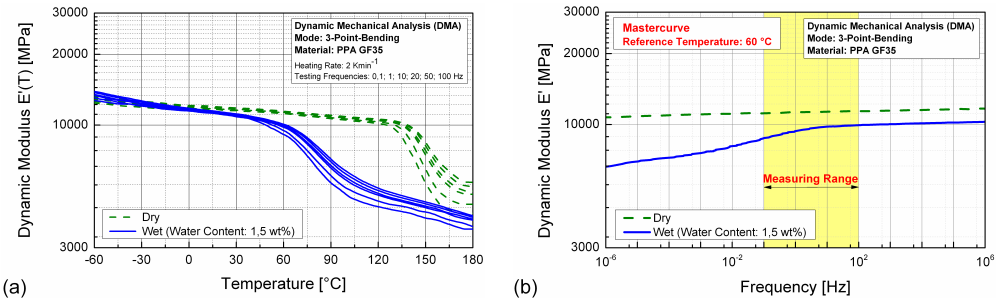

Figure 1. Dynamic Mechanical Analysis (DMA) for PPA-GF35: (a) Temperature dependency of dynamic modulus for various frequencies; (b) Modulus mastercurves for a reference temperature of 60 °C, determined by TTS principle out of (a)

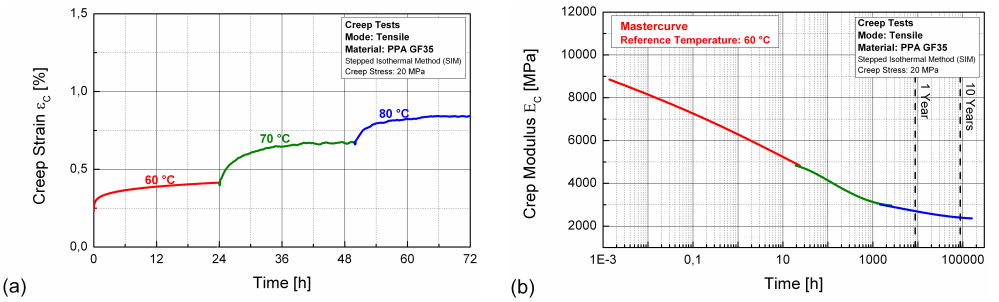

Figure 2. Creep behavior for PPA-GF35 at 20 MPa: (a) creep strain e_C vs. time t for test temperatures of 60, 70 and 80 °C; (b) creep modulus mastercurve for a reference temperature of 60 °C, determined by TTS principle out of (a).

4. Conclusions

For materials selection especially for high demand applications and media influence polymer specific properties such as time and temperature dependency of the elastic modulus have to be considered. Dynamic mechanical analysis represents an efficient method for the characterization of the thermo-mechanical behaviour of polymers at application relevant conditions. By DMA-tests at various frequencies and an extended temperature range, frequency and temperature dependent modulus data can be provided efficiently at suitable time ranges, even for preconditioned materials. Proper evaluation methods based on the time/temperature superposition principle can be used for the further evaluation of frequency-dependent behaviour. Furthermore the presented exemplary material characterization of PPA-GF35 shows significant creep behaviour at 60 °C and wet material state. Hence, DMA and Creep tests are efficient methods for the determination of application relevant material properties which are not available in ordinary data sources but which are decisive for material selection.

Acknowledgements

The research work was performed at the Chair of Materials Science and Testing of Polymers in cooperation with the Materials Center Leoben Forschung GmbH and the ANDRITZ AG. Financial support by the Austrian Federal Government (in particular from the Bundesministerium für Verkehr, Innovation und Technologie and the Bundesministerium für Wirtschaft, Familie und Jugend) and the Styrian Provincial Government, represented by Österreichische Forschungsförderungsgesellschaft mbH and by Steirische Wirtschaftsförderungsgesellschaft mbH, within the research activities of the K2 Competence Centre on "Integrated Research in Materials, Processing and Product Engineering", operated by the Materials Center Leoben Forschung GmbH in the framework of the Austrian COMET Competence Centre Programme, is gratefully acknowledged.

References

[1] M.F. Ashby, Materials Selection in Mechanical Design, 4th ed., Elsevier; Butterworth-Heinemann, Amsterdam, Boston, Burlington, Mass, 2011.
[2] CES Selector 2012 software, Granta Design Limited, Cambridge, UK, 2011.
[3] UL IDES, URL: http://www.ides.com/.
[4] CAMPUS, URL: http://www.campusplastics.com.
[5] D. Cebon, M.F. Ashby, C. Bream, L. Lee-Shotham: CES Selector 2012 User's Manual, Release 1: Granta Design Limited, Cambridge, UK, 2011.
[6] ASTM D6992-03. Standard Test Method for Accelerated Tensile Creep and Creep-Rupture of Geosynthetic Materials Based on Time-Temperature Superposition Using the Stepped Isothermal Method, ASTM International, West Conshohocken, PA, 2009.

S11-L28
Comparison of crack growth kinetics in different polypropylene grades using linear elastic fracture mechanics

Florian Arbeiter (1)*, Gerald Pinter (1), Frank Andreas (2)
(1) Chair of Material Science and Testing of Polymers, Otto-Glöckel-Str. 2, 8700 Leoben, Austria
(2) Polymer Competence Center Leoben GmbH, Roseggerstrasse 12, 8700 Leoben, Austria
*Florian.Arbeiter@unileoben.ac.at

1. Introduction

Polypropylene is a widely used thermoplastic polymer. Due to its manifold applications extensive knowledge of material properties is necessary. Especially in structural applications it is of utmost importance to regard long term mechanisms which can lead to unexpected failure. Crack initiation and Slow Crack Growth can cause this kind of failure over long time frames and must not be neglected when considering possible applications for the material. The high local ductility of Polypropylene, however, makes it very hard to determine long term properties, such as crack initiation and growth in feasible time frames. Therefore faster methods are needed to describe these vital material properties. One of the possibilities is the use of Linear Elastic Fracture Mechanics (LEFM). It can be used to determine crack kinetics of materials. Depending on the crack kinetics, material parameters can be derived and used to calculate life times of actual structural applications under similar loading conditions. Crack initiation is not considered in this approach and acts as an additional safety factor. The specimens used in this work are Cracked Round Bar Specimens (CRB) which provide a strong constraint at the notch root and are therefore able to induce brittle crack growth even in rather ductile materials such as Polyethylene and Polypropylene.

2. Theory

The proper application of LEFM requires global loads which are in the range of linear viscoelasticity and that there are only small and localized plastic deformations at the crack tip [1]. The distribution of stress around the crack tip can then be described with the Stress Intensity Factor (K). K is dependent on the global loading s, the general crack length a and a geometric factor Y which describes the development of K in relation to specimen geometry and crack length as can be seen in equation 1 . The factor K is usually specified according to the loading condition [2]. All specimens in this work are tested under pure tensile load and marked

with $_I$.

$$K_I = \sigma \cdot \sqrt{a} \cdot Y$$

Equation 1. Generalized Stress Intensity Factor under pure tensile load (= mode I) with the crack length a, global load s and the geometric factor Y

In a double logarithmic diagram crack growth over time can be plotted as a function of K_I. According to theory there are three different areas in these plots. The first area is the so called threshold. Below this load value the crack does not start to grow. Increasing the load leads to crack initiation and stable crack growth which marks the second area. The third area is the unstable crack growth. At this loading level the crack growth rates increase drastically and the specimen fractures abruptly. The constant slope of the second area can be described by equation 2 where A and m are material constants and da/dt is the crack extension per time frame [3]. When conducting cyclic testing to shorten testing times da/dt is usually replaced by da/dN where dN is the number of cycles needed for the crack extension da. Additional the Stress Intensity Factor K is replaced by DK which considers the cyclic loading. Another important factor when conducting cyclic testing is the loading ratio F_{min}/F_{max} which is 0.1 in the current work and therefore results in $DK = K_{max} - K_{min} = K_{max} \cdot 0.9$ [4, 5].

$$\frac{da}{dt} = A \cdot K_I^{\,m}$$

Equation 2. Crack Growth Kinetics with the material parameters A and m, the Stress Intensity Factor K_I and crack extension da over passed time dt

3. Experimental

The examined materials can be seen in Table 1. All three are made of Polypropylene with different reinforcements and or base material compositions. Materials were chosen according to demands in real application. All cyclic tests were performed on servo-hydraulic fatigue testing machines (MTS Table Top (MTS Systems GmbH, Germany)). The frequency for the test was 5 Hz to minimize increase of temperature due to hysteretic heating while testing.

Table 1. Composition of all examined materials

Material	Polymer	Reinforcement
PP 1	PP-Block	~ 50% Talc
PP 2	PP-Block / PP-Homo	~ 50% Talc
PP 3	PP-Blend	~ 20% Wollastonite

Actual crack length a(N) during the test could not be observed optically and was therefore calculated by means of a compliance calibration method [6]. The geometric factor Y = f(b/r) which is mentioned in Equation 1 was calculated according to Benthem and Koiter and is shown in Equation 3 [7].

$$f\left(\frac{b}{r}\right) = \frac{1}{2} \cdot \left[1 + \frac{1}{2} \cdot \left(\frac{b}{r}\right) + \frac{3}{82} \cdot \left(\frac{b}{r}\right)^2 - 0.363 \cdot \left(\frac{b}{r}\right)^3 + 0.731 \cdot \left(\frac{b}{r}\right)^4\right]$$

Equation 3. Calculation of the geometric factor for CRB-Specimen according to Benthem and Koiter where r is the radius of the specimen and b the current concentric crack length

4. Results and discussion

Using the compliance method mentioned earlier it was possible to generate crack growth kinetic data for all three materials. In Figure 1a the kinetics for all materials can be seen for the loading conditions of R=0.1 and f=5 Hz. According to LEFM theory the applied load is irrelevant for the results as long as the requirements of LEFM which are explained in the Theory section are met. In Figure 1b crack kinetics data for the same material are shown for different loading levels. Lines of both tests coincide in the second area where stable crack growth is measurable and therefore indicate the applicability of LEFM for this test. At higher values of DK_I the slopes change which is an indication of high local plasticity which disagrees with the requirements of LEFM.

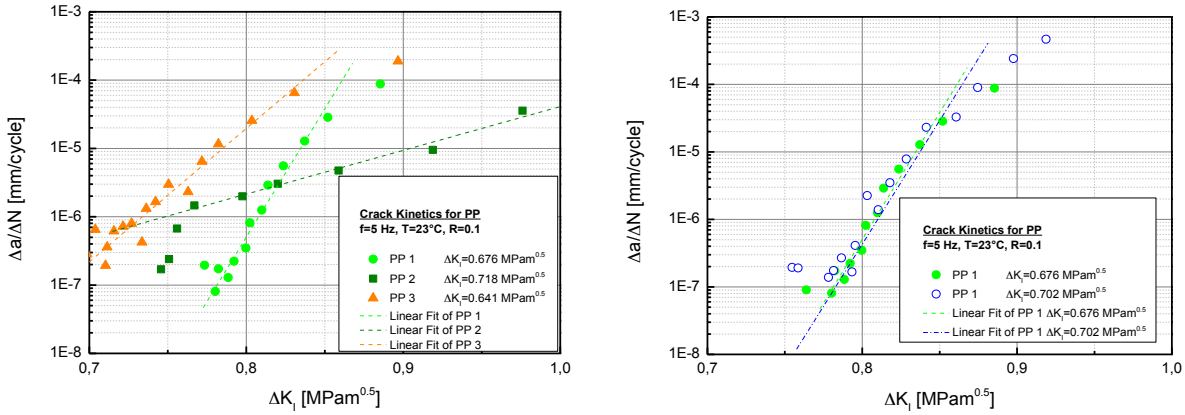

Figure 1. Comparison of crack growth kinetics of all three materials (a) and validation of applicability of LEFM by use of different loading levels for the test (b)

Acknowledgements
The research work of this publication was performed at the Chair of Materials Science and Testing of Polymers (University of Leoben, Austria) within the framework of the FFG program of the Austrian Ministry of Traffic, Innovation and Technology and the Austrian Ministry of Economy, Family and Youth with contributions of the Österreichisches Forschungsinstitut für Chemie und Technik (Austria), Martin-Luther-Universität Halle-Wittenberg (Germany) and the Polymer Competence Center Leoben GmbH (Austria)

References
[1] Lang, R.W.: Applicability of linear elastic fracture mechanics to fatigue in polymers and short-fiber composites (**1984**)
[2] Hertzberg, R.W.: Deformation and fracture mechanics of engineering materials, 4th edn. J. Wiley & Sons, New York (**1996**)
[3] Paris, P., Erdogan, F.: A critical analysis of crack propagation laws. Transactions of the ASME. Journal of Basic Engineering **1963**(85), 528–534
[4] Broek, D.: Elementary engineering fracture mechanics, 3rd edn. Martinus Nijhoff; Distributed by Kluwer Boston, The Hague, Boston, Hingham, Mass (**1982**)
[5] Anderson, T.L.: Fracture mechanics. Fundamentals and applications, 3rd edn. CRC, Taylor & Francis, Boca Raton [u.a.] (**2005**)
[6] Frank, A., Freimann, W., Pinter, G., Lang, R.W.: A fracture mechanics concept for the accelerated characterization of creep crack growth in PE-HD pipe grades. Engineering Fracture Mechanics 76(18), 2780–2787 (**2009**).
[7] Benthem, J., Koiter, W. (eds.): Method of Analysis and Solutions of Crack Problems, 3rd edn. (**1973**)

S11-L29
Ion mobility mass spectrometry, an enabling technology for polymeric characterisation

Matthew Kennedy*
Waters Corporation, Simonsway, M22 5PP, Manchester, United Kingdom
*matt_kennedy@waters.com

1. Introduction
Polymeric materials are inescapable in our modern societies and cover a broad range of applications, in areas such as automobiles, textiles, packaging, medicine and pharmacy, to name just a few. The increasing complexity of such applications has generated a requirement for highly complex polymeric materials. Accurate and detailed polymer characterisation is therefore vital to this process. Recently, a great deal of time and effort has been invested in polylactide research due to their bio-compatible and bio-degradable nature [1].
The utility of both mass spectrometry (MS) and ion mobility spectroscopy (IMS) to characterise polymeric materials is well documented; however, although the combination of these techniques provides significant advantage, compared to the individual techniques. It should be noted, significant limitations must be overcome to produce a viable analytical tool. As a result it is only recently that a commercial IMS-MS instrument has been available (ASMS 2006).
This instrument utilises alternative technologies that overcome the main limitations of a classical IMS-MS system but retains the benefits of the union [2]. Such an instrument is ideal for characterising complex polymeric materials such as polylactide.

2. Theory

The inclusion of ion mobility functionality along with mass spectrometry provides an additional, orthogonal mode of separation, which affords the analyst increased peak capacity. Ions can be separated by their mass, their shape, and also their charge.

3. Results and discussion

Polylactide samples were introduced to the ElectroSpray (ESI) source via direct infusion. Due to the nature of ion formation in ESI, ions with different charge states are generated. This phenomenon makes data analysis extremely complicated. By utilizing the mobility separation, it is possible to deconvolute different charge states within the polymeric ion series, thus simplifying data handling.

We are also able to show that the folding patterns observed in the travelling wave region (IMS) of the instrument is consistent with published literature based on theoretical calculations and experiments carried out on classical IMS devices (a linear drift tube) [3]

4. Conclusions

In this work, we demonstrate that the additional mode of separation offered by ion mobility can be used to aid the characterisation of polymeric materials as well as provide a greater understanding of the 3-dimensional structure of polymers.

References

[1] *J Am Soc Mass Spectrom* **2010**, 21, 1159–1168
[2] K.Giles, J.Wildgoose, J.Langridge, I. Campuzano, *Int.J.Mass.Spectrom.* **2010,** 298, 10-16
[3] *Chem. Eur. J.* **2011**, 17, 9738 – 9745

S11-L30

MALDI (matrix-assisted laser desorption ionization) and ES(I) (electrospray (ionization)) techniques for the characterization of natural (latex surfaces, gelatin nano particles and polysaccharides) and synthetic (UHMW-PE) polymers

Martina Marchetti-Deschmann (1), Sophie Fröhlich (1), Angela Lehner (1), Victor U. Weiss (1), Wladek Szymanski (2), Matthew A. Kennedy (3), Guenter Allmaier (1)*

(1) Vienna University of Technology, Institute of Chemical Technologies and Analytics, Getreidemarkt 9/164, A-1060 Vienna, Austria
(2) University of Vienna, Faculty of Physics, Boltzmanngasse 5, A-1090 Vienna, Austria
(3) Waters, Atlas Park, M22 5PP Manchester, UK
*guenter.allmaier@tuwien.ac.at

1. Introduction

In the characterization of polymers and polymeric nano particles of synthetic origin as well as of natural sources molecular weight determination, size determination, heterogeneity of the sample and finally primary structural elucidation are the starting point in any case. During the last decades several techniques based on electrospraying (ES) combined with charge reduction of aqueous polymer solutions, electro spray ionization (ESI) of soluble polymer solutions and matrix-assisted laser desorption ionization (MALDI) of insoluble (directly from polymeric solids) as well as soluble polymers were introduced. These techniques allowed the generation of gas-phase singly or multiply charged species even in size range beyond 5 nm and in the molecular weight range above 1 million Dalton. The so generated ionic species were transferred to different separation devices, namely time-of-flight (TOF) analyzer, quadrupole-reflectron TOF (QRTOF) analyzer with and without prior ion mobility (IM) separation and high flow differential mobility analyzer (DMA). The goal of the presentation is to show achievements and also limitations of the mentioned combination of techniques for the first characterization steps of synthetic and natural polymers [1, 2].

2. Experimental

Natural latex used in medical glove production [3] and ultrahigh molecular weight (UHMW) PE used as human implants were used as solid material for mass spectrometric imaging (IMS) by means of UV-MALDI. Specific sample preparation protocols were used to perform direct desorption/ionization from the MALDI-matrix covered solid samples. The MALDI mass spectrometers applied were either a Synapt HDMS or G2 QRTOF (Waters, Manchester, UK) and a Axima CFR$^+$ or Axima Tof^2 (Shimadzu Kratos Analytical, Manchester, UK). For ESI mass spectrometry of soluble polymeric materials (e.g. gelatin or intact virus nano particles) a Synapt G2 QRTOF (Waters, Manchester, UK) was selected with a 32 kDa RF quadrupole device. The combination of ES with a Po-201 source (for charge reduction) and a high flow DMA followed by a condensation particle counter (CPC) as detector (independent of the chemical composition of the sample) is called MacroIMS (ion mobility spectrometer) or GEMMA (gas-phase molecular mass analyzer) provided by TSI Inc (Shoreview, MI, USA). This device was used for all analysis were the samples (e.g. gelatin, intact virus, polysaccharides) were soluble in aqueous solutions or suspensions [1, 2].

3. Results and discussion

We will show the results of the analysis of challenging polymeric samples – direct analysis (Imaging MS by MALDI) of latex [3] and UHMW-PE used in the medical field, i.e. the distribution of small organic and biological molecules on the polymeric surfaces as well as the structural characterization of them by tandem MS. Limitations and outlooks of these approaches will be presented.
For the synthetic gelatin nano particles, intact virus particles and polysaccharides, all dissolved or suspended in aqueous solution systems ES with charge reduction and DMA analysis will be presented up to a particle size of 40 nm and a molecular mass of several mega Daltons. Successful attempts to use ESI in combination with a QRTOF mass analyzer (32 kDa RF quadrupole can do this only) to analyze the identical samples will be presented, too.

4. Conclusions

What we want to present is that new techniques and unusual combination of techniques are allowing to bridge the existing gap between analysis of small polymeric molecules and of high molecular mass polymer-based nano particles. Analytical characterization is essential before these materials are entering the field of applications. This is of particular importance due to the fact that more and more synthetic or semi-synthetic materials (e.g. polymer (PE or latex)-based implants) and nano particles (e.g. drug delivery) are used in various fields of nanotechnology

Acknowledgements

This work was supported by a grant of the Austrian Science Foundation (TRP29-N20 to WS and GA). Further we thank D. Blaas (Medical University, Vienna, Austria) for providing the virus samples.

References

[1] G. Allmaier, C. Laschober and W. Szymanski, *J. Am. Soc. Mass Spectrom.* 2008, 19, 1062-1068.
[2] R. Müller, C. Laschober, W. Szymanski and G. Allmaier, *Macromolecules* 2007, 40, 5599-5605.
[3] M. Marchetti-Deschmann and G. Allmaier, *J. Mass Spectrom.* 2009, 44, 61-70.

Session 9: Polymer Degradation and Stabilization

S9-IL31
Odor perception and polymer degradation

Anders Höglund (1)*, Ann-Christine Albertsson (1), Anna Lindqvist (2), Birgitta Berglund (2,3)
(1) KTH Royal Institute of Technology, Department of Fibre and Polymer Technology, Teknikringen 56-58, SE-100 44 Stockholm, Sweden
(2) Stockholm University, Department of Psychology, Frescati Hagväg 8, SE-106 91, Stockholm, Sweden
(3) Karolinska Institutet, Institute of Environmental Medicine, P.O. Box 210, SE-171 77, Stockholm, Sweden
*anhog@kth.se

1. Introduction

Modern instrumental analytical methods have provided a good understanding of polymer degradation, both during early and later stages of degradation. The straight-forward approach is to subject polymer samples to natural or accelerated degradation environments and measure one or several polymer properties as a function of time. An alternative method is to correlate the degradation products formed during ageing to simultaneous molar mass changes and changes in mechanical properties.[1] Such a correlation allows the assignment of certain indicator products to predict the degree of degradation of polymers. Indicator products can also be used to show the degree of degradation of chemically cross-linked networks,[2] to identify surface grafting of polymers,[3] or to discriminate different polymer types.[4] The indicator products are identified after extraction and subsequent GC-MS analysis. Drawbacks with these procedures include limited instrumental detection limits, the need for careful sample taking, proper method development, and high instrument costs.
Our main aim is to develop a rapid and straight-forward method to detect polymer degradation. The hypothesis is that the odorous volatile compounds released from the polymers during ageing can be used as a link to relate odor quality to polymer degradation. To verify this, odor intensity measures were compared with GC-MS and tensile testing results. In addition, pure compounds of the degradation products were studied as binary and higher order mixtures in order to reveal key information about the human olfactory code.

2. Theory

When exposed to e.g. UV-light or heat, polymers degrade. This results in a deterioration of material properties and formation and release of degradation products. These substances are subsequently emitted to the indoor air were they may affect human health. In addition, the degradation products may also be useful to reveal information about the status of the polymer they originate from. The use of odor perception as a detection method has been proven useful in other research fields. Odor perception is widely used in the wine industry to discriminate and categorize the wines.[5] Changes in wine odor profiles during oxidative ageing are also

studied with parallel odor perception and GC-MS.[6] In medicine, disease-specific compounds have been shown to be useful for olfactory diagnosis.[7] A relatively well-known example is the acetone-like breath of diabetes patients resulting from ketone compounds generated by fatty acid metabolism. If successful for detecting wine oxidation and various diseases, odor perception may also be useful for detecting polymer degradation.

3. Experimental

Strips of Polyamide 66 (PA66) were thermo-oxidized at 90 °C for 12, 72, 168, and 288 hours. Odor stimuli consisted of aged polymers, two to five-order mixtures of PA66 degradation products, and blanks. Each subject measured odor intensity, odor similarity, and odor pleasantness/unpleasantness by free magnitude estimation. Arithmetic means for the group were calculated. The low molar mass products from the polymer samples were extracted by HS-SPME and subsequently analyzed by GC-MS. Tensile testing of the polymer materials were performed on an Instron 5566, the thermal properties of the polymers were determined with a DSC, and FTIR spectra of the thermo-oxidized polymer materials were also recorded.

4. Results and discussion

The perceived odor intensity of PA66 during the initial stages of the degradation (up to 72 h) was relatively low but increased approximately 150% after 168 h (Figure 1, left).[8] In parallel, a total of eight degradation products increased in extracted amount with increased degradation time. Five of these were identified as odorous in the odor experiments: pentanoic acid, 2-metyl-pyridine, butanamide, pentanamide, and dibutyl phthalate. Both tensile strength and elongation at break decreased with increased degradation time (Figure 1, right). This deterioration in mechanical properties was continuous. However, it was not until after 168 hours that a significant deterioration in mechanical properties was observed. Interestingly, this deterioration in mechanical properties coincided with the 150% increase in perceived odor intensity of the aged materials and also with the increase in extracted amounts of degradation products. During the same time period, negligible changes in thermal and surface properties of PA66 were observed. Odor perception was, thus, demonstrated to be a useful tool to detect polymer degradation at an early stage.
Binary and higher-order mixtures of the PA66 degradation products were also studied.[9] The perceived odor qualities of the binary mixtures were intermediary vectors relative to their single component-odor vectors in a three-component principal components analysis (PCA). Three of the PA66 degradation products and their odor qualities contributed profoundly to their binary mixtures: the “floral/fruity” 2-pentylcyclopentan-1-one, the “sharp/cheese-like” pentanoic acid and the “minty” cyclopentanone but in fewer cases. The “ether-like” 2-methyl pyridine and the “nutty” butanamide had much less influence. Odor similarity was shown to be caused by odor quality, rather than odor intensity. The profoundly contributing degradation products formed distinct clusters of odors and were therefore interpreted to be key degradation products of PA66. In contrast to the binary mixtures, the higher-order mixtures created new odor qualities which were completely different and untraceable to their various parts as perceived alone.

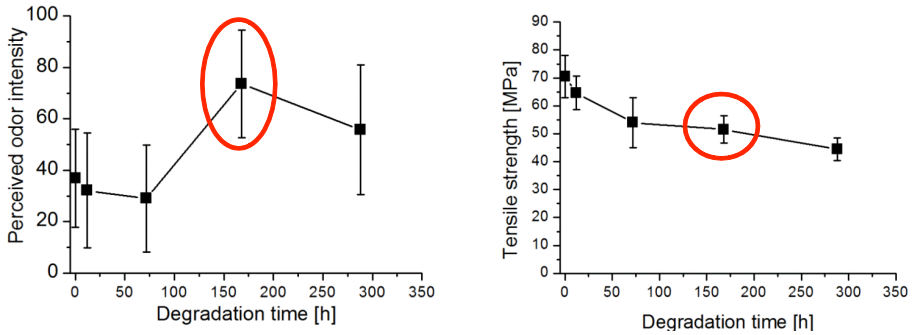

Figure 1. Perceived odor intensity (left) and tensile strength (right) of polyamide 66 during thermal oxidation at 90 °C.

5. Conclusions

Odor perception was demonstrated to be rapid and straight-forward method to reveal early degradation of Polyamide 66. A significant deterioration in mechanical properties correlated with a 150% increase in perceived odor intensity and an increase in the amounts of a total of eight of the degradation products released from the polymer matrix. Very small changes in thermal and surface properties of PA66 were observed during the same time period. Three of the PA66 degradation products: 2-pentylcyclopentan-1-one, pentanoic acid, and cyclopentanone can be viewed as key degradation products because they have a substantial impact on the perceived odor quality when being part of a mixture. The research of the perception of natural mixtures are just as essential as the odors of single chemical compounds and contributes to the understanding of the human olfactory code.

Acknowledgements

The authors greatly acknowledge the Swedish Council for the Environment, Agricultural Sciences and Spatial Planning (FORMAS) [Grant ID: 242-2007-763], the Royal Institute of Technology (KTH), and also the EU FP6 NEST projects MINET [043297] and SysPAQ [028936] for financial support of this work.

References
[1] Hakkarainen M, Albertsson A-C. *Biomacromolecules* **2005,** 6, 775-779.
[2] Höglund, A.; Hakkarainen, M.; Kowalczuk, M.; Adamus, G.; Albertsson, A.-C. *J. Polym. Sci., Part A: Polym. Chem.* **2008,** 46, 4617-4629.
[3] Höglund, A.; Hakkarainen, M.; Edlund, U.; Albertsson, A.-C. *Langmuir* **2010,** 26, 378-383.
[4] Willoughby, B. G.; Golby, A.; Davies, J.; Cain, R. *Polym. Test.* **2003,** 22, 553-570.
[5] Chollet, S.; Valentin, D. *Ann. Psychol.* **2000,** 100, 11-36.
[6] Zea, L.; Moyano, L.; Medina, M. *Int. J. Food Sci. Technol.* **2010,** 45, 2425-2432.
[7] Shirasu, M.; Touhara, K. *J. Biochem.* **2011,** 150, 257-266.
[8] Höglund, A.; Lindqvist, A.; Albertsson, A.-C.; Berglund, B. *Polym. Degrad. Stab.* **2012,** 97, 481-487.
[9] Lindqvist, A; Höglund, A.; Berglund, B. *Perception* **2012**, 41, 1373-1391.

S9-L32

Plastic materials for solar thermal applications monitoring the degradation of stabilization systems after exposure to heat

S. Beißmann (1)*, W. Buchberger (1), G. Wallner (1), K. Grabmayer (1), D. Nitsche (2)
(1) Johannes Kepler-University Linz, Altenbergerstraße 69, A-4040 Linz, Austria
(2) AGRU Kunststofftechnik GmbH, Ing.-Pesendorfer-Str. 31, 4050 Bad Hall, Austria
*Susanne.beissmann@jku.at

1. Introduction

The implementation of novel polymeric materials in solar-thermal systems is considered to have an extraordinary potential as they provide substantial advantages in comparison to traditional materials. A key challenge is to maintain required durability for extended lifetimes, since these materials are prone to degradation when exposed to heat or sunlight. Therefore, the addition of different stabilizers is essential. Since it is not yet fully clear which additive package provides the best performance for a specific application, characterization of degradation pathways is of significant importance. The present work aimed at a detailed study on the formation of degradation products of commonly used antioxidants to provide a better insight into the stabilization mechanism.

2. Theory

Nowadays there are various different analytical tools for analyzing polymer additives, which generally require the extraction from the particular matrix as a first step. Of the different procedures to analyze polymer additives, chromatographic methods play a dominant role. Besides the application of gas chromatography (GC) and pyrolysis coupled to gas chromatography (Py-GC) [1, 2], high performance liquid chromatography (HPLC) in combination with ultraviolet (UV) [3, 4] detection or mass spectrometric (MS) [5, 6] detection is commonly applied.

3. Experimental

HPLC experiments were carried out using an Agilent 1260 Infinity Quaternary LC system with a 50 mm x 4.6 mm I.D. Phenomenex Kinetex C18 column, packed with 2.6 µm particles. A binary gradient with ACN / water was used for the chromatographic separation of the investigated analytes. Atmospheric pressure chemical ionization (APCI) was selected as it provides very good performance for substances with low polarity. All aging experiments were performed with a Binder FD 53 material test chamber.

4. Results and discussion

The applicability of different analytical methods for the determination of polymer additives and their degradation products in plastic materials during accelerated aging tests was investigated. Commercial anti-oxidant systems have been examined regarding migration and chemical reaction in several polyolefin materials during aging in different environments at elevated temperatures (95°C-135°C). The degradation of the additives was monitored by the analysis of the aged polymer samples as well as the ageing fluid taken after certain periods of time using various detection methods such as UV-absorbance and tandem mass spectrometry.
Numerous degradation products of commercial additives could be identified. For materials containing ®Irganox 1330 three new species, identified as oxidation products, were found within the material. From their structure it can be concluded that two of them still have antioxidant capacity. The behavior of other stabilizers was different, for example, predominantly hydrolyzed products were found in samples stabilized with ®Irganox 1010. It is suggested that this stabilizer forms degradation products which are able to migrate out into the surrounding aging fluid. To prove this assumption, the migration of substances into the aqueous ageing fluid was investigated. As the migration of substances into water is supposed to be low, an enrichment step using solid phase extraction was conducted. Several compounds could be identified and assigned to the corresponding stabilizer.

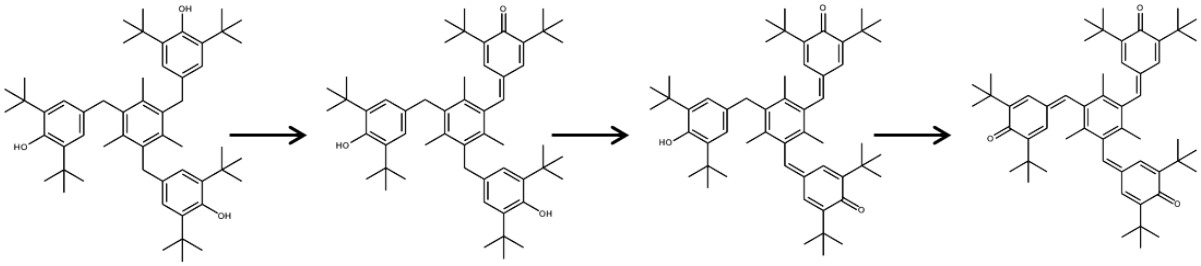

Figure 1. Structure formula of Irganox 1330 and its oxidation products

5. Conclusions

The potential of highly sensitive APCI-MS/MS detection in combination with HPLC could be clearly demonstrated for detection and identification of various common stabilizers and degradation products. For materials containing sterically hindered phenols (used as antioxidants) some previously unknown degradation products could be identified. These included compounds with a quinone-type structure, hydrolysis products, or products generated by reaction with hydroxy radicals.

Acknowledgements

This research work was performed in work package AP-01 *" Test Methods"* of the fundamental research project *SolPol-1* and work package AP-05 *"Durable Compounds"* of the cooperative research project *SolPol-2* on *Solar-thermal Systems based on Polymeric Materials* (www.solpol.at). This Project is funded by the Austrian Climate and Energy Fund (KLI.EN) within the program "Neue Energien 2020". The authors wish to express their acknowledgements to the Scientific Partners JKU-Institute of Polymeric Materials and Testing (JKU-IPMT), JKU-Institute of Analytical Chemistry (JKU-IAC) and the Company Partners AGRU Kunststofftechnik GmbH (AGRU) und APC Advanced Polymer Compounds (APC).

References

[1] M. Herrera, G. Matuschek, A. Kettrup, J *Anal Appl Pyrol*, 70, 2003, 35-42.
[2] F.C.Y. Wang, J Chromatogr A, 891 (2000) 325-336.
[3] M.S.D. Garcia, J.M. Lopez, R. Bouza, M.J. Abad, E.G. Soto, M.V.G. Rodriguez, *Anal Chim Acta,* 521, 2004, 179-188.
[4] B.H. Kim, D.K. Yang, J.H. Ok, *Journal of Chromatographic Science*, 45 (2007) 16-21.
[5] C. Block, L. Wynants, M. Kelchtermans, R. De Boer, F. Compernolle, *Polym Degrad Stabil*, 91, 2006, 3163-3173.
[6] M.J. Carrott, D.C. Jones, G. Davidson, *Analyst*, 123, 1998, 1827-1833.

S9-L33
Degradation of composite materials based on low-density polyethylene and Mora tree (Maclura tinctoria)

Svetlana Nikolaeva (1)*, José Saavedra-Arias (1), Silvia Mau (2)
(1) Laboratorio de Materiales Industriales (LAMI), Universidad Nacional, Apdo.86-3000, Heredia, Costa Rica
(2) Laboratorio de Microbiología, Escuela de Ciencias Biológicas, Universidad Nacional, 86-3000, Heredia, Costa Rica
*snikolaeva17@gmail.com

1. Introduction

The aim of this research was the biodegradation of low-density polyethylene (LDPE) composite film with different parts (leaves, peel and stems) of mora tree (Maclura tinctorea) like filler, by action of 6 strains of fungi: Penicillium sp., Aspergillus niger, Microsporum sp., Aspergillus sp., Fusarium sp. and Trichoderma sp. Synthetic plastics are resistant to degradation, hence the development of biodegradable polymers may be an option to reduce the environmental impact caused by them. The composite materials in which a polymer matrix forms a dominant phase around a filler material, is designed with the goal of more rapid degradation than synthetic plastics, it can be consumed by microorganism of natural macromolecules within plastic matrix with further degradation. The mora tree was used as filler in a composite polymeric material, and the influence of this plant as a degrading agent is being studied.

The use of biodegradable polymer materials begins with a conceptual application in different sectors like packaging, agriculture and medicine, and the subsequent introduction of these materials in the industry.

2. Theory

As defined by the American Society for Testing of Materials (ASTM) and the International Standards Organization (ISO) the degradable plastics are considered as such when presented a significant change in chemical structure under specific environmental conditions. These changes result in a loss of physical and mechanical properties or from the action of naturally occurring microorganisms like fungi.

Mora tree Maclura tinctoria (L.) is a native tree of America and can be found in the tropical and subtropical humid and dry forests (Trees of Central America, 2004), distributed in Mexico, Central America, the West Indies and parts of Brazil.
According to Usha [1] low density polyethylene (LDPE) is one of the major sources of environmental pollution and many investigations [2-4] are carried out to find alternatives for their degradation. The processes: degradation and biodegradation have been studied as a possible solution to the problem of polymer products, for example, in 2010, Remersaro *et. al.* [4] analyzed the degradation of polyethylene grocery bags, by simulating solar radiation with controlled temperature and humidity, concluding that there is a change of physical and chemical properties to those that have an oxy-biodegradable additive in half the time than those not containing it. Salgado *et. al*. [5] evaluated composite biodegradation of LDPE with modified sugarcane bagasse by alkali treatment and acetylation, providing an hydrophobic character of the latter, likewise the biodegradation study on exposure to weathering and soil for 1, 2 and 3 months, producing a wear in the mechanical properties. Mendez and Łabużek [6,7] used the micromicetas and fungi for LDRE degradation.

3. Experimental
6 strains of fungi: Penicillium sp., Aspergillus niger, Microsporum sp., Aspergillus sp., Fusarium sp. and Trichoderma sp. were used in this study. The fungi were isolated from soil and were identified by the Microbiological Laboratory of the School of Biological Sciences at Universidad Nacional. These were cultivated on Potato-dextrose Agar at 21°C for two weeks. The samples of composite material (1 cm2) were aseptically placed as a sole carbon source at the surface of the modify Czapek-Dox agar. After that, the plates were incubated at 28°C. After the incubation, the samples were observed with an optical microscope and SEM, to evaluate the colonization and conidia production. A FTIR analysis was made to evaluate the degradation of the composite film.

4. Results and discussion
The macroscopic observation showed that the initial growing of the fungus was at the edges of the samples. After weeks of incubation, the colonization of *Penicillium* sp., *Aspergillus niger*, *Microsporum* sp., *Aspergillus* sp., *Fusarium* sp. and *Trichoderma* sp. covered the sample surface.
To evaluate the fungal growth, the colonization and conidia production from the samples an analysis in the optical microscope and SEM was made. The entire surface of the polymer was examined; the strains *Penicillium* sp., *Fusarium* sp., *Trichoderma* sp., *Aspergillus* sp. and *Aspergillus niger* showed a complete colonization, the *Microsporum* sp. is the only one which has an abundant growth of the fungus at the edges, but not at the center of the polymer. In the case of Aspergillus sp., Aspergillus niger and Fusarium sp. the conidiophores and conidia were observed at the surface and around the samples as show Fig.1. The results show that the fungal growth was established through the use of the samples as a carbon source leading to its biodegradation.

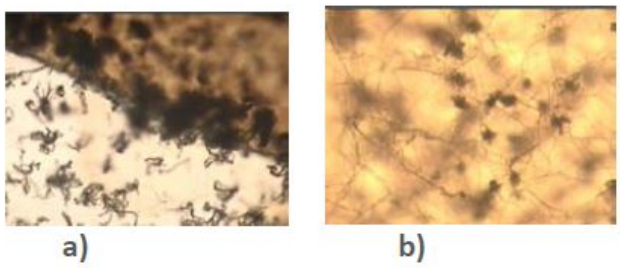

Figure 1. a) *Aspergillus* sp. and b) *Penicillium* sp. observed with an optical microscope with 10x in magnification showed a complete colonization of the sample.

5. Conclusions
The result of the study has proven that fungi were capable of degrading polyethylene using it like carbon source for their reproduction and growth.

Acknowledgements
Researchers acknowledge the financial support by the National University of Costa Rica, CONICIT and MICIT of Costa Rica.

References
[1] Usha R, Sangeetha T, Palaniswamy M, (2011) Screening of Polyethylene degrading microorganisms from garbage soil-Libian Agriculture research center journal internation 2 (4) ISSN 2219-4304.
[2] Uribe D, Giraldo D, Gutierrez S, Merino F (2010) Biodegradacion de polietileno de baja densidad por accion de un consorcio microbiano aislado de un relleno sanitario, Lima,Peru.Rev.peru.biol.17(1):133-136. ISSN 1727-9933.
[3] Pantyukhov P, Monakhova T, Kolesnikova N, Popov A, Nikolaeva S (2012) The oxidative and biological destruction of composite materials based on low-density polyethylene and lignocellulosic fillers, Chemistry& chemical technology Vol.6,No3,349-354.
[4] Remersaro J, Medina D, Hernandez M, Latronica L, (2010) Ensayos fisico-quimicos para el studio de la degradacion de bolsas de supermercado. Revista del laboratorio tecnologico de Uruguay, INNOTEC,5.

[5] Salgado R,Coria L, Garcia E, Vargas Z,Rubio E, Crispin I (2010) Elaboracion de materiales reforzados con character biodegradable a partir de polietileno de baja densidad y bagazo de caña modificado, Revista iberoamericana de polimeros, SLAP.
[6] Mendez C, Vergary G, Bejar V, Cardenas K (2007) Aislamiento y caracterizacion de micromicetas biodegradadores de polietileno Rev.peru.biol. 13(3):203-205. ISSN 1727-9933.
[7] S. Łabużek, B. Nowak, J. Pająk. (2004) The Susceptibility of Polyethylene Modified with Bionolle to Biodegradation by Filamentous Fungi. Polish Journal of Environmental Studies 13 (1): 59-68.

S9-L34
Photocatalytic and antimicrobial activity of surface modified ZnO nanoparticles in nanocomposite coatings

Jerneja Godnjavec (1)*, Bogdan Znoj (1,2), Marjeta Simončič (3), Zorica Crnjak Orel (1,3), Peter Venturini (1,2)
(1) Centre of Excellence PoliMaT, Tehnološki park 24, 1000 Ljubljana, Slovenia
(2) Helios Domžale d.d., Količevo 2, 1230 Domžale, Slovenia
(3) Kemijski inštitut Ljubljana, Hajdrihova 19, 1000 Ljubljana, Slovenia
*jerneja.godnjavec@polimat.si

1. Introduction
The application of nanoscale materials and structures, usually ranging from 1 to 100 nanometers, is an emerging area of nanoscience and nanotechnology. Zinc oxide (ZnO) nanoparticles have attracted much interest because they possess various remarkable physical and chemical properties that are distinct from those of conventional bulk materials formulation [1].

2. Theory
ZnO is widely used for paint and cosmetic application because it is chemically stable and environmentally friendly material that has good transparency and UV-blocking properties [2, 3]. ZnO nanoparticles are also useful as antibacterial and antifungal agents when incorporated into materials, such as surface coatings - paints, textiles, and plastics [4].
The drawback of nano ZnO is its photocatalytic activity which can facilitate the generation of reactive species, which can degrade organic compounds in the formulation. The surface modification of nanoparticles to enhance its chemical and physical properties is the key for the successful applications of nanomaterials [5]. Therefore, it is necessary to modify the surface of ZnO nanoparticles to reduce the agglomeration, to decrease its photocatalytic activity and to obtain wide UV shielding ability.

3. Experimental
In this study ZnO nanoparticles were coated with silanes in order to determine its effect on phtocatalytic and antibacterial properties of nanoparticles. The surface treatment of ZnO nanoparticles was characterized with FTIR. Microstructural analysis was done by AFM. The size, particle size distribution and zeta potential of ZnO nanoparticles in water dispersion was measured by DLS method. UV–VIS spectroscopy was employed to evaluate the transmittance of the nanocomposite coatings in the wavelength range of 200 – 800 nm. The photocatalytic activity of ZnO in nanocomposite was determined by accelerated weathering test. Antibacterial activity was evaluated by Escherichia coli test method.

4. Conclusions
The results showed that surface treatment of ZnO nanoparticles with silane decreases its photocatalytic activity, improves nanoparticles dispersion and UV protection of the clear polyacrylic composite coating.

Acknowledgements
The authors acknowledge the financial support from the Ministry of Higher Education, Science and Technology of the Republic of Slovenia through the contract No. 3211-10-000057 (Center of Excellence Polymer Materials and Technologies).

References
[1.] A. Nasu, Y. Otsubo, J. Colloid Interface Sci., 2007, 310, 617-623
[2.] Sosa I. O., Noguez C., Barrera R. G., J. Phys. Chem., 2003, B107, 6269-6275.
[3.] M. Rashvanda, Z. Ranjbara, S. Rastegarb, Prog. Org. Coat., 2011, 71 362–368.
[4.] Y. H. Leung, C. M. N. Chan, A. M. C. Ng, H. T. Chan, M. W. L. Chiang, A. B. Djurisišić,Y. H. Ng, W. Y. Jim, M. Y. Guo, F. C. C. Leung, W. K. Chan, D. T. W. Au, Nanotechnology, 2012, 23, 475703 (12pp).
[5.] W. Posthumus, P.C.M.M. Magusin, J.C.M. Brokken-Zijp, A.H.A. Tinnemans, R. van der Linde, J. Colloid Interface Sci., 2004, 269, 109–116.

Session 8: Theory, Modeling and Simulations

S8-L35
A network-analysis-based comparative study of viscous fluid flow in barrier screw geometries

Michael Aigner*, Christoph Kneidinger, Thomas Köpplmayr, Jürgen Miethlinger
Institute of Polymer Extrusion and Building Physics, Altenberger Str. 69, 4040 Linz, Austria
*michael.aigner@jku.at

Abstract
We present a systematic approach based on complex networks that uses tensor algebra and numerical methods to model and calculate selected barrier screw geometries in terms of pressure, mass flow, and residence time. In addition, we report the results of three-dimensional simulations using the commercially available ANSYS Polyflow software.

1. Introduction
Barrier screws are widely used in the plastics industry. Due to the extreme diversity of their geometries, describing the flow behavior is very difficult and normally not done in practice. Network theory and parameterized geometries, however, allow both the flow and the pressure/throughput behavior to be described.

2. Theory
The major drawbacks of three-dimensional FEM simulations are that they require great computational power, a large memory, and considerable time to create CAD-geometries and complete the flow calculation. Consequently, a modified 2.5-dimensional finite volume method termed *network analysis* is preferable. Michaeli et.al. [1] described the basic procedure that underlies network analysis; Köpplmayr et. al. [2] and Schöppner [3] added descriptions of the calculation for extrusion dies and barrier screws, respectively. In general, the flow behavior in a complex geometry can be solved by subdividing the geometry into smaller, geometrically simpler parts for which analytical formulae based on constitutive equations are available. The resulting 2.5-dimensional flow resistance network can be solved in a manner analogous to network analysis of electrical circuits. Pressure flow and drag flow, both caused by screw rotation, must also be taken into account. The latter is considered by introducing an additional boundary condition.
Figure 2 shows the geometry and the resistance network of the current flow problem. We cannot take advantage of any symmetry and must therefore consider the whole geometry in the calculation. For illustration purposes, the geometry is divided into four sections (n=4), which results in a flow resistance network consisting of 10 (3n+1) elements.

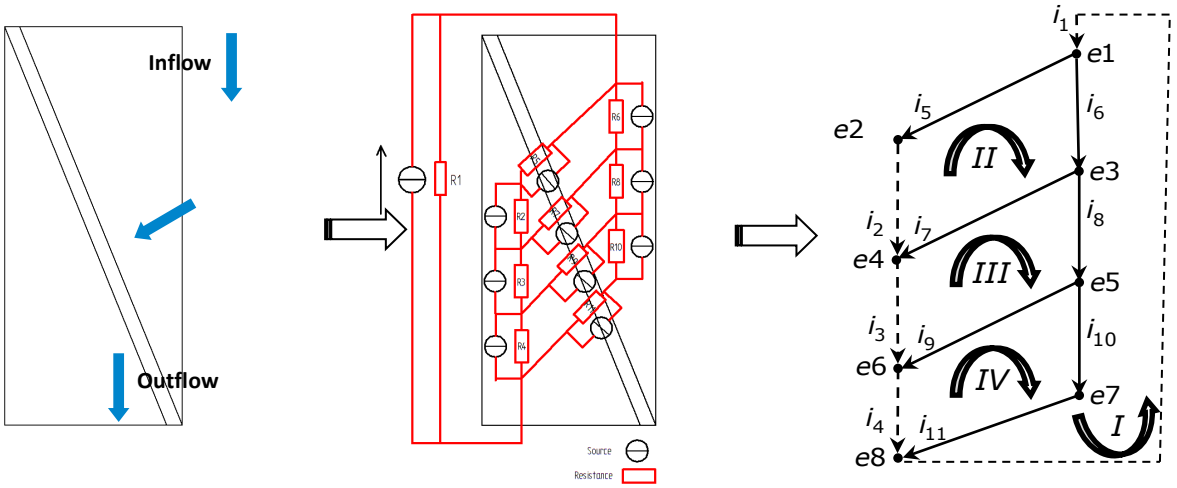

Figure 2: Geometry and resulting flow resistance network of a barrier cross-section and the tree of its directed graph

Two analytical methods, *Cut-Set* and *Loop-Analysis*, can be used to calculate the resistance network. Figure 3 shows the basic steps for calculating the pressure drop and the volume throughput along the resistance network for both methods.

The following analogies are used for calculation: $u \triangleq \Delta p;\ i \triangleq \dot{V}$

Cut Set-Analysis

$$\underline{\underline{G}} = \begin{pmatrix} G_1 & 0 & 0 & 0 & 0 \\ 0 & G_2 & 0 & 0 & 0 \\ 0 & 0 & \mathrm{K} & 0 & 0 \\ 0 & 0 & 0 & G_{z-1} & 0 \\ 0 & 0 & 0 & 0 & G_z \end{pmatrix};\ \underline{i}_0 = \begin{pmatrix} i_{01} \\ i_{02} \\ \mathrm{K} \\ i_{z-1} \\ i_z \end{pmatrix};\ \underline{u}_0 = \begin{pmatrix} u_{01} \\ u_{02} \\ \mathrm{K} \\ u_{z-1} \\ u_z \end{pmatrix}$$

$$\underbrace{\underline{Q} \cdot \underline{\underline{G}} \cdot \underline{\underline{Q}}^T}_{\underline{\underline{Y}}} \cdot \underline{e} = \underbrace{-\underline{Q} \cdot \underline{i}_0 + \underline{Q} \cdot \underline{\underline{G}} \cdot \underline{u}_0}_{\underline{i}_q} = 0$$

$$\underline{\underline{Y}} \cdot \underline{e} = \underline{i}_q \rightarrow \underline{e} = \underline{\underline{Y}}^{-1} \cdot \underline{i}_q$$

$$\underline{u} = \underline{\underline{Q}}^T \cdot \underline{e}$$

$$\underline{i} = \underline{\underline{G}} \cdot \underline{u} + \underline{i}_0 - \underline{\underline{G}} \cdot \underline{u}_0$$

Loop-Analysis

$$\underline{\underline{R}} = \begin{pmatrix} R_1 & 0 & 0 & 0 & 0 \\ 0 & R_2 & 0 & 0 & 0 \\ 0 & 0 & \mathrm{K} & 0 & 0 \\ 0 & 0 & 0 & R_{z-1} & 0 \\ 0 & 0 & 0 & 0 & R_z \end{pmatrix};\ \underline{i}_0 = \begin{pmatrix} i_{01} \\ i_{02} \\ \mathrm{K} \\ i_{z-1} \\ i_z \end{pmatrix};\ \underline{u}_0 = \begin{pmatrix} u_{01} \\ u_{02} \\ \mathrm{K} \\ u_{z-1} \\ u_z \end{pmatrix}$$

$$\underline{\underline{B}} \cdot \underline{\underline{R}} \cdot \underline{\underline{B}}^T \cdot \underline{j} = \underbrace{-\underline{\underline{B}} \cdot \underline{u}_0}_{u_q} + \underline{\underline{B}} \cdot \underline{\underline{R}} \cdot \underline{i}_0 = 0$$

$$\underline{\underline{Z}} \cdot \underline{j} = \underline{u}_q \rightarrow \underline{j} = \underline{\underline{Z}}^{-1} \cdot \underline{u}_q$$

$$\underline{i} = \underline{\underline{B}}^T \cdot \underline{j}$$

$$\underline{u} = \underline{\underline{R}} \cdot \underline{i} + \underline{u}_0 - \underline{\underline{R}} \cdot \underline{i}_0$$

G... Die conductance matrix
Q... Fundamental cut-set matrix
R... Die resistance matrix
B... Fundamental loop matrix

Figure 3: Basic procedure for calculating pressure drop and volume throughput [4]

4. Results and discussion

The isothermal flow of material in barrier screw geometries was simulated numerically using a novel code based on network analysis. For comparison, we carried out three-dimensional simulations using the commercially available CFD software ANSYS 14 Polyflow©, which is based on the finite element method. Our simulation routine provided three types of results: the mass flow rate and the pressure profile of any flow path, and the residence time at the end of the barrier section. The accuracy of the calculation was analyzed by computing the total pressure as a function of flow rate and screw speed, as shown in Figure 4 and the pressure profile in flow direction. In the operational range of the extruder, the results were found to be in good accordance with the numerical study.

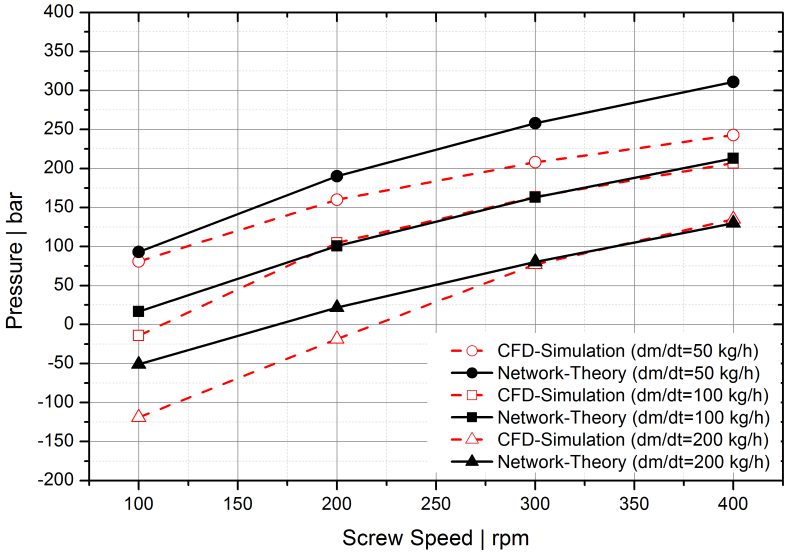

Figure 4: Comparison of the pressure/throughput behavior calculated using CFD-Simulation and the Network-Theory

5. Conclusions

The results obtained by network analysis and FEM Simulations correlated well. Network analysis provides an efficient alternative to complex FEM software in terms of computing power and memory consumption. Furthermore, typical barrier screw geometries can be parameterized and used for flow calculations without time-consuming CAD-constructions.

Acknowledgements

Financial support by WOOD K-plus is gratefully acknowledged. WOOD K-plus is funded by the Austrian Government and the Provincial Government of Upper Austria within the COMET program.

References

[1] W. Michaeli, F. Pöhler, *Die Verwendung der Netzwerktheorie bei der Werkzeugauslegung*, Plaste und Kautschuk 40, 1993, pp. 61-65.
[2] T. Köpplmayr, M. Aigner, J. Miethlinger, *A comparitative study of viscous flow in slit-exit cross-section dies using network analysis*, Journal of Plastics Technology 8, 2012, pp. 53-74.
[3] V. Schöppner, *Simulation der Plastifiziereinheit von Einschneckenextrudern*, Dissertation, Paderborn, 1995.
[4] D. Naunin, *Einführung in die Netzwerktheorie*, Vieweg, 1985.

S8-L36

A novel approach to simulate melt homogeneity in a single-screw plasticizing unit of an injection molding machine

Klaus Straka*, Bernhard Praher, Georg Steinbichler
Johannes Kepler University, Institute of Polymer Injection Molding and Process Automation, Altenberger Straße 69, 4040 Linz, Austria
*Klaus.straka@jku.at

1. Introduction

In polymer processing both the thermal homogeneity and the optical- mechanical homogeneity (mixing quality) of the polymer melt play a key role on the part quality. For most injection molding applications mixing is performed in the single screw plasticizing unit of the injection molding machine. Thus, the quality of the product is strongly dependent on the ability of the plasticizing unit to generate a homogenous melt pool in the screws ante chamber. We present a new approach to investigate melt homogeneity in the screw chamber by means of CFD simulations.

2. Theory

The principles of mixing in the metering section of single screw extruders are described by the well known unwound channel concept – an upper wall is moved across an unwound stationary screw channel [1,2]. In more complex geometries like pin mixing sections [3] or chaotic screws [4], numerical simulations are used to get an insight into the mechanics of flow and mixing. Numerical studies of color mixing in the metering zone of a single screw extruder and their validation have been done by Alemaskin et al. [5].

The methods above mentioned have in common that they describe mixing mechanisms within the screw channels but neither of them investigates the thermal homogeneity nor the optical- mechanical homogeneity of the melt in the screws ante chamber.

We intend to show a method how to simulate the melt flow from the screw into the chamber. On basis of the calculated pressure and velocity field of the polymer melt we investigate the distribution of tracer particles within the screw chamber and compare it with the optimum distribution. The comparison is done utilizing the discrete pairwise correlation function and the cluster distribution index [6,7], which is a measure for the optical homogeneity of the melt pool in front of the screw tip. Thermal inhomogeneities arise from the residence time distribution of the screw, the reduction of the effective screw length during plasticizing and viscous heating of the polymer melt due to the shear rate within the screw channels. Analysis of the temperature distribution is evaluated by extending the solvers of the CFD simulation with the energy balance equation.

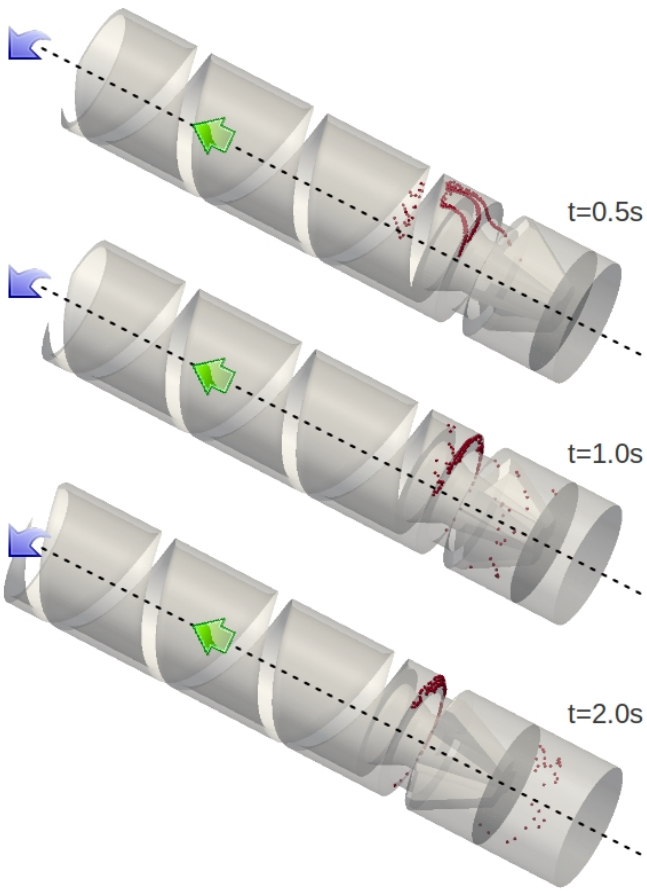

Figure 1. Position of screw and increase of the length of the chamber at t=0.5, 1.0 & 5.0s

3. Experimental

In our approach, the fluid volume (the CFD mesh) is decomposed in two parts, the screw, consisting of the screw channels, non return valve and the screw tip, and the chamber representing the screws ante chamber. The screw volume rotates to simulate the rotation of the plasticizing screw whereas the topology of the chamber changes in axial direction to simulate the growth of the chamber during the plasticizing process (see Figure 1). The simulation of tracer particles is done by Lagrangian particle tracking algorithm which calculates the position of the tracer particles on basis of the pressure and velocity distribution in the flow domain. Furthermore we give an outlook on how to validate the simulation results for the temperature distribution in the chamber by means of novel ultrasonic temperature measuring device.

This measurement system is based on the fact that the speed of sound in a polymer melt depends on the pressure and the temperature of the melt. Thus knowing the transit times of ultrasonic pulses through as well as the pressure in the polymer melt, one can calculate the (mean) temperature of the melt.

5. Conclusions

We have developed a framework for CFD analysis of the melt flow in single-screw plasticizing units in injection molding machines. Within this framework it is possible to analyze the effect of different geometries of the screws metering zone or mixing heads on the melt homogeneity in the screw chamber. Using these methods as a prototyping tool will certainly reduce the prototype costs in engineering as well as the time to market of newly developed screw / mixing head geometries in injection molding.

References

[1] Z. Tadmor, C. G. Gogos, Principles of Polymer Processing, 2nd Ed., John Wiley & Sons, New Jersey, 2006
[2] C. Rauwendaal, Polymer Extrusion, 4th Ed., Carl Hanser, Munich, 2001
[3] W. G. Yao, S. Tanifuji, K. Takahashi, K. Koyama, Mixing efficiency in a pin mixing section for single-screw extruders, Polym. Eng. Sci., 2001, 41/6, p. 908–917
[4] W. R. Hwang, T. H. Kwon, Dynamical modeling of chaos single-screw extruder and its three-dimensional numerical analysis, Polym. Eng. Sci., 2000, 40/3, p. 702–714
[5] K. Alemaskin, I. Manas-Zloczower, M. Kaufman, Color mixing in the metering zone of a single screw extruder: Numerical simulations and experimental validation, Polym. Eng. Sci., 2005, 45/7, p. 1011–1020
[6] T. A. Witten, L. M. Sander, Diffusion-Limited Aggregation, a Kinetic Critical Phenomenon, Phys. Rev. Lett., 1981, 47/19, p. 1400
[7] T. H. Wong, I. Manas-Zloczower, Two-Dimensional Dynamic Study of the Distributive Mixing in an Internal Mixer, International Polymer Processing, 1994, 11/1, p. 3–10

S8-L37
Influence of material condition on processing of rubber compounds and its representation in simulation

Michael Fasching (1)*, Walter Friesenbichler (2), Gerald Berger (2)
(1) Polymer Competence Center Leoben GmbH, Roseggerstrasse 12, 8700 Leoben, Austria
(2) Montanuniversität Leoben, Chair of Injection Moulding of Polymers, Otto-Gloeckelstrasse 2, 8700, Leoben
*Michael.fasching@pccl.at

1. Introduction

The injection moulding simulation of rubber compounds is composed by the description of the filling phase and the modeling of the chemical reaction of cross-linking during the heating phase. As rubber compounds are usually manufactured in a discontinuous batch process, material variations play a more important role than in processing thermoplastics. In addition, they are usually highly filled with fillers like carbon black or silica which interact with one and another and with the rubber polymer. In addition, both the material processing and storage prehistory which affect the filler-filler-interactions as well as the material storage period which generally reduces the processing time impede the setup of a suitable rubber injection moulding process.
The objective of this work is to determine the influences of the rubber material condition on the material behaviour and to show the resulting effects on the injection moulding simulation using a NBR compound filled with carbon black.

2. Theory

For the accurate description of the filling phase, the most important factor is the shear viscosity which corresponds to the flow behavior. In this work, the Carreau-WLF is used for the approximation of the viscosity curves.
For the highly filled NBR-compound, the polymer viscosity as well as filler-filler interactions and filler-polymer interactions contribute to the macroscopic shear viscosity [1]. Especially the filler-filler interactions depend on the material processing and storage prehistory. While on the high pressure capillary rheometer (HPCR), a certain stress is always applied on the compound by the inlet flow in the actual measurement capillary, the shear stress prior to the measurement can be varied using a rubber process analyzer (RPA) in a dynamic mode for shear viscosity measurements by applying the Cox-Merz-Rule [2].
To characterize the curing process, the RPA is used with a constant amplitude and frequency. The torque transmitted in phase with the oscillation by the material sample is proportional to the curing degree. The torque values are then scaled to corresponding curing degrees between 0 and 1 to be approximated with the Deng-Isayev-model [3].

3. Experimental

For the measurement of shear viscosity at medium shear rates (100-5000 s^{-1}), a Goettfert Rheograph 2000 HPCR was used with some modifications to standard thermoplastic viscosity measurements. First, the calculation of the entrance pressure loss by applying the Bagley plot was replaced by the pressure losses using an orifice die. Second, data below shear rates of 100 s^{-1} were not

recorded due to the dominance of elastic effects of the rubber compound over the pressure loss of the capillary. For the measurement of the viscosity at higher temperatures, a batch without cross-linking agent was used in addition.
For the measurement of lower shear rates (5-100s^{-1}), a RPA Montech D-RPA 3000 was used. To determine the influence of preshearing on the viscosity, tests were performed both based on ASTM 6204/A and with different shear stress levels (amplitude and frequency of oscillation) prior to the actual measurement.
The cross-linking measurements were performed according to ASTM 5289 with a frequency of 1.67 Hz and an amplitude of 0.502 °. Therefore, fresh material samples as well as samples stored for 4 months at room temperature were compared.
The obtained material data are used in systematic simulations using response surface experiment designs to obtain a set of virtual process parameters for the injection moulding process, depending on the material state including disturbing values such as compound prehistory. By means of a non-linear software optimiser (Minitab 16, Minitab Inc.), the process parameters are optimised in a way, called as robust process, that all predefined quality criteria (scorch, minimum degree of cross-linking, difference of degree of cross-linking between surface and core zones of the part) are suited in the best possible way.

4. Results and discussion

The measurement results show a significant influence of preshearing on the dynamic viscosity measurements of the RPA (figure 1). With the application of stress before the actual measurement, a good correlation to the HPCR could be achieved.

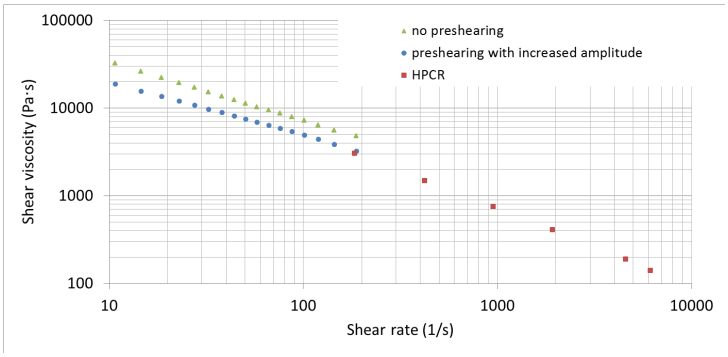

Figure 1. Effect of preshearing on the viscosity measurements of the RPA in comparison to the HPCR of an NBR-compound at a temperature of 140°C

Figure 2 shows the effect of material storage time at room temperature on the incubation time. The reduction of the incubation time that can easily be seen here naturally affects the possible processing parameters as the processing time at one temperature of the compound is reduced substantially.

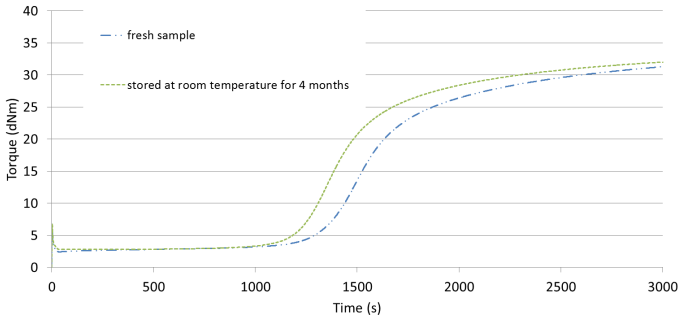

Figure 2. Influence of material storage at room temperature on the curing behavior of an NBR-compound at a temperature of 120°C

Both effects could also be shown performing injection moulding simulations on a test part with the software Cadmould 3D-F by Simcon. Detailed simulation results will be presented in the extended version.

5. Conclusions

It is quite obvious that the material processing prehistory substantially affects the shear viscosity. As both the rubber process analyzer and the high pressure capillary rheometer cannot display the shear stress applied on the material during plastification by the injection moulding screw, new measurement technologies for the direct measurement of viscosity in an injection moulding machine have to be developed, similar to concepts in use for thermoplastics [4,5].
It could be proven that material storage does significantly reduce the incubation time of the investigated rubber compound and thereby it's processing time. It is therefore required to reduce the material and mould temperatures to be able to process aged materials, which leads to a higher injection pressure which the injection moulding machine needs to deliver.

These effects can also be taken into account in injection moulding simulation and therefore this method enables to determine a virtual processing window with a maximum robustness against disturbing values such as material changes.

Acknowledgements
The research work of this abstract was performed at the Polymer Competence Center Leoben GmbH (PCCL, Austria) within the framework of the COMET-program of the Federal Ministry for Transport, Innovation and Technology and Federal Ministry for Economy, Family and Youth with contributions by the Chair of Injection moulding of Polymers, Montanuniversitaet Leoben and company partners SKF Group, Engel Austria GmbH, Simcon kunststofftechnische Software GmbH and Dr. Gierth Ingenieursgesellschaft mbH. The PCCL is funded by the Austrian Government and the State Governments of Styria and Upper Austria.

References
[1] J.L. Leblanc, *Prog. in Poly. Sci.,* 2002, 27, 627-687
[2] W.P. Cox, E.H. Merz, *J. Pol. Sci.* 1958, 28-118, 619-622
[3] A.I. Isayev, M. Sobhanie, J.S. Deng, *Rub. Chem. a. Tech.,* 1988, 61-5, 906-937
[4] W. Friesenbichler, I. Duretek, R. Jegadeesan, R.K. Selvasankar, *Polimery,* 2011, 56, 58-62
[5] W. Friesenbichler, I. Duretek, R. Jegadeesan, *Kunststoffe,* 2010, 3, 37-40

Session 11: Advances in Polymer Analysis, Characterisation and Testing

S11-L38
Mechanical and thermal characterization of the solvent activation effect on cyclo-olfin-polymer surfaces to seal microfluidic chips

Martin Laher (1)*, Dario Borovic (2), Werner Balika (2) and Sabine Hild (1)
(1) Institute of Polymer Science/JKU Linz, Altenbergerstraße 69, 4040, Linz, Austria
(2) Sony DADC Austria AG, BioSciences, Sonystraße 20, 5081 Anif, Austria
*martin.laher@jku.at

1. Introduction
Microfluidic devices for bioanalytical and medical applications are of major interest today. The crucial fabrication step for the production of polymer microfluidic chips is the sealing of a microstructured substrate with a cover plate. The main task thereby is to reach bonding strengths able to withstand internal pressures of up to several bars while maintaining precisely the geometry and functionality of microchannel structures. Different bonding techniques based on surface activation methods like plasma or solvent treatment have been presented in literature [1-4]. A reported successful fabrication process is usually quantified by the achieved bonding strength of the chip. However, a profound mechanical and thermal characterization of the surface activation process itself as well as resulting bonding areas is still missing. In this study, we investigated the time-dependent mechanical and thermal progression of solvent activation effects. Different parameters like activation time and post-treatments are studied. Furthermore mechanical, thermal and chemical imaging of bonding area- and micro-channel cross-sections with nanometer scale resolution are presented. Atomic force microscopy and confocal raman imaging was used. The aim of this study was to explore the reason for non satisfying bondability of activated chips after storage.

2. Theory
The ability to produce microstructured polymer chips by injection molding allows mass-production of polymer based chips to be accessible to industrial scale. Automatization and high reproducability of the injection molding process renders polymer chips to be affordable and disposable after usage. For medical applications cross-contamination and sterility are fundamental points. Analytical purposes like DNA replication and protein separation are much more efficient and faster when processed on microfluidic chips.
The fabrication of these devices in principle consist of the conjunction of a structured substrate with a flat cover plate to form and seal the channels of the chip. The bonding process needs to be irreversible, needs to provide required bonding strength without leakage and needs to avoid any change in channel geometry or transparency required for optical detection systems. Mere thermal bonding by temperature and pressure can not meet these criteria because too high temperatures soften and deform the whole chip whereas too low pressure does not result in adequate bonding and bonding strength. The solution is to provide a very thin layer of micrometer or nanometer thickness on the polymer surface acting as a kind of glue while bulk properties remain unchanged and provide stiffness and geometrical stability. Polymer surfaces can be modified in order to lower the softening temperature, the mechanical stiffness or to increase surface energy. Solvent activation or plasma treatment are applicable techniques for this purpose. Here only solvent activation is studied.
Polymeric material is going to swell when solvent molecules and polymer chains are of similar chemical structure. Solvent molecules penetrate into the polymer network and increase chain segmental mobility. Interdiffusion of polymer chains is facilitated which generates a homogeneous bonding area. Lower softening temperatures of activated surface layers and higher temperature

further help and facilitate this process. Considering the necessity of surface activation effects to assist thermal bonding of polymer surfaces in order to reach required bonding strength provokes the following three questions: 1) what is the effect of solvent exposure on the polymer surface and how can it be characterized? 2) how deep does the solvent penetrate into the surface? 3) can residual solvent be detected in the bonding area or channel cross-sections after sealing the chip? Considering changes in nano- and micrometer thick layers underlines the need for analytical tools able to probe with similar resolution. Atomic force microscopy (AFM) and confocal raman imaging have been chosen in this study.

3. Experimental

Microstructured cyclo-olefin-polymer (COP) chips injection molded and provide by Sony DADC Austria AG, BioSciences, Sonystraße 20, 5081 Anif, Austria have been analyzed throughout this study. A self-built solvent activation device allows reproducible surface treatment of chips for defined activation times. Bonded chips also provided by Sony DADC have been roughly cut with a saw and polished with a razor blade to access cross-sections of micro-channels as well as bonding areas. These regions of interest have been cut with an utra-microtom with freshly prepared glass knives and a diamond knife for finish.

4. Results and discussion

The effect of solvent activation on mechanical properties of cyclo-olefin-polymer surfaces can be monitored and characterized by force-distance measurements with atomic force microscopy (AFM). A special method of AFM with heatable cantilever probes called local thermal analysis (LTA) allows to measure softening temperatures in the nanometer scale. Applying both techniques immediately after solvent activation provides information about the swelling process and its decay with time. Initially lowered softening temperatures, lower hardness and lower stiffness quickly increase with time after activation but do not reach the level of untreated samples anymore. The longer the activation time the more distinct this effect is. Analysis of confocal Raman spectroscopic data reveal that the maximum of residual solvent resides some micrometer below the surface. Longer activation times correlate with higher residual solvent concentration but do show identical distribution profiles of solvent with depth. Annealing or evacuation could not remove sub-surface confined solvent. The penetration depth of the solvent front into the polymer surface could be imaged with LTA and Raman and is in accordance with confocal Raman depth scans. Local thermal analysis as well as Raman imaging of cross-sections of bonded areas could proof the existence of a solvent containing bonding area (figure 1).

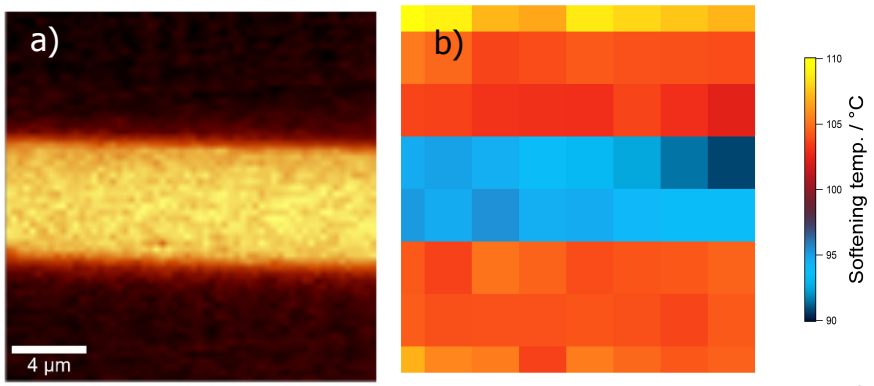

Figure 1. a) Raman image of solvent peak intensity (yellow = high, red = low) of a 20 µm^2 cross-section to the bonding area. **b)** Local thermal softening temperatures of a matrix of 8 x 8 local thermal measurements over a cross-section of 20 µm^2.

5. Conclusions

Atomic force microscopy and confocal Raman imaging showed to be suitable techniques to investigate changes in mechanical and thermal properties of the polymer surface due to solvent activation. Decreased softening points increase quickly after treatment but do not reach the level of untreated samples. Analogous behavior was found for mechanical parameters like contact stiffness and hardness. Increasing activation time increases the concentration of solvent found below the surface. Raman depth scans and cross-section investigations are in good agreement about solvent penetration depths. The existence of confined residual solvent forming a bonding area of several micrometer thickness inside the bonded chip could be proofed and imaged with Raman spectroscopy as well as local thermal analysis.

Acknowledgements

This investigation was financially supported by the Austrian FFG (Project no. 2682742) and Sony DADC Austria AG, BioSciences, Sonystraße 20, 5081 Anif, Austria. Measurements were made on a MFP-3D Stand Alone AFM (Asylum Research).

References
[1] Bhattacharyya et al., Lab on a Chip, 2007, 7, 876-882
[2] L. Brown et al., Lab on a Chip, 2006, 6, 66-73.
[3] S. Miserere et al., Lab on a Chip 2012, 12, 1849-1856.
[4] Wu et al,. Lab on a Chip, 2005, 5, 1393-1398.

S11-L39
Evaluation of Raman spectroscopy to characterize heat ageing in thermoplastic polyurethanes

Katharina Bruckmoser*, Katharina Resch
Materials Science and Testing of Polymers, University of Leoben, Austria
*Katharina.Bruckmoser@unileoben.ac.at

1. Introduction
Thermoplastic polyurethanes (TPU) are widely used in sealing industry due to beneficial mechanical and excellent tribological properties [1,2]. Usage conditions of TPU include exposure to friction heat and elevated temperatures. It is well known that predominately the crystalline morphology of TPU is sensitive to thermal treatment: massive changes in crystallinity or shifting of melting temperature range may occur [3,4]. Moreover, elevated temperatures give rise to chemical decomposition [5]. Ageing mechanisms in TPU are today frequently studied applying spectroscopic methods. Especially IR spectroscopy is well established [6,7]. However, IR spectra cover merely parts of the whole of chemical and morphological information. In recent years, Raman spectroscopy emerged as powerful tool in the characterization of polymeric materials, with specific regard to chemical and crystalline structure. However, only some studies are dealing with Raman spectroscopy of TPU [8,9,10]. Therefore, the overall objective of the present study was to evaluate Raman spectroscopy to characterize heat ageing in TPU. Additionally, in order to quantify spectroscopic effects referring to crystalline morphology, Differential Scanning Calorimetry (DSC) was applied.

2. Experimental
Material
An ester based TPU grade formulated from 4,4`-methylene diphenyl diisocyanate (MDI), 1,4-butanediol (BD) and polycaprolactone (PCL) with a melting temperature of 156 °C and a melting temperature range from 120 to 194 °C was investigated.
Thermal Treatment
Thermal treatment of TPU was performed on a Differential Scanning Calorimeter DSC 821e (Mettler-Toledo AG, Schwerzenbach, CH). Ageing temperatures were systematically varied between 120 to 210 °C. Heat ageing times from 5 to 360 minutes were chosen. After thermal treatment the samples were cooled to ambient temperature with a rate of 50 °C/min to reduce reorganization effects. Experiments were conducted in nitrogen atmosphere. Sample mass was 6 mg ± 1 mg. After spectroscopic investigations DSC thermograms of aged samples were recorded between 23 and 200 °C. For higher heat ageing temperatures the DSC thermograms have been recorded between 23 and 250 °C. A heating rate of 10 °C/min was applied and the experiments were conducted in nitrogen atmosphere. The melting temperature was evaluated according to ISO11357-3.
Spectroscopic Investigations
Fourier Transform Infrared (FT-IR) spectroscopy was performed in Attenuated Total Reflection mode (ATR) within a wavenumber range from 650 to 4000 cm^{-1} at a resolution of 4 cm^{-1} using a diamond crystal (Spectrum One, Perkin Elmer Instruments GmbH, Uberlingen, GER).
Raman spectra of DSC samples were recorded on a Labram confocal Raman spectrometer (Horiba Jobin Yvon GmbH, Bensheim, GER) equipped with a helium neon laser. The line at 632,8 nm with a power of 6 mW on the sample surface was used for excitation. Furthermore, a diffraction grating with 1800 grooves/mm was applied. Position of hole and slit with 500 µm and 200 µm were chosen. Spectra were recorded in the range of 500 to 3200 cm^{-1} using integration time of 20 s with 10 iterations and a 100x objective. Lateral and spectral resolutions of 1 µm and 0,5 cm^{-1} were achieved, respectively. A baseline correction of Raman spectra was applied using the software LabSpec V.5 (Horiba Jobin Yvon GmbH, Bensheim, GER).

3. Results and discussion
In Figure 5a representative ATR and Raman spectra of unaged and heat aged (210 °C, 60 min) TPU are shown. ATR spectroscopy doesn`t reveal any significant differences between the two samples. However, Raman spectroscopy reveals an additional bond at 1154 cm^{-1} for the heat aged sample. Additionally, several hidden bonds around the aromatic stretching vibration of the C-C bonding at 1617 cm^{-1} arise in the heat aged sample, which are responsible for the broadening of this bond. Moreover, heat ageing yields formation of chromophoric groups (represented by bonds at e.g. 1143, 1154, 1587, 1604 and 1643 cm^{-1}), which indicates significant yellowing of the sample [11].
In Figure 5b the melting characteristics of unaged and heat aged sample are shown schematically. Heat ageing provokes considerable changes in crystalline morphology of TPU. Whereas the unaged sample exhibits a melting enthalpy DH_m of 18 J/g, heat ageing at 210°C for 60 min yields in melting enthalpy DH_m of 10 J/g. Furthermore, a shift in melting temperature is observable. In general, for the samples investigated within the present study, systematic interrelationships between melting characteristics and

ageing temperature and time were observed.

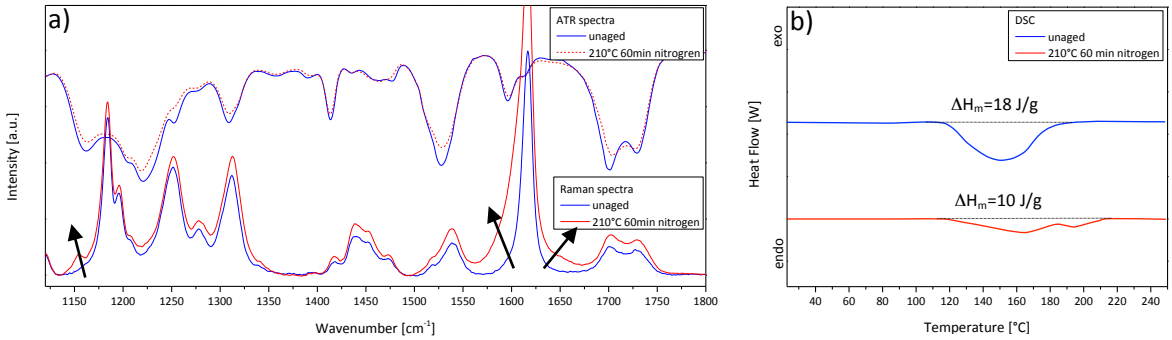

Figure 5: (a) ATR and Raman spectra of unaged and heat aged TPU. (b) DSC characteristics of unaged and heat aged TPU.

4. Conclusions and Outlook

It has been shown that Raman spectroscopy is a powerful method to characterize heat ageing in TPU. Especially chemical ageing mechanisms were detectable. With DSC significant differences in crystallinity were observed for the aged samples. However, a distinct correlation between DSC thermograms and Raman spectra was not established yet. Thus, to get a deeper insight in the morphology of TPU various characterizations including temperature controlled Raman spectroscopy, Light microscopy and Atomic Force microscopy are currently in progress. By this way detailed interrelationships between ageing conditions, chemical degradation mechanisms and changes in morphology (crystalline superstructure and crystallinity) shall be established.

Acknowledgements

The research work of this paper was performed at the Polymer Competence Center Leoben GmbH (PCCL, Austria) within the framework of the COMET-program of the Austrian Ministry of Traffic, Innovation and Technology with contributions by the Chair of Materials Science and Testing of Polymers at the University of Leoben and SKF Sealing Solutions Austria GmbH. The PCCL is funded by the Austrian Government and the State Governments of Styria and Upper Austria.

References

[1] Oertel, G., Polyurethane Handbook, Hanser Publishers, Munich, Germany (1994).
[2] Holden, G., Kricheldorf, H.R., Quirk, R.P., Thermoplastic Elastomers, Hanser Publishers, Munich, Germany (2004).
[3] Seymour, R.W. and Cooper, S.L., DSC Studies of Polyurethane Block Copolymers, J. Polym. Sci. B Polym. Lett., 9 (1971) 689-694.
[4] Seymour, R.W. and Cooper, S.L., Thermal Analysis of Polyurethane Block Polymers, Macromolecules, 6(1) (1973) 48-53.
[5] Montaudo G, Puglisi C, Scamporrino E, Vitalini D., Mechanism of Thermal Degradation of Polyurethanes. Effect of Ammonium Polyphosphate, Macromolecules, 17 (1984) 1605–1614.
[6] Yang, W.P; Macosko, C.W; Wellinghoff, S.T, Thermal Degradation of Urethanes Based on 4,4'-Diphenylmethane Diisocyanate and 1,4-Butanediol (MDI/BDO), Polymer, 27 (1986) 1235-1240.
[7] Rosu, D., Tudorachi, N., Rosu, L., Investigations on the Thermal Stability of a MDI Based Polyurethane Elastomer, J. of analytical and applied pyrolysis, 89 (2010), 152-158.
[8] Ferry, A.; Jacobsson, P.; van Heumen, J.D; Stevens, J.R., Raman, Infra-red and D.S.C. Studies of Lithium Coordination in a Thermoplastic Polyurethane, Polymer, 37 (No. 5) (1996), 737-744.
[9] Janik, H.; Pałys, B.; Petrovic, Z. S., Multiphase-Separated Polyurethanes Studied by Micro-Raman Spectroscopy, Macromolecular Rapid Communications, 24 (No. 3) (2003), 265-268.
[10] Parnell, Shane; Min, K.; Cakmak, M., Kinetic Studies of Polyurethane Polymerization with Raman Spectroscopy, Polymer, 44 (2003), 5137-5144.
[11] Bruckmoser, K., Resch, K., Effect of Heat Ageing on the Morphology of Thermoplastic Polyurethanes, In Proc. Polymeric Materials 2012, Kressler, J., Kausche, H., Deutsche Bibliothek, Halle (Saale), Deutschland (2012).

S11-L40

Non-destructive determination of EVA crosslinking in PV modules by Raman-spectroscopy

Boril S. Chernev (1)*, Christina Hirschl (2) and Gabriele C. Eder (3)
(1) Graz Centre for Electron Microscopy and Research Institute for Electron Microscopy and Nanoanalysis, Graz University of Technology, Steyrergasse 17, 8010 Graz, Austria
(2) CTR Carinthian Tech Research, Europastraße 4/1, 9524 Villach, Austria
(3) Austrian Research Institute for Chemistry and Technology, Franz Grill Straße 5, 1030 Wien, Austria
*boril.chernev@felmi-zfe.at

1. Introduction and Theory

For the determination of the degree of crosslinking, vibrational spectroscopy is a suitable method for a number of polymeric materials. The requirement for the applicability of this detection method is that a reactive group is consumed during the crosslinking reaction step which exhibits a vibrational spectrum clearly distinguishable from that of the formed cross-linked polymer. In polymeric EVA materials, however, the situation is significantly different: EVA initially consists of linear copolymeric chains of ethylene and vinyl acetate and does not contain any dedicated cross linking groups. A 3-dimensional network of an elastomer is build up from the originally linear EVA chains in the presence of a crosslinking agent during the lamination process at temperatures of ~150°C. The crosslinking proceeds via a radical pathway and involves the reaction of the terminal methyls of the acetate groups of the copolymer chains by forming -CH_2-CH_2- bridges between the individual chains leading to the built up of a 3-dimensional network. Thus, upon crosslinking, the relative concentration of the methyl groups is expected to decrease in intensity. However, as the density of crosslinking is quite low in cured EVA, the only expectable spectroscopic change will be that of the relative intensities of the characteristic CH_3/CH_2 bands.
The aim of the work presented here was to find an analytical approach which allows for the non-destructive determination of the degree of crosslinking of EVA embedded within a PV-module in order to permit quality control and pre-delivery inspection of manufactured solar modules.

2. Experimental

EVA test samples (cured foils) with different degrees of crosslinking were manufactured in a standardized process in a manual laminator. The degree of crosslinking of the polymeric sheets was controlled *via* the lamination time. These samples were investigated by Soxhlet extraction (=standard method for the determination of the degree of crosslinking of EVA), thermal analysis (DSC-measurements) and Raman spectroscopy. The Raman spectra were calibrated against (i) the gel content as obtained by the Soxlhet extraction and (ii) the degree of crosslinking as calculated from the DSC-results by applying a chemometric evaluation.
In order to test for the applicability of this analytical approach to measure the crosslinking of EVA embedded within a module, sample laminates (mini modules) were produced with one crystalline solar cell embedded between two sheets of EVA which were covered with a glass front sheet and a polymeric back sheet. These test items were treated in the manual laminator with increasing lamination times to achieve gradually increasing crosslinking. Raman spectra (measured in the confocal mode) of the encapsulated EVA were recorded and their degree of crosslinking subsequently determined by evaluating the spectra by using the chemometric calibration as described above.

3. Results and discussion

The spectral changes in the EVA-Raman spectra with increasing lamination time (which equals to increasing degree of crosslinking) were mainly detected in the CH-stretching vibration region (2800-3000 cm^{-1}). For the chemometric evaluation, however, in addition to the spectral regions of the CH-stretching and deformation vibrations also the fingerprint region was taken into account. The comparison of the Raman data with the results obtained from the thermal analysis (DSC) resulted in a very promising correlation (r^2= 95). Using a calibration of the Raman spectra versus DSC data to determine the progress of crosslinking in the EVA foils embedded in various mini-modules showed an increasing degree of crosslinking with increasing lamination time. However, the statistical spread of the results obtained for different measurement points within one mini module is rather large (especially for short lamination times), for longer lamination times a good accordance was found.
Confocal Raman spectroscopy was identified to be a suitable analytical tool which allows for the in situ determination of the degree of crosslinking of the EVA encapsulate within a PV-Module. However, a rather elaborate calibration of the Raman spectra of the EVA material with a reference method (Soxhlet or DSC) is required. In addition, one has to bear in mind that the calibration is only valid for a given quality of EVA foils, meaning the demand for a new calibration when changing the supplier or the type of EVA used. In order to ensure reliable results, the uniformity of the foils (unchanging composition of the foil, especially with regard to the concentration of the cross-linker) delivered by the supplier has to be verified in an intake control procedure.

Acknowledgements

This investigation was performed as part of the K-Project IPOT (co-funded by the Federal Ministries of Transport, Innovation and Technology (BMVIT) and Economics and Labour (BMWA). The Raman microscope was financially supported by the European Regional Development Fund (EFRE), Graz University of Technology and the Government of Styria.

Session 6: Polymer Composites and Nanotechnology

S6-L41
Microwave response properties of epoxy resin composites filled with nano- and micro-sized carbonaceous materials

S. Bellucci (1)*, A. Cataldo (1), F. Micciulla (1), E. Stefanutti (1), P.Kuzhir (2), A.Paddubskaya (2), A. Plyushch (2), S. Maksimenko (2), V. Fierro (3) and A. Celzard (3)

(1) Frascati National Laboratory, National Institute of Nuclear Physics, Via E. Fermi 40, 00044 Frascati, Italy
(2) Research Institute for Nuclear problems of Belarusian State University (INP BSU), Belarus
(3) IJL – UMR CNRS 7198, Université de Lorraine - ENSTIB, France
*bellucci@lnf.infn.it

The main goal of the present communication is to optimize the way of producing electromagnetic (EM) materials of coating-type providing high EM interference (EMI) shielding effectiveness in microwave frequency range caused by as low as possible content of conductive graphitic inclusions (up to 2 wt.%). For that purpose, a series of composite samples were prepared, based on epoxy resin (Epikote 828), a curing agent called A1 (a modified TEPA) and 0.25, 0.5, 1.0 and 2.0 wt.% content of exfoliated graphite (EG), thick graphene (TG) and commercial single-walled carbon nanotubes (CNT) from Heji for reference. EG was obtained by intercalation of natural graphite flakes, subsequently submitted to a thermal shock. Accordion-like particles were thus produced, leading to a material of low packing density, around 3 g/L [1]. EG particles have the form of distorted accordion-like cylinders, having a typical diameter within the range 0.3 - 0.5 mm, and an aspect ratio around 20. TG was prepared by suspending EG particles in cyclohexane, and submitting the suspension to a series of grinding and ultrasonic dispersion steps [2]. After freeze-drying, disk-shaped particles, having diameter and thickness around 10 and 0.1 µm, respectively, were obtained.
The spectra of S–parameters of epoxy/carbon composites were measured in microwave range (26-37 GHz) with scalar network analyzer. It was found that the highest EMI shielding effectiveness similar to that provided by 20 wt. % of carbon fibers, 7 wt.% of carbon filaments, and 12-20 wt.% of single-walled and multi-walled CNTs [3-4] embedded into polymer matrix, corresponds to Epoxy/EG composites. The average value of power transmitted through the samples is 60%, 30%, and close to 0 for 0.25, 1 and 2 wt.% of EG embedded, respectively (see Fig.1.). Along with relatively high EM performance in microwave range, graphene platelets are much more easily processable than composites filled with CNTs [5]. Concluding, giving the benefit of being lightweight, graphitic materials, especially exfoliated graphite, lead to exceptionally good EM attenuation ability to epoxy resin matrix, along with high electrical conductivity (3 orders of magnitude higher than for epoxy filled with single-walled CNTs [6]).

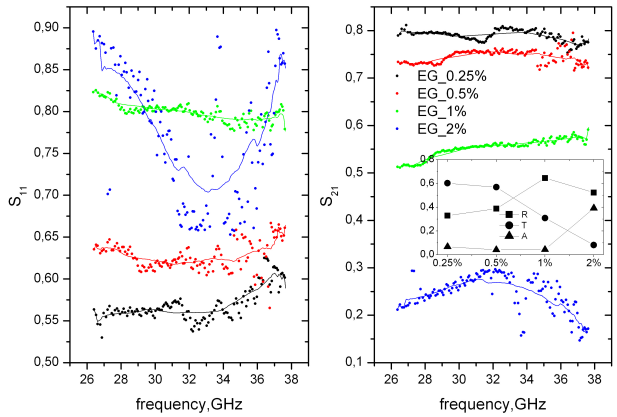

Figure 1: S-parameters vs frequency for epoxy/EG composites with different content of EG inclusions (0.25-2 wt.%). Transmittance, absorbance and reflectance of epoxy/EG at 30 GHz.

Acknowledgements
The work was partially supported by the EU FP7 projects PIRSES-GA-2012-318617 FAEMCAR, FP7-266529 BY-NanoERA.

References
[1] A. Celzard, J.F. Marêché, G. Furdin, Progress in Materials Science 50 (2005) 93-179.
[2] French Patent CNRS N° PCT/EP 92 / 023117.
[3] D.D.L. Chung, Carbon 39 (2001) 279–285
[4] Y. Yang, M. C. Gupta, K. L. Dudley and R. W. Lawrence, NANO LETTERS 5 (2005) 2131-2134
[5] G.D. Bellis, A. Tamburrano, A.Dinescu, M. L. Santarelli, M. S. Sarto, Carbon 49 (2011) 4291–4300
[6] A. Paddubskaya, D. Bychanok, A. Plyushch, et al., Journal of Nanoelectronics and Optoelectronics 7 (2012) 1–6

S6-L42

The influence of montmorillonite organosilane functionalization on the properties of epoxy/montmorillonite nanocomposites

Miroslav Huskić (1,2)*, Majda Žigon (1,2), Marica Ivanković (3)
(1) Center of Excellence PoliMaT, Tehnološki Park 24, 1000 Ljubljana, Slovenia
(2) National Institute of Chemistry, Hajdrihova 19, 1000 Ljubljana, Slovenia
(3) University of Zagreb, Faculty of Chemical Engineering and Technology, Marulićev trg 19, HR-10001 Zagreb, Croatia
*miro.huskic@ki.si

1. Introduction

In the last decades, extensive research has been devoted to organically modified clay minerals as reinforcements for polymers. Their platelet morphology and high aspect ratio lead to improved heat resistance, mechanical, thermal, gas diffusion barrier properties, etc. One of the most widely used clay minerals is montmorillonite (MMT) [1]. MMT and other clay minerals contain active sites such as silanols and exchangeable interlayer cations, typically Na^+ and/or Ca^{2+}. The surface of the MMT layers is hydrophilic, and therefore has to be modified to ensure good intercalation with mostly hydrophobic commercial polymers. The most common method of MMT modification is cation exchange using organic ammonium salts. Since the ammonium salts are not stable at elevated temperatures, at which polymers are commonly processed, the silylation reaction of MMT has attracted a great interest [2]. In this work, MMT was modified by (3-aminopropyl)triethoxy silane (APTES) and used as a nanofiller for epoxy resins. The influence of the reaction time and the aminosilane concentration on the silylation efficiency was studied by means of XRD, FTIR, NMR and TGA. Epoxy-based nanocomposites were prepared with different amounts of silylated MMT and the nanocomposite mechanical properties were compared with those of epoxy systems with commercial organically modified MMT, Nanofil 2® and Nanofil 8®.

2. Experimental

To perform the silylation of MMT (Nanofil 757®) by APTES different reaction conditions were used, varying the reaction time (4h and 24 h) and the amount of APTES (mass ratio MMT:APTES = 1:0.33, 1:0.5, 1:1, and 1.1.5). Silylated MMT (S-MMT) was labeled according to the amount of aminosilane and the reaction time: S0.3 _4h (24h); S0.5_4h (24h); S1.0_4h (24h); S1.5_4h (24h). Nanofil 2® (N2) and Nanofil 8® (N8) are organically modified MMTs intercalated with stearylbenzyldimethyl ammonium chloride and distearyldimethyl ammonium chloride, respectively. Slow curing epoxy resin for infusion was used.
Epoxy-based nanocomposites were prepared with different amounts (1, 3, and 5 weigh parts to 100 weigh parts of epoxy/curing agent matrix) of silylated MMT or commercial organically modified MMT and characterized by dynamic mechanical analysis (DMA), X-ray diffraction (XRD), thermogravimetric analysis (TGA), and ^{29}Si CP MAS NMR.

3. Results and discussion

Silylation of MMT was confirmed by FTIR and ^{13}C CPMAS NMR. With increasing reactant ratio the layer thickness of S-MMT and the quantity of bound silane also increase, which was confirmed by TGA. In the XRD spectra of epoxy/S-MMT nanocomposites the basal signal seems to be shifted to higher angles indicating a partial deintercalation of APTES out of the silicate gallery during the curing process. Decrease in interlayer spacing can be explained by further condensation of ethoxy groups with MMT or between neighboring silane molecules. The intercalation of epoxy resin in the MMT galleries could also be prevented by the cross-linking reaction, which probably takes place during the addition of silylated MMT into the epoxy resin. For epoxy/N2 nanocomposite, the basal signal is shifted to lower angle (from 2θ =4.5° to 2θ= 3°) indicating the formation of intercalated nanocomposite. Contrary to that, no obvious change in position of basal spacing is observed for epoxy/N8 nanocomposite.
The storage modulus of the nanocomposite containing S-MMTs at 25 °C is higher for 5 to 15 % with respect to the pristine epoxy matrix and increases with increasing filler loading. Contrary to that, when 1wt. % of N2 or N8 is added to epoxy resin the modulus is decreased up to 4 %. By increasing N2 and N8 content to 5 % the modulus increases to the level of pure epoxy. The glass transition temperatures of all prepared nanocomposites, determined from the maximum value of the loss modulus (*E*"), are slightly higher (2 to 5 °C) than that of the cured epoxy matrix but do not change with increased S-MMT content.

Acknowledgements

The authors acknowledge the financial support from the Ministry of Education, Science, Culture and Sport of the Republic of Slovenia through the contract No. 3211-10-000057 (Center of Excellence Polymer Materials and Technologies) and the Ministry of Science, Education and Sports of the Republic of Croatia (project 125-1252970-3005: «Bioceramic, Polymer and Composite Nanostructured Materials»)

References

[1] S.S. Ray, M. Okamoto, *Prog. Polym. Sci.* 2003, 28, 1539–1641.
[2] A.B. Bourlinos, D.D. Jiang, E.P. Giannelis, *Chem. Mater.* 2004, 16, 2404-2410.

S6-L43

Effect of different nanomaterials on the durability and mechanical properties of LDPE nanocomoposite

Mohammad Nahid Siddiqui (1)*, Halim Hamid Redhwi (2)
(1) Chemistry Department and Center of Excellence in Nanotechnology (CENT),
(2) Chemical Engineering Department, King Fahd University of Petroleum & Minerals, Dhahran 31261, Saudi Arabia,
*mnahid@kfupm.edu.sa

1. Introduction

Reinforcing fillers are commonly used in polymer formulations to improve the modulus and other mechanical properties of the material. It is the interaction of the filler particle surface with the plastic matrix and the ensuing formation of an interfacial layer that yields the anticipated improvement of properties. Therefore, decrease in average particle size of fillers and the consequent increase in specific surface area is desirable in designing better composites as it increases the polymer/nanofiller interfacial volume. Therefore, thermoplastic nanocomposites often show superior mechanical properties compared to the conventional composites at a lower loading of the filler. Using nanoscale fillers can also improve the weatherability of nanocomposites by providing more efficient light-shielding by the filler particles during outdoor exposure. Higher specific surface area of nano-filler results in more efficient shielding of underlying polymer matrix compared to conventional fillers at the same volume fraction. Superior weatherability of PP/ZnO nanocomposites [1] and PP/double hydroxide nanocomposites [2] has been reported. Rutile-based nanocomposites of polyurethane [3] and poly (methyl methacrylate) [4] also show markedly improved weatherability. ZnO nanocomposite coatings used as a protective lacquer on pine wood surface afforded a level of stabilization even superior to that afforded by even conventional UV absorbers or the hindered-amine light stabilizers (HALS) [5]. However, in clay-based systems such as PP/montmorillonite (MMT), the weatherability of the nanocomposite was poorer compared to the unfilled PP matrix. A similar observation was reported for polyethylene as well. The objective of the present study was to study the mechanical and weathering characteristics of three polyethylene nancomposites based on commercially available nanoscale fillers (montmorillonite clay (MMT), silica and zinc oxide). Part I of the paper addresses the mechanical characteristics of the nanocomposite and the Part II will be on the weatherability of the nanocomposite materials under outdoor and accelerated weathering exposure.

2. Experimental

Three nanoscale fillers were commercially procured and used as-received with no modification: MMT Clay- Cloisite 20 A (Nanocor, Hoffman Estates, IL), Zinc Oxide (Advanced Materials, Manchester, CT), NanoSilica Aerosil OX 50 (Evonik, Addison, IL). Cloisite20 isnatural montmorillonite clay modified with a quaternary ammonium salt. The specific surface areas of the fillers used, according to the manufacturers, are as follows: Closite20=10.9 sq.m./g. [Gonzales et al., 2008]; Nanosilica = 50 sq.m./g; Nano Zinc Oxide =35 sq.m./g.

3. Results and discussion

Incorporation of the nano-fillers into the LDPE even at the 5wt% level results only in small changes in the FTIR spectra of composites. Incorporating filler generally does not chemically affect the polymer and large changes in the infra-red spectra are not anticipated. An overlay of the FT-IR spectra for the different composites shown in Figure 1 is consistent with this expectation. However, comparing the FT-IR spectrum of LDPE-ZnO nanocomposite with the control LDPE sample, the absorption band at 2364 cm^{-1} appears to be more intense in the former spectrum. This peak is generally attributed to sorbed CO_2 on the nanoparticles. Also a new peak at around 500 cm^{-1} is apparent; this is likely from prismatic microstructure of the filler [Abdullah et al., 2009] that obtains a peak at 512 cm^{-1}. In the case of LDPE-nano-SiO_2nanocomposite, the peak at 3730 cm^{-1} is more intense and sharp probably due to the contribution of O-H groups in the silica filler that was incorporated. There is also an intense peak at 1117 cm^{-1} due to C-O functional group. LDPE-nanoclay nanocomposite shows two sharp and intense peaks at 3724 and 3703 cm^{-1}which are likely due to the N-H functional groups in the amine-functionalized clay.

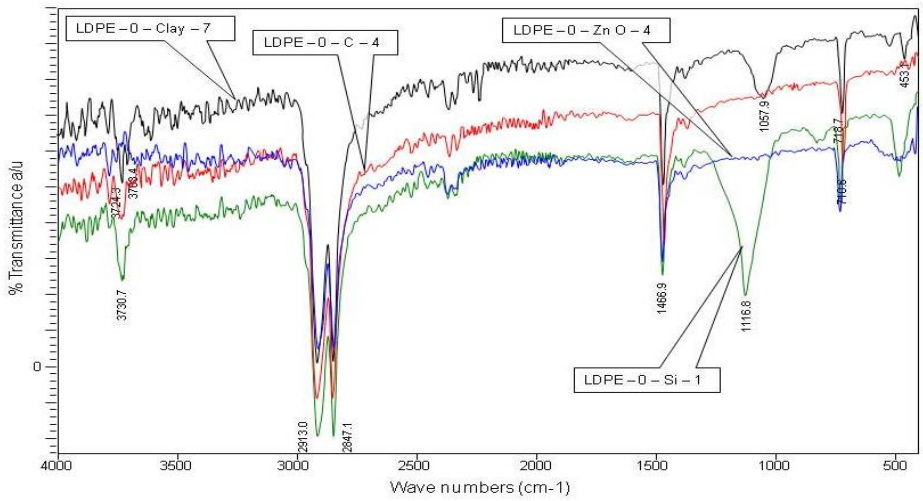

Figure 1. Overlay of FT-IR spectra of control and nanocomposite LDPE samples

The DSC studies of crystalline melting cycles did not show any significant differences between the thermal behaviors of the nanocomposites. In each case, during the first heating the melting started early, to yield a peak at about 112–113 °C. In these instances the change in thermal behavior was attributed to increased nucleation facilitated by the nano-clay particles. The minimal change in the thermal behavior of present nanocomposites is primarily because of the minimal volume fraction of nanofiller used in these compositions and the consequent small fraction of interfacial volume created in the composite.

4. Conclusions

All three nanoscale fillers melt blended into LDPE resulted in reinforcement of the matrix. Calculated reinforcement efficiencies suggest the surface-modified nanoclay filler with also the largest specific surface area, to perform the best with LDPE matrix. However, the nano-zinc oxide filler appears to be the most efficient reinforcing filler even though it has the smallest specific surface area of the fillers studied. It also has a lower hydrophobicity compared to the MMT clay and has no specific filler surface characteristics that would obtain a superior interaction with polyethylene. As expected, untreated silica with its relatively more hydrophilic surface was least efficient in reinforcing. The results show that in addition to filler-matrix interactions, the dispersion of filler in the matrix also must be taken into account in assessing relative efficiencies of reinforcement.

Acknowledgements

The authors would like to acknowledge the support provided by the Deanship of Scientific Research at King Fahd University of Petroleum & Minerals (KFUPM), Dhahran, Saudi Arabia, for funding this work through project number IN100021.

References

[1] Zao H. and Li R.K.Y. (**2006**) *Polymer, 47,* 3207–3217.
[2] Peng D. and Qu B. (**2006**) *Polymer Engineering & Science,* 46(9), 1153–1159
[3] Chen X.D., Wang Z., Liao Z.F., Mai Y.L., Zhang M.Q. (**2007**) *Polymer Testing*, 26:202–8.
[4] Zan L., Liu Z., Fa W. and Peng T. (**2006b**) *Wuhan University Journal of Natural Sciences*, 1(2), 415-418.
[5] Weichelt F., Emmler R., Flyunt R., Beyer B., Buchmeiser M.R., Beyer M. (**2009)** M*acromolecularMaterials and Engineering,* 295(2): 130-136.

S6-L44

Effect of particle surface functionalities on the mechanical properties of magnetoelastomers

Franz Hiptmair (1)*, Zoltan Major (1), Rudolf Haßlacher (2), Sabine Hild (2), Kerstin Schindler (3), Christian Wolfrum (3)

(1) Johannes Kepler University of Linz, Institute of Polymer Product Engineering, Altenbergerstraße 69, 4040 Linz, Austria
(2) Johannes Kepler University of Linz, Institute of Polymer Science, Altenbergerstraße 69, 4040 Linz, Austria
(3) Eckart GmbH, Güntersthal 4, 91235 Hartenstein, Germany
*franz.hiptmair@jku.at

1. Theory

Magnetorheological elastomers (MREs) are SMART materials that consist of an elastomer matrix, reinforced with magnetoactive particles. When subjected to an external magnetic field, MREs exhibit a reversible change of mechanical or rheological properties, which is known as the magnetorheological effect. This behavior makes these materials interesting for industrial applications such as active dampers of acoustic waves or vibrations in mechanical structures [1][2]. Currently MREs, based on non-recyclable silicone or rubber matrices, are dominant because of their straightforward fabrication. Using thermoplastic matrices instead would provide the advantage of repeated processing.

The MRE material behavior is not only influenced by the particle size, shape and their distribution/arrangement (degree of anisotropy) within the elastomeric matrix, but also the by particle-matrix interface, which can be selectively manipulated via different surface functionalities (coatings) [3]. In this work, the effect of various particle coatings on the magnetomechanical properties is investigated for several PDMS and thermoplastic elastomer based MRE types.

2. Experimental

Polydimethylsiloxane (PDMS) and Polyolefin-elastomers (Engage grades, DOW) were selected as matrix materials for the magnetoelastomers. The PDMS materials were mixed with 10 vol% of spherical iron particles of various surface treatments and a crosslinking agent. Afterwards, they were cured in a cast form to prepare specimens. The thermoplastic elastomers were compounded with the filler particles in a mixer and then dog-bone specimens were prepared via die cutting from compression molded sheets.

To study the magnetomechanical behavior of the SMART elastomers, comprehensive dynamic mechanical analysis (DMA) of the MRE specimens was carried out using a BOSE modular test bench, which can apply static or dynamic tensile/compressive and torsional loading. To allow for mechanical tests under magnetic fields, a mangle type permanent magnet Halbach array has been developed and implemented into test bench. The magnetic loading device can apply a field of 430 mT at any direction and is compact enough to fit in a temperature chamber, which makes measurements from -60 °C to +80 °C possible.

The time/frequency, temperature and load dependent viscoelastic properties (stiffness and damping) are varied over a wide range using the selected elastomer matrices. The DMA data acquisition includes the dynamic modulus values from 0.01 to 50 Hz as well as the hysteresis loop graphs in the stress-strain system, which are directly related to the material's energy losses and consequently to the material's damping capacity.

Acknowledgements

This research work was performed within the framework of the K_{APMT} project. The K_{APMT} is funded by the Austrian Government and the State Government of Upper Austria.

References

[1] U. Cakmak, F. Hiptmair, Z. Major, Mech. Time-Depend. Mater., in press.
[2] J. Kaleta, M. Królewicz, D. Lewandowski, Smart Mater. Struct. 2011, 20, 085006.
[3] R. Haßlacher, V. Barroso, S. Hild, F. Hiptmair, Z. Major, K Schindler, C. Wolfrum, Proc. 8th Annual European Rheology Conference (AERC 2013), Leuven, Belgium.

Session 5: Polymers for Technically Advanced Applications and Energy

S5-L45
Advanced printing devices based on the polymer hydrogels

Grigoriy A. Mun*, Ibragim E. Suleimenov, Laura Agibayeva, Maral Tsoy, Rauash A. Mangazbayeva
Al-Faraby Kazakh National University, 71 Al-Farabi ave, 050040 Almaty, Kazakhstan
*mungrig@yandex.ru

1. Introduction

Polymer hydrogels are well-known type of so-called "intelligent materials". They are able to swell in water and water solutions accumulating large amounts of liquid [1-3]. Swelling ratio (the ratio of mass gel containing water to mass of dry gel) may change in wide range, from 10 up to 5 000 times under different external influences. The ability of polymer gels to undergo substantial swelling or collapsing, as function of their environment, is one of the most remarkable properties of these materials. The phenomenon of hydrogel collapse is investigated very widely. The detailed fundamental review of responsive gels is given in the two-volume book of the same name edited by Dusek [4].

Advance applications of polymer gels for different purposes discussed in reports devoted to the problem [5-7]. Nevertheless, main part of polymer gel produced all over the word is currently using in hygienic aims (baby napkins, etc.).

Any commercially significant device actually based on polymer hydrogels using as "intelligent materials" is not described yet. In particular, well-known robotics systems described in [5-7] actually represents some advance application looking in quite far future.

2. Results and discussion

In present article, we propose the simplest construction of printer based on polymer hydrogels, which can be building up in nearest future. The effect of gel collapse [8,9] taking place due to direct electric current is rather simple for understanding. Negatively charged network attract to oppositely charged electrode. This phenomenon may be described correctly by Faraday's law analog, which was firstly obtained experimentally in [10]; its theoretical background was described in [11].

It is known well that hydrogel may swell not only in water but in different water solutions too. In particular, usual acrylic acid gel swells in ink practically in the same manner as in water.

In present report, we are aimed to show, that phenomenon of contraction of hydrogel in water solutions may be employed in printing devices. Moreover, such devices may be made much more effective than existing ones.

Figure 1 illustrates principle of action of proposed method of printing. Paper sheet (1) is placed between gel that swell in ink (2) and electrode (3) having the opposite sigh in respect to the sign of network charge. The second electrode (4) is placed under gel. In initial state (Figure 1a) ink solution does not penetrates in paper, while degree of bonding of liquid y polyelectrolyte network is very high. I.e. paper sheet stays white without additional influences.

Direct current (DC) causes contraction of gel just near electrode (2), and ink solution releases from gel penetrating in paper (Figure 1a). Consequently just near the electrode ink spot is forming.

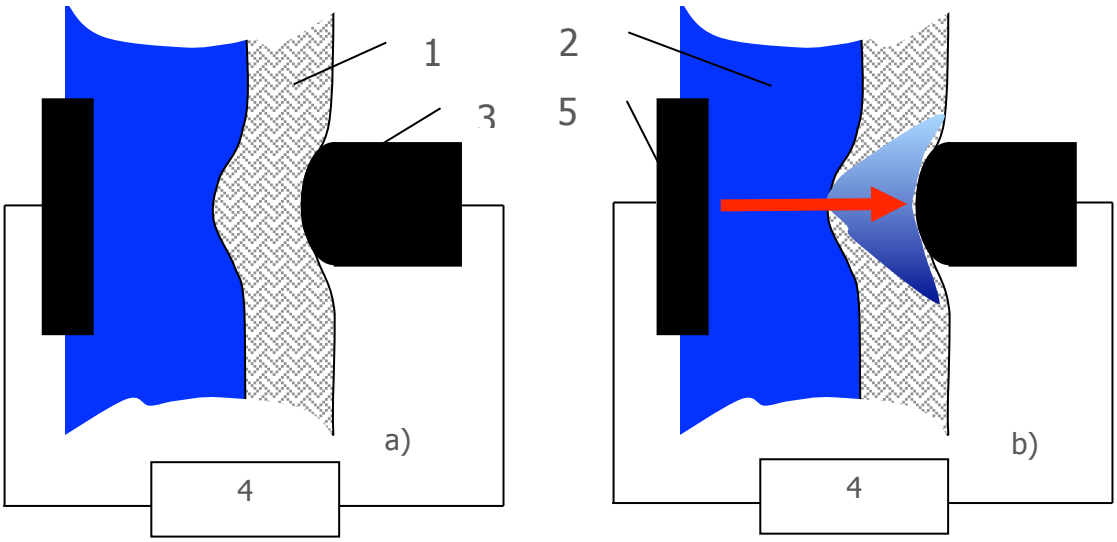

Figure 1. Penetration of ink inside paper sheet under the influence of DC; 1 – paper, 2 – gel plate swelled in ink, 3,4 – positive and negative electrode.

A matrix (Figure 2) contains correspondent set of such electrodes, obviously, will form some image at the paper sheet in the same manner as a well-known ink printer. Electric scheme governing by DC distribution in the matrix may use the same principles as, for example, well-known plasma of liquid crystal screens.

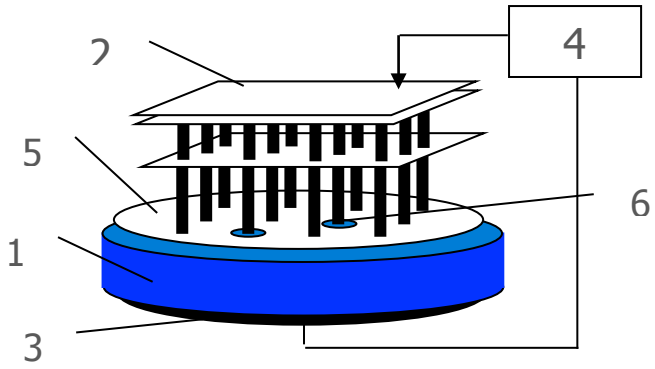

Figure 2. Matrix employed in the method of printing with the help of hydrogel managed by electric current

Experimental model, which was used, consists gel dispersion cowered by membrane that is penetratable for ink solution and DC (1), electrode matrix (2), common electrode placed under gel (3) and DC source (4). This source allow making arbitrary distribution of currents among electrodes of matrix (2).
Paper sheet (5) was placed between electrodes of matrix (2) and gel (1). DC cause appearance of ink spot (6) just near correspondent electrode.
The test experiment by using such experimental model has been carried out. Voltage 2.2 V for all electrodes was used, all the electrodes were identical. Polyacrylic gel produced by ATOFINA, France was used in order to show that proposed method is workable with wide-used hydrogels. It was shown that ink spots are easy visible at the paper sheet. Traces of mechanical influence of electrodes are visible at the same photo too. Comparison of this traces and ink spots shows that printing actually is due to influence of DC rather than any other factors.

2. Conclusions

Thus, the method of printing based on polyelectrolyte hydrogels is actually workable. Preliminary experiments describing in the report shows that some weak parasite ink releasing may take place. Nevertheless, proposed method may be easy improved with the help of interpolymer complexes forming at gel surface. Such complexes [12-14] is widely investigated during last few decades too; they are able to block parasite ink releasing.
The main advantage of proposed method if ability of direct managing by electric current; there is no necessity to use some mechanical systems to organize printing, while the electrode matrix may have the same size as standard paper sheets.

References

[1] T. Tanaka, B. Fillmore, I. Riehie, Phys. Rev. Lett., 1980, 45,20, 1636-1639.
[2] A.Suzuki, Adv. Polym. Sci.1993, 110, 199-237.
[3] S. Saito, M. Konno, H. Inomata, Adv. Polym. Sci. 109, 207-232.
[4] S.Dusek, Adv. Polym. Sci. 199, 109, 3-97.
[5] Y. Osada, J. P. Gong, Prog. in Polym. Sci., 1993, 18, 187-226.
[6] Y. Osada, J. P. Gong, K. J. Sawahata, Macromol. Sci.-Chem. 1991, A28, 1189-1205.
[7] Y. Osada, H. Okuzaki, J. P. Gong, Trends in Polym. Sci. 1994, 2, 61-66.
[8] M. Doi, M.Matsumoto, Y. Hirose, Macromolecules. 1992, 25, 5504-5511.
[9] M. Hirai, T.Hirai, A. Sukumoda, H. Nemoto, Y. Amemiya, K. Kobayashi, T. Ueki, *J. Chem. Soc.-Faraday Trans.* 1995, 91, 473-477.
[10] T.V. Budtova, I.E. Suleimenov, S.Ya. Frencel, Polymer Gels and Networks. 1995, 3, 387-393.
[11] I. E. Suleimenov, I. Pereladov, E. Bekturov, Euroasian Chem. Tech. J. 2002, 243-247.
[12] E. Tsuchida, K. Abe // Adv. Polym. Sci. 1982, 45, 1-99.
[13] E. A. Bekturov, L.A. Bimendina, Adv. Polym. Sci. 1981, 41, 99-163.
[14] G. A. Mun, Z.S. Nurkeeva, V.V. Khutoryanskiy, G.S. Azhgozhinova, E.M. Shaikhutdinov, Kinam Park, Macromol. Rapid Commun. 2002, 23, 965-967.

S5-L46
Hidden holograms in light-sensitive liquid crystal elastomers

M. Gregorc (1), H. Li (2), V. Domenici (3), G. Ambrožič (4), M. Čopič (1) and I. Drevenšek-Olenik (1)*

(1) Faculty of Mathematics and Physics, University of Ljubljana, Jadranska 19 and J. Stefan Institute, Jamova 39, SI-1000 Ljubljana, Slovenia
(2) Nankai University, TEDA APS, 23 Hongda Street, Tianjin 300457, P. R. China
(3) Dipartimento di Chimica e Chimica Industriale, Università degli studi di Pisa, via Risorgimento, 35, 56126 Pisa, Italy
(4) Center of Excellence for Polymer Materials and Technologies, Tehnološki park 24, SI-1000 Ljubljana, Slovenia
*irena.drevensek@ijs.si

1. Introduction

Light-sensitive liquid crystal elastomers (LS-LCEs) exhibit peculiar opto-mechanical properties, which are direct consequences of the specific coupling mechanisms present in these materials [1-3]. When exposed to optical irradiation, they change their size and shape, flip between different shapes, oscillate, or even move on supporting surface. Investigations of possible use of these effects in various devices, such as photo-mechanical transducers, actuators, cantilevers, microfluidic tools, etc., are rapidly expanding.
Another very interesting feature of the LS-LCEs is their large opto-optical response, which is at present still practically unexplored. Our recent investigations show that light-induced modifications of optical refractive index in LS-LCEs provide a possibility for fabrication of optical diffraction structures (volume holograms), which can be easily tuned by various external stimuli [4-6]. In the work reported in this contribution, we focus on light-induced patterning of LS-LCEs in the temperature region close to the nematic-paranematic phase transition, in which several special phenomena, such as a possibility of recording "hidden holograms", are observed. By hidden holograms we mean holograms that can be made either visible or invisible, depending on the external parameters, for instance temperature. Such holograms are very interesting for different watermarking applications.

2. Theory

In order to compute the diffraction efficiency of recorded holographic gratings as a function of temperature or time after the recording process, we use the approach combining paraxial wave equation to describe propagation of the optical electromagnetic field and nonlinear absorption to describe photo-induced modifications in the recording material. The spatial distribution of the *cis*-isomer as a function of space and time $c_c(\mathbf{r},t)$ is determined by the absorption of the two UV laser beams crossed in the sample. As the modification in the isomer distribution is slow compared to the propagation time of light through the sample, we can model the recording process by first calculating the electromagnetic field $E(\mathbf{r},t)$ in the sample at a certain distribution of the *cis* isomers $c_c(\mathbf{r},t)$, and then calculate the corresponding local change in their distribution $\Delta c_c(\mathbf{r},t)$. The effect of $\Delta c_c(\mathbf{r},t)$ on local absorption coefficient is then taken into account in the calculation of the light field $E(\mathbf{r}, t+\Delta t)$.

3. Experimental

Monodomain side-chain LCE films with a thickness of 150 μm were prepared using a polymer back-bone based on a commercial hydroxymethyl-polysiloxane, which is crosslinked by 1,4-bis (undec-10-en-1-yloxy) benzene used as crosslinker unit. The side-chain LC moieties are composed of usual rod-like mesogens (4-methoxyphenyl 4-(but-3-en-1-yloxy) benzoate) and light-sensitive azomesogens (1-(4-(hex-5-enyloxy)phenyl)-2-(4-methoxyphenyl) diazene) in the ratio of 9:1. Details of the sample preparation and characterization procedures are described in [7].
Optical experiments were performed with films of the size of 3 mm x 5 mm. The upper edge of the film was fixed to the frame on the heating stage, while the lower edge was free to move. However, to prevent bending of the film, the lower edge was loaded with the small weight of a mass of 0.5 g. Diffraction gratings were recorded with either two or four intersecting UV laser beams from an argon ion laser operating at a wavelength of λ_R=351 nm. The average power density of UV light on the sample was around 20 mW/cm^2. The lattice distance Λ of the resulting 1D and 2D transmission gratings was in the range 1 μm < Λ < 15 μm. The polarization of the recording beams was parallel to the nematic director **n**, i.e., the beams were extraordinarily polarized. The diffraction properties of the gratings were probed with a low-power beam from a HeNe laser operating at a wavelength of λ_P=632.8 nm. The probe beam entered the film at normal incidence and was also extraordinarily polarized. The diameter of the probe beam was about 0.2 mm. The intensities of selected diffraction peaks were detected either with a CCD camera or with photodiodes.

4. Results and discussion

Figure 1 shows a result demonstrating a hidden square optical lattice with lattice distance of 13.2 μm. The recording took place in the paranematic phase at T=85°C via 3 min of exposure to the UV intensity pattern. Then the sample was cooled to the T=71°C i.e. to the nematic phase by cooling rate of 2°C/min. Solid circles represent an average diffraction intensity of the first order diffraction peaks (see inset of Fig. 1). In the beginning of the cooling process (at T=85°C) diffracted intensity is very low and rapidly decreases to the background level. The initial diffraction is a consequence of the thermally induced grating structure, which vanishes within about 1 minute. The diffraction intensity then remains zero down to T=80°C. On further cooling it rapidly increases, reaches a pronounced maximum at T=77°C and then decreases. This decrease is a consequence of the two phenomena: (i) cooling below the temperature of the maximum refractive index modulation and (ii) cis to trans back-isomerization of the azomesogens.

Azomesogens used in our material are relatively short-lived, i.e. their relaxation time in the vicinity of T_0 is about 5 min.
Figure 2 shows the calculated value of the square of the depth-averaged first Fourier component of optical dielectric tensor modulation, which is proportional to the diffraction efficiency of the first order diffraction peaks $\eta_{\pm1}=I_{\pm1}/I_0$ (where I_0 is incident intensity of the probe beam and $I_{\pm1}$ the intensity of the first order diffracted beams) as a function of temperature for a grating that was recorded in the paranematic phase. At $T>T_0$ there is practically no diffraction. The sudden increase of the calculated value of $\eta_{\pm1}$ below T_0 is very similar to the abrupt increase of the diffracted intensity observed in the experiment (Fig. 1). Since the cooling rate in the experiment was on the same time scale as the rate of the *cis* to *trans* back-relaxation, the spontaneous decay of the grating during cooling process was also included in the computation. With this addition a very good agreement between the computational and the experimental result is obtained.

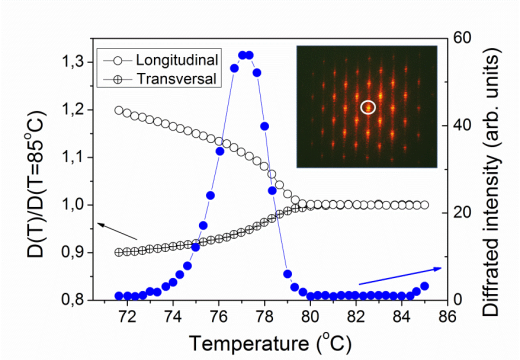

Fig. 1 Average intensity of the first order diffraction peaks (solid circles) and relative length of lattice diagonals (open and crossed circles) as a function of temperature during cooling of the sample from T=85°C to T=71°C. The inset shows a far field diffraction pattern at T=77°C. A white circle designates the transmitted beam.

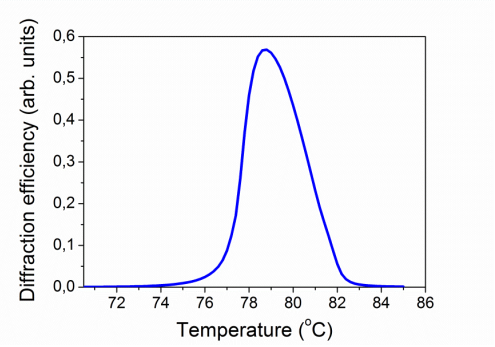

Fig. 2 Calculated diffraction efficiency during cooling from T=85°C to T=71°C.

Acknowledgements
We acknowledge the financial support from the Ministry of Higher Education, Science and Technology of the Republic of Slovenia through the contracts: No. 3211-10-000057 (Centre of Excellence for Polymer Materials and Technologies) for financing the research on synthesis of LS-LCEs; research programme P1-0192 - Light and Matter for financing research on optical properties; and bilateral project BI-CN/11-13-012 for supporting the visit of H. Li to Ljubljana.

References

[1] M. Warner, E. M. Terentjev, in *Liquid Crystal Elastomers,* revised ed.; Oxford University Press: New York, USA, 2007.
[2] H. Finkelmann, E. Nishikawa, G.G. Pereira, M. Warner, *Phys. Rev. Lett.* **2001**, *87*, 015501
[3] D. Corbett, M. Warner, *Liq. Cryst.* **2009**, 36, 1263.
[4] M. Devetak, B. Zupancič, A. Lebar, P. Umek, B. Zalar, V. Domenici, G. Ambrožič, M. Žigon, M. Čopič, I. Drevenšek-Olenik, *Phys. Rev. E* **2009**, *80*, 050701.
[5] M. Gregorc, B. Zalar, V. Domenici, G. Ambrožič, I. Drevenšek-Olenik, M. Fally, M. Čopič, *Phys. Rev. E* **2011**, *84*, 031707.
[6] M. Gregorc, H. Li, V. Domenici, G. Ambrožič, M. Čopič, I. Drevenšek-Olenik, *Materials* **2012**, *5*, 741.
[7] V. Domenici, G. Ambrožič, M. Čopič, A. Lebar, I. Drevenšek-Olenik, P. Umek, B.Zalar, B. Zupančič, M. Žigon, *Polymer* **2009**, *50*, 4837-4844.

S5-L47

Photosensitive polymers in organic electronics: Towards the modulation of the performance of organic devices

T. Griesser (1), M. Edler (1), S. V. Radl (2), W. Kern (1,2), T. Rath (3), G. Trimmel (3), M. Kratzer (4), A. Pavitschitz (4), C. Teichert (4), M. Marchl (5), E. Zojer (5), G. Schwabegger (6), C. Simbrunner (6), H. Sitter (6)

(1) Chair of Chemistry of Polymeric Materials, University of Leoben, A-8700 Leoben.
(2) Polymer Competence Center Leoben GmbH, Roseggerstraße 12, 8700 Leoben, Austria
(3) Institute for Chemistry and Technology of Materials, Graz University of Technology, A-8010 Graz
(4) Institute of Physics, University of Leoben, A-8700 Leoben.
(5) Institute of Solid State Physics, Graz University of Technology, A-8010 Graz
(6) Institute of Semiconductor and Solid State Physics, University of Linz, A-4040 Linz

The tuning of material properties such as surface energy, surface reactivity, refractive index and electric conductivity in thin polymer films is crucial for modern organic electronic and optical devices.
In this study we report on photoreactive polymer films that offer the possibility of a patterned modulation of these properties by means of UV-light. The investigated photoreactions undergo either an isomerisation reaction [1] or a photo-cleavage reaction [2,3] which results in polar and chemically reactive products. These photoproducts increase the surface polarity and surface reactivity in the investigated polymer layers. In this context, we could show that the change in the surface energy influences the morphology of deposited organic small molecule semiconductors which is important for the performance of OTFTs.[3] In addition, the photo-induced change in the chemical reactivity offers the possibility of an immobilization of a luminescent Ru(II) complex in the emission layer of a polyfluorene based OLED, which paves the way towards a selective modulation of its electroluminescence as shown in Figure 1.[1]
Furthermore, we report on a novel polyaniline derivative bearing photosensitive N-formamide groups.[4] UV-illumination of this polymeric material leads to a decarbonylation reaction resulting in polyaniline which can be subsequently protonated to yield the conductive emeraldine salt. Due to the fact that the conductivity depends on the conversion of the photoreaction, a selective adjustment of the conductivity by means of UV-light is feasible. This polymeric material could be used as photo-patternable charge injection layer for structured organic light emitting diodes (see Figure 2).

Figure 1. Photograph of an OLED using a blend of the photosensitive polymer and polyfluorene as emitting layer before (left) and after (right) the photochemical immobilization of the Ru(II) complex.

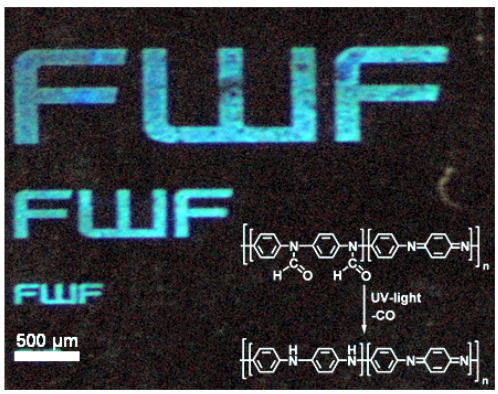

Figure 2. Photograph of a structured OLED using a photo-patternable polyaniline derivative as charge injection layer.

References

[1] T. Köpplmayr, M. Cardinale, T. Rath, G. Trimmel, E. Zojer, S. Rentenberger, W. Kern, T. Griesser, *Macromol. Chem. Phys.* **2012**, *213*, 367.
[2] M. Marchl, M. Edler, A. Haase, A. Fian, G. Trimmel, T. Grießer, B. Stadlober, E. Zojer, *Adv. Mater.* ***2010***, *22*, 5361.
[3] M. Marchl, A. W. Golubkov, M. Edler, T. Griesser, P. Pacher, A. Haase, B. Stadlober, M. R. Belegratis, G. Trimmel, E. Zojer *Appl. Phys. Lett.* **2010**, 96, 213303.
[4] T. Griesser, S. V. Radl, M. Kratzer, A. Pavitschitz, C. Teichert, M. Edler, T. Koepplmayr, T. Rath, G. Trimmel, G. Schwabegger, C. Simbrunner, H. Sitter, W. Kern, *J. Mater. Chem.* **2012**, *22*, 2922.

S5-L48

Polymer science in the development of printed noble metal structures on flexbile substrates using digital and additive manufacturing technologies

Stefan Köstler (1)*, Simon Lenz (2), Daniela Fuchs (2), Andrea Lassenberger (2), Valbonë Mehmeti (2), Heinz Pichler (1), Andreas Rudorfer (1), Kurt Kalcher (2), Volker Ribitsch (2)

(1) JOANNEUM RESEARCH, MATERIALS – Institute of Surface Technologies and Photonics, Steyrergasse 17, 8010 Graz, Austria
(2) Karl-Franzens University Graz, Institute of Chemistry, Heinrichstrasse 28, 8010 Graz, Austria
*stefan.koestler@joanneum.at

1. Introduction

We report on the application of polymer science and –technology in the development of printing inks and processes for noble metal structures. Such noble metal structures on flexible polymer substrates are applied as e.g. electrodes in medical technology or chemical- or biosensors.

Processing of functional materials by printing technologies is a fascinating field of research and development, gaining more and more importance. A great variety of different functional materials such as polymers, nanoparticles, or biomolecules can be printed [1]. Among them, the use of conductive inks for printed electronics is about the most promising and important field. According to a recent forecast, a rapid growth of the printed electronics market is expected, reaching a volume around 50 mio. USD in 2020 [2]. So far, applications were mainly dominated by electrical interconnects for printed circuit boards, solar cells, and displays.

Future trends in the field of printed electronics point towards novel applications taking direct advantage of the unique integration opportunities of printing technologies and printable materials. Such applications are expected on the one hand in printed energy- and data storage and on the other hand in sensors and medical technology. Regarding the applied printing technologies, direct and additive structuring methods like e.g. inkjet or aerosol jet printing increasingly outperform more traditional techniques like screen printing.

Inkjet printing allows the precise and repeatable deposition of small droplets. Digital control allows the printing of complex graphics in high resolution. After the great success of desktop inkjet printers for office use, the potential of the inkjet technology in other fields than graphical printing was recognized in the recent past. Various benefits of inkjet printing lead to a rapid increase of research and implementation in industrial applications. The most striking advantages are the additive, non-contact process, high precision, digital control and relatively cheap and simple equipment.

The relatively new Aerosol-Jet technology is based on the nebulization of an ink to form an aerosol. The aerosol is then transported to the nozzle by a carrier gas stream and focussed on the substrate by a sheath gas stream. Compared to the inkjet technology, smaller aerosol droplets are produced and narrower lines can be printed. Furthermore, an even broader range of different materials and formulations can be applied and structures with higher thickness and aspect ratio can be printed.

Polymer science plays a crucial role in many aspects of inkjet and Aerosol-Jet printing technology. On the one hand, for many applications flexible polymeric substrates (e.g. foils, textiles, etc.) are used. Many of these substrate show rather poor wettability and printability in their pristine state. Therefore, surface pretreatments using e.g. chemical, photochemical, or plasma modification of the polymers are required. In some cases, also the application of polymeric coatings as wetting and adhesion promoting layers is possible. At least equally important is the use of polymeric materials as active components and ingredients for the formulation of noble metal inks.

Polymers are used for example as:

- Polymeric stabilizers for metal nanoparticle based inks
- Responsive polymers as reducing agents for metal-organic decomposition (MOD) inks
- Polymer additives and ink modifiers

We discuss the application of surface modification methods and polymer science in ink formulation in a few examples of gold and platinum inks developed for applications in medical technology and sensors. This includes the formulation of metal nanoparticle as well as metal organic decomposition (MOD) inks. Polymer additives used in such MOD inks can either be simple viscosity modifiers, adhesion promotors or even active compounds and reducing agents. Examples for active stimuli-responsive polymers used in MOD inks are polyaldehydes. Polyaldehydes are a very special class of polymeric materials which can be depolymerized following a well defined unzipping reaction and are converted back into the monomers at moderate temperatures [3]. If applied in MOD printing inks, such polyaldehydes decompose after printing in the subsequent thermal treatment step releasing monomeric aldehydes. These aldehydes can act as reducing agents in order to convert the precursors into metals [4].

2. Experimental

Printing of noble metal inks on polymer substrates with very different surface properties were investigated and compared. A polyimide (Kapton®) and a fluoropolymer (fluorinated ethylene-propylene copolymer, FEP) were investigated and their surfaces were modified using techniques such as different plasma treatments, UV-ozone treatment, and polyelectrolyte coatings. Metal organic decomposition (MOD) inks were prepared from gold and platinum salts and precursors in organic or mixed aqueous/organic solvents and suitable polymeric additives. Gold and Platinum nanoparticle based inks were synthesized by borohydride reduction of the respective metal salt precursor in presence of different stabilizers.

3. Results and discussion

Printability on such different polymer substrates as Kapton and FEP has been achieved using surface modification techniques.
Gold and platinum based nanoparticle and MOD ink formulations were successfully developed and printed using inkjet printing technology. Especially in the MOD inks, polymeric materials such as polyaldehydes were found to be essential components in order to ensure proper printability, adhesion, and reduction of the precursor.
Using these formulations gold and platinum patterns for application as electrodes in e.g. biosensors could be printed on flexible polymer substrates and subsequently transformed into electrically conductive metal films by thermal treatment (Figure 1).

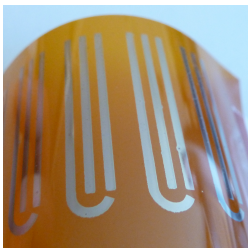

Figure 1. inkjet printed platinum electrodes on flexible polymer substrate (Kapton®) for use as biosensors.

Acknowledgement

The Styrian Government (Department 3: Science and Research) is gratefully acknowledged for funding under the project HTI – JetBioSens and the Austrian Research Promotion Agency (FFG) for funding under the project ESMI.

References

[1] E. Tekin, P.J. Smith, U.S Schubert, Soft Matter, **2008**, 4, 703-713.
[2] R. Das, „Printed, Organic & Flexible Electronics Forcasts, Players & Opportunities 2010-2020," IDTechEx Ltd., 2010.
[3] S. Köstler, Polym. Int. **2012**, 61, 1221-1227.
[4] S. Köstler, D. Wachter, A. Rudorfer, H. Pichler, AT 50929, WO 2011079329, EP 108015520.

Session 11: Advances in Polymer Analysis, Characterisation and Testing

S11-L49
Application of deflectometry for surface inspection of high-glossy injection-molded facing parts

Johannes Macher (1)*, Dieter P. Gruber (1), Gerald Berger (2), Walter Friesenbichler (2)
(1) Polymer Competence Center Leoben GmbH, Roseggerstrasse 12, 8700 Leoben, Austria
(2) Montanuniversität Leoben, Department of Polymer Engineering and Science, Chair of Injection Molding, Otto Glöckel-Straße 2, 8700 Leoben, Austria
*johannes.macher@pccl.at

1. Introduction

Injection molding facilitates the fast and reproducible production of parts with increasingly complex shaping. Nevertheless, even small deviations of the process' parameters can lead to defects on the parts' surface marring their appearance which is becoming one of the major quality criterions for plastic parts presently. Texture, color and illumination are additional factors which influence the results of human evaluation. Solutions exist for the automatic measurement of the perceptibility of defects on diffuse reflecting surfaces [1]. Specular reflecting surfaces, however, are still often manually inspected by looking for distortions in the reflection of a light source or the surroundings. Defects which would be almost invisible on diffuse reflecting parts are easily detected on specular reflecting surfaces [2]. The phase measuring deflectometry, which derives from the reflection grating method, is a surface measurement method enabling the detection of surface defects using structured light provided by a screen or a monitor [3]. In contrast to fringe projection methods the camera is not focused on the surface the pattern is projected on but on the image of the light source which is reflected from the surface. The inspected part becomes part of the optical system and distorts the pattern. Therefore, the imaging of the monitor on the camera sensor depends wholly on the shape of the part.

2. Theory

The basic deflectometric measurement setup mainly consists of a monitor which serves as a light source, the highly reflective sample and a camera. The camera is not focused on the surface of the sample but on the image of the light source which is reflected by the surface. Therefore, the sample can be considered to be part of the optical setup whose geometry influences the image [3, 4].

The monitor generates four sinusoidal patterns which are phase shifted by π/2 for each direction. The images of the patterns which are captured with one camera are mathematically described by

$$b_k = f_0 + f_1 \cdot cos\left(\phi(u) + k \cdot \frac{\pi}{2}\right) \quad k = 0 \dots 3 \tag{1}$$

where f_0 denotes the offset in the image due to backlight illumination, f_1 denotes the captured amplitude and ϕ denotes the targeted phase information. The phase information is calculated from the four images with

$$\phi(u) = \tan^{-1}\frac{b_3 - b_1}{b_0 - b_2} \tag{2}$$

Knowing the periodic length of the monitor sinusoidal patterns in pixel, it is simple to convert the phase information into monitor pixel coordinates for the respective directions.

Since the light of the image is reflected according to the law of reflection, a tilt of the slope in a specific region of a surface would change the imaging of the monitor on the camera sensor and, thus, change the measurement. Consequently, the information about a surface in the measurement is proportional to the first derivative of the surface. This is advantageous for defect inspection since only one derivation of the data is needed to obtain the curvature of the surface which is proportional to the perceptibility of defects [1].

3. Experimental

Successful in-line defect detection of high-quality injection-molded parts requires the inspection of the entire surface. Thereby, curvature of the parts makes the application of additional cameras and thus additional measurement images necessary. However, due to the lack of space only the inspection of one region of the surface is introduced in the examples. The sinusoidal pattern for the measurements was generated using an off the shelf LCD-monitor. Industrial cameras of the type AVT Prosilica 2450C and Matlab by MathWorks, Inc. were used for the acquisition and processing of the measurement images. Figure 1 displays the facing part (developed by Kunststoff-Institut Lüdenscheid and Wittmann Battenfeld GmbH) which was used in the tests as well as one of the fixing aids on the backside of the parts which caused sink marks. Series of parts with comparable perceptibility of the sink marks were produced by varying the holding pressure during the manufacturing process.

a) b)

Figure 1. a) Inspected part (manufactured by Kunststoff-Institut Lüdenscheid and Wittmann Battenfeld GmbH) b) Backside of the part with a fixing aid which causes a sink mark on the facing side of the part

4. Results and discussion

Figure 2 displays one measurement image as well as the curvature of the part which was calculated from the results of the measurement. Only the region of the part which reflects the pattern of the monitor into the camera can be evaluated. The sink mark emerges because of its increased curvature in relation to the background. Comparison with a "golden sample" gives an objective reproducible value for the perceptibility of the sink mark using algorithms which relate the curvature to the perception of human observers.

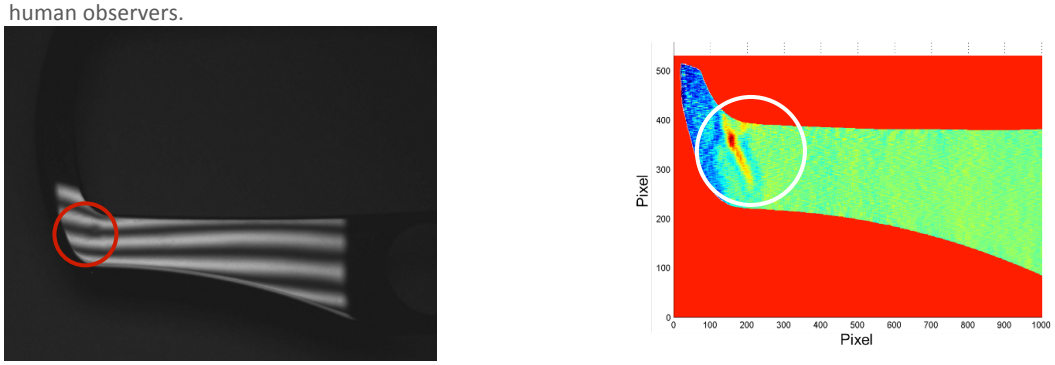

a) b)

Figure 2. a) Measurement image of a single sinusoidal pattern. The pattern is deformed by a sink mark. b) Curvature of the part. The sink mark of the fixing aid is strongly perceptible.

5. Conclusions

Inspection of high-glossy injection-molded facing parts with deflectometric measurement shows considerable potential for the application in in-line measurement setups for high-glossy injection-molded parts. Since the measurements give the first derivative of the parts' surfaces, the curvature which can be related to the perceptibility of surface defects is acquired numerically stable compared to other methodologies. Future work will contain the implementation of the deflectometric measurement in a process line and its combination with additional optical inspection methodologies.

Acknowledgements

The research work of this paper was performed at the Polymer Competence Center Leoben GmbH (PCCL, Austria) within the framework of the COMET-program of the Federal Ministry for Transport, Innovation and Technology and the Federal Ministry of Economy, Family and Youth with contributions by Institute of Plastics Processing, Montanuniversitaet Leoben and Schöfer GmbH, Alicona Imaging GmbH, Hans Höllwart - Forschungszentrum für integrales Bauwesen AG, Payer International Technologies GmbH and Wittmann Battenfeld GmbH. The PCCL is funded by the Austrian Government and the State Governments of Styria and Upper Austria.

References

[1] D. P. Gruber, G. Berger, G. Pacher, W. Friesenbichler, Polymer Testing. 2011, 30, 6, 651–656.
[2] S. Kammel, F. Puente León, IEEE Transactions on Instrumentation and Measurement. 2008, 57, 4, 763-769
[3] H. Rapp and C. Stiller, Forum Bildverarbeitung, 2010
[4] J Balzer and S Werling, Measurement, 2010, 43, 1305–1317

S11-L50

Local thermal analysis as a tool for morphological investigation of propylene-hexene copolymer

Thomas Fischinger*, Martin Laher and Sabine Hild
Institute for Polymer Science, Johannes Kepler University, Altenbergerstraße 69, 4040 Linz, Austria
*Thomas.Fischinger@jku.at

1. Introduction

Thermal analysis methods are generally used to provide important and reliable data about softening temperature of polymeric materials. However, up to now mainly bulk properties of polymers have been detected. Conventional methods reach a limit for applications such as the investigation of crystal structures. Therefore, a method is proposed for nano-thermal characterization of polymers using scanning probe microscopy (SPM) in combination with heatable cantilever probes. In this study, the structure and morphology of randomly distributed isotactic propylene-1-hexene-copolymer (PHCP) were investigated with a focus on local thermal properties. In this article it will be shown that it is possible to investigate the different softening point of α- and γ- structure of PHCP.

2. Theory

Resistively heated cantilever were initially developed for data storage [1, 2] and is now applicable for thermal analysis of polymers [3] allowing a resolution in the nm-scale. SPM permits to engage the probe with a constant force on the polymer surface (Figure 1a), and heating the tip. Due to thermal expansion of the sample, the Z-sensor signal starts to decrease in order to maintain a predetermined cantilever deflection (Figure 1b).

Several groups have developed SPM based techniques to investigate thermal properties of polymers. These are transition temperature microscopy [4], scanning thermal expansion microscopy [5], dynamic localized thermo-mechanical analysis [5], thermally assisted atomic force acoustic microscopy [6] as well as shear modulation force microscopy combined with heated tip atomic force microscopy [7]. All these approaches depend on a reliable calibration of the tip temperature.

In a PHCP, the incorporation of a comonomer acts as a stereo-error in the polymer chain.

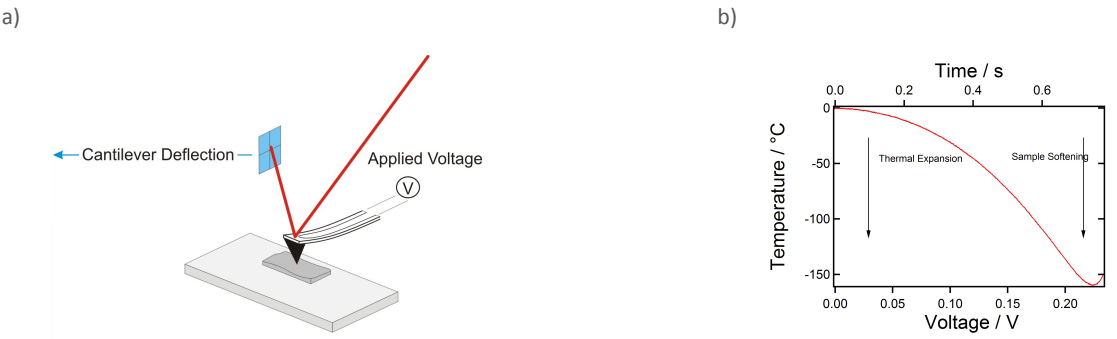

Figure 1. a)Basic experimental set-up for conventional local thermal analysis. b) Z-Sensor signal as a function of time and temperature (heating rate: 2 V^{-1}).

3. Experimental

Local thermal analysis was performed on a MFP 3D SA (Asylum Research) using resistively heated cantilever (ThermaLever A200). Fundamental for this method is a suitable temperature calibration. In this study a standard polymer method is presented using thermoplastic polymers as calibration materials. Defined thermal properties provided by the supplier were cross-checked by differential scanning calorimetry (DSC; Perkin Elmer 8000) measurements. Table 1 summarizes specific transition points of each polymer used for calibration.

Table 1. Overview of transition temperatures of standard samples in use determined by DSC.

Polymer	Molar mass	T_S [°C]
PS-1	1,300	44,1
PS-3	4,000	82,7
PC	45,000	147,5
Nylon 12		170,4
Nylon 6/6		254,4

For temperature correlation 16 measurements on each calibration sample were performed on an area of 20 μm^2 applying a voltage rate of 0.3 Vs^{-1}. Constant contact force, trigger point and substrate temperature ensure a reproducible outcome for calibration.
The PHCP sample granules have been melt-pressed at 180°C between to glass plates to produce a film of about 500 µm with a plain surface. The sample were re-melted and crystallized using a cooling rate of 0.5 °C min^{-1}.

4. Results and discussion

Different methods for temperature calibration of heatable cantilever are still under discussion for local thermal analysis [3, 8-11]. However, methods such as Raman thermometry calibration methodology with an expected uncertainty of 5 °C [8, 10] reported a polystyrene softening point of 120 °C compared to 100 °C measured with bulk ellipsometry. This difference is caused by the fact that measurements in air do not take into account thermal contact resistance. We therefore propose a methodological approach on the basis of the same experimental set-up as the thermal analysis method itself. For this reason systematic errors of measurement coming from different set-up and environmental condition are eliminated.

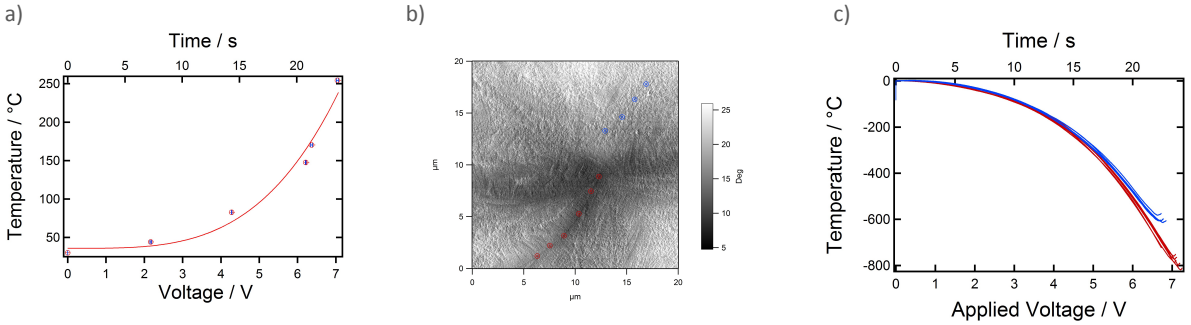

Figure 2. a) Correlation of the applied voltage and melting temperature of the polymer standards. b) Phase image of the PHCP sample with indicated measuring points on the α-form (red) and on the γ-modification (blue). c) Comparison of LTA-curves of the α- and γ-form demonstrating a difference in the softening behavior.

The polypropylene (PP) homopolymers is expected to crystalize a high content of α-form (red), whereas the comonomer should

crystallize with a γ-modification (blue) [12], which can be seen in **Figure 2b**. The aforementioned calibration method is used for the investigation of the isotactic propylene-1-hexene-copolymer. It could be realized for the first time to measure the softening temperature of different modification and lamella.

5. Conclusions

This article as has clearly shown an accurate calibration method for polymer samples. From the research that has been carried out, we can conclude that it is possible to distinguish between α- and γ- crystal structure. Furthermore, exact melting point determinations of single lamella are possible.

References

[1] Vettiger, P.; Cross, G.; Despont, M.; Drechsler, U.; Durig, U.; Gotsmann, B.; Haberle, W.; Lantz, M.; Rothuizen, H.E.; Stutz, R. *IEEE Transactions on nanotechnology* **2002**, *1*, 39–55.
[2] Dürig, U.; Cross, G.; Despont, M.; Drechsler, U.; Häberle, W.; Lutwyche, M.I.; Rothuizen, H.; Stutz, R.; Widmer, R.; Vettiger, P. *Tribology Letters* **2000**, *9*, 25–32.
[3] Souier, T.; Samad, Y.A.; Lalia, B.S.; Hashaikeh, R.; Chiesa, M. *J. Phys. Chem. C* **2012**, *116*, 8849–8856.
[4] Kevin Kjoller, *Transition temperature microscopy*, 2010.
[5] Hammiche, A.; Price, D.M.; Dupas, E.; Mills, G.; Kulik, A.; Reading, M.; Weaver, J.M.; Pollock, H.M. *Journal of microscopy* **2000**, *199*, 180-190.
[6] Oulevey, F.; Gremaud, G.; Semoroz, A.; Kulik, A.J.; Burnham, N.A.; Dupas, E.; Gourdon, D. *Review of Scientific Instruments* **1998**, *69*, 2085.
[7] Gray, T.; Killgore, J.; Luo, J.; Jen, A.K.Y.; Overney, R.M. *Nanotechnology* **2007**, *18*, 44009.
[8] Nelson, B.A.; King, W.P. *Review of Scientific Instruments* **2007**, *78*, 23702.
[9] Zhou, J.; Berry, B.; Douglas, J.F.; Karim, A.; Snyder, C.R.; Soles, C. *Nanotechnology* **2008**, *19*, 495703.
[10] Nelson, B.A.; King, W.P. *Sensors and Actuators A: Physical* **2007**, *140*, 51–59.
[11] Lee, J.; Beechem, T.; Wright, T.L.; Nelson, B.A.; Graham, S.; King, W.P. *J. Microelectromech. Syst* **2006**, *15*, 1644–1655.
[12] Rosa, C. de; Auriemma, F.; Ruiz Ballesteros, O. de; Luca, D. de; Resconi, L. *Macromolecules* **2008**, *41*, 2172–2177.

S11-L51
Cooling rate effects on crystal modification development in ß-nucleated polypropylene

Daniela Mileva (1)*, Markus Gahleitner (1), Davide Tranchida (1), Ayret Mollova (2), René Androsch (2)
(1) Borealis GmbH, St.-Peter-Str 25, 4021 Linz, Austria
(2) Martin Luther University Halle-Wittenberg, 06217 Merseburg, Germany
*daniela.mileva@borealisgroup.com

1. Introduction

The present work provides comprehensive information about the condition of formation and the stability of different polymorphs in isotactic polypropylene (iPP) containing a b nucleating agent. Cooling the quiescent melt at rates lower than 50 K s^{-1} resulted in formation of b-crystals. Solidification at rates between 50 and 300 K s^{-1} let to replacement of the b-phase by a-crystals. Faster cooling was connected with formation of mesophase. Fast scanning chip calorimetry revealed different mechanisms of nucleation at low and high supercooling, confirmed by the different crystal geometry demonstrated by atomic force microscopy analysis.

2. Theory

Isotactic polypropylene (iPP) is a semicrystalline polymer, which ordered phase can adopt several polymorphic modifications. In absence of nucleating agents, cooling of the quiescent melt of iPP at rates lower than 150 K s^{-1} triggers formation of monoclinic lamellar crystals, which are replaced by mesomorphic nodular domains at larger cooling rates. Suppression of crystallization and mesophase formation is achieved in case, the quench is performed below the glass transition temperature of iPP at rates larger than 10^3 K s^{-1} [1,2]. In the present study, the focus is placed on the analysis on the conditions for crystallization, mesophase formation and full vitrification of iPP in presence of b-phase nucleating agent. Furthermore, the thermal stability and reorganization of quenched and slowly cooled b-nucleated iPP were analyzed.

3. Experimental

The commercial b-nucleated iPP grade BE60 from Borealis was analyzed. Films of different cooling history were prepared using a special cooling device described elsewhere [2,3]. Wide angle X-ray scattering (WAXS) was employed for characterization of the crystal structure of films with different thermal history. Atomic force microscopy was used for analyzing the morphology of quenched and slowly cooled films of b-nucleated iPP. Standard differential scanning calorimetry (DSC) and fast scanning chip calorimetry (FSC) were applied for collecting information about the crystallization behaviour of b-nucleated iPP in a wide range of cooling rates from 10^{-1} to 10^3 K s^{-1}.

4. Results and summary

The nucleation efficiency of g-quinacridone was analyzed by FSC. Isothermal crystallization experiments revealed a bimodal distribution of the rate of crystallization as a function of temperature, as shown in Figure 1.

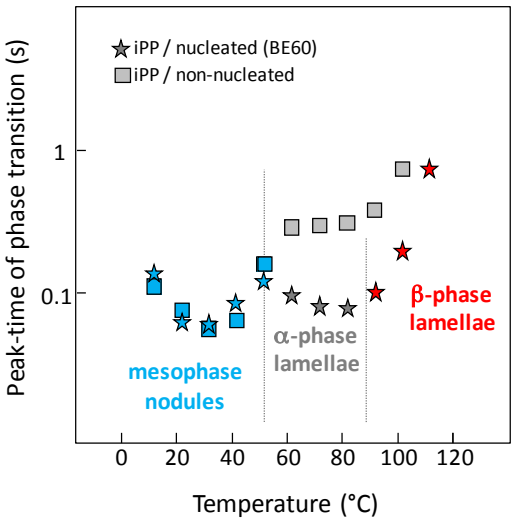

Figure 1. Peak-time of isothermal crystallization of iPP containing b-nucleating agent (stars). For the sake of comparison data of non-nucleated iPP are included [].

Figure 1 shows a plot of the peak-time of phase transition as a function of temperature of isothermal crystallization. The plot contains data collected on nucleated (stars) and non-nucleated (squares) iPP. In both of the cases, bimodal distribution of the peak-times as a function of temperature is observed. The minimum at 60–80 °C is related to formation of crystals via heterogeneous nucleation, while the minimum at 30 °C is related to mesophase formation via homogeneous nucleation. In the temperature range of homogeneous nucleation between the glass transition temperature and around 20 °C, data collected on unmodified iPP and iPP containing b-phase nucleating agent are identical. In other words, the b-phase nucleating agent does not affect the rate of mesophase formation at high supercooling. In contrast, the rate of crystallization at temperatures higher than about 60 °C is remarkably lower in the non-filled iPP. This observation supports the notion that crystallization at high supercooling, at temperatures close to the glass transition temperature, is governed by homogeneous nucleation.

The crystallization behaviour, structure and morphology of beta-nucleated iPP were analyzed at cooling rates close to melt processing. Addition of g-quinacridone invokes formation of b-phase lamellar crystals at rates of cooling below 50 K s^{-1}. The b-phase is replaced by a-phase with preservation of the lamellar morphology at further increase of the cooling rate. Solidification of the quiescent melt at rates larger than 300 K s^{-1} suppresses the crystallization and allows generation of mesomorphic nodular domains. The polymorphism of iPP containing b-phase nucleator, that is, the formation of different ordered structures, can further be controlled by heating, or annealing at elevated temperature. Heating the mesophase leads to their reorganization to a-crystals. The mesophase – crystal phase transition which has been related to a local chain reorganization process within the ordered phase is not affected by the presence of the b-phase nucleator.

References

[1] S. Piccarolo, *J. Macromol. Sci.*, Phys 1992; B31, 501–511.
[2] Q. Zia, R. Androsch, H.-J. Radusch, *Polymer* 2006, 47, 8163–8172.
[3] A. Mollova, R. Androsch, D. Mileva, M. Gahleitner, S. Funari, *E. Polym. J.*, submitted.

S11-L52
Investigation the polymer of environmental capacity of surface water

Rizah Hajdini*
Str Clirimit, 40000 Mitrovice- Kosovo
*tomi-ri@hotmail.com

This paper presents comparative characteristics of integrated performance assessment of water quality of the Sitnica River in the Republic of Kosovo .
The increase of anthropogenic impact on water resources causes increase of adverse natural phenomena and processes. Actually, the human activities that generated global climate change is the cause of the current effects - significant reduction in water content for certain periods of the year, the loss of small streams, reducing the degree of dilution of reused waters that are discharged into water bodies, and as a result – declining of their self-cleaning ability.
Water quality monitoring of the River Sitnica is necessary to assess environmentally balanced condition. The paper presents comparative characteristics of the complex criteria such as Index of Water Pollution (IWP), Environmental Index of Water Quality (EIWQ) and Hydro-ecological Potential (HEP).
Assessment of environmental safety is the likelihood of natural and man-made hydro-ecosystem to maintain resistance under the influence of anthropogenic factors (to maintain positive value of hydro-ecological potential).
In 2010 and 2012 pre-production thermoplastic resin pellets and post-consumer plastic fragments were collected and analyzed for contamination for persistent organic pollutants (POPs). Samples were taken from the different river water, and selected sites in Kosovo. The total concentration of PCBs ranged from 27 to 886 ng/g; DDTs from 21 to 6130 ng/g and PAHs from 23 to 964 ng/g.

Session 6: Polymer Composites and Nanotechnology

S6-L53
New templated hydrophilic / hydrophobic material: Polyacrylic acid hydrogels on porous polyethylene films

Vili Bukošek (1)*, M. A. Smirnov (2), I. Yu. Dmitriev (2), G. K. Elyashevich (2)
(1) Faculty for Natural Sciences and Engineering, University of Ljubljana, Snežniška ul. 5, 1001 Ljubljana, Slovenia
(2) Institute of Macromolecular Compounds, Russian Academy of Sciences, Bolshoi pr. 31, 199004 Saint-Petersburg, Russia
*vili.bukosek@ntf.uni-lj.si

Abstract
Hydrogels of crosslinked polyacrylic acid (PAA) polymers are in focus of research interest as “stimuli responsible” materials due to their unique physical and chemical properties - high swelling, pH sensitivity, capability to swelling/contraction regulated by chemical and electrochemical interactions and high selectivity as membranes for pervaporation of water-organic liquid mixtures. However, PAA gels have a very low mechanical strength. In this work the hydrogel materials were prepared by synthesis of crosslinked PAA onto hydrophobic porous polyethylene (PE) films which provided high mechanical characteristics at maintenance of hydrogel properties as active component of the material.
Porous polyethylene films were obtained in the ecologically safe technological process based on polymer melt extrusion, followed by isometric annealing, uniaxial extension at the room temperature and thermal fixation [1]-[3]. The commercial grade of linear PE (M_w = 170000, M_w/M_n = 4-5, T_m = 132 ^oC) were used. Overall porosity of the films was 45-50%. A strongly developed relief-like surface of these films and through pores (average sizes 200-250 nm) in the film structure provide a high adhesion of the matrix to PAA gel and also give the possibility of the efficient fixing a large amount of PAA inside the matrix. As a result the new effective hydrophilic-hydrophobic film material was formed.
High swelling hydrogels have been fabricated by free-radical copolymerizaion of acrylic acid with bifunctional crosslinkers and ammonium persulfate – sodium sulfate – Moore salt as initiator. In the result of the PAA gel formation on the film surface and also inside the pores the milk-white opaque PE porous film became transparent due to the filling of pores by hydrogel. Thickness of PE matrix and the PE/PAA composite was 15 and 50 μm, respectively. Mass fraction of hydrogel in the material was 80-90%. It is shown that the composites PE/PAA have the higher swelling degree in water, acid and alkali than monolitic PAA gel films.
It was established that monolitic gel PAA films are characterized by the low mechanical strength and high britlleness (break elongation was only 1.5%). Porous PE matrix provides the samples PE/PAA a significant increasing of elasticity - break elongation grows up to 20%. Moreover, PE/PAA samples have the higher elastic modulus than PE support. The structure of PE/PAA samples was investigated by SEM and DMA techniques. It is proved that PAA layer in the composites has the smooth homogeneous defectless surface and completely masks the developed relief of the PE support. DMA curves demonstrate the first transition temperatures of PE in the range -126 ^oC to -115 ^oC and second transition in the range 29 ^oC to 45 ^oC, depends on draw ratio l= 48 to

l= 78, and the orientation degree of supporting membrane. Glass transition of PAA in composites at a frequency of 1 Hz is 62 ^{o}C to 75 ^{o}C depending on the crosslinking PAA.
The work was supported by Bilateral Project (Slovenia/Russia) “Structure and properties of polymer porous films, high swelling hydrogels and their composites” (BI-RU/12-13-032) and Russian Foundation for Basic Research (Grant № 10-03-00421).

References

[1] G.K. Elyashevich, E.Yu. Rosova, E.A. Karpov. Patent of Russian Federation № 2140936, 1997.
[2] V.Bukošek, G.K.Elyashevich. Morphology of conductive composite systems: PE/PPY and PE/PANI. European Polymer Congress- 2007, Portoroz, Slovenia, July 1-7, 2007, p. 255.
[3] G.K. Elyashevich, I.S. Kuryndin, V.K.Lavrentyev, A.Yu.Bobrovsky, V.Bukošek. Physics of Solid State, 2012, v.54, #9, p. 1907-1916.

S6-L54

Synthesis, physical-chemical and physico-mechanical properties of some of copolymers chitosan with acrylates for composition is subjected to biodegradation and soluble in organic solvents

Uryash V.F.*, Smirnova L.A., Kokurina N.Yu., Mochalova A.E., Larina V.N., Kalashnikov I.N., Kashtanov E.A.

Research Institute of Chemistry, Nizhny Novgorod State University, Gagarin prosp. 23/5, 603950 Nizhny Novgorod, Russia
*ltch@ichem.unn.ru

1. Introduction

Biological stability and biodegradability of different polymeric materials is an important environmental and technological problem. There are several aspects of this problem. One of them - the elimination of waste, industrial waste products. It is known that an important role in the destruction of the material belongs to microorganisms, namely microscopic fungi. Capacity of enzyme systems, their diversity and lability allow this group of living organisms used as power sources of various polymers, both natural and synthetic origin. Therefore, in recent years a lot of attention is paid to the preparation of polymer compositions based on natural (chitin, chitosan, starch, cellulose) and synthetic polymers, such as acrylic and methacrylic. The advantage of these materials is their adjustable resistance to microorganisms, which allows to obtain a composition as biopersistence, and on the contrary, easily biodegradable.

In connection with the purpose of the work was to study the thermodynamic properties, physico-chemical, physico-mechanical properties of hybrid composites based on copolymers of polysaccharides, acrylic and methacrylic monomers for constructing biodestruktiruemyh and organic-based materials.

To address this goal are synthesized block- and graft copolymers of polysaccharides (chitosan, starch) with acrylic and methacrylic monomers (methyl methacrylate, oktilmetacrylate, nonilmetacrylate, methyl acrylate, ethylhexyl acrylate) of different composition, measured their heat capacity of 10-330 K, calculated enthalpy, entropy, and function of Gibbs defined the standard enthalpy of combustion and formation, studied temperature relaxation transitions and decomposition, the effects on these characteristics under the influence of biodegradation micromycetes.

2. Theory

The term "biodamage" refers to situations in which living organisms and the presence of their activities cause changes in the structural and functional characteristics of the objects of human or natural origin, used as raw materials [1]. Biodamage occur in the ecological environment and, therefore, are closely related and depend on a number of related environmental factors. In each case, these features are reflected in the biocenotic contacts that occur between the object, its damaging organisms and the environment. These contacts can strengthen or weaken the effect of organisms on an object or even completely block it. The most important components, the presence of which creates a situation biodamage are living organisms that can be a source biodamage impact on the object.

In nature, there are two ways of catabolism of chitin. One way is in the degradation of chitin by the action of chitinases chitooligosaccharids initially to continue to chitobiosy, followed by its transformation into N-acetylglucosamine in the presence of N-acetyl-β-glucosaminidase and glucosoamin the action of N-acetylglucosoamino-deacetylase. The second way, so-called "chitosan" postulated by analogy with the degradation of other natural polymers. Key enzyme in this case is chitindeacetylase, which is responsible for the conversion of chitin chitosan. This enzyme has been found in some microorganisms, particularly fungi. Formed under the influence of chitosan chitosanase glukosoamin degraded to dimers, the latter, in turn, to monomers in the presence of the enzyme - glucosaminidase [2].

3. Experimental

Synthesised block and graft copolymers of chitosan (CTS) and methyl acrylate (MA) of various compositions. As biodestruktor used *Aspergillus terreus*, *Penicillium cyclopium*, and *Aspergillus niger*. Examined the effects of abiotic factors (humidity, low and high temperature) on the physico-chemical properties of the block-copolymer (CTS-MA). As a method of the study of physico-chemical

properties of the composites CTS and MA used differential thermal analysis (DTA) in the area from -190 to 400° C. In the experiments, the standard was a quartz. Sample and reference sample were 0.2-0.3 g. The temperature was measured with a chromel-copel thermocouple with an error of 0.5 degrees. The experiment was conducted in an atmosphere of helium. Heating rate in the experiments was 5 deg./min.

4. Results and discussion

Comparison of the physico-chemical properties of CTS and its block-copolymer with MA and mixed compositions CTS with PMA showed that the polysaccharide has virtually no effect on the second component, while the MA changes the temperature relaxation transitions CTS. MA in the block-copolymer t_β lowers and raises the glass transition temperature ordered microregions CTS. In a mixture of PMA blocks fluctuations CTS pyranose rings, and thus suppresses the β-transition of the latter. In addition, there is a mixture of plasticizing effect of water sorption on the PMA. His tg decreases proportionally to the concentration of H_2O.

Conducted by DTA studies of the impact of micromycetes *Aspergillus terreus* in the block-copolymer and *Penicillium cyclopium* on graft copolymer of CTS with MA showed that the observed changes in the physico-chemical properties of the copolymer. While fungi are processed first CTS as namely its temperature relaxation transitions change the most. An important indicator of the impact on CTS micromycetes it is the disappearance of the exothermic peaks in the thermograms of its destruction and the appearance of these endothermic peaks decomposition PMA.

Climatic factors of aging can be used to enhance bioutilization polymer compositions, both in developing new recipes and creations of new biotechnology to accelerate their bioutilization.

The dependence of the standard enthalpy of combustion and formation of the block-copolymer CTS-MA on its composition.

Acknowledgements

The reported study was partially supported by RFBR, research project No. 13-03-00900 a.

References

[1] V.D. Ilichev. Biodamage, Graduate School, Moskow, 1987, 352 p

[2] S. Dinter, U. Bunger, E. Siefert; in Peter, M.G., Domard, A., Muzzarelli, R.A.A. (Eds.), Advan. Chitin Sci. University of Potsdam, Potsdam, 2000, v.4, p.506-510.

S6-L55
Preparation of UV reactive montmorillonite and characterisation of its nanocomposites with poly(vinyl alcohol)

Jörg Guido Schauberger*, Gisbert Riess, Wolfgang Kern

University of Leoben, Chair of Chemistry of Polymeric Materials, Otto-Gloeckel-Strasse 2/4,8700 Leoben, Austria

*joerg.schauberger@unileoben.ac.at

1. Introduction

The effects of photochemical crosslinking of Poly(vinyl alcohol) (PVA) using iron(III)chloride as crosslinking agent have been well investigated by Kuncser, Filoti et al [1–3]. Also the application of organo-modified and cation-exchanged Montmorillonites (MMT) and their effects on the polymer matrix of PVA are well known [4]. The first aim of the present work was to prepare an iron(III) cation exchanged montmorillonite clay (Fe^{3+}-MMT), by mixing it with an appropriate metal salt. The cation exchange reaction was performed in accordance to Rozenson, McBride and Gerstl [5,6,7].

The second objective of this work was the preparation of UV curable PVA composite containing Fe^{3+}-MMT, with a filler content of up to 50 wt.-%. A major advantage of this new material is an improved of PVA to water in two different ways: strong polymer-filler interactions on the one hand [4] and covalent crosslinking by UV exposure on the other [1,8,9]. A further advantage is the absence of organic photoinitiators which will be beneficial in the field of food packaging and biomedical applications.

2. Theory

Two different reaction mechanisms of photochemical crosslinking of iron(III)chlorine doped PVA have been suggested in literature: Manivannan et al. [10] state that the mechanism of crosslinking is based on a charge transfer from excited Fe^{3+} ions to the polymer subsequent radical generation (see **Figure 6a**). Whereas Kowalonek et al. [11] claim that chlorine radicals are generated during irradiation of $FeCl_3$ and react with PVA to give macroradicals. These macroradicals subsequently recombine (see **Figure 6b**) and form crosslinks. [10,11]

It is assumed that the photochemical crosslinking mechanism of iron(III) doped PVA via charge transition and reduction of Fe^{3+} to Fe^{2+} is the prevalent mechanism (as depicted in **Figure 6a**). This lead us to the intention, that cation exchanged montmorillonite clay loaded with Fe^{3+} could be applied as a nanoscaled filler material which releases iron(III) ions and thus makes additional UV crosslinking of the PVA matrix feasible.

This novel concept will combine physical polymer filler interactions by hydrogen bonding between PVA and the Si-OH groups of the MMT surface and covalent crosslinking of the polymer through UV-induced radical crosslinking.

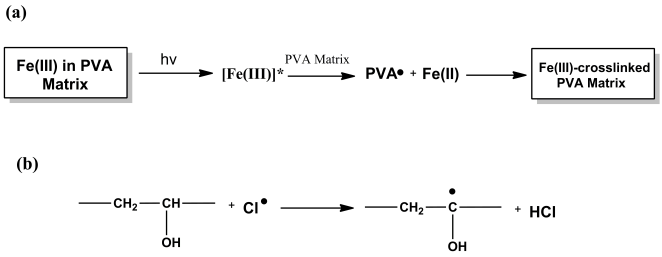

Figure 6: Reaction mechanisms for the photochemical crosslinking of iron(III)chloride doped PVA according to Manivannan [10] (a) and Kowalonek [11] (b).

3. Experimental

The preparation of Fe^{3+}-MMT performed in accordance to known procedures [5,6,7], one part of Na^{+}-MMT clay and two parts of $FeCl_3$-solution were dispersed at room temperature, followed by filtration and repeated rinsing with deionised water until no excess Fe^{3+}-ions were detected in the rinsing fluid by complexation, using potassium thiocyanate. Incorporated Fe-ions were detected by SEM/EDX-measurements. The functionalized MMT was dispersed into PVA with filler contents up to 50 wt.-% with regard to the dry matter. Changes of the absorption of the Fe^{3+}-ions at a wavelength of 360 nm upon UV exposure were observed by UV-VIS spectroscopy.

Thin films were obtained by casting of the dispersions on polypropylene petri dishes followed by drying under a constant air flow at room temperature. The particle distribution in the PVA matrix was evaluated by SEM microscopy and changes of the swelling behaviour of the composite material upon UV irradiation were investigated.

4. Results and discussion

Upon UV exposure of PVA/Fe^{3+}-MMT dispersions the absorption of the liquid sample was decreasing as depicted in **Figure 7a**. This results suggested that a photobleaching effect was occurring, due to the UV-induced reduction of Fe^{3+} to Fe^{2+}. Self-supporting PVA/Fe^{3+}-MMT films were yellowish and hazy, but still permit the passage of light (**Figure 7b**). Scanning electron microscopy of self-supporting PVA/Fe^{3+}-MMT composite films revealed that the modified clay particles were exfoliated in the matrix with perpendicular orientation to the cross section of cryogenically broken samples (**Figure 7c**).

Due to the good intercalation and the resulting exfoliation of the filler particles gel contents ranging between 65 and 75 wt.-% were obtained without UV-exposure. Subsequent UV irradiation lead to a strong increase of the gel content up to 98 wt.-% for composite samples containing of 30 wt.-% Fe^{3+}-MMT (**Figure 7**:.

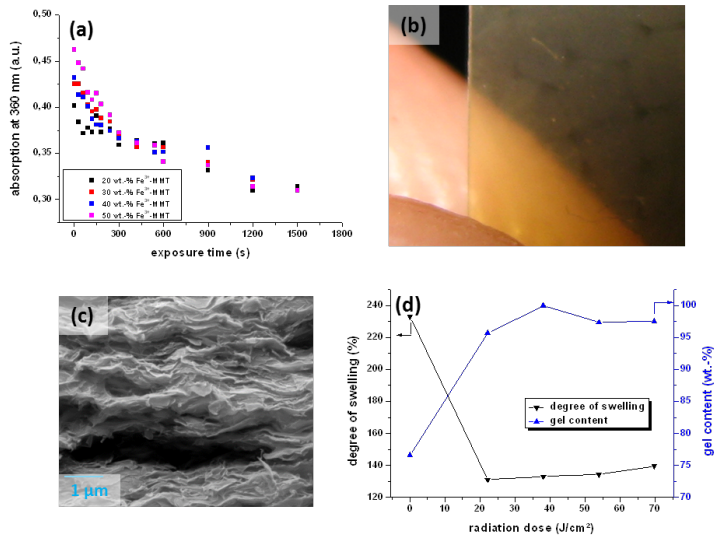

Figure 7: (a) decrease of absorption of aqueous PVA/Fe3+-MMT dispersions upon UV exposure (b) PVA/Fe3+-MMT composite film with 20 wt.-% MMT content (c) SEM micrograph of a broken sample with 50 wt.-% of Fe^{3+}-MMT (d) degree of swelling and gel content of PVA/Fe^{3+}-MMT samples (30 wt.-% filler content)

5. Conclusions

It is demonstrated that it is possible to prepare photoreactive PVA/Fe3+-MMT nanocomposites with filler contents of up to 50 wt.-% of modified clay. The change of absorption at 360 nm can be assigned to a charge transition of the Fe^{3+} to Fe^{2+} ions, which leads to radical generation and further crosslinking of the polymer matrix. Hence non-toxic photoactive species are applied and non-

volatile scission products are formed. This new material can be considered as biocompatible and environmentally benign.

Acknowledgements
The authors want to thank their collegues at the Chair of Chemistry of Polymeric Materials for their support and Mr. Bernhard Sartory for performing the SEM measurements and for sharing his expertise concerning mineralogy.

References
[1] V. Kuncser, G. Filoti, A. Avramescu, R. Podgorsek, M. Biebricher, H. Franke, Investigation of the light induced refractive index changes in Fe:PVA, Journal of Alloys and Compounds 257 (1997) 285–292.
[2] V. Kuncser, A. Avramescu, G. Filoti, P. Rotaru, R. Podgorsek, M. Biebricher, H. Franke, Optical and Mössbauer study of the real time holographic organometallic material Fe:PVA, Journal of Alloys and Compounds 256 (1997) 269–275.
[3] G. Filoti, V. Kuncser, H. Franke, T. Kardinahl, G. Manivannan, Optical induced modifications in thin films of Fe:PVA, Journal of Radioanalytical and Nuclear Chemistry 190 (1995) 315–320.
[4] C.M. Paranhos, B.G. Soares, R.N. Oliveira, L.A. Pessan, Poly(vinyl alcohol)/Clay-Based Nanocomposite Hydrogels: Swelling Behavior and Characterization, Macromol. Mater. Eng. 292 (2007) 620–626.
[5] I. Rozenson, Reduction and Oxidation of Fe3+ in Dioctahedral Smectites—1: Reduction with Hydrazine and Dithionite, Clays and Clay Minerals 24 (1976) 271–282.
[6] M.B. McBride, Perturbation of Structural Fe3+ in Smectites by Exchange Ions, Clays and Clay Minerals 23 (1975) 103–107.
[7] Z. Gerstl, Fe2+-Fe3+ Transformations in Clay and Resin Ion-Exchange Systems, Clays and Clay Minerals 28 (1980) 335–345.
[8] P. Obreja, D. Cristea, E. Budianu, R. Rebigan, V. Kuncser, M. Bulinski, G. Filoti, Effect of dopant on the physical properties of polymer films for microphotonics, Progress in Solid State Chemistry 34 (2006) 103–109.
[9] M. Bulinski, I. Iova, A. Belea, V. Kuncser, G. Filoti, Experimental investigation of the nonlinear optical response in Fe:PVA, Journal of Materials Science Letters 19 (2000) 27–28.
[10] G. Manivannan, O. Nikolov, T. Kardinahl, W. Keune, H. Franke, R. Changkakoti, R.A. Lesssard, Charge transfer phenomenon in optical storage material: Fe3+-doped poly(vinyl alcohol) | Publications: SPIE, SPIE Proc. (1994) 98–109.
[11] J. Kowalonek, H. Kaczmarek, D. Bajer, Surface Properties of Poly(vinyl alcohol) with Iron(III)chloride Before and After UV-Irradiation, Macromol. Symp 295 (2010) 114–118.

S6-L56
Preparation of water vapor barrier coatings employing a water based layer-by-layer approach

Gerald Findenig (1)*, Simon Leimgruber (1), Anna Dunkl (1), Rupert Kargl (1), Karin Stana Kleinschek (2), Volker Ribitsch (1)
(1) University of Graz, Institute of Chemistry, Heinrichstraße 28, AT-8010 Graz, Austria
(2) University of Maribor, Faculty of Mechanical Engineering, Smetanova Ulica 17, SI-2000 Maribor, Slovenia
*gerald.findenig@uni-graz.at

1. Introduction
Due to their renewability, biodegradability and the diminishing availability of fossil resources, the interest of applying biopolymers in the field of packaging has been growing during the last years. However, in comparison to their synthetic counterparts like PET or PP packaging materials derived from biopolymers exhibit poor barrier properties to water vapor. In the scope of current manufacturing processes hydrophobic polymers like polyvinylidene chloride (PVDC) are used to improve the barrier properties to water vapor of such renewable materials. The application of hydrophobic polymers depends on organic solvents and quite harsh chemistry (formaldehyde based resins) for adhesion promotion. The presented study reports the development of an ecologically friendlier alternative utilizing a water-based Layer-by-Layer approach [1, 2]. **Figure 1** shows the basic principle of the applied coating technique.

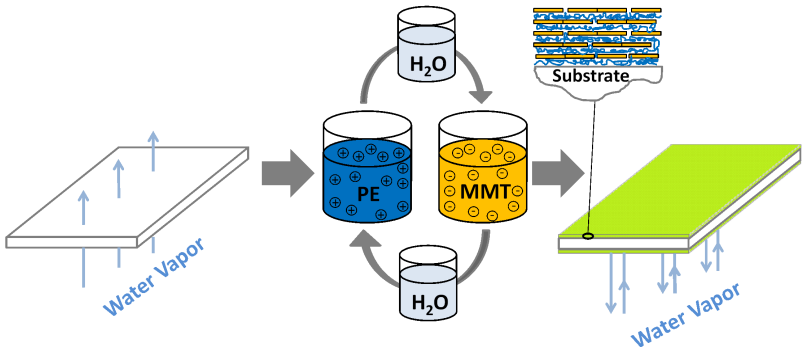

Figure 1. Basic principle of the coating procedure [2].

3. Experimental

Four different polyelectrolytes, namely polyethyleneimine (PEI), polydiallyldimethylammonium chloride (pDADMAC), 2-hydroxy-3-trimethylammonium propyl chloride starch (HPMA starch) and chitosan were used to investigate their capability to prepare water vapor barrier coatings in combination with montmorillonite (MMT) clay platelets on regenerated cellulose films. Furthermore the influence of the ionic strength of the polyelectrolyte solutions, the concentration of the coating solutions/suspensions, the coating technique (dip vs. spray coating) and the coating time on the water vapor transmission was elaborated.

4. Results and discussion

The best barrier properties were achieved when PEI as polyelectrolyte was used. The experiments using HPMA starch also showed a decrease in the water vapor transmission rate, whereas the coatings containing pDADMAC and chitosan did not lead to a significant barrier improvement on the cellulose substrate. A higher ionic strength in the polyelectrolyte solutions lead to thicker coatings and subsequently to better barrier properties. As a result a correlation between the coating thickness and the barrier properties was found. The coatings feature a high degree of transparency, flexibility and mechanical stability.

5. Conclusions

Our work demonstrated the development of flexible water vapor barrier coatings using the LbL-technique with positively charged polyelectrolytes and negatively charged MMT clay platelets. The whole coating process is using water as solvent or dispersing media. Additionally, the films are keeping their properties also after rigorous bending of the substrate due to their brick and mortar structure. The developed surface coatings are suitable for applications like packaging and flexible electronics.

Acknowledgements

The research leading to these results has received funding from the European Union Seventh Framework Programme (FP7/2007-2013) under grant agreement n° 214653. Prof. Thomas Heinze from the University of Jena is highly acknowledged for providing the HPMA starch.

References

[1] G. Decher, J. D. Hong, J. Schmitt, *Thin Solid Films* ***1992***, 210-211, 831-835.
[2] G. Findenig, S. Leimgruber, R. Kargl, S. Spirk, K. Stana-Kleinschek, V. Ribitsch, *ACS Appl. Mater. Interfaces* ***2012***, 4, 3199-3206.

Session 10: Polymer Processing and Recycling

S10-L57
Influence of injection molding process setup on cooling efficiency and its relevance to part geometry

Michael Nindl, Gregor Stadler, Michael Stricker*
Johannes Kepler University Linz, Institute of Polymer Injection Moulding and Process Automation, Altenberger Strasse 69, 4040 Linz, Austria
*michael.stricker@jku.at

1. Introduction

In injection molding, part geometry is one of the main quality factors. The main influencing ones are inner stress, shrinkage and crystallinity for semi-crystalline polymers. These factors are affected by the solidification of the polymer within the injection mold [1]. The solidification takes places, depending on pressure and temperature of the polymer. These result from the process setup and the pvT-properties of the polymer. A main factor influencing shrinkage is the demolding temperature of the injection molded

part [2]. Up to now, no measurement strategy for determination of the mean demolding temperature is known. Therefore, a method based upon calorimetry has been developed to investigate cooling efficiency of injection molding processes.

2. Measurement Equipment

The mean demolding temperature can be measured with a calorimeter. The main components of the developed calorimeter are an insulated container and one or multiple temperature sensors (fig. 1). The container is filled with an appropriate fluid, which temperature is measured by the temperature sensors. For measurement of the mean demolding temperature, the injection molded part is transformed into the calorimeter directly after demolding. After a certain time, thermal equilibrium is reached. The mean part temperature, at the time of entering the fluid, can be calculated by initial and final temperature of the fluid, part and fluid mass and heat capacities of the components [3]. The measured temperature corresponds to the mean demolding temperature.

Part geometry of complex shaped injection molded parts can be investigated with 3D-digitizing system operating on a fringe projection principle with high accuracies. Such a system projects a fringe pattern onto the measuring object. Due to the geometry of the measuring object, the pattern is distorted and acquired by a camera system [4,5]. The geometry of the measuring object is then calculated by triangulation of the acquired image data.

Measurement errors for the calorimeter and the 3D-digitizing systems have been investigated experimentally and theoretically in detail [3,5].

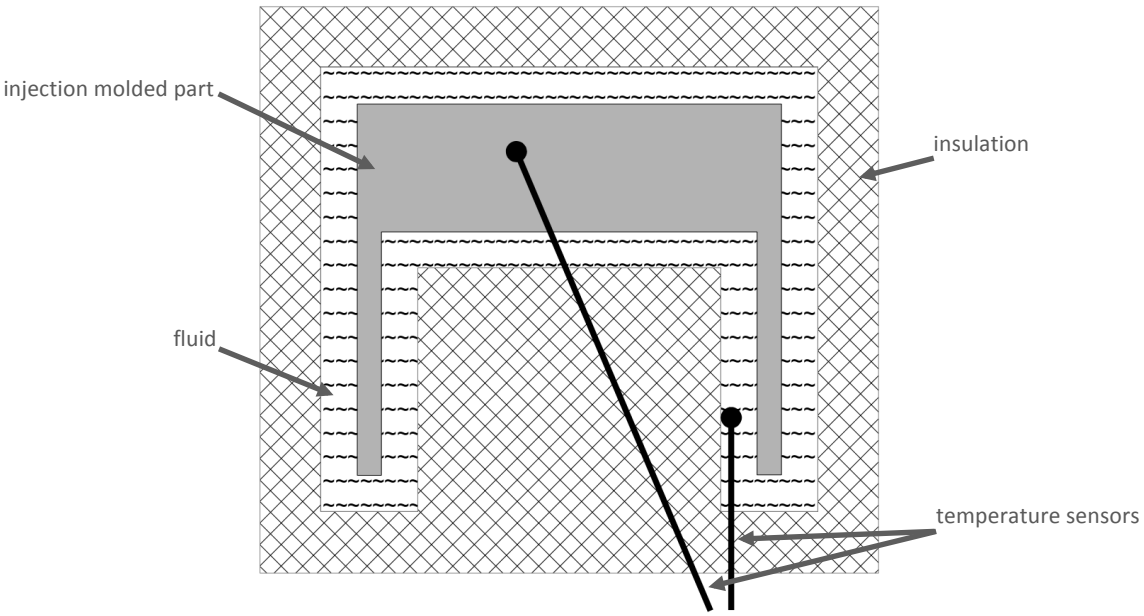

Figure 1. Schematic view of the developed calorimeter

3. Experimental Results

The influence of process setup on the demolding temperature and part geometries has been investigated in a series of molding trials and correlated to each other. The process parameters influencing part geometry or demolding temperature the most correspond in a great measure. Holding pressure, cooling time and mold temperature as the most influencing process parameters and the nonexistence of interactions could be confirmed [6]. Apart from cooling time and mold temperature, holding pressure has a significant impact on demolding temperature.

4. Conclusion and Outlook

In the current work a state-of-the-art 3D-digitizing system is utilized to investigate the impact of process setup on part geometry. As demolding temperature has a major influence on part geometry, measurement of this parameter is of great interest. Therefore, an apparatus for measurement of the demolding temperature has been developed. This system enables to evaluate the efficiency of cooling systems in injection molding processes. Results of calorimetric and geometric measurements have been correlated.

In future work, the calorimetric apparatus will be used for the determination of heat transfer coefficients on the polymer-mould interface, in order to improve accuracy of numerical simulations. Another application for the calorimeter is to evaluate effective thermal diffusivities of polymeric materials.

References

[1] J. Moller, J. Swartz, M. Carlson, R. Alterovitz, Post-Ejection Cooling Behavior of Injection Molded Parts, ANTEC 1993
[2] D.O. Kazmer, Injection Mold Design Engineering, Hanser, 2007
[3] G. Stadler, Entwiclung eines Kalorimeters zur Messung der Entformungstemperatur spritzgegossener Formteile, Bachelor Thesis at Johannes Kepler University Linz, 2012

[4] F. Raschke, M. Stricker, Potenziale in der Werkzeugtemperierung zur Produktivitaets- und Qualitaetssteigerung, Presentation at Von der Vision zur Realitaet im Spritzgiessen, Schwertberg (AT), 2012
[5] N. Nindl, Der Einfluss von Prozessparametern auf die Geometrie eines spritzgegossenen Formteils, Bachelor Thesis at Johannes Kepler University Linz, 2012
[6] S. Kulkarni, Robust Process Development and Scientific Molding: Theory and Practice, Hanser, 2010

S10-L58
Application of D-optimal design of experiments on process optimization of an automotive part

Gerald Berger(1)*, Hans-Jürgen Luger (1), Walter Friesenbichler (1), Irmgard Beytollahi (2), Michael Gierth (3), Paul Filz (4)

(1) Montanuniversität Leoben, Department of Polymer Engineering and Science, Chair of Injection Molding of Polymers, Otto-Gloeckel-Strasse 2, 8700 Leoben, Austria
(2) Magna Auteca AG, Elin Süd Str. 14, A-8160 Krottendorf/Weiz, Austria
(3) Dr. Gierth Ingenieurgesellschaft mbH, Annastr. 17, 52062 Aachen, Germany
(4) Simcon Kunststofftechnische Software GmbH, Schumanstr. 18a, 52146 Würselen, Deutschland
*gerald.berger@unileoben.ac.at

1. Introduction

Mold proving of new plastics parts in industry is commonly done by experimental try and error method. Although a favorable working point, resulting in quality features, e.g. part dimensions, warpage, and weight within their tolerance ranges may be determined, no one knows if this is the best and robust process setting and what are the most influencing effects. Therefore, Design of Experiments (DoE) methods with systematic determination of process influences (input factors) on the part quality (output factors) are applied to find mathematical polynomial process functions. These enable to predict part quality everywhere within the examined test window, even there where no test was done. By using multivariate regression and adequate optimization algorithms a process optimum is found, where every tested part quality parameter is as close to its nominal value as possible. To reduce test time and costs a two-level D-optimal screening DoE combined with replicated center point is applied. This methodology was performed both in reality and in injection molding simulation based on an existing injection molded part and its mold in the frame of funded Cornet project “Advanced Part Sim II” together with Austrian, Slovenian and German industrial and scientific partners.

2. Methodology

Fig. 1 shows the methodology to find a process optimum by means of injection molding simulation or real injection molding experiments.

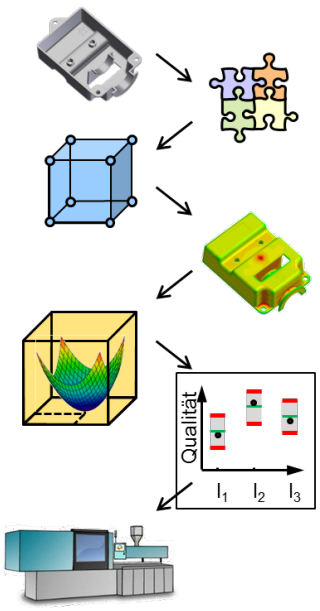

1. Definition of part and quality parameters (geometry, cycle time, surface properties)
2. Problem classification and definition of input parameters (machine settings)
3. Definition of input parameter steps and choice of an appropriate DoE
4. Systematic real part manufacturing or virtual part manufacturing by injection molding simulation
5. Real or virtual measurement of part quality parameters. Calculation of polynomial mathematical models to describe each quality parameter as a function of the input parameters = Mathematical model of the injection molding process.
6. Combined mathematical optimization of all quality parameters to bring them as close as possible to their nominal value. Determination of optimum process point.
7. Validation of models by comparison of predicted and measured quality parameters.

Š **Robust process window.**

Fig. 1: Methodology to find a robust process window [1].

3. Experimental

The chosen part was an existing automotive mirror drive component, made of PET (Fig. 2). The experiments were done on an ENGEL injection molding machine, by systematically varying cooling fluid temperature, nozzle and hot-runner temperature, injection rate, back pressure, holding pressure, holding pressure time, and cooling time in a 10 settings D-optimal Design of Experiments with twice-replicated center point. A similar DoE was done in injection molding simulations using Cadmould 3D-F 6.0 [3] without back pressure.

Two diameters and part weight with known nominal values and tolerances were chosen as quality parameters. They were either measured by GAGE-proved gauge and balance or calculated from the simulation results. Statistical analysis, model building and optimization were done in VARIMOS® [4] and CQC® [5] Continuous Quality Control software.

Tab. 1: DoE parameters and levels (left) and experimental DoE plan (right).

Machine setting/process parameter	Unit	Code	Center level	Level variation
Cooling fluid temperature	°C	A	140	±10
Hot runner temperature	°C	B	307.5	±7,5
Back pressure	bar	C	90	±20
Injection rate	cm^3s^{-1}	D	30.4	±10
Holding pressure	bar	E	600	±200
Holding pressure time	s	F	9	±3
Cooling time after holding p.	s	G	7	±2

	A	B	C	D	E	F	G
1	0	0	0	0	0	0	0
2	-	-	-	-	-	-	-
3	-	-	-	+	+	+	+
4	-	+	+	+	+	-	-
5	-	+	+	-	-	+	+
6	+	+	-	-	+	+	-
7	+	+	-	+	-	-	+
8	+	-	+	+	-	+	-
9	+	-	+	-	+	-	+
10	0	0	0	0	0	0	0

4. Results and discussion

In reality the most important process influence on the both diameters was holding pressure (~ 42%), followed by cooling temperature, hot runner temperature, injection rate and cooling time (16 to 10%). Part weight is determined by holding pressure (73 %), holding pressure time (19%), and injection rate (8%).

The simulation showed nearly the same influence order on the diameters: holding pressure, cooling temperature, holding pressure time, hot runner temperature, and injection rate but with 70%, 12%, 11%, 4%, and 3%, respectively. The simulated part weight is determined by holding pressure, holding pressure time, injection rate, hot-runner temperature and cooling temperature by 38%, 30%, 13%, 12%, and 7%, respectively.

Table 1 compares the optimum simulated process setting, the optimum experimental process setting, and the trial-and-error determined optimum, made by the partner enterprise. Table 1 displays further the resulting quality parameters.

Tab. 1: Comparison of different optimum determination methods and resulting part quality.

Machine setting/process parameter	Unit	Simulated optimum	Experimental optimum	Trial and error optimum
Cooling fluid temperature	°C	132	140	140
HR nozzle/melt temperature	°C	300	307	307
Back pressure	bar	-	90	90
Injection rate	cm^3s^{-1}	20	34	30
Holding pressure	bar	800	550	510
Holding pressure time	s	12	6.0	6
Cooling time after hp	s	0.4	5.0	6.4
Quality results				
Cycle time	s	17.61	16.42	17.61
D_1 +/- 3 x standard deviation s	mm	83.753	83.770 +/- 0.040	83.771 +/- 0.036
D_2 +/- 3 x standard deviation s	mm	83.747	83.750 +/- 0.040	83.748 +/- 0.036
Part weight	g	21.910	20.248 +/- 0.034	20.466 +/- 0.034

5. Conclusions

The systematic DoE experiments suggest minor changes of machine settings to reach a reduction in cycle time of 1.2 s and in part weight of 0.22 g, however, at the cost of a higher dimension variation. The validation of the suggested optimum will be done. The systematic DoE based simulation proposes another process setting optimum, which has to be verified again.

Acknowledgements

The authors are very grateful to the Austrian Research Promotion Agency (FFG), the German AIF and the Slovenian Ministry of

Technology for the public funding and to all 35 company partners, especially Magna Auteca AG for their financial and technical support.

References

[1] M. Gierth, B. Gruemer, *Project documentation of Robust Process Methodology,* Collective Research Network Project "Advanced Part Sim II", 2011.
[2] H.-J. Luger, *Real and virtual process optimization of a mirror drive component*, Master thesis in progress, Montanuniversität Leoben, Austria, 2012.
[3] www.simcon-worldwide.com/pages/en/products/cadmould.php
[4] http://www.simcon-worldwide.com/pages/en/products/varimos.php
[5] www.dr-gierth.de

S10-L59
Fluorescence marker based measurement of the residence time distribution and its statistical moments

Gregor Gerstorfer (1)*, Bernhard G. Zagar (1), Thomas Schmidt (2)
(1) Institute for Measurement Technology, University of Linz, Altenbergerstreet 69, A-4040 Linz, Austria
(2) Tiger Coatings GmbH & Co. KG, Negrellistreet 36, A-4060 Wels, Austria
*gregor.gerstorfer@jku.at

1. Introduction

One of the key parameters in the quality assurance of the polymer extrusion process is the retention or residence time defined as the first statistical moment of the residence time distribution (RTD). The shape of the residence time distribution depends on the combined effect of the flow pattern developed, the mixing mechanisms and the reaction and heat transfer processes. By studying the shape of the RTD one might be able to infer otherwise hidden properties of the extrusion process.
We report on a highly sensitive fluorescence marker based system that allows us to characterize the RTD function to fluorescence levels close to baseline thus enabling to better determine the standard deviation and skewness of the RTD which are thought to also convey important information [1].

2. Theory

In polymer extrusion, the extrusion process can be controlled by several parameters, which all affect the final polymer properties. Those parameters are – beside the design related characteristics of the extruder – the volumetric throughput, the rotational speed of the screws, the temperatures at given zones of the extruder and the configuration of the screw elements, to name just a few. The main tasks of an extruder are the melting and the mixing of the compounds, which have to be kept within tight tolerances. Mixing can be separated into two different kinds known as distributive versus dispersive mixing. Distributive mixing is responsible for having the same amount of each ingredient in each volume element. Dispersive mixing is responsible for homogeneous distribution of all ingredients within each volume element including the process of disaggregating of agglomerates. The mixing quality therefore is an important factor which is not easily accessible via measurement processes.
To classify the mixing behavior of an extruder, several statistical moments of the RTD in combination with other parameters are an important indicator [2, 3, 4, 5]. To obtain the RTD one could resort to simulations or acquire it experimentally. Often, the experiment is used to verify the simulations. For the experimental determination of the RTD different groups report on using some kind of tracer particles [2, 5, 6] injected impulsively at the intake zone of the extruder at known concentrations and measured highly time resolved at the output. The type of tracer specifies the required sensor, for example a dielectric tracer requires a capacitance sensor, PZT powder effects the dielectric permittivity (measured with a dielectric sensor), iron powder effects the magnetic susceptibility (measured via induced currents), color pigments effect the color intensity (measured with a colorimeter), fluorescent dyes under UV light fluoresce in the visible spectrum with concentration dependent intensity (measured by a spectrometer), $CaCO_3$ filler affects the ultrasound attenuation, radioactive tracers can be traced by radiation detectors even in 3D and along the entire extruder, etc. [7, p. 195].
Viewed in a system theoretical way, the RTD can be modeled as the impulse response of a time invariant system with the screw elements representing ideal mixers and ideal conveyors. By convoluting those ideal elements to model their series connection, the RTD can be obtained.

3. Experimental

In this paper fluorescent pigments and a UV–VIS–spectrometer will be employed to determine various statistical moments that define in some sense the shape of the RTD. As tracer a fluorescent pigment is employed, particularly a daylight fluorescent pigment (Swada HMP Lunar Yellow 27) which is moderate in prize and also nontoxic.

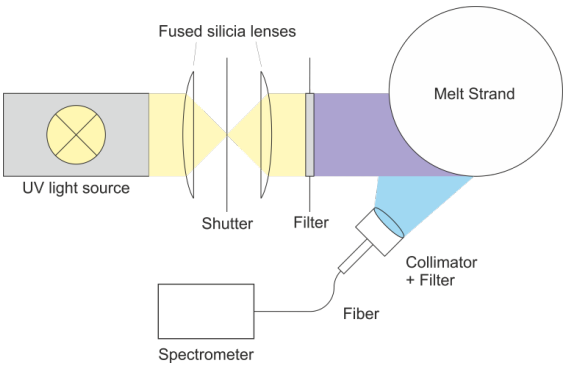

Figure 1 Schematics of the experimental setup

Figure 1 shows the experimental setup, where a UV light source (a high pressure mercury vapor lamp in combination with a UV-pass filter) providing several tens of mW of collimated light to illuminate via an electromechanical shutter the melt strand to induce fluorescence which is picked up and coupled into an optical fiber by a high–aperture collimating optics to be transferred to a high-speed spectrometer for analysis. The spectrometer is a Czerny–Turner spectrometer (Hamamatsu Mini--Spectrometer C10082CAH) with enhanced anti–etaloning and a spectral range from 200nm to 800nm with a spectral resolution of 1 nm. The total setup can be geometrically arranged into a cubicle less than 100 mm on a side and is thus perfectly well suited for inline process control. The acquired spectra are read into MATLAB for subsequent data processing.

4. Results and discussion

Figure 2 shows a set of acquired data (left) and the derived residence time distributions (right) for a range of tracer concentrations but otherwise equal configurations and settings: a Coperion ZSK26 co—rotating twin—screw extruder processing 4 kg/h of pure polyester resin at a screw speed of 800 rpm. The RTDs are approximately equal and the first statistical moment – i.e. the mean residence time – is also approximately equal and amounts to after averaging the different $\hat{t}_{\mathrm{mean}} = (22.90 \pm 0.38)\,\mathrm{s}$ experiments.

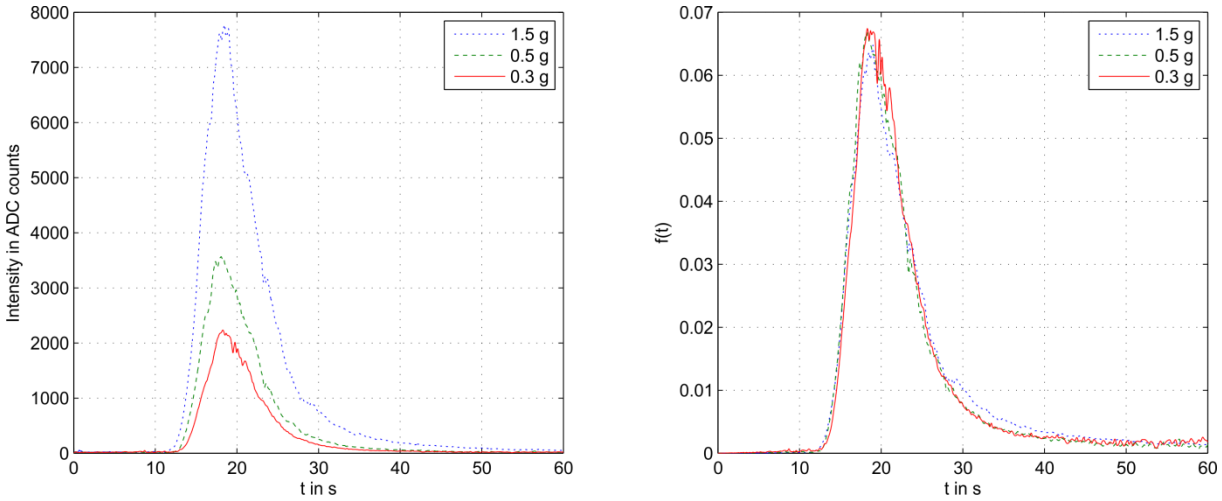

Figure 2 Left: Comparison of acquired data for RTD calculation for varying concentrations of tracer particles (mass added impulsively in g for typical flow rates of 4 to 10 kg/hour). Right: The calculated RTDs are approximately equal for different quantities of tracer and deliver approximately equal mean residence times for each experiment.

5. Conclusions

We could show that a measurement setup compact and small enough to be adapted for an inline quality control is able to deliver reliable residence time distributions within seconds of applying low–cost fluorescence tracers.

Acknowledgements

The authors gratefully acknowledge the partial financial support for the work presented in this contribution by the Austrian Center of Competence in Mechatronics (ACCM).

References

[1] Yijie Gao, Fernando J. Muzzio, Marianthi G. Ierapetritou. "A review of the residence time distribution (RTD) applications in solid unit operations", Powder Technology, 228(0):416–423, 2012.

[2] O.S. Carneiro, J.A. Covas, J.A. Ferreira, M.F. Cerqueira, "On-line monitoring of the residence time distribution along a kneading block of a twin-screw extruder", Polymer Testing 23 (2004) 925–937.

[3] Ajay Kumar, Girish M. Ganjyal, David D. Jones, Milford A. Hanna, "Digital image processing for measurement of residence time distribution in a laboratory extruder", Journal of Food Engineering 75 (2006) pp.. 237–244

[4] P. Cassagnau, M. Courmont, F. Melis, J.P. Puaux, "Study of Mixing of Liquid/Polymer in Twin Screw Extruder by Residence Time Distribution", Polymer Engineering and Science, vol. 45, 2005, pp 926-934

[5] Xian-Ming Zhang, Zhong-Bin Xu, Lian-Fang Feng, and Xiao-Bo Song, "Assessing Local Residence Time Distributions in Screw Extruders Through A New In-line Measurement Instrument", Polymer Engineering and Science, vol. 46, 2006, pp 510-519

[6] Xian-Ming Zhang, Lian-Fang Feng, Sandrine Hoppe, Guo-Hua Hu, "Local Residence Time, Residence Revolution, and Residence Volume Distributions in Twin-Screw Extruders", Polymer Engineering and Science, vol. 48, 2008, pp 19-28

[7] Martin Bastian, "Einfärben von Kunststoffen: Produktanforderungen — Verfahrenstechnik — Prüfmethodik", Hanser, Munich, 2010.

S10-L60
Improving the foamability of a styrene butadiene copolymer

Bernd Geissler (1)*, Anna Uray (1), Stephan Laske (2), Clemens Holzer (2) and Guenter R. Langecker (2)

(1) Polymer Competence Center Leoben GmbH., Roseggerstraße 12, 8700, Leoben, Austria

(2) Montanuniversitaet Leoben, Department of Polymer Engineering and Science, Chair of Polymer Processing, Otto Gloeckel-Strasse 2, 8700, Leoben, Austria

*bernd.geissler@pccl.at

1. Introduction

Due to increasing material prices and the possibility to achieve unique material properties, physical foaming is getting more and more important in the field of plastic processing. During the last 20 years a lot of scientific work has been done in the field of foam extrusion, but still not everything is understood. The complex relationship between material properties, processing conditions, processing equipment and the interaction of the polymer with the blowing agent makes it difficult to achieve the desired foam structure and the required properties. Therefore it is necessary to develop strategies to improve or develop material formulations for physical foaming.

2. Theory

Physical foaming is a complex process, which involves various thermodynamic and kinetic phenomena [1]. Fundamentally all foaming processes consist of four main steps: First of all a foamable composition must be formed. In the next step the phase separation between polymer and blowing agent (cell nucleation) must be initiated due to a thermodynamic instability. This step is followed by the foam growth and the last main step the stabilization of foam structures [2]. The first key component in the development of a material formulation for physical foaming is the choice of a suitable nucleating agent. Normally nucleating agents are inorganic fillers, foreign polymer phases or chemical blowing agents, which are used to archive small cell sizes, high cell density and uniform cell size distribution [3]. According to McClurg [4] ideal nucleating agents are easily dispersable in the polymer matrix, having a uniform size and shape, a non-wetting surface and are plentiful enough to promote heterogeneous nucleation. Besides talc [5] and chemical blowing agents [6], calcium carbonate ($CaCO_3$) [7] is often used as a nucleating agent. The second key components are the rheological properties of the used polymer. Especially the melt strength is very important for the manufacturing of high quality foams. Therefore the addition of high molecular polymers is an often used strategy to improve the foamability [8].

3. Experimental

In this study a blend of two styrene butadiene block copolymer (SBC-blend with a MVR (200 °C/5 kg) of 11 g/10 min and a density of 1.02 g/cm³) and carbon dioxide (CO_2, 99% pure) as blowing agent were used. As nucleating agent three different grades of calcium carbonate ($CaCO_3$) with the same coating, but different particle size and a chemical blowing agent masterbatch were examined. The preparation of the $CaCO_3$ masterbatches was carried out on a co-rotating twin screw extruder with a diameter of 25 mm and a screw length of 40D. To investigate the effect of a higher molecular polymer on the nucleation effect of $CaCO_3$ a fourth masterbatches was manufactured with 20 wt.-% of $CaCO_3$-2 and 80 wt.-% of a higher molecular polystyrene grade (PS with a MVR (200 °C/5kg) of 7 g/10 min). The properties and composition of the used nucleating masterbatches are summarized in table 1.

Table 1. Properties and composition of the nucleating masterbatches

	MB-1	MB-2	MB-3	MB-4	MB-5
Nucleating Agent	$CaCO_3$-1	$CaCO_3$-2	$CaCO_3$-3	$CaCO_3$-2	Endothermic chemical blowing agent (CBA)
d_{50} in µm	0.08	1.8	6	1.8	-
Carrier polymer	SBC-Blend	SBC-Blend	SBC-Blend	PS	LDPE
Amount active ingredient in wt.-%	20	20	20	20	40

For the foaming experiments a Rosendahl RE 45 mm grooved feed single screw extruder with a screw length of 32D and a static mixer was used. For these experiments we used a capillary die with a diameter of 2.5 mm and length of 10.5 mm. The blowing agent was injected by a positive displacement pump at a fixed amount of 0.4 wt.-% CO_2 for each formulation. All master batches were dry blended and carefully diluted with the SBC-Blend to achieve a filler content of 5 wt.% for the $CaCO_3$ and 0.6 wt.% for MB-5. After reaching a steady state the melt was collected and 2 mm thick sheets were prepared for the rheological tests with a vacuum hot press. Next the volume flow rate was measured and the blowing agent injection was started. A sufficient time was given to stabilize the process until no further change was noticeable. For every setting the whole process was repeated three times. The rheological properties of the samples were measured with a rotational rheometer at 180°C with cone plate geometry. Creep recovery measurements were done to determine the material's elasticity at 180°C. The creep recovery test consists of a 300 s creep phase with a constant load of 200 Pa followed by a 700 s recovery phase.
For the morphology characterization the samples were fractured in a brittle manner and the microstructure of the fracture surface was examined with an infinite focus microscope (Alicona IFM) to determine the cell density and the mean cell size. Furthermore the density of the foamed samples was measured with a high precision balance.

4. Results and discussion

Figure 1 represents the time dependent strain of the different formulations during creep and recovery. With increasing particle size of the $CaCO_3$ grade, there is an increase in the calculated zero viscosity. During the recovery phase all formulations shows a similar behavior. The addition of the higher molecular PS based masterbatch had the most significant effect on the zero viscosity. It was possible to improve the foam morphology due to the addition of the different masterbatches (Fig. 2). In this study the cell density increases with increasing filler size. The cell size shows the similar tendency, compared to the results from the creep and recovery experiments. With increasing zero viscosity the cell size decreases. However MB-5 shows a dissimilar behavior, because MB-5 caused no change in the creep and recovery behavior, but led to the best foam morphology. We assume that the nucleation mechanism is different for the mineral fillers and the chemical blowing agent. Furthermore the addition of the high molecular PS at amount of 16 wt.-% improved significant the nucleation rate of $CaCO_3$-2.

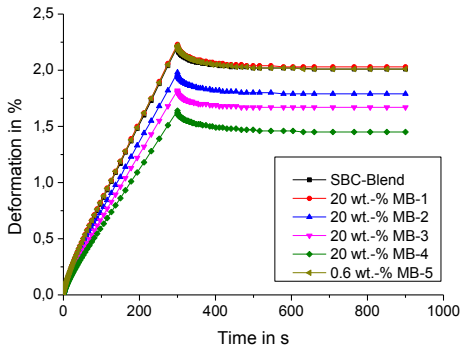

Figure 1. Time dependent strain during creep and recovery for different formulations

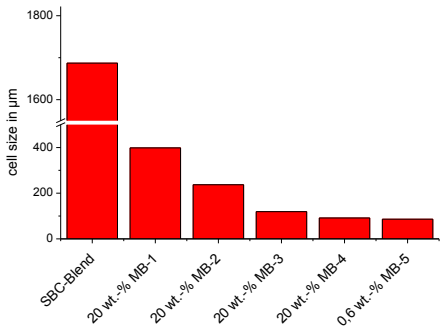

Figure 2. Mean cell size in µm

5. Conclusions

The effect of different nucleating agent masterbatches on the foaming behavior of a SBC-blend was studied. It was found out that the nucleation rate increases with increasing particle size of the $CaCO_3$ grade and that the creep and recovery experiments correlate with the foaming results for the mineral fillers. However this was not found for the chemical blowing agent masterbatch due to a different nucleating mechanism. The results showed that the increasing apparent zero viscosity due to the addition of the fillers led to an increase in the cell density and a decrease in the mean cell size. We think that the higher apparent zero shear viscosity led to higher stresses at the same deformation rate in the flow field of the capillary die, which leads to local pressure fluctuations. We assume this is also a possible explanation for the improved foaming behavior because of the addition of the high molecular polystyrene.

Acknowledgements
The research work of this abstract was performed at the Polymer Competence Center Leoben GmbH (PCCL, Austria) within the framework of the COMET-program of the Federal Ministry for Transport, Innovation and Technology and the Federal Ministry of Economy, Family and Youth with contributions by Department of Polymer Engineering and Science, Chair of Polymer Processing, Montanuniversitaet Leoben. The PCCL is funded by the Austrian Government and the State Governments of Styria and Upper Austria.

References

[1] S. T. Lee, C. B. Park, and N. S. Ramesh, Polymeric foams: science and technology, **2006**, 45, 1.
[2] J. S. Colton, The nucleation of microcellular thermoplastic foam, Massachusetts Institute of Technology, **1985**.
[3] A. Behravesh and C. Park, Challenge to the production of low-density, fine-cell HDPE foams using CO2, Cellular polymers, **1998**
[4] R. MCCLURG, Design criteria for ideal foam nucleating agents, Chemical Engineering Science, **2004**, 59, 5779–5786
[5] H. E. Naguib, C. B. Park, and P. C. Lee, "Effect of Talc Content on the Volume Expansion Ratio of Extruded PP Foams," Journal of Cellular Plastics, **2003**, 39, 6, pp. 499–511
[6] A. H. Behravesh, C. B. Park, L. K. Cheung, and R. D. Venter, "Extrusion of polypropylene foams with hydrocerol and isopentane," Journal of Vinyl and Additive Technology, **1996**, 2, 4, pp. 349–357
[7] M. Abbasi, S. N. Khorasani, R. Bagheri, and J. M. Esfahani, Microcellular foaming of low-density polyethylene using nano-CaCo3 as a nucleating agent, Polymer Composites, **2011**, 32, 11, pp. 1718–1725,.
[8] H. E. Naguib, C. B. Park, and N. Reichelt, Fundamental foaming mechanisms governing the volume expansion of extruded polypropylene foams, Journal of Applied Polymer Science, **2004**, 91, 4, pp. 2661–2668.

Session 2: Surfaces, Interfaces and Structures

S2-L61
Photochemical engineering of polypropylene surfaces

Katrin Fohringer (1)*, Milana Đukić (2), Katja Schuler (2), Vanessa Winmer (2), Inge Eberhard (2), Simone Knaus (1)

(1) Vienna University of Technology, Institute of Applied Chemistry, Division Macromolecular Chemistry, Getreidemarkt 9, 1060 Vienna, Austria
(2) HTBLVA Dornbirn, Institution of Higher Education of Chemical Engineering, Höchsterstrasse 73, 6851 Dornbirn, Austria
*katrin.fohringer@ias.tuwien.ac.at

1. Introduction

The performance of polymer-based materials for both traditional and modern applications depends not only on structure-related properties, such as malleability, thermal stability and mechanic resistance, but also on their surface properties and interface behaviour. Applications in which the surface properties play a protagonist role, such as wettability, adhesion, adsorption, lubrication, biocompatibility and permeability, depend substantially on chemical nature of the polymer device. [1] Polyolefins, such as polyethylene and polypropylene (PP), possess desirable properties including good mechanical strength, chemical resistance, thermal stability and low cost. Their attributes make them promising candidates for various applications involving functional textiles, filtration devices, medical implants, and many others. Unfortunately, the major drawback of polyolefins is their low surface energy, which results in incompatibility with other natural or synthetic polymers, no adhesion to metal, poor wettability and hemocompatibility. [2] There are many methodologies that have been developed over last decades with the purpose of producing polyolefin devices that exhibit specified surface properties. One of the most appropriate and versatile methods to modify the properties of PP surfaces is UV initiated surface grafting. The aim of the present work was the epoxy-functionalization of PP surfaces (**Figure 1**), which allows tailoring of the surface properties with regard to wettability, hemocompatibility, biological activity and thermosensitivity by subsequent covalent bonding of, for example, carbohydrate moieties, maleimide residues and initiators for surface-initiated atom transfer radical polymerization (ATRP).

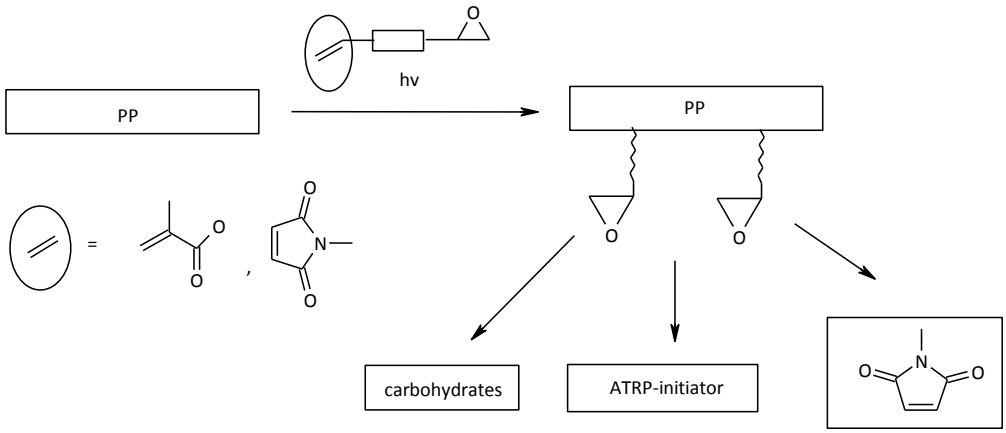

Figure 1. Photochemical engineering of PP surface

2. Results and discussion

PP films were epoxy-functionalized by surface photografting of commercially available glycidylmethacrylate (GMA) and monomers containing epoxy-groups and methacrylate or maleimide residues, respectively, linked by long-chain aliphatic spacers to improve the affinity to PP surfaces (Met-Epo, Mi-Epo). Mi-Epo was obtained by esterfication of maleimidoundecanoic acid with undecenol in emulsion droplets in water. Epoxidation of the vinyl group with m-chloroperoxy benzoic acid was feasible in nearly quantitative yield. Met-Epo was synthesized by epoxidation of undecenol, followed by reaction of this precursor with methacrylic anhydride.

All monomers were immobilized by UV irradiation using benzophenone as hydrogen abstracting initiator. Covalent attachment of carbohydrates ("glycoengineering") was achieved by reaction with N-methyl-D-glucamine (MG) and N-(2-aminoethyl)-gluconamide (AEG). Maleimide residues and ATRP-surface initiators were immobilized by reaction with maleimido undecanoic and bromoisobutyric acid, respectively.

The epoxy-functionalized PP films and all post-modified samples were characterized by ATR-IR spectroscopy, atomic force microscopy (AFM) and contact angle measurements.

Epoxy-functionalization resulted in enhanced wettability (e.g. PP 92°, PP-g-Epoxy 71-75°) and after glycoengineering, which improves the hemocompatibility of PP because of the hydrophilicity [3], contact angles decreased to 56-61°C. AFM revealed a different structure of the grafted layers depending on the polarity and the type of polymerizable group. As can be seen in **Figure 2**, grafting of GMA results in very rough surfaces compared to films modified by grafting of the more hydrophobic monomer Met-Epo.

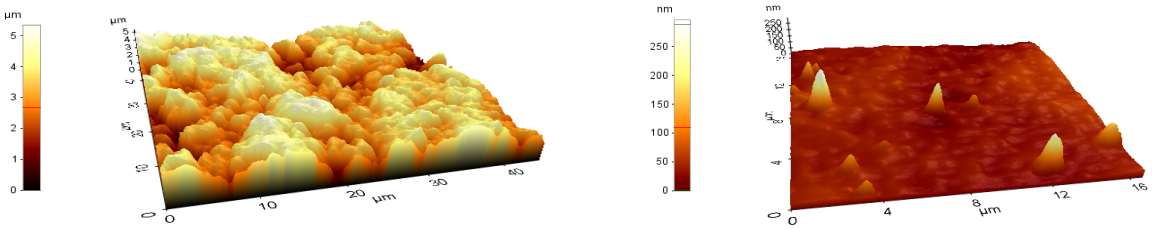

Figure 2. AFM of PP-g-GMA –MG (left) and PP-g-Met-Epo-MG (right)

Maleimide finishing (MI) of epoxy-functional foils led to products allowing spatially controlled UV surface pattering and, for example, covalent bonding of SH-functional bioactive molecules. [4] MI-functionalized films were successfully labeled with a mercapto-fluorescence marker (FLU-SH; **Figure 3**) [5] to prove the homogeneity of the modified surface.

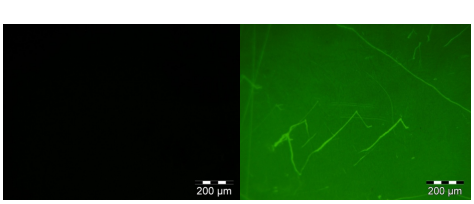

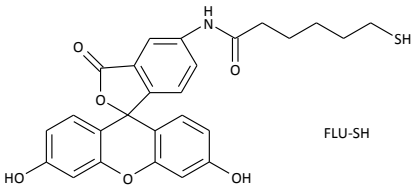

Figure 3. Fluorescence microscope image of FLU-SH labeled blank (left) and PP-g-GMA-MI (right)

First results of surface initiated graft copolymerization with (i) acrylic acid leading to surfaces suitable for immobilization of TiO_2 photocatalysts [6] and (ii) N-isopropylacrylamide leading to thermosensitive surfaces [1] will be presented, showing that UV-grafting of epoxy-functional monomers is a versatile tool for surface engineering of PP.

Acknowledgements
Part of this work was done within the frame of "Sparkling Science", a research program of the Austrian Federal Ministry of Science and Research (project "Green Chemisry").

References
[1] Thelma S. P. Cellet, Marcos R. Guilherme, Rafael Silva, Guilherme M. Pereira, Marcos R. Mauricio, Edvani C. Muniz, Adley F. Rubira, *Journal of Colloid and Interface Science*, 2012, 367(1),494-501.
[2] Kiran K. Golin, Orlando J. Rojas, Evren A. Özcam, Jan Genzer, *Biomacromolecules*, 201213, 1371-1382.
[3] Q. Yang, Zhi-Kang Xu, Zheng-Wei Dai, Jian-Li Wang, Mathias Ulbricht,*Chemistry of Materials*, 2005,17(11),3050-3058.
[4] K.Joonyeong, C. Joungmo, Paul M. Seidler, Nicholas E. Kurland, Vamsi K. Yadavalli,*Langmuir* , 2010,26(4),2599-2608.
[5] P. Knaack, Synthesis and Applications of Functional Dyes, Diploma Thesis, Vienna University of Technology, 2010.
[6] S.Yang, Gu Jia-Shan, Yu Hai-Yi, Zhou Jin, Li Shi-Feng, Wu Xiu-Min, Wang Liang, *Separation and Purification Technology*, 2012, 83, 157-165.

S2-L62
Photoinduced cross-linking of polynorbornenes for 3D microstructuring and applications in organic electronics

Archim Wolfberger (1)*, Thomas Griesser (1), Ute Daschiel (1,2), Andreas Petritz (3), Volker Schmidt (3), Abdellatif Jerrar (4), Christian Teichert (4), Wolfgang Kern (1,2)
(1) University of Leoben, Chair of Chemistry of Polymeric Materials, Otto Glöckel-Straße 2, 8700 Leoben, Austria
(2) Polymer Competence Center Leoben GmbH, Roseggerstraße 12, 8700 Leoben, Austria
(3) Joanneum Research GmbH, Institute for Surface Technologies and Photonics, Franz Pichler-Straße 30, 8160 Weiz, Austria
(4) University of Leoben, Institute of Physics, Franz Josef-Straße 18, 8700 Leoben, Austria
*archim.wolfberger@unileoben.ac.at

1. Introduction
The ring-opening metathesis polymerization (ROMP) technique offers a versatile tool for the synthesis of highly defined polymers and enables the realization of ambitious polymer architectures.[1] In general, this living polymerization method provides the possibility for the fabrication of polymers with low polydispersity without protecting group chemistry and is also highly tolerant regarding functional groups.[2] In this contribution, we focus on the microstructuring of polynorbornene films using one- and two-photon induced cross-linking. In a first step polynorbornene derivatives bearing aromatic ester groups were synthesized by means of ROMP. These polynorbornenes are capable of undergoing the photo-Fries rearrangement reaction, which proceeds through a radical mechanism and thus leads to cross-linking of the macromolecules caused by recombination of the photogenerated radicals without the requirement of photoinitiators. In a further approach the residual double bonds in ROMP derived polymeric materials were exploited for a photoinduced thiol-ene reaction in order to achieve a selective cross-linking of the macromolecules.[3] To demonstrate the versatility of this reaction for the realization of 3D polymeric microstructures, polynorbornene films were structured via two-photon induced cross-linking [4].

2. Results and discussion
The photoinduced thiol-ene reaction and the photo-Fries reaction were both investigated by means of FTIR spectroscopy. Additionally, the cross-linking of the macromolecules and thus the change in solubility was assessed by means of sol-gel analysis. Thin polynorbornene films were laterally patterned using conventional single photon lithography followed by development, leading to resolutions in the µm range. Furthermore, polynorbornenes bearing aromatic ester groups were used as photopatternable dielectrics in organic thin film transistors (OTFTs), which exhibited sufficient field effect mobilities at low operating voltages.
Going a step beyond the 2D-patterning of polymeric materials, the photoinduced thiol-ene reaction was also used for realizing polynorbornene 3D microstructures by employing the two-photo absorption (TPA) writing technique, using a highly active TPA-photoinitator. The obtained 3D features were investigated by scanning electron microscopy (SEM) and atomic force microscopy (AFM) and exhibited well-defined geometries in the µm-regime (see Figure 1).

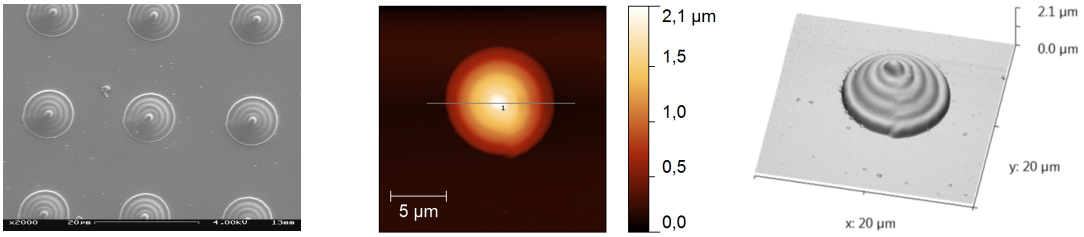

Figure 1. SEM micrograph of an array of polynorbornene 3D-microstructures (A); AFM image (B) and 3D-reconstructed AFM image (C) of an individual microstructure.

3. Conclusions

The versatility of the investigated cross-linking approaches for ROMP-derived polymers paves the way towards novel strategies for the realization and implementation of polymeric 2D and 3D microstructures. It has been shown that the photo-Fries rearrangement reaction in polynorbornenes can be utilized for 2D-microstructuring applications and allows a direct photolithographic patterning without the need of photoinitiators. Additionally, these intrinsically photopatternable polynorbornene films turned out to be promising candidates for novel polymeric dielectric materials in organic thin film transistors.
Moreover, the reactivity of the polynorbornene main chain double bonds in the photoinduced thiol-ene reaction can also be exploited for a selective crosslinking of polynorbornene macromolecules. In combination with the two-photon excitation technique this photoreaction offers novel strategies for the fabrication of polymeric 3D microstructures.

Acknowledgements

Financial support by the Austrian Science Fund (FWF) (Project TRP 181-N19) is gratefully acknowledged. Part of this work was performed at the Polymer Competence Center Leoben GmbH (PCCL) within a strategic research project (IV-4S1).

References

[1] C. W. Bielawski, R. H. Grubbs, *Prog. Polym. Sci.* 2007, 32, 1.
[2] G. Black, D. Maher, W. Risse, Living Ring-Opening Olefin Metathesis Polymerization, in: R. H. Grubbs, (Ed.); Handbook of Metathesis, Vol. 3, 1st edition, Wiley-VCH, Weinheim, 2003, p. 2.
[3] A. Wolfberger, B. Rupp, W. Kern, T. Griesser, C. Slugovc, *Macromol. Rapid Comm.* 2011, 32, 518.
[4] T. Griesser, A. Wolfberger, U. Daschiel, V. Schmidt, A. Jerrar, C. Teichert, W. Kern, Cross-linking of ROMP derived Polymers Using the Two-Photon Induced Thiol-Ene Reaction: Towards the Fabrication of 3D- Polymer Microstructures. (Submitted to *Polymer Chemistry*)

S2-L63

Microencapsulation by electrostatic layer by layer deposition of chitosan and sodium dodecyl sulfate to encapsulate linseed oil from oil-in-water emulsion

Sudipta Chatterjee (1,2), Fabien Salaün (1,2), Christine Campagne (1,2)*
(1) GEMTEX – ENSAIT, Roubaix, France
(2) University of Lille - North of France, Villeneuve d'Ascq, France
*christine.campagne@ensait.fr

1. Introduction

Microencapsulation is a method to encapsulate active agents such as drugs, enzymes, hormones, and living cells in a polymer covert to provide a physical barrier against adverse environmental conditions with desired release properties [1]. Microcapsules have multidisciplinary applications such as biomedical, biotechnology, food, textiles, cosmetics, and printing. The choice of microencapsulation method is function of nature of active agent, and is guided by environmental, physiological and commercial constraints. Among two hundreds of encapsulation methods described in literatures, the methods based on oil-in-water emulsion such as interfacial polymerization, coacervation, phase separation are widely used for microencapsulation [2]. Our objective is to develop microcapsules using natural biopolymer for encapsulating linseed oil and integrate in textiles for developing functionalized textiles to bring a certain comfort for the skin to prevent inflammations during physical activities. Chitosan (CS) obtained from alkaline deacetylation of crustacean chitin shows exquisite encapsulating and release properties for various active materials [3]. In our study, microcapsules are developed using CS to encapsulate linseed oil for textile applications.

2. Theory

The multilayer microcapsules with core-shell morphology are developed by electrostatic interaction between polycationic CS and anionic sodium dodecyl sulfate (SDS) in layer by layer (LBL) deposition process [4]. The LBL process is combined with oil-in-water

emulsification at the beginning using SDS as an anionic emulsifier which develops negatively charged oil droplets in the emulsion, and the addition of CS in the emulsion results in the formation of microcapsules by electrostatic interaction between CS and SDS on the surface of oil droplets [5]. The multilayer shell formation on the microcapsules involves alternate addition of SDS and CS by electrostatic interaction and molecular rearrangement on the surface as well. The mild alkali treatment after harvesting microcapsules from LBL process causes rigidification of the microcapsules on the outermost shell. 1-Butanol is used as stabilizer to control drying step during alkali treatment of microcapsules to impede microcapsules aggregation and gelation of CS molecules. The trisodium citrate treatment after the alkali treatment of microcapsules centers around the charge stability of microcapsules on the surface.

3. Experimental

The microencapsulation method to encapsulate linseed oil was initiated by preparing oil in water emulsion under homogenizing (16000 rpm, 30 min, and 50 °C) condition using 20 wt % of linseed oil and 80 wt % of aqueous SDS (10 g/l) solution. The microcapsules were formed in the emulsion under the same condition as before by adding requisite amount of CS solution (3%, w/v in 2%, v/v acetic acid) in 100 ml of emulsion. The multilayer formation on microcapsules was carried out by step by step addition of CS and SDS solution in the required amount under stirring condition (1500 rpm) at 50 °C [5]. The LBL deposition was continued maximum up to 10 cycles, and each cycle of SDS and CS addition was considered as addition of 1 layer on the surface of microcapsules. The mild alkali treatment of microcapsules was done by adding 5 ml of microcapsules suspension in the mixture of 20 ml of 0.02 (N) NaOH and 1 ml of 1-butanol at 30 °C for 10 min under 1500 rpm in order to rigidify outermost shell of microcapsules without aggregate formation by microcapsules. The alkali treated microcapsules were subject to citrate treatment by reacting 25 ml trisodium citrate solution 0.1 (M) with as prepared 25 ml of alkali treated microcapsules suspension under 1500 rpm at 30 °C for 30 min for charge stabilization.

The morphology and properties of microcapsules were determined using zeta potential technique, optical microscopy, scanning electron microscopy (SEM), atomic force microscopy (AFM) with surface roughness (*Ra*) measurement and contact angle experiments for surface energy.

4. Results and discussion

The zeta potential measurement of microcapsules suspension during LBL showed that oil-in-water emulsion had strong negative zeta potential (-53.8 mV) as SDS was used as an anionic emulsifier in the system and formation of microcapsules with addition of CS solution caused increase in zeta potential from -53.8 to +35.6 mV due to positive charges of CS molecules in 1 layer sample [5]. The addition of anionic SDS during formation of multilayer microcapsules in LBL could not get it to switch to negative zeta potential value as overcharging occurred due to CS. However some differences in zeta potential values were found with SDS and CS addition during LBL indicating electrostatic interaction on the surface. The zeta potential of microcapsules after alkali treatment showed less positive zeta potential than that of sample just after LBL before alkali treatment due to charge neutralization of polar groups of CS molecules on the surface by alkali [5]. The SEM analysis of alkali treated microcapsules indicated presence of microcapsules on the sample surface after drying as found up to 4 layers and after that whole network was collapsed due to too much addition of CS in the suspension during LBL.

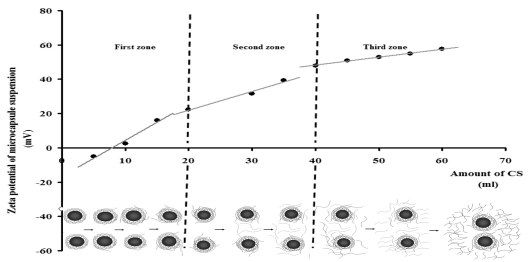

Figure 1: Zeta potential variation of oil-in-water emulsion with CS addition during microencapsulation process

As shown in Figure 1, zeta potential variation of microcapsules suspension during CS addition followed three distinct zones and the first zone showed strong zeta potential variation with CS addition during 1 layer formation suggesting that first zone was the active zone of shell formation by interaction of CS and SDS on the surface as other two zones did not exhibit any significant change in zeta potential with CS addition in oil-in-water emulsion. Thereby, optimized CS amount for further layer formation was considered to be 15 ml (3%, w/v in 2%, v/v acetic acid) in 100 ml of emulsion. The microencapsulation process was subject to dilution after 2 layers to confirm the maximum deposition of SDS and CS on the surface during LBL process as the microcapsules got again overcharged with CS molecules after 2 layers. The stepwise dilution was applied by diluting the microcapsules by 10 times with de-ionized water before SDS addition during each layer formation. The microcapsules were spinning around their zeta potential values during LBL depending on charge of wall materials on the surface up to 6 layers. The method was continued up to 6 layers as dilution after each layer deceased the population in suspension. Also, optical microscope of microcapsules during LBL indicated microcapsules were not aggregated due to dilution and rid microcapsules suspension of undesired complex formation of CS and SDS. Moreover, the population was lessened due to dilution. The SEM analysis of microcapsules revealed that microcapsules were to some extent aggregating to form raspberry type structure and alkali treatment of microcapsules resulted in formation of nanocapsules from microcapsules as shown in SEM image of 6 layers because apparently visible microcapsules are indeed clusters of nanocapsules that

are adhered to each other by CS chains.
The AFM images of optimized microcapsules suspension showed presence of individual microcapsules on the surface of 4 and 6 layers after drying, suggesting that dilution had a positive effect on the arrangement of microcapsules on surface after drying. The contact angle experiments revealed that polar groups of CS were more exposed on the surface due to added layer numbers because 4 layers and 6 layers microcapsules samples showed higher values of γ^P (polar component of surface energy) of than that of 2 layers. Also, surface roughness (*Ra*) was less for 4 layers (37.2 nm) and 6 layers (41.4 nm) than 2 layers (65.9 nm), indicating dilution exerted positive effect on decreasing the roughness of surface after dilution. However, SDS addition during LBL made the surface rough for 4.5 layers (119.0 nm) due to uneven distribution of SDS molecules on the surface of microcapsules.
The addition of small amount of 1-butanol during alkali treatment of microcapsules significantly reduced both aggregation of microcapsules and undesired gel formation of CS molecules in alkaline condition as evidenced by optical microscopy. 1-butanol acts as stabilizer to control drying step during rigidification of outermost shell of microcapsules by alkali treatment. The addition of trisodium citrate solution to the microcapsules suspension after alkali treatment was mainly to impart same charge on the microcapsules having different added layer numbers as evidenced by zeta potential analysis. The zeta potential values of alkali treated microcapsules after citrate treatment were always close to 0 mV irrespective of added layer numbers due to buffering action of trisodium citrate in microcapsules suspension.

5. Conclusions
The multilayer microcapsules formed by electrostatic interaction of oppositely charged CS and SDS in combined oil-in-water emulsification and LBL deposition process showed different morphologies depending on the added layer numbers as well as the amount of added wall materials in the suspension during LBL. The alkali treatment of microcapsules sample with 6 layers gave rise to nanocapsules as alkali solution caused ripping of CS link between them. The process of rigidification of outermost shell of microcapsules by alkali treatment was made more effective amending 1-butanol and citrate solution as microcapsules suspension got rid of unwanted gel formation by CS molecules and aggregation of microcapsules as well.

Acknowledgements
We gratefully acknowledge financial support from the project ACHILLE (Applied comfort and Health in light leisure equipment) – A crosstexnet ERA-NET project (transnational call 2010 - convention Feder n°11002645).

References
[1] K. Bouchemal, S. Briançon, E. Perrier, H. Fessi, I. Bonnet, N. Zydowicz, *Int. J. Pharm.* 2004, 269, 89-100.
[2] P. J. Watts, M. C. Davies, C. D. Melia, *Crit. Rev. Ther. Drug* 1990, 7, 235-259.
[3] H. Peng, H. Xiong, J. Li, L. Chen, Q. Zhao, *J. Food Eng.* 2010, 101, 113–119.
[4] T. Aoki, E. A. Decker, D. J. McClements, *Food Hydrocolloid.* 2005, 19, 209–220.
[5] S. Chatterjee, F.Salaün, C. Campagne, S. Vaupre, A. Beirão, *Carbohyd. Polym.* 2012, 90, 967-975.

S2-L64
Application and characterization of microstructured cellulose thin films

Rupert Kargl (1)*, Tamilselvan Mohan (2), Aleš Doliška (2), Karin Stana-Kleinschek (2), Volker Ribitsch (1)
(1) University of Graz, Institute of Chemistry, Heinrichstraße 28, AT-8010 Graz, Austria
(2) University of Maribor, Faculty of Mechanical Engineering, Smetanova Ulica 17, SI-2000 Maribor, Slovenia
*rupert.kargl@uni-graz.at

1. Introduction
Cellulose thin films (< 100 nm thickness) were used for interfacial studies and as sensor matrices within the last two decades. Their advantage is a large hydrophilic surface area combined with the insolubility in water and most organic solvents. Cellulose thin films exhibit a relatively low unspecific binding of for instance (bio-)molecules which is attributed to their uncharged highly hydrated surface [1]. For that reason these films are interesting substrate for the preparation of (bio-)sensor supports. Several methods are known to prepare such thin films on diverse materials [2]. One of these methods is spin coating of cellulose derivatives and subsequent regeneration to pure cellulose. The organo-soluble cellulose derivative trimethylsilyl cellulose can easily be spin coated and converted to pure cellulose upon exposure to vapors or solutions of hydrochloric acid [3]. These desilylation can be exploited in the manufacturing of micro-structured cellulose surfaces which can further be applied in the field of (bio-)molecule arrays [4].

2. Experimental
The regeneration of thin spin coated trimethylsilyl cellulose (TMSC) films on solid substrates was monitored by determining the mass-loss during the desilylation reaction with a quartz-crystal microbalance with dissipation detection (QCM-D). Contact angle measurements and X-ray photoelectron spectroscopy were employed to confirm a complete regeneration and to characterize the obtained pure cellulose material. TMSC was further coated on microscope glass slides and micro-structured by applying a metal mask during the regeneration. Cellulose patterns were structured by exposure to cellulase solutions leading to digestion of

cellulose and remaining TMSC patterns. The patterned surfaces were applied in the detection of fluorescent labeled DNA from solution.

3. Results and discussion

Desilylation of cellulose via treatments with vapors of hydrochloric acid occurs within two distinct reaction steps as revealed by QCM-D. In the first, fast step the major amount of trimethylsilyl moieties is cleaved whereas a complete and slow desilylation is only obtained after longer incubation with $HCl_{(g)}$. Completely hydrolyzed TMSC consist of pure cellulose with its characteristic elemental composition and wettability. A coating of TMSC on conventional microscope glass-slides is stable and can be regenerated in a patterned way, by placing lithographic masks on the substrate. These masks protect the TMSC layer from being regenerated. The patterns formed represent a spatially distributed wettability and chemical reactivity as a result of the conversion to hydrophilic cellulose (**Figure 1**). Pure cellulose patterns can also be digested by cellulases which can be exploited for a further structuring method. Owing to the spatial separation and chemical differences, cellulose patches can be used for the immobilization and detection of DNA from solution at a concentration of 80 nmol l^{-1}.

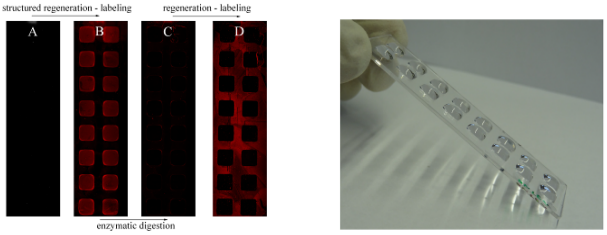

Figure 1. Left: micro-structured cellulose slides; right: wettability pattern on a cellulose/TMSC slide.

Acknowledgements

The research leading to these results has received funding from the European Union Seventh Framework Programme (FP7/2007-2013) under grant agreement no. 214653. Prof. Thomas Heinze from the University of Jena is highly acknowledged for providing the TMSC.

References

[1] I. Filpponen, E. Kontturi, S. Nummelin, H. Rosilo, E. Kolehmainen, O. Ikkala, J. Laine, *Biomacromolecules* 2012, 13, 736-742.
[2] E. Kontturi, P. C. Thüne, J. W. Niemantsverdriet, *Langmuir* 2003, 19, 5735-5741.
[3] T. Mohan, R. Kargl, A. Doliška, A. Vesel, V. Ribitsch, K. Stana-Kleinschek, *J. Colloid Interface Sci.* 2011, 358, 604-610.
[4] R. Kargl, T. Mohan, S. Köstler, S. Spirk, A. Doliška, K. Stana-Kleinschek, V. Ribitsch, *Adv. Funct. Mater.* 2012, DOI: 10.1002/adfm.201200607

Session 6: Polymer Composites and Nanotechnology

S6-L65
Photochemical cross-linking of polymer materials via functional inorganic particles

Jakob Manhart (1)*, Sandra Schlögl (1), Jörg Schauberger (2), Raimund Schaller (3), Armin Holzner (3), Wolfgang Kern (1,2)

(1) Polymer Competence Center Leoben GmbH, Roseggerstraße 12, A-8700 Leoben, Austria
(2) University of Leoben, Chair of Chemistry of Polymers, Otto Glöckel-Straße 2, A-8700 Leoben, Austria
(3) Semperit Technische Produkte GmbH, Triester Straße 26, A-2632 Wimpassing, Austria
*Jakob.Manhart@pccl.at

1. Introduction

The present work aims at the UV assisted cross-linking of poly(vinyl alcohol) (PVA) and poly(isoprene) using functionalized inorganic particles as cross-link agents. For this purpose, two different cross-link mechanisms were employed. The photochemical cross-linking of poly(vinyl alcohol) involves the excitation of a selected photoacid generator (triphenyl sulfonium salt) with ultra-violet (UV) light to release Brønsted acids [1,2]. Once formed, the generated protons were used for the cationic ring opening of epoxy moieties attached to inorganic SiO2-particles (**Figure 1a**). Due to this UV-initiated reaction mechanism, a cross-linking of the poly(vinyl alcohol) chains is accomplished resulting in the formation of three-dimensional polymer networks. With respect to the second approach, the thiol-ene reaction was applied for the cross-linking of poly(isoprene) using mercapto-functionalized SiO2-particles. In the presence of a photoinitiator, free radicals are formed upon UV exposure that react with the mercapto moieties of the particles. Once generated, the thiyl radicals react with the C=C double bonds of the poly(isoprene) under the formation of thioether links, and a cross-linking of the polymer chains is achieved (**Figure 1b**) [3,4].

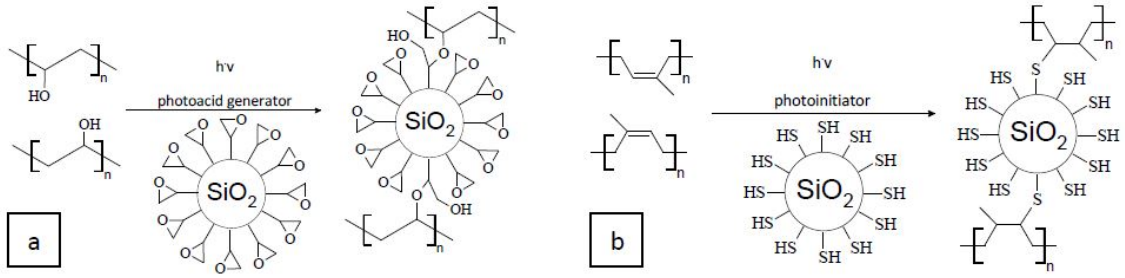

Figure 1. Mechanism of the cross-link reaction of poly(vinyl alcohol) (a) and poly(isoprene) (b) with inorganic particles

2. Experimental

Poly(vinyl alcohol) was dissolved in dimethyl sulfoxide by stirring the solution at 45°C for 5 hrs. After cooling to room temperature, epoxy-modified SiO2-particles and the photoacid generator were dispersed into the poly(vinyl alcohol) solution. Poly(isoprene), photoinitiator and mercapto-modified particles were dissolved in chloroform and stirred at room temperature for 10 hrs. After sonicating the mixtures, thin films were either spin cast on CaF2-substrates or prepared with a coating knife before removing the solvents at 25°C under vacuum. UV irradiation was performed using a conventional mercury emitter as UV-lamp. Structured illumination was achieved with a 100 µm-patterned quartz mask. The illuminated poly(vinyl alcohol) samples were further post-baked at 70°C for 1 h. The patterned and cross-linked specimens were then developed with deionized water (poly(vinyl alcohol)) or petroleum naphtha (poly(isoprene)).

Reaction kinetics were characterized by means of FTIR-spectroscopy and the cross-link densities were determined by equilibrium swelling measurements. Further, tensile properties of photochemically cross-linked natural rubber (NR) latex films prepared by a coagulant dipping process were investigated. Structured specimens were analyzed by means of optical microscopy using polarized light and phase contrast techniques. Furthermore, the surface topography of patterned and developed poly(vinyl alcohol) films was investigated with confocal microscopy.

3. Results and discussion

The UV-induced cross-linking of poly(vinyl alcohol) employing inorganic epoxy-functionalized particles as cross-linkers was determined by equilibrium swelling measurements in water. The results clearly show that the degree of swelling decreases with an increasing amount of particles. As the degree of swelling correlates to the network density, the results give evidence that the photo-induced cross-linking of PVA films with inorganic particles is feasible. In order to assess the photochemical cross-linking of poly(isoprene) samples based on the thiol-ene reaction the addition reaction of thiols to C=C double bonds was investigated by real time FT-IR spectroscopy. The results reveal that the characteristic C=C peak (835 cm-1) significantly decreases upon UV illumination. In addition, by increasing the amount of particles from 5 to 25 wt.-% the consumption of C=C double bonds can be increased considerably. Similar results are achieved by swelling measurements where the degree of swelling declines with an increased illumination dose and the level of particles. By optimizing both the process parameters as well as the concentration of the photochemicals, cross-linked NR latex films with good tensile properties ranging from 20 ± 2 to 24 ± 2 MPa are obtained. In order to demonstrate the excellent controllability of the cross-linking with inorganic particles regarding its functionality and processing, patterned illuminated samples were prepared to design structured polymer materials with tailored topography. The optical micrograph (using phase contrast) of a structured illuminated and developed poly(isoprene) film cross-linked with 5 wt.-% mercapto-modified SiO2-particles is illustrated in **Figure 2a**. The clearly visible contrast between the illuminated and non illuminated areas shows a change in the refractive index which is caused by the thiol-ene reaction during UV-irradiation. The micrograph illustrates that a structured cross-linking of elastomer materials can be achieved with functional inorganic particles. **Figure 2b** provides a confocal micrograph of a patterned illuminated and developed PVA film containing 20 wt.-% epoxy-functionalized particles. From the results it can be concluded that structured surfaces are accomplished. It should be noted that the resolution depends on the diameter of the employed functional particles.

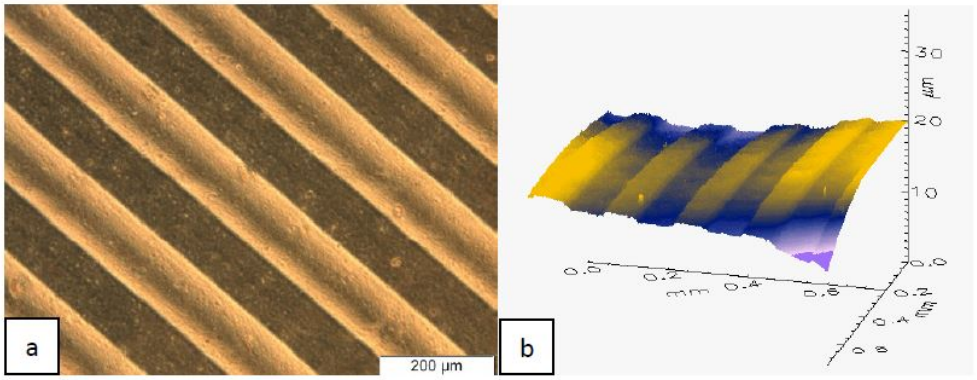

Figure 2. Patterned illuminated and developed polymer films: poly(isoprene) (a) and poly(vinyl alcohol) (b)

4. Conclusions

The results give evidence that photochemical cross-linking and patterning of poly(isoprene) and poly(vinyl alcohol) materials can be achieved using surface-modified SiO2-particles as cross-link agents. As poly(vinyl alcohol) is water-soluble, the UV cross-linking of PVA offers a promising way with regards to the manufacture of water-developable photo resists.

Based on the UV cross-linking of poly(isoprene) with the inorganic particles, tensile strength as well as cross-link density can be significantly enhanced. As the particles exhibit a reduced extractability, the biocompatibility of the NR latex films can be improved considerably. Consequently, the photochemical cross-linking of poly(isoprene) by means of inorganic particles offers a new approach for manufacturing elastomeric articles with good mechanical properties and reduced extractable chemical levels.

Acknowledgements

This study was performed at the Polymer Competence Center Leoben GmbH (PCCL, Austria) within the framework of the COMET-program of the Federal Ministry for Transport, Innovation and Technology and the Federal Ministry for Economy, Family and Youth with contributions by the University of Leoben and Semperit Technische Produkte GmbH. The PCCL is funded by the Austrian Government and the State Governments of Styria and Upper Austria.

References

[1] Y. Yağci, I. Reetz, Prog. Polym. Sci. 1998, 23, 1485-1538.
[2] H. Kura, K. Fujihara, A. Kimura, T. Ohno, M. Matsumara, Y. Hirata, T. Okada, J. Polym. Sci., Part B: Polym. Phys. 2001, 39, 2937-2946.
[3] C. E. Hoyle, C. N. Bowman, Angew. Chem. Int. Ed. 2010, 49, 1540 – 1573.
[4] S. Schlögl, A. Temel, R. Schaller, A. Holzner, W. Kern, Rubber Chem. Technol. 2010, 83, 133-148.

S6-L66
Polymer-based nanocomposite fibers as a precursor for non-woven fabrics

Paulina Latko*, Rafał Kozera , Anna Boczkowska
Faculty of Materials Science and Engineering/Warsaw University of Technology
Woloska 141 Street; 02-507 Warsaw, Poland
*paulinalatko@interia.pl

1. Introduction

The intense progress in the field of nanomaterials contribute to search repeatedly novel combinations between the various classes of materials. As a result the nanocomposites are obtained that is two component system where in the matrix at least one dimension of the filler is located at the nano-scale. The main target of our study was the manufacturing process of nanocomposites fibers consist of thermoplastic polymer matrix -polyamides 11(PA11) and carbon nanotubes (MWCNTs) as a filler. The one of the major features of the polymer nanocomposites with CNTs is low percolation threshold, therefore the three-dimensional carbon nanotubes are able to conduct electrical charges even at low nanofiller contents. While the composites are produced as a fiber, the applied form of target product is veil - kind of fabric composed of previous extruded fibres with carbon nanotubes (Figure 1).

2. Method

The method of manufacturing includes, first of all, the homogenization process of carbon nanotubes with thermoplastic polymer then extruding the fibers from the previously made pellets and pressing them into the desired veil with specific weight and dimensions. Due to even a slight addition of carbon nanotubes into the polymer melt, the viscosity of the mixture significantly increases. Therefore the parameters of all processes were firstly adjusted and then optimized according to the stock of the filler.

We managed to obtain the thin fibers containing CNTs from the range of 1% - 6 wt.%.

Figure 1. Conductive veil, fabricated from polyamide with 1% wt. of CNTs.

3. Results

The resulting material, both pellets and fibers, were measured using the DSC and TGA analysis. Also tensile tests were done, and microscopic observation were carried out with the application of Scanning Electron Microscopy (SEM). It was observed the uniform distribution of CNTs in a polymer matrix without the presence of agglomerates. This fact is extremely important, because evidences of the mutual compatibility of components in the fabricated nanocomposites. It also confirms that melt-processing of nanocomposite could be the appropriate pathway for the industry scale. The electrical conductivity as well as mechanical performance of produced fibers were examined.

4. Conclusions

Further research in the production and improvement of the performance described non-woven nanocomposite veils is justified by their potential application in the aerospace industry. Thanks to its low density and relatively easy method of fabrication, may soon replace the currently used copper mesh. But above all, increased electrical properties must qualify as innovative materials against thunderbolt.

References

[1] M. Moniruzzaman, K.I.Winey- Polymer Nanocomposites Containig Carbon Nanotubes- *Macromolecules* 2006, *39,* 5194-5205
[2] Z.Spitalsky, D. Tasis, K.Papagelis, C.Goliotis- Carbon nanotube-polymer composites: Chemistry, processing, mechanical and electrical properties- Progress in Polymer Science 35 (2010) 357–401
[3] B.G.Min, H.G.Chae, M. L. Minus and S. Kumar- Polymer/carbon nanotube composite fibers- An overview- Functional Composites of Carbon Nanotubes and Applications, 2009: 43-73
[4] P. J.Hogg- Toughening of thermosetting composites with thermoplastic fibers, Materials Science and Engineering A 412 (2005) 97–103
[5] Z.Han, A.Fina- Thermal conductivity of carbon nanotubes and their polymer nanocomposites: A review - Progress in Polymer Science 36 (2011) 914–944
[6] B.Krause, P. Pötschke , L.Häußler- Influence of small scale melt mixing conditions on electrical resistivity of carbon nanotube-polyamide composites- Composites Science and Technology 69 (2009) 1505–1515

S6-L67
Friction and wear of poly-ether-imide polymers

H. Unal (1)* and A. Mimaroglu (2)
(1) University of Sakarya, Faculty of Technology, Esentepe Kampusu, Adapazari, Turkey
(2) University of Sakarya, Faculty of Engineering, Esentepe Kampusu, Adapazari, Turkey
*unal@sakarya.edu.tr

Abstract

In this work, the dry sliding wear behaviour of poly-ether-imide composites PEI+15%PTFE and PEI+20% GFR rubbing against PPS+40%SGFR, BMC+15%LGFR and AISI D2 steel were investigated using a pin–on–disc rig. The main purpose was to study the influence of disc material, sliding distance, applied load parameters on the wear performance of the poly-ether-imide polymers.. Tests conditions were 20, 40 and 60N loads and at 0.5,1.0 and 1.5 m/s sliding speeds. It was observed that, for all material combinations used in this investigation, the coefficient of friction decreases linearly with the increase in load. The specific wear rate increases with the increase in sliding speed and shows no change with the increase in load value. In general, the specific wear rate showed very little sensitivity to the varying load and sliding speed. Finally it is concluded that the wear behaviour of poly-ether-imide polymers is much dependant on the physical and mechanical properties of the polymer.

Keywords: Tribology; PEI; PPS, BMC;AISI D2 Steel

S6-L68

Rheological properties of styrene acrylic copolymer based silica nanocomposites for coatings industry application

Urban Šegedin (1)*, Klemen Burja (2), Franci Malin (1), Saša Skale (1), Bogdan Znoj (1), Peter Venturini (1)
(1) Central R&D of Helios Group, Helios Domžale d.d., Količevo 2, 1230 Domžale, Slovenia
(2) Centre of Excellence for Polymeric Materials and Technologies, Tehnološki park 24, 1000 Ljubljana, Slovenia
*urban.segedin@helios.si

1. Introduction

Present study focuses on rheological properties of silica nanocomposites based on styrene acrylic copolymer (SAC). Nanocomposites prepared by post synthesis blending of nanoparticles and SAC (MNP) in comparison with the *in situ* prepared nanocomposites (INP) were investigated in this work. A novel explanation on nanoparticle behavior in nanocomposites is proposed. The close relation between rheological properties and nanoparticle agglomeration is shown. Obtained results imply that the copolymer - nanoparticle interactions are limited and cannot be the sole reason for non-Newtonian behavior of nanocomposites.

2. Theory

Silica nanoparticles can be used in coatings industry to enhance hardness, thermal stability, anticorrosion protection, UV stability and resistance to abrasion. Different approaches in preparation of organic copolymer based surface modified silica nanocomposites are described in the literature [1-9]. Maximal effectiveness of nanoparticles can be achieved by proper dispersing process. Improved distribution through the copolymer matrix is reached by surface modification of nanoparticles. Surface modification with methacryloxypropyltrialcoxysilanes provides better distribution, stabilization and fixation of nanoparticles, therefore keeping the dispersion transparent. Agglomeration of nanoparticles leads to deterioration of optical properties of nanocomposites [1-9].
Thus far, nanoparticles have been regarded as very small filler particles with extremely high surface to volume ratio. This is displayed in strong effects on properties at low concentrations (usually below 5 %) [1]. Behaving as fillers, added nanoparticles affect the rheological properties of prepared nanocomposites [10]. Viscosity and pseudoplasticity of such nanocomposites are increasing with nanoparticle concentration due to the fact that intermolecular interactions (noted as loss modulus, G'') rise. Intramolecular interactions are displayed in terms of elasticity (storage modulus, G'). With rheological characterization effects of nanoparticles on large scale can be assessed (in contrary to electron microscopy and X-ray diffraction where structures on small scale are observed) [11]. General understanding on how nanoparticles affect rheological properties of nanocomposites is limited to increase of the viscosity, pseudoplasticity and occurrence of thixotropy, yield point and also decrease in transparency [12, 13]. Decrease in elasticity has also been reported [14]. On the other hand, for as much as 15 % of incorporated silica nanoparticles no effect on elasticity characterized by storage modulus G' has been detected [8]. Intensive agglomeration at higher nanoparticle concentrations is reported as well [14] and some propositions are made for application of silica nanoparticles as matting agents [12]. This is in contradiction with conserved transparency [8] that also has been observed in present research.
In present work new concept is introduced. As proposed, nanoparticles smaller than 100 nm in all dimensions have limited interactions with SAC. Observed effects on rheological properties are a consequence of nanoparticle agglomeration leading to formation of submicron and micron size particles. These act as classical fillers but remain rather small and as such have a large surface to volume ratio. Therefore, the changes in rheological properties are expected. If proposed assumption is correct, stable nanocomposites with proper nanoparticle distribution will remain transparent with no effect on viscosity and pseudoplasticity. Newtonian liquid shows the phase angle of 90° throughout the frequency range in oscillatory tests and constant viscosity at different shear conditions at flow tests [10]. With insufficient dispersing, nanoparticles form agglomerates that affect rheological properties. When more nanoparticles are added the effect is even stronger. Agglomeration of nanoparticles leads to pseudoplasticity and phase angle drops well below 90° at low angular frequencies. During the storage time larger agglomerates are formed in poorly stabilized nanocomposites. Therefore, smaller surface is available for copolymer – particle interactions. Such decrease in internal structure of nanocomposite can be observed as reduced viscosity and pseudoplasticity in flow tests.

3. Experimental

Syntheses of SACs and INP nanocomposites were performed on RC1*e*^{TM} reaction calorimeter (Mettler-Toledo). Triple wall glass reactor AP01-2-RTC was used for syntheses under reflux conditions. In addition, stainless steel high pressure reactor HP60 was used for high solid SAC and INP nanocomposite syntheses at elevated pressures. MNP nanocomposites were prepared by post synthesis blending of SAC and silica nanocomposites under dissolver stirrer accompanied by sonification.
Rheological properties of prepared nanocomposites were evaluated by Physica MCR301 rheometer (Anton Paar) with cone-plate sensor geometry. Agglomeration and distribution of nanoparticles through the copolymer matrix were observed by scanning (SEM) and transmission electron microscopy (TEM). Optical properties of prepared nanocomposites were analyzed by UV/VIS spectrometer. Thermal properties of nanocomposites were determined by thermal gravimetric analysis (TGA) and differential scanning calorimetry (DSC). Storage stability of nanocomposites after one year was also evaluated.

4. Results and discussion

The results of flow tests are presented in **Figure 1** (right). It can be seen that mixed nanoparticles with polysiloxane modified surface (MNP) have an effect on pseudoplasticity due to agglomerate formation (confirmed by SEM). On the other hand, incorporated nanoparticles modified with 3-methacryloxypropyltriethoxysilane (INP) have no effect on rheological properties. In fact, viscosity of INP nanocomposite is even lower when compared to plane high solid SAC (SAC 2 HS) even though the solid content is slightly higher (75.0 w/w % compared to 71.3 w/w %). MNP nanocomposites show lower viscosity when compared to copolymer (SAC 1, 62.4 w/w % solids) due to dilution with additional solvent. **Figure 1** (left) represents the oscillatory measurements in form of phase angle versus angular frequency plot. Model Newtonian fluid is showing 90° phase angle in entire frequency range. Both SACs are practically Newtonian whereas both MNP nanocomposites show strong pseudoplastic behavior. INP nanocomposite behaves like a Newtonian fluid. Other analyses such as transparency (UV/VIS), thermal properties (TGA and DSC) and storage stability (rheology) also support our assumption on the behavior of silica nanoparticles.

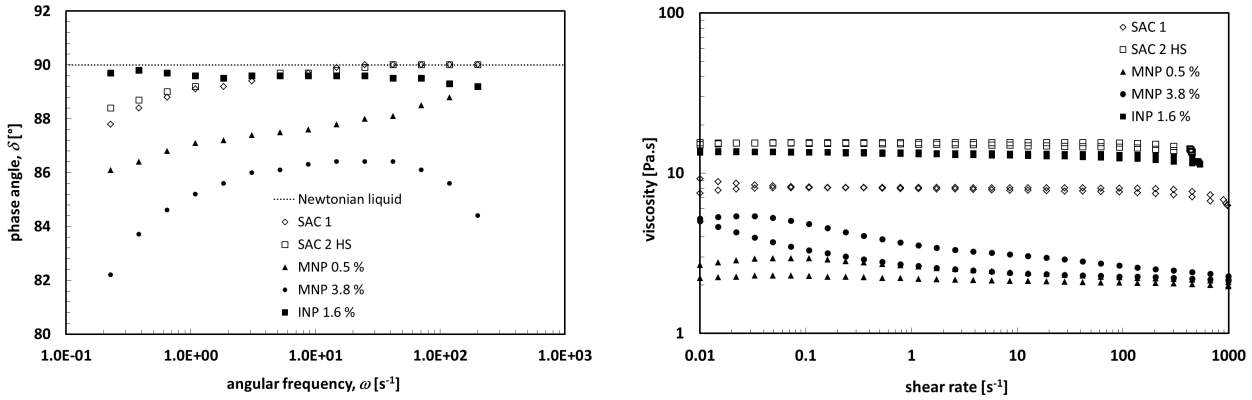

Figure 1. Oscillatory (left) and rotational measurements – flow curves (right) of SACs and silica nanocomposites.

6. Conclusions

In present study a novel explanation on behavior of silica nanoparticles in nanocomposites is introduced. The results support the idea of limited interactions between copolymers and nanoparticles smaller than 100 nm in all directions. This is reflected in rheological properties of nanocomposites and also confirmed by evaluating their thermal and optical properties.

Acknowledgements

Operation was part financed by the European Union, European Social Fund. Operation implemented in the framework of the Operational Program for the Human Resources Development for the Period 2007-2013, Priority axis1: Promoting entrepreneurship and adaptability, Main type of activity 1.1.: Experts and researchers for competitive enterprises.

The authors acknowledge the support from CE PoliMaT (financially supported by the Ministry of Education, Science, Culture and Sport of the Republic of Slovenia through the contract No. 3211-10-000057 (Centre of Excellence for Polymer Materials and Technologies)) where syntheses on RC1*e*™ were performed.

References

[1] D. K. Chattopadhyay, K. V. S. N. Raju, *Prog. Polym. Sci.* **2007,** 32, 352-418.
[2] E. Amerio, P. Fabbri, G. Malucelli, M. Messori, M. Sangermano, R. Taurino, *Prog. Org. Coat.* **2010,** 62, 129-133.
[3] D. Li, Q. Liu, L. Yu, X. Li, Z. Zhang, *Appl. Surf. Sci.* **2009,** 255, 7871-7877.
[4] Z. J. Ma, J. Hu, Z. J. Zhang, *Eur. Polym. J.* **2007,** 43, 4169-4177.
[5] W. Tanglumlert, P. Prasassarakich, P. Supaphol, S. Wongkasemjit, *Surf. Coat. Technol.* **2006,** 200, 2784-2790.
[6] K. Xu, S. Zhou, L. Wu, *Prog. Org. Coat.* **2010,** 67, 302-310.
[7] T. Yu, J. Lin, J. Xu, T. Chen, S. Lin, X. Tin, *Compos. Sci. Technol.* **2007,** 67, 3219-3225.
[8] O. Pyrlik, A. Nennemann, *Pitture e Vernici – European Coatings* **2010**, 86, 52.
[9] L. Reijnders, *Polymer Degradation and Stability* **2009,** 94, 873-876.
[10] T. G. Mezger; The Rheology Handbook, 3rd revised edition, Vincentz Network, Hanover, **2011**.
[11] S. Ceccia, E. A. Turcato, P. L. Maffettone, R. Bongiovanni*, Prog. Org. Coat* **2008**, 63, 110-115.
[12] S. Bussell, *Polym. Paint. Col. J.* **2010,** December, 26-28.
[13] B. Essen, *Polym. Paint. Col. J.* **2010,** December, 22-24.
[14] A. K. Mishra, R. S. Mishra, R. Narayan, K. V. S. N. Raju, *Prog. Org. Coat.* **2010,** 67, 405-413.

S6-L69
Ageing monitoring of nanosized aqueous polyurethane dispersion

Martin Ocepek (1)*, Jožefa Zabret (2,3), Janez Kecelj (2,3), Saša Skale (1), Peter Venturini (1,3), Bogdan Znoj (1,3), Janvit Golob (4)

(1) Helios Domžale d.d., Količevo 2, 1230 Domžale, Slovenia
(2) Helios TBLUS d.o.o., Količevo 65, 1230 Domžale, Slovenia
(3) CO PoliMaT, Tehnološki park 24, 1000 Ljubljana, Slovenia
(4) UL, Faculty of Chemistry and Chemical Technology, Aškerčeva cesta 5, 1000 Ljubljana, Slovenia
*martin.ocepek@helios.si

1. Introduction

Polyurethane water dispersions are used as resins in coatings of higher quality. Their benefits are: low environmental impact, as they contain little or no volatile organic components, good coating properties achieved only through physical drying at room temperature, wide range of applications and easy modification of physical and application properties by changing monomers ratio [1-7].

2. Theory

There have been several processes developed for PUDs synthesis but on the industry scale prepolymer and acetone processes are preferred. Prepolymer process can be divided into substages. First is the polymerization of poliols and diicocyanate performed in organic solvent. Typically N-methylpirolidone is used because it can efficiently dissolve internal emulsifying monomer and reduces the viscosity of the prepolymer. Next step is neutralization of functional groups in order to increase the hydrophilicity of the polymer chains. Then the isocyanate (NCO) terminated prepolymer is dispersed in cold water using high shear forces. In the final stage, water-soluble diamine is added as a chain extender in order to increase molecular weight [1-7].

We have observed that free NCO groups were present even for hours after synthesis had ended. Described phenomena was studied also by J. Yoon Jang et al. [6]. They made a conclusion that the conversion of NCO groups in chain extending step is around 50% as the chain extender cannot reach the NCO groups buried inside particles. However, NCO groups eventually react via competitive reaction with water even in a reaction that is slower for the factor from 200 to 1000 [7]. In both cases urea linkages are formed but in case of reaction of NCO with water, undesirable gaseous CO_2 is formed as a side product [1-7]. Nevertheless, some authors report full disappearance of NCO until the end of chain extension process but under different synthesis parameters [8].
According to relative kinetics constants [7], side reactions of free NCO groups with carboxyl groups and even with existing and newly formed urethane or urea groups are possible. That causes crosslinking in the system, which additionally raises molecular weight.
For the purpose of our study, only 50% of theoretically needed amine groups (-NH_2) were added, according to residual NCO groups.

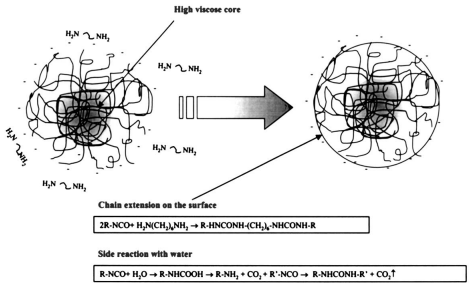

Figure 1. Chain extension step [6].

3. Experimental

PUD preparation

Polymerization was carried out via prepolymer process at 82°C. Equimolar amount of Triethylamine, according to carboxyl groups was used. For the chain extension step we employed 50% of theoretically needed Isophoronediamine (IPDA), according to residual NCO groups which were determined by di-n-dibutylamine back titration method [4] at the end of first stage.

PUD monitoring

After the synthesis, PUD has been put into 1L plastic container and kept at room temperature (20°C ± 1°C) for the whole aging process. Container was sealed, except when samples for aging parameters measurements were taken.

Characterizations

FTIR spectra were measured with FTIR Nexus, Thermo Nicolet spectrometer using ZnSe pellets in a range between 650 and 4000 cm^{-1} with resolution 4 cm^{-1}. For particle size and zeta potential measurements we used ZetaSizer nano series, Malvern. Atomic Force Microscope, Park was used for particle size validation. Conductivity and pH measurements were performed without any

sample preparation with SevenMulti, Mettler Toledo. Viscosity was measured with MCR301, Anton Paar rheometer at 20°C. Size exclusion chromatography was employed for molecular weight determination.

4. Results and discussion

Fig. 2 presents recorded FTIR spectra in a period of three days after the synthesis. The spectra are normalized to unchanging C-H peak at wavenumbers from 2820 to 3010 cm^{-1}. It is shown that majority of free NCO groups at wavenumber 2270 cm^{-1} disappear after one day and that required time for total disappearance is 3 days.

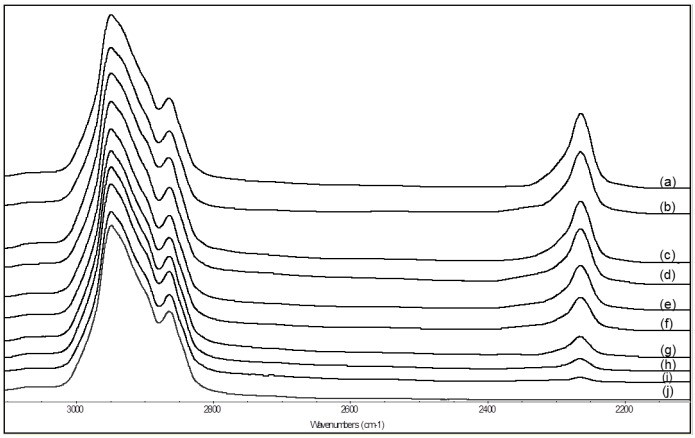

Figure 2. Disappearance of NCO groups during ageing (normalized to C-H peak).

5. Conclusions

Polyurethane dispersions prepared via industrial prepolymer process were monitored by several chemical and physical parameters to investigate the behaviour of the material. We showed that free NCO groups mainly disappear after approximately one day and that a full conversion occurs in 3 days. The ageing mechanism was confirmed by pH and conductivity measurements showing expected drop of pH and conductivity increasement. During aging process particle size and its distribution did not significantly changed.

Acknowledgements

Funding for this research was provided by Helios d.d.

References

[1] D. K. Chattopadhyay, K.V.S.N. Raju, *Prog. Polym. Sci.* 2007, 32, 352–418.
[2] B. K. Kim, *Colloid Polym. Sci.* 1996, 274, 599-611.
[3] Y. K. Jhon et al., *Colloids and Surfaces, A: Physicochem. Eng. Aspects* 2001, 179, 71-78.
[4] G. Oertel, Polyurethane handbook, Hanser Publishers, Munich, Germany, 1985, p. 22-25, 31.
[5] S. A. Madbouly, J. U. Otaigbe, *Prog. Poly. Sci.* 2009, 34, 1283-1332.
[6] J. Yoon Jang et al., *Colloids and Surfaces A: Physicochem. Eng. Aspects* 2002, 196, 135–143.
[7] M. Ionescu, Chemistry and Technology of Polyols for Polyurethanes, Rapra Technology, Shropshire, UK, 2005, p. 18.
[8] K. K. Yee, Aqueous polyurethane dispersion with non-yellowing and good bonding strength for waterborne polyurethane footwear adhesives applications, Acadia University, Canada, 2005.

Session 5: Polymers for Technically Advanced Applications and Energy

S5-L70
Mechanical properties of thiolated hydrogel assemblies: the effect of polymer modification and structural architecture

James P. Best*, Frank Caruso
Department of Chemical and Biomolecular Engineering, The University of Melbourne, Parkville, Victoria 3010, Australia
*bestj@student.unimelb.edu.au

Introduction

Soft nanostructured planar and colloidal hydrogel systems are promising for biomedical applications due to their precise engineering, low cytotoxicity, and tunable hydration and rigidity [1, 2]. Increasingly, research is focusing on the influence of advanced material physicochemical properties on cellular and biological interactions [3]. In the work presented in this abstract, we chemically modified a well-studied polymeric hydrogel (poly(methacrylic acid), PMAA) with varying degrees of thiol functionality. We then studied how tuning the crosslinking degree in these systems, along with the film architecture, affected the system mechanical properties, quantified using atomic force microscopy (AFM) force spectroscopy.

Results and discussion

1. PMAA modification and characterization

Utilizing carbodiimide chemistry, PMAA was modified with (2-pyridinyldithio)ethanamine (PDA) in order to introduce a thiol functionality to the hydrogel [4]. The reaction stoichiometry was varied for four PMAA batches as to achieve functionalization extents of 5, 10, 15 and 20 %, as shown in Figure 1.

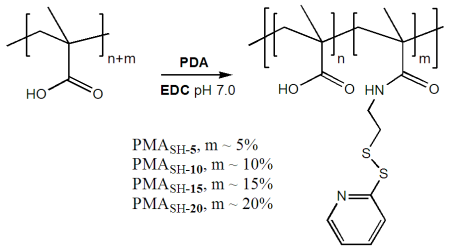

Figure 1. Preparation of PDA modified PMAA (PMAA-*co*-PPDAMA) with varying amounts of covalently attached PDA.

The extent of PDA modification was accurately quantified using ^{1}H-NMR. PMAA-*co*-PPDAMA could then be reduced to "PMA_{SH}" through cleavage of the disulfide linkage. Using the layer-by-layer technique it was adsorbed sequentially with a hydrogen bonding partner, poly(*N*-vinylpyrrolidone) (PVPON), onto poly(ethyleneimine) (PEI) coated planar or colloidal/mesoporous SiO_2 substrates. The film was then crosslinked using a strong oxidizing agent, and the PVPON removed under basic conditions. Hollow PMA_{SH} capsules or mesoporous particles were subsequently formed through etching of the silica substrate for colloidal deposition.
The charge and hydrophobicity of the modified polymers were investigated using ζ-potential analysis on colloidal beads, and inverse captive bubble measurements on planar films (results shown in Figure 2). The thiol modification of PMAA had a negligible effect on PMA_{SH} surface charge, while the hydrophobicity of the hydrogel surface increased slightly as expected.

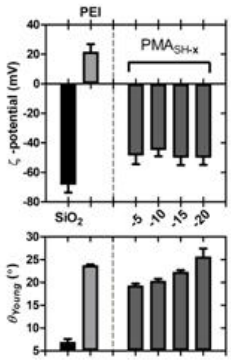

Figure 2. ζ-potential (top) and hydrophobicity (bottom) results for SiO_2, PEI and modified PMA_{SH} batches.

2. Mechanical properties of variable PMAA-*co*-PPDAMA

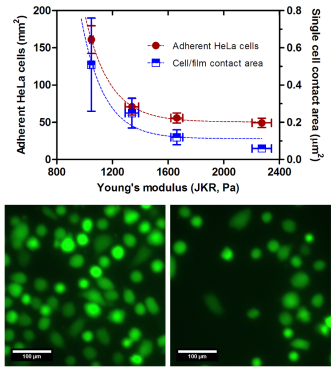

Figure 3. HeLa cell adhesion on PMA_{SH} substrates. Cancer cell adhesion was promoted through tuning the rigidity of the planar support network. Fluorescence images show stained HeLa adhesion to low (5%, left) and high (20%, right) E_Y films after 6 h.

Incubation with HeLa cervical cancer cells suggested that cell adhesion could be promoted through tuning of the PDA modification of PMAA, as shown in Figure 3. The promoted adhesion was linked to the mechanical properties of the hydrogel films. In order to quantify the difference in mechanical properties of the films, a colloidal probe AFM technique was utilized. The Young's modulus (E_Y) of the films increased with increasing PDA modification using a Johnson-Kendall-Roberts (JKR) model. As the spring constant of the film decreased, settled cells were able to affect a larger deformation on the film substrate, enhancing the contact area.

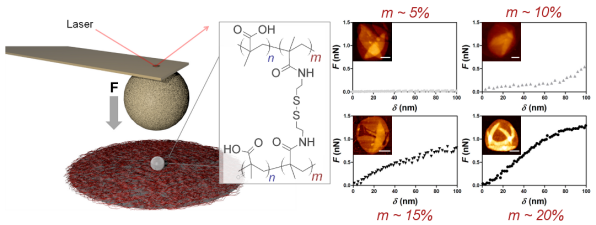

Figure 4. Colloidal probe (CP) AFM technique (left) for hydrogel capsule indentation. Force-deformation curves (right) for capsules with variable PDA modifications.

In addition, the influence of crosslinking extent in free-standing PMA_{SH} capsules was studied using CP-AFM. As shown in Figure 4, capsule systems with a greater number of crosslinks showed increased rigidity, witnessed in both AFM imaging of collapsed capsules, and force-deformation curves.

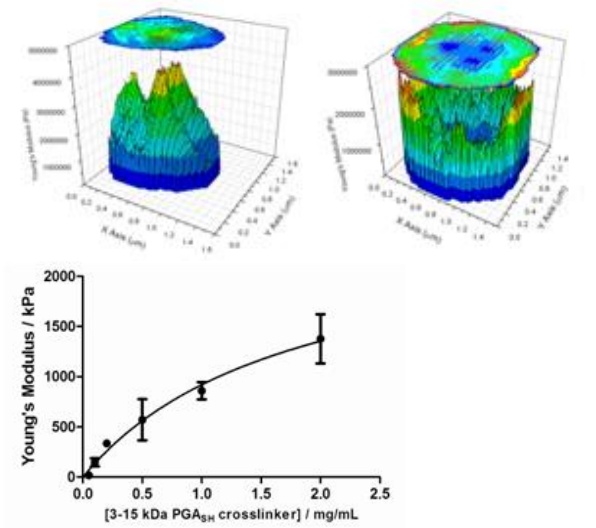

Figure 5. High-resolution force tomography images representing E_Y maps for hydrogel particles with 2.0 mg/mL (left) and 0.2 mg/mL (right) crosslinker, and E_Y/crosslinker relationship (bottom).

Mesoporous hydrogel particles were also fabricated using thiolated poly(*L*-glutamic acid) (PGA_{SH}), analagous to PMA_{SH}, and studied using a high-resolution AFM technique. For these systems, 800 nm mesoporous silica templates were infiltrated with the hydrogel polymer in solution, and then crosslinked using different concentrations of the thiolated polymer. The spring constant (1.4 – 52.7

mN/m) and E_Y (17.7 – 1377.3 kPa) of the PGA_{SH} particles could be effectively tuned, as shown in Figure 5. In addition, the detailed morphology and deformation of the particles could also be studied using the high-resolution force technique.

3. Mechanical properties of variable PMA_{SH} architectures

In order to study the effect of the crosslinked hydrogel architecture on the mechanical properties, 20 % modified PMAA-*co*-PPDAMA was built upon planar and colloidal substrates, and the mechanical properties compared, as shown in Figure 6. Interestingly, hollow capsules had the greatest system spring constant, whereas core-shell particles had a film constant half that of planar film deformation. This difference in force resistance is expected to be due to membrane bending tensors (T_1, T_2) in the shell systems, which do not occur in either film or core-shell architectures. It is anticipated that through characterizing the mechanical properties of these architectures, physical parameters relating to the surface tension and membrane pre-tensions of the polymer films may be elucidated.

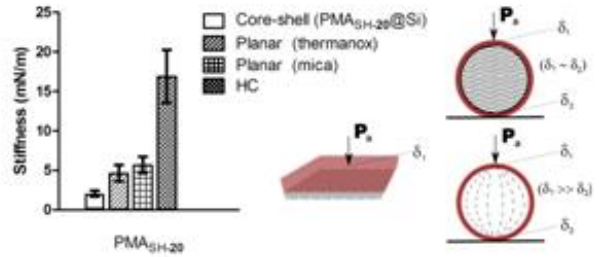

Figure 6. Mechanical stiffness comparison for planar film, core-shell, and hollow capsule compression.

Acknowledgements.
This work was supported by the Australian Reasearch Council within the Federation Fellowship and Discovery Project schemes.

References

[1] Hoare, T.R. and D.S. Kohane, *Polymer* 2008, 49, 1993-2007.
[2] Becker, A.L., A.P.R. Johnston, and F. Caruso, *Small* 2010, 6, 1836-1852.
[3] Best, J.P., Y. Yan, and F. Caruso, *Adv. Health. Mater.* 2012, 1, 35-47.
[4] Becker, A.L., et al., *Langmuir* 2009, 25, 14079-14085.

S5-L71
Novel silicone thermoplastic elastomers with tailored permeation properties

Katrin Berger (1)*, Gisbert Riess (2), Wolfgang Kern (2)
(1) Polymer Competence Center Leoben, Roseggerstrasse 12, 8700 Leoben, Austria
(2) Chair of Chemistry of Polymeric Materials, Montanuniversität Leoben, Otto-Glöckl-Straße 2, 8700 Leoben, Austria
*katrin.berger@unileoben.ac.at

1. Introduction

Polysiloxanes such as polydimethylsiloxane (PDMS) combine several unique properties. They exhibit a low glass transition temperature, high thermal and oxidative stability, high UV-resistance, low surface energy and strong hydrophobicity as well as high permeability to many gases [1]. These characteristics are independent over a wide temperature range. Our research deals with the synthesis and properties of polymers containing soft segments of dimethylsiloxane and hard urea segments. In order to determine structure-property relations, regarding to permeation properties, the chemical structure was varied.

2. Experimental

In this study thermoplastic silicone elastomers, based on polydimethylsiloxane oligomers with amino groups and different diisocyanates, were synthesized according to figure 1 [2]:

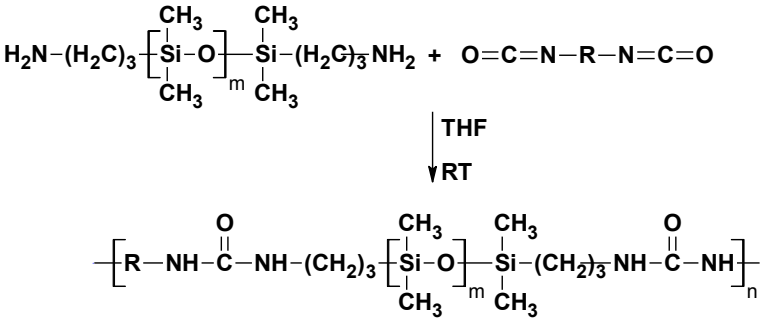

Figure 1: Scheme of synthesis of the main-chain urea-siloxane polymer [2]

The polymers were characterized by nuclear magnetic resonance (NMR) and infrared (FTIR) spectroscopy. The formation of hydrogen bonding of the hard segments was investigated by temperature dependent FTIR-spectroscopy, which displayed the thermal stability of the elastomer. The main-chain urea-siloxane copolymers listed in table 1 were synthesized and characterized in the described manner.

Table 1: Synthesized main-chain urea-siloxane copolymers

	α,ω-diamino siloxane (1400 g/mol)	α,ω-diamino siloxane (2800 g/mol)
hexamethylene diisocyanate	HMDI-1400	HMDI-2800
isophorone diisocyanate	IPDI-1400	IPDI-2800
2,4-toluene diisocyanate	TDI-1400	TDI-2800

3. Results and discussion

Thin membranes of thermoplastic main-chain urea-siloxane copolymer were prepared and investigated with respect to the permeation properties of organic solvents. Vials were filled with a mixture of an aromatic (toluene) and an aliphatic hydrocarbon (iso-octane) and were sealed with the polymer films. The weight of the vials was periodically measured to investigate possible barrier properties of the polymers against organic solvent mixtures. The weight loss of solvent over a period of 7 days was determined. No correlation between chemical structure and solvent permeation was found, whereas the composition of the residual solvent mixture showed strong variations. This was investigated by the GC-MS-technique.

Shorter siloxane units led to lower permeability of organic solvents. Urea-siloxanes with isophorone diisocyanate depicted higher permeation rates compared to other urea-siloxanes. The permeation of single solvents was investigated and the results are shown in the following figure 2.

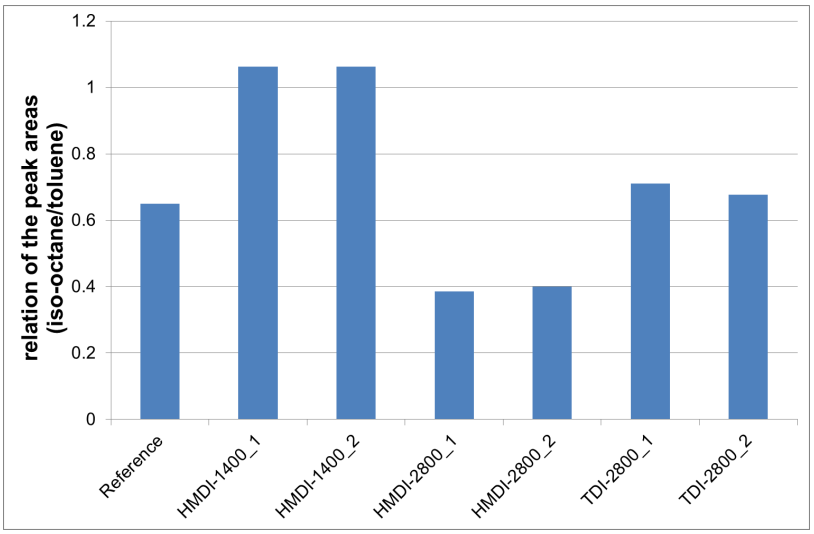

Figure 2: GC-MS data of the residuals solvent mixture in the vials per two samples

The concentration of residual solvent mixture was measured by the relation of the peak area of the two solvents. Figure 2 depicts that a separation of the solvent mixture occurred. Hexamethylene diisocyanate with short siloxane units (HDMI-1400) exhibited a

higher permeability of aromatic solvent, while the opposite effect took place for the sample with longer siloxane-chains. Toluene diisocyanate with longer siloxane units showed no effect. Therefore the permeation properties can be tailored with regard to the field of application. These siloxane polymers can be used as semipermeable membranes for separation of solvent mixtures.

4. Conclusions

In conclusion, we have successfully synthesized novel main-chain urea-siloxane elastomers with selective barrier properties. These polymers are highly permeable for organic solvents depending on the chemical structure. The permeation properties are important with respect to the application as membrane material in oil field applications.

Acknowledgements

This study was performed at the Polymer Competence Center Leoben GmbH (PCCL, Austria) with contributions of the Chair of Chemistry of Polymeric Materials (University of Leoben). PCCL is funded by the Austrian Government and the State Governments of Styria and Upper Austria.

References

[1] I. Yilgör, A. K. Sha´aban, W. P. Steckle, D. Tyagi, G. L. Wilkes, J. E. McGrath, *Polymer* **1984**, 25, 1800.
[2] G. Riess, H.-W. Schmidt, *Chem. Mon*. **2006**, 137, 935-941

S5-L72

Photochemical cross-linking of XNBR-latex using the thiol-ene reaction – a new approach for the manufacture of low allergenic latex gloves

Dietmar Lenko (1)*, Sandra Schlögl (1), Raimund Schaller (2), Armin Holzner (2), Wolfgang Kern (1,3)
(1) Polymer Competence Center Leoben GmbH, Roseggerstrasse 12, A-8700 Leoben, Austria
(2) Semperit Technische Produkte GmbH, Triester Bundesstraße 26, A-2632 Wimpassing, Austria
(3) University of Leoben, Chair of Chemistry of Polymeric Materials, A-8700 Leoben, Austria
*Dietmar.Lenko@pccl.at

1. Introduction

Currently synthetic latices such as carboxylated acrylonitrile butadiene rubber (XNBR) latex are cured via thermal processes generating covalent and ionic cross-links using sulfur or peroxides in conjunction with accelerators and activators and ZnO. The combination of these two systems is required to generate both ionic and covalent cross-links to ensure good mechanical properties of elastomer materials. Covalent bonds are generated with the sulfur curing of the butadiene units whereas ionic links are achieved with a reaction of zinc ions with the carboxylic acid groups of the latex at higher pH values [1]. However, residual accelerator levels in dipped XNBR-latex goods can lead to allergenic reactions [2-4]. In the present work a new photochemical curing process based on the thiol-ene addition reaction has been developed to avoid skin irritating and skin sensitizing process chemicals. The reaction mechanism involves the excitation of a photoinitiator with UV light followed by a bond cleavage and the formation of free radicals which generates thiyl radicals due to a proton abstraction from multi-functional thiols. These thiyl radicals react with the C=C double bonds of the butadiene units of a conventional XNBR-latex, which is taken without any pre-treatment, under the formation of thioether links [5]. In addition ionic links were generated by a thermal curing step with ZnO to ensure high tensile strength of the cross-linked elastomer materials (see **Figure 1**).

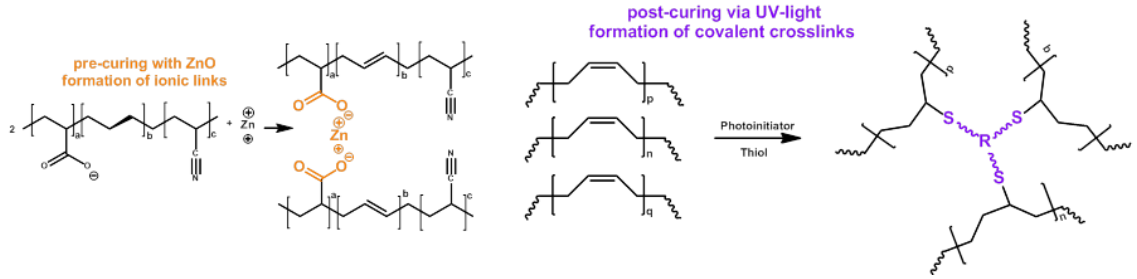

Figure 8: Dual cross-linking of XNBR-latex

2. Experimental

The UV assisted cross-linking of XNBR latex was carried out both in liquid (pre-vulcanization) as well as in solid (post-vulcanization) phase. For the photochemical vulcanization a selected photoinitiator (Lucirin TPO-L) and a tri-functional thiol (trimethylolpropantris-3-mercaptopropionate) were added to the XNBR latex. The photochemical pre-vulcanization was carried out in a falling film photoreactor providing a homogeneous and continuous UV illumination of the latex mixture. The lamp power ranged from 800 and 3500 W with wave lengths between 250 and 480 nm [6]. For the thermal pre-vulcanization a KOH solution (1 wt.-%) was added to the XNBR latex under stirring to raise the pH-value from 8.3 to 10 and a ZnO dispersion was admixed,

obtaining ZnO levels of 0.5, 1.0 and 2.0 phr (parts per hundred parts rubber). The mixture was stirred for 2 hours at 50 °C. The latex films were prepared via a conventional coagulant dipping process. Both thermally as well as photochemically pre-cured XNBR latex films were then post-vulcanized employing the UV assisted reaction pathway. The post-vulcanization was carried out under air with a medium pressure Hg lamp (Hereaus) using a light intensity in the range from 0.3 to 1.2 J/cm^2.
The characterization of the UV cross-linking reaction was performed with real time FT-IR spectroscopy. Swelling measurements according to the Flory-Rehner method were carried out to determine the cross-link density of the cured XNBR films.[7] The mechanical properties of cross-linked XNBR latex films including Young's modulus, tensile strength and ultimate elongation were determined with a Zwick tensile tester Z010 in compliance with ASTM standard.[8]

3. Results and Discussion

Since the decrease of the thiol-bands and the appearance of thioether signals, which arise when forming the thiol-ene networks in XNBR films, cannot be detected quantitatively (both moieties show weak absorption signals in their infrared spectra) the decrease of the C=C double bonds was monitored during UV exposure. The real time FT-IR spectroscopy clearly reveals that the control sample containing neither photoinitiator nor thiol does not show a significant decrease (1 %) of the C=C band (see **Figure 2a**). With 5.0 phr photoinitiator added the decrease of the relative peak area amounts to 8 % attributed to the formation of short chain carbon-carbon cross-links. However, the maximum depletion of the peak area (12 %) is observed in the presence both of photoinitiator and thiol. In the first step the XNBR-latex was photochemically pre-cured. Although a considerable increase of the network density and the Young's modulus is observed with increasing UV exposure, the tensile properties could not be improved (<4 MPa). Therefore we combined the UV assisted pre-curing of the

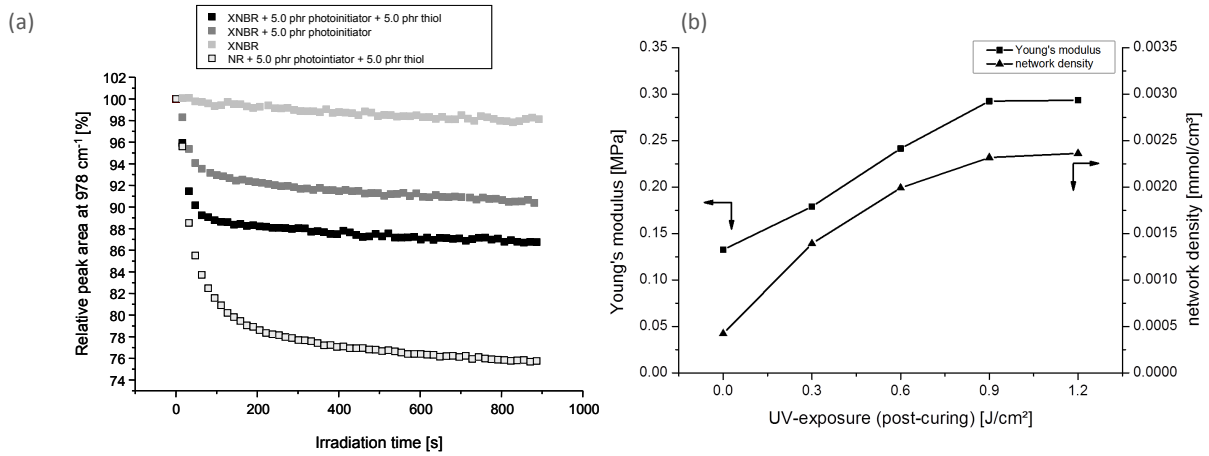

Figure 9: (a) Monitoring the thiol-ene reaction in XNBR films with real time FT-IR spectroscopy: Depletion of the C=C band at 968 cm^{-1} upon UV irradiation (b) Young's modulus and network density in dependence on the UV post-curing of XNBR-latex (thermal pre-vulcanization with 0.5 phr ZnO)

liquid state with a photochemical post-curing of the solid films. Whilst the network density, the Young's modulus and the ultimate elongation at break correlate with the UV exposure dose used in the post-curing step, the tensile strength cannot be enhanced significantly. Several authors have proposed that both covalent as well as ionic cross-links are required to obtain good mechanical properties and ageing stabilities.[9] As a consequence we combined a thermal pre-curing step employing ZnO with a UV assisted post-curing step. In **Figure 2b** the network density of the thermal pre-cured samples (0.5 phr ZnO) is depicted in dependence on the UV exposure used in the post-curing. It is evident, that the network density as well as the Young's modulus are increasing with higher UV exposure doses.
With respect to the tensile properties a substantial increase of the tensile strength and Young's modulus is observed, that is attributed to the additional formation of ionic cross-links. It can be observed that the concentration of ZnO strongly influences the tensile properties of the XNBR films and that the photochemical post-curing step leads to a further increase of the tensile strength. In particular, the tensile strength of XNBR films thermally pre-cured with 2.0 phr ZnO can be improved from 26 ± 2 MPa to 30 ± 2 MPa. From the results it can be concluded that the tensile properties of dual cross-linked XNBR films meet the quality requirements of the European Standard EN 455-2 for medical and surgical gloves.[45] Since conventional vulcanization agents are substituted by photochemicals, allergenic reactions related to accelerator residues can be avoided. Consequently the dual cross-linking of XNBR represents a new way towards the production of low allergenic medical gloves.

4. Conclusions

It is clearly shown that the photochemically cross-linking of XNBR-latex using the thiol-ene reaction is feasible. The two step process (thermal pre-curing & UV post-curing) is required to ensure high tensile strength, which is mainly governed by the light intensity and the concentration of the photochemicals. The new UV process offers a new approach for the manufacture of low allergenic latex articles (e.g. gloves), with tailored donning properties.

Acknowledgements
The research work of this paper was performed at the Polymer Competence Center Leoben GmbH (PCCL, Austria) within the framework of the COMET-program of the Federal Ministry for Transport, Innovation and Technology and Federal Ministry for Economy, Family and Youth with contributions by the Chair of Chemistry of Polymeric Materials (University of Leoben, Austria) and the Semperit Technische Produkte GmbH (Wimpassing, Austria). The PCCL is funded by the Austrian Government and the State Governments of Styria and Upper Austria.

References
[1] H. P. Brown, Rubb Chem Technol 1963, 36 (4), 931–962.
[2] C. Peixinho, British Journal of Dermatoloy 2008, 159, 132.
[3] A. Yagami, K. Suzuki, H. Saito, K. Matsunaga, *Allergol Int* 2009, 58, 347.
[4] D. Ownby, *The Journal of allergy and clinical immunology*. 2002, 27, 110.
[5] C. E. Hoyle, T. Y. Lee, T. Roper, *Journal of Polymer Science, Part A.* 2004, 21, 5301.
[6] S. Schlögl, A. Temel, R. Schaller, A. Holzner, W. Kern, *Rubb Chem Technol* 2010, 83, 133.
[7] P. J. Flory, J. Rehner, *J. Chem. Phys.* 1943, 11, 521.
[8] ASTM. D412-06ae2 Test Methods for Vulcanized Rubber and Thermoplastic Elastomers—Tension
[9] L. Ibarra, M. Alzorriz, J. Appl. Polym. Sci. 2002, 84, 605.
[10] EN. 455-2 Medical gloves for single use - Part 2: Requirements and testing for physical properties

S5-L73
Improvement of light shielding performance of thermotropic glazings by adaption of material composition and curing parameters

Andreas Weber (1)*, Katharina Resch (2)
(1) Polymer Competence Center Leoben GmbH, Roseggerstraße 12, 8700, Leoben, Austria
(2) University of Leoben, Department Polymer Engineering and Science, Otto Glöckel-Straße 2, 8700, Leoben, Austria
*Andreas.Weber@pccl.at

1. Introduction
Thermotropic glazings change their light transmittance from transparent to opaque upon exceeding a threshold temperature reversibly [1]. Thus, they can prevent buildings and solar thermal collectors from overheating [2,3]. Thermotropic glazings based on UV-curable resin systems consist of a thermotropic additive that is finely dispersed in a resin matrix [1]. Below the threshold temperature refractive indices of matrix and thermotropic additive are almost equal, resulting in transparent appearance [1]. Upon exceeding the threshold temperature refractive index of thermotropic additive changes significantly with the onset of light-scattering [1]. Consequently, the layer turns opaque. However, recent research revealed formation of vacuoles at the interface of matrix material and scattering domains formed by thermotropic additive for specific thermotropic glazings [4]. As a consequence transition from opaque to transparent occurred above the switching threshold [4]. Thus, the overall objective of this study was to investigate formation of vacuoles in detail and subsequently to establish strategies for preventing it.

2. Experimental
Thermotropic layers based on UV-curable resin matrix were prepared by dissolving the thermotropic additive (paraffin) in the UV-crosslinkable matrix solution. Matrix consisted of polyester acrylate oligomer, reactive diluent and photo-initiator. The dissolutions were poured in the intervening space between two glass panes which were sealed around the edge, stored for 10minutes at room temperature, and cured by UV light. Afterwards free standing layers with a thickness of 900µm were obtained by removal of the glass panes. The theoretical additive content was 5wt%.

Hemispheric solar transmittance as a function of temperature of the formulated thermotropic layers were determined applying UV/Vis/NIR spectrometry. The spectrophotometer was equipped with a heating stage in order to maintain sample temperature. Prior to measurement, the samples were allowed to equilibrate for five minutes at the selected temperature. Morphology was investigated applying optical and scanning electron microscopy, respectively.

3. Results
Thermotropic layer produced from 57wt% oligomer, 40wt% reactive diluent trimethylolpropane triacrylate (TMPTA) and 3wt% conventional photo-initiator blend (benzophenone and 1-hydroxy cyclohexyl phenyl ketone) and cross-linked with a dose of 2.1J/cm² from mercury lamp of Light Hammer 6 (Fusion UV Inc., Gaithersburg, MD, USA) showed solar hemispheric transmittance of 70% at room temperature (see Fig. 1, left). Upon exceeding the threshold temperature of 50°C, solar hemispheric transmittance increased to 85%. Optical and scanning electron micrographs revealed vacuoles at the interface of matrix and thermotropic additive (see Fig. 1 left, insert: domain with vacuole; vacuole is depicted black). These vacuoles are likely to be formed due to different coefficients of thermal expansion (CTE) of matrix and additive: Upon irradiation with 2.1J/cm² (mercury lamp) temperature of glass panes comprising the thermotropic mixture increases. This is attributable primarily to an increase of

temperature of the thermotropic mixture due to absorption of radiation emitted by the mercury lamp. Upon cooling after curing procedure thermotropic additive may contract more intensely than the surrounding matrix. In combination with limited adhesion of matrix and thermotropic additive vacuoles are formed.
To prevent vacuole formation, several strategies have been applied:

- Increasing matrix flexibility by replacement of tri-functional TMPTA by another tri-functional reactive diluent with longer spacers between acrylate moieties (OTA)
- Reduction of heat generation in thermotropic mixtures due to absorption by
  - variation of irradiation intensity
  - replacement of conventional photo-initiator by a photo-bleaching one which allows a more efficient curing process for thick layers

Thermotropic layer formulated with conventional photo-initiator blend and cured by a dose of 1.2J/cm² from mercury lamp of Light Hammer 6 featured hemispheric solar transmittance of 80% and 83% below and above the threshold temperature, respectively. Replacement of reactive diluent TMPTA by OTA yielded transmittance of 79% at room temperature which increased to 85% upon exceeding the threshold temperature. Both, replacement of TMPTA by OTA and reduction of curing dose to 1.2J/cm², yielded transmittance of 84 and 87% below and above the threshold temperature, respectively. In general a stronger impact of UV dose on light shielding properties was observed. However, further reduction of curing dose would yield partially uncured samples due to lacking depth of cure resulting from absorption of conventional photo-initiator and its fragments. Hence a photo-bleaching photo-initiator was utilised in order to maintain sufficient conversion and depth of cure in the 900µm thick thermotropic layers also on low levels of irradiance. Thermotropic layer produced from 57wt% oligomers, 40wt% reactive diluent OTA and 3wt% photo-bleaching photo-initiator (ethyl 2,4,6-trimethylbenzoyl phenyl phosphinate) was cured by low intensity UV-radiation from Universal-UV-Lampe (Camag, Muttenz, CH) for 30 minutes displayed a hemispheric solar transmittance of 81% at room temperature (see Fig. 1, right). Upon exceeding the threshold temperature, a slight reduction in hemispheric solar transmittance to 79% was attained. The improvement in switching characteristics is attributable to suppression of vacuole formation (see Fig. 1 right, insert: domain is lacking a vacuole).

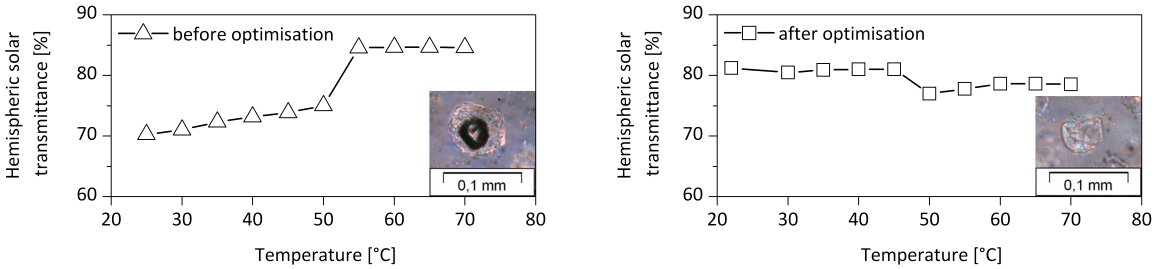

Figure 1. Hemispheric solar transmittance as a function of temperature and corresponding optical micrographs (inserts) of thermotropic layers before (left) and after (right) optimisation of curing parameters.

4. Conclusions

Especially by reducing the irradiation dose and correspondingly adapting the resin formulation, specifically in terms of photo-initiator, an improvement of the light shielding efficiency of thermotropic glazings was obtained. Thus, a processing-structure-property-relationship is deducible: Curing by low intensity UV-radiation suppresses vacuole formation successfully. This may be ascribed to reduced heat generation and thus lower temperature increase of the matrix material. Hence, different CTE of matrix and additive have minor effect on the development of layer morphology. The lack of vacuoles yields improved switching characteristics.

Acknowledgements

This research project is funded by the State Government of Styria, Department Zukunftsfonds. The authors wish to acknowledge the contributions of BASF SE (Ludwigshafen, D), Cytec Surface Specialities (Drogenbos, B) and Sasol Wax GmbH (Hamburg, D).

References

[1] P. Nitz, H. Hartwig, *Sol. Energy* **2005**, 79, 573–582.
[2] J. Yao, N. Zhu, *Build. Environ.* **2012**, 49, 283–290.
[3] G.M. Wallner, K. Resch, R. Hausner, *Sol. Energy Mater. Sol. Cells* **2008,** 92, 614–620.
[4] A. Weber, K. Resch, *Energy Procedia* **2012**, 30, 471-477.

S5-L74
Spectroscopic, thermal and (thermo)mechanical analysis of multilayer backsheets

Klaus J. Geretschläger*, Gernot M. Wallner, Jörg Fischer
Johannes Kepler University Linz (JKU), Institute of Polymeric Materials and Testing (IPMT)
Altenberger Strasse 69, 4040 Linz, Austria
*klaus_jakob.geretschlaeger@jku.at

1. Introduction
For backsheets and frontsheets of PV modules currently a variety of polymeric materials is used. Polyester and fluoropolymers are dominating. Alternative materials are currently developed and introduced into the market. Interestingly, no comprehensive property profiles of multilayer backsheets are available in the literature. Hence, it is the main objective of this work to characterize commercially relevant backsheets as to their spectroscopic, thermal and (thermo)mechanical behaviour and to derive application oriented properties.

2. Experimental
Various multilayer backsheet materials were selected and analysed by ultraviolet/visible/near infrared spectroscopy (UV/VIS/NIR), infrared spectroscopy in attenuated total reflection mode (IR-ATR), differential scanning calorimetry (DSC), thermal gravimetric analysis (TGA), dynamic mechanical analysis (DMA) and tensile testing.

3. Results and discussion
The hemispherical solar reflectance of the white pigmented backsheets was ranging from 0,539 to 0,800. By IR-spectroscopy and DSC the polymeric materials of the various layers were identified. Furthermore, it was shown for the thermoplastic EVA layers (inner surface of polyester backsheets), that two different EVA grades with VA contents of 7 $\%_m$ and 17 $\%_m$ are used. By TGA an inorganic filler and pigment content of about 6 $\%_m$ at room temperature was detected. Figure 10 displays representative DMA curves and tensile test curves of a polyamide based multilayer backsheet. The highest Young's modulus was found in polyvinylfluoride based multilayers while the lowest values had been detected for polyamide based structures. Depending on the backsheet type softening was revealed in the service relevant temperature range (from -50 to 100°C). Significant differences in the thermo(mechanical) behaviour were also observable in the PV module lamination temperature range (from 100 to 160°C).

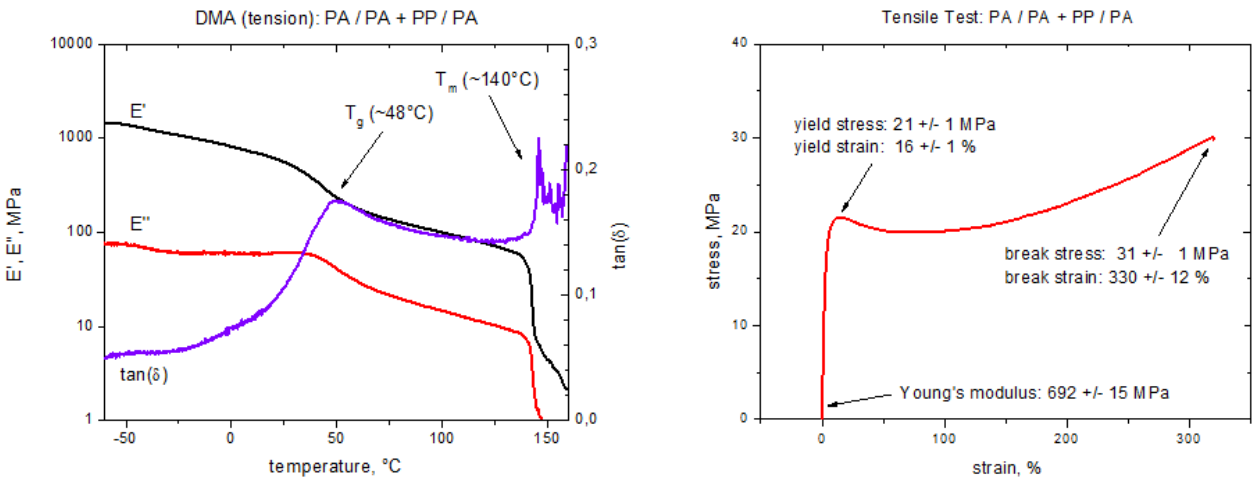

Figure 10. DMA curve (left) and tensile testing curve (right) of a polyamide based multilayer backsheet

4. Conclusions
While the material properties given in the data sheets of commercially relevant backsheets for PV modules are hard to compare due to a lack of data and different testing methods and parameters used, in this paper for the first time a comprehensive and comparable property profile is provided for the main backsheet types.

POSTERS

Session 1: Advances in polymer synthesis and modification

S1-P1
Purification of invertase from Saccharomyces cerevisiae with poly(ethyleneimine)-attached monolithic cryogel columns

Kemal Çetin (1)*, Işık Perçin (2), Deniz Türkmen (1), Adil Denizli (1)
(1) Department of Chemistry, Biochemistry Division, Hacettepe University, Ankara, Turkey
(2) Deparment of Biology, Molecular Biology Division, Hacettepe University, Ankara, Turkey
* kemalcetin@hacetepe.edu.tr

1. Introduction
Poly(2-hydroxyethyl methacrylate) – poly(ethylene imine) (PHEMA-PEI) cryogel columns were produced to have an efficient, cost effective and rapid purification of invertase from *Saccharomyces cerevisiae*. The PHEMA cryogels were prepared by free radical polymerization in a syringe at sub-zero temperature. Poly(ethyleneimine) (PEI) was attached with ester groups of PHEMA cryogel. Then, the metal ions were chelated on the PHEMA-PEI cryogel column. Invertase adsorption was performed on the metal chelating monolithic columns.

2. Theory
Invertase (β-D-fructofuranosidase fructohydrolase, EC 3.2.1.26) which is efficient enzyme to catalyse the hydrolysis of sucrose into glucose and fructose [1]. The hydrolyzed sugar mixture obtained by invertase has the advantage of being colourless in contrast to the coloured products obtained by acid hydrolysis. [2] Invertase generally exists in microorganisms and plants. It is widely used in the food and beverage industry. The enzyme is also used in the manufacture of artificial honey and plasticizing agents [3]. Immobilized metal ion affinity chromatography (IMAC) is a powerful method for the purification of proteins, peptides, nucleic acids, hormones, and enzymes [4]. The separation is based on the interaction of a Lewis acid (electron pair acceptor), i.e., a chelated metal ion, with an electron donor atoms (N, O and S) on the surface of the protein [5]. Proteins are assumed to bind through the imidazole group of histidine, the indoyl group of tryptophan and the thiol group of cysteine. Co-operation between neighboring aminoacid side chains and local conformations play important roles in protein binding [6].
Cryogels are natural or synthetic polymers which are synthesized in moderately frozen solutions of monomeric or polymeric precursors [7]. Since cryogels have some advantages such as having macropores, short diffusion path, low pressure drop and very short residence time, they are very good alternative to purify invertase from *Saccharomyces cerevisiae.* In this study, metal ions-chelated poly (hydroxyethyl methacrylate)/poly(ethyleneimine) [mPHEMA/PEI] monolithic cryogel columns are prepared for the adsorption of invertase. PEI is attached on the PHEMA columns in order to have high adsorption capacity for invertase. It was showed that the attachment of polymer chains such as PEI onto the adsorbent to form tentacle-type supports could sufficiently increase the adsorption capacity of biomolecules [8].

3. Experimental
To prepare PHEMA cryogel, 1.3 ml HEMA and 0.3 g MBAAm were dissolved in 5 ml deionized water and the mixture was degassed under vacuum for 5 min to eliminate soluble oxygen. The PHEMA cryogel was prepared by free radical polymerization initiated by TEMED and APS in a plastic syringe. And then polymerization solution was frozen at −12 °C for 24 h. After thawing at room temperature, it was washed with 200 ml of water [9]. The swelling degree of the cryogel was determined by sucking the cryogel dry and then transferred to a pre-weighed vial and weighed. After drying to constant mass in the oven at 60 °C, the mass of dried sample was determined and then the swelling degree was calculated. The morphology of a cross section of the cryogel was investigated by scanning electron microscope (SEM).
2 ml of 0.5 M sodium carbonate buffer (pH 10.5) was recirculated through the column at 1.0 ml/min at room temperature. Then, the PEI solution (10% (w/w), pH 10.6) was recirculated through the column at 1.0 ml/min at 55 °C and attachment procedure was continued for 6 h. The PHEMA-PEI cryogel was washed with distilled water to remove any physical adsorbed PEI from the polymeric structure. Amino (−NH2) content of PEI-modified PHEMA cryogel was determined by elemental analyzer.
Then, metal ions were chelated on the cryogel columns. Invertase adsorption was performed on the metal chelating monolithic columns for different metal ions with their different amounts of loadings.

4. Results and discussion
The PHEMA cryogel was prepared by polymerization of 2-hydroxyethyl methacrylate with cross-linker in the presence of initiator. According to the SEM images of the pore structure of the cryogel, it has non-porous and thin polymer walls while having large continuous interconnected pores (10–200 µm in diameter) that provide channels for the mobile phase to flow through. Because cryogel columns have macroporous structure, it allows the solution to pass easily. Pore volume in the PHEMA cryogel was 67.5%.
The ester groups on the PHEMA cryogel help us attach poly(ethyleneimine) (PEI) via imine groups in the presence of $NaHCO_3$.

Amino (−NH2) amount of PHEMA-PEI cryogel was determined as 82 mg PEI/g. Different metals with different amounts are studied to have effective purification of invertase. Elution of invertase from the PHEMA-PEI-Metal cryogel was also carried out in cryogel column.

5. Conclusions

Slow diffusional mass transfer and the large void volume between the beads are the main limitations of the conventional packed-bed column. Therefore, monolithic cryogel columns having supermacroporous structure are gaining in popularity for proteomic studies, and purification of biological subtances. Immobilized metal ion affinity chromatography (IMAC) is a low-cost technique with its affinity-like selectivity, simplicity and stability. Besides these, IMAC has a higher recovery yield with the use of mild, non-denaturing elution conditions. In this work, a new PHEMA cryogel carrying PEI and chelated metal ions is designed for the purification of invertase from *Saccharomyces cerevisiae*. Our this new column system can be a candidate for purification of invertase.

References

[1] B. Akkaya, L. Uzun, E.B. Altıntaş , F. Candan, A. Denizli, J. Macromol. Sci. 46 (2009) p.232.
[2] S. Akgöl, Y. Kaçar, A. Denizli, M.Y. Arıca, Food Chemistry 74 (2001) 281–288
[3] E. Akardere, B. Özer, E. B. Çelem, S. Önal, Separation and Purification Technology 72 (2010) 335–339
[4] N. Tüzmen, T. Kalburcu, A. Denizli, Process Biochemistry 47 (2012) 26–33
[5] D. Turkmen, H. Yavuz, A. Denizli, International Journal of Biological Macromolecules 38 (2006) 126–133
[6] D. Çimen, A. Denizli, Colloids and Surfaces B: Biointerfaces 93 (2012) 29–35
[7] V.I. Lozinsky, I.Y. Galaev, F.M. Plieva, I.N. Savina, H. Jungvid, B. Mattiasson,Trends Biotechnol 2003;10:445-451.
[8] D. Türkmen, H. Yavuz, A. Denizli, Int. J. Biol. Macromol. 38 (2006) 126
[9] E. Özgür, N. Bereli, D. Türkmen, S. Ünal, A. Denizli, Materials Science and Engineering C 31 (2011) 915–920

S1-P2

Synthesis and properties of a new poly(aryleneethynylene)s from the cross-coupling condenstation of 4-[(tert-butyldimethylsiloxy)methyl]-1,6-heptadiyne and p-diiodobenzene

Yeong-Soon Gal (1)*, Sung-Ho Jin (2)
(1) Chemistry Division, Kyungil University, Hayang, Gyeongsan 712-701, Gyeongsangbuk-do, Korea
(2) Department of Chemistry Education, Pusan National University, Busan 609-735, Korea
*ysgal@kiu.ac.kr

1. Introduction

Poly(phenylene-ethynylene)s, a new class of conjugated polymers, have attracted much attention because of their fascinating properties [1]. It was demonstrated that poly(phenylene-ethynylene)s with their unique properties are fantastic materials in such different areas as explosive detection, molecular wires in bridging nanogaps, and polarizers for LC displays. Some ethynylene polymers were also prepared by palladium-catalyzed coupling reaction between the p-diiodobenzene and diethyldipropargyl malonate in high yield. Curing of crystalline polyacetylenes results in the formation conjugated networks of alternating double and triple bonds still in crystalline arrays transverse to the polymer backbone. Fluorene-based low-band gap copolymers were prepared for bulk heterojunction photovoltaic cell applications. The poly(fluorenyleneethynylene)s were prepared by alkyne metathesis of (9,9-dialkyl)fluoren-2,7-yleneethynylenes. The diacetylenic polymer via oxidative coupling of 9,9-dipropargylfluorene was prepared and characterized. And also, poly(9,9-dipropargylfluorenylene-phenylene) and poly(9,9-dipropargylfluorenylene-biphenylene) were prepared by cross-coupling condensation polymerization. Poly(arylene-ethynylene)s with ferrocene unit were also synthesized by the reaction of 1,1'-bis(ethynyldimethylsilyl)ferrocene and aromatic dihalides. Here, we report on the synthesis of a new poly(aryleneethynylene)s from the cross-coupling condensation of 4-[(tert-butyldimethylsiloxy)methyl]-1,6-heptadiyne and p-diiodobenzene and its electro-optical and electrochemical properties.

2. Experimental

p-Diiodobenzene, bis(triphenylphosphine)palladium(II) dichloride, cuprous iodide, piperidine, and benzyltriethylammonium chloride were obtained from Aldrich Chemical Co. and used as received. The analytical grade solvents were dried with an appropriate drying agent and distilled. The synthesis of 4-[(tert-butyldimethylsiloxy)methyl]-1,6-heptadiyne was carried out according to the literature method [2]. The palladium-catalyzed reaction of 4-[(tert-butyldimethylsiloxy)methyl]-1,6-heptadiyne and *p*-diiodobenzene was performed in a 100 mL glass pressure vessel with a magnetic stirrer and carried out by the following procedure. After the reactor was charged with 45.0 mL of piperidine, 2-4-[(tert-butyldimethylsiloxy)methyl]-1,6-heptadiyne (1.0 g, 4.23 mmol), and *p*-diiodobenzene (1.395 g, 4.23 mmol), 45 mg of $(PPh_3)_2PdCl_2$, and a catalytic amount of CuI was added. Then the reaction was performed at 70 ^{o}C oil bath under nitrogen atmosphere and stirring was continued at this temperature for 24 h. At the end of reaction, the crude product was isolated by precipitation into methanol. After filtration, the crude polymer was purified with Soxhlet in methanol to remove the residual monomers and oligomers. The collected yellow powder was dried under vacuum

overnight at 40 °C to afford the corresponding polymer in 92 % yield.

3. Results and discussion

The palladium-catalyzed reaction of 4-[(tert-butyldimethylsiloxy)methyl]-1,6-heptadiyne and *p*-diiodobenzene proceeded well in homogeneous manner under mild reaction condition to give a high yield of polymer. The reaction mechanism between an aromatic dihalide and a terminal acetylenic comonomer in the presense of copper(I) iodide, base, and palladium catalyst involves in-situ formation of a copper acetylide. In most cases, copper acetylides are insoluble in common organic solvents, which are expected to the reduced with respect to their reactivity and the low molecular weight of the resulting polymer. However, in the present polymerization, insoluble copper salt was not formed during the reaction. The soluble copper salt reacts with palladium aryl complexes produced by the oxidative addition of aryl iodide to a zero valent palladium intermediate under transfer of acetylide group to paddadium. The cross-coupling product is produced by the reductive elimination, regenerating the zero valent palladium species [1,2].

The molecular weight (Mn) and polydispersity (Mw/Mn) of the resulting polymer were 9.3 x 10^3 and 2.1, respectively. This polymer was completely soluble in common organic solvents such as chloroform, chlorobenzene, tolune, and xylene. In the X-ray diffractogram of polymer powder, the peak in the diffraction pattern is broad and the ratio of the half-height width to diffraction angle ($\Delta 2\theta/2\theta$) is greater than 0.35 [3-5], indicating that the present polymer is amorphous. The thermal behavior of polymer was examined by differential scanning calorimeter and thermogravimeter. From the DSC thermogram of polymer, it was found that a broad exothermic peak was observed around 205 °C (started at 140 °C) in the first heating, whereas there was no exothermic peak in the second heating. The broad exothermic peak is probably due to the thermal crosslinking of the internal ethynyl groups in the polymer main chain. The TGA thermogram of polymer revealed that this polymer is thermally stable up to 250 °C. The char yield of this polymer was 16.6% even after heating up to 600 °C.

The chemical structure of polymer was characterized by such instrumental methods as infrared and NMR spectroscopies. The IR spectrum of polymer did not show any absorption frequency at 3284 cm^{-1} due to the acetylenic ≡C-H stretching absorption frequency, which had been observed in the IR spectrum of 4-[(tert-butyldimethylsiloxy)methyl]-1,6-heptadiyne. The ^{1}H-NMR spectrum of polymer showed the peaks of methylene protons adjacent to ethyne group and methine proton peak at 2.40-3.02 ppm and 3.50-3.98 ppm, respectively. Three methyl proton peaks of t-butyl group and the aromatic proton peaks of phenylene moieties were also observed at 1.38-1.80 ppm and 7.20-7.75 ppm, respectively. On the other hand, the acectylenic proton peak (≡C-H) of 4-[(tert-butyldimethylsiloxy)methyl]-1,6-heptadiyne was disappeared. In the ^{13}C-NMR spectrum of polymer, the signals for both the ethynylene carbons of 4-[(tert-butyldimethylsiloxy)methyl]-1,6-heptadiyne were disappeared, and the new signals of internal ethynylene carbons were appeared at 82.23 ppm and 88.71 ppm, the first one is assigned to the signal of ethynylene carbon adjacent to phenylene group in the main chain of the polymer. One of several motivation issues in terms of design and synthesis of poly(aryleneethynylene) is optically clear material in the range of visible light. Optically clear compound is very important in the application of display such as LCD and OLED, because it can be widely used as a coating material to protect device surface. Moreover, optically clear compound is able to expand its application field to not only coating but also optical retardation calibration as well as filling material between display device layers.

The UV-visible absorption of polymer exhibited no absorption in the range of visible light at all and showed only absorption in 272nm wavelength. When it was also excited at 272nm, it gave PL maximum emission with 327 and 380nm. Considering short excitation wavelength, this polymer has vivid advantage for optically clear material. Also, this material includes silicon atom and it is expected that this polymer has superior interface contact property as silicon atom always shows that. In order to examine the electrochemical property of this polymer, cyclic voltammetry (CV) data was obtained. This polymer includes a phenyl ring and two triple bonds at each main chain unit, but oxidation and reduction was not appeared largely. Although the scan rate was increased up to 150mV/sec and maintained by consecutive scans of 30, CV curves were not changed. It means that when this polymer is used for electronic layer, it is inert and stable.

4. Conclusions

A new poly(aryleneethynylene) with acetylenic and arylene moieties was easily prepared by the cross-coupling condensation of 4-[(tert-butyldimethylsiloxy)methyl]-1,6-heptadiyne and *p*-diiodobenzene by using $PdCl_2(PPh_3)_2$/CuI. This polymer was completely soluble in common organic solvents such as chloroform, chlorobenzene, tolune, and xylene. This polymer was found to be amorphous from the X-ray diffractogram analysis of polymer powder. The UV-visible absorption spectrum showed that this polymer exhibited no absorption in the range of visible light at all and showed only absorption in 272nm wavelength. This material can expand its application field to not only coating but also optical retardation calibration and filling material between display device layers.

Acknowledgements

This work was supported by a grant (M2009010025 and) from the Fundamental R&D Program for Core Technology of Materials of the Ministry of Knowledge Economy (MKE). This work was also supported by the National Research Foundation of Korea (NRF) grant funded from the Ministry of Education, Science and Technology (MEST) of Korea (No. 2011-0028320 and 2012-001846). The authors thank Mrs S. A. Chae of Korea Basic Science Institute (Daegu) Branch for the measurement of the 500 MHz NMR spectra polymer.

References
[1] U.H.F. Bunz, *Chem. Rev*. **2000**, 100, 1605.
[2] S.H. Jin, S.H. Kim, Y.S. Gal, *J. Polym. Sci.: Part A: Polym. Chem*. **2001**, 39, 4025.
[3] T. Masuda, T. Higashimura, *Acc. Chem. Res*. **1981**, 17, 51-56.
[4] S.K. Choi, Y.S. Gal, S.H. Jin, H.K. Kim, *Chem. Rev*. **2000**, 100, 1645-1681.
[5] Y.S. Gal, S.H. Jin, J.W. Park, K.T. Lim, *J. Polym. Sci.: Part A: Polym. Chem*. **2009**, 47, 6153-6162.

S1-P3
Synthesis of ionic polyacetylenes via the uncatalyzed polymerization of ethynylpyridines by using functional alkyl halides

Yeong-Soon Gal (1)*, Sung-Ho Jin (2), Jong Wook Park (3), Kwon Taek Lim (4)
(1) Chemistry Division, Kyungil University, Hayang, Gyeongsan 712-701, Gyeongsangbuk-do, Korea
(2) Department of Chemistry Education, Pusan National University, Busan 609-735, Korea
(3) Department of Chemistry, The Catholic University of Korea, Bucheon 420-743, Korea
(4) Division of Image and Information Engineering, Pukyong National University, Busan 608-739, Korea
*ysgal@kiu.ac.kr

1. Introduction
The polymers having a conjugated backbone shows such unique properties as electrical conductivity, paramagnetism, migration and transfer of energy, color, and chemical reactivity and complex formation ability [1-5]. In 1991, a new family of ionic polyacetylenes was synthesized through the activated polymerization of ethynylpyridines by using alkyl halides [6,7]. We have also reported the preparation of various ionic conjugated polymers having different functionalities [8-10]. Due to their extensive conjugation and ionic nature, these ionic polyacetylenes have potentials as materials for mixed ionic and electronic conductivity, energy storage devices such as batteries, permselective membrane, and light-emitting devices.
Here, we report on the synthesis of new ionic conjugated polymers with functional alkyl substituents by the uncatalyzed polymerization of 2-ethynylpyridine by using the corresponding alkyl halides and the characterization for chemical structure and physical properties of resulting polymers.

2. Experimental
2-Ethynylpyridine was prepared by the bromination of 2-vinylpyridine and the consecutive dehydrobromination reaction according to the literature method [11]. Poly(N-alkyl-2-ethynylpyridinium halide)s were prepared by the activated polymerization of 2-ethynylpyridine with the corresponding alkyl halides in DMF solvent without any additional initiator or catalyst. The resulting viscous polymer solution was diluted by additional DMF and the diluted polymer solution was precipitated into an excess amount of ethyl ether. The precipitated polymer was filtered and dried under vacuum at 40 ^{o}C for 24 hrs. The polymer yields were calculated by gravimetry.
FT-IR spectra were obtained with a Bruker EQUINOX 55 spectrometer using a KBr pellet. NMR spectra were recorded on a Varian 500 MHz FT-NMR spectrometer (Model: Unity INOVA) in DMSO-d_6. The inherent viscosities of polymers were determined at a concentration of 0.5 g/dL in DMF at 30 ^{o}C. The electrical conductivity of the sample was determined by using a standard four-point probe measurement without extensive pumping of the doped pellets with a Hewlett-Packard 3490 multimeter and a Keithley 616 Digital Electrometer. Conductivity was calculated from the measured resistance of the sample. The optical absorption spectra were measured by a HP 8453 UV-visible Spectrophotometer. The photoluminescence spectra were obtained by Perkin Elmer luminescence Spectrometer LS55 utilizing a lock-in amplifier system with a chopping frequency of 150 Hz. Xenon lamp was used as the excitation source, and the incident beam took the maximum absorption peak of the polymers. The electrochemical measurements were performed in 0.1M tetraethylammonium tetrafluoroborate [$(t\text{-}Et)_4NBF_4$] containing DMF solution. Ag wire and platinum foil were used as a reference and a counter electrode, respectively. Cyclic voltammetric waves were produced by using a Hokuto Denko HA-301 potentiostat/galvanostat (AUTOLAB/PG-STAT12) equipped with a HA-301 functional generator and a X-Y reorder.

3. Results and discussion
All polymerization reactions involve the quaternization of pyridine nitrogen in ethynylpyridines [12]. Ethynyl pyridinium monomers are spontaneously polymerized to form highly conjugated, charged polyacetylenes without any additional catalyst or initiator. Here, various conjugated ionic polymers were easily prepared from the uncatalyzed polymerization of 2-ethynylpyridine by using such functional alkyi halides as iodomethane, 2-bromomethyl-1,3-dioxolane, 4-(phenylazo)benzoyl chloride , etc. The polymerization proceeded well to give a high yield of polymer. As the reaction proceed, the solution became viscous and the color of reaction mixture was changed from the light brown of the initial mixture into dark red.
The polymerization behaviors are very similar with those of polymerization of 2-ethynylpyridine by using propargyl bromide and 5-[(5-bromopenthoxy)methyl-2-norborene [8]. The polymerization has been known to contain the first quarternarization of 2-ethynylpyridine by alkyl or carbonyl halides. The initial step involves a nucleophilic attack by the nitrogen atom of unreacted 2-

ethynylpyridine and/or the halide anion on the activated electrophilic N-ethynyl triple bond of the quaternized acetylenic monomer [12]. The activated acetylenic triple bond of monomeric species formed at the initial reaction time is susceptible to the linear polymerization, followed by a consecutive propagation step that contains the produced macroanion and the quaternized monomeric species. Finally, this reaction is terminated by a reaction of macroanioic species with alkyl halide and/or other components. This polymer was completely soluble in such organic solvents as DMF, DMSO, and NMP and the inherent viscosities of polymers were in the range of 0.10-0.17 dL/g.

The chemical structure of polymers was characterized by such instrumental methods as NMR, infrared, and UV-visible spectroscopies. The FT-IR spectrum of polymer did not show the acetylenic C≡C bond stretching (2110 cm^{-1}) and acetylenic ≡C-H bond stretching (3293 cm^{-1}) frequencies of 2-ethynylpyridine. Instead, the C=C stretching frequency peak of conjugated polymer backbone around 1600 cm^{-1} became relatively more intense than those of the C=C and C=N stretching frequencies of 2-ethynylpyridine itself. The UV-visible and photoluminescence spectra of polymer with azobenzene moieties were measured and discussed (UV-visible: 1.1×10^{-3} wt. % PL: 1.1×10^{-2} wt. %, DMF). The absorption spectrum exhibits strong absorption maximum value of 330 nm and broad absorption in the range of 450 ~ 550 nm, which is due to the π→ π* interband transition of this conjugated polymer. The photoluminescence spectrum of this ionic conjugated polymer showed the maximum peak of 597 nm corresponding to the photon energy of 2.07 eV when PL was checked with excitation of 526 nm wavelength. The electrochemical kinetic behavior through the cyclic voltammograms of polymer solution with various scan rates (30 mV/s ~ 150 mV/s) was also investigated. As the scan rate was increased, the oxidation and reduction potentials are slightly shifted to higher potentials because of higher speed of scan rate. The oxidation of polymer occurred at 0.46 V and 1.34 V (*vs* $Ag/AgNO_3$), where the vinylene and pyridinium bromide units of the conjugated polymer could be oxidized in the scan. Polymer also shows reduction at –0.40 and –1.00 V. The redox current value was gradually increased as the scan rate was increased. This result suggests that the electrochemical process of polymer is reproducible in the potential range of –1.2~ 1.6 V *vs* $Ag/AgNO_3$ and there are two vivid redox peaks. The kinetics of the redox process of polymer was very close to a diffusion process from the experiment plotting the oxidation current density of PEPABPC *versus* the scan rate.

4. Conclusions

New ionic conjugated polymers were easily prepared by the activated polymerization of 2-ethynylpyridine by using the corresponding alkyl halides. This polymerization proceeded well in mild reaction conditions to give high yield of polymer. This method do not use any additional initiator or catalyst, thereby originally eliminating the contamination of samples by catalyst residues. This polymer was completely soluble in organic solvents, thus well-processable. Due to its good solubility and conductivity, these pyridyl-containing polyacetylene has potentials as materials for mixed ionic and electronic conductivity, energy storage devices such as batteries, permselective membrane, light-emitting devices, and photovoltaic cells.

Acknowledgements

This work was supported by a grant (M2009010025) from the Fundamental R&D Program for Core Technology of Materials of the Ministry of Knowledge Economy (MKE). The authors thank Mrs S. A. Chae of Korea Basic Science Institute (Daegu) Branch for the measurement of the 500 MHz NMR spectra polymer.

References

[1] T. Masuda, T. Higashimura, *Acc. Chem. Res*. **1981**, 17, 51-56.
[2] S.K. Choi, Y.S. Gal, S.H. Jin, H.K. Kim, *Chem. Rev*. **2000**, 100, 1645-1681.
[3] M.R. Buchmeiser, *Chem. Rev*. **2009**, 109, 303-321.
[4] J. Liu, J.W.Y. Lam, B.Z. Tang, *Chem. Rev*. **2009**, 109, 5799-5867.
[5] M. Goh, S. Matsushita, K. Akagi, *Chem. Soc. Rev*. **2010**, 39, 2466-2476.
[6] S. Subramanyam, A. Blumstein, *Makromol. Chem.-Rapid Commun*. **1991**, 12, 23-30.
[7] A. Blumstein, L. Samuelson, *Adv. Mater*. **1998**, 10, 173-176.
[8] Y.S. Gal, W.C. Lee, S.Y. Kim, J.W. Park, S.H. Jin, K.N. Koh, S.H. Kim, *J. Polym. Sci.: Part A: Polym. Chem*. **2001**, 39, 3151-3158.
[9] Y.S. Gal, S.H. Jin, J.W. Park, K.T. Lim, *J. Polym. Sci.: Part A: Polym. Chem*. **2009**, 47, 6153-6162.
[10] Y.K. Ko, W. Kwon, D.M. Kim, K. Kim, Y.S. Gal, M. Ree, *Polym. Chem*. **2012**, 3, 2028-2033.
[11] Y.S. Gal, H.N. Cho, S.K. Kwon, S.K. Choi, *Polymer (Korea)*, **1988**, 12, 30-36.
[12] Y.S. Gal, S.H. Jin, K.T. Lim, J.W. Park, *J. Appl. Polym. Sci*. **2011**, 122, 987-992.

S1-P4

Influence of different Al-alkyls on the polymerization of ethene with Ziegler-Nata catalyst

Thomas Höchfurtner (1)*, Christian Paulik (2)
(1) Competence Center Wood Kplus, Altenbergerstr. 69, 4040, Linz, Austria
(2) Johannes Kepler University, Institute for Chemical Technology of Organic Materials, Altenbergerstr. 69, 4040, Linz, Austria
*t.hoechfurtner@kplus-wood.at

1. Introduction

The main objective of this work is the homo-polymerization of ethene with Ziegler-Natta (ZN) catalysts. The influence of different co-catalysts Triethylaluminium (TEA), Triisobutylaluminium (TIBA), Tri-n-octylaluminium (TNOA) and Tri-n-hexylaluminium (TNHA) on the polymerization of ethene with a commercial Ziegler-Natta catalyst (ZN) has been studied.

2. Theory

The polymerization of olefins with Ziegler-Natta catalysts plays an important role in the production of plastics, especially of polyolefines. These catalysts consist of $TiCl_4$, immobilized on an inert carrier ($MgCl_2$ or SiO_2) and magnesium- or aluminumalkyls as co-catalyst. Thereby the alkyls are decisive for the reduction of the catalyst and the formation of the active centers (C^*). At these centers the polymerization takes place by insertion of the monomer into the existing polymer chain [1].

3. Experimental

A bi-supported Ziegler-Natta catalyst of SiO2/MgCl2/TiCl4 type was used for slurry polymerization of ethene in purified propane and heptane solvents. The polymerization experiments were performed in a compensation-calorimetric controlled 5 l steel reactor at monomer pressure of 7.5 ± 0.04 bar [2]. Different Al/Ti ratios were prepared by varying the co-catalyst concentrations, whereas the amount of catalyst remained constant. Experiments were performed under isothermal steady state conditions (T_R = 80 ± 0.08 °C).
The influence of co-catalyst and solvent was quantified by measuring the polymerization rate (R_p). Physical properties of reactor powders, such as molecular weight, melting point, degree of crystallinity and bulk density were characterized as well.

4. Results and discussion

As shown in Figure 1, with increasing co-catalyst concentration up to 4.5 mol dm^{-3} an increase in polymerization rate was found. When using TEA or TNOA a further increase leads to a drastically drop in R_p, in contrast to the use of TIBA, where the polymerization rate remains almost constant. Nevertheless, no relation between a maximum R_p and a particular Al/Ti ratio could be identified (Figure 2).

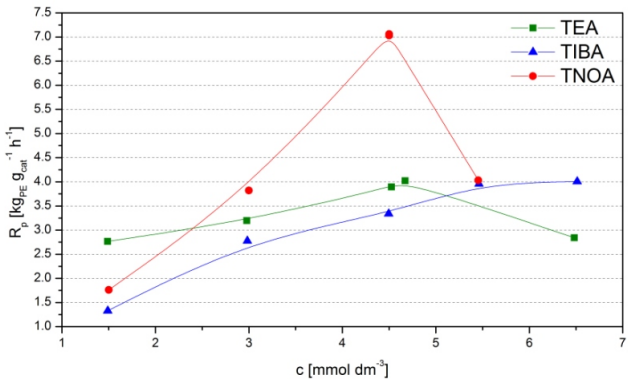

Figure 1: Polymerization rate (R_p) versus co-catalyst concentration (c) of TEA, TIBA and TNOA.

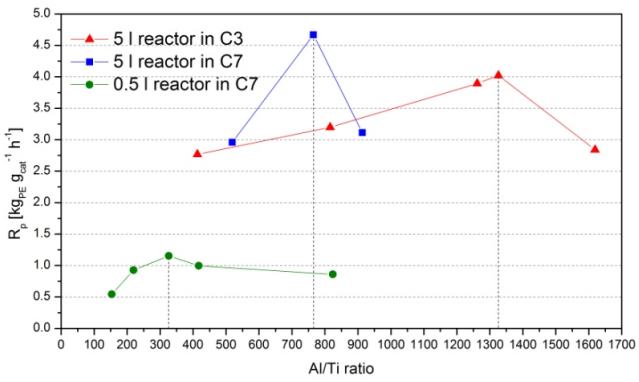

Figure 2: Polymerization rate (R_p) vs. Al/Ti ratio in slurry polymerization with TEA as co-catalyst. Experiments were performed in a 5 l and a 0.5 l reactor.

The molecular weights of the polymer powders were evaluated by intrinsic viscosity measurement, Figure 3. It is shown that the use of TIBA and TNOA leads to much higher molecular weight than the use of TEA. This is due to the sterical hindrance of the larger alkyl groups, which prohibit the determination of the chain propagation on the catalyst surface.
Further studies were performed with differential scanning calorimetry (DSC) to evaluate the melting point and the crystallinity. No direct correspondence on the used co-catalysts was found, but on the molecular mass; the higher the molecular mass of the polymer, the lower the crystallinity.

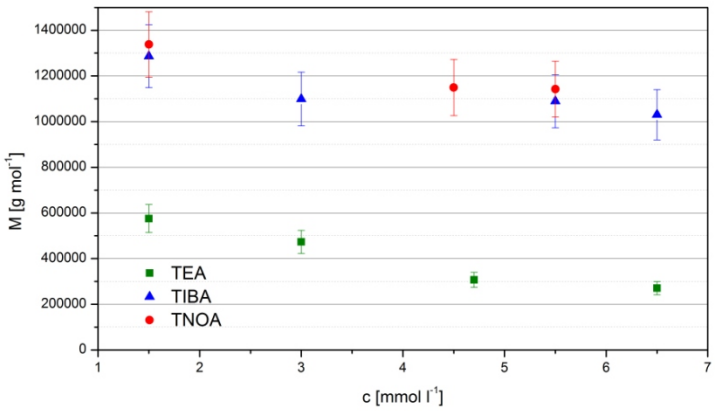

Figure 3: Molecular weight (M) vs. co-catalyst concentration (c) of TEA, TIBA and TNOA.

5. Conclusions

A clear dependency of the polymerization rate on the co-catalyst concentration was found for the used catalyst system and the used polymerization setup. Not as assumed, and as it is used in industrial polymerization, in this study the Al/Ti ratio had almost no effect. The area for an optimum polymerization rate is relatively small. Exceeding a critical TEA and TNOA concentration leads to a decrease in productivity, whereas Triisobutylaluminium (TIBA) shows a constant activity beyond this point.
The reason for this behavior can be found in the property of Triethylaluminium (TEA) and Tri-n-octylaluminium (TNOA) forming a dimer species beyond the critical concentration, which leads to a reduced number of active centers and a drop in polymerization rate (R_p). Because of sterical hindrance TIBA is not able to form dimers, hence no drop in activity was observed.

Acknowledgements

The authors thank Competence Center Wood Kplus and Borealis for financial support.

References

[1] Steinborn, D., Grundlagen der metallorganischen Komplexkatalyse, **2007**, 1. Aufl., B.G. Teubner Verlag/GWV Fachverlage, Wiesbaden, Wiesbaden, 137-15.
[2] Ruff, M., Paulik, C., Controlling polyolefin properties by in-reactor blending: 1. Polymerization process, precise kinetics and molecular properties of UHMW-PE polymers, Macromol. React. Eng., **2012**, 6, 302–317.

S1-P5
GMA based polyHIPEs: Influence of polymerisation factors on morphology

Sebastjan Huš (1), Mitja Kolar (1,2), Aleš Podgornik (3,4), Peter Krajnc (1,2)*
(1) University of Maribor, Faculty of Chemistry and Chemical Engineering, PolyOrgLab, Smetanova 17, SI-2000 Maribor, Slovenia
(2) Centre of Excellence PoliMaT, Tehnološki park 24, SI-1000 Ljubljana, Slovenia
(3) Centre of Excellence COBIK, Velika pot 22, SI-5250 Solkan, Slovenia
(4) BIA Separations d.o.o., Teslova 30, SI-1000 Ljubljana, Slovenia
*peter.krajnc@um.si

1. Introduction

Porous poly(glycidyl methacrylate-co-ethyleneglycol methacrylate) polymers were prepared by the polymerisation of high internal phase emulsions (HIPEs), where the internal phase exceeds 74% of total emulsion volume [1]. Futures of morphology like cavity and interconnecting pore diameter were investigated and successfully controlled by changing the surfactant ratio, initiator system, monomers ratio, pore volume ratio, stirring rate and reaction mixture temperature.

2. Experimental

Glycidyl methacrylate (GMA) and ethyleneglycol methacrylate (EGMA) were passed through the layer of Al_2O_3 to remove the inhibitors. The surfactant Synperonic PEL 121, potassium persulfate (KPS), calcium chloride hexahydrate, N,N,N',N'-tetramethylethylenediamine (TEMED), ammonium persulfate (APS) and azobisisobutyronitrile (AIBN) were used as received.
GMA, EGMA, AIBN (optional) and Synperonic PEL 121 were placed in a 250ml round-bottomed three-necked reactor. The aqueous phase was prepared separately by dissolving appropriate initiator (APS or KPS) and calcium chloride hexahydrate. The organic

phase was stirred at various stirring rates with an overhead stirrer. An appropriate amount of aqueous phase was added under continuous stirring. After complete amount of aqueous phase was added, stirring was continued for 1 h. TEMED was added few seconds before the end of mixing. Than the emulsion was transferred into a PP tube and left in an oven for 24 h. PolyHIPEs were extracted in a Soxhlet apparatus with water for 24 h and absolute ethanol for another 24 h. After that they were dried in vacuum at 40°C for 24 h.
Resulting polymers were characterized by nitrogen adsorption / desorption and mercury intrusion porosimetry to determine pore size distribution. Porous structure typical for polyHIPEs was determined using scanning electron microscopy (SEM).

3. Results and discussion

In order to successfully control the futures of morphology, influence of different polymerisation factors was investigated. The surfactant ratio was varied between 10 and 50% (based on monomer volume). Initiators used in experiments were AIBN, KPS and APS in combination with TEMED. Monomer ratio (GMA:EGMA) was varied between 60:40 and 85:15. Pore volume was changed from 75% to 91%, which was also the maximum pore volume. Stirring rate was varied from 100 to 300 rpm and reaction mixture temperature was varied from 20 °C to 50 °C.
We can conclude that the biggest influence on morphology futures was made by changing the initiator system from KPS (and APS) to AIBN, where cavity diameter could be tailored in the range between sub micron and 50 µm. The biggest influence on interconnecting pore diameter was obtained by changing the surfactant and pore volume ratio. With increasing the surfactant and pore volume ratio the resulting polymers had increased number of interconnecting pores.

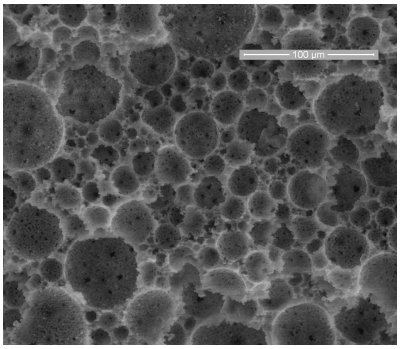

Figure 1. SEM image of GMA-co-EGMA polyHIPE

4. Conclusions

PolyHIPEs prepared from glycidyl methacrylate (GMA) and ethyleneglycol methacrylate (EGMA) monomers have till now mainly been used in chromatography [2-6]. With the efficient control of polyHIPEs morphology the range of application will expand.

References

[1] Lissant, K. J., Emulsions and Emulsion Technology, Part 1. Marcel Dekker: New York, 1974.
[2] Krajnc, P.; Leber, N.; Štefanec, D.; Kontrec, S.; Podgornik, A., Preparation and characterisation of poly(high internal phase emulsion) methacrylate monoliths and their application as separation media. Journal of Chromatography A 2005, 1065 (1), 69-73.
[3] Junkar, I.; Koloini, T.; Krajnc, P.; Nemec, D.; Podgornik, A.; Strancar, A., Pressure drop characteristics of poly(high internal phase emulsion) monoliths. Journal of Chromatography A 2007, 1144 (1), 48-54.
[4] Majer, J.; Krajnc, P., Amine Functionalisations of Glycidyl methacrylate Based PolyHIPE Monoliths. Macromolecular Symposia 2010, 296 (1), 5-10.
[5] Yao, C. H.; Qi, L.; Yang, G. L.; Wang, F. Y., Preparation of sub-micron skeletal monoliths with high capacity for liquid chromatography. Journal of Separation Science 2010, 33 (4-5), 475-483.
[6] Pulko, I.; Smrekar, V.; Podgornik, A.; Krajnc, P., Emulsion templated open porous membranes for protein purification. Journal of Chromatography A 2011, 1218 (17), 2396-2401.

S1-P6

Influence of addition of 2-ethylhexyl acrylate on characteristics and chromatographic properties of glycidyl methacrylate based polyHIPE monoliths

Simona Jerenec (1), Mario Šimić (2,1), Aleš Podgornik (3,2), Jiří Kotek (4), Peter Krajnc (5,1)*
(1) Centre of Excellence PoliMaT, Tehnološki park 24, SI-1000 Ljubljana, Slovenia
(2) BIA separations d. o. o., Mirce 21, SI-5270 Ajdovščina, Slovenia
(3) Centre of Excellence COBIK, Velika pot 22, SI-5250 Solkan, Slovenia
(4) Institute of Macromolecular Chemistry AS CR, v.v.i., Heyrovského nám. 2, Prague, Czech Republic
(5) PolyOrgLab, Faculty of Chemistry and Chemical Engineering, University of Maribor, Smetanova 17, SI-2000, Maribor, Slovenia
*peter.krajnc@um.si

1. Introduction

Emulsions with high internal phase are known as HIPEs where internal phase occupies over 74 vol. %. By polymerisation of HIPE emulsions, polyHIPE materials are obtained. Resulting materials are solid, characterized by a highly porous open cellular structure. Poly(glycidyl methacrylate-co-ethylene glycol dimethacrylate-co-ethylhexyl acrylate) monoliths were prepared from water-in-oil emulsions (w/o). Monoliths were cross-linked with ethylene glycol dimethacrylate (EGDMA) (25 mol. %). The influence of 2-ethylhexyl acrylate (EHA) on emulsion stability and morphology of the resulting monoliths was studied in the range of 0 to 20 mol. %. The addition of 2-ethylhexyl acrylate leads to a higher free volume of polymeric chains which gives a less rigid material and consecutively elasticity of the material is increased. Open-cell structure was confirmed by scanning electron microscopy.

2. Experimental

Chemicals

Monomers: glycidyl methacrylate (GMA, Aldrich), ethylene glycol dimethacrylate (EGDMA, Aldrich), 2-ethylhexyl acrylate (EHA, Aldrich).

Aluminum oxide to remove the inhibitors (Al_2O_3, Acros Organics), initiators potassium persulfate (PPS, Fluka) and N,N,N`,N`-tetramethylethylenediamine (TEMED, Fluka) salt calcium chloride haxahydrate ($CaCl_2$ $6H_2O$, Sigma-Aldrich), surfactant Synperonic PEL 121 (Aldrich), solvent toluene (Sigma-Aldrich).

Prepartion of polyHIPE material - EGDMA/GMA/EHA monoliths

Organic phase consists of monomers EGDMA, GMA and EHA, surfactant PEL 121 to stabilise the emulsions and solvent toluene. A aqueous phase contains $CaCl_2$ $6H_2O$, initiator PPS and deionised water. Aqueous phase was added dropwise to the organic phase. The emulsion was stirred with an overhead stirrer at 250 rpm one hour after all aqueous phase was added. At the end initiator TEMED was used.

The emulsion was sheded to the PET container and cured at 40 °C for 24 h. Monoliths were purified with ethanol for 48 h and dried under vacuum.

Initiators potassium persulfate (PPS, 0,11 mas. % / aqueous phase) and N,N,N`,N`- tetramethylethylenediamine (TEMED, 0,13 vol. % / aqueous phase), salt calcium chloride hexahydrate ($CaCl_2$ $6H_2O$, 1,79 mas. % / aqueous phase), surfactant Synperonic PEL 121 (20 vol. %/ monomers), solvent toluene (25 vol. % / organic phase) were added. The amounts of remaining components are presented in the table 1.

3. Results and discussion

Preparation of poly(glycidyl methacrylate-co-ethylene glycol dimethacrylate) monoliths is already known. However, mechanical properties of such highly porous carriers can present a problem with flow trough applications. By the addition of 2-ethylhexyl acrylate, monoliths with better mechanical properties were prepared. Addition of 2-ethylhexyl acrylate does not influence the stability of emulsion.

Samples with varied amount of 2-ethylhexyl acrylate and aqueous phase were prepared (*Table 1*).

Table 1: Morphological characteristics and data of prepared polyHIPE samples

Sample	EGDMA (mol. %)	GMA (mol. %)	EHA (mol. %)	Aqueous phase (vol. %)	Cavities, d[µm]	Interconnecting pores, d [*µm*]	Protein binding capacity [*mg/mL*]
SJ-120	25	75	0	90	16	1,4	/
SJ-121	25	75	0	85	15	2,4	7,1
SJ-122	25	75	0	75	14	0,8	8,4
SJ-123	25	70	5	75	15	2,2	10,6
SJ-124	25	70	5	85	20	1,9	6,1
SJ-125	25	70	5	90	26	2,2	6,9
SJ-126	25	65	10	75	24	2,3	6,5
SJ-127	25	65	10	85	21	2,9	/
SJ-128	25	65	10	90	8	1,1	10,6
SJ-129	25	55	20	75	9	0,7	8,1
SJ-130	25	55	20	85	18	1,3	/
SJ-131	25	55	20	90	5	1,3	/

We can see from the table 1 that amount of aqueous phase influences the pore size. The range of aqueous phase was between 75 vol.% and 90 vol.%. By increasing the amount of aqueous phase, monoliths with larger cavities were obtained. Increasing the amount of aqueous phase from 75 vol. % to 90 vol. % the average cavities diameter increases (from 15 to 26 *µm*) (Sample SJ-123 and SJ-125), in the presence of 5 mol. % 2-ethylhexyl acrylate. Diameters of interconnecting pores are between 0,7 *µm* and 2,9 *µm*. Addition of 2-ethylhexyl acrylate does not substantially the change chromatographic properties. Chromatographic properties were tested the addition of monomer 2-ethylhexyl acrylate does not significantly change protein binding capacity (ranging from 6,1 *mg/mL* to 10,6 *mg/mL*).

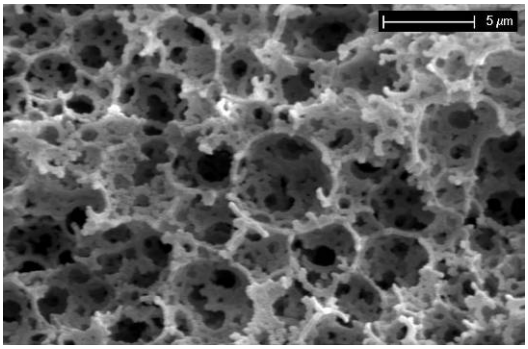

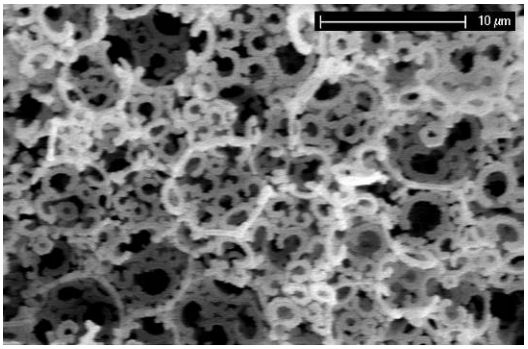

Samples SJ-131 and SJ-128 (90 vol. % of aqueous phase)

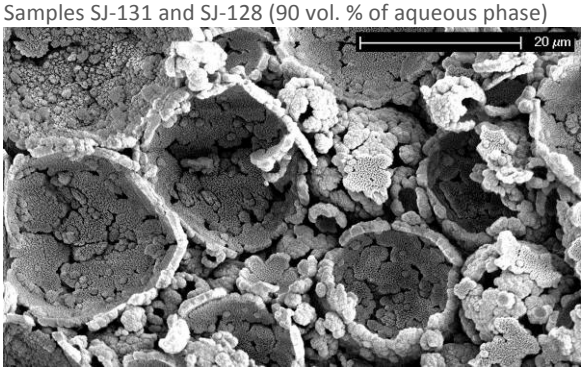

Sample SJ-126 (75 vol. % of aqueous phase)

Figure 11: SEM images of samples with different volume of aqueous phase

As seen from the SEM images (*Figure 1*), larger ratio of added aqueous phase causes a more open cellular structure.

4. Conclusions

Monoliths consisting 2-ethylhexyl acrylate were successfully prepared. Obtained material is stable and does not collapse by the chromatographic applications. Such material is appropriate for separations of proteins.

Acknowledgements

The financial support of the Ministry of Science, Higher Education and Technology of the Republic of Slovenia (Centre of Excellence PoliMaT) through the contract No. 3211-10-000057 is gratefully acknowledged.

References

[1] N. R. Cameron, D. C. Sherrington, *Adv. Polym. Sci.* **1996**, 126, 165 – 213.
[2] N. R. Cameron, P. Krajnc, M. S. Silverstein, Colloidal Templating in Porous Polymers, (Eds: M. S. Silverstein, N. R. Cameron, M. A. Hillmyer), John Wiley & Sons Inc .Hoboken, NJ, USA **2011**.
[3] I. Pulko, P. Krajnc, Macromol. Rapid Commun. **2012**, 33, 1731.
[4] P. Krajnc, N. Leber, D. Štefanec, S. Kontrec, A. Podgornik, *J. Chromatogr. A* **2005**, 1065, 69 – 73.

S1-P7
Glucose oxidase immobilisation on dye attached cyrogel discs

Işık Perçin (1)*, Gülsu Şener (2), Nilay Bereli (2), Adil Denizli (2)
(1) Hacettepe University, Department of Biology, Molecular Biology Division, 06800, Ankara/Turkey
(2) Hacettepe University, Deparment of Chemistry, Biochemistry Division, 06800, Ankara/Turkey
*ipercin@hacettepe.edu.tr

1. Introduction

As it produces gluconic acid and hydrogen peroxide, glucose oxidase (GOX) (beta-D-glucose:oxygen-1-oxidoreductase, EC 1.1.3.4) is an important enzyme in industry. It has many commercial and industrial applications. Baking, dry egg powder production, wine production, gluconic acid production are some examples of applications in which GOX used in food industry. Main objective of enzyme immobilization is to make enzymes reusable in industry. Immobilized enzymes are more durable to pH and temperature changes and more stable when compared to free enzymes.
Dye ligands which are commercially available can bind many proteins, especially enzymes. They are inexpensive and can easily be immobilized on matrices carrying hydroxyl groups. In this study poly(hydroxyethyl methacrylate) (PHEMA) cryogel discs were prepared by free radical cryopolymerization. Cibacron Blue F3GA (CB F3GA) was chosen as the dye ligand and GOX was immobilized on CB F3GA attached cryogel disc. Free enzyme and immobilized enzyme were compared in terms of activity and stability.

2. Theory

GOX catalyses the oxidation of glucose to hydrogen peroxide and D-gluconolactone. GOX is naturally found in some organisms like fungi and insects. GOX usually occurs as a glycoprotein. GOX has two identical subunits and its molecular weight ranges from 130-175 kDa. Improving the stability and reusability of GOX is important due to its common industrial usage.
Reactive dyes which are usually used in textile industry are synthetic but they interact with active sites of many proteins. Based on these features, reactive dyes are used as affinity ligands in biochromatography systems. Dye ligands are important alternatives to specific ligands like proteins, substrates, nucleic acids and coenzymes. Reactive dyes contain a chromophore linked to a reactive group. They also have sulfonic acid groups which are negatively charged at all pH values. The interactions between dye ligands and proteins are non-covalent.

3. Experimental

PHEMA based cryogel discs were typically prepared as follows: Both HEMA was methylenebisacrylamide (MBAA) were dissolved in deionized water. After adding APS and TEMED polymerization was achieved at -16°C for 24 h. CB F3GA was attached to cryogel disc under basic conditions at 70°C. Excess dye was removed by washing the discs with deionized water. Washed cryogel discs were used for GOX immobilization. Effects of pH and temperature on enzyme immobilization were investigated. Storage stability of immobilized GOX was also tested.

4. Results and Discussion

The PHEMA cryogel discs have interconnected large pores (10-100 µm in diameters) and its structure is elastic like a sponge. The equilibrium swelling degree of the PHEMA cryogel disc was 9.5 g H2O/g cryogel. The PHEMA cryogel discs can easily release the water inside its pores when it is compressed by hand. Maximum GOX immobilization was achieved at 25°C and pH 5.0. Immobilized enzyme has advantages over free enzyme in terms of reusability and storage stability.

5. Conclusions

Affinity chromatography systems take advantage of specific non-covalent interactions between dye ligands and proteins. Because of their cheapness and easy immobilization dyes are preferred as ligands. In this study a triazine dye CB F3GA was attached to PHEMA cryogel discs and its efficiency for GOX immobilization was investigated. Immobilization of the enzyme made it reusable and increased its stability. According to the obtained results CB F3GA attached cryogel discs are suitable materials for GOX immobilization.

References

[1] Denizli A, Pişkin E. Dye-ligand affinity systems. J Biochem Biophys Methods. 2001;49:391-416.
[2] Perçin I, Sağlar E, Yavuz H, Aksöz E, Denizli A. Poly(hydroxyethyl methacrylate) based affinity cryogel for plasmid DNA purification. Int J Biol Macromol. 2011;48:577-582.
[3] Perçin I, Yavuz H, Aksöz E, Denizli A. Mannose-specific lectin isolation from Canavalia ensiformis seeds by PHEMA-based cryogel. Biotechnol Prog. 2012;28:756-761.
[4] Bankar SB, Bule MV, Singhal RS, Ananthanarayan L. Glucose oxidase-an overview. Biotechnol Adv. 2009;27:489-501.
[5] Wong CM, Wong KH, Chen XD. Glucose oxidase: natural occurrence, function, properties and industrial applications. Appl Microbiol Biotechnol. 2008;78:927-938.
[6] Alkan H, Bereli N, Baysal Z, Denizli A. Antibody purification with protein A attached supermacroporous poly(hydroxyethyl methacrylate) cryogel. Biochem. Eng. J. 2009;45:201-208.
[7] Andac M, Galaev I, Denizli A. Dye attached poly(hydroxyethyl methacrylate) cryogel for albumin depletion from human serum. J Sep Sci. 2012;35:1173-1182.

S1-P8

Effect of additive acid H_3PO_4 on the properties and the storage time of compound for the production of ureaurethanes

Kamila Pietrzak*, Małgorzata Markiewicz, Joanna Ryszkowska
Warsaw University of Technology, Faculty of Materials Science and Engineering, Woloska 141, 02-507, Warsaw, Poland
*kpietrzak@inmat.pw.edu.pl

1. Introduction

Polyurethane elastomers are used in many industrial applications due to excellent physical and mechanical properties like good resistance to abrasion and to oil, grease and weather conditions [1]. To produce them two methods are used, namely one-step and two-step methods [2]. In the case of the two-step method, the first step in the formation of prepolymer is the reaction of a polyol with a diisocyanate. The second step involves the reaction of the prepolymer isocyanate groups with a compound containing at least two active groups with active hydrogen atoms. From water, extending agents and crosslinking agents in the course of the reaction urethane groups are formed. The side reactions may form allophanate and biuret groups [3]. The rate of reaction will depend on the pH of the environment (Fig.1) and the presence of metal compounds. Reactivity towards isocyanate compound depends on the type of active hydrogen atom, the presence and nature of the substituents, the reaction temperature and the nature of the catalyst [4]. Isocyanates are highly reactive compounds, can easily react with water (even react with water contained in the air), which makes it difficult to store. Isocyanate "locked" other non-reactive substance; it normally does not react with reactive groups and can be stored indefinitely and subjected safely to long pre-treat in processes [5]. Blocking agents used here include phenols, esters of acetic acid or maleic acid, ethyleneimine, caprolactam, and many other compounds.

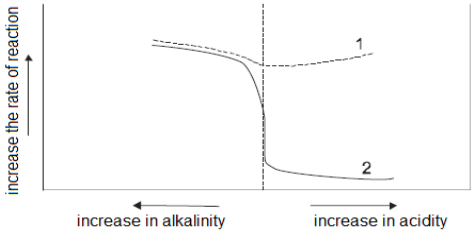

Figure 1. Effect of pH on the rate of the reaction of polyols and diisocyanates [3]

2. Experimental

Ureaurethanes (PURMs) synthesis were used: poly (ethylene adipate) (PAE) with an average molecular weight ok.1950 - Alfa Alfaster Systems T620, 4,4 '-diisocyanate difenylonometanu (MDI) from Aldrich, used as a chain extender dicyjandiamidu (DCDA) of Aldrich, and inhibitor in the form of phosphoric acid (V). Ureaurethanes synthesis was performed with a different molar ratio of reactants. For the production of polyurethane prepolymer is made by a mixture containing 50%PAE and 50%DCDA and prepolymer containing 50%PAE, 50%DCDA and 100%MDI. A prepolymer was made in two versions: with and without acetic acid. The prepolymer was stored in a sealed container at a temperature of -5°C over a period of 2 weeks. After this time ureaurethanes were

prepared.
The following characteristics were examined: density (ρ) determined by hydrostatic weighing in accordance with ISO 2781, the hardness (H) determined using a Shore A durometer in accordance with ASTM D2240-75, resilience (η) carried out by Schobe'a according to PN-71/C-04255 and wear resistance (ΔV) made by ISO 4649. The mechanical properties were examined in a static tensile test. This study was performed on testing machine, in accordance with ISO 527, at a speed of 500mm/min. Thermal analysis was performed using thermogravimetry (TGA) and differential scanning calorymetry (DSC). Was performed the dynamic-mechanical thermal analysis (DMA) to determine the cross-link density ureaurethanes. The analysis was carried out by observing the structure of the brittle fracture using a scanning electron microscope (SEM).

3. Results and discussion
Selected properties of the produced PURM are shown in the following tables. Table 1 lists the materials without the addition of phosphoric acid (V). Table 2 lists the values for PURM without inhibitor. The materials that were prepared and tested, as indicated in tables A, B, C - ureaurethanes without acid, containing rigid segments in sequence: 17.6%, 20.4% and 23%. However, determinations of A1, B1, C1 concern the materials with the addition of orthophosphoric acid (V).

Table 1. Physical, mechanical and thermal properties of ureaurethanes without acid

Samples	ρ [g/cm^3]	H [°ShA]	ΔV [dm^3]	η [%]	$T_{2\%}$ [°c]	$T_{5\%}$ [°c]	T_{max1} [°c]	T_{max2} [°c]	Tg [°c]
A	1.1930	60	34	19	271	297	363	422	-33.9
B	1.2388	73	36	35	270	297	309	371	-33.3
C	1.2458	71	39	32	268	298	311	367	-33.5

Table 2. Physical, mechanical and thermal properties of ureaurethanes with acid

Samples	ρ [g/cm^3]	H [°ShA]	ΔV [dm^3]	η [%]	$T_{2\%}$ [°c]	$T_{5\%}$ [°c]	T_{max1} [°c]	T_{max2} [°c]	Tg [°c]
A1	1.2346	65	41	40	273	298	308	402	-33.6
B1	1.2398	63	43	38	269	295	306	366	-33.0
C1	1.2471	74	49	32	269	297	311	367	-32.5

During the casting of 14 days after production of the prepolymer it is noted that ureaurethanes inhibitor had a significantly lower viscosity than the material without the inhibitor.
Physical properties such as hardness and density increased in both cases with increasing content of hard segments. Flexibility for PURM acid is higher than that of free acid PURM and decreases with increasing content of hard segments, which confirms the increase in hardness and density. Abrasive wear resistance decreases with increasing content of hard segments for PURM with acid. Thermal analysis showed that both types PURM temperature resistance is higher at the lower share of rigid segments. However, the glass transition temperature of the soft segments (Tg) for PURM acid increases with increasing hard segments.

Table 3. R index and the degree of phase separation (SSF) for ureaurethane content of 17.6% hard segments

Samples	C=O related	C=O free	R	SSF
A	9.20	9.38	0.98	0.50
A1	10.54	6.91	1.52	0.60

Table 3 shows the values for PURM hard segments content of 17.6% with and without acid, in order to illustrate the differences. We found that the hydrogen bonding index (R) and the degree of phase separation (SSF) for PURM without acid, increase with increasing hard segments. However, in the case of materials with an acid, these values decrease with increasing hard segments. The addition of phosphoric acid (V) to ureaurethanes resulted in an increase in the hydrogen index value as compared to PURM without acid.

4. Conclusions
Adding phosphoric acid (V) to ureaurethanes resulted in a change of the structure and some properties of obtained PURM. Apparently, it decreased the viscosity of mixtures, which allowed them easy casting into molds.

Acknowledgements
The study has been financed by the framework of the project Nr PBS1/A5/3/2012, titled: "Elastomer composite materials for applications in friction systems transmitting the drive in extreme load conditions used in transport machines and equipment".

References
[1] D.K. Chattopadhyay, K.V. Raju, *Prog. Polym. Sci.* **2007**, 32, 352-418.
[2] Z. Wirpsza, PTR Prentice Hall, London, 1993.
[3] M. Markiewicz, Warsaw University of Technology, 2010, p.33

[4] K. Pietrzak, Warsaw University of Technology, 2010, p. 26-30.
[5] I. Gruin, J. Ryszkowska, B. Markiewicz, PW Publishing House, Warsaw, 1996.

S1-P9
Influence of reaction conditions on the hypercrosslinking of porous poly (4-vinylbenzyl chloride) monoliths

Irena Pulko (1,2)*, Silvester Bolka (2), Peter Krajnc (2,3)
(1) Polymer Technology College, Pod gradom 4, 2380 Slovenj Gradec, Slovenia
(2) Centre of Excellence Polymer Materials and Technologies, Tehnološki park 24, 1000 Ljubljana
(3) University of Maribor, Faculty of Chemistry and Chemical Engineering, PolyOrgLab, Smetanova 17, 2000 Maribor, Slovenia
*irena.pulko@vstp.si

1. Introduction
PolyHIPE materials are produced from high internal phase emulsions (HIPEs), where the dispersed phase occupies > 74% of the emulsion volume. PolyHIPEs have been prepared from either oil-in-water (o/w) or water-in-oil (w/o) emulsions and have been used in a flow through manner as scavengers,[1] reagents,[2] solid phase synthesis supports[3] and chromatography media.[4] PolyHIPEs are porous, but due to relatively large pores surface area is rather low. Different methods are known to increase surface area of polyHIPEs and one of them is hypercrosslinking reaction (Figure 1). Hypercrosslinked polyHIPE is a potentially attractive catalyst support material due to the combination in one material of an interconnected network of macropores, facilitating access of reagents to the surface, with an ultra-high surface area produced by the hypercrosslinking induced microporosity.

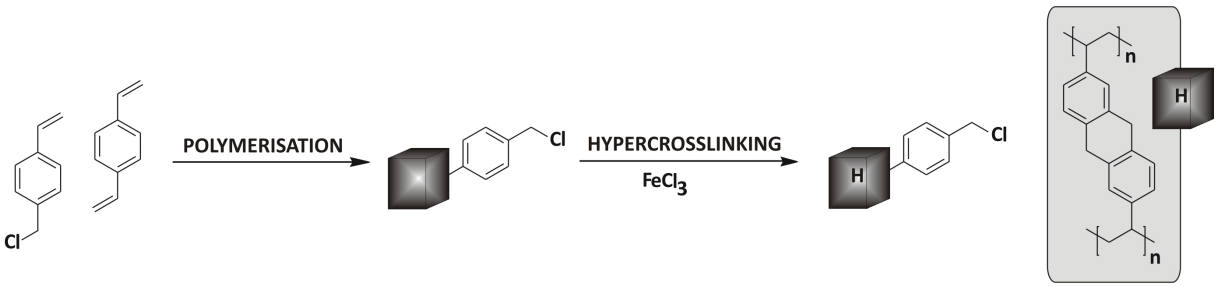

Figure 1. Formation of hypercrosslinked PolyHIPE

2. Experimental
100 mL of an aqueous phase, consisting of 0.11 g $K_2S_2O_8$ in 100 mL of deionised water, was added dropwise with continuous stirring at 300 rpm to an oil phase, consisting of 30.0 g 4-vinylbenzyl chloride, 0.70 g divinylbenzene and the surfactant sorbitan monooleate (Span 80; 7.01 g). The emulsion was stirred for another 30 min. After addition of the aqueous phase then transferred to a mold for curing (24 h at 60°C). The resulting polyHIPE was purified by Soxhlet extraction (deionised water and acetone, both for 24 h) then dried for 24h.
Hypercrosslinking of polyHIPE: 1 g of cubic polyHIPE was placed in a flask, 80 mL of 1,2-dichloroethane was added and the neck was fitted with a rubber septum. The mixture was degassed under a stream of nitrogen for 15 min with constant stirring (magnetic or ultrasound), after which time the nitrogen supply was removed and the sealed flask left for a further 45 min to swell the polymer. The flask was then placed in an ice bath and $FeCl_3$ (equimolar ratio to chlorine content in PolyHIPE) was added quickly through the neck of the flask. The flask was then resealed and degassed again for a period of 15 min. After removal of the nitrogen supply, the flask was left stirring in the ice bath for a further 45 min to ensure uniform dispersion of $FeCl_3$. The sealed flask was then placed in an oil bath at 80˚C and heated for a different period of time (1h – 7h). The reaction was then quenched by the addition of 40 mL of methanol then filtered under gravity. It was then washed with methanol and 0.1 M HNO_3 (aq) then in soxhlet apparatus with acetone for 24 hours. The product was then dried at 50˚C for 24 h.

3. Results and discussion
Lightly crosslinked polyHIPEs were prepared by polymerization of continuous phase of high internal phase emulsion consisting of surfactant and 2 mol% of divinylbenzene and 98% of vinylbenzene and influence of stirring (magnetic stirrer or ultrasonic treatment) on hyperrcosslinking were investigated. Hypercrosslinking reaction (chlorine content) was monitored by FTIR spectroscopy and potentiometric titration. Chlorine content in starting polymer was determined to be 21.70%. By adding $FeCl_3$ to the reaction mixture and using ultrasound treatment chlorine content decreased to 8.67% after 1h (Scheme 1). After 7h of mixing chlorine content was 3.10%. Similar results were obtained when using magnetic stirrer, e.g. chlorine content after 5h mixing with magnetic stirrer was 3.98% and 3.88% when using ultrasound. It can be concluded that both mixing methods are efficient. Due to the damaging of the sample when using magnetic stirrer, ultrasonic treatment is preferred.

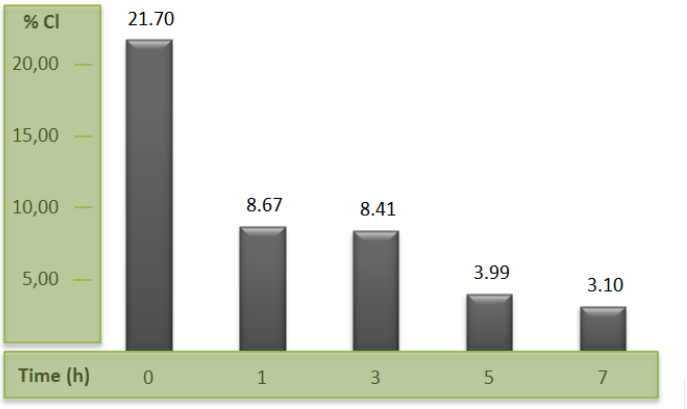

Scheme 1. Chlorine loading with progress of hypercrosslinking reaction

4. Conclusions

Lightly crosslinked polyHIPEs (high internal phase emulsion) based on vinylbenzyl chloride were prepared by the polymerisation of the continuous phase of a high internal phase emulsion and hypercrosslinked in dichloromethane using $FeCl_3$ as a catalyst. The influences of mechanical and ultrasonic stirring of polymer and $FeCl_3$ were examined. Hypercrosslinking reaction was monitored by FTIR spectroscopy and potentiometric titration. It was found that there is no significant difference in the degree of hypercrosslinking using mechanical or ultrasonic stirring. Because magnetic stirrer damages lightly crosslinked polymer, ultrasonic treatment is a more convenient method.

References

[1] P. Krajnc, J. F. Brown, N. R. Cameron, *Org. Lett.* 2002, 4, 2497-2500; P. Krajnc, D. Štefanec, J. F. Brown, N. R. Cameron, *J. Polym. Sci., Part A: Polym. Chem.* 2005, 43, 296-303.
[2] N. R. Cameron, D. C. Sherrington, I. Ando, H. Kurosu, *J. Mater. Chem.* 1996, 6, 719-726.
[3] P. W. Small, D. C. Sherrington, *J. Chem. Soc., Chem. Commun.* 1989, 1589-1591; J. F. Brown, P. Krajnc, N. R. Cameron, *Ind. Eng. Chem. Res.* 2005, 44, 8565-8572.
[4] P. Krajnc, N. Leber, D. Štefanec, S. Kontrec, A. Podgornik, *J. Chromatogr. A* 2005, 1065, 69-73.

S1-P10
Reversible crosslinking of anthracene functionalized polynorbornenes

Simone Viola Radl (1)*, Benjamin Hirschmann (1), Thomas Griesser (2), Wolfgang Kern (1,2)
(1) PCCL GmbH, Roseggerstraße 12, 8700 Leoben, Austria
(2) University of Leoben, Chair of Chemistry of Polymeric Materials, Otto-Glöckel-Straße 2, 8700 Leoben, Austria
*simone.radl@pccl.at

1. Introduction

The photoinduced dimerization reaction of anthracene is one of the oldest known photoreactions. Fritzsche in 1867 discovered that solar irradiation of a saturated benzenic solution of anthracene leads to microscopic crystals which adhere firmly to the side of the vessel.[1] Remarkably, this photoproduct was observed to revert back entirely to the starting compound thermally and under UV illumination. A few years later Coulson, Hengstenberg and Ehrenberg constituted the dimerization reaction mechanism of anthracene. [1,2,3]

In general, anthracene molecules undergo a photodimerization reaction upon irradiation with light λ>300 nm, leading to a [4+4] cyclo adduct (see Figure 1). This dimerization reaction is reversible and thus a thermal treatment (≥ 150 °C) or an illumination λ<300 nm results in a dissociation reaction to the initial compound.

In this contribution, we report on the synthesis of polynorbornene based polymers bearing anthracene groups capable of undergoing the reversible dimerization reaction, which offers the possibility of a reversible cross-linking of the polynorbornene macromolecules. Besides the [4+4] dimerization reaction, which was investigated by means of UV-VIS measurements, also the influence of the glass transition temperature on the reversibility of the photoreaction was studied.

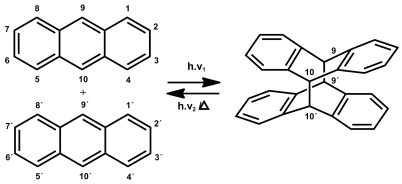

Figure 1. Reversible dimerization reaction of two anthracene molecules

2. Experimental

The photoreactive monomer mono-**1** is easily accessible by an esterification reaction of norbornene-2,3-dicarboxylic acid dichloride with 9-anthracene methanol (mono-**1**, see Figure 2), analogous to the synthesis of endo,exo-bicyclo[2.2.1]hept-5-ene-2,3-dicarboxylic acid, bis[2-[2-(2-ethoxyethoxy)ethoxy]ethyl] ester (mono-**2**) as reported elsewhere.[4] Mono-**1** was purified by column chromatography and was obtained in high yield (82%). ^{1}H NMR, ^{13}C NMR and FTIR-spectroscopy are in accordance with the proposed structure.

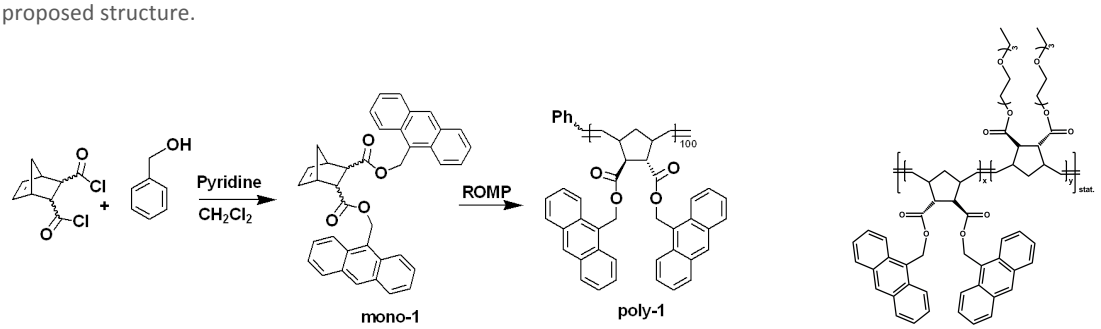

Figure 2. Synthesis of poly-**1** (left) and the structure of poly(**1**-co-**2**) (right) **poly-(1-co-2)**

The polymers were prepared by ring opening metathesis polymerization (ROMP) using Umicore M31 as initiator for ROMP. The polymerizations were performed in dichloromethane under inert atmosphere at room temperature in a glove box. A homopolymer, poly-**1**, with a theoretical polymerization degree of X_n= 100 and a glass transition temperature of T_g=140°C as well as a statistical copolymer poly(**1**-co-**2**) (Figure 2, X_n= 100, mono-**1** : mono-**2**= 50:50, T_g= 23°C) were prepared by this method.

3. Results and discussion

The photodimerization reaction of the anthracene molecules in thin films of poly-**1** and poly(**1**-co-**2**) was observed by monitoring the anthracene UV absorption peaks in the region between 310 – 410 nm. Figure 3 shows the UV-Vis spectra of poly-**1** and poly(**1**-co-**2**) prior to illumination (blue), after illumination (red) and after a thermal treatment (vacuum oven, 150°C, 90 min). During irradiation the intensity of the four absorption peaks decreases as a result of the dimerization reaction of the anthracene moieties. The subsequent thermal treatment leads to a partial dissociation of the built dimers to the initial anthracene moieties.

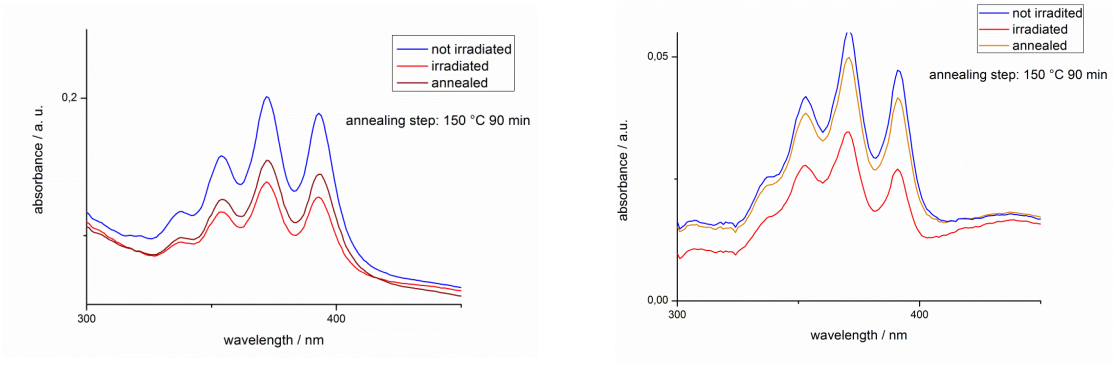

Figure 3. UV-Vis spectra of poly-**1** (left) and poly-(**1**-co-**2**) (right) after irradiation (dimerization) and annealing (dissociation)

The UV-Vis spectra in Figure 3 reveal that the dimerization reaction and also the thermal induced dissociation reaction in poly-(**1**-co-**2**) proceeds more efficient compared to the reactions in poly-**1**. This expected result can be explained by the lower glass transition temperature of poly-(**1**-co-**2**) (Tg = 23°C) which leads to a higher mobility of the anthracene moieties, facilitating the dimerization and dissociation reaction of the anthracene molecules in this polymeric material.

Acknowledgements
The research work was performed at the Polymer Competence Center Leoben GmbH (PCCL, Austria) within the framework of the COMET-program of the Federal Ministry for Transport, Innovation and Technology and the Federal Ministry of Economy, Family and Youth with contributions by the University of Leoben.

References
[1] H. D. Becker, *Chem. Rev.* **1993**, 93.
[2] M. Ehrenberg, *Acta Crystallogr.* **1966**, 20.
[3] H. Bouas-Laurent, A. Castellan, J. P. Desvergne, R. Lapouyade, *Chem. Soc. Rev.* **2000**, 29, 43.
[4] R. M. Kriegel, W. S. Rees, M. Weck, *Macromolecules*, **2004**, 37, 6644.

S1-P11
Creating hierarchical porosity in poly(styrene-co-divinylbenzene) polyHIPEs via post polymerization treatment

Urška Sevšek (1), Karel Jerabek (2), Peter Krajnc (1,3)*
(1) PolyOrgLab, Faculty of Chemistry and Chemical Engineering, University of Maribor, Smetanova 17, SI-2000, Maribor, Slovenia
(2) Institute of Chemical Process Fundamentals of the ASCR, Rozvojova 2/135, CZ-165 02, Prague, Czech Republic
(3) Centre of Excellence PoliMaT, Tehnološki park 24, SI-1000 Ljubljana, Slovenia
*peter.krajnc@um.si

1. Introduction
Styrene and divinylbenzene are common monomers used for preparation of high internal phase emulsions that can be polymerised into porous polymeric material. High internal phase emulsions (HIPEs) are known as emulsions containing more than 74,05 vol% of internal phase. By polymerising the emulsion, a porous material is prepared, containing larger pores, named voids. They are created by internal phase droplets that are removed after polymerisation. A polyHIPE material also contains smaller, interconnecting voids, often referred to as windows that occur due to shrinkage process because of the difference between monomer and polymer densities. Until now only in two cases polymer derived from a HIPE emulsion has been hypercrosslinked and further used for catalyst support and gas storage. [1][2] Most of the hypercrosslinking studies have been done via Friedel Crafts alkylation using ferric chloride as the catalyst. In one case stannic tetrachloride was used as the catalyst [3] and also a peroxy radical initiator was used [4].
Besides having a material that is porous, which enables easier access of reagents, hypercrosslinking gives a higher degree of pores, micropores, which increase the surface area and therefore make the material more appropriate for separation of small molecules. The latter is one of the most common applications for using hypercrosslinked material.
Poly(styrene-co-divinylbenzene) polyHIPEs with different ratios of monomers have been prepared and treated after polymerization with a peroxy iniciator to induce formation of smaller pores and therefore enlarge the surface area of the material, making it more applicable for separation of small molecules.

2. Experimental
Preparation of STY-co-DVB monoliths
Surfactant (sorbitan monooleate), styrene and divinylbenzene were placed in a reactor. Their amounts are given in *table 1*. The mixture was stirred with an overhead stirrer at 300 rpm for 10 minutes. The aqueous phase was prepared separately by dissolving calcium chloride hexahydrate (1.78 g) and initiator (KPS, 0.11 g) in deionised and degased water (100 mL). An approproate amount of aqueous phase (80 vol. %) was added dropwise and under constant stirring to the organic solution. Once all the aqueous phase had been added, stirring was continued for a further 60 min, to produce a uniform W/O emulsion. The emulsion was transferred into a PP tube and exposed to high temperature (60°C). The resulting polyHIPE was then extracted in a Soxhlet apparatus with water for 24 h and absolute ethanol for a further 24 h. The monolith was dried in vacuo at 30°C for 72 h.
Functionalisation of monoliths
From 0,6 g to 1,4 g of powdered (p) or monolithic (m) polymer was placed in a 50 mL flask fitted with a reflux condenser. 20.0 mL of solvent (toluene (T), acetonitrile (A) or N,N-dimethylformamide (D)) was added and left mixing for 2h in order to get the solvent to swell the polymer. Then di-tert-butyl peroxide (0,1 g/g polymer) was added. The mixture was stirred and heated under reflux for 20 h at 104°C (78°C when using acetonitrile). The resulting polymer was filtered and washed with tetrahydrofurane (3 × 50 mL). The material was dried in vacuo at 70°C for 24 h to give hypercrosslinked polyHIPE. Nitrogen adsorption/desorption measurements were done.

3. Results and discussion

Table 1. Compositions of emulsions

Sample	Crossl. [mol %]	Organic phase			Surface area[b] [m^2/g]	Surface area of the functionalised samples [m^2/g]
		m (STY) [g]	m (DVB)[a] [g]	m (Span 80) [g]		
A1	80	/	9,114	1,824	66,9	355,8
A2	72	0,754	8,206	1,787	81,3	330,0
A3	64	1,457	7,297	1,760	42,0	300,5
A4	52	2,558	5,929	1,697	68,6	170,2

For previously prepared styrene/divinylbenzene polyHIPEs (Table 1), radical initiator has been used to induce hypercrosslinking. Jerabek *et al*. have previously used a peroxy initiator, namely di-tert-butyl peroxide, for hypercrosslinking a poly(divinylbenzene-co-styrene) material, derived from bulk polymerisation. Mentioned peroxy initiator has a specific mechanism of initiation.[4] Primary t-butoxy radicals initiate the polymerisation of the residual vinyl bonds and furthermore abstract labile hydrogen atoms from an aliphatic chain. This creates new radicals which are able to initiate further polymerisation. [5] Surface area of our porous materials has substantially increased (see Table 1). As can be seen from Figure 1, the polyHIPE structure has not been severly damaged, therefore the increase of the surface area is mostly due to hypercrosslinking.

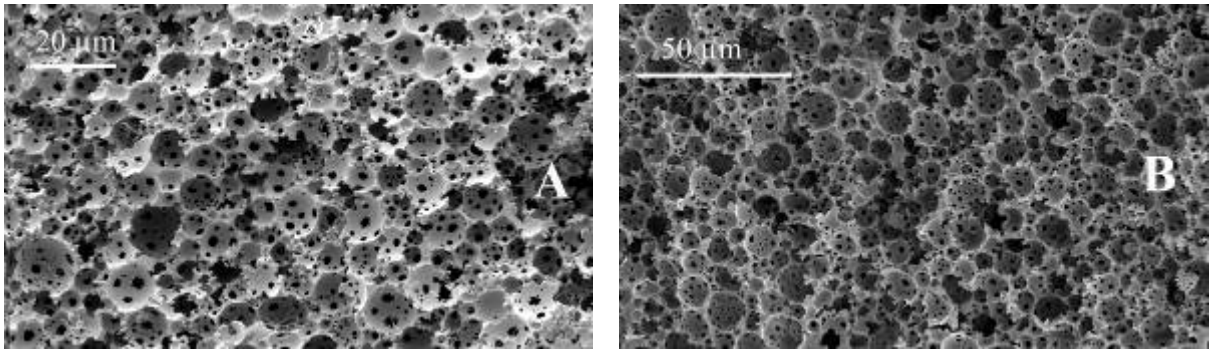

Figure 1. SEM images of sample A1 before (A) and after hypercrosslinking (B)

4. Conclusions

We prepared hypercrosslinked porous poly(STY-co-DVB) monoliths with high surface areas up to 355 m^2/g. We were able to preserve the porous polyHIPE structure during and after the hypercrosslinking reaction. Using di-tert-butyl peroxide as the radical initiator leads to enlargement of BET surface area for even as high as 7-folds. Our results show that the initial crosslinking degree influences on the surface area and pore structure of the polymer.

Acknowledgements

Financial support of the Slovenian Research Agency (scholarship to Urška Sevšek, contract number 1000-08-310094 is gratefully acknowledged.

References

[1] I. Pulko, J. Wall, P. Krajnc, N.R. Cameron, *Chem. Eur. J.* **2010**, *16*, 2350-2354.
[2] M.G. Schwab, I. Senkovska, M. Rose, N. Klein, M. Koch, J. Pahnke, G. Jonschker, B. Schmitz, M. Hirscher, S. Kaskel, *Soft Matter* **2009**, *5*, 1055-1059.
[3] A. V. Pastukhov, M. P. Tsyurupa, V. A. Davankov, *J. Polym. Sci., Part B: Polym. Phys.* **1999**, *37*, 2324-2333.
[4] K. Soukupova, A. Sassi, K. Jerabek, *React. Funct. Polym.* **2009**, *69*, 353-257.
[5] E.H. Farmer, C.G. Moore, *J. Chem. Soc.* **1951,** 131-141.

S1-P12

Thiol-ene chemistry and emulsion templating for microcellular open porous polymer preparation

Maja Sušec (1,2), Robert Liska (3), Peter Krajnc (2,1)*
(1) Centre of Excellence PoliMaT, Tehnološki park 24, Ljubljana, Slovenia
(2) University of Maribor, Faculty of Chemistry and Chemical Engineering, PolyOrgLab, Smetanova 17, Maribor, Slovenia
(3) Vienna Technical University, Institute of Applied Synthetic Chemistry, Getreidemarkt 9/63, Vienna, Austria
*peter.krajnc@um.si

1. Introduction

High internal phase emulsions (HIPE) are emulsions with a volume fraction of the droplet phase higher than 74 %. A method for the preparation of highly porous monolithic polymers is the polymerisation of the continuous phase of a HIPE.[1, 2] PolyHIPEs are materials with an open cellular structure and with interconnecting pores, which is the result of the internal phase being trapped inside the continuous phase during the polymerisation. After the extraction of internal phase, the porous structure is observed. Such monolithic polymers were initially prepared as styrene/divinylbenzene copolymers for applications such as precursors for reactive species,[3] as column for filtrations or separations,[4] as media for tissue engineering[5] and also as a media for 3D cell cultures.[6]

2. Experimental

Pentaerythritol tetrakis(3-mercaptopropionate) (tetrathiol, TT, Sigma Aldrich), divinyladipate (DVA, TCI Europe), toluene (TOL, from 20 % to 60 %, Sigma Aldrich), Irgacure 819 (I819, BASF), calcium chloride ($CaCl_2$, Sigma Aldrich), poly(ethylene glycol)-block-poly(propylene glycol)-block-poly(ethylene glycol) (Pluronic L-121, Sigma Aldrich), sorbitan tristearate (Span 65, Merck), ethanol (Merck) were all used as received.

To organic phase, consisting of DVA and TT, initiator (Irgacure 819), surfactants (Pluronic L-121 and Span 65) and toluene, different amount of aqueous phase (80, 85, 90, 95 %) was added drop wise. The mixture was stirred with an overhead stirrer at 250 rpm during the addition of aqueous phase and for further 30 min after the addition of all aqueous phase. Emulsions were then transferred to silicon mould and polymerised in UV chamber for 140 s. Prepared polymers were purified with Soxhlet extraction in water for 24 h and in ethanol for 24 h. Figure 1 presents formulas of used monomers to prepare polyHIPEs.

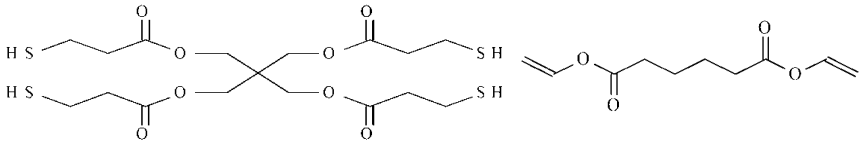

Figure 1. Formulas of used monomers

3. Results and discussion

Polymers with different amount of toluene were prepared. The amount of solvent was changed from 20 to 60 %. Table 1 shows that the samples with different percentage of toluene have different average diameter of cavities. We found that with increasing amount of toluene, the average diameter of cavities also increases.

Table 1. Varying the amount of added toluene

SAMPLE ID	AQUEOUS PHASE [%]	POROGEN [%]	DIAMETER OF CAVITIES [µm]
A20	85	20	8
A30	85	30	12
A50	85	50	18
A60	85	60	12

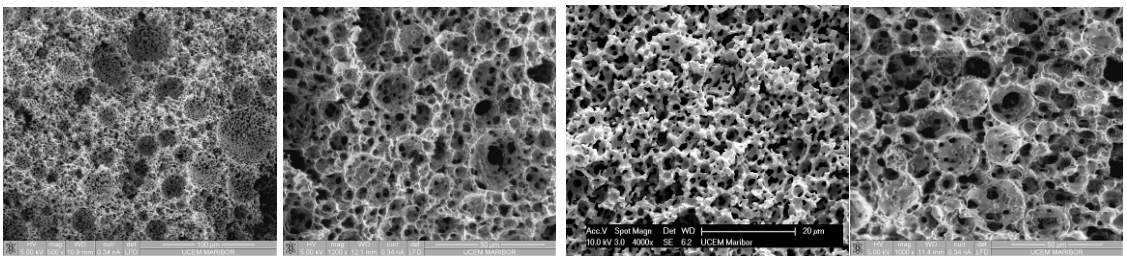

A20 AK30 A50 A60

Figure 2. SEM figures of samples with different amount of solvent

Table 2 presents prepared polyHIPEs with different amount of aqueous phase (80, 85, 90 and 95 %). We have shown that the optimal amount of aqueous phase for polyHIPE material is 85 %, and we also shown the emulsion with 95 % of aqueous is not stable.

Table 2. Varying the amount of added aqueous phase

SAMPLE ID	AQUEOUS PHASE [%]	POROGEN [%]
B80	80	50
B85	85	50
B90	90	50
B95	95	50

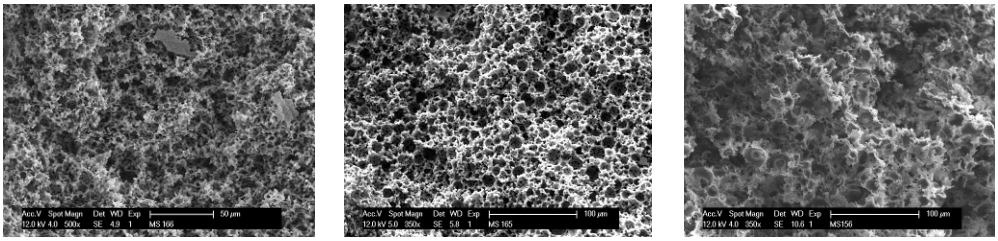

B80 B85 B90

Figure 3. SEM figures of samples with different amount of aqueous phase

4. Conclusions

We have shown that highly porous monolithic structures can be prepared from divinyl adipate and pentaerythritol tetrakis(3-mercaptopropionate) by using thiol-ene chemistry and emulsion templating. It was found that adding of 30 % and 60 % vol (with regards to oil phase) of toluene can produce polymer with a typical polyHIPE structure. We have shown that the optimal amount of aqueous phase is 85 % and that addition of 50% vol. of toluene yields monoliths with largest cavities.

Acknowledgements

The financial support of the Ministry of Science, Higher Education and Technology of the Republic of Slovenia (Centre of Excellence PoliMaT) through the contract No. 3211-10-000057 is gratefully acknowledged. Slovene Human Resources Development and Scholarship Fund is acknowledged for scholarship to Maja Sušec.

References

[1] N. R. Cameron, P. Krajnc, M. S. Silverstein, Colloidal Templating in Porous Polymers, (Eds: M. S. Silverstein, N. R. Cameron, M. A. Hillmyer), John Wiley & Sons Inc .Hoboken, NJ, USA 2011.
[2] I. Pulko, P. Krajnc, Macromolecular Rapid Communications 2012, 33, 1731.
[3] H. F. M. Schoo, G. Challa, B. Rowatt, D. C. Sherrington, Reactive Polymers 1992, 16, 125.
[4] I. A. Katsoyiannis, A. I. Zouboulis, Water Research 2002, 36, 5141.
[5] A. Barbetta, M. Dentini, M. S. De Vecchis, P. Filippini, G. Formisano, S. Caiazza, Advanced Functional Materials 2005, 15, 118.
[6] M. W. Hayman, K. H. Smith, N. R. Cameron, S. A. Przyborski, Journal of Biochemical and Biophysical Methods 2005, 62, 231.

S1-P13
Microcellular open porous poly(divinyl adipate)

Marko Turnšek (1), Peter Krajnc (1,2)*

(1) PolyOrgLab, Faculty of chemistry and chemical technology, University of Maribor, Smetanova 17, SI-2000 Maribor, Slovenia
(2) Centre of excellence PoliMaT, Tehnološki park 24, SI-1000 Ljubljana, Slovenia
*peter.krajnc@um.si

1. Introduction

Divinyl adipate (DVA) is a reactive difunctional vinyl ester that can be used as a monomer and a crosslinker. As reported in literature, DVA is used mainly with UV polymerization producing polymer networks. DVA contains ester linkages that could be utilized for biodegradation of prepared polymer. In order to study the morphology and degradation of porous poly(DVA), high internal phase emulsion templating was utilized and factors such as surfactant concentration, phase volume ratio and amount of initiator were studied. PolyHIPE[1] polymers have an open cellular structure with interconnecting pores, which is the result of the

internal phase being trapped inside the continuous phase during the polymerisation. After the extraction of internal phase, the porous structure is observed. PolyHIPE's have so far been used in various applications, such as filtration media[2], chromatography media[3], support for biological cells[4], etc.

2. Experimental

DVA has been used in the continuous phase along with solvent (toluene), surfactant (PEL-121) and initiator (AIBN). Internal phase consisted of water and salt (CaCl2x5H2O). Internal phase was added drop wise to the organic phase in a round bottom flask, under constant steering with an overhead stirrer at 300 rpm. After the addition of the internal phase stirring was continued for further half an hour. Emulsion was then transferred into silicone mold and put in an oven for 24 hours at 60° C. PolyHIPE was purified via Soxhlet extraction with ethanol and water for 24 hours respectively. We confirmed porous HIPE structure with scanning electron microscope (figure 1) and furthermore nitrogen adsorption was used to determine surface area of monoliths.

3. Results and discussion

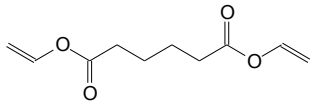

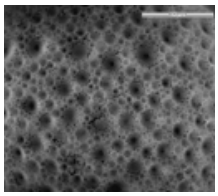

Figure 1. DVA monomer and SEM picture of prepared polyHIPE.

	Continuous phase DVA [g] Initiator [%]	Solvent [g]		Surfactant [%]	Internal phase [%]
S1	1,5	1,5	20	1	80
S2	1,5	1,5	30	1	80
S3	1,5	1,5	20+10	1	80
S4	1,5	1,5	20+10	1	90
S5	2	2	25	1	80
S6	2	2	40	1	80
S7	1,5	1,5	30	3	80
S8	1,5	1,5	30	1	80
S9	1,5	1,5	30	1	90

Emulsion stability was the main focus. With 20% surfactant ratio emulsion collapsed, so we increased surfactant ratio to 25% and got semi stable emulsion but once in an oven degradation started rapidly, while 30% surfactant was enough for emulsion stability. We also tried to mix two different surfactants but emulsions were not stable. Emulsions form internal volume ratios of 90% were stable, but monoliths were mechanically unstable. We concluded that optimal amount of surfactant is 30% and the amount of initiator is not a major influencing factor for morphology tuning.

Biodegradation of obtained monoliths were tested in solution of PBS buffer, 3M NaOH and 0,1M NaOH. We prepared 3 batches of each monolith in all 15 samples for PBS buffer, 12 samples for 3M NaOH and 12 samples for 0,1M NaON. In PBS buffer degradation is undetected until now (graph 1), In 3M NaOH monoliths degraded completely in 2 to 3 days. In 0,1M NaOH the degradation is slower, we monitored it on a weekly base (graph 2) and after 5 weeks material has completely degraded.

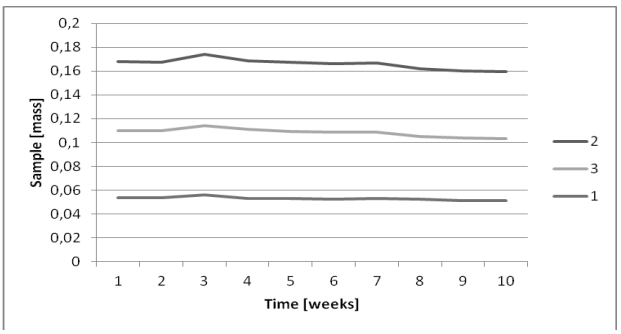

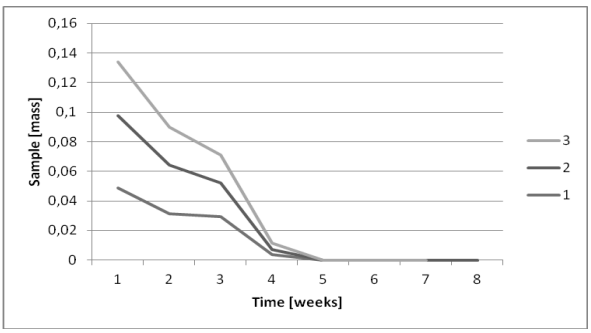

Graph 1. Monomer in PBS buffer

Graph 2. Monomer in 0,1M NaOH

4. Conclusions

DVA has proven that it can be used as monomer and crosslinker in forming a stable polyHIPE. We can use formed polymer for multiple purposes, such as flow through studies and tissue engineering. Because of ester bonds the material is suitable for biodegradation.

Acknowledgements
Financial support of the Slovenian Research Agency (scholarship to Marko Turnšek) is gratefully acknowledged.

References
[1] PULKO, I., KRAJNC, P. Macromol. rapid commun., 26. Oct. 2012, vol. 33, iss. 20, str. 1731-1746.
[2] D. C. Walsh, J. I.T. Stenhous, L. P. Kingsbury, E. J. Webster, J. Aerosol Sci. 1996,27, 629
[3] P. Krajnc, N. Leber, D. Štefanec, S. Kontrec, A. Podgornik, J. Chromatogr. A 2005, 1065, 69
[4] W. Busby, N. R. Cameron, C. A. B. Jahoda, Polym. Int. 2002,51, 871

Session 2: Surfaces, interfaces and structures

S2-P14
Use of mathematical method to describe topographics properties of polymers

M. Babič (1)*, P. Kokol (2), M. Milfelner (3), P. Panjan (4), Igor Belič (5)
(1) Emo-Orodjarna d.o.o., Slovenia,
(2) University of Maribor, Faculty of Health Sciences, Slovenia,
(3) Tic-Lens d.o.o., Slovenia,
(4) Institute Jozef Stefan, Slovenia,
(5) Institute of Materials and Technology, Slovenia
*babicster@gmail.com

1. Introduction
Mathematics and computer science are very useful in many other sciences. We use the mathematical method of fractal geometry in chemical engineering to analyze microstructure of polymers. In this work, we have used a scanning electronic microscope (SEM) to search and analyse the fractal structure of the polymers. The present study is intended to use new method, fractal geometry and to describe completely topographics properties of polimers. Finally, concept of fractal geometry is applied to characterize the microstructure and derive the useful relationship between fractal dimension and microstructural features.

2. Theory
Characterization of surface topography is important in applications involving friction, lubrication, and wear (Thomas, 1999). In general, it has been found that friction increases with average roughness. Roughness parameters are, therefore, important in applications such as automobile brake linings and floor surfaces. The effect of roughness on lubrication has also been studied to determine its impact on issues regarding lubrication of sliding surfaces, compliant surfaces, and roller bearing fatigue. Finally, some researchers have found a correlation between the initial roughness of sliding surfaces and their wear rate. Such correlations have been used to predict the failure time of contact surfaces. A section of standard length is sampled from the mean line on the roughness chart. The mean line is laid on a Cartesian coordinate system wherein the mean line runs in the direction of the x-axis and magnification is the y-axis.The value obtained with the formula on the right is expressed in micrometers (Om) when y=f(a).

3. Experimental
Fig. 1 presents the calculation of the fractal dimension. Firstly, we convert the SEM micrograph into a binary picture. To calculate the fractal dimension we use a box-counting algorithm. The log-log plot presents the fractal dimension.

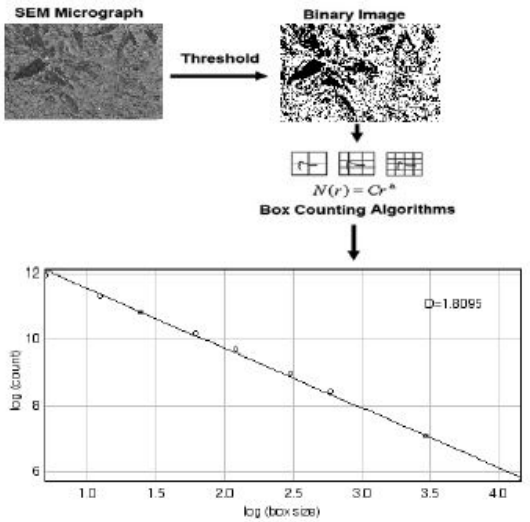

Figure 1. Calculation of fractal dimension with box-counting method

4. Results and discussion

Roughness one of many topographic properties is good predictor of the performance of a mechanical component, since irregularities in the surface may form nucleation sites for cracks or corrosion, but roughness may promote adhesion. We analysed this roughness using the mathematical method of fractal geometry. Fractal geometry is becoming increasingly popular in materials science to describe complex objects. With fractal geometry, we analysed roughness of polymers. Contact profilometry is a quantitative technique known to reflect the irregularities of the surface profile of the polymers.

5. Conclusions

The paper present using mathematical method to describe mechanical properties of robot laser hardened specimens. We use relative new method, fractal geometry to describe complexity of microstructure of polymers specimens. The main findings can be summarized as follows:

1. There exist a fractal structure in the microstructure of polymers.
2. We describe complexity with fractal geometry of microstructure of polymers.
3. We use box-couting method to calculated fractal dimension microstructure of polymers .

Relationship between topographics properties and polymers we may be better understand through exploration the fractal dimensions of the microstructure.

Acknowledgements

The present work was supported by the European Social Fund of the European Union.

References

[1] G. E. Totten, PhD., FASM, Steel heat treatment, second edition, 2006.
[2] Xu, Z., Leong, K.H. & Reed, C.B. 2008, "Nondestructive evaluation and real-time monitoring of laser surface hardening", Journal of Materials Processing Technology, vol. 206, no. 1-3, pp. 120-125.
[3] Kennedy, E., Byrne, G. & Collins, D.N. 2004, "A review of the use of high power diode lasers in surface hardening", Journal of Materials Processing Technology, vol. 155-156, pp. 1855-1860.
[4]Kennedy, E., Byrne, G. & Collins, D.N. 2004, "A review of the use of high power diode lasers in surface hardening", Journal of Materials Processing Technology, vol. 155-156, pp. 1855-1860.
[5]John C Ion, “Laser processing of Engineering Materials- Principles, procedures and industrial applications ”, Elsevier, 2005.

S2-P15

Electrical characterisation of conductive composites material based incompatible polymer matrix

A. Merzouki, N. Haddaoui
L.P.C.H.P. Dépt. Génie des Procédés, Facultés des Sciences de l'Ingénieur,
Université Ferhat ABBAS de Sétif. 19000 ALGERIE

1. Introduction

Polymer blends and composites are major areas of academic and industrial research, because of the ability to pre-design and achieve property Improvements surpassing their homopolymer counterparts. A new emerging field of polymer blending still largely unexplored focuses on polymer immiscible blends comprising three and more component systems (polymers and fillers). A major characteristic of immiscible (phase separated) polymer blends is the multi-phase morphology, and its formation sensitivity to the proccessing conditions. Polymer blends offer an effective route for the production of new engineering materials, with electrical and mechanical properties, which can be tailored to satisfy a large variety of applications [1-2].
It is well known that the electrical resistivity of insulating polymers can be decreased by dispersing a conductive filler, e.g., carbon black (CB) throughout the polymer matrix.
Polymers filled with the carbon black have a big antistatic power. However, it is a problem to reach a certain conductivity by addition of particles of carbon black while preserving the mechanical properties of the polymer and to reduce most possible the price of the final Composite, the carbon black is a relatively expensive load. It is in this objective that news techniques were developed to prepare some composite materials with a lowest threshold of percolation possible. Among these techniques we can mentioned the selective distribution of the load in an interface of an incompatible polymer blend.

2. Theory

There are several ways to decrease the percolation threshold of GB particles in polymers. They are mainly based on the use of additives, the optimization of processing conditions, and the size distribution and porosity of GB particles. This work focuses on a completely different approach, which relies upon the selective localization of GB particles in multiphase polymeric materials. This approach bas already been considered by some authors, who reported very encouraging results [1-3].
Incorporation of a filler to a binary immiscible polymer system can lead to several morphologies: the filler particles may disperse in the matrix along with the minor dispersed polymer phase, the filler may locate at the interfaces between the matrix and the dispersed polymer phase. The filler may be encapsulated by the minor phase.
In this work we prepared and studied the electric behaviour of this composite material type (Polypropylene/ Polyethylene/ Carbon Black) and (Polypropylene/ Polystyrene/ Carbon Black) at different filler concentration and different sample thickness. The two polymeric phases of composites are known as an incompatible polymer, the third phase represents the filler.

3. Expermental

-Polymers: - Polypropylene (PP): Vestolene, (Italy) d=0.9
- Polyethylene (PE): law density, B21 (Algeria) d=0.93
- Polystyrene (PS): B.A.S. 143 E F (Germany) d = 1.05.

Incompatible blend composition (wt %): PP/PS : 80/20 and PE/PP : 80/20
- Filler: Carbon Black (CB): Super Battery Black, S.A.Ensagry, WILLEBROEK N.V (Belgium), surface area = 42 m2.gr-1 .
The polymers granulates were melted and banded on an electrically heated two-roll mill at 190 °C. After 5 min of mixing, the carbon black was then added and mixed into the polymer blend for time periods of 10 min.
After the designated mixing time was achieved, the polymer - carbon black mixture was removed as a sheet from the mill.
These sheets were crushed into granulates of 3-5 mm diameter, then compression molded into Plaques 15 cm x l0 cm with different thickness for electrical property testing.
Sample plaques (2.5 cm x 1.5 cm) were tested for transversal resistivity by placing the samples between to cupper electrodes connected to a digital multimeter. The same pressure is exercised on the two electrodes during the résistance lecture. The resulting resistance R is converted to transversal resistvity by the following relationship.

4. Results and discussion

Results showed the role of the nature of the matrix on the electric properties of the final material and that a matrix presenting the adequate structure can improve the conductivity or same times to decrease the threshold of percolation. Percolation was detected at lower carbon concentrations in PP/PS system, than in The PE/PP system.

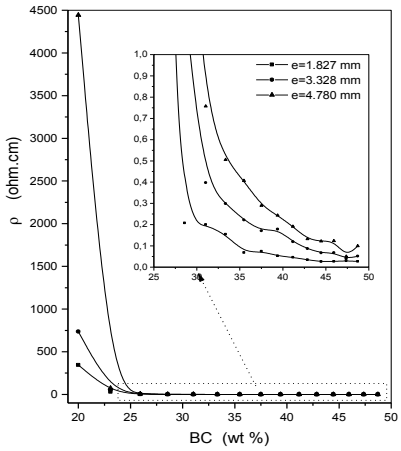

Fig 1: Resistivity (ρ) Vs wt % CB in PP/PS blend (80/20) having different thickness

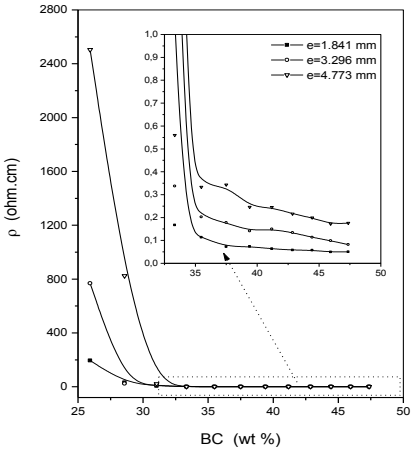

Fig 2: Resistivity (ρ) Vs wt % CB in PE/PP blend (80/20) having different thickness

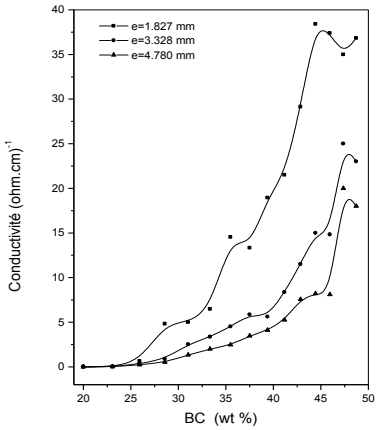

Fig 3: Conductivity (σ) Vs wt % CB in PP/PS blend (80/20) having different thickness

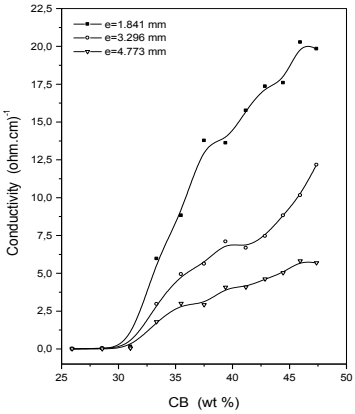

Fig 4: Conductivity (σ) Vs wt % CB in PE/PP blend (80/20) having different thickness

5. Conclusion

- Below 20 wt % CB in PP/PS composites and 25 wt % CB in PE/PP composites, the samples have a high resistivity. Filler grains are note in contact. Filler network is note achieved.
- PE/PP composites have a higher resistivity then PP/PS composites for the same filler ratio.
- At law concentrations the difference between composites resistivity is considerable for the comparable filler concentrations.
- Thickness increases considerably the resistivity in both composites.
- At high filler concentrations the composites based PP/PS are more conductive than the composites based PE/PP.
- At high filler concentration the thickness has a lower effect on the conductivity than on the resistivity at lower concentration.
- The second critical concentration is retched at 45 wt % for the PP/PS composites, whereas in the PE/PP composites it is observed only in the samples with lowest thickness.
- Composites with an appreciable conductivity have a filler ratio more than 20 wt % for the PP/PS composite and more than 25 wt % for the PE/PS composites.
- Results show the effect of matrix nature on the filler distribution, CB distribution is more efficient in PP/PS. It has a higher conductivity, percolation threshold is observed at a lower concentration than in PE/PP composites.

References:

[1] I. FISHER, J. ZOLTAN and A. SIEGMANN, Polymer Composites, (2000) 21, 396-416
[2] C. Chen, J.C. LaRue, R. D. Nelson, L. Kulinsky, and M. J. Madou., Journal of Applied Polymer Science DOI 10.1002/app
[3] R. T. Subramaniam1, L. Chiam-Wen, L.P. Yee and E. Morris., Recent Advances in Plasticizers, Dr. M. Luqman, 2009, p 165
[4] Z.M. Li, S.N. Li, B. Xu. And A0 Lu., Polymer-Plastics Technology and Engineering, (2007), 46, 129–134.

S2-P16
Microstructural morphology of EVA-copolymer modified bitumen

S.N. Nahar (1)*, A.J.M. Schmets (1), A. Scarpas (1) and G. Schitter (2)
(1) Structural Mechanics, Faculty of Civil Engineering & Geosciences, Delft University of Technology. Stevinweg 1, 2628 CN, Delft, The Netherlands
(2) Automation and Control Institute (ACIN), Vienna University of Technology. Gusshausstrasse 27-29; A-1040 Vienna, Austria
*s.n.nahar@tudelft.nl

Bitumen is the binder of asphalt concrete which provides the viscoelastic nature of the material. In many pavement applications, polymer is incorporated into bitumen and the use of this modified binder increases the structural strength of asphalt and its service life under high thermal and mechanical stresses. The modified bitumen improves the deformation, cracking resistance, low temperature properties and the fatigue characteristics of the material. Ethylene-vinyl-acetate (EVA) is a thermoplastic polymer which is used as one of the polymer modifiers of bitumen for more than two decades. EVA modified bitumen provides improved workability during mixing process of asphalt and increase the life time of the pavement. It gives the material higher stiffness, low sensitivity in temperature variations and good binding properties. The blending of the modifier with bitumen is the most important parameter in achieving desired performance of the material. The modifier should be physically and chemically stable during processing, storage, application and service. In this context of research atomic force microscope (AFM) is used as a surface-morphology characterization tool to understand the blending of EVA with pure bitumen.

Pure bitumen is a complex organic matter which is macroscopically homogeneous but microscopically heterogeneous. It exhibits distinct microstructural morphology depending on the crude origin and process conditions. One of the scanning probe techniques, AFM has revealed that this microstructural morphology is a unique fingerprint of the material type. These microstructural domains are different in stiffness and adhesion properties than the matrix which is qualitatively proved by the change in probe-sample interaction found in AFM phase images. The microstructural properties are directly related to the mechanical properties of the material.

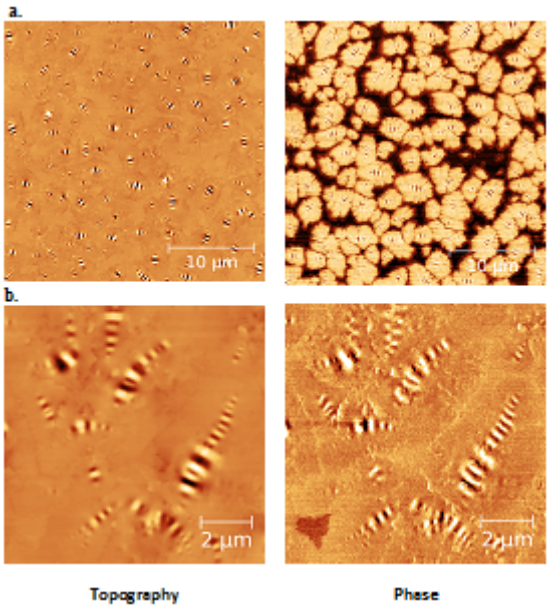

Figure 1. AFM topography and phase images of 70/100 penetration grade pure bitumen at 25°C a) 30×30 µm and b) 10×10 µm scan size

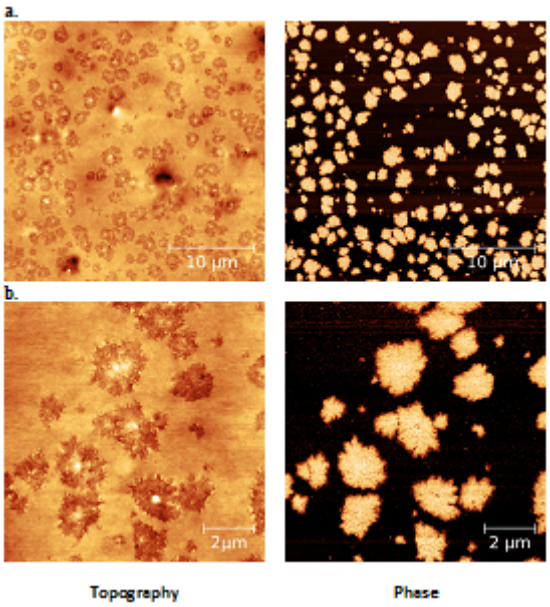

Figure 2. AFM topography and phase images of EVA 5% (w/w) polymer modified 70/100 bitumen at 25°C a) 30×30 µm and b) 10×10 µm scan size

A 70/100 penetration grade (a measure of hardness) bitumen is selected for this study which is widely used bitumen grade for the pavement applications in Europe. EVA 5% (w/w) polymer is mechanically blended to the 70/100 pure bitumen at 170°C. The surface morphology of both the pure and EVA modified bitumen is studied by AFM. The obtained AFM images are presented in Figure 1 and Figure 2. In Figure 1, the pure bitumen was found to have 2 to 5 µm domains of elliptical shapes with an oscillating topography pattern in the middle of the domain ('bee'-like structure). The high resolution image of the pure bitumen (Figure 1.b) clearly shows the morphological details. The presence of EVA is observed to alter the microstructural morphology by changing the domain size, shape and topography. In Figure 2, the 5% EVA modified bitumen showed microstructures of uniform sizes in which the oscillating pattern or the bee-structure is no more pronounced. Instead the high resolution AFM topography image (Figure 2.b) of the modified bitumen reveals the presence of many small circular (diameter with 10 to 20 nm) particles inside the microstructures. However the blending of EVA and the microstructural morphology will vary with different penetration grades of bitumen and their thermodynamic history.

AFM is a very promising tool to understand the blending of polymer with bitumen in microscopic level at higher precision. To understand the performance of the binder and the extent of blending, AFM can be used in combination with the traditional mechanical tests available for the polymer modified bitumen.

S2-P17
Anchoring of alkylsilanes and alkylphosphonic derivates on copper surfaces

Nothdurft Philipp (1)*, Feldbacher Sonja (1), Kern Wolfgang (1,2)
(1) Polymer Competence Center Leoben GmbH, Roseggerstraße 12, 8700 Leoben, Austria
(2) Montanuniversität Leoben, Franz-Josef-Straße 18, 8700 Leoben, Austria
*Philipp.Nothdurft@pccl.at

1. Introduction

Copper is used in different industrial applications due to its excellent thermal and electrical conductivity. In printed circuit boards (PCBs) conductive pathways are produced by etching copper foils on insulating materials. The stability of such bilayer depends mainly on mechanical strength and adhesion. To improve the binding strength between copper and the insulating material, which is an epoxy resin, modification of the copper surface can be an interesting approach. For functionalization of a solid surface a powerful and simple method are self assembled monolayers (SAMs). They are formed by immersion of a substrate into a solution of a reactive molecule in an organic solvent. In case of copper numerous reports exist about formation of SAMs with alkanethiols, monochlorosilanes, trichlorosilanes, triethoxysilane, alkylphosphonic derivates [1][2][3][4]. Because one requirement of the produced SAMs is thermal stability, alkanethiols were not used for further research. In this study we concentrated on silanes and phosphonates for copper modification. Both substance classes seem to meet the needed requirements. To characterize SAMs, X-ray photoelectron spectroscopy (XPS), attenuated total reflectance (ATR) and contact angle measurements were used. For simplicity in XPS measurements and checkability if a reaction occurred, silanes and phophonates were chosen with a fluorinated

tail group. For further research the fluorinated tail groups will be modified to functional groups, which can interact with molecules in an epoxy resin.

2. Theory

The chemisorption of silanes and phosphonates is relied on a hydroxylated copper surface, where a condensation reaction can occur. The silanes are hydrolyzed by water and form silanols and finally form a siloxy-copper bond (Cu-O-Si). Phosphonates react with copper and form copper-phosphonates (Cu-O-P). The number of the bonds is dependent on the molecule properties and the molecular grafting mode (mono-, bi- or tridentate).

3. Experimental

The received copper foils were polished to remove the protecting layer, and afterwards cleaned with ethyl acetate, isopropyl alcohol and milipore water. The samples were further placed in nitric acid solution and oxidized in 5% aqueous H_2O_2 solution. Chemisorption of the silanes and phosphonic derivates were performed by immersion of the prepared copper foils for a period of time in the respective solution. Afterwards the coated copper foils were washed and blown dry with CO_2. The experimental procedure was mainly adopted from Hoque [1][2]. Prior to further surface modification, an optimization of the oxidation process was necessary. The dipping time of HNO3 respectively the H2O2 solution was varied. In Figure 1 a scheme of the reaction is shown. The characterization of the manufactured SAMs was done by XPS, ATR and contact angle measurements.

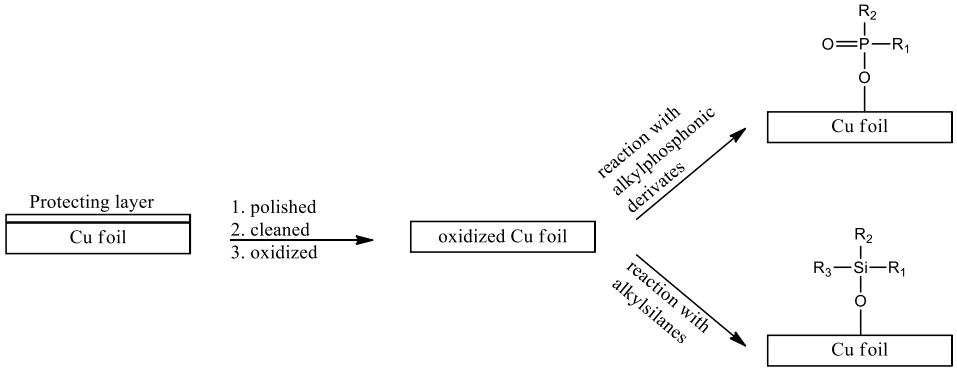

Figure 1. Scheme of reaction

4. Results and discussion

For the oxidation procedure with nitric acid and hydrogen peroxide solution the best process conditions were found with dipping times of 10 minutes per solution. XPS data show a complete removal of Cu(II) oxides on the surface after polishing and nitric acid treatment. Cu(II) oxides are formed again after H2O2 treatment which can be further used for copper modification. Copper modification is successful with trichlorosilanes on oxidized copper. This can be clearly seen by a XPS F1s spectrum and in other spectra such as C2s, Si2p in accordance witho Hoque [1][2]. Contact angle measurements showed a hydrophobization of the surface after silanization. After oxidation a contact angle of ~ 18° is obtained and can be increased to ~125° after SAM formation with fluorinated silanes. Monochlorosilanes and triethoxysilanes need optimization of the reaction conditions to attach to the surface. So far trichlorosilanes showed the best results for copper modification. Phosphonates also show a good workability and first results confirm the SAM formation on copper.

5. Conclusions

Copper modification via functional silanes and phosphonates is an interesting field of research and our first results seem to be promising to meet our requirements. SAMs could be formed on copper surface, for the use of adhesive forces enhancement between copper and an epoxy resin. In our first experiments we used fluorinated silanes and phosphonates, where here the fluoro groups are used as a tracer in the XPS measurements. In further experiments functional instead of fluorinated groups will be used to perform covalent bonding between the copper and the epoxy resin.

Acknowledgements

The research leading to these results has received funding from AT&S and Atotech.

References

[1] E.Hoque, J.A. DeRose, B.Bhushan, K.W. Hipps , *Ultramicroscopy* 2009, 109, 1015-1022
[2] E.Hoque, J.A. DeRose, R. Houriet, P. Hofmann, H.J. Mathieu, *Chem. Mater.* 2007, 19, 798-804
[3] G. Fonder, I.Minet, C. Volcke, S. DEvillers, J. Delhalle, Z. Mekhalif, *Applied Surface Science*, 2011, 257, 6300-6307
[4] W. Guo, S.Chen, H. Ma, *J.Serb. Chem. Soc.* 2006, 71, 167-175

S2-P18

Silica nanoparticles bearing a photoreactive shell for crosslinking of polymers and immobilization of polymer surfaces

Gisbert Riess (1)*, Nina Muhr (1), Jörg G. Schauberger (1), Wolfgang Kern (1)
(1) Chair of Chemistry of Polymeric Materials, University of Leoben, Otto-Glöckl-Straße 2, 8700 Leoben, Austria
*riess@unileoben.ac.at

1. Introduction

The modification of inorganic nanoparticles (e.g. nanoplates and spheres) is increasing in importance especially for surface functionalization. It is a prerequisite for achieving enhanced properties and designing materials with new characteristics. If photoactive groups are attached to the surface of nanoparticles, the surface can be modified by UV irradiation. Therefore, in our research, nanoparticles bearing a photo reactive shell have been synthesized and investigated with respect to their behavior and potential applications. For this purpose compounds with nitrogen-nitrogen double bonds such as phenylazide or aromatic diazosulfonate groups are used, these are well known for their photo reactivity. [1, 2]

2. Experimental

For hydrophobic polymers nanoparticles (SiO_2-NP) bearing azido surface groups (SiO_2-C_6H_4-N_3) were prepared from amino functionalized SiO_2-NP and 4-azidophenyl isothiocyanate. The photoreaction of the azido group has been applied to attach the photoreactive nanoparticles to polymer surfaces. Upon UV irradiation with wavelengths $\lambda < 280$ nm, the azido (N_3) group splits off a nitrogen (N_2) molecule to give high reactive nitrene moieties.
In the second approach, silica nanoparticles have been modified with diazosulfonate groups (SiO_2-C_6H_4-N_2-SO_3Na) for hydrophilic polymers. First 3-(m-aminophenoxy)propyltrimethoxysilane was attached to silica nanoparticles (SiO_2-NP). The bonded amino phenyl groups were converted in an additional step to a phenyl diazosulfonate. Depending on the matrix, the photolysis of the diazosulfonate group yields phenyl and/or phenol units, following free radical or ionic pathways [2].

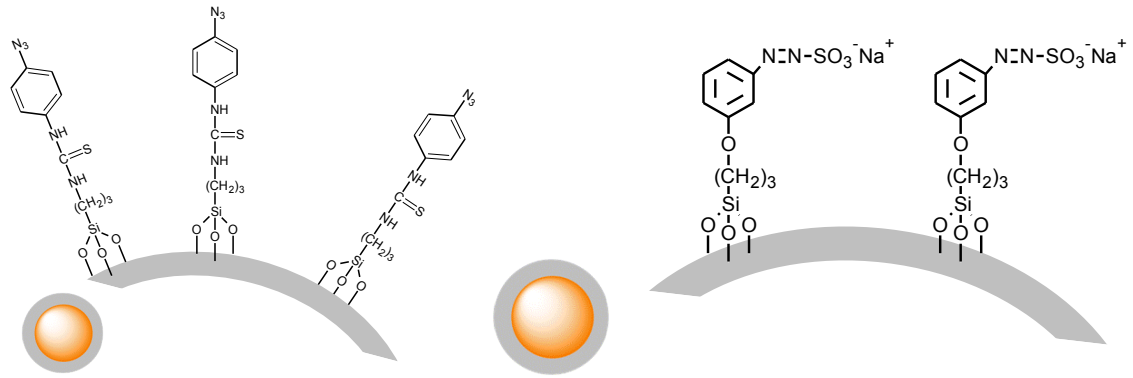

Figure 1: Azidophenyl silica nanoparticles and diazosulfonate silica nanoparticles.

3. Results and discussion

The azidophenyl functionalized nanoparticles (SiO_2-C_6H_4-N_3) which bearing an UV reactive ligand shell, were used to crosslink various hydrophobic polymers, such as polyisoprene and a polynorbornene derivate. Furthermore, azidophenyl functionalized NP are capable to immobilize of inert polymer surfaces, e.g. polyethylene. Depending on the reaction time, different amounts of SiO_2-C_6H_4-N_3 were deposited on the illuminated areas of polyethylene, whilst no immobilization of SiO_2-C_6H_4-N_3 was observed in the non-illuminated areas:

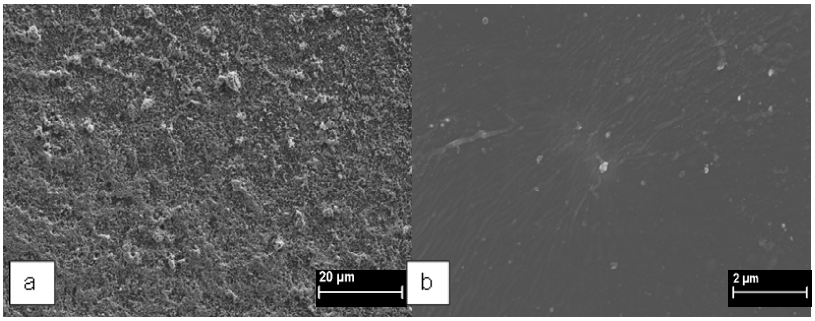

Figure 2: SEM micrographs of an UV irradiated PE-LD foil (a) and a non-irradiated (b) PE-LD foil.

The nanoparticels with diazosulfonate groups were synthesized based on different concentrations of modifying agent and silica nanoparticles, to determine the optimum ratio of surfactant and particles for surface functionalization.

Table 1: Synthesized silica nanoparticles with different concentrations of diazosulfonate groups.

composition	silica nanoparticles	3-(m-aminophenoxy)propyltrimethoxy silane
(-)	(wt.-ratio)	(wt.-ratio)
NP1	1	1
NP2	1	2
NP3	1	4

After functionalization and conversion to diazosulfonates, the nanoparticles were dispersed with polyvinyl alcohol (95 wt.%). The resulting films are irradiated and then swelling properties were determined. After the swelling, the films were dried and the gel content was calculated. The results clearly show that upon irradiation the gel content rises due to crosslinking of the PVA matrix. In contrast to these results pristine PVA remains water soluble.

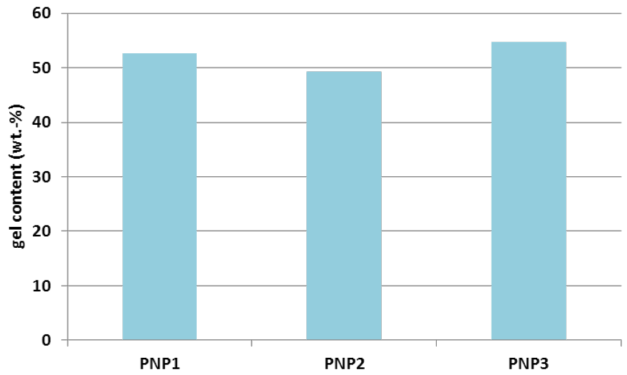

Figure 3: Gel content of illuminated films based on polyvinylalcohol and different silica nanoparticles with diazosulfonate groups (SiO_2-C_6H_4-N_2-SO_3Na)

The gel content after irradiation is independent from the used concentration of modifying agent, but polyvinyl alcohol is cross-linked. Therefore the lowest concentration of the modifying agent is able to functionalize all suitable locations of the nanoparticle surface, which are related to the crosslinking of polyvinyl alcohol.

4. Conclusions

In conclusion, we have demonstrated the application of nanoparticles, bearing a photo sensitive shell, for the cross-linking of polymers and for selective immobilization on foils. It was shown, that silica nanoparticles were successfully modified with diazosulfonate units or azido groups. Using azidophenyl functionalized nanoparticles an immobilization on the surface of a hydrophobic polymer was achieved. On the other hand diazosulfonated nanoparticles are capable of reacting with numerous polymer matrices and thus it is possible to obtain photo curable nanocomposites. The particles were used to prepare UV-crosslinked composites with hydrophilic polymers such as polyvinyl alcohol. It was demonstrated that photoactive core shell nanoparticles were synthesized for polymer composites with a wide range of polymer types.

References

[1] C.H. Lee Go, W.H. Waddel, *J. Am. Chem. Soc*. **1984**, 106, 715-718.
[2] O. Nuyken, B. Voit, *Macromol. Chem. Phys.* **1997**, 198, 2337.

S2-P19
Integrated approach at snap fit design

Jože Tavčar (1)*, Gašper Resman (2), Jože Duhovnik (1)
(1) University of Ljubljana, Faculty of Mechanical Engineering, Aškerčeva 6, SI-1000 Ljubljana, Slovenia
(2) Iskra Mehanizmi, Lipnica 8, SI-4245 Kropa, Slovenia
*jtavcar@iskra-mehanizmi.si

1. Introduction
Snap fits have an important role at small appliances, toys and other assemblies made from polymer materials. Integrated approach need to consider specifics of materials properties, ergonomics and molding tool design. In this way robust design can be achieved that use all the advantages of polymer materials. A systematic analysis of different snap fit constructions has been done by comparison between numerical analyses, experimental data and results of others authors. The summary of research work was edited into compact procedure that guides engineers through snap fit design.

2. Snap fit design process
In the first step a compact overview of basic functions of snap fit elements was prepared that help a designer to select an optimal construction. Functions of snap fit elements: locaters, lock function that prevents motion, enhancements for assembly, guidance elements, operator feedback, guard elements and retainers. In the next step operator ergonomic needs to be studied. A snap fit designer has to answer several questions: are assembly steps logical to the operator, are parts well guided during assembly process, does the operator get feedback information of final position? In the next step comes design of details that includes determination of stiffness, deformations and calculation of mechanical loads. At the end tool design limitations and injection molding technology need to be considered.

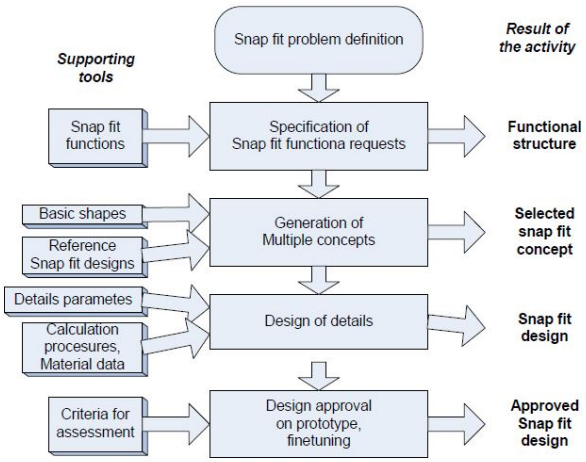

Figure 1. Snap fit design process diagram.

Summary of snap fit design process is presented in figure 1. The main activities of the process are similar to steps in methodology of design (VDI 2222). On the left side there are specific supporting tools for each activity. Supporting tools were developed during our research project. They are in a form of systematic review of different shapes for conceptual phase or as a computer program for design details calculation. By using systematic approach the snap fit solution is better. It does not depend only on designers` intuition and past experiences. On the right side of the diagram there are results of activities.

3. Supporting tools
Snap fit designers need complex knowledge from tool design, polymer properties to snap fit solutions. Supporting tools were developed specifically to company production program which is based on personal care appliances and mechatronic modules. The structure of snap fit design knowledge database is flexible. That mean all new findings and experiences are periodically added to supporting tools. It is a useful tool for beginners – they do not need to repeat all typical mistakes; and for senior designers – they are more productive and snap fit solutions are optimized.
An example of systematically designed snap fit connection (figure 2):
- Slope level of cantilevers locks enable connection at user-friendly force
- Round end and tube are guiding the elements during assembling stroke
- Lock design (negative angle) is preventing opening the connection (non-releasing lock) by an average user
- Specific tool that press all the lock hooks concurrently need to be used for opening connection (second option are blind holes for shapers release -> holes are marked but not drilled through)
- Length of cantilevers enables elastic deformation during assembly and braking at misuse

- Bigger radius at the cantilevers root enable better processing at injection molding and reduce stress concentrations

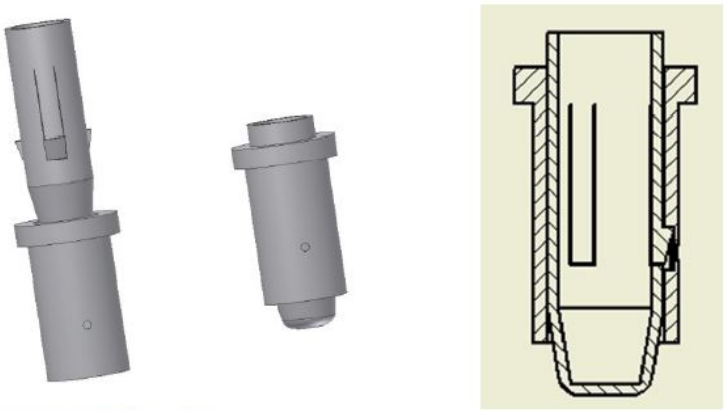

Figure 2. Tube snap fit connection.

4. Conclusions

Nowadays manufacturing companies cannot afford delays at entering the market, product design has to be good the first time. This is possible only by applying integrated and systematic approach through all steps of product development. Snap fit design is a typical activity that requires specific, interdisciplinary knowledge. Permanent collecting of knowledge and setting up supporting tools improve quality of design solutions and it reduces number of expensive engineering changes (5).

References

[1] Jordan Rotheiser, Joining of Plastics, Hanser 2009, Munich.
[2] Gottfried W. Ehrenstein. Mit Kunststoffen Konstruieren, Carl Hanser Verlag Muenchen, 3. Auflage, 2007
[3] Schreyer, Guenter. Konstruieren mit Kunststoffen, Carl Hanser Vrlag Muenchen, 4. Auflage, 2008
[4] James C. Gerdeen, Engineering Design with Polymers and Composites, Taylor& Francis, 2006
[5] J. Tavčar, J. Duhovnik, Engineering change management in individual and mass production. Robot. comput.-integr. manuf. [Print ed.], 2005, Vol. 21, No. 3, pp. 205-215
[6] VDI 2222-1, Methodic Development of Solution principles, Association of German Engineers, VDI Verlag, 1997

S2-P20

Structural rearrangements in membranes of anionic liposomes induced by their adsorption on the spherical polycationic brushes

Olga Zaborova (1)*, Andrey Sybachin (1), Viktor Orlov (2), Alexander Yaroslavov (1)
(1) Department of Chemystry, Lomonosov Moscow State University, Leninskie Gory, 1, 119991, Moscow, Russia
(2) A.N. Belozersky Institute, Lomonosov Moscow State University, Leninskie Gory, 1, 119991, Moscow, Russia
*olya_z_88@mail.ru

1. Introduction

Liposomes represent an important category of nano-sized systems for biomedical applications. Due to unique structure, liposomes are used for encapsulation of different substances for improving their physical, chemical and operational characteristics. Hydrophobic molecules can be incorporated into the liposomal membrane, hydrophilic – into the inner water cavity. These features make liposomal containers promising for encapsulation and delivery of various therapeutic, diagnostic and cosmetic agents.

A spherical polycationic brush (SPB) is made by graft-polymerizing a cationic monomer onto the surface of a 100 nm polystyrene bead. It is possible to adsorb small unilamellar anionic liposomes (40–60 nm diameter) onto the SPBs while maintaining the liposome integrity. The liposomes were constructed with electroneuthral dipalmytoylphosphatidyl choline (DPPC) admixed with 0.1–0.5 mol fraction of an anionic lipid, phosphatidylserine (PS^{1-}).

In this work it was demonstrated that SPBs are able to adsorb up to 40 liposomes that dramatically increase effective volume of liposomal container. It was demonstrated earlier that complexation of anionic liposomes with polycations may result in structural rearrangements in liposomal membrane such as lateral segregation of lipids and their trance-membrane migration (flip-flop). Such rearrangements may result even in disruption of liposomes.

By differential scanning calorimetry (DSC) it was shown that increase of molar fraction of anionic lipid in liposomes drastically change the structure of membrane after complexation with SPBs while interaction with linear polycation – poly-N-ethyl-4-vinylpyrydinium bromide – is not affected by PS^{1-} fraction.

By means of fluorescence quenching the stability of complexes towards dissociation in water salt media was studied for wide range of anionic lipid content. The integrity of liposomal membrane in complexes was controlled by using liposomes with inner cavity filled with 1 M NaCl solution and measuring of conductivities of unbound liposomes and complexes.
The results obtained allows one to choose optimal composition for the containers potential for the delivery of biological active substances – high number of adsorbed liposomes, stability in physiological media and integrity of liposomal container`s membrane in complex.

This work was supported by Russian Foumdation of Basics Researches (projects № 11-03-92487-IMST and № 12-03-31401)

Session 3: Polymers from renewable resources

S3-P21
Studies on the kinetics of synthesizing palm stearin alkyd resin

A.R.N. Azimi*, Rosiyah Yahya, Seng – Neon Gan
Faculty of Science, Chemistry Department, University of Malaya , 50603 Kuala Lumpur , Malaysia

Abstract: The kinetics of synthesizing three long oil alkyd resins based on palm oil , dehydrated castor oil , and linseed oil , individually , was studied at 240 – 245 degree Celsius. Synthesizing process was alcoholysis. Kinetic treatment of polyesterification of each alkyd was studied as a function of conversion and reaction time. The progress of reaction was monitored through measuring the acid value of sample of the reaction mixture at specified time intervals. Kinetic results showed that three alkyds synthesis have similar kinetic behavior , greatly, and follow second order rate law at the initial stage of process and thereafter deviation were observed.

Key words: Palm alkyd resin , Palm stearin , Alkyd kinetics , Organic coatings, Polyesterification.

S3-P22
Polyurethane foams from liquefied cork at atmosferic pressure

N. V. Gama (1)*, B. Soares (1), C. S. R. Freire (1), I. Brandão (2), A. Barros-Timmons (1), A. Ferreira (1,3), C. Pascoal Neto (1)
(1) CICECO and Department of Chemistry, University of Aveiro – Campus Santiago, 3810-193 Aveiro, Portugal
(2) Sapec-Química SA, Zona Industrial de Ovar – Lote 18, 3880 Ovar, Portugal
(3) Escola Superior de Tecnologia e Gestão de Águeda - Rua Comandante Pinho e Freitas, nº 28, 3750 – 127 Águeda, Portugal.
*nuno.gama@ua.pt

1. Introduction
Polyurethanes (PUs) are versatile engineering materials which find a wide range of applications because their properties can be readily tailored by the type and composition of their components. PU is the general name for a polymer having urethane linkages in their chain structure and is prepared by the step polymerization between –NCO groups of an isocyanate and the hydroxyl groups (-OH) of a molecule.
The general route to synthesize these polymers is reacting a polyol with an isocyanate. To obtain polyurethane foams (PUFs), the isocyanate and polyol, as well as catalysts, surfactants and blowing agents are all blended together under vigorous stirring and transferred into a mold. The foaming occurs when the blowing agents reacts with isocyanate groups, which spontaneously lose CO2, thus, generating the foam bubbles. As well-known, PUFs are produced within an extensive range, which allows them to be used in a wide diversity of consumer and industrial applications. Foams can be flexible, semi-flexible (or semi-rigid) or rigid depending on the chemical composition and functionality both of the polyol and the isocyanate.
Like other polymers, PUFs rely on petroleum feedstocks and the increasing concern over environmental impact and the supply of petroleum has motivated the development of PUFs from bio and renewable raw materials.

2. Theory
Oxypropylated lignin, oxypropylated cork, starch, soybean, sugar beet pulp and data seeds have been used as replacements of petroleum feedstocks in the synthesis of polyurethane foams (PUFs) and the results demonstrated that replacing a typical petroleum-based polyol with this type of materials, foams had comparable foaming kinetics, density, cellular morphology, and thermal conductivity [1-5]. In the present study we investigated the valorization of cork via their liquefaction at atmospheric pressure, using acid catalyst as opposed to previous reports which involved harsher liquefaction conditions for subsequent use as polyol in the production of PUFs. Figure 1 shows the raw material used in this work and the PUFs obtained.

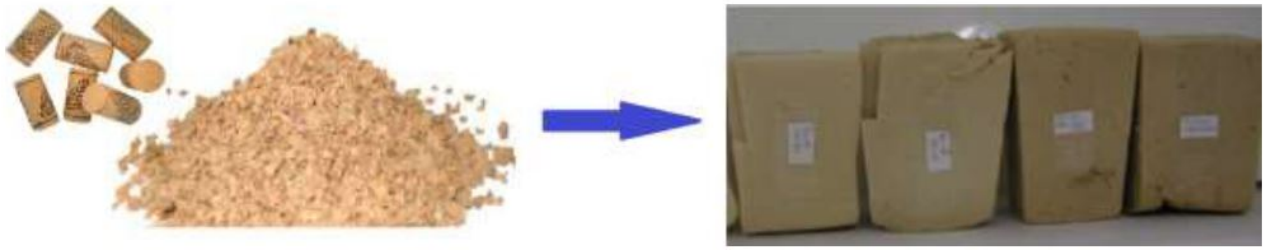

Figure 1. Raw material and polyurethane foam

3. Experimental

Cork liquefaction was carried out at atmospheric pressure using polyethylene glycol and glycerol as solvents and sulphuric acid as a catalyst. The resulting polyol, TEGOSTAB B 8404 (EVONIK) surfactant, POLYCAT 34 (Air Products) catalyst and blowing agent (Water) were placed in a polypropylene cup. The mixture was homogenized using an IKA Ost Basic mixer with rotating blades, for about 10 seconds at 700 rpm. Then the methylene diphenyl diisocyanate (MDI) was added to the mixture and mixed again for more 10 seconds at 700 rpm. Foams were obtained by free expansion in the mold, at room temperature.

4. Results and discussion

To evaluate the possibility of using liquefied cork in the production of PUFs, different formulations have been prepared. Their chemical composition was monitored by FTIR, the morphology by SEM, whilst the thermal and mechanical properties of PUFs were evaluated by thermal conductivity, TGA, DMA and compressive strength.

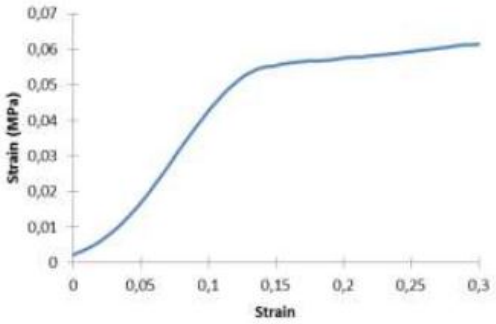

Figure 2. Compressive stress-strain curve of a PUF

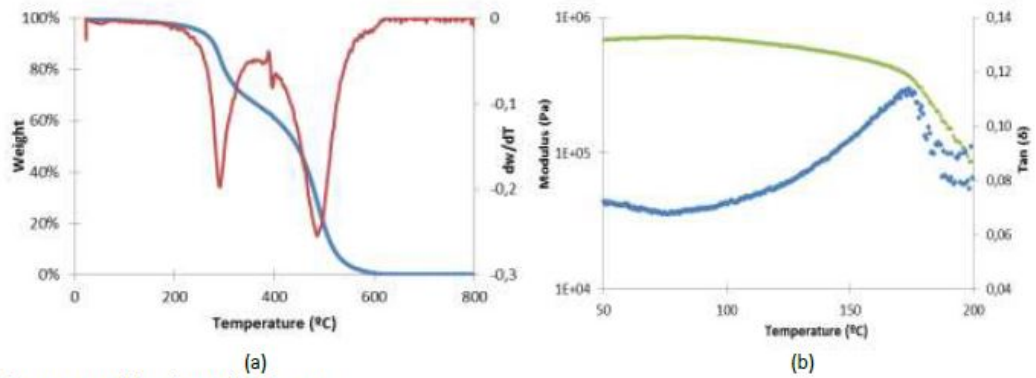

Figure 3. TGA (a) and DMA (b) of a PUF

SEM revealed that the cells of the foams are mainly closed having identical sizes and well-defined cell walls. PUFs, with a density of 25 Kg/m3 and a thermal conductivity of 33 mW/mK, demonstrated good mechanical properties as can beseen in Figure 2. The thermal stability of the PUFs up to 280 ºC and high elastic modulus till 170 ºC, as can been seen in
Figure 3 suggest their potential applications as insulation materials [6].

5. Conclusions

Polyurethane foams were prepared using liquefied cork under milder conditions than those used in previous reports [3] and their characteristics and properties were studied by FTIR, SEM, density, thermal conductivity, compressive strength, TGA and DMA. The experimental results demonstrated that replacing the petrochemical polyols by liquefied cork, yields foams with adequate structure, thermal and mechanical properties.

Acknowledgements
The authors would like to acknowledge QREN/FEDER for funding the Ecopolyols project (Nº 11435) and to Dow Chemical for kindly supplying the isocyanate. CICECO acknowledges FCT for the Pest-C/CTM/LA0011/2011 project.

References
[1] A.A. Abdel Hakim, Mona Nassar, Aisha Emam, Maha Sultan, Preparation and characterization of rigid polyurethane foam prepared from sugar-cane bagasse polyol, Materials Chemistry and Physics, 129, (2011) 301-307.
[2] Suqin Tan, Tim Abraham, Don Ference, Christopher W. Macosko, Rigid polyurethane foams from a soybean oil-based Polyol, Polymer, 52, (2011) 2840-2846.
[3] M. Evtiouguina, A. Barros-Timmons, J.J. Cruz-Pinto, C. Pascoal Neto, M. N. Belgacem, A. Gandini, The oxypropylation of cork and the use of the ensuing polyols in polyurethane formulations, Biomacromolecules, 3, (2002) 57-62.
[4] Shengjun Hu, Caixia Wan, Yebo Li, Production and characterization of biopolyols and polyurethane foams from crude glycerol based liquefaction of soybean straw, Bioresource Technology, 103, (2012) 227-233.
[5] Claire Pavier, Alessandro Gandini, Urethanes and polyurethanes from oxypropylated sugar beet pulp I. Kinetic study in solution, European Polymer Journal, 36, (2000) 1653-1658.
[6] Nihal Sarier, Emel Onder, Thermal insulation capability of PEG-containing polyurethane foams, Thermochimica Acta, 475, (2008) 15-21.

S3-P23
Enzymatic processing and exploitation of lignocellulose materials

GS. Nyanhongo (1), V. Perz (2)*, E. Nugroho Prasetyo (1), GM. Guebitz (1,2,3)
(1) Graz University of Technology, Institute of Environmental Biotechnology, Petersgasse 12/1, A-8010, Graz, Austria
(2) ACIB GmbH, Petersgasse 14, 8010 Graz, Austria
(3) Institute of Environmental Biotechnology, University of Natural Resources and Life Sciences, Vienna, Konrad Lorenz Strasse 20, 3430 Tulln, Austria
*veronika.perz@acib.at

1. Introduction
Industrial exploitation of lignocellulose based products is becoming extremely given its renewable nature and bioprocessability, regarded as green chemistry technologies.[1] Accordingly, our group is developing laccase-mediator based processes for upgrading lignin properties to be suitable for industrial application. Lignin is a major industrial waste product whose economic exploitation is only limited to 2 % and the rest is usually burnt.[2] Existing applications of lignin are currently limited to below 10 % in polymer blends (mortar, construction systems, adhesives, biodegradable plastics, polyurethane, paints, dyes, pesticides and printed circuit boards). Further, we are also involved in developing a cellobiose dehydrogenase bleaching system aimed at replacing chemical bleaching chemicals. Cellobiose dehydrogenase (CDH) is a fast emerging enzyme in the field of biotechnology recognized for its ability to produce hydrogen peroxide and also reduction of phenolic radicals and quinones.[3] In this study, CDH from *Myriococcum thermophilium* (MtCDH) was assessed for its ability to use desizing effluents resulting from the cotton processing industry during the later bleaching step as shown in Fig 1.

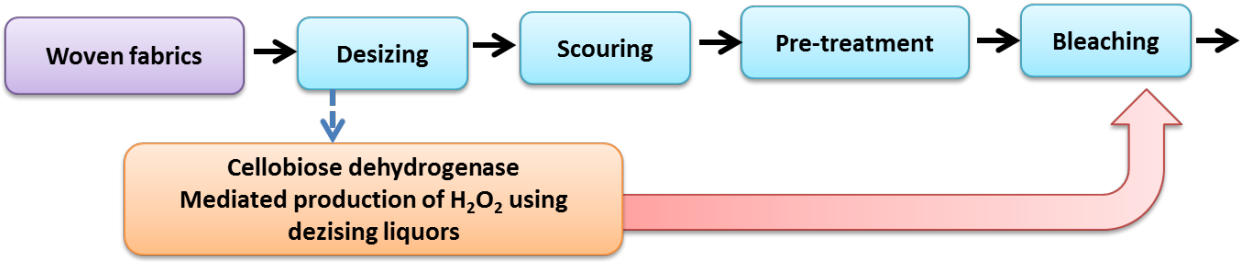

Figure 1. Effluents resulting from the desizing process were incubated with CDH and the produced hydrogen peroxide used to bleach the same fabrics.(Adopted from Flitsch et al 2012)

2. Experimental
Laccase mediated modification of lignin
Calcium lignosulfonates (1 g) sample were incubated with laccase in the presence or absence of either 1 M 1-hydroxybenzotriazole (HBT) or 1 mM ABTS final concentration. Lingin reaction and modifications were monitored by measuring fluorescence intensity at (Ex 355 nm/Em 400 nm), FTIR spectra in the 4000–600 cm−1 range, Size exclusion chromatography sing three TSK-gel columns (3000 PW, 4000 PW, 3000 PW) coupled in series and characterized using ^{1}H NMR, ^{13}C NMR and heteronuclear single quantum correlation (HSQC) 2D-NMR spectra

Bleaching studies with CDH

Desized and scoured fabrics were first bleached and then incubated with either MtCDH or glucose oxidase and desizing liqours. Different experimental conditions were investigated including production of H_2O_2 under optimal enzyme conditions followed by bleaching, simultaneous production of H_2O_2 and bleaching, production of H_2O_2 and bleaching in the presence of metals and of TAED (N,N,N,N-tetraacetylethylendiamine). The samples were incubated for 1 h, rinsed with deionized water and dried at 40 °C for 24 h before measuring weight loss. The change in color that is whiteness (Berger whiteness), color differences (ΔE) was measured by using a ColorLite Sph850 Spectrophotometer (Colorlite GmbH, Vienna, Austria).

3. Results and discussion

A recombinant MtCDH with a specific activity of 3.1 U mg^{-1} was able to oxidize many different cellooligosacharides commonly found in desizing waste waters including some cellulose fragments pilling off from the garment. Further studies based on the obtained results a one-pot enzymatic scouring/bleaching process for cotton fabrics was developed using pectinases as scouring agent and MtCDH to produce H_2O_2 for bleaching. An average increase in whiteness (Berger) ΔE of 26 and an average 95% increase in wettability were observed in all MtCDH treated fabrics. In addition, MtCDH oxidized typical colored cotton flavonoids (morin, rutin, isoquercitrin).[4] The MtCDH has several advantages as a bleaching agent for cellulose based polymers as compared to glucose oxidase which only uses glucose as substrate. Further the presence of the cellulose-binding module locates the H_2O_2 production directly to the fiber, which even explains the high impact observed in cotton bleaching even with low levels of H_2O_2. The ability of CDH to use the desizing effluents implies reduction in waste discharged from the desizing process.

Size exclusion chromatography showed an extensive increase in molecular weight of laccase treated lignin samples incubated with TvL and ThL by 107% and 572% from 28400 Da after 17 h of incubation, respectively.[2] Interestingly, FTIR spectroscopy, ^{13}C NMR and Py-GC/MS analysis of the treated samples suggested no substantial changes in the aromatic signal of the lignosulfonates, a good indication of the ability of TvL/ThL-HBT systems to limit their effect on functional groups without degrading the lignin backbone. Further, the enzymatic treatments led to a general increase in the dispersion properties, a welcome development for its application in polymer blends. The observed extensive polymerization was attributed to the formation of new ether and C-C aryl-aryl or aryl-alkyl linkages as confirmed by FTIR, ^{13}C-NMR spectra and Py-GC/MS chromatograms. The mixing of the laccase modified lignins with siloxane resulted in hybrid copolymers in homogenous interpenetrating polymers with increased viscosity, shorter curing time, higher tensile strength, improved dispersion and miscibility properties.[5] This shows that the laccase modification of lignin resulted in increasing its miscibility with siloxane.

4. Conclusions

MtCDH is highly promising enzyme for the development of an *in situ* bleaching system with several advantages including its ability to use a wide variety of cellooligosachrides resulting from the desizing process. Laccase mediated modification of lignin increases its molecular weight, reactivity, miscibility and dispersion properties. All these properties can be controlled depending on the desired polymer blends required.

Acknowledgements

Acknowledgements: Authors are thankful for the financial support offered by EU Biorenew, Cottonbleach project and ACIB.

References

[1]. Nyanhongo GS, Nugroho Prasetyo E, Herrero Acero E, Guebitz GM (2012) Advances in the application of oxidative enzymes in biopolymer chemistry and biomaterial research In: Felber F. et al. eds. "Functional Materials from Renewable Sources", ACS symposium series, American Chemical Society Washington DC, 2012, pp 329 - 349

[2] Nugroho Prasetyo E, Kudanga T, Rencoret J, Gutiérrez A, del Río JC, Santos JI, Nieto L, Jiménez-Barbero J, Martínez AT, Li J, Gellerstedt G, Lepfire S, Silva C, Kim SY, Cavaco-Paulo A, Seljebakken Klausen B, Frode Lutnaes B, Nyanhongo GS*, Guebitz GM (2010) Polymerisation of lignosulfonates by the laccase-HBT (1-hydroxybenzotriazole) system improves dispersibility. Bioresource Technology 101: 5054-5062

[3] G. Henriksson, G. Johansson, G. Pettersson A critical review of cellobiose dehydrogenases Journal of Biotechnology, 78 (2000), pp. 93–113

[4] Flitsch A, Sygmund C, Ludwig R, Nugroho Prasetyo E, Nyanhongo GS, Guebitz GM. (2013) Cellulose oxidation and bleaching processes based on recombinant Myriococcum thermophilum cellobiose dehydrogenase. Enzyme and Microbial Technology 52:60-7

[5] Nugroho Prasetyo E, Kudanga T, Fischer R, Eichinger R, Nyanhongo GS, Guebitz GM (2012) Enzymatic synthesis of lignin-siloxane hybrid functional polymers. Biotechnology Journal 7: 284–292

Session 4: Polymers for biomedical applications

S4-P24
Preparation of calcium phosphate/poly (acrylamide – co – acrylic acid) composites by hydrogel calcification

B. M. Abd El-Hady*, M. A. Oraby and W. E. Abd El Fattah
National Research Center, Dokki, Cairo, Egypt
*bothaina11@yahoo.com

ABSTRACT
A novel type of calcium phosphate / copolymer composite was prepared by the calcification of a poly (acrylamide – co – acrylic acid) hydrogel . An organic gel containing phosphate ions was transformed into an opaque solid material by the diffusion of calcium ions. The formation of crystals of hydroxyapatite on the opaque products was observed. Three copolymers of acrylamide (AAm) and acrylic acid (AAc) were synthesized by the free radical solution polymerization technique. Feed ratios of the monomers were 90:10 (w/w), 70:30 (w/w), and 50:50 (w/w) of acrylamide: acrylic acid, respectively. All reactions were carried out in aqueous media. The copolymers and composites were characterized by X - ray diffraction (XRD) and infrared (FT-IR). SEM was employed to analyze the morphological characteristics of the organic template and inorganic/organic composites. SEM-associated with EDS area analyses were performed in order to study the the characteristic components of the organic / inorganic composites. Swelling behavior of composites was evaluated by gravimetric analysis. The influences of reaction conditions , such as cross-linker concentrations, initiator concentrations, bath temperature, and time of reaction on the water absorbency of the organic/ inorganic composites were investigated for the as prepared (90:10 (w/w)) composite. The *in – vitro* bioactivity of that composite was evaluated by soaking samples in simulated body fluid. The formed apatite layer on the surface of the composites was observed.

Keywords: copolymer; hydroxyapatite; crosslinking; hydrogels; poly(acrylamide- co - acrylic acid); swelling.

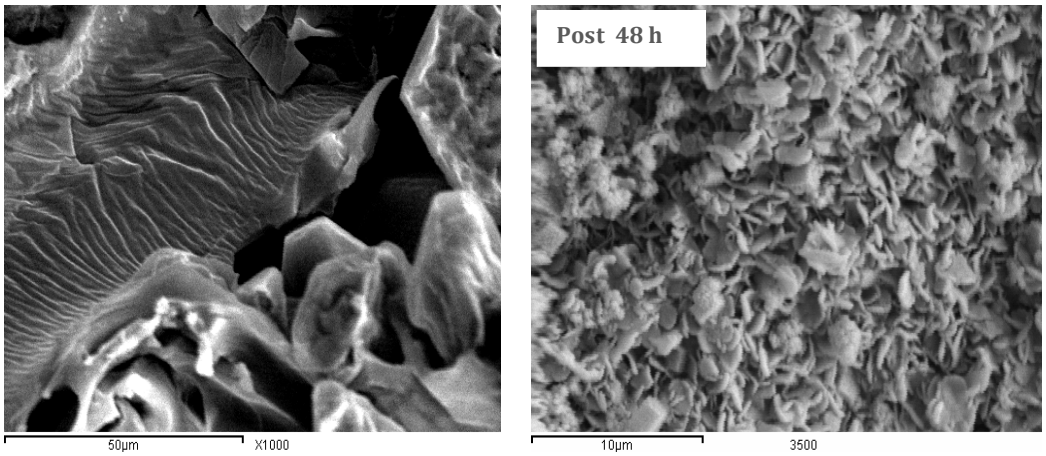

Figure1. SEM images of organic/inorganic composite pre- and post - immersion in SBF for 48 h proving the formation of a bio-layer on the specimen surfaces.

S4-P25

Preparation and properties of porous polyureaurethanes based on rapeseed polyol and different types of isocyanates

Monika Auguścik (1)*, Milena Zieleniewska (1), Aleksander Prociak (2), Joanna Ryszkowska (1)
(1) Warsaw University of Technology, Faculty of Materials Science and Engineering, Wołoska 141, 02-507 Warsaw, Poland
(2) Cracow University of Technology, Faculty of Chemical Engineering and Technology, Warszawska 24, 31-155 Cracow, Poland
*mauguscik@inmat.pw.edu.pl

1. Introduction

Recent studies on polyurethanes aim at replacing the petrochemical polyols with ingredients from renewable raw materials. This would be advantageous from both economic and environmental points of view. Application of petrochemical polyols is unfavorable in respect of production, energy and costs. That is why various methods are being developed for the synthesis of polyols from vegetable oils such as soybean oil, rapeseed oil, castor oil and palm oil. There are some known works involving the use of polyols from vegetable oils in the manufacture of polyurethanes for industrial applications [1,2]. Attempts have also been made to develop bio-tech materials for use in medicine. [3,4].
The object of the study was to develop a porous material containing a polyol with the rapeseed oil used as a scaffold for bone tissue engineering (scaffolds). For their production a solvent-free method was applied using NaCl and CO2 as porogen. It should be emphasized that the chosen method allows the production of large samples. The ureaurethanes were produced using three types of isocyanates. The aim of this study was to investigate the effect of the type of isocyanate on the properties of materials. Also examined was the influence of prepolymer mixing time with chain extender on the structure of the scaffolds.

2. Experimental

The subject of the research were polyureaurethanes (PURM) intended for use as substrates for bone tissue engineering. RZ2E was used as polyol produced from rapeseed oil, which was developed at the Department of Chemistry, Technical University of Cracow. Three types of diisocyanates were used for synthesis of diisocyanates: 4,4 '-dicyclohexylmethane diisocyanate (HMDI), hexamethylene diisocyanate (HDI) and isophorone diisocyanate (IPDI) (respectively materials HM, HD and IP) with water used as an extender; sodium chloride and carbon dioxide were used as porogen.
Properties of scaffolds were examined using various testing techniques such as Differential Ccanning Calorimetry (DSC), Dynamic Mechanical Analysis (DMA), Thermogravimetric Analysis (TGA), Fourier Transform Infrared Spectroscopy (FTIR). The microstructure of the materials was characterized by the Scanning Electron Microscope(SEM) and Micro-Computerized Tomography (µCT); porosity was determined using the Archimedes method. Since bioactivity and ability to degrade are much-desired features of substrates in tissue engineering therefore, also scheduled were material tests after incubation in the liquid simulating human plasma (SBF) and in phosphate buffered saline (PBS). Cell culture tests are also planned.

3. Results and discussion

SEM image analysis was used to evaluate the influence of performance parameters and the type of isocyanate on the microstructure of the scaffolds. Exemplary images of materials are shown in Figure 1.

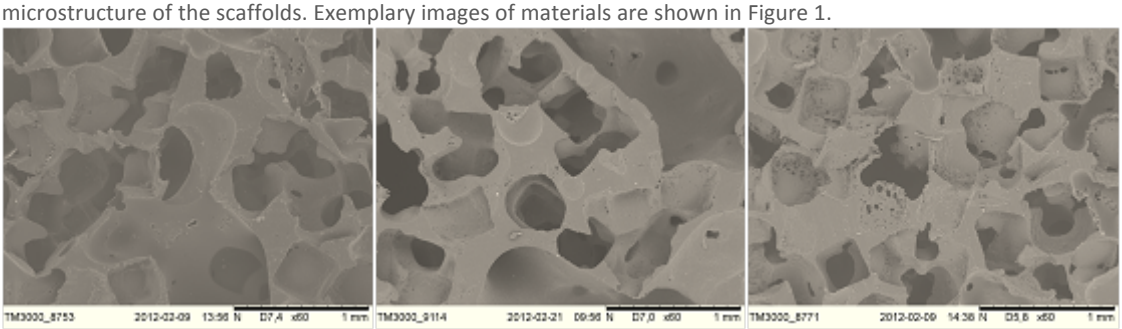

Figure 1. SEM images of materials HM, HD and IP.

Performed observations allowed to state the presence of an open-cell architecture, while differences were observed in size, shape, volume and thickness of the macro-pores depending on the type of produced materials. The most uniform distribution of the macro-pores and their largest number was observed in materials in which HMDI isocyanate was the substrate. Macro-pore walls of this material have the least thickness and show the largest micro-porosity in comparison with the materials in which HDI and IPDI were used. The architecture of HD is similar to HM though the amount of macro-pores in its structure is reduced and the wall thickness is greater as compared to the HM. With the increasing time of mixing the prepolymer with water the shapes of macro-pores are more regular, which demonstrates the significant effect of selection of this parameter on the final appearance of the microstructure.
In order to determine the chemical structure of the obtained materials infrared spectroscopy was used. FT-IR spectroscopy was also used to determine the degree of phase separation. The results show that the degree of phase separation is variable depending

on the isocyanate SSFHDI <SSFIPDI <SSFHMDI.
Thermal analysis was also performed on the materials. Peaks on DTG curve were observed in thermograms of the analysed PURM being the result of decomposition of urethane and urea bonds and the soft phase. Materials in which HMDI isocyanate was used show the highest initial breakdown temperature and after combustion process there remains the smallest weight. The initial breakdown temperature is the lowest in the materials in which HDI was used as one of the reactants. Basing on DSC thermograms it was found that materials having a high content of hard segments have a higher dissociation temperature of the hard phase and the lowest glass transition temperature of the soft phase.
Images of the surface of the materials after exposure in SBF allow to conclude that first apatites appear on the samples after a month. With the increasing exposure time in simulated body fluid their quantity increases. On the materials in which HMDI and HDI were used as isocyanate much more apatite accumulated than on the material with IPDI following a three-month's period. FTIR analysis confirms the presence of peaks characteristic of the apatite.
On the surface of the materials there are also additional micro-pores and local loss of material, suggesting a hydrolytic degradation process. Also, decreasing temperature at the beginning of the process of thermal decomposition after 3 months of exposure in SBF, as well as lowering the temperature of maximum rate of degradation for all the samples seem to confirm the changes in the structure of the investigated materials during hydrolytic degradation.
The materials were also tested for DMA compression. Polyurethanes HM and IP show a much greater stiffness compared to the materials synthesized from HDI. For both IP and HD materials increased elasticity and loss modules were observed along with the increasing mixing time of the prepolymer. For material HM the modules decreased with the increasing time of mixing of the prepolymer with chain extender. The analysis of the research results carried out for the materials after a 3-months exposure in SBF shows an increase in the both modules.

5. Conclusions
The research and tests indicate the possibility of using RZ/2E polyol to produce polyureaurethanes with porous structure. It was possible to successfully develop a material based on renewable raw materials (rapeseed oil) with a structure suitable for dedicated applications. Studies have found that the properties of obtained materials are dependent on the type of isocyanate and mixing time prepolymer with chain extender.
Out of the tested materials the best properties were obtained in the material prepared by using isocyanate HMDI with the longest mixing time of the prepolymer.
Summarizing the results obtained in this study it can be concluded that the obtained polyureaurethanes have great potential as a product for bone tissue engineering.

Acknowledgements
The work was funded by the project Era NET Matera pt.: „Bio-based Polyurethane Materials" – BBPM, Nr NCBiR/ERA-NET-MATERA/06/2011Thank you for your contributions.

References
[1] J.M.E. Rodriguesa, M.R. Pereirab, A.G. de Souzac, et. al., *Thermochimica Acta*, 2005, 427, 31–36
[2] Maria Kuranska, Aleksander Prociak, *Composites Science and Technology*, 2012, 72, 299-304
[3] M.K Mitha, M. Jayabalan, *J. Mater. Sci.: Mater. Med*, 2009, 20, 203-211
[4] P.S. Sathiskumar, Giridhar Madras, *Polymer Dagradation and Stability*, 2011, 96, 1695-1704

S4-P26
Improving polyethylene biocompatibility by adsorbing sulfated polysaccharides

Aleš Doliška (1,2)*, Volker Ribitsch (3), Simona Strnad (2), Karin Stana Kleinschek (1,2)
(1) Center of Excelence PoliMaT, Tehnološki park 24, 1000 Ljubljana, Slovenia
(2) University of Maribor, Laboratory for Characterization and Processing of Polymers, Smetanova 17, 2000 Maribor, Slovenia
(3) University of Graz, Institute for Chemistry, Graz, Austria
*ales.doliska@polimat.si

1. Introduction
Cardiovascular diseases are one of the leading causes of mortality in the developed countries. One of the most common cardiovascular diseases is atherosclerosis. The medical treatment is usually surgical by bypassing the affected vessels to restore blood flow or in case of smaller defects stents from different materials are often used. Vascular grafts are mainly made from polyester (polyethylene terephthalate- PET) in tube shape. Dacron® is the best known fabric and grafts can be either knitted or woven, however the smaller diameter grafts became the nemesis of research and a symbol for limitations of modern biotechnology. Currently the best solution is surface modification with anticoagulants.

2. Theory
When foreign material is exposed to blood, the blood proteins adsorb to surface followed by activation of clotting system, activation of platelets, thrombolysis and activation of complement system [1].
Surface properties influencing blood interaction at polymer interfaces are described by wettability (surface free energy), surface chemistry, charge and roughness. These entire surface characteristics are important and can be modified in way to improve the hemocompatibility.
Intensive investigation is ongoing [2-6] to define and develop polymeric materials with proper hemocompatibility. Generally it is accepted that a hydrophilic environment at the blood polymer interface is beneficial in reducing platelet adhesion and thrombus formation.
Current methods to create hemocompatible surfaces are those with attachment of an anticoagulant such as heparin to the surface. There are several techniques available to utilize the anticoagulant activity of heparin in conjunction with blood contacting materials. Those methods are: heparin releasing surfaces, heparin immobilized surfaces and coatings with heparin copolymers.
Owing to certain adverse effects caused by heparin, such as the abnormal bleeding of treated patients or, potential contamination since it is derived from mammalian sources, alternative biopolymers derived from plants are investigated in order to develop new anticoagulant and antithrombotic drugs [7]. The alternative anticoagulants from non-animal source are therefore of great scientific interest. Plant polysaccharides such as fucoidan, dextran[8] carrageenan [9] and others are increasingly used for medical application. Polyethylene terephthalate (PET) is one of the most frequently used materials in cardiovascular surgery. It is well-known that uncoated PET possesses moderate biocompatibility, which is insufficient for cardiovascular replacements. But so far no surface modification has produced satisfactory results.

3. Experimental
In order to improve the biocompatibility of the PET surfaces they were coated with different polysaccharides with anticoagulant properties, such as heparin and dextran sulfate. Model PET surfaces were prepared from Mylar® foil to facsimile PET used in medical devices. Surfaces were prepared with spin coat technique on the quartz crystals (supplied by Q Sense AB) with gold plate electrodes and with gold on the active surface. Model PET film thicknesses were estimated by measuring the mass of spin coated film in air with QCM-D (QSense E-4) and were found to be 48 ± 10 nm. The AFM imaging of model PET films showed that films were smooth and uniform with an average roughness, Sa = 0.25 nm.
Crystals coated with PET films were first washed with milliQ water, at a flow rate of 0.2 ml/min for 20 minutes, followed by adsorption of Chitosan from 0.05 % solution at a flow rate of 0.1 ml/min. This was followed by a rinsing step with milliQ water, and after that the adsorption of heparin (200 mg/l) or dextran sulphate (200 mg/l) was done at a flow rate of 0.1 ml/min. The QCM crystals were then rinsed with milliQ water and ready to be used for the QCM-D coagulation analyses and water contact angle measurements.

4. Results and discussion
Figure 1 shows the in situ modification of model PET films with Chitosan solution (0,05 %) and rinsing step, followed by adsorption of sulfated polysaccharides (Heparin and Dextran sulfate) and final rinsing step. The frequency change in both cases is similar, after Chitosan adsorption, surface was rinsed with MilliQ water. Using Sauerbrey equation [10] the calculated adsorbed mass per area of Chitosan layer after rinsing was 90 ±10 ng/cm2. The second layer of sulfated polysaccharides increase the adsorbed mass after final rinsing step to 220 ±10 ng/cm2 in case of heparin and to 140 ±10 ng/cm2 when Dextran sulfate was used.

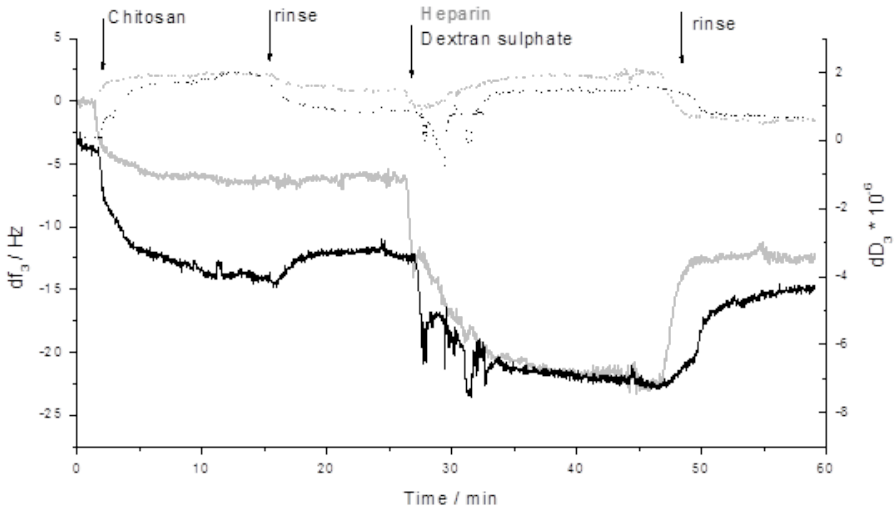

Figure 1. Frequency (solid line) and dissipation changes (dot line) at third overtone during adsorption of Chitosan (0,05 %), followed by adsorption of Heparin, 200 mg/l (black lines) and Dextran sulfate, 200 mg/l (grey lines) onto model PET films, monitored by QCM-D (times of polymer solutions' additions, as well as rinsing steps are market by arrows)[11].

In **Figure 2**, the typical time dependent frequency and dissipation change curves (df=f(t) and dD=f(t)) of the blood coagulation cascade on the non-modified PET film after initiation with Ca^{2+} ions are presented. From these kinds of measurements valuable information about surface dependent coagulation can be gained [11]. Information about the so-called onset-time (the time needed for thrombin formation) and fibrinogen cleavage to fibrin molecules, which formed the fibrin network-blood clot, can be obtained from the functions

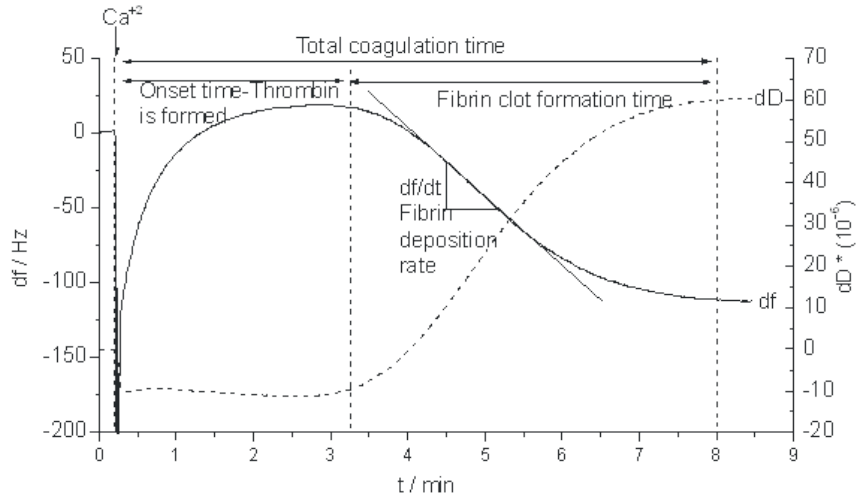

Figure 2. Frequency and dissipation change (at third overtone) during coagulation on non-modified PET surface

The coagulation times determined from the frequency and dissipation changes during the blood plasma coagulation process in contact with the non-modified and modified PET surfaces are presented in **Figure 3**. Significant differences between the coagulation times on the different PET surfaces can be observed.

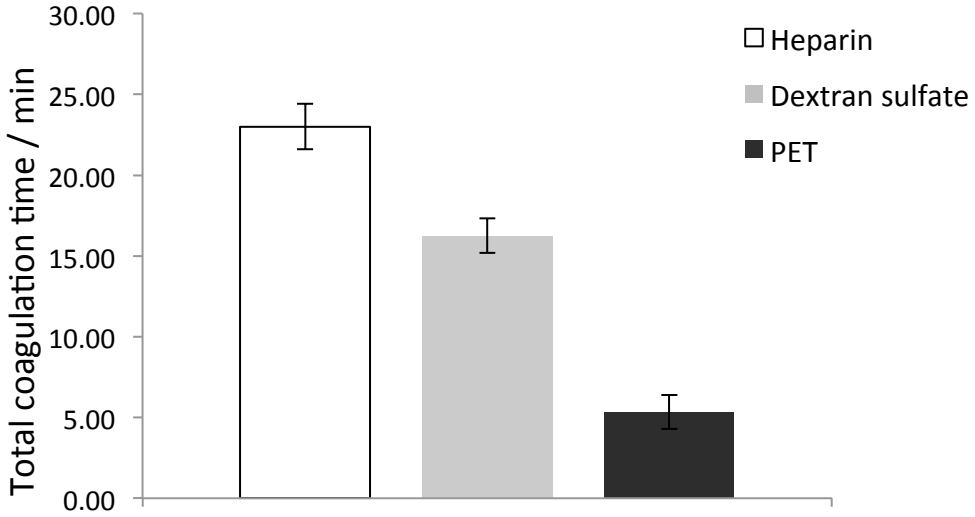

Figure 3. Total coagulation time of citrated blood plasma, triggered with $CaCl_2$, on the surfaces of differently modified PET films, monitored with QCM-D

5. Conclusions

The results showed that QCM-D is a valuable tool for investigation of the surface activities of different surfaces and is a well suited technique for adsorption studies. As such, QCM-D can be used to study the coagulation procedure under physiological environment. Blood coagulation kinetics parameters such as fibrin deposition rate can be obtained with QCM-D. Results show prolonged total coagulation times for PET surfaces treated with anticoagulants. The main drawback is its limitation to model surfaces, which often differ from real ones.

Acknowledgements

The authors acknowledge the financial support from the Ministry of Higher Education, Science and Technology of the Republic of Slovenia through contract No. 3211-10-000057 (Center of Excellence Polymer Materials and Technologies) and funding from the program group Textile chemistry (P2-118), University of Maribor, Faculty for mechanical engineering.

References

[1] B. D. Ratner, A. S. Hoffman, F. J. Schoen, J. E. Lemons. Biomaterials Science, An introduction to Materials in Medicine: Academic press, 1996.
[2] P. Zilla, D. Bezuidenhout, P. Human. Biomaterials 2007;28:5009-5027.
[3] M. Chaouat, C. Le Visage, A. Autissier, F. Chaubet, D. Letourneur. Biomaterials 2006;27:5546-5553.
[4] I. Junkar, A. Vesel, U. Cvelbar, M. Mozetic, S. Strnad. Vacuum 2009;84:83-85.
[5] I. Junkar, U. Cvelbar, A. Vesel, N. Hauptman, M. Mozetič. Plasma Processes and Polymers 2009;6:667-675.
[6] A. Vesel, I. Junkar, U. Cvelbar, J. Kovac, M. Mozetic. Surface and Interface Analysis 2008;40:1444-1453.
[7] D. Wall, S. Douglas, V. Ferro, W. Cowden, C. Parish. Thrombosis Research 2001;103:325-335.
[8] T. Indest, J. Laine, L. S. Johansson, K. Stana-Kleinschek, S. Strnad, R. Dworczak, V. Ribitsch. Biomacromolecules 2009;10:630-637.
[9] F. R. F. Silva, C. M. P. G. Dore, C. T. Marques, M. S. Nascimento, N. M. B. Benevides, H. A. O. Rocha, S. F. Chavante, E. L. Leite. Carbohydrate Polymers 2010;79:26-33.
[10] A. Doliška, A. Vesel, M. Kolar, K. Stana-Kleinschek, M. Mozetič. Surface and Interface Analysis 2011:n/a-n/a.
[11] A. Doliska, S. Strnad, J. Stana, E. Martinelli, V. Ribitsch, K. Stana-Kleinschek. Journal of biomaterials science. Polymer edition 2011.

S4-P27
Elastic polymer substrates for cell migration research

Daniel Dziob (1,2)*, Justyna Nowak (1), Karolina Zamora (2), Jadwiga Laska (2) and Zenon Rajfur (1)
(1) Jagiellonian University, Institute of Physics, Reymonta 4, 30-059 Krakow, Poland
(2) AGH University of Science and Technology, Faculty of Materials Science and Ceramics, Mickiewicza 30, 30-059 Krakow, Poland
*daniel.dziob@uj.edu.pl

1. Introduction
Cell motility plays an important role in normal and pathological biological processes. Embryonic development, immunological processes or tumor metastasis are inherently connected to cell migration phenomenon. Migrating cells mechanically interact with the substrate. They transmit forces generated by the active actomyosin system through cell adhesions to the substrate which leads to the cell traction formation. We can determine the resulting tractions employing elastic substrate method in which deformation of elastic substrate caused by crawling cells is translated to the cell traction map.

2. Theory
Migrating adherent cells exert forces on the substrate. Recently, it was shown that migration parameters like cell velocity, directional persistence or even cell shape depend on the mechanical properties of the substrate. Especially, elasticity of the substrate seems to be an important factor in defining the cellular response to the mechanical properties of the substrate (2, 3). In this work we performed systematic studies on how migration parameters of fish epithelial keratocytes depend on the elasticity of the substrate.

3. Experimental
Elastic substrate preparation: the preparation of acrylamide substrates was based on the radical polymerization reaction, where acrylamide was a monomer and bis-acrylamide was a crosslinking agent. *N*,*N*,*N*',*N*'- tetramethylethylenediamine (TEMED) and ammonium persulfate (APS) were catalysts. Specific elasticity of the polymer was achieved by varying the acrylamide to bis-acrylamide molar ratio. Substrates were prepared in the form of thick coatings on silanized and glutaraldehyde-activated glass coverslips. The substrates were stored in PBS solution (1, 4).
Cell migration assay: epithelial fish keratocytes were used as model migrating cells. They were prepared according to the standard procedures (5). In short, single scales from Molly fish were incubated sandwiched between two coverslips, then after 48 hrs. migrating keratocytes were separated from the cell sheet by short immersion in the PBS buffer. Afterwards, time lapse of single migrating cell was recorded and migration parameters were calculated from collected images.

4. Results and discussion
The goal of these studies was to determine mechanical properties of different polymer substrates and to correlate them with the appropriate parameters describing keratocyte migration. Young modulus of polymer substrates was determined by AFM and/or indentation method and their surface topology was visualized by AFM. Hydrophobicity/hydrophility was determined by wetting angle (contact angle) measurements.
Keratocytes migrate differently on different substrates - for example, they tend to have much higher directional persistence on the glass substrate than on plastic or acrylamide. Velocity of migration also correlates with the elasticity of the substrate.

5. Conclusions
There are clear differences between basic set of keratocyte migration parameters like migration velocity, directional persistence and cell shape depending on the mechanical properties of a substrate. Future works will determine the detailed biophysical mechanism of interactions between migrating cell interactions and the substrate.

Acknowledgements
We would like to acknowledge Tomasz Kolodziej and Piotr Cyzio for their help with cell cultures and imaging. All experimental work was done in prof. Jozef Moscicki lab. This work was supported by VENTURES grant 2012-9/3 from Polish Science Foundation.

References
[1] Damljanovic V., Lagerholm C.B., Jacobson K. Bulk and micropatterned conjugation of extracellular matrix proteins to characterized polyacrylamide substrates for cell mechanotransduction assays. Biotechniques. 2005 Dec;39(6):847-51.
[2] S. F. Gilbert, Ed., Developmental Biology (Sinauer, Sunderland, MA, ed. 7, 2003)
[3] Ridley AJ, Schwartz MA, Burridge K, Firtel RA, Ginsberg MH, Borisy G, Parsons JT, Horwitz AR. Cell migration: integrating signals from front to back. Science. 2003;302:1704–1709.
[4] Tse J.R., Engler A.J.. Preparation of Hydrogel Substrates with Tunable Mechanical Properties. Current Protocols in Cell Biology 10.16.1-10.16.16, June 2010
[5] Roy P., Rajfur Z., Jones D., Marriott G., Loew L. and Jacobson K. Local photorelease of caged thymosin b4 in locomoting keratocytes causes cell turning. Journal of Cell Biology, 2001;153;1035-1047

S4-P28
Extremely non-equilibrium gaseous plasma for sterilization of polymer materials

Kristina Eleršič*, Aleksander Drenik, Martina Modic, Ita Junkar, Zdenka Peršin, Alenka Vesel, Uroš Cvelbar, Janez Trtnik, Karin Stana – Kleinschek, Miran Mozetič
Centre of excellence PoliMaT, Tehnološki part 24, 1000 Ljubljana, Slovenia
*Kristina.elersic@ijs.si

1. Introduction
Non-equilibrium gaseous plasma is nowadays widely used in different industrial branches. Plasma is created from parent equilibrium gas at low pressure using appropriate electrical discharges. Plasma parameters depend on particularities of discharges such as DC glow discharge, low-frequency, radio-frequency and microwave discharges. The ionization fraction depends predominantly on applied discharge power per unit volume of the discharge chamber, while many other parameters depend also on particularities of discharge configuration, the type of materials facing plasma, the gas pressure and flow rate as well as properties of materials under plasma treatment. Electrical parameters of discharges such as voltage, current, phase shift and vacuum parameters are measured rather precisely while the characterization of plasma itself is a difficult task due to the lack of appropriate measuring techniques. That's why modeling is an important tool applied in order to estimate the plasma parameters and thus understand interaction of plasma with solid materials.

2. Theory
Destruction of bacteria on polymer materials could be performed effectively without damaging polymer substrates using plasma with right parameters [1]. The destruction by ions is very efficient but the ions also cause important modifications of substrates due to acceleration to moderate kinetic energy in the sheath between unperturbed plasma and substrates. Also, the hard ultraviolet radiation which is emitted at transition of highly excited atoms and molecules to lower states or the ground state is effective but causes irrevisable modification of polymer materials. Best plasma particles suitable for destruction of bacteria are therefore neutral reactive particles found in oxygen plasma, i.e. atoms in the ground as well as metastable excited states of low excitation energy. The atoms interact with bacteria constituents causing slow and controlled removal of organic materials including the sugars, proteins and other hydrocarbons which are present in the capsule, bacterial cell wall as well as the cytoplasm [2]. The oxidation and thus etching of these materials could be performed at any temperature but best results should be obtained at room temperature in order to preserve the original properties on polymer substrates [3].

3. Experimental
Destruction of selected bacteria was studied experimentally using a small plasma reactor. The discharge chamber was of cylindrical shape with inner diameter 36 mm and length 250 mm, and was connected to the afterglow chamber through a glass tube of inner diameter 5 mm in order to assure surface neutralization of charged particles. Both discharge and afterglow chambers were made from borosilicate glass. A copper coil was wrapped around the discharge chamber and connected to a radiofrequency generator of nominal power 700 W and standard industrial frequency 27.12 MHz. The afterglow chamber was pumped continuously during experiments using a Leybold fore-pump with ultimate pressure of 0.1 Pa. Oxygen of commercial purity was leaked continuously into the discharge chamber through a manually adjustable needle valve. The pressure in discharge chamber was estimated with a Pirani gauge and was about 2 mbar while in the afterglow chamber it was about 1 mbar. Plasma parameters were estimated with electrical and catalytic probes as well as by optical emission spectroscopy. Both hydrogen and oxygen atomic lines were observed in spectra indicating the presence of excited atoms with excitation energy exceeding 10 eV. The density of charged particles was of the order of 10^{16} m^{-3} and the electron temperature was close to 40000 K. The density of neutral oxygen atoms in the discharge chamber was $7x10^{21}$ m^{-3} while in the afterglow chamber at the position of substrates it was $4x10^{20}$ m^{-3}[4, 5].

4. Results and discussion
Bacteria were exposed to both glowing plasma in the discharge chamber and neutral oxygen atoms in the afterglow chamber for different periods. Prior and after exposure they were imaged by atomic force microscopy (AFM) as well as scanning electron microscopy (SEM). No deposition of conductive film onto samples was performed prior to SEM characterization. Untreated bacteria were covered with a micrometer thick capsule. The capsule surface was visible very well from AFM images, while SEM images of untreated bacterial capsule were rather dim. Although we used the primary electron beam of kinetic energy only 1 keV we never managed to obtain sharp images. This could be explained either by poor scattering of primary electrons on the capsule surface, or modification of surface properties during acquisition of the SEM images, or rich morphology at the nanoscale level, or the combination of these effects. Even a brief exposure of samples to glowing oxygen plasma caused degradation of both capsule and bacteria. Obviously, oxygen plasma interacts aggressively with organic materials. Such an aggressive interaction is explained by synergistic effects of different reactive plasma particles. Charged particles accelerated in the sheath between unperturbed plasma and the solid materials facing plasma are accelerated across the sheath and thus bombard the surface with the kinetic energy corresponding to the difference between plasma and floating potentials, in our particular case about 20 eV. Also, charged particles are neutralized immediately upon touching the surface thus release also their potential energy, which, for the case of singly charged molecular oxygen positive ions, is 12 eV. Each ion reaching the surface, thus brings over 30 eV of energy which is dissipated

on the surface. The energy is used for a variety of surface effects, but finally it is observed as increased surface temperature. The surface temperature also increases upon the treatment with glowing oxygen plasma due to relaxation of different molecular and atomic excited states. Finally, radiation from plasma in the wide range from far infrared to vacuum ultraviolet range is absorbed in the material facing plasma so they are actually exposed to a rather high thermal flux. The increased surface temperature facilitates chemical reactions and eventually opens new channels for surface heating. An important mechanism which is usually neglected at room temperature and becomes effective at elevated temperature is heterogeneous surface recombination of neutral oxygen atoms in the ground state. The probability for such surface reaction depends enormously on the surface temperature due the increasing surface mobility of atoms. Finally, the surface temperature becomes so large that regular oxidation with neutral molecules in the ground electronic state but different vibrational as well as rotational states becomes effective and the oxidation control is lost. The bacteria have been burned.

Exposure of bacteria to oxygen plasma therefore assures for sterilization of any object treated so it represents a powerful alternative to classical sterilization methods. Unfortunately it is not a very appropriate technique for sterilization of delicate polymer materials which cannot stand elevated surface temperatures. Increased surface temperature often leads to destruction of original polymer chemical, physical and mechanical properties. In combination with UV radiation the subsurface layers of polymer are damaged, too. In order to avoid this unwanted effects but still use advantage of low temperature gaseous sterilization with pure oxygen it is advisable to perform experiments in the afterglow region. This region is characterized by the absence of charged particles, UV radiation and highly excited oxygen molecules and atoms. Since these particles causes major thermal load, thermal effects can be avoided if oxidation of organic materials is performed in the afterglow chamber.

A systematic study on destruction of bacteria in the afterglow chamber was performed. Bacteria were exposed to a reactive oxygen atmosphere rich in neutral oxygen atoms in the ground state for different times up to 500 s. The bacteria were then imaged by SEM and AFM. The first effect observed is gentle removal of the capsule materials. This is explained by oxidation of sugars, proteins and alike materials with oxygen atoms. The interaction probability at room temperature is low at the value below about 10^{-3} so the samples essentially remain at room temperature. As soon as the capsule is removed an almost perfectly sharp image is observed by SEM. Also, AFM shows the structure of the bacteria wall free from capsule materials. Furthermore, stretching bacterial structures such as pilli are removed upon brief interaction with neutral oxygen atoms. After completing the capsular removal and upon further treatment the bacterial cell wall is slowly degraded as revealed by both SEM and AFM. The cell wall becomes full of structures not foreseen in the classical biological picture. Such a rich surface morphology is explained by inhomogeneous etching which in turn is explained by inhomogeneous structure of the bacterial cell wall. Finally, after about 250 s of treatment in the afterglow chamber, the cell wall is almost completely removed and the only indicator of its existence are ring like shapes as revealed from SEM images. The bacterial cyto-skeleton is clearly observed and the bacteria are not functional any more. The treatment in the afterglow therefore allows for destruction of bacteria at room temperature where the effects on polymer substrates are negligible.

5. Conclusions

A method for destruction of bacteria without causing damage to delicate polymer materials was presented. The method is based on application of neutral oxygen atoms for slow degradation of organic materials. First, capsule is removed, followed by inhomogeneous etching of the bacterial cell wall until the cyto-skeleton is revealed. The bacteria is damaged so much by oxidation with oxygen atoms that the substrates of any type and composition becomes sterile without increasing their temperature measurably. The method is particularly useful for sterilization of biomedical materials that do not stand prolonged treatment at high temperature in autoclavs, especially polymer materials. The right treatment time assuring sterility depends solely on the fluence of oxygen atoms onto the surface of treated materials. At our particular experimental conditions the optimal treatment time is about 250 s. Taking into account the measured density of O atoms in the afterglow chamber used for our experiments, i. e. $4x10^{20}$ m^{-3} it is possible to calculate the recommended oxygen atom fluence, which is $1.5x10^{25}$ atoms per m^2.

Acknowledgements

The authors acknowledge the financial support from the Ministry of Education, Science, Culture and Sport of the Republic of Slovenia through the contract No. 3211-10-000057 (Centre of Excellence for Polymer Materials and Technologies).

References

[1] L. Q. Yang; J. R. Chen; J. L. Gao; Y. F. Guo. *Appl Surf Sci* 2009, 255, (22), 8960-8964.
[2] F. Sohbatzadeh; A. H. Colagar; S. Mirzanejhad; S. Mahmodi. *Appl Biochem Biotech* 2010, 160, (7), 1978-1984.
[3] A. Vesel; I. Junkar; U. Cvelbar; J. Kovac; M. Mozetic. *Surf Interface Anal* 2008, 40, (11), 1444-1453.
[4] U. Cvelbar; N. Krstulovic; S. Milosevic; M. Mozetic. *Vacuum* 2007, 82, (2), 224-227.
[5] I. Junkar; U. Cvelbar; A. Vesel; N. Hauptman; M. Mozetic. *Plasma Process Polym* 2009, 6, (10), 667-675.

S4-P29

Application of dissipative particle dynamics method on pH-responsive drug delivery dystem

GUO Yingying (1,2,3)*, Robert K. Y. Li (1,3)

(1) Department of Physics and Materials Science, City University of Hong Kong, Hong Kong, People's Republic of China
(2) Department of Physics, University of Science and Technology of China, Hefei, Anhui, People's Republic of China
(3) USTC-CityU Joint Advanced Research Centre, Suzhou, Jiangsu, People's Republic of China
*gyy.happy@hotmail.com

1. Background

The drug delivery systems have been developed for reasons that some drugs have an optimum concentration range within which maximum benefit is derived and some drugs will degrade before it arrived to the target [1]. Among those drugs carriers, polymeric microspheres self-assemble from amphiphilic copolymers could be used as a good candidate for this purpose. The microspheres encapsulate the drug inside the core and release them as they are arrive at the target sites. The stimulus in the target sites could play an important role for drug release. Different organs, tissues and cellular compartments may have large differences in PH, which makes the PH a suitable stimulus. During the last few years, PH-sensitive micelles have attracted attentions widely both in experiment and simulation [2-7]. Computer simulation could be an efficient tool to study the self-assemble behavior and the release process for the drug delivery system. It could help us to understand the formation and release mechanism for the drug carriers which could not be shown in experiment. It also could offer some guide to experiment on design new structures for different purpose of drug release system such as control release or prolong release. The simulation method we used here is the dissipative particle dynamics method which allows us to simulate large scale like polymer system.

2. Results and discussion

Our system comprises of PLA-b-PEG diblock copolymer, IBU drugs and water. The coarse-grained method is taken to simplify all the components in the system (Fig. 1). The IBU-loaded micelle which acts as a drug delivery vehicle is placed in an acid environment. The concentration of HCL is about 5% in the solution. Figure 2 shows the evolution of the drug-loaded micelle subjects to acid environment with $1*10^6$ steps. The affinities of each component to HCL disrupt the thermodynamic equilibrium that is achieved in water environment (Fig. 2a). With the dynamic stimulation progress, the micelle evolves and we observe the drug release process as time increased to 25000 steps (Fig. 2b) and there are more and more drugs could be found in the acid environment as the time step goes further (2c, 2d).

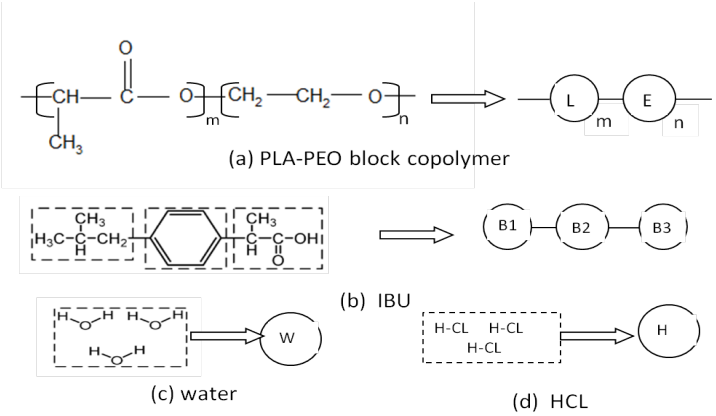

Figure 1. Coarse-grained method for all components in our system

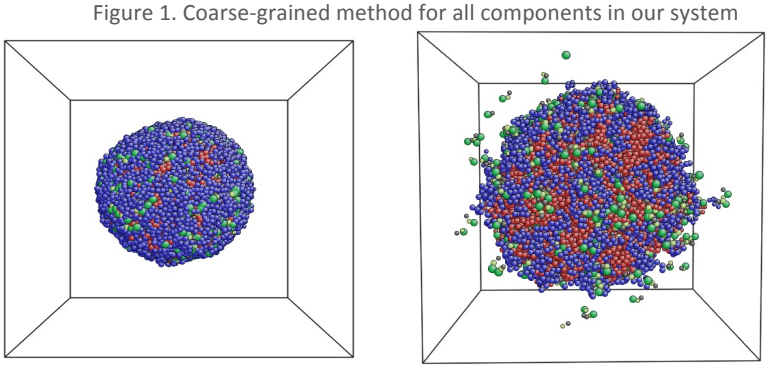

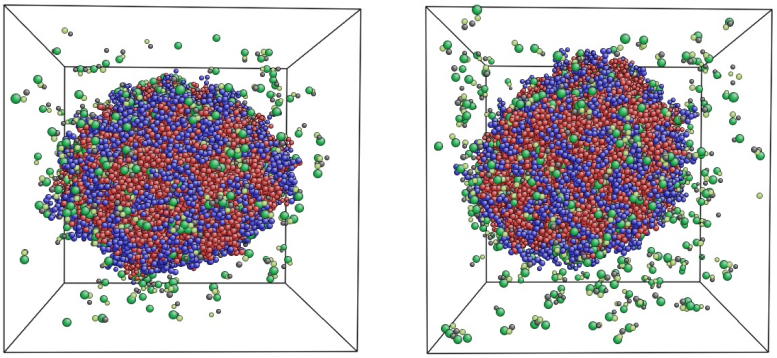

(c) (d)

Figure 2. Snapshots of the drug release mechanism of the drug-loaded micelle in an acid environment. (a) initial step, (b) 25000 steps, (c) 100000steps, (d) 1000000 steps. Color legend: blue, PEG blocks; red, PLA blocks; green-light yellow-grey, IBU molecules. Water and HCL are omitted for clarification.

Figure 3 shows the variation of drug concentration in and outside the micelle with different time steps. Initially, the drugs are mainly concentrated at the center of the micelle. Then, by putting it into acid environment for a short time (25000 steps), the drugs begin to diffuse from the core. As time increases, more drugs are diffuse into the acid environment.

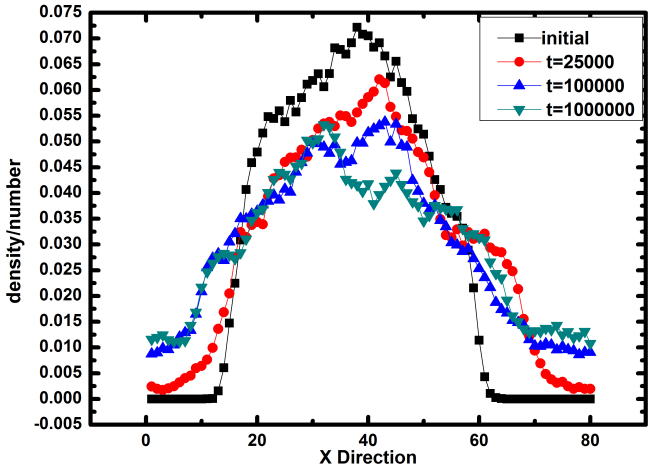

Figure 3. Density profile of IBU molecules with different time steps

3. Conclusions

The PH responsive release of the drug happens via the diffusion mechanism. Due to the compatibility between the acid molecules and polymer-drug formed micelles, the acid solutions disperse into the inside of the polymeric carriers gradually, which causes the swell of the micelle. As a result, the swelling micelle generates more free space for the drug to release itself to the acid environment.

References

[1] C. Kaparissides, S. Alexandridous, K. Kotti, S. Chaitidou Journal of Nanotechnology Online, volume 2, March 2006
[2] M.J. Abdekhodaie, X.Y. Wu, Biomaterials 29 (2008) 1654.
[3] J. Lin, J. Zhu, T. Chen, S. Lin, C. Cai, L. Zhang, Y. Zhuang, X.S. Wang, Biomaterials 30 (2009) 108.
[4] Y.Y. Li, S.H. Hua, W. Xiao, H.Y. Wang, X.H. Luo, C. Li, S.X. Cheng, X.Z. Zhang, R.X. Zhuo, J. Mater. Chem. 21 (2011) 3100.
[5] J.S. Lu, N.J. Li, Q.F. Xu, J.F. Ge, J.M. Lu, X.W. Xia, Polymer 51 (2010) 1709.
[6] T.H. Qu, A.R. Wang, J.F. Yuan, Q.Y. Gao, J. Colloid Interface Sci. 336 (2009) 865.
[7] K. Van Butsele, P. Sibret, C.A. Fustin, J.F. Gohy, C. Passirani, J.P. Benoit, R. Jerome, C. Jerome, J. Colloid Interface Sci. 329 (2009) 235.

S4-P30
Light-switchable polymers for applications towards proteins

Benjamin Horstmann*, Franz-Josef Meyer-Almes
University of Applied Sciences, Department of Chemical Engineering Biotechnology, Schnittspahnstrasse 12, 64287, Darmstadt, Germany
*Benjamin.Horstmann@h-da.de

Abstract
Bioconjugated stimuli responsive polymers are an interesting field for polymer research combined with biomedical application [1,2,3]. To switch the macrostructure of a stimulus responsive polymer a specific stimulus is required. Temperature is a well known example thereof. Above specific temperature (LCST, low critical solution temperature), temperature sensitive polymers undergo a phase transition from hydrophilic to hydrophobic. This leads to a collapse of the polymer. The LCST is depended on the polymer and can be tuned by copolymerisation with polar or unpolar monomers. Polyacrylamides, for example poly(*N*-isopropylacrylamid) (PNIPAAM), are known to have this feature. PDMA (poly(*N,N*dimethylacrylamide) is an excellent water soluble unreactive polymer, but it does not show a LCST between 5 and 100 °C. Via copolymerisation with a hydrophobic monomer, a thermoresponsive polymer can be generated. In addition, the polarity can switched upon a light stimulus, is a photo-responsive monomer (eq.: 4-phenylazophenyl acrylate, AZAA) is incorporated [4]. This leads to a dual responsive polymer. Here, the copolymer shows two different LCST values, depending on the configuration of azobenzene. Thus, the temperature-responsive polymers can be switched, in a specific temperature range, by radiation with UV- or Vis-light. Combination of these polymers with biochemical targeting groups offers different interesting opportunities towards protein-polymer conjugates. Light-switchable, bioconjugable polymers are a tool to take control over a protein in an aqueous solution, at mild temperatures and without any addition of further additives. Here, two examples are presented: The coupling of such a functional polymer to an enzyme enables the control over its activity by light induced switch. Another application is the incorporation of a targeting unit, like an inhibitor, into the polymer. Here, fishing of specific proteins from cell lysate or catch-and-release systems are possible applications.

References
[1] M.A. Cohen Stuart, W. T. S. Huck*, et al., Nature Materials* **2010***,* 9, 101-113*.*
[2] J.-F. Lutz, H. G. Börner, *Prog. Polym Sci*. **2008**, 33, 1-39.
[3] E. Cabane, X. Zhang, K. Langowska, C. G. Palivan, W. Meier, *Biointerphases* **2012**, 7, 9.
[4] R. Kröger, H. Menzel, M. L. Hallensleben*, Macromol. Chem. Phys*. **1994**, 195, 2291-2298.

S4-P31
Novel modeling approach to generate a hybrid nanocomposite scaffold of collagen/polyvinyl alchohol/florohydroxy apatite for bone tissue engineering

Imanieh Hossein (1)*, Gheibi Nematolah (2), Alavi Sajede (1)
(1) Department of Chemistry, Faculty of Science, imam Khomeini international university, Qazvin, Iran
(2) Assistant Professor, Department of Biochemistry and Biophysics, Qazvin University of Medical Sciences, School of Medicine, Qazvin, Iran
*hosseinimanieh@hotmail.com

1. Introduction
Tricomponent scaffold systems prepared by natural and synthetic materials especially, Collagen the most widely found protein in mammals and is the major provider of strength to tissue. A novel scaffold (Coll- PVA- FHA) containing collagen(Coll), flurohydroxy apatite (FHA) and polyvinyl alcohol (PVA) was prepared using freeze-drying and lyophilization method. This work presents the synthesis and the characterization of collagen-polyvinyl alcohol/flurohydroxy apatite hybrid materials with various weight ratio of the components. The considerable properties can be explained due to the presence of strong interaction between components. [1],[2]

2. Theory
Different kind of composites were obtained according to D-optimal design for three accompanying component mixture. design of experiment (DOE) was used for understanding the structural characteristics and mechanical properties in the porous nanocomposite. This novel scaffold was characterized biophysicochemically for their comparative significance in bone grafting applications. we used freeze drying to prepare scaffolds using collagen, polyvinyl alcohol and flurohydroxy apatite. Using a (DOE) approach, system and process parameters were optimized concurrently and their effects on the porosity and mechanical properties of the resulting scaffold were computed.[3]

3. Experimental

General procedure: collagen solution (0.52 gr coll in dionized water, (SERVA Co.) extracted from calf skin) was added to 6.5 gr 10% solution of PVA (Denki kagoku kogyo Co, M.W:26000) and vigorously stirred at ambient temperature and pressure to ensure complete mixing. In the second step 0.13 gr synthesized FHA added into PVA-GEL solution. The ratio of material to solvent should be 1 to 6.

4. Results and discussion

The structural composition of the scaffolds were characterized by Fourier Transform Infrared spectroscopy. Homogeneous dispersion of FHA in PVA and Coll matrix with interconnected porosity of 200-300 µm was observed by Scanning Electron Microscopy, X-ray diffraction, and optical microscopy. Cell proliferation in composite scaffolds observed by MTT assay.

5. Conclusions

We conclude that the nanocomposite could be optimized by the method of experimental design (DOE). DOE helped to identify the effect of components on properties evaluated on the base of this method.

These data indicate that Nanocomposite scaffolds promote required critical properties and suggest that the novel Coll-PVA-FHA composite scaffolds are promising design for matrix-based bone repair and bone augmentation. This study additionally provides a method for efficient production of scaffolds for general application in tissue engineering.

References

[1] M. Kikuchi, T. Ikoma, S. Itoh, H.N. Matsumoto, Y. Koyama, K. Takakuda, K.Shinomiya, J. Tanaka, Compos. Sci. Technol. 64 (2004) 819– 825.
[2] Q. Zheng, L.W. Zhou, J. Dent. Res. 82 (2003) 349.
[3] Giesbrecht, F. and M. Gumpertz. 2001. Planning, Construction, and Statistical Analysis of Comparative Experiments. North Carolina State University.
[4] DuMouchel, W.; Bradeley, J. A simple Bayesian modification of D-optimal designs to reduce dependence on an assumed model. Technometrics, 36:37-47, 1994.

S4-P32
Platelet morphology and adhesion on functionalized surfaces

Ita Junkar*, Martina Modic, Kristina Eleršič, Miran Mozetič, Uroš Cvelbar, Zdenka Peršin, Aleš Doliška, Karin Stana Kleinschek
Centre of Excellence PoliMat, Tehnološki park 24, 1000 Ljubljana, Slovenia
*ita.junkar@polimat.si

1. Introduction

Activation and adhesion of platelets on artificial surfaces is highly influenced by surface properties. In order to produce surfaces with hemocompatible properties adhesion and activation of platelets to artificial surfaces should be minimized. At the beginning it was thought that surfaces should be inert in order to prevent undesired reactions; however it is now believed that surfaces should promote certain biological interactions. Designing surfaces with antitrhomogenic properties is a highly challenging task as even in the 21. century there are no clear rules what kind of surfaces will be hemocompatible. One way to evaluate the *in vitro* hemocompatibility of surfaces is to study the morphological changes of platelets after adhesion and to determine the number of adherent platelets on the artificial surface. The aim of the present study was to observe the effects of platelet adhesion on virgin poly(ethylene terephthalate) (PET) surface and on PET surface after incorporation with oxygen or nitrogen functional groups.

2. Theory

Hemocompatibility of vascular implants is still problematic due to undesired thrombotic reactions, which often occur on vascular grafts with diameters smaller than 6 mm [1]. In such cases another surgical procedure is needed, which is unpleasant for the patient and is connected with high health care costs. Optimization of vascular graft surface to improve hemocompatibility is thus crucial for implementation of vascular implants with smaller diameters. The problem of vascular grafts is also unsatisfactory endothelization of the inner side of the artificial wall. Endothelial cells line the inner side of our natural blood vessels and are thought to be an ideal antithrombogenic material. Plasma treatment and incorporation of nitrogen functional groups on the surfaces was already shown to improve proliferation of endothelial cells [2,3]. By optimizing plasma treatment technique and thus concentration of incorporated functional groups on the surface it is also possible to influence on the adhesion of platelets and their activation.

3. Experimental

The PET foils with the thickness of 250 µm were treated by highly reactive oxygen and nitrogen plasma. The plasma was created with an inductively coupled RF generator, operating at a frequency of 27.12 MHz and an output power of about 200 W.

Immediately after treatment the surfaces were incubated with the whole blood from healthy volunteers. The incubation was done at room temperature for 15 min. After incubation the weakly adherent platelets were removed by washing with phosphate buffer saline (PBS). Surface morphology of platelets was determined by atomic force microscopy (AFM) as well as by optical microscopy (OM), while the number of adherent platelets was counted from the images taken by OM.

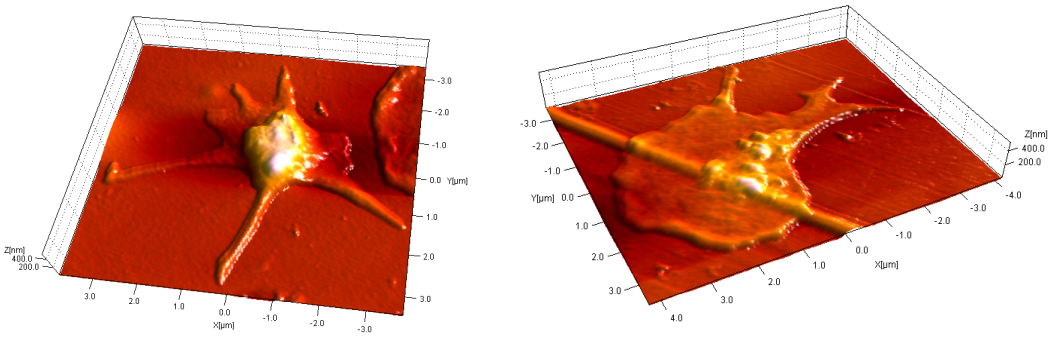

a) b)

Figure 1. Atomic force microscopy image of platelet morphology: a) platelet in dendritic form, b) platelet in a spread form (highly activated form).

4. Results and discussion

Our study showed that platelet morphology was different on differently treated surfaces. Highly activated platelets were in a large number observed on the untreated PET surfaces and surfaces with nitrogen incorporated functional groups. There were high numbers of platelets on these surfaces as observed from images taken by OM. Interestingly the morphology of platelets on surfaces incorporated with oxygen functionalities was rather different. On these surfaces mostly round and dendritic form of platelets were observed and their number was significantly lower. The changes in morphology of platelets were studied in details also by AFM. From **Figure 1 a)** it can be observed that platelet is in dendritic form and it starts to form pseudopodia. In Figure 1 b) the platelet is in highly activated spread form, which will with high probability lead to undesired thrombotic reactions.

5. Conclusions

Our study showed that AFM is a valuable technique for studying the morphology of soft biological samples such as platelets. Moreover it was shown that changes in platelet morphology were influenced by different treatment techniques and that oxygen incorporated PET surfaces seemed to reduce platelet adhesion and activation.

References

[1] H. Kito, T. Matsuda, *J. Biomed. Mater. Res.* 1996;30:321-30
[2] H.E. Roald, R.M. Barstad, I.J. Bakken, B. Roald, T. Lyberg, K.S. Sakariassen, *Blood Coagul. Fibrinolysis*. 1994, 5, 355-63.
[3] M.J.B. Wissink, R. Beernink, A.A. Poot, G.H.M. Engbers, T. Beugeling, W.G. van Aken, et al. *J. Control. Release.* 2000, 64, 103-14.

S4-P33
Preparation and characterization of hydroxyapatite/chitosan/collagen composites

A. Sionkowska*, I. V. Antoniac, B. Kaczmarek
Nicolaus Copernicus University, Faculty of Chemistry, Gagarina 7, 87-100 Toruń, Poland
*as@chem.umk.pl

1. Introduction

The goal of bone tissue engineering is to repair bone defects, which are difficult or even impossible to be treated by conventional methods. Bone tissue engineering employs a multidisciplinary approach, drawing on the principles of cell biology, molecular development biology, materials science and biomechanics, to aid in the repair of tissues damaged beyond the natural healing capacity of the bone.

The development of successful composite biomaterials for bone regeneration requires a concurrent engineering approach that combines different research fields. During the last decades, researchers have tailored that composite materials with natural polymers are useful for a wide variety of medical and dental applications.

2. Theory

Nowadays, there are few main compounds, from which are made biomaterials used to produce implants. Natural polymers are used in variety forms as a matrix for other compounds. They are biocompatible and biodegradable. This group of components includes such compounds as chitosan and/or collagen. [1] Collagen is the most important biopolymer in living organisms. [2] Chitosan is a polysaccharide and natural polymer made from chitin. [3,4]. This two components are biocompatible and biodegradable in human body. They are non-toxic and don't inhibit the growth of bone, because can be used to obtain the porous structure. [5,6] Hydroxyapatite in a major component of human bone. It is used to produce implants, because it increases the biocompatible and biodegradable properties of materials. [7]

3. Experimental

Composites of hydroxyapatite/chitosan/collagen were prepared as a film after the solvent evaporation from appropriate solutions. Hydroxyapatite was mixed with chitosan which was used in 1% concentration. Ratio of hydroxyapatite was 5% based on chitosan. Collagen was isolated from rat tails tendon. It was added to the mixture in different ratios: 75/25, 50/50, 25/75. Solution were put on the glass plate and solvent was evaporated. For obtained films different analysis were done. FTIR spectra were recorded by spectrometer JASCO 6200 type and SEM images were obtained by FEI-PHILIPS XL30 ESEM.

4. Results and discussion

The FTIR spectra for films of chitosan, collagen and its composites with hydroxyapatite are shown below in Figure 1. SEM images obtained for the composites are shown in Figure 2.

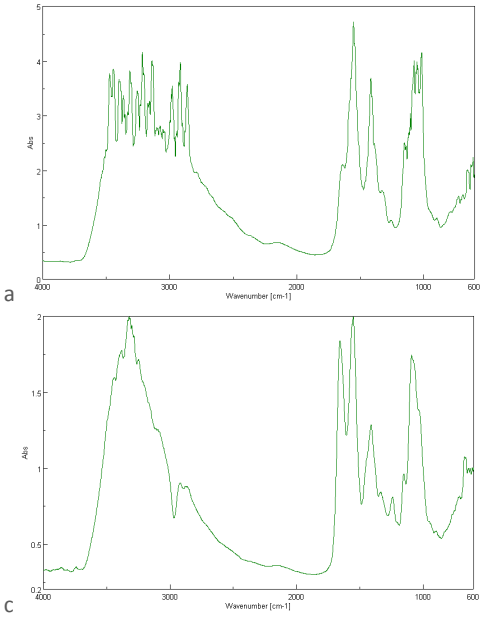

a

c d

Figure 1. FTIR spectra of a) chitosan film b) collagen film c) chitosar ıgen composites in ratio 25/75 with hydroxyapatite

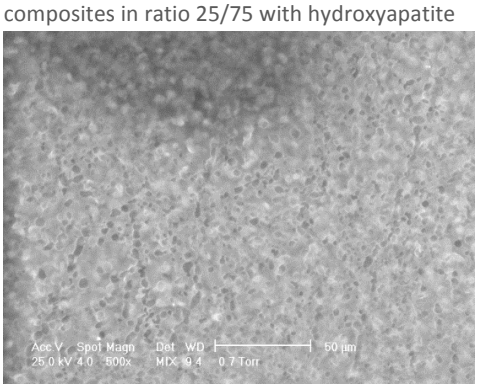

b

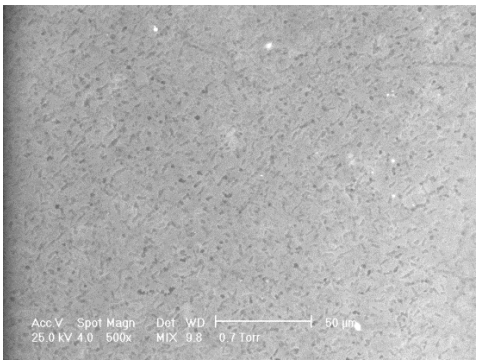

Figure 2. SEM images of a) chitosan/collagen composites in ratio 25/75 b) chitosan/collagen composites in ratio 25/75 with hydroxyapatite

5. Conclusions

FTIR spectra show the peaks from characteristic groups in collagen and chitosan. Different ratios of chitosan and collagen in the composites lead to alteration of FTIR bands positions. SEM images show that the composites are homogeneous. There are changes

in composite structure due to the presence of hydroxyapatite in the composite, what can be a result of appearance the new chemical bonds.

References

[1] Swetha M, Sahithi K, Moorthi A, Srinivasan N, Ramasamy K, Selvamurugan N. Inter. J. Biol. Macromol. 2010, 47, 1-4.
[2] Van der Rest R, Garrone M. FASEB J. 1991, 5, 2814-2823.
[3] Chen F, Wang ZC, Lin CJ. Mater. Lett. 2002, 57, 858-861.
[4] Sionkowska A. Progress Polym. Sci. 2011, 36, 1254-1276.
[5] Taravel MN, Domard A. Biomat. 1996, 17, 451-455.
[6] Zhu X, Zhou D, Guan S, Zhang P, Zhang Z, Huang Y. J. Mater. Sci. Mater. Med. 2012, 23, 983- 990.
[7] Nikpour MR, Rabiee SM, Jahanshahi M. Comp. 2012, 43, 1881-1886.

S4-P34
Antibiotic release from hydroxyapatite/chitosan/collagen composites

A. Sionkowska*, B. Kaczmarek
Nicolaus Copernicus University, Faculty of Chemistry, Gagarina 7, 87-100 Toruń, Poland
*as@chem.umk.pl

1. Introduction

Natural polymers are mostly isolated from plants and animal body. They are commonly called as biopolymers. These materials are used to produce implants, which can be applied for reconstruction of bone or teeth. Compounds which are used in medicine should be biocompatible and nontoxic for human body.

2. Theory

Hydroxyapatite (HAp) is important compound for biomedical implants, because its chemical composition is similar to the major component of human bone. [1-5] Chitosan (CTS) is a polysaccharide and natural polymer made from chitin. [6,7] Hydroxyapatite and chitosan are commonly used as a biomaterials. [8] They both are biocompatible, nontoxic and biodegradable. [1,6,9-11] They degrades in body without any destruction of living organism, that's why theirs composites are used the most often in medical care. [1,2,6] Pure hydroxyapatite is not used, because of its brittleness. Materials made from hydroxyapatite and chitosan are more flexible, what means that they have better mechanical properties. They don't inhibit growth of bone and can form chemical bonds with surrounding tissues. [2,12] Poly(methyl methacrylate) (PMMA) is used as a component of biomaterials. It forms a strong chemical bond with implants and it is not absorbed by the body. Use of PMMA is limited because of its no bioactivity. [13-15]

3. Experimental

Composites of hydroxyapatite/chitosan/PMMA were prepared as a film after the solvent evaporation. Hydroxyapatite was mixed with chitosan which was used in different concentration: 0.5, 1 and 2%. Ratio of hydroxyapatite was 5% based on chitosan. Moreover, poly(methyl methacrylate) was added because it can form a strong bonds with other components. It was added as a 15, 50, 85% based on chitosan. Solution were put on the glass plate and solvent was evaporated. For obtained films different analysis were done. Mechanical properties such as a Young's modulus (E_{mod}), elongation at break (dl) and tensile force (F_{max}) were measured using a mechanical testing machine (Z.05, Zwick/Roell, Germany). Images of hydroxyapatite/chitosan films with and without PMMA were obtained using Scanning Electron Microscopy (SEM) (LEO Electron Microscopy Ltd, England).

4. Results and discussion

Changes in Young's Modulus of composite obtained on the base of hydroxyapatite/chitosan/PMMA are shown as a bars in Figure 1. Scanning Electron Microscopy images of the composite are shown in Figure2.

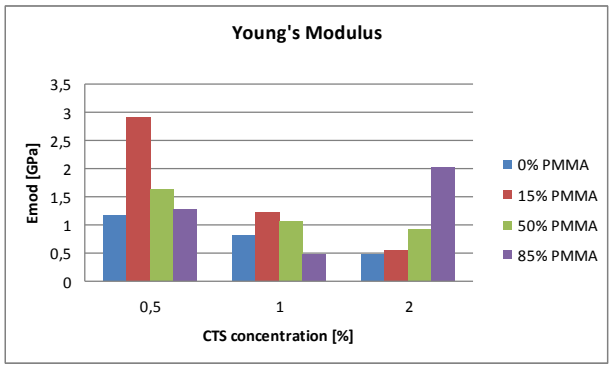

Figure 1. Changes of mechanical properties of composites with different ratios of PMMA.

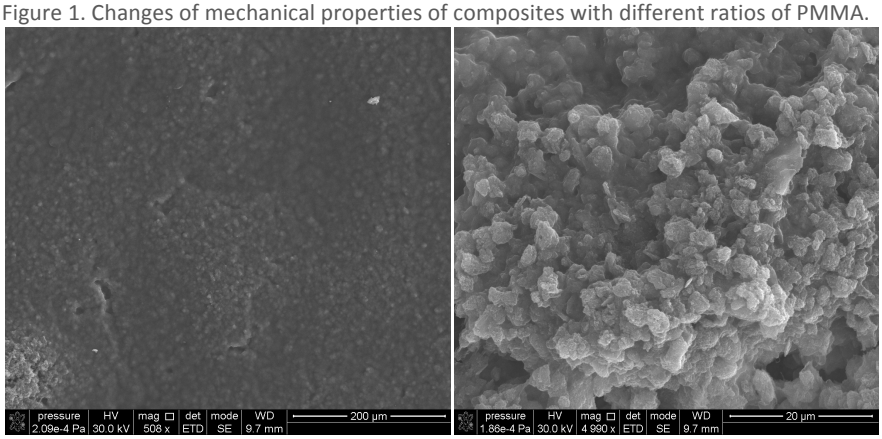

Figure 2. SEM images of HAp/CTS composite.

5. Conclusions

Mechanical properties of composite films depend on the concentration of chitosan solution used for film preparation and depend on the ratio of PMMA in composite. Using mechanical property measurements and Scanning Electron Microscope images one can find which composite can be the best for future applications. Antibiotic release from selected composites was recorded.

References

[1] Pan X, Zhitomirasky I., Mater. Chem. Phys. 2005, 94, 245-251.
[2] Kong L, Gao Y, Cao W, Gong Y, Zhao N, Zhang X. J. Biomed. Mater. Res. A. 2005, 75, 275-282.
[3] Zhang Y, Venugopal JR, El-Turki A, Ramakrishna S, Su B, Lim T., Biomater. 2008, 32, 4314-4322.
[4] Martins VCA, Goissis G, Ribeiro AC, Jr EM, Bet MR., Artif Organs 1998, 22, 215-221.
[5] Chen F, Wang ZC, Lin CJ., Mater. Lett. 2002, 4, 858-861.
[6] Sionkowska A., Prog. Polym. Sci. 2011, 36, 1254-1276.
[7] Wang L, Li C., Carbohydr. Polym. 2006, 68, 740-745.
[8] Zhu X, Zhou D, Guan S, Zhang P, Zhang Z, Huang Y., J. Mater. Sci. Mater. Med. 2012, 23, 983-990.
[9] Wan Ngah WS, Teong LC, Wong CS, Hanafiah MAKM., J. Appl. Polym. Sci. 2012, 125, 2417-2425.
[10] Yan X, Evenocheck HM., Carbohydr. Polym. 2011, 87, 1774-1778.
[11] Zhao F, Yin Y, Lu WW, Leong C, Zhang W, Zhang J, Zhang M, Yao K., Biomat. 2002, 23, 3227-3234.
[12] Itokazu M, Yang W, Aoki T, Ohara A, Kato N., Biomat. 1998, 19, 817-819.
[13] Kim SB, Kim YJ, Yoon TL, Park SA, Cho IH, Kim EJ, Kim IA, Shin JW. Biomat. 2004, 25, 5715-5723.
[14] Sivakumar M, Manjubala I, Rao KP., Carbohydr. Polym. 2002, 49, 281-288.

S4-P35
Poly(2-oxazoline)-hydrogels as matrices for stimuli-triggered substance release

Andrew M. Kelly (1,2)*, Angela Hecke (2), Bianca Wirnsberger (2) and Frank Wiesbrock (1,2)
(1) Polymer Competence Center Leoben GmbH, Roseggerstrasse 12, 8700 Leoben, Austria.
(2) Graz University of Technology, Institute for Chemistry and Technology of Materials, Stremayrgasse 9, 8010 Graz, Austria.
*andrew.kelly@pccl.at

Summary. Crosslinked poly(2-oxazoline) hydrogels can be prepared from monofunctional 2-ethyl- and 2-phenyl-2-oxazoline as well as bisfunctional phenylene-1,3-bis-(2-oxazoline) in a single-mode microwave reactor. Swelling degrees of the hydrogels varied according to the ratio of monomers in the polymerization mixtures. These hydrogels can incorporate organic substances after diffusion strategies at room temperature. The substances are released from the dried gels only if stimuli such as solvent or pH changes are applied.

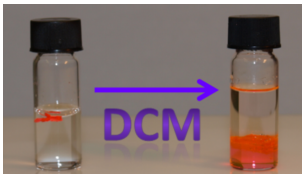

1. Introduction
Hydrogels are crosslinked polymer networks with the ability to absorb water or comparable biological fluids in a manner similar to living tissue [1]. Due to their insolubility in water and their porous structure, numerous applications in the medical field are possible. The status of these materials as ideal candidates for medical applications stems from the possibility of drug release by diffusion through or degradation of the hydrogels in addition to their biocompatibility and degradability reported in literature [2,3]. Poly(2-oxazoline)s (**Scheme 1**) are interesting candidates in hydrogel synthesis: It is possible to synthesize tailor-made hydrogels for specific functions including slow delivery of medications due to effect of the crosslinking degree on the hydrogel properties [4]. The recent growth in the investigation of poly(2-oxazoline)s has resulted from advances in microwave-assisted chemistry which enables accelerated syntheses [5]. Here, the microwave-assisted synthesis and characterization of a 32-membered library of poly(2-oxazoline)-based hydrogels is described showing the possible variance in swelling degrees as well as their capability in compound uptake and release.

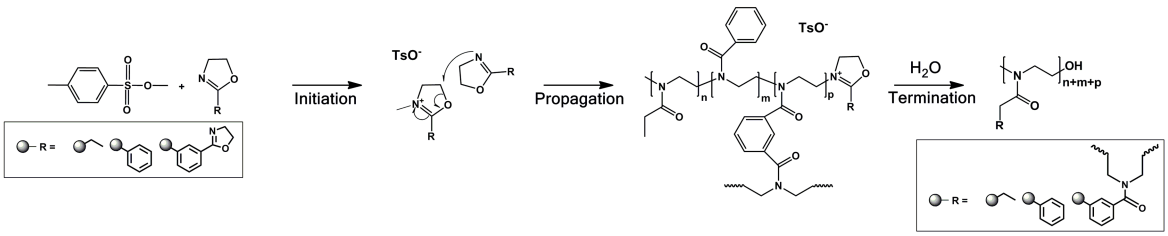

Scheme 1. Living cationic ring-opening copolymerization of 2-ethyl-2-oxazoline **EtOx**, 2-phenyl-2-oxazoline **PhOx**, and phenylene-1,3-bis-(2-oxazoline) **PBO**, yielding crosslinked hydrogels of the composition p**EtOx**$_n$-p**PhOx**$_m$-p**PBO**$_q$.

2. Experimental
EtOx, **PhOx**, and methyl tosylate were purchased from Aldrich, purified by distillation over sodium sulfate and stored under an inert atmosphere. **PBO** from Evonik (Hanau, Germany) was used without purification. Polymerizations were performed in the microwave reactor Initiator Eight from Biotage in sealed vials dedicatedly designed for the single-mode microwave system at 140 °C. **MonOx** ratios were selected from [**EtOx**]:[**PhOx**] = 150:0, 100:50, 50:100, or 0:150 (4 ratios), whilst the ratio [**MeOTs**]:[**PhOx+EtOx**] remained constant at 1:150. The ratio of monomers [**PhOx+EtOx**]:[**PBO**] was varied according to 150:30, 150:15, 150:10, 150:7.5, 150:6, 150:3, 150:2, or 150:1.5 (8 ratios). For a typical procedure, 1.34 g (13.5 mmol, 100 eq) **EtOx**, 0.99 g (6.7 mmol, 50 eq) **PhOx**, 0.22 g (1 mmol, 7.5 eq) **PBO**, and 0.0242 g (0.13 mmol, 1 eq) **MeOTs** produced the hydrogel **EtOx**$_{100}$**PhOx**$_{50}$**PBO**$_{7.5}$. The products were recovered as colorless to slightly yellow solids and subjected to repeated swelling/drying cycles in DCM until weight constant. The yield was equal to or greater than 95%.

3. Results and discussion
Swelling Degrees of the p**EtOx**$_m$-p**PhOx**$_n$-p**PBO**$_q$ **Hydrogels.** For the synthesis of the 32-membered library of **PBO** crosslinked hydrogels (**Scheme 1**), optimized reaction conditions were considered [6]. The hydrogels were prepared via one-pot syntheses of the monomer mixtures under solvent-free conditions. To determine the swelling degrees of each hydrogel, the test solvents water, ethanol and dichloromethane were employed (**Figure 1)**. Maximum swelling degrees were obtained within 24 h. Hardly any swelling in water was observed for hydrogels of the compositions p**PhOx**$_{150}$-p**PBO**$_q$ and p**EtOx**$_{50}$-p**PhOx**$_{100}$-p**PBO**$_q$. Hydrogels of the composition p**EtOx**$_{100}$-p**PhOx**$_{50}$-p**PBO**$_q$ exhibited swelling degrees in water up to a maximum value of 2.7 for p**EtOx**$_{100}$-p**PhOx**$_{50}$-p**PBO**$_{1.5}$. For the p**EtOx**$_{150}$-p**PBO**$_q$ series, the maximum swelling in water was observed; with lower degrees of crosslinking swelling increased to a maximum of 14 for p**EtOx**$_{150}$-p**PBO**$_2$. Notably, p**EtOx**$_{150}$-p**PBO**$_{1.5}$ was soluble in all test solvents.

The correlation between swelling degree and hydrogel composition was most obviously illustrated when using ethanol as test solvent. With a decrease in crosslinking, an increase in swelling was observed for each of the four series with **EtOx**:**PhOx** variation. Swelling degrees also increased with decreasing **PhOx** content. Hence, maximum swelling degrees of 11.7 were observed for p**EtOx**$_{100}$-p**PhOx**$_{50}$-p**PBO**$_{1.5}$. In dichloromethane, however, it was noted that only the degrees of crosslinking influenced the swelling degrees; the ratio of **EtOx**:**PhOx** did not influence the swelling degree in dichloromethane. Consequently, accessible pore sizes (due to different size of the ethyl and phenyl side-chains) and pore (size) distribution (due to the different reactivity of **EtOx** and **PhOx**) were not influential for swelling in this solvent [7]. Maximum swelling degrees of 20 were observed for the lowest crosslinking degrees in the hydrogels p**EtOx**$_m$-p**PhOx**$_n$-p**PBO**$_{1.5}$ ($m \leq 100$; $n \geq 50$).

Dye Inclusion. Due to the higher swelling in dichloromethane it was possible to post-synthetically load the example hydrogel p**EtOx**$_{150}$-p**PBO**$_3$ with organic molecules allowing for the diffusion-mediated capture of dissolved molecules in the hydrogels. Loading of the hydrogels with Eosin Y, for example, was achieved by storing the hydrogels for 24 h in 0.5 wt% dichloromethane/ethanol solutions of the dye. According to UV/Vis spectroscopy, the Eosin Y concentration in solution was barely altered during the loading, indicating that high swelling degrees of the hydrogels corresponded with sufficiently high diffusion through the swollen gels. The amount of loaded Eosin Y in each hydrogel could be calculated from the swelling degrees of the hydrogels: Loading of p**EtOx**$_{150}$-p**PBO**$_3$ yielded a hydrogel of the composition p**EtOx**$_{150}$-p**PBO**$_3$·[Eosin Y]$_{1.25}$.

Stimuli-Triggered Release. Release from the post-synthetically impregnated hydrogels was dependent upon stimuli. Changing the solvent from water to chloroform or chloroform/water biphasic systems triggered immediate release of Eosin Y by diffusion, exploiting the hydrophilic/hydrophobic character of **EtOx**/**PhOx**. Eosin Y, however, was not released from accordingly loaded p**PhOx**$_{150}$-p**PBO**$_3$ in water. Lowered pH values alternatively allowed for slow degradation of the hydrogels observed in aqueous environments, yielding the four components poly(ethylene iminium chloride), propionic acid, benzoic acid, and phthalic acid and the release of included organic molecules (Eosin Y).

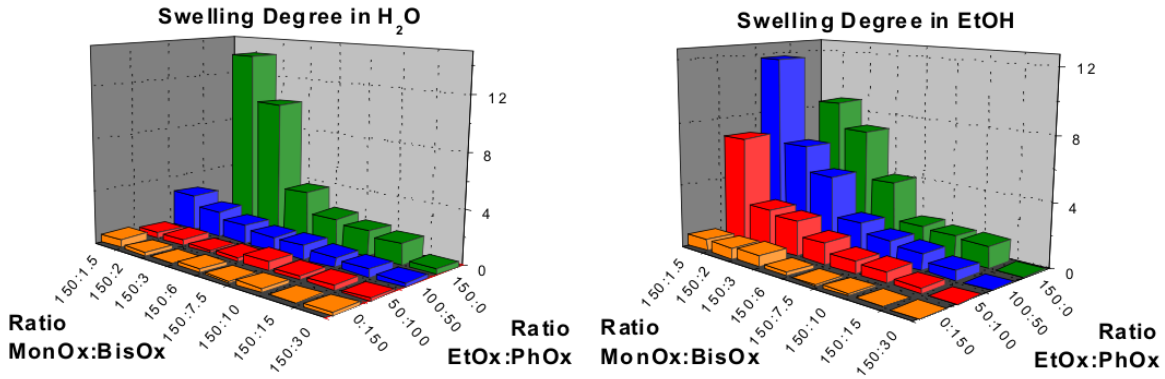

Figure 1. Maximum swelling degrees of the 32 p**EtOx**$_m$-p**PhOx**$_n$-p**PBO**$_q$-based hydrogels in water (left) and ethanol (right).

4. Conclusions

A 32-membered library of 2-oxazoline-based hydrogels was synthesized from monofunctional **EtOx** and **PhOx** and bisfunctional **PBO**. All syntheses were performed in a single-mode microwave reactor with reaction times as short as 1 h. Swelling degrees in water, ethanol, and dichloromethane depended on the hydrogels' compositions and could be varied over a broad range dependent on the crosslinking degree and monomer ratios. Hydrogels were shown to be capable of both uptake of model organic compounds and their triggered release through either diffusion or degradation.

Acknowledgements

This study was performed at the Institute for Chemistry and Technology of Materials at the Graz University of Technology with funding and contributions from the Polymer Competence Center Leoben GmbH (PCCL, Austria) within the framework of the COMET-program of the Austrian Ministry of Traffic, Innovation and the Ministry of Economy, Family and Youth. PCCL is funded by the Austrian Government and the State Governments of Styria and Upper Austria.

References

[1] Y. Qiu, K. Park, *Adv. Drug Delivery Rev*. 2001, 53, 321-339.
[2] L. Brannon-Peppas, N.A. Peppas, *J. Controlled Release* 1989, 8, 267-274.
[3] J.E. Puskas, Y. Chen, *Biomacromolecules* 2004, 5, 1141-1154
[4] A.M. Kelly, F. Wiesbrock, *Macromol. Rapid Commun.* 2012, 33, 254-288.
[5] C. Ebner, T.Bodner, F. Stelzer, F. Wiesbrock, *Macromol. Rapid Commun.* 2011, 32, 1632-1647.
[6] F. Wiesbrock, R. Hoogenboom, M.A.M. Leenen, M.A.R. Meier , U.S. Schubert, *Macromolecules* 2005, 38, 5025-5034.
[7] A.M. Kelly, A. Hecke, B. Wirnsberger, F. Wiesbrock, *Macromol. Rapid Commun*. 2011, 32, 1815-1819.

S4-P36
Stabilized micellar carrier as a delivery vehicle of cisplatin

Neli Koseva (1)*, Ekaterina Stoyanova (2), Violeta Mitova (1), Petar Petrov (1), Rossen Donev (3)
(1) Institute of Polymers, Bulgarian Academy of Sciences, 103 Acad. G. Bonchev Str., 1113 Sofia, Bulgaria;
(2) Faculty of Chemistry and Pharmacy, Sofia University "St. Kliment Ohridski", 1 J. Bourchier Blvd, 1164 Sofia, Bulgaria
(3) Institute of Life Science, College of Medicine, Swansea University, Swansea SA2 8PP, UK;
*koseva@polymer.bas.bg

1. Introduction
The use of polymeric nanocarriers for drug delivery has shown significant therapeutic potential to improve the efficiency and the specificity of drug action [1] . Cis-Dichlorodiamminoplatinum(II) ([PtCl2(NH3)2], cisplatin) is the most widely used platinum-based antineoplastic agent [2]. However, disadvantages such as severe toxic side effects, short circulation period in the blood, intrinsic or acquired resistance of some tumors to the drug, et. are associated with cisplatin clinical use. The aim of the present investigation is an evaluation of the applicability of a polymer micelle-like particles as cisplatin carrier addressing different aspects: tolerability, drug payload, dispersion stability, release profile.

2. Theory
Drug conjugation to a macromolecular carrier is a promising strategy especially in the field of cancer therapy. It has been demonstrated that long-circulating polymeric carriers can preferentially and effectively accumulate in solid tumors – a phenomenon known as the "Enhanced Permeability and Retention (EPR) effect" (Matsumura and Maeda, 1986; Maeda et al. 2003). Polymeric micelles are one of the most extensively studied for delivering hydrophobic drugs. They serve as drug containers with sufficient dispersion stability due to the hydrophilic shell. Significant advance in the construction of multifunctional and/or stabilized micellar entities has been made by use of mixtures of block copolymers or/and cross-linking methods [3, 4].
In this study we have examined stabilized polymeric micelles (SPMMS) composed of poly(ethylene oxide)-b-poly(propylene oxide)-b-poly(ethylene oxide) ($PEO_{19}PPO_{29}PEO_{19}$) and poly(acrylic acid)-b-poly(propylene oxide)-b-poly(acrylic acid) ($PAA_{18}PPO_{34}PAA_{18}$). The polymeric nanoparticles bear carboxylic groups and afford possibility for cisplatin conjugation. Cisplatin undergoes ligand exchange reactions with carboxylate ions, and the resulting species are able to undergo the reverse exchange reaction with chloride ions to regenerate cisplatin at physiological salt concentrations (Howe-Grant and Lippard, 1980). The cisplatin-incorporated micelles are extremely stable in distilled water whereas in physiological saline the drug is released in a sustained manner.
The stabilized polymeric micelles are composed of biocompatible polymers (PEG and PAA), however, there are other biological features which need to be considered prior employing the nanoparticles in drug delivery - the activation of complement system by the drug carriers and influence on neuronal expression of genes related to neurogenesis and neurodevelopment.

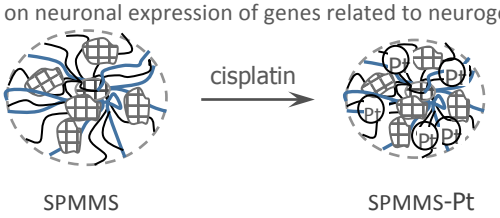

Figure 1. Schematic presentation of SPMMS loading with cisplatin.

3. Experimental
Stabilized micelles with a mixed shell were obtained as follows: a binary mixture of diblocks $PEO_{19}PPO_{29}PEO_{19}$/PAA_{18}-PPO_{34}-PAA_{18} (1:1 molar ratio) was dissolved in THF; the organic solvent was evaporated and bi-distilled water (pH=9) was added; then the micellar solution was irradiated with a full spectrum UV light in the presence of pentaerythritol tetraacrylate (PETA). The stabilized polymeric micelles were purified by dialysis against bi-distilled water for 14 days.
Cisplatin was added to an aqueous solution of the stabilized micelles (2 mg/ml) at pH 8.0 at a molar ratio of cisplatin to carboxylate groups 1:4 followed by stirring of the mixture for 24 h at room temperature. Unbound cisplatin was removed by dialysis against deionized water for 2 days. The release of platinum(II) complexes from the polymer carrier was studied at pH 7.4 (10 mM PBS, 0.14 M NaCl) and at pH 5 (0.1 M citrate buffer solution).
The experiments for assessment of the ability of the nanoparticles to activate the complement system and their neurotoxicity are described in [were].

4. Results and discussion
An efficient and fast approach for stabilizing the mixed PEO–PPO–PEO/PAA–PPO–PAA micelles was applied. It involved UV-induced free radical polymerization of a multifunctional monomer PETA loaded in the micelles. PETA was used as cross-linking agent because of its ability to form an interpenetrating network, in which the polyether chains are physically entrapped. The interpenetrating network was restricted to nanodomains randomly dispersed within the micelles.
The construction of mixed micelles affords opportunity of increasing the functionality of the nanocarrier and imparting new

features. In the case of the mixed PEO–PPO–PEO/PAA–PPO–PAA micelles, pH responsiveness of the shell was added to the thermosensitive properties of the core. The pH sensitivity determines also the pH range of SPMMS dispersion stability, i.e. at pH > 5 when the PAA chains are ionized and contribute to the stabilization of the solution. Moreover, neither complement activation nor a significant apoptotic or necrotic effects on cultured human neurons were detected for SPMMS.

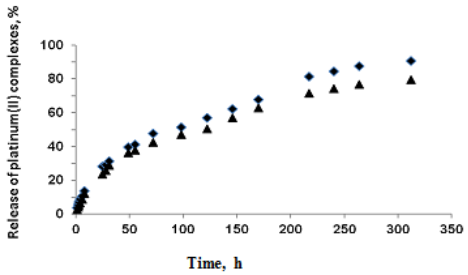

Figure 2. Release of Pt(II) complexes from drug loaded SPMMS at 37 °C: _ pH 7.4 (10 mM PBS, 0.14 M NaCl) and ▲ pH 5 (0.1 M citrate buffer solution).

The SPMMS were loaded with cisplatin by mixing of the aqueous micellar solution with the drug. The solution of the loaded particles was colorless and transparent. Under the experimental conditions drug loading efficiency equal to 76 % was achieved. The corresponding amount of the immobilized cisplatin was determined to be 20 % of the mass of the loaded particles. The size of the loaded nanoparticles was about 180 nm measured by DLS.
The obtained release profiles in both media indicate sustain manner of drug release from the nano-carrier. No clearly expressed initial burst effect was observed. This could be an indication that the whole amount of the drug was complexed to the carrier via ligand exchange. More than 80% of the loaded drug was released within 13 days of incubation.

5. Conclusions
The stabilized mixed micelles display a combination of key features for cisplatin conjugation - hydrophilic shell with high density of carboxylate groups that are able reversibly to exchange ligands with cisplatin and therefore to regenerate the agent at physiological salt concentrations. The platinum(II) complexes were released in a sustained manner without initial burst effect. Considering the overall features of the tested nanoparticles, SPMMS seem to be applicable for drug delivery without having an adverse effect on neurogenesis, neurodevelopment and activation of complement system.

Acknowledgements
The support by the NSF of Bulgaria (Contract no DCVP 02/2009) and EC (Grant agreement no: 316086, Project POLINNOVA) is highly acknowledged.

References
***[1] T. M. Allen, P. R. Cullis*, Science**, 2004, 303, ***1818–1822, 2004*.**
[2] A.-M. Florea, D. Büsselberg, *Cancers* 2011, 3, 1351-1371.
[3] C. A. Fustin, V. Abetz, J. F. Gohy, *Eur. Phys. J.* E 2005, 16, 291–302.
[4] G. Riess, *Prog. Polym. Sci*., 2003, 28, 1107.
[5] R. Donev, N. Koseva, P. Petrov, A. Kowalczuk, J. Thome, *World J. Biol. Psychiatry* 2011, 12 (SUPPL. 1), 44-51.

S4-P37
Tailor-made components for dental adhesives

Norbert Moszner*, Jörg Angermann, Iris Lamparth, Yohann Catel, Urs Fischer
Ivoclar Vivadent AG, Bendererstrasse 2, FL-9494 Schaan, Liechtenstein
*norbert.moszner@ivoclarvivadent.com

Self-etching enamel-dentin adhesives (SEAs) are used in restorative dentistry to achieve a strong bond between the filling composite and dental hard tissues. The main components of currently used SEAs include strongly acidic adhesive monomers, such as methacrylate group-containing phosphoric acids, and crosslinking dimethacrylates. The visible-light photoinitiators of SEAs are based on mixtures of camphorquinone (CQ) and tertiary amines. Water is primarily used as solvent or co-solvent in SEAs. Thus, especially in the case of one-bottle adhesives, the methacrylates may undergo hydrolysis of the methacrylate ester bonds in the presence of the strongly acidic adhesive monomers. Moreover, in SEAs the acid-base reaction of the acidic monomers with the basic amine co-initiator of the photoinitiator may significantly impair the formation of initiating radicals. In order to improve the performance of SEAs, we were looking for new tailor-made adhesive monomers and photoinitiators with improved stability under strongly acidic aqueous conditions.

For producing hydrolytically stable, strongly acidic monomers, we synthesized monomers, which contain hydrolytically stable ether or amide bonds as linking groups between the strongly acidic and the polymerizable group, for example, the very hydrolytically stable phosphonic acid **A** and bis(methacrylamido) dihydrogen phosphate **B.** These monomers showed a high reactivity in the free-radical polymerization, a very good solubility in water and polar solvents, a low cytotoxicity and no mutagenic effect. Furthermore, they enabled a fast interaction with enamel and dentin, produce corresponding Ca^{2+} salts of low solubility and therefore generate strong bonds to the dental hard tissue.

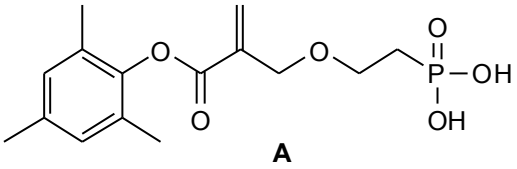

A

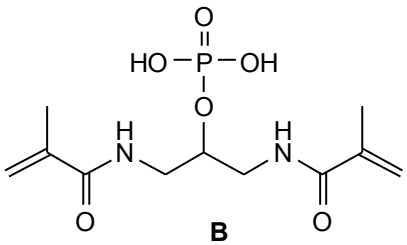

B

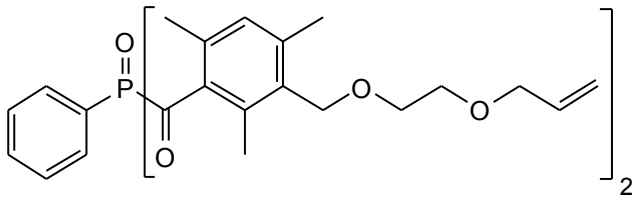

C

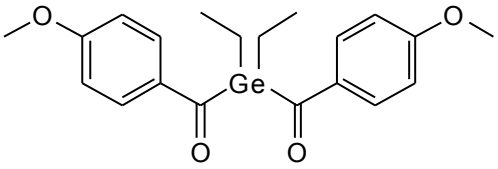

D

Because of the poor photoreactivity of CQ-amine based photoinitiator systems in acidic aqueous dental primer formulations, new amine-free Norrish-Typ-I photoinitiators were synthesized. So, we synthesized the substituted bisacylphosphine oxide derivative bis(3-{[2-(allyloxy)ethoxy]methyl}-2,4,6-trimethylbenzoyl)phenylphosphine oxide **C**. Moreover, the novel visible-light Norrish-Typ-I photoinitiator bis(4-methoxybenzoyl)diethylgermane **D** was synthesized. In the presence of monomers, this photoinitiator undergoes monomolecular photodecomposition under formation of germyl and 4-methoxybenzoyl radicals, which may initiate the polymerization. The main benefits of the diacylgermanium compounds are the strong blue light absorption, their high stability and high photoinitiating efficiency in aqueous acidic solutions.

S4-P38
Bioactive biomaterials with anti-oxidative stress and antimicrobial properties

E. Nugroho Prasetyo (1)*, GS. Nyanhongo (1), GM. Guebitz (1,2)
(1) Graz University of Technology, Institute of Environmental Biotechnology, Petersgasse 12/1, A-8010, Graz, Austria
(2) Institute of Environmental Biotechnology, University of Natural Resources and Life Sciences, Vienna, Konrad Lorenz Strasse 20, 3430 Tulln, Austria
*nugrohoprasetyo@tugraz.at

1. Introduction

Many diseases including cardiovascular, cancers, neurodegenerative including in ability of chronic wounds to heal have as their main underlying cause free radicals generated either *in vivo* or from exogenous sources. For example, although iron is essential for many metabolic functions in humans, it is also potentially toxic because of its role in the generation of free radicals responsible for the development of oxidative stress related diseases[1]. Chronic wounds (defined as wounds that do not heal, remaining in the inflammatory phase for an unpredictable time) are also characterized by elevated levels of reactive oxygen species (produced by neutrophils, macrophages, resident fibroblasts and endothelial cells), persistent inflammation, high level of proteases (e.g. neutrophil- derived elastase and matrix metalloproteases produced by macrophages, fibroblasts, neutrophils, epithelial cells, and endothelial cells) as well as high amounts of exudates which promote bacterial infection[2]. These reactive oxygen species (ROS) continuously oxidize biomolecules thus continuously damaging newly synthesized and old biomolecules[2]. Chronic wounds constitute a major health care challenge all over the world with costs for caring patients estimated to be between £2.3bn–3.1bn in the UK and US$25 billion per year in the USA[3]. Although reasonable success has been achieved in controlling exudates and inhibiting bacteria; inflammation, proteases and ROS remain a big challenge. Similarly, although a lot of effort has been directed at synthesizing iron effective iron chelators, up to now ideal drug has been found. Here we present two novel systems we developed for controlling excessive production of free radicals in chronic wounds thereby promoting healing and novel therapeutic phenolic functionalized chitosan microspheres for “free iron” chelation.

2. Experimental

Gelatin, carboxymethylcellulose and alginate hydrogels loaded with cellobiose, cellobiose dehydrogenase (CDH) and phenolic antioxidants were synthesised. These hydrogels were incubated in the presence of a free radical generating system ($O_2^{\bullet-}$, OH•, •NO) in the absence or presence of cellobiose. The synthesis of phenolic functionalized chitosan microspheres was achieved by grafting laccase oxidized phenolic iron chelator molecules (catechol, hydroxybenzoic acid) onto chitosan. The microspheres were then made from the phenolic functionalized chitosan by dropping small microspheres into an alkaline solution.

3. Results and discussion

Multilayered gelatin, carboxymethylcellulose and alginate hydrogels were synthesized with in-built antioxidant regenerating system for continuous quenching of free radicals ($O_2^{\bullet-}$, OH•, •NO)) and antimicrobial system based on a versatile enzyme cellobiose dehydrogenase were synthesized. *In vitro* incubation of a radical generating system with sinapic acid, guaiacol, vanillic acid or 2,6-dimethoxyphenol resulted in the oxidation of the respective phenolic antioxidants. Addition of the antioxidant regenerating system (CDH and cellobiose) to the oxidized phenolic antioxidants resulted in the regeneration of the parent compound [4,5]. Incubation of an NO generating systems with hydrogels loaded with sinapic acid, guaiacol, vanillic acid or 2,6-dimethoxyphenol showed that the antioxidant regenerating system (CDH + cellobiose) was able to continuously quench $O_2^{\bullet-}$, OH•, •NO radicals. In addition studies with CDH-loaded hydrogels free of oxidized phenolic antioxidants was able to use O_2 to produce H_2O_2, an antimicrobial agent which was able to completely inhibit the growth of *Stapylococcus aureus, Bacillus subtilis, Pseudomonas putida* and *Cellulomonasmicrobium cellulans* [5].

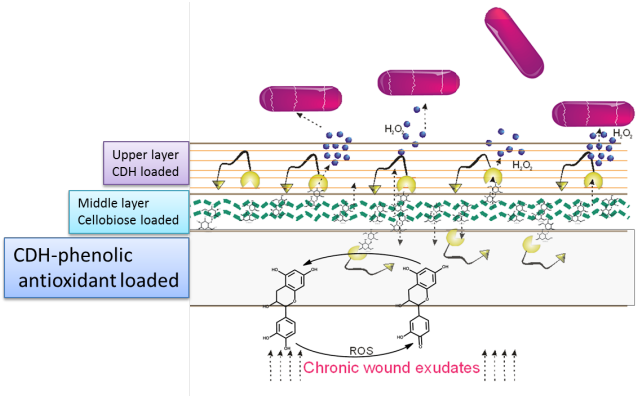

Fig.1. Structural and functional design of the hydrogel for the management of the chronic wounds. The chronic wound exudates activates the CDH and also triggers the diffusion of cellobiose into both the lower and upper layers of the gels where it is used to regenerate oxidized phenolic in the lower and to produce H_2O_2 in the upper part. Modified from Nyanhongo et al [4].

In vitro studies showed the ability of laccase to mediate the coupling of phenolic molecules (catechol, caffeic acid, and 2,5-dihydroxybenzoic acid) onto glucosamine as model substrate of chitosan. The coupling was in a 1:1 ratio. Furthermore, coupling of these molecules onto chitosans of different sizes was demonstrated, resulting in decrease in $–NH_2$ groups as quantified via Derivatization and a concomitant increase in iron-chelating capacity from below 3% to up to 70% upon phenolic functionalization was measured for the chitosan based on reduced ferrozine/Fe2+ complex formation.

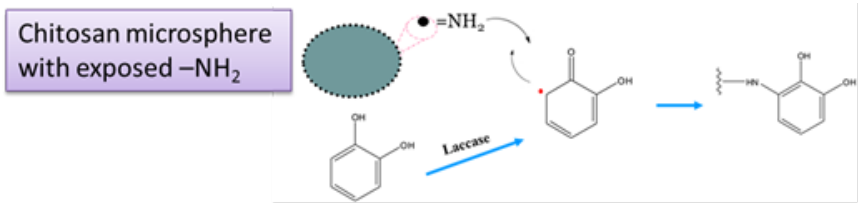

Fig 2: Carboxic acid and catechol highly functionalized microspheres. Modified from Brzonova et al [6]

4. Conclusions

The results presented in this work therefore opens-up new strategies aimed at developing a new generation of iron-chelating biomedical polymers as well as the first ever continuous self- regenerating free radical quenching system that could find applications in many biomaterial systems.

Acknowledgements

Acknowledgements: Authors are thankful for the financial support offered by EU NOVO project and ACIB.

References

[1]. D.S. Kalinowski, D.R. Richardson, The evolution of iron chelators for the treatment of iron overload disease and cancer, *Pharmacol. Rev*. 57 (2005) 4547–4583.

[2] Bjarnsholt T et al (2008) Why chronic wounds will not heal: a novel hypothesis. *Wound Rep Reg* 16 2–10

[3] Posnett J., Franks P.J. (2008) The burden of chronic wounds in the UK. Nursing Times; 104: 3, 44–45.
[4] Nyanhongo GS, Sygmund C, Ludwig R, Prasetyo EN, Guebitz GM. An antioxidant regenerating system for continuous quenching of free radicals in chronic wounds. *Eur J Pharm Biopharm*. doi: 10.1016/j.ejpb.2012.10.013
[5] Nyanhongo GS, Sygmund C, Ludwig R, Prasetyo EN, Guebitz GM. (2012) Synthesis of multifunctional bioresponsive polymers for the management of chronic wounds. *JBMR :B*. DOI: 10.1002/jbm.b.32893
[6] Brzonova I, Steiner W, Zankel A, Nyanhongo GS*, Guebitz GM (2011) Enzymatic synthesis of catechol and hydroxyl-carboxic acid functionalized chitosan microspheres for iron overload therapy. *Eur J Pharm Biopharm* 79: 294 - 303

S4-P39
Crosslinked 2-hydroxyethyl methacrylate within emulsion templating

Muzafera Paljevac (1), Karel Jeřabek (2), Peter Krajnc (1,3)*
(1) University of Maribor, Faculty of Chemistry and Chemical Engineering, PolyOrgLab, Smetanova 17, SI-2000 Maribor, Slovenia
(2) Institute of Chemical Process Fundamentals of the Academy of Sciences of the Czech Republic, Department of Catalysis and Reaction Engineering, Rozvojová 135, 16502 Praha, Czech Republic
(3) Centre of Excellence PoliMaT, Tehnološki park 24, SI-1000 Ljubljana, Slovenia
*peter.krajnc@um.si

1. Introduction

Emulsion templating is a versatile method for the preparation of highly porous organic polymers, inorganic materials, and inorganic-organic composites. In general, the technique involves forming a high internal phase emulsion (HIPE). HIP emulsions are defined as emulsions wherein the volume of the droplet (internal) phase is higher than 74.05% of the total emulsion volume [1, 2]. HIPEs are commonly used for the preparation of hydrophobic polymer materials, namely, from water in oil (w/o) emulsions. Hydrophilic polyHIPEs cannot be prepared using w/o HIPEs, since monomers are normally water soluble. For the preparation of hydrophilic polyHIPEs an oil in water (o/w) HIPE is needed, where the external phase is aqueous. In this case, monomers are oil soluble and the aqueous phase serves as the porosity template [3, 4].

Poly(2-hydroxyethyl methacrylate) (poly(HEMA)) is a widely used biocompatible polymer [5] and is commercially used for contact lenses [6], drug delivery [7] and artificial cornea [8]. For many applications permanent porosity of poly(HEMA) with controlled pore size distribution would be highly desired. Use of emulsion templating for poly(HEMA) synthesis, using both o/w and w/o HIPEs, has been recently described [4, 9].

Herein, we report the preparation of porous polyHIPE materials based on HEMA using different types of crosslinkers, namely N,N'-methylene bisacrylamide (MBAA) and glutaraldehyde (GA). The influence of crosslinkers on the morphological structure of poly(HEMA) material is reported.

2. Experimental

The polymerisation reaction was conducted using 250 ml round-bottomed flask. In a typical polymerisation reaction deionized H_2O was loaded into the flask along with monomer HEMA (2.215 g), crosslinker MBAA (0.397 g), initiator APS (2 wt% based on monomer) and surfactant Pluronic F68 (20 wt% of water phase). Cyclohexane (75 vol% of emulsion) was added drop wise to the monomer solution while stirring with an overhead stirrer at 250 rpm (D-shaped paddle stirrer). Once all cyclohexane has been added, stirring was continued for a further 60 minutes to form a milky white o/w emulsion. Stirring rate was then reduced to 20 rpm and the reducing agent TMEDA (60 mL) was added. In the case of monoliths, the emulsion was then transferred to the mould (polyethylene container) and cured at room temperature for 24 h. All obtained monoliths were purified via Soxhlet extraction with isopropanol for 24 h, and dried for at least 24 h in air and then under vacuum.

For poly(HEMA-co-MBAA)membrane synthesis, emulsions were cast on the glass support using doctor blades (with dimensioned slit 1000 µm) and covered with a glass plate, polymerized at room temperature for 24 h and purified with isopropanol via Soxhlet extraction.

The emulsions for poly(HEMA-co-GA) were prepared in the same way as emulsions for the poly(HEMA-co-MBAA) monoliths and membranes with the exception that GA was used as the crosslinker (Scheme 1). Furthermore, curing time was 72 h. All obtained monoliths based on HEMA/GA were purified via Soxhlet extraction with water for 24 h, and dried in air and then under vacuum.

3. Results and discussion

Firstly, MBAA was utilized as the crosslinking agent for HEMA chains. HIPE formulations, containing HEMA as monomer, MBAA as the crosslinking agent, ammonium peroxodisulfate (APS) as the initiator and Pluronic F68 (HLB value ~24) as the surfactant (20 wt% with respect to the water phase), resulted in kinetically stable emulsions. Obtained polymers had a homogeneous morphological and macroscopic structure. Various degrees of crosslinking were used, namely between 10 and 13 mol% with regards to monomers. With the use of Pluronic F68, kinetically stable HIPEs were obtained with volume share of internal phase up to 90%. For the obtained polymer materials no shrinkage upon drying was noted. The SEM image of prepared poly(HEMA-co-MBAA) (74.8 %PV, 13.1 mol%) revealed an open cellular structure (Figure 1) with cavity diameter sizes between 6-9 mm and interconnecting pore diameters between 2-3 mm. Nitrogen adsorption/desorption measurements for the same sample resulted in an average BET surface area of 8.9 m^2/g.

Secondly, crosslinked poly(HEMA) with the aid of emulsion templating, was prepared, with the incorporation of GA into the continuous phase of HIPEs before the curing procedure. For that purpose, the HIPEs were prepared in the same way as for MBAA crosslinked HEMA. Soft monoliths were obtained without observable shrinkage. SEM microscopy was performed on the wet sample (74.8 %PV, 21 mol%). By using GA as a crosslinker, the polyHIPE structure was less pronounced in comparison to Poly(HEMA-co-MBAA). However, on SEM images the cavities with average diameter of approximately 12 mm and interconnecting pores with average pore size of approximately 3 mm, were seen.

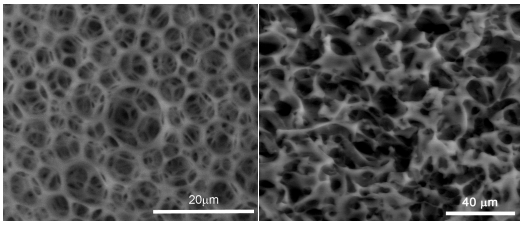

Figure 1. SEM images for a poly(HEMA-co-MBAA) monolith (left) and for a poly(HEMA-co-GA) monolith.

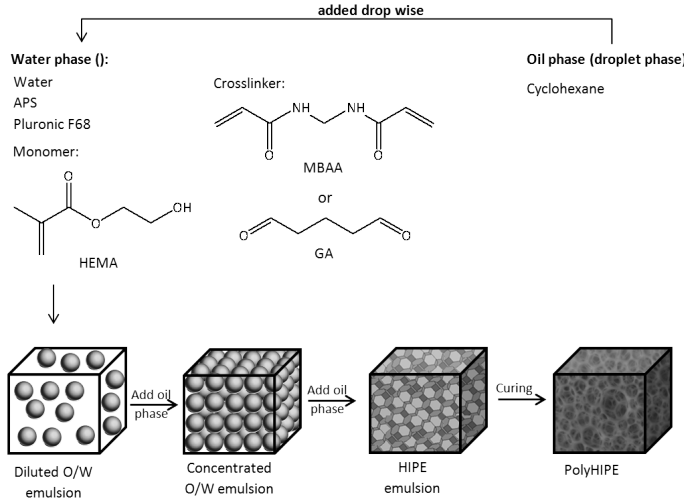

Scheme 1: emulsion preparation.

4. Conclusions

We have shown that both, N,N'-methylene bisacrylamide and glutaraldehyde, can be used to crosslink poly(HEMA) chains within the high internal phase emulsion templating approach. The morphology of glutaraldehyde crosslinked poly(HEMA) differ from material obtained using N,N'-methylene bisacrylamide as a crosslinker. However, interconnected porous structure is still evident.

Acknowledgements

Financial support of the Slovenian Research Agency and the Czech Grant Agency through the projects L2-2008 and BI-CZ 11/12-05 is gratefully acknowledged.

References

[1] I. Pulko , P. Krajnc, *Macromol. Rapid Commun.* 33 (2012) 1731–1746.
[2] S.D. Kimmins and N.R. Cameron, *Adv. Funct. Mater*. 21 (2011) 211-225.
[3] P. Krajnc, D. Štefanec, I. Pulko, *Macromol. Rapid commun.*, 26 (2005) 1289-1293.
[4] S. Kovačič, D. Štefanec and P. Krajnc, *Macromolecules* 40 (2007) 8056-8060.
[5] I. Gibas and H. Janik, *J. Chem. Chem. Technol*. 4 (2010) 297-303.
[6] J.P. Bergmanson, C.M. Ruben and L.W. Chu, *J. Ophthalmol*. 69 (1985) 373-379.
[7] A.J. Cadotte and T.B. DeMarse, *J. Neural. Eng*. 2 (2005) 114-122.
[8] T.V. Chirila, *Biomaterials*, 22 (2001) 3311-3317.
[9] M. Paljevac, K. Jeřabek, P. krajnc, *J. Polym. Environ.* 20 (2012) 1095–1102.

S4-P40

Degradation in vitro of polyurethanes based on atactic polyhydroxybutyrate in simulated body fluids

Maria Rutkowska (1)*, Joanna Brzeska (1), Aleksandra Heimowska (1), Henryk Janeczek (2), Marek Kowalczuk (2)

(1) Gdynia Maritime University, Department of Chemistry and Industrial Commodity Science, Gdynia, Poland
(2) Polish Academy of Sciences, Centre of Polymer and Carbon Materials, Zabrze, Poland
*rutmaria@am.gdynia.pl

1. Introduction

Polyurethanes are commonly used in medicine as non- and degradable implants [1]. Their biocompatibility can be accelerated by using appropriate substrates for their building. Atactic poly([*R,S*]-3-hydroxybutyrate) - the synthetic analog of natural polyhydroxybutyrate - is known as biodegradable and biocompatible polymer [2] and as OH-terminated polyol can be incorporated into polyurethane structure.

The aim of the present study was to estimate the influence of synthetic, atactic poly[(*R,S*)-3-hydroxybutyrate] used as a part of soft segment of polyurethanes on their degradability in simulated body fluid (SBF) (containing Na^+, K^+, Mg^{2+}, Ca^{2+}, Cl^-, HCO_3^-, HPO_4^- and SO_4^{2-}) [3] and in Ringer solution (containing Na^+, K^+, Ca^{2+} and Cl^-) [4].

2. Experimental

Polyurethanes were synthesized using two-step method. The obtained polymers differed in soft segments structure and in molar ratio of NCO:OH in prepolymer [5]. The soft segments were built with polyoxytetramethylenediol - PTMG, polycaprolactonediol - PCL and a-PHB (with 23 % of a-PHB in soft segments). The hard segments of all polymers were built with 4,4'-methylene dicyclohexyl diisocyanate (H_{12}MDI) and 1.4-butanediol (1.4-BD). For comparison PURs without a-PHB were also synthesized.

PUR	The soft segments composition	Molar ratio of NCO:OH in prep.	Before incubation			After 36 weeks in SBF			After 36 weeks in Ringer		
			Tg [°C]	Tm_1[°C] ΔH [J/g]	Tm_2[°C] ΔH [J/g]	Tg [°C]	Tm_1[°C] ΔH [J/g]	Tm_2[°C] ΔH [J/g]	Tg [°C]	Tm_1[°C] ΔH [J/g]	Tm_2[°C] ΔH [J/g]
$PUR_{PTMG+a-PHB/3.7}$	PTMG+a-PHB	3.7:1	-55.3	37.8 0.7	136/158 16/2	-12.7	64.5 10.8	151.1 22.0	-43.0	- -	80-135 15.7
$PUR_{PCL+a-PHB/3.7}$	PCL+a-PHB		-32,4	50.7 3.6	90/138 4.7/9.1	-19.7	61.9 4.2	133.2 21.4	-49.1	- -	127.9 25.5
$PUR_{PTMG+a-PHB/2}$	PTMG+a-PHB	2:1	-61.5	- -	126.6 27.1	-69.1	48.8 1.8	143.2 16.6	not estimated		
$PUR_{PCL+a-PHB/2}$	PCL+a-PHB		-29.0	- -	- -	-19.5	49.7 30.4	104.2 8.6	-15.0	53.8 28.3	104.0 12.3

Tg-temperature of the glass transition of soft segments, Tm_1-soft segments melting temperature, Tm_2-hard segments melting temperature, ΔH-melting enthalpy

The incubation of polyurethanes samples was carried on in 37°C and ambient pH for 4, 12, 24 and 36 weeks in two simulated body fluids: SBF and Ringer solution. After degradation the mass changes of the polymers samples and their thermal properties (using DSC) were estimated. The polymer surface was observed under optical microscope.

3. Results and discussion

The presence of poly([*R,S*]-3-hydroxybutyrate) in polyurethane structure accelerated their degradation in SBF and in Ringer solution and protected against the calcification process.

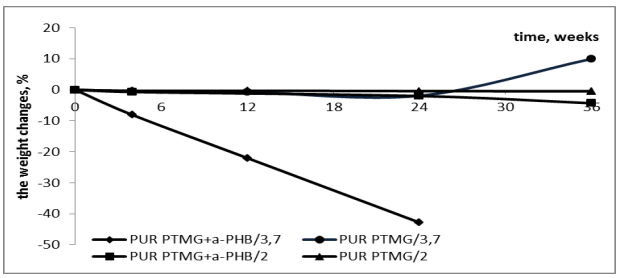

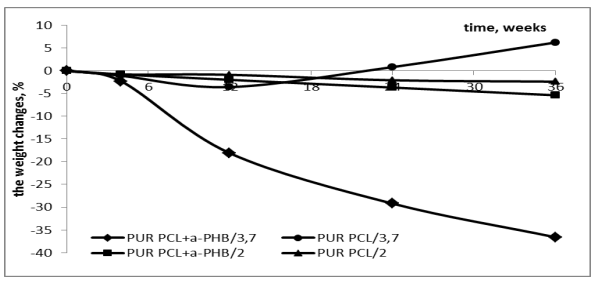

Figure 1. The weight changes of polyether-ester-urethane(A) and polyesterurethane (B) samples during incubation in SBF

The mass changes of polymer samples with a-PHB after incubation in SBF indicated that polyurethanes with high content of hard segments were degraded faster than in case of polyurethanes with lower molar ratio of NCO:OH in prepolymer (Fig.1). The observed increase in mass weight for PUR without a-PHB could be explained by solid salt confined in polymer network. The same tendency of weight changes could be observed for incubation process in Ringer solution (Fig.2).

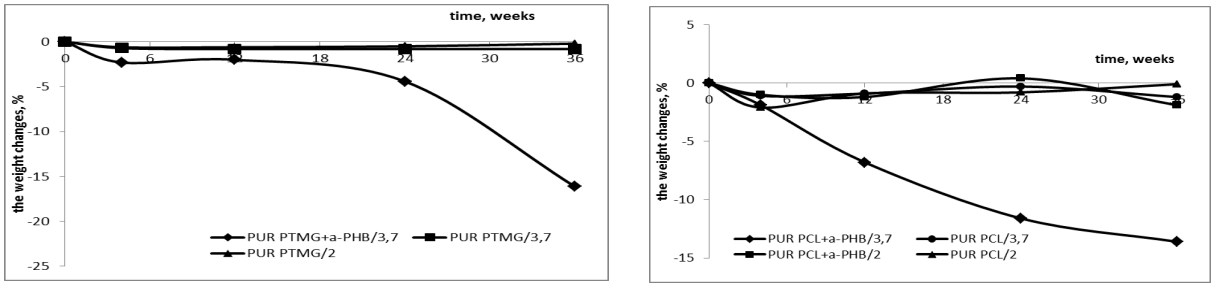

Figure 2. The weight changes of polyether-ester-urethane(A) and polyesterurethane (B) samples during incubation in Ringer solution

before degradation **after 36 weeks of incubation in SBF**

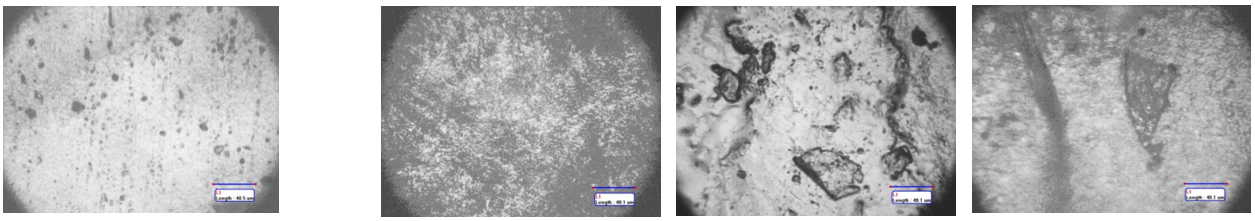

$PUR_{PTMG+a-PHB/3.7}$ **$PUR_{PTMG+a-PHB/3.7}$** **$PUR_{PTMG/2}$** **$PUR_{PTMG+a-PHB/2}$**

Fig. 3. The microscopic observations of surface of polyurethane samples before and after 36 weeks of degradation in SBF

It was observed that the sediment of solid salt on the polymer surface was larger for PURs synthesized with NCO:OH=3.7:1 than for PUR with NCO:OH=2:1 after the incubation in SBF. Presence of a-PHB in soft segments seemed to protect polyurethanes against the salts sediment (Fig.3).
The obtained polyurethanes were almost completely amorphous (Table 1). During incubation in both solutions some macrochains were cut, then reorganized and some small degree of crystallinity disappeared (e.g. $PUR_{PTMG+a-PHB/3.7}$ and $PUR_{PCL+a-PHB/3.7}$) whereas another - appeared (e.g. $PUR_{PTMG+a-PHB/2}$ and $PUR_{PCL+a-PHB/2}$). Generally the changes of Tg of polyurethanes during incubation also indicated on the reduction of chains lengths (Table 1).

4. Conclusion

The presence of poly([*R,S*]-3-hydroxybutyrate) in polyurethanes structure accelerated their degradation in simulated body fluid (SBF) and in Ringer solution, protected against the calcification process and affected their morphology.
It could be stated that polyurethane based on atactic poly[(*R,S*)-3-hydroxybutyrate] displayed the properties appropriate for further investigations for medical application.

References

[1] Chan-Chan LH., et al, "Degradation studies on segmented polyurethanes prepared with HMDI, PCL and different chain extenders" *Acta Biomaterialia* 6 (2010): 2035.
[2] Piddubnyak V., et al, "Oligo-3-hydroxybutyrates as potential carriers for drug delivery" *Biomaterials* 25 (2004): 5271.
[3] Kokubo T., Takadama H. "How useful is SBF in predicting in vivo bone bioactivity?" *Biomaterials* 27 (2006): 2907

[4] Wan Y., Wen D., "Preparation and characterization of porous conducting poly(dl-lactide) composite membranes" *Journal of Membrane Science* 246 (2005): 193.
[5] Brzeska J. et al., "Influence of synthetic polyhydroxybutyrate on selected properties of novel polyurethanes for medicine. Part II. Polyurethanes based on aliphatic diisocyanate in hard segments" *Polimery* 1 (2011): 27.

S4-P41
Chitosan nanoparticles with the inhibiting effect on carbonic anhydrase in tumor diagnosis and treatment

V. Semak (1)*, D. Vnuková (1), P. Kasák (1), L. Janikovičová (1), M. Takáčová (2), M. Zaťovičová (2), S. Pastoreková (2), I. Lacík (1)*

(1) Polymer Institute SAS, Dúbravská cesta 9, 845 41 Bratislava, Slovak Republic
(2) Institute of Virology SAS, Dúbravská cesta 9, 845 05 Bratislava, Slovak Republic
*Vladislav.Semak@savba.sk, Igor.Lacik@savba.sk

1. Introduction
Carbonic anhydrase IX (CA IX) is a cell surface protein that is present in solid tumors but not in the corresponding normal tissues. CA IX is considered to be one of the best cellular biomarkers of hypoxia and this feature makes it a proper target for the tumor diagnosis and/or treatment [1].

2. Theory
To date a variety of low molecular weight selective CA IX inhibitors is known [2]. Sulfanilamide core is a common leading structure of these inhibitors. An active site of the CA IX is on its extracellular part; however, the enzyme blocked by the inhibitor is transported to the cell and replaced by a new active molecule of CA IX. The cells are able to internalize particles up to the size of 200 nm. Hence, in order to provide a sustained inhibition of CA IX, chitosan nanoparticles with diameter > 200 nm have been under development with the aim to provide both long-term and continuous delivery of inhibitor either by direct interactions of CA IX molecule with the sulfanilamide moiety at the nanoparticle surface or by degradation of chitosan nanoparticles followed by the release of sulfanilamide inhibitor.

3. Results and discussion
The inhibitor is covalently bound *via* appropriate linker to a chitosan chain. For subcellular tracing of the nanoparticles, a fluorescent label, fluorescein isothiocyanate, was attached to the chitosan by an analogical strategy. The isothiocyanate functionality permits direct bonding of fluorescein moiety to a chitosan *via* thiourea bridge [3]. Both modified chitosans are mixed with an unmodified chitosan in selected ratio shown in **Figure 1.** Chitosan particles are formed by *i*) precipitation from the acidic solution either upon addition of sodium triphosphate or by pH adjustment, or by *ii*) reverse emulsion techniques.

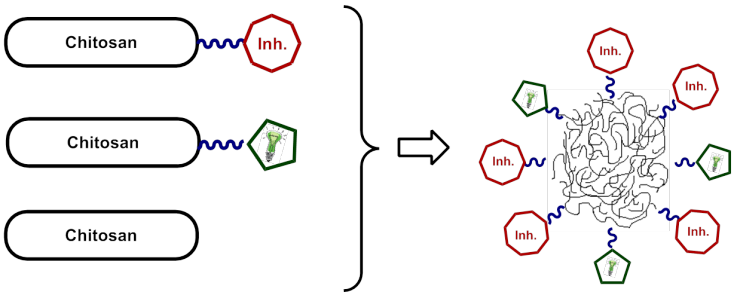

Figure 1. General strategy for the preparation of chitosan nanoparticles.

4. Conclusions
This contribution discusses the principles and results on preparation and characterization of chitosan nanoparticles containing inhibitor and fluorescence reporter molecules. Inhibition activity of prepared compounds and nanoparticles with different amount of modified chitosans (inhibitor & fluorescent label) is under evaluation.

Acknowledgements
This work was supported by the Slovak Research and Development Agency under the contract No. APVV-0658-11. Mrs. M. Kimličková is acknowledged for help with DLS measurements.

References
[1] (a) Supuran, C. T. *World J. Clin. Oncol.* **2012**, *3*, 98-103. (b) Supuran, C. T. *Nat. Rev. Drug Discov.* **2008**, *7*, 168-181. (c) Opavsky, R.; Pastorekova, S.; Zelnik, V.; Gibadulinova, A.; Stanbridge, E. J.; Zavada, J.; Kettmann, R.; Pastorek, J. *Genomics* **1996**, *33*, 480-487.
[2] (a) Ohradanova, A.; Vullo, D.; Pastorekova, S.; Pastorek, J.; Jackson, D. J.; Wörheide, G.; Supuran, C. T. *Bioorg. Med. Chem.* **2012**, *20*, 1403–1410. (b) Vullo, D.; Scozzafava, A.; Pastorekova, S.; Pastorek, J.; Supuran, C. T. *Bioorg. Med. Chem. Lett.* **2004**, *14*, 2351-2356. (c) Pastorekova, S.; Casini, A.; Scozzafava, A.; Vullo, D.; Pastorek, J.; Supuran, C. T. *Bioorg. Med. Chem. Lett.* **2004**, *14*, 869-873.
[3] (a) Tallury, P.; Kar, S.; Bamrungsap, S. Huang, Y.-F.; Tan, W.; Santra, S. *Chem. Commun.* **2009**, 2347-2349. (b) Huang, M., Khor, E.; Lim, L.-Y. *Pharmaceut. Res.* **2004**, *21*, 344-353.

S4-P42
Moleculary surface-imprinted nanofibres for hemoglobin depletion

Emel Tamahkar (1,2), Monir Bakshphour (3), Müge Andaç (3), Adil Denizli (3)
(1) Hacettepe University Chemical Engineering Department Bioengineering Division, 06800 Ankara, Turkey
(2) Hitit University Chemical Engineering Department, 19030 Çorum, Turkey
(3) Hacettepe University Chemistry Department, 06800 Ankara, Turkey
*emeltamahkar@gmail.com

1. Introduction
The aim of this study is to prepare molecularly imprinted nanofiber membranes for selective depletion for hemoglobin from human serum with high capacity. Bacterial cellulose is a biocompatible, highly swollen network and inexpensive biomaterial with a high surface area. Molecularly surface-imprinted nanofiber membranes are prepared with functional monomer and template molecule based on non-covalent interaction. When polymerized, the functional monomer (vinyl imidazole) which was complexed with a template (hemoglobin) via a metal ion (Ni^{2+}), was positioned on the nanofiber surface for the selective binding of proteins.

2. Theory
Molecularly surface-imprinting is a promising method for creating recognition sites of analyte on the surface of the polymer possesing high selectivity. Nanofibers have been gaining more attention since they avoid intraparticle diffusion resistances with high surface area. This is useful for fast separation of proteins. Surface imprinting and adopting nanomaterial are two effective approaches to overcome mass transfer resistances especially for proteins. Vinyl imidazole was used as the metal-coordinating monomer due to the affinity of imidazole nitrogen donor atoms towards Ni^{2+} ions. The pre-complexation process was performed between hemoglobin and this vinyl imidazole-Ni^{2+} complex.

3. Experimental
A series of solutions were prepared with a specific concentration of hemoglobin and different amounts of vinyl imidazole-Ni^{2+} complex in water-ethanol mixture. The UV spectra of these solutions with and without a hemoglobin solution were determined. The characterization of the complex was investigated by UV and FT-IR spectrophotometry. Prior to polymerization, the bacterial cellulose nanofiber membranes were silaned with 3-MPS (3-methacryloxypropyltrimetoxysilane) in toluene and washed with methanol for several times. For the synthesis of molecularly surface-imprinted nanofiber membranes, the silanized bacterial cellulose nanofiber membranes were immerged into the vinyl imidazole-Ni^{2+}-hemoglobin complex solution and allowed to polymerize under UV light source for 2 h. The template removal was performed by 0.5 M NaCl solution and template removal was screened spectrophotometrically. The morphology of bacterial cellulose nanofiber membranes were characterized by SEM and AFM.

4. Results and discussion

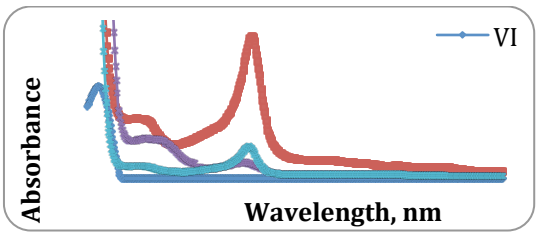

Figure 1. The UV spectra of Hb (hemoglobin), VI-Ni (vinyl imidazole and Ni^{2+}), VI-Ni^{2+}-Hb complex.

As seen from the figure above, the complex of vinyl imidazole and Ni^{2+} was formed since vinyl imidazole peak is shifted to right and one new peak was formed. Also the results indicated that hemoglobin was complexed with vinyl imidazole-Ni^{2+} complex.

References
[1]H. He, G. Fu, Y. Wang, Z. Chai, Y. Jiang, Z. Chen, Biosens. Bioelectr., 2010, 26, 760-765.
[2]M. Kempe, M. Glad, K. Mosbach, J. Mol. Recognit., 1995, 8, 35-39.
[3]T.A. Sergeyeva, H.Matuschewski, S.A.Piletsky, J.Bendig, U.Schedler, M. Ulbricht, 2001, J. Chromatog. A, 907, 89-99.
[4]V.P.Joshi, M.G. Kulkarni, R.A. Mashelkar, Chem. Eng. Sci., 2000, 55, 1509-1522.

S4-P43
RGD-functionalized poly(2-oxazoline) microgels: preferred adhesion to cancer cells

Frank Wiesbrock (1,2)*, Verena Schenk (1,2), Elisabeth Rossegger (1,2) and Michael Höpfner (3)
(1) Polymer Competence Center Leoben GmbH, Roseggerstrasse 12, 8700 Leoben, Austria.
(2) Graz University of Technology, Institute for Chemistry and Technology of Materials, Stremayrgasse 9, 8010 Graz, Austria.
(3) Charité - Universitaetsmedizin Berlin, Department of Physiology, Campus Benjamin Franklin, Thielallee 71, 14195 Berlin, Germany.
*frank.wiesbrock@pccl.at

1. Introduction
Chemotherapeutics for the treatment of cancer commonly are non-selective DNA intercalators that, due to their non-selectivity, cause severe side-effects in patients. Crosslinked three-dimensional polymer networks that are water-swellable but not soluble, so-called hydrogels, can act as carriers for drug delivery [1]. Poly(2-oxazoline)-based hydrogels, the surfaces of which were functionalized with the RGD peptide recognition motif, were tested for selective adhesion to cancer cells.

2. Experimental
Hydrogels were synthesized under microwave irradiation from 2-ethyl- (**EtOx**), 2-nonyl- (**NonOx**), and 2-9'-decenyl-2-oxazoline (**Dc$^{=}$Ox**) as well as tetramethylene-bis(2-oxazoline) (**TMBO**) as crosslinker (**Figure 1**). The hydrogels were ground in a Retsch S1000 planetary ball mill as aqueous suspensions. Particle sizes were determined with a CILAS 1180 Particle Size Analyzer. 50 mg of the ground hydrogel samples were suspended in 5 mL of water and mixed with 2.5 mg of c(RGDfC) (Bachem, Switzerland) and one drop of photoinitiator Lucirin TPO-L prior to polychromatic irradiation with 4500 mW cm^{-2}.

3. Results and discussion
The adhesion of ground microgels was tested against endothelial Eahy- and pancreatic cancer BON cells. BON cells were chosen for their high surface expression of highly active a_vb_5-integrins according to fluorescence-activated cell sorting measurements. The a_vb_5-integrin like its a_vb_3-congener has been reported to show interaction of supreme strength with the RGD motif in peptoide pentacycles. Eahy cells were chosen as a counterpart with comparably low expression of the respective integrin-composition. BON and Eahy cells were grown on glass cover slips and incubated with the hydrogel suspensions prior to a washing procedure. The poly(2-oxazoline)-based networks bearing the c(RGDfC) pentapeptide showed significant and time-dependent adhesion to BON cells, while poly(2-oxazoline) networks lacking the RGD-motif did not show a significant adhesion to BON cells (**Figure 1**). In n = 5 independent experiments the adherence of RGD-positive versus RGD-negative hydrogels to BON cells after 24 h was analyzed, resulting in a 4.3-fold higher adhesion of RGD-bearing hydrogels as compared to the RGD-negative ones.

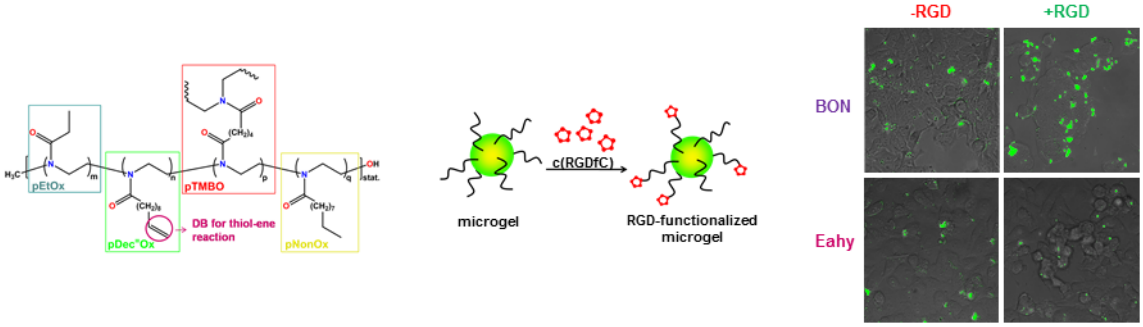

Figure 1. Structural formula of the crosslinked microgel that can be RGD-functionalized by thiol-ene reactions (left and middle). Photographies of BON and Eahy cells that were incubated with the RGD-functionalized microgel (right).

Acknowledgements
This study was performed at the Institute for Chemistry and Technology of Materials at the Graz University of Technology with funding and contributions from the Polymer Competence Center Leoben GmbH (PCCL, Austria) within the framework of the

COMET-program of the Austrian Ministry of Traffic, Innovation and the Ministry of Economy, Family and Youth. PCCL is funded by the Austrian Government and the State Governments of Styria and Upper Austria.

References

[1] A.M. Kelly, F. Wiesbrock, *Macromol. Rapid Commun.* 2012, 33, 1632-1647.
[2] C. Mas-Moruno, F. Rechenmacher, H. Kessler, *Anti-Cancer Agents in Medicinal Chemistry* 2010, 10,753-768.
[3] V. Schenk, E. Rossegger, F. Bangerl, H. Kren, K. Reichmann, B. Hoffmann, M. Höpfner, F. Wiesbrock, *Macromol. Rapid Commun.*, submitted.

S4-P44
Polyphosphazenes with pH-promoted degradation

Sandra Wilfert*, Oliver Brüggemann, Ian Teasdale
Institute of Polymer Chemistry, Johannes Kepler University Linz, Welser Strasse 42, 4060 Leonding, Austria
*sandra.wilfert@jku.at

1. Introduction

Functional polymers play a decisive role in the area of biomedicine. For example, for the intravenous delivery of anti-cancer drugs, polymeric drug carriers with molecular weights above the renal clearance limit enhance the blood circulation time and enable an increased tumor uptake via the EPR effect [1, 2]. For this purpose, the development of biodegradable polymeric drug carriers is important, in particular where high polymer doses are required, in order to prevent accumulation of the high molecular weight macromolecules in the body and any side-effects this may cause [3].
To use these effects, the design of polymeric drug carriers with biodegradability, biocompatibility and controlled molecular weight is essential. Polyphosphazenes offer a degradable backbone, structural diversity and adjustable properties that can be varied by the side groups attached to the polyphosphazene backbone by macromolecular substitution [4].

2. Results and discussion

In this contribution a series of hydrophilic polyphosphazenes are presented that offer a tunable rate of degradation in a pH-promoted response, i.e. the degradation is faster at lower pH-values. The precursor polymers, poly(dichlorophosphazenes), were obtained via the living cationic polymerization of chlorophosphoranimine with controlled molecular weights and narrow polydispersities [5]. The chlorine atoms were then replaced with suitable substituents. The synthesized polymers showed excellent solubility in water. The hydrolytic degradation behavior was controlled by selective choice of the attached side groups to the polymer backbone. In this work, we show not only the rate of degradation can be tailored by subtle changes to the chemical structure of the polymer [6, 7], but also how a pH-promoted response can be induced to prepare functional polyphosphazenes with controlled degradability.

Acknowledgements

S. Wilfert gratefully acknowledges the Johannes Kepler University Linz for the “JKU Goes Gender” dissertation fellowship. NMR measurements were carried out with Wolfgang Schöfberger at the Austro-Czech RERI-usab NMR center which was established with financial support from the European Union through the EFRE INTERREG IV ETC-AT-CZ programme (project M00146, "RERI-uasb").

References

[1] R. Haag, F. Kratz, *Angew. Chem. Int. Ed.,* **2006,** 45, 1198-1215.
[2] H. Maeda, J. Wu, T. Sawa, Y. Matsumara.,*J. Controlled Release,* **2000,** 65, 271-284.
[3] R. Duncan, *Curr. Opin.Biotechnol.,* **2011,** 22, 492-501.
[4] H. R. Allcock, N. L. Morozowich, *Polym. Chem.,* **2012,** 3, 578-590.
[5] H. R. Allcock, C. A. Crane, C. T. Morrissey, J. M. Nelson, S. D. Reeves, C. H. Honeyman, I. Manners, *Macromolecules,* **1996,** 29, 7740-7747.
[6] I. Teasdale, S. Wilfert, I. Nischang, O. Brüggemann, *Polym. Chem.,* **2012,** 2, 828-834.
[7] I. Teasdale, S. Wilfert, I. Nischang, O. Brüggemann, WO 2012/031609.

S4-P45
The synthesis of water soluble dextran phosphates

Yurkshtovich N.K.*, Golub N.V., Alinovskaya V.A., Yurkshtovich T.L., Kosterova R.I.
The Research Institute for Physical Chemical Problems of the Belarusian State University, 220050, Minsk, Leningradskaya str,14.
*yurkshtovich@tut.by

The development of polymeric materials of medical use to posses prolonged and adjustable therapeutic effect is an actual and perspective direction in modern Macromolecular Chemistry. Natural polysaccharides and their derivatives, in particular the products of etherification of polysaccharides by phosphoric acid are of considerable interest among polymer mediums.[1,2]
In this work the of study phosphorylation of dextran using melt H_3PO_4 - $(NH_2)_2CO$ by the method described[3] was carried out. The influence of the etherification reaction conditions on the functional composition and yield of the zol-fraction was investigated.
The regularities of the etherification reaction of dextran, depending on composition of the mix, temperature and pressure of the reaction zone (0,15-1,0 bar) were studied. Materials with the degree of substitution by phosphate (DS_P) and carbamate groups (DS_N) 0,29-0,67 and 0,13-0,30 respectively and zol-fraction of 23,5-100 % yield were obtained.
The dextran phosphates were established to be mono-and dibasic mono-and diphosphates, which percentage depends on the system conditions. Optimum conditions for the obtaining of the stable viscous solutions of dextran phosphates have been defined.

References
1. Granja, P.L.; Pouysegu, L.; Defficux,D; Daude, G; Jeso, B.D.; Labrugere, C., Barbosa, M.A.. *J. of Appl. Pol. Sc.* 2001, **82**, 3354-3368.
2. Denizli, B.K.; Kaplan, C.H.; Zakir, M.O.; Guner Ali. *Polymer.* 2004, **45**, 6431-6435.
3. Heinze, U.; Klemm, D.; Under, E.; Piescher, F. *Starch.* 2003, **55**, 55-60.

Session 5: Polymers for technically advanced applications and energy

S5-P46
Long-term stable flexible polymeric optical waveguides

Sonja Feldbacher (1)*, Rachel Woods (1), Valentin Satzinger (2), Gregor Langer (3) and Wolfgang Kern (1,4)
(1) Polymer Competence Center Leoben GmbH, Roseggerstrasse 12, A-8700 Leoben, Austria
(2) Institute of Nano structured Materials and Photonics, Joanneum Research, A-8160 Weiz, Austria
(3) AT&S AG, Fabriksgasse 13, A- 8700 Leoben, Austria
(4) Institute of Chemistry of Polymeric Materials, University of Leoben, A-8700 Leoben, Austria
*Sonja.Feldbacher@pccl.at

1. Introduction
Polymeric optical waveguides are becoming increasingly important in the developing area of broadband communications [1]. The field of electronics is advancing rapidly, leading to further demands for faster speeds, larger data storage, smaller components and a better design of integrated optical circuits. The integration of optical interconnections on printed circuit boards (PCB's) requires precise technologies to make this emerging field possible. The microfabrication technique, two-photon photopolymerisation (2PP) can be used to produce three-dimensional structures in the sub-micron region [2]. The used material needs to fulfill a number of requirements to be a suitable candidate in this field. This includes having a high refractive index contrast between the matrix cladding material and the written waveguide core and the material must have sufficient flexibility and high thermal stability to withstand harsh processing conditions. High chemical and long-term stability is also required. This work concerns the development and characterisation of a new polysiloxane material, which is used in the application of the integration of optical interconnections on printed circuit boards.

2. Theory
To produce optical interconnects, two-photon photopolymerisation, induced by a femto-second laser is utilised in the fabrication of three-dimensional optical waveguides, embedded in a silanol terminated polysiloxane matrix material [3]. Due to the non-linear TPA (two photon absorption) process, the interaction is confined to the laser focus, making it possible to fabricate three-dimensional structures inside the optical material. The high photon density obtained in the focus of the laser results in the polymerisation of acrylate functional groups, which are attached to a polysiloxane backbone, causing an increase in the refractive index. The light guiding effect is based on the high refractive index contrast between the matrix cladding material and the written waveguide core.

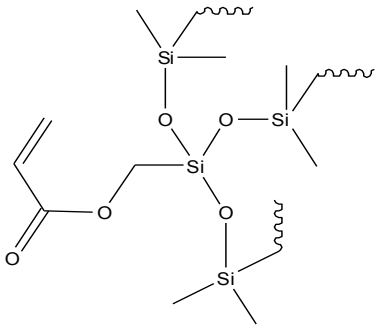

Figure 1. Acrylic functionalised polysiloxane material

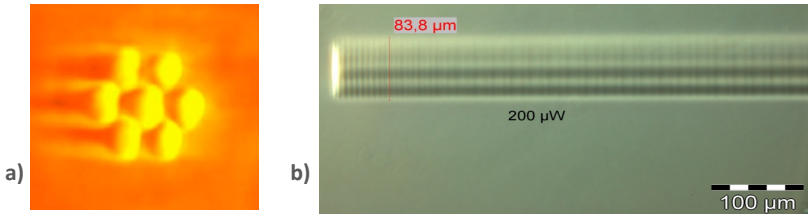

Figure 2. a) microscope image of a 2PP-sturctured waveguide bundle cross-section b) phase constrast microscope image of a waveguide bundle side view

3. Experimental

In all experiments, material mixtures were based on the silanol terminated polysiloxane cross linked with 20 wt. % acryloxymethyl trimethoxy silane (Fig. 1). 0.025-wt %N-DPD (1,5-bis(4-(dimethylamino)phenyl penta-1,4-diyn-3-one, 2PP-photoinitiator) was dissolved in the cross linker, and the polymer and cross linker were stirred for one hour during which a pre curing occurs, increasing the viscosity of the material and making the application of the material onto substrates easier to produce thin layers. Following the sample preparation, thin films were prepared by scraping the material onto substrates to give film thicknesses of between 300 and 500 µm and cured at room temperature for one hour. To structure optical waveguides, an ultra fast Ti-sapphire laser system (Mai Tai, pulse duration 120 fs, repetition rate: 1 kHz) was utilised, at a wavelength of 800 nm. Laser powers between 160-260 µW were used. The phase contrast images of the waveguide structures were studied using an Olympus BX 51 optical microscope and images were captured using a Colour View IIIu digital camera. Specially designed FR-4 PCB's were used to produce working demonstrators. The demonstrators were 10 cm x 5 cm, and consisted of a rigid base and a flexible polyimide foil. The optical interconnections on the boards consist of a VCSEL (vertical-cavity surface-emitting laser), which is mounted upright and emits light at 850 nm parallel to the substrate surface, and a photodiode. In order to structure waveguides, the optical components are fully embedded in the optical material. A bundle of waveguides were inscribed between the diodes, consisting of a centre waveguide surrounded by six waveguides (Fig. 2). Photocurrents of the demonstrators were recorded before and directly after TPA structuring using a Keithley 6485 Picoameremeter, with the laser diode driven with 6 mA by a Newport 505B Laser Diode Driver. The demonstrators were all stored in dark conditions, and the photocurrent was monitored regularly for about two years.

4. Results and discussion

The produced waveguides were characterised by phase contrast microscopy and cut back investigations to determine the optical losses. The laser powers used to structure the waveguides affected not only the size of the cross section, but also the optical loss. Cut back measurements performed on a number of different waveguides revealed that higher laser powers resulted in waveguides with low optical losses, with two waveguides structured with a laser power of 230 and 210 µW having propagation losses of 0.43 +/- 0.30 dB/cm and 0.22 +/- 0.57 dB/cm. To investigate the cross section, short sections of waveguides were inscribed over breakable parts on the substrate, which could then be cut to obtain a clean surface. Waveguide diameters of up to 45µm were obtained. Produced demonstrators, consisting of optical interconnects mounted on fully flexible as well as on rigid substrates, yielded extremely high photocurrents of up to 200 µA respectively 300 µA, which remain stable even at elevated temperatures and during long term storage. In all measured demonstrators an increase in the photocurrent was observed after a long period of storage, proving that the waveguides improve after the TPA (two photon absorption) has taken place, giving higher photocurrents and a stronger contrast of the waveguides observed by phase contrast microscopy. It is likely the interconnecting network of the polymerised acrylate functionality in the waveguide core improves during storage.

5. Conclusions

We have developed and characterised an optical material, utilised for applications in the fabrication of three dimensional waveguides by two photon induced polymerization. The matrix material is stable enough to withstand processing requirements, is easily produced and is suitable for uses in 3D microfabrication (eg. 2PP). The waveguides were characterised by phase contrast microscopy and cut-back techniques. Optical interconnects have been fabricated by two-photon photopolymerisation (2PP) on specially designed substrates, with waveguide structures aligned correctly between optoelectronic components. Such produced demonstrators yielded high photocurrents of up to 300 µA, which remain stable even at elevated temperatures and during long-term storage.

Acknowledgements

Thanks to the partner company AT&S for attending this project and a very special thank you to Valentin Satzinger for his tireless effort and support in this project.

References
[1] M. Usui, M. Hikita, T. Watanabe, M. Amano, S. Sugawara, S. Hayashida and S. Imamura, J. Ligthwave Technol. 14 (1996), 2348.
[2] H.G. Sun, S. Kawata, APS 170 (2004) 169.
[3] R. Woods, S. Feldbacher, G. Langer, V. Satzinger, V. Schmidt, W. Kern, Polymer 52 (2011), 3031.

S5-P47
Raman and Infrared microscopical analysis of multilayer backsheets

Klaus J. Geretschläger*, Gernot M. Wallner, Jörg Fischer
Johannes Kepler University Linz (JKU), Institute of Polymeric Materials and Testing (IPMT)
Altenberger Strasse 69, 4040 Linz, Austria
*klaus_jakob.geretschlaeger@jku.at

1. Introduction
For backsheets and frontsheets of PV modules currently a variety of polymeric materials is used. Fluoropolymers which exhibit good chemical and physical properties are still dominating. However, this material is cost intensive. Therefore, alternative materials have been developed and introduced into the market. Besides, TPT backsheets based on PVF (T) and Polyester (P) many other backsheet types, also without fluoropolymers, are now commercially available. The main objective of this work is to investigate commercially relevant backsheets as to their layer structure and material composition.

2. Experimental
Various multilayer backsheet laminates were selected and categorized. Raman and Infrared microscopical techniques were implemented and applied to analyze the layer structure and materials used.

3. Results and discussion
The results showed that multilayer backsheets are mainly three layer assemblies with an average total thickness of 350 µm. The predominant core component is PET with a layer thickness of about 220 µm. Backsheets with high performance fluoropolymers exhibit often a symmetric structure. In contrast, fluoropolymer-free backsheets based on engineering thermoplastics, such as polyester (PET) or polyamide (PA) show also an asymmetric buildup, also with thermoplastic EVA as an inner layer material. The most important inorganic modifier is the white pigment TiO_2 used in the outer layers. In only two backsheets TiO_2 was identified in the middle layer. Figure 12 illustrates the typical structure of a multilayer backsheet.

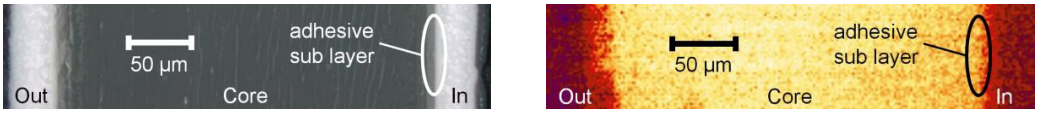

Figure 12. True colour image (Raman) and false colour image (Infrared) of a multilayer backsheet

4. Conclusions
Raman microscopy is suitable for the simultaneous identification of inorganic crystalline modifiers and organic polymeric components. Infrared microscopy is only capable to detect organic compounds. So the combination of these two techniques provides a powerful tool for backsheet analysis and classification. Due to the small thickness of the adhesive layers in further work special focus is given on high resolution Raman microscopical techniques.

S5-P48

Crosslinked poly(2-oxazoline)s as membranes with high Li^+ ion conductivity

Andrew M. Kelly (1,2)*, Bianca Wirnsberger (1,2) and Frank Wiesbrock (1,2)
(1) Polymer Competence Center Leoben GmbH, Roseggerstrasse 12, 8700 Leoben, Austria.
(2) Institute for Chemistry and Technology of Materials, Graz University of Technology, Stremayrgasse 9, 8010 Graz, Austria.
*andrew.kelly@pccl.at

1. Introduction

Lithium ion batteries are the major energy source for mobile devices and are under increasing challenges in terms of power efficiency and safety. Separators are required in these devices in order to shield the electrodes whilst still allowing for the flow of ions [1]. Polymer-based membranes are of increasing interest as materials for this purpose due to their ability to allow ion transfer and maintain thermal stability.

2. Experimental

2-Ethyl-2-oxazoline **EtOx**, 2-phenyl-2-oxazoline **PhOx**, and phenylene-1,3-bis-(2-oxazoline) **PBO** were used to prepare hydrogels under solvent-free conditions utilizing methyl tosylate as initiator for the cationic ring-opening polymerization. Copolymers from reaction mixtures containing varying reactant ratios were prepared. The reactants were added to a screw vial (4 mL, d = 12 mm) under an inert atmosphere and heated at 140 °C for 45 minutes yielding the required hydrogel.

3. Results and discussion

Crosslinked poly(2-oxazoline)-based hydrogels were chosen as materials in this study due to their well-defined 3-D structures that meet many prerequisites of applicable separator materials [2,3]. The example gel p**EtOx**$_{100}$p**PhOx**$_{50}$p**PBO**$_6$ was synthesized and subsequently impregnated with solutions of $LiClO_4$ through diffusion into the gel in its swollen state. The gels were swollen in 5/10/20 wt.-% aqueous $LiClO_4$ solutions on the one hand and in 5/10 wt.-% solutions of $LiClO_4$ in propylene carbonate on the other. Lithium ion conductivities of the impregnated gels were determined by impedance measurements (frequencies of 1 kHz to 1 MHz). In case of the water systems, the conductivity increased with electrolyte content to a maximum of $1.46 \cdot 10^{-3}$ S×cm^{-1} for 20 wt.-% $LiClO_4$. Both propylene carbonate gels displayed conductivities of around $1.75 \cdot 10^{-4}$ S×cm^{-1}. Gels swollen in aqueous solutions were characterized using scanning electron microscopy showing pore sizes in the range of 0.2 to 1.5 microns, meeting the dimensions of commercial membranes [4]. Mechanical tests revealed elastic moduli in the range from 19.3 to 33.3 MPa.

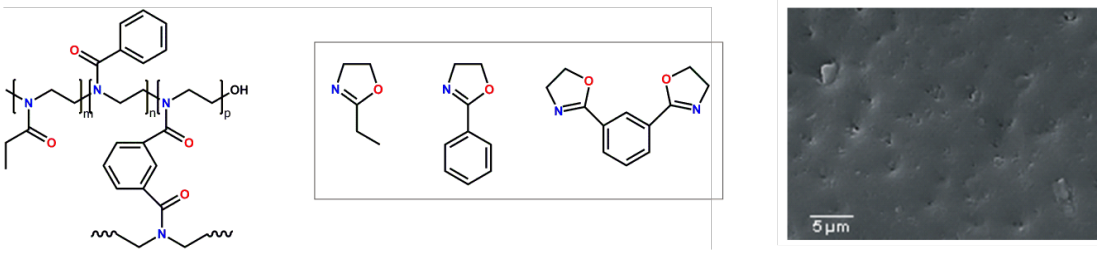

Figure 1: Structure of the poly(2-oxazoline)-based hydrogels (left), monomers used in their syntheses (center), and SEM images of a gel impregnated with an aqueous 10 wt.-% $LiClO_4$ solution showing its pore structure (right).

4. Conclusions

Poly(2-oxazoline)-based hydrogels are candidates for a wide variety of applications including membrane materials for lithium ion transfer. Suitable hydrogels were reproducibly prepared and post-synthetically swollen in lithium salt solutions. The swollen polymer networks exhibited maximum values of lithium ion conductivity in the range of 1 mS×cm^{-1} as well as well defined pore structures with pore diameters in the range of a micron, which correspond to current industry standards.

Acknowledgements

This study was performed at the Institute for Chemistry and Technology of Materials (ICTM) at the Graz University of Technology with fundings and contributions from the Polymer Competence Center Leoben GmbH (PCCL, Austria) within the framework of the COMET-program of the Austrian Ministry of Traffic, Innovation and the Ministry of Economy, Family and Youth. PCCL is funded by the Austrian Government and the State Governments of Styria and Upper Austria.

References

[1] J. Kaiser, A. Gutsch, C.-R. Hohenthanner, T. Schaffer, Lithium-Ion-Battery WO2011/009620 (2011)
[2] A.M. Kelly, F. Wiesbrock, *Macromol. Rapid Commun.* 2012, 33, 254-288.
[3] B. Unal, R.J. Klein, K.R. Yocca, R.C. Hedden, *Polymer* 2007, 48, 6077-6085.
[4] M. Park, X. Zhang, M. Chung, G.B. Less, A.M. Sastry. *J. Power Sources* 2010, 195, 7904-7929.

S5-P49
Aspects of the photophysical behavior of MEH-PPV in thin films, solution and blends: a multicolored signature

Henrique Camargo, Tatiana D. Martins*
Chemistry Institute/Federal University of Goias, campus II, P.O. Box 24242, zip code 74690-970, Goiania/GO, Brazil
*tatiana@quimica.ufg.br

1. Introduction
This work presents an detailed description of the poly[2-methoxy-5-(2'-ethylhexyloxy)-p-phenylene vinylene] (MEH-PPV) photophysical behavior, at distinct forms, from dilute solutions in good and non-solvents to thin films obtained from these very solutions and when part of a blend. Samples were evaluated by several spectroscopic methods, including steady-state, and time-resolved fluorescence spectroscopies, electronic, confocal and fluorescence microscopies and nuclear magnetic resonance. Data showed that spectral behavior of these samples, combined with microscopy information can be used to identify singular emitting species into the bulk of MEH-PPV.

2. Theory
Poly(phenylenevinylene) derivatives has attracted the attention of the scientific community specially due to their mechanical, morphological and optical properties. Solutions, thin and thick films of these materials, prepared by several methods have been reported and they have been classified over their optical responses. Although considering the enormous aspects influencing their properties that are related to the preparation methods choice, there is a consensus around the influence of preparation over molecular conformation, which is responsible for aggregation and, consequently, to the inter and intrachain communications in the system.
Although conformational issues are closely related to the photophysical behavior of PPV derivatives, electronic and energetic aspects are expected to govern the efficiency of the luminescence of such species and, for MEH-PPV, numerous singlet excited states are expected to be involved in energy migration processes even to triplet states. In this case, fluorescence lifetime measurements are useful to identify the presence of a single or multiple emitting species in a solid or solution sample and are useful to identify interchain exciton formation[1-3].

3. Experimental
MEH-PPV solutions were prepared at a concentration range from $1x10^{-9}$ to $1x10^{-7}$ mol L^{-1} in chloroform, dichloromethane, ethanol, tetrahydrofuran, acetonitrile, methanol. Thin films were spin-coated and blend with poly(methylmethacrylate) in 1% of MEH-PPV were prepared from chloroform solutions.

4. Results and discussion
Steady-state fluorescence measurements evidenced a very important blue-shift as polarity of the liquid environment increases. It follows the Lippert equation, if non-oxygenated solvents are treated separately from the oxygenated ones. This behavior is replicated in thin films produced from these same solutions.
Time-correlated single photon counting measurements evidenced that fluorescence lifetime curves as bi or multi-exponential, evidencing the presence of several emitting species in both films and solutions. These species are result of inter and intrachain communications, derived from aggregation. Aggregates emitting in the blue region are also contribute to the total emission even in good solvents.

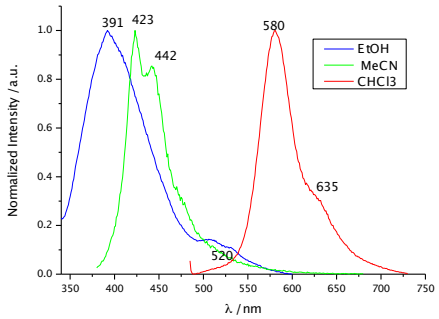

Figure 1. Fluorescence spectra of 10-7 mol.L-1 solutions of MEH-PPV in three distinct solvents.

5. Conclusions

In this work, we observed that memory of the chain conformation and the extent of aggregation of MEH-PPV in solution is carried into cast films. Also, in tightly entangled chains, the exciton migration occusr three-dimensionally whereas in extended chains, migration is in one-dimension.

Acknowledgements

Thanks to Professor Teresa Atvars from Unicamp/Brazil for time resolved fluorescence measurements and CNPq for financial support.

References

[1] A. Dogariu, D. Vacar, A. J. Heeger, *Phys. Rev. B*,**1998**, 58 10218- 10224.
[2] G.Kranzelbinder, M. Nisoli, S. Stagira, S. D. Silvestri, G. Lanzani, K. Mullen, U. Scherf, W. Graupner, G. Leising, *Appl. Phys. Lett*. **1997,** 71, 2725-2727.
[3] I. D. W. Samuel, G. Rumbles, C. J. Collison, R. H. Friend, S. C. Moratti, A. B. Holmes, *Synth. Met.***1997,** 84, 497-500.

S5-P50
Controlling film morphology for best FET sensor response

Pramod Kumar (1), Vlad Medvedev (1)*, Olga Solomeshch (1), K. N. Shivananda (2), Yoav Eichen (2), Nir Tessler (1)

(1) Nanoelectronic Center, Electrical Engineering Department, Technion, Haifa 32000, Israel
(2) Schulich Faculty of Chemistry, Technion, Haifa 32000, Israel
*medvedev@ee.technion.ac.il

1. Introduction

Organic field effect transistor (OFET) sensing devices combine many advantages of organic electronics, such as semiconductor diversity, and low-cost processing. In this study, the degree of crystallization and grain boundaries are varied through structural modifications as well as solution processing and the effect on sensing capabilities is analyzed. The chemical structure synthetic modifications are based on “Click chemistry” where the preparation of organic electronic materials takes place similar to LEGO bricks assembled to form various structures. This has allowed us to build complex π-conjugated structures and fine-tune these materials1. Using this method one can “click” in units that would react with specific analytes so that when incorporated within an OFET structure it would function as molecular sensor.

It is established that for sensing to be efficient the analytes should penetrate the film so that they can affect the transistor channel region, In this context, the role of grain boundaries has been shown to be important in providing diffusion paths as well as reaction sites. To this end we studied the crystallization and grain boundary formation for a range of chemical structures and a series of processing conditions. In the first part of this study, we do not “click” in specific recognition sites and analyze the effect of grain boundaries through the transistor response to the presence of oxygen and water vapors.

2. Experimental

Using click-chemistry approach we synthesized the molecule in figure 1 the synthesis procedure of which is described in [1]

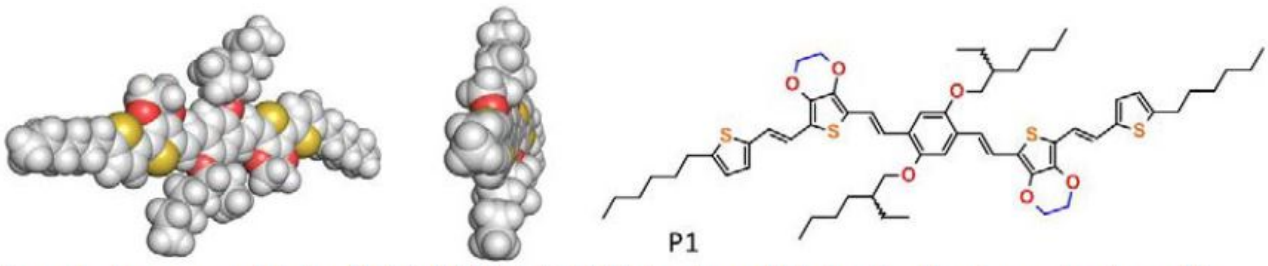

Figure 1. An energy minimized (DFT, B3LYP/6-31G(d)) structure of P1 showing the planer structure of it.

We found that the microstructure formation has two distinct regimes. First, the potential instantaneous crystallization of the oligomer during the spin coating process which is highly dependent on the solution concentration. Second, The crystallization during the post annealing which is highly temperature dependent. The effect of these two regimes is depicted in figure 2.

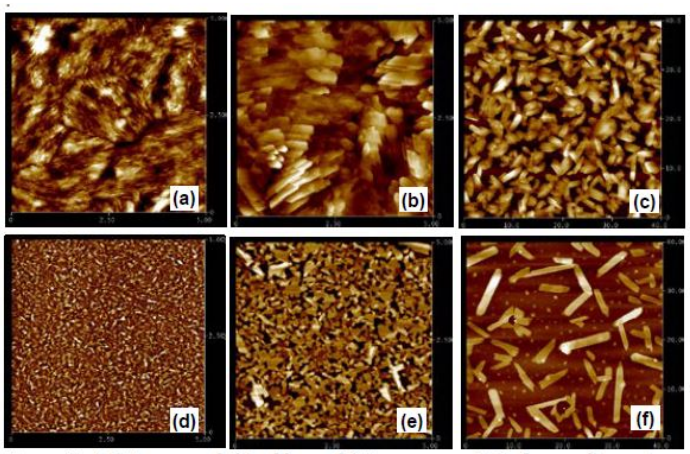

Figure 2. AFM scans of thin films of P1 grown on SiO_2 from after spin-coating films from two different THF solutions having concentrations: 10mg/mL (a, b and c) and 1mg/mL (d, e and f). the films were annealed at different temperatures: 30°C (a and d); 110°C (b and e) and 150°C (c and f).

As the figure 3 shows we found a high selectivity for diffusion of analytes which is correlated to inter-grain spaces or voids. "Clicking" in specific recognition sites allows to extend this study to effects associated with the detection of TNT related vapors. **-30-20-**

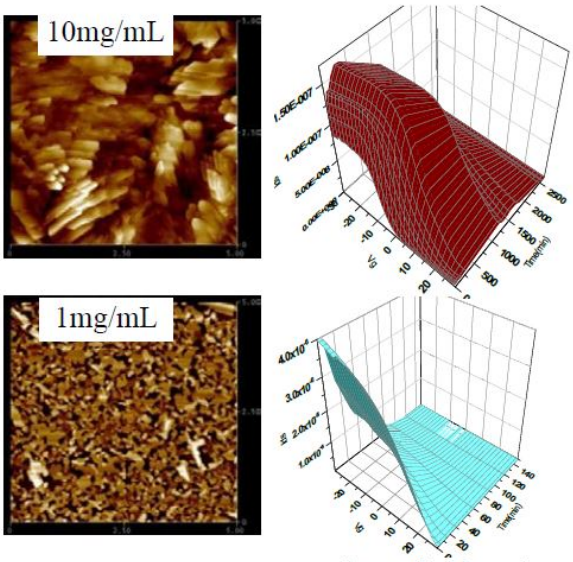

Figure 3. Response current curve upon exposure to gas flow and its dependence on the film morphology

5. Conclusions

By controlling the film morphology one can optimize the device performance in terms of mobility or in terms of sensitivity to analytes.

Acknowledgements

This work was supported by the European Commission under the FP7 Security Project CommonSense (261809).

References

[1] Kammasasndra Nanjunda Shivananda , Irit Cohen , Elena Borzin , Yulia Gerchikov , Michal Firstenberg , Olga Solomeshch , Nir Tessler , and Yoav Eichen, Adv. Func. Mater. 22, 1489(2012).

[2] Firstenberg, M.; Shivananda, K. N.; Cohen, I.; Solomeshch, O.; Medvedev, V.; Tessler, N.; Eichen, Y. Adv. Funct. Mater. 2011, 21, 634

S5-P51

Anomalous ion exchange phenomenon

Talkybek Jumadilov (1), Dina Shaltykova (2)*, Ibragim Suleimenov (2)
(1) Institute of Chemical Sciences, 106 Valikhanova Str., 050100, Almaty, Kazakhstan
(2) Almaty University of Power Engineering and Telecommunications, 126 Baitursynov st., 050013, Almaty, Kazakhstan
*dina_65@mail.ru

1. Introduction

Electrochemical processes usually occur under condition of electric neutrality of a system as whole and its macroscopic parts separately. A set of electrochemical reactions may be quite complicated, but the deviations from neutrality usually have scale determined by Debye length only. Now we report that organic chemical reaction directly resulting in charging of a macroscopic specimen is observed. Non-zero macroscopic charge appears during long-distance interactions between two polymer hydrogels, when one network is a cross-linked polyacid, which generates moveable hydrogen ions, and another cationic hydrogel can take part in a chemical reaction of bonding of mentioned ions.

2. Experimental

A polyethyleneymine (PEI) gel having =NH groups (gel-1) was placed at the bottom of cylindrical tube filled by distillated water (or low molecular salt solution), and cross-linked polyacrylic acid (PAA, gel-2) was placed on the glass filter just above the first specimen under the upper level of water. Initially both gels were swollen in distillated water up to equilibrium state. Variations of swelling ratio as well as changing of chemical composition were measured.

3. Results and discussion

The main result of long-distance interactions between gel-1 and gel-2, which are placed in pure water, is an additional swelling, i.e. resulting swelling ratio of PAA gel is about 1.2-1.5 times higher than without interaction. Besides, additional swelling of PAA gel sufficiently depends on the distance between specimens. Here we should underline that typically swelling ratio has maximum just in pure water (in comparison with other solvents). In other words, obtaining much higher swelling ratio is surprising fact as it is. Long-distance interaction between polymer networks results in anomalous behavior of swelling ratio with increasing of salt concentration too (Fig.1). Normally the adding of salt leads to decreasing of swelling ratio [1,2]. Nevertheless, in our experiments swelling ratio increase in salt solution of relatively low concentration.

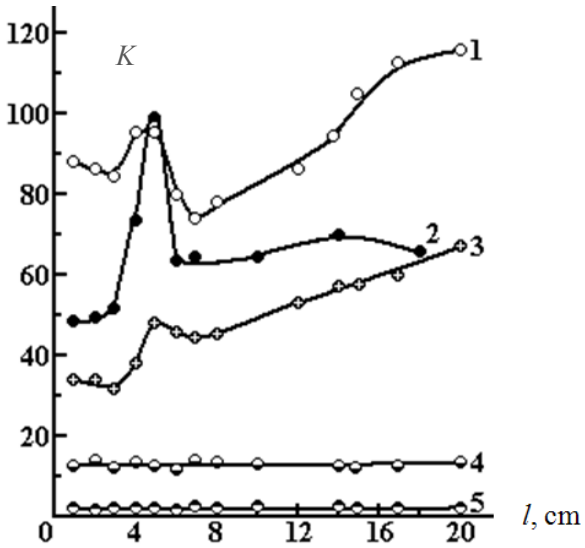

Figure 1. Formation of macroscopic charge at long-distance interaction between acceptor and donor networks

Pair of next reactions may explain long-distance interactions between two hydrogel specimens:

$R_1\text{-}COOH \leftrightarrow R_1\text{-}COO^- + H^+$ (1)

$R_2{=}NH + H^+ \leftrightarrow R_2{=}NH_2^+$ (2)

Normally reactions (1) and (2) do not break up the electric neutrality of a system, but in our case the first reaction takes place in

volume of one specimen, and the other occurs in volume of specimen which is placed at relatively long distance. Hydrogen ions generated in volume of the first sample are chemically bonding by neighboring specimen. In other words, polyacrylic acid gel (reaction 1) may be considered as a donor, and the gel-2 as an acceptor of protons (reaction 2). Consequently, in idealized case both gels obtain non-zero electrostatic charge (Fig 2), and behavior of the system now is determined by macroscopic charge distribution.

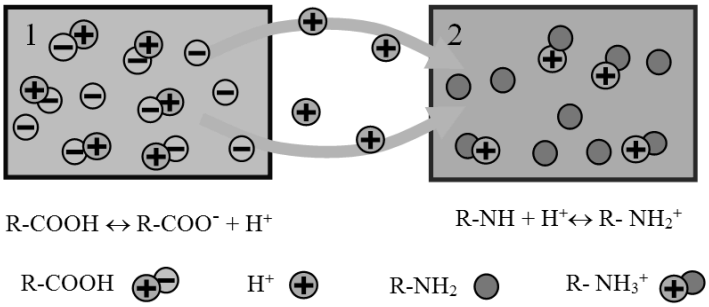

Figure 2. Formation of macroscopic charge at long-distance interaction between acceptor and donor networks

Let us supposed, that low-molecular electrolyte, potassium chloride, for example, is added in solution surrounding both gels. Obviously, negative ions will be attracted to positively charged gel, and positive ones – to PAA gel.
Next reaction may present such process schematically:

R_1-COO- + R_2=NH_2^+ + NaCl → R_1-COONa + R_2=NH_2Cl (3)

Low-molecular ions are separated between hydrogel pair in this reaction (3); besides, low-molecular salt is removed from solution into gel pair volume, i.e. anomalous ion exchange actually takes place. Normally reaction (3) cannot take place at all, but in the case of long-distance interactions between hydrogels it became quite understandable. Indeed, reaction (3) is a total of two different processes, which take place in different specimens.

We should underline that such ion exchange is namely anomalous one, while during reactions gathered by scheme (3) in PAA gel volume takes place the process correspond to next ion exchange reaction:

R_1-COOH + Na^+ → R_1-COONa +H^+ (4)

Normally such ion exchange reaction occurs in opposite direction, while degree of dissociation of R1-COOH groups is much less than degree of dissociation of R1-COONa groups.
The most obvious applications of observed phenomenon lie practically in the same field that for ion exchange (water purification, enrichment technologies, etc). Nevertheless, anomalous ion exchange has some sufficient preferences. First, the ionic exchange system based on phenomenon of long-distance interactions between hydrogels is easy renewable. Indeed, it is enough to apply mechanical stress for releasing concentrated salt solution. Second, anomalous ion exchanging gives possibility to get out arbitrary salt from solution, etc.

4. Conclusions

Thus, interactions between acid and protonized polymer hydrogels demonstrate an example of chemical process, which results in appearance of macroscopic electric charge, which can lead to anomalous ion exchange phenomena.

References

[1] A.R.Khokhlov, E.Yu.Kramarenko, *Macromolecules*, 1996, 29, 681-685.
[2] T.V.Budtova, N.G.Bel'nikevich, I.E. Suleimenov, S.Ya. Frenkel, Concentration redistribution of low molecular weight salt of metals in presence of strongly swelling polyelectrolyte hydrogels, Polymer, 1993, 34, 5154-5157.

S5-P52
Perspectives of using the Suleimenov – Mun waves in power

Bayana B.Yermukhambetova (1), Roman S.Ivlev (2), Daulet B.Kaldybekov (1,3)
(1) Scientific-research Institute of New chemical technologies and material at Al-Farabi Kazakh National University, 71 Al-Farabi ave,. 050040 Almaty, Kazakhstan
(2) Kazakh British Technical University, 59 Tole Bi str., 050000 Almaty, Kazakhstan
(3) K.I. Satpaev Kazakh National Technical University, 22 Satpaev str., 050013 Almaty, Kazakhstan

1. Introduction

The Suleimenov – Mun waves (SM waves) were originally discovered [1] in the study of surface phenomena occurring at the contact of a solid state and a cross-linked polymer network. Currently, both theoretically and experimentally, proved that there are some types of these waves [2,3] that capable to develop including in homogeneous environments at least.

On the basis of the data, at present, it is already possible to give a correct definition of the SM waves. It consists in the following. The SM waves is called that oscillation of an arbitrary nature developing in an arbitrary type of media in the area of critical parameter values. It is corresponded to phase transition occurrence and caused by the inertia of medium response to the variation of controlling parameters.

The given definition is convenient to explain on the example of thermo-sensitive macromolecule solutions possessing an upper critical solution temperature of the phase transition.

In this case, phase transition takes place at a certain temperature value of the solution. As applied to the equilibrium conditions this point can be measured with high accuracy [4]. However, at the transition to a dynamic regime there is appear a particular time delay between the moment when solution acquires the critical temperature and the time when there is a proper phase transition. This factor [4] relates to the fact that at temperature up to the phase transition macromolecules are in swollen coils which the degree of swelling can be easily evaluated based on the degree of swelling of cross-linked polymer networks (10,000 grams of water per one gram of dry matter). The phase transition is resulted by partial or complete loss of solubility of the polymer molecules. As a rule, it is accompanied by a sharp increase in the optical density of the medium. Loss of solubility it is due to the establishment of intramolecular micelles which cannot occur without the formation of significantly more compact structures than the original swollen coil.

The transition from one state to another requires, as a minimum, movement of certain part of macromolecule fragments in a space which resulted to the appearance of phase transition inertia factor, respectively. And existence of this factor leads to the Suleimenov – Mun waves in the above mentioned temperature range.

2. Results and discussion

In this paper the behavior of copolymer solutions of acrylic acid (AA) and N-isopropylacrylamide (NIPAAM) in the phase transition have been experimentally studied.

In Figure 1, the experimental results of the measurement of electrical conductivity dependence on temperature at different pH values of above mentioned copolymer solutions were shown. Polymers with different mass ratios of hydrophobic and hydrophilic groups were used. As an example, the data for copolymer containing 80 mol.% NIPAAm and 20 mol.% AA was given.

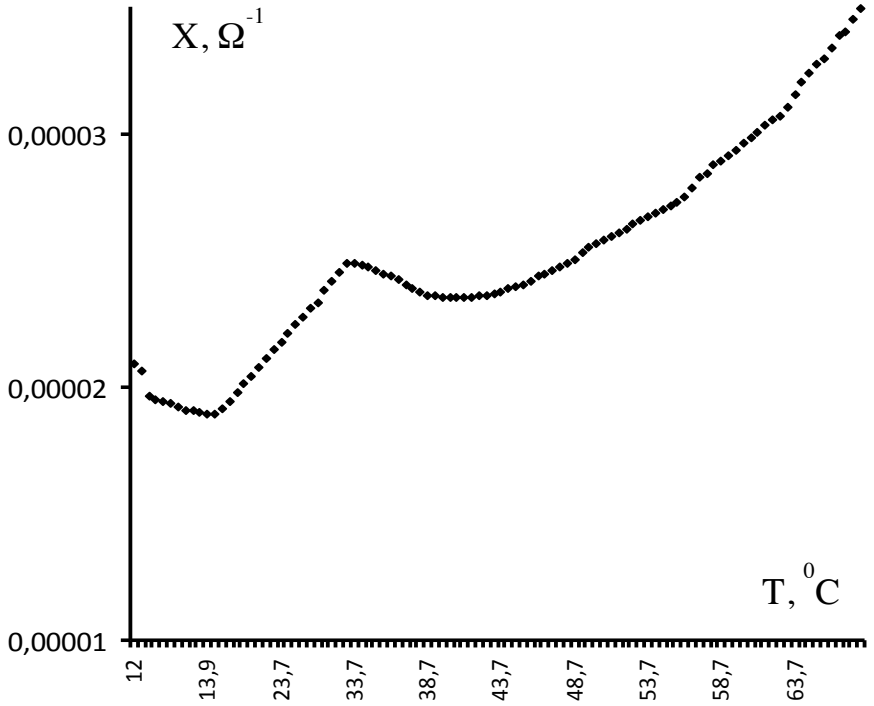

Figure 1. Dependence of electrical conductivity of NIPAAm-AA copolymer solution on temperature; [NIPAAm]:[AA]=80:20 mol.%, pH=5,5

It is seen that with increasing temperature there is a general tendency towards growth the electrical conductivity which is associated with raise of ionization degree of carboxyl groups in copolymer. Yet, the behavior of conductivity on temperature, as shown in Figure 1, indicates a significant drop in the number of mobile ions in the system in phase transition area (33,7 ^{o}C). It is expressed in the anomalous decline of electroconductivity of the solution caused, obviously, with compaction of thermo-sensitive macromolecules followed by precipitation.

Essentially, this type of waves can be excited spontaneously, and what is more it is possible to regulate the conditions of activation, in particular due to the change the phase transition temperature by adding into the solution an additional quantities of low molecular weight salt. The mechanism of this effect, as shown in this paper, is related to the change in the difference of osmotic pressure between the inner regions of the coil and the media.

In this paper, the wave character of electrical conductivity change as well as the concomitant transform in the value of osmotic pressure can be used for realization of new systems for utilization of solar radiation was shown.

The simplest example of such system is a device that converts oscillation difference of electrostatic potentials arising at propagation of the SM waves between two electrodes, in source of a direct-current or alternating-current voltage.

References

[1] I.E. Suleimenov, G.A. Mun, Izvestiya nauchno-tehnicheskogo obshestva “KAHAK”, 2012, 3 (37), 109-113.

[2] B.B. Yermukhambetova, N.V. Semenyakin, R.A. Abdykalykova, A.V Timofeyev, M.A. Dergunov, D.K. Kaldybekov, 8th International Conference on Nanosciences & Nanotechnologies ", 7 - 15 July 2011 Thessaloniki, Greece, P. 117.

[3] G. Yeligbayeva, A. Shaikhutdinova, G. Irmukhametova, V. Bublik, E. Shaikhutdinov 7th IUPAC International Conference on Novel materials and their Synthesis (NMS-VII) & 21st International Symposium on Fine Chemistry and Functional Polymers (FCFP-XXI), Shanghai, 16-21 October, 2011, P.97.

[4] Suleimenov I., Mun G., Ivlev R., Panchenko S., Kaldybekov D. Autooscillations in Proc. 2012 AASRI Conference on Modeling, Identification and Control, December, 10-20, Hong Kong, accepted

Session 6: Polymer composites and nanotechnology

S6-P53
Synthesis and properties of PVA/Au° films in the discharge of electrical alternating current

Shamshiya Amerkhanova*, Rustam Shlyapov, Aitolkyn Uali
Buketov Karagandy State University, University Street, 28, 100028, Karagandy, Kazakhstan
*amerkhanova_sh@mail.ru

1. Introduction
The rapid development of the field of polymeric materials devoted on the development of methods of synthesis and optimization of the conditions for obtaining composite polymeric materials, having in its composition nanoscale structures, and the study of their properties, is in recent decades. It is known that some of the methods aimed at obtaining nanoparticles in condensed matter, based on the use of physical effects, such as photoreduction, laser ablation, and ultrasonic treatment [1]. In this paper, the possibility of using an electric alternating current in the synthesis of gold nanoparticles in the matrix of polyvinyl alcohol was been considered.

2. Experimental
Synthesis of gold nanoparticles in a polymer matrix was carried out by the classical Turkevich method, but the reaction was influenced electric alternating current. The platinum electrodes connected to the low-frequency oscillator were immersed for creation a discharge of electric alternating field in the solution. Current frequency is 50, 500 and 5000 Hz. The duration of exposure was 1 hour.

3. Results and discussion
The dispersive analysis of gels showed that amount of the gold particle size of 25 nm is ≈ 85% at use of alternating current of 50 Hz. The exposing the gel up to 20 hours amount of particles (with size until 20 nm) is up to 45%. The amount of the particles (25 nm) was ≈ 30% after 50 hours of exposure.
It was also established that the frequency of electrical alternating current to 500 Hz, and 5000 Hz, then, does not lead to any changes. Also the sorption capacity of films based on these gels to the saturated vapor of inorganic electrolytes was been researched.

Acknowledgements
The researches were funded by a grant from the Committee of Science, Ministry of Education and Science of the Republic of Kazakhstan (state registration number 0112RK006674).

References
[1] A.Yu. Olenin, G.V. Lisichkin, *Rus. Chem. Reviews*. **2011,** 80(7)635-662.

S6-P54
PMMA nanocomposites with poly(dimethyl siloxane) surface modified ZnO

A. Anžlovar (1,2)*, Z. Crnjak Orel (1,3), M. Žigon (1,2)
(1) Center of Excellence for Polymer Materials and Technologies, PoliMaT, Tehnološki park 24, SI-1000, Ljubljana, Slovenia
(2) National Institute of Chemistry, Laboratory for Polymer Chemistry and Technology, Hajdrihova 19, SI-1000, Ljubljana, Slovenia
(3) National Institute of Chemistry, Laboratory for the Spectroscopy of Materials, Hajdrihova 19, SI-1000, Ljubljana, Slovenia
*alojz.anzlovar@ki.si

1. Introduction
Zinc(II) oxide, ZnO, is an environmentally friendly and technologically important inorganic material. Being a wide gap semi-conductor with optical band gap in the UV region it is highly efficient UV absorber. Poly(methyl methacylate), PMMA, is an amorphous optically clear thermoplastic material which is used as a substitute for inorganic glass. It undergoes ductile rather than brittle fracture, it shows higher impact strength and it has favourable processing conditions compared to inorganic glass. The composites of both ZnO and PMMA have potential applications in antireflection coatings, UV protecting films and transparent barrier/protective layers[1,2]. For the preparation of homogeneous PMMA/ZnO nanocomposites it is crucial to achieve good dispersion stability. The aim of our work is first a development of a coating procedure of nano ZnO to form an elastomer layer of poly(dimethyl siloxane) dimethacrylate, PDMS, on its surface. ZnO was synthesized from zinc acetate in various diols (ethylene glycol, 1,2-propane diol). Second, we developed the extrusion and moulding procedure or the preparation of PMMA/ZnO nanocomposites as materials with high UV absorption and enhanced mechanical properties for various outdoor applications.

2. Experimental

PMMA granulate (M_w = 100000 g/mol) was purchased from Polyciences. Nano ZnO with particle size between 20 – 50 nm was synthesized by the polyol method in EG using p-toluene sulphonic acid as an end capping agent[3,4]. It was characterized by the HR TEM and SEM microscopy, FTIR spectroscopy and XRD diffraction. ZnO nanoparticles were coated with poly(dimethyl siloxane) dimethacrylate by the precipitation from ethyl methyl ketone solution using methanol as the precipitating agent. PDMS coated nano ZnO was deposited on PMMA granules by sedimentation from dispersion in methanol. After the evaporation of methanol, the prepared PMMA granules were extruded at 210 °C in MiniLab twin screw extruder at 20 rpm. Subsequently extruded molten material was moulded at 230 °C on Mini Jet at pressure of 950 bars to prepare specimen. The distribution of ZnO nanoparticles in the PMMA matrix was studied by STEM microscopy of ultramicrotomed sections. Optical transparency and UV absorption of nanocomposites were studied by UV-VIS spectroscopy while thermal and mechanical properties (Young's modulus) were studied dynamic mechanical analysis – DMA.

3. Results and discussion

FTIR spectroscopy of coated nano ZnO confirmed the presence of PDMS elastomer coating. The distribution of ZnO nanofiller in PMMA matrix was studied by STEM microscopy of crio-ultramicrotome sections. STEM micrographs of nanocomposites with coated nano ZnO compared to those containing uncoated filler showed its more uniform distribution in polymer matrix. STEM micrographs also showed the presence of filler particles with broad particle size distribution from 100 nm to few µm indicating that nano ZnO is agglomerated during the preparation of nanocomposites. UV-VIS spectroscopy showed that PMMA granulate is UV stabilized but despite this pure PMMA material is partially transparent for UV light. By increasing the concentration of nano ZnO, the transmittance for UV light is substantially reduced (96-97%) at 0.1 wt.% and almost stopped (99%) at 0.5 wt. % of ZnO. The transparency for visible light of these specimens is also substantially reduced indicating that large ZnO agglomerates are formed which is in accordance with electron micrographs observations. DMA analysis showed that coated nano ZnO increases the Young's modulus by 15-25% in the temperature region from 35 to 65 °C while in the region between 65 and 90 °C modulus is increased by 20-40% at low concentrations of PDMS (2.4-5.2%). The largest increase in the Young's modulus was observed for specimen containing 1 wt. ZnO coated with 5.2 wt.% of PDMS. Obviously, the optimal amount of PDMS lies between 2.4 and 5.2 wt. %. On the curves of tan δ as a function of temperature the glass transition temperature shifts towards higher temperatures for 2-4 °C, but almost independently of the ZnO concentration as well as of the amount of PDMS coating.

4. Conclusions

The addition of nano ZnO coated with PDMS elastomer enhances the Young's modulus properties of PMMA/ZnO nanocomposites but the concentration of ZnO nanofiller as well as the amount of PDMS elastomer should be optimised. The UV absorption of PMMA/ZnO nanocomposites is substantially increased even at low ZnO concentrations but visible light transparency is poor either due to agglomeration of nano ZnO or due to degradation of PMMA during extrusion and moulding.

Acknowledgements

The authors acknowledge the financial support from the Ministry of Higher Education, Science and Technology of the Republic of Slovenia through contract No. 3211-10-000057 (Center of Excellence for Polymer Materials and Technologies, PoliMaT). The authors also thank Miroslav Huskić, Ph.D., of the National Institute of Chemistry for the DMA measurements, and Igor Djerdj, Ph.D., of the Rudjer Bošković institute, Zagreb, Croatia for HR-TEM microscopy.

References

[1] A. Anžlovar, Z.C. Orel, M. Žigon, *Eur. Polym. J.* 2010,46(6),1216-1224.
[2] A. Anžlovar, Z.C Orel, M. Žigon, *Materiali in Tehnologije* 2011,45(3),269-274.
[3] A. Anžlovar, K. Kogej, Z.C. Orel, M. Žigon, *e-XPRESS Polym. Lett*. 2011,5(7),604-619.
[4] A. Anžlovar, Z.C. Orel, K. Kogej, M. Žigon, *J. Nanomater.,* 2012,2012,760872.

S6-P55

The influence of mechanical activation on the thermal properties of composite polymer materials

Y. Auchynnikau (1)*, Y. Trusova (2), T. Grigorieva (3), V. Struk (1), N. Malay (2), N. Lyahov (3)

(1) Grodno State University, Faculty of engineering innovation, Ozeshko 22, 230023 Grodno, Belarus
(2) Belgorod State University, Faculty of Engineering Physics, Pobeda 85, 308015 Belgorod, Russia
(3) Institute of Solid State Chemistry and Mechanochemistry of the Siberian Branch of the Russian Academy of Sciences, Kutateladze 18, 630128 Novosibirsk, Russia
*ovchin_1967@mail.ru

1. Introduction

Mechanochemical activation of various nature to give them specific performance has a number of advantages over traditional chemical approaches to solid-phase synthesis of organic compounds. Of particular importance to the solid-phase organic synthesis using the mechanical activation (MA) has to carry out reactions that are impossible to implement in the liquid-phase version of the traditional methods and chemistry. These reactions include, in particular, surface reactions are relatively rare in terms of the formation of chemical bonds in normal media with polymeric materials. Such reactions are very promising for the preparation of compositions based on polymer matrices, modified Nanophase silicate particles. Introduction of mechanically activated silicate particles grafted polymer layer will reach a high thermodynamic compatibility of the materials in the composition, which in turn would increase the valuesof the physical and mechanical characteristics of the composite material [1-2].

2. Theory

Apply heat spectroscopy allows us to study a number of features of the structure and physico-chemical characteristics of polymeric materials and compositions thereof: melting temperature and melting temperature range, the heat of melting, annealing, and the phenomenon of relaxation, lowering the melting temperature, the degree of crystallinity, stereoregularity, identify the composition of polymer blends [7-14]. It is interesting to study the thermal characteristics of nylon, mechanically activated under different conditions. Presence in its structure of unsaturated bonds, not symmetrical structure that determines its polarity and should allow actively engage in mechanochemical reactions of interest in the formation of composite materials based on polyamides with improved performance characteristics.
The aim of this work is to study thermal properties of mechanically activated polymer particles.

3. Experimental

As the object of the investigation polymer powders and silicate. Powder polyamide 6 were obtained by cryogenic grinding granulated PA6-210/310 (JSC "Khimvolokno"), cooled to the temperature of liquid nitrogen. Dispersion of the powder used for coating, ranged from 80 to 200 microns. Mechanical activation was carried out in a planetary ball mill AGO-grade type 2. Mechanical activation time is 6 to 60 seconds, with acceleration 60 g. The polymer particles were mechanically activated together with ultra SiO_2 and kaolinite. Dispersity silicate particles ranged from 5 to 60 microns, depending on the type of modifier. Determination of thermal properties and phase transitions of the test substances was performed on the thermal analyzer SDT Q600, the heating rate of the sample was 5 º C / min.

4. Results and discussion

When combined mechanical activation of kaolinite and polyamide 6 is an interaction of radical groups and unsaturated bonds polyamide with active sites on the surface of the kaolinite crystals, which in turn increases thermal oxidation stability of the composition. Replacing kaolinite superdispersed silicate (Aerosil) in combination with polyamide 6 leads to minor changes of thermophysical properties of the composite material. Home oxidative processes in the composition is observed at 165 º C, but the intensity of the process, the melting temperature corresponds to the values as for powdered polyamide 6. Oxidation processes in the polymer melt starts from 240 º C, which indicates the low oxidative stability of the composition.

5. Conclusions

Found that the main structural component of the crystalline portion cryogenic grinding polyamide 6 is γ'-form. Conducting mechanoactivation particulate cryogenic grinding polyamide 6 increases the resistance of the polymer to thermal oxidation. Joint mechanoactivation particulate polyamide 6 with silicate particles of different nature leads to mixed results for changing thermal characteristics of polyamide. Introduction to the composition of kaolinite improves resistance to oxidation and thermal degradation, while the use of Aerosil impairs resistance to the effects of the initial polymer oxidative environment

References

[1.] Mechanochemical synthesis of dispersed layered composites based on kaolinite and higher carboxylic acids / TF Grigorieva [etc.] / / Proceedings of the Russian Academy of Sciences. - 1995. - T. 341, № 1. - S. 66-68.
[2.] Mechanochemical synthesis of dispersed layered composites based on kaolinite and a number of organic and inorganic acids. The study by IR spectroscopy / TF Grigorieva [etc.] / / Inorganic Materials. - 1996. - T. 32, № 2. - S. 214-220.

S6-P56

Synthesis, characterization and catalytic activity of gold nanoparticles protected by poly(n-vinylpyrrolidone)

Sarkyt Kudaibergenov (1,2)*, Nurlykyz Yesmurzayeva (3), Elmira Baygazieva (4)

(1) Laboratory of Engineering Profile, K.I. Satpaey Kazakh National Technical University, Satpayev Street 22, 050013 Almaty, Republic of Kazakhstan

(2) Institute of Polymer Materials and Technology, Satpayev Street 22, 050013 Almaty, Republic of Kazakhstan

(3) Department of Chemical Technology, K. I. Satpayev Kazakh National Technical University, Satpayev Street 22, 050013 Almaty, Republic of Kazakhstan

(4) Al-Farabi Kazakh National University, al-Farabi Street 271, 0500 Almaty, Republic of Kazakhstan

*ipmt-kau@usa.net

1. Abstract

Gold nanoparticles (AuNPs) stabilized by poly(N-vinylpyrrolidone) (PVP) were prepared and characterized by UV-Vis spectroscopy, DLS, and SEM. The catalytic activity of PVP-AuNPs nanoparticles supported on the surface of aluminum oxide was evaluated with respect to decomposition of hydrogen peroxide.

2. Introduction

Nowadays, gold nanoparticles (AuNPs) due to their unique properties such as optical, mechanical, electrical and catalytic activity play crucial role for industries [1-3]. Catalytic activity of AuNPs is well known since 1980's when the pioneering work of Haruta has been published [4]. Catalysts based on AuNPs and supported on metal oxides have attracted researcher's attention because of their high catalytic activity for various oxidation and reduction reactions under mild conditions [5]. In the present communication we stabilized AuNPs with poly(N-vinylpyrrolidone) having different molecular weights, determined their sizes, prepared aqueous solutions of AuNPs, immobilized them on aluminum oxide by impregnation method and studied the catalytic activity.

3. Experimental

Standard aqueous solution of tetrachloauric acid HAuCl4 with concentration 100 mg L-1 was purchased from Sigma- Aldrich. Poly(N-vinylpyrrolidone) (PVP) with different molecular weights 10 103, 40 103, 350 103 and aluminum oxide were also purchased from Sigma-Aldrich. Absorption spectra of AuNPs were determined at room temperature by UV-Vis spectroscopy (Specord 210 plus BU, Germany). The sizes of AuNPs were determined with the help of DLS device Malvern Zetasizer Nano ZS90 (UK). Concentration of Au in supernatant was determined by ion-coupled plasma atomic emission spectroscopy ICP-AES "Optima 5100DV" (Perkin Elmer, USA). Scanning electron microscopy (SEM) image was recorded on a JEOL JSM–6490LA (Japan). PVP stabilized AuNPs were obtained by "one-pot" synthetic protocol [10]. Aqueous solutions of HAuCl4 (5 mL), 0.5 M KOH (4 mL), and 4% PVP (5 mL) were mixed, stirred and heated up to 100 C during several minutes. As a result the colored solutions of AuNPs stabilized by PVP (PVP-AuNPs) were obtained as shown in Fig.1. PVP-AuNPs were supported on Al2O3 by impregnation method. For this 0.5 g of Al2O3 was added to 5 mL of PVP-AuNPs and stirred during 5 hours. After the precipitate was separated by preparative centrifuge "Eppendorf 5810R" (Germany) at 10 103 rpm, then it was washed out 5 times with distilled water. The content of Au in supernatant was determined by the ICP-AES. The precipitate was dried at 50 °C. The powders of Al2O3 with supported PVP-AuNPs (Al2O3/PVP-AuNPs) were used as catalysts for decomposition of H2O2 (Fig.2).

Figure 1. Samples of AuNPs stabilized by PVP with $M_n = 10 \cdot 10^3$ (1), $40 \cdot 10^3$ (2) and $350 \cdot 10^3$ (3)

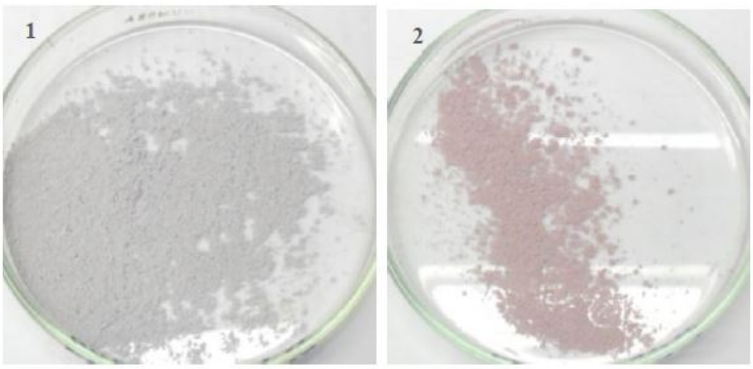

Figure 2. Samples of Al_2O_3 with immobilized PVP-AuNPs. $M_n = 40 \cdot 10^3$ (1) and $350 \cdot 10^3$ (2)

4. Results and discussion

Visible spectra of freshly prepared PVP-AuNPs show the bands with maxima at 520-550 nm corresponding to so-called "plasmon resonance" spectra that are specific for AuNPs. Figs.3 and 4 represent the size distribution of pristine AuNPs-PVP and SEM image of PVP-AuNPs supported on the surface of Al2O3.

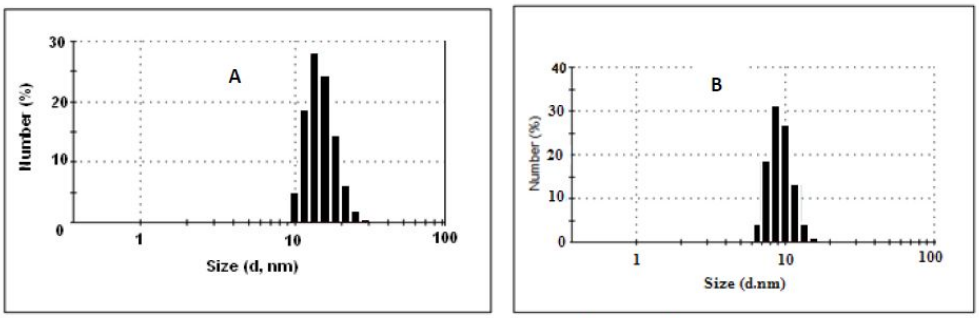

Figure 3. Size distributions of AuNPs stabilized by PVP with $M_n = 10 \cdot 10^3$ (A) $40 \cdot 10^3$ (B)

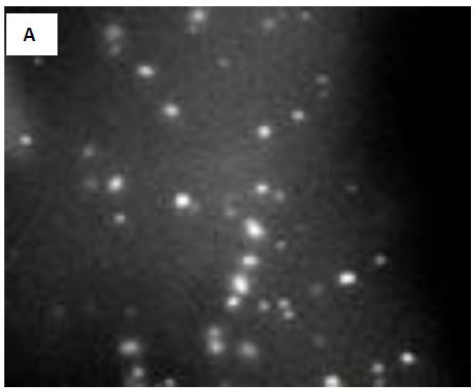

Figure 4. SEM images of PVP-AuNPs

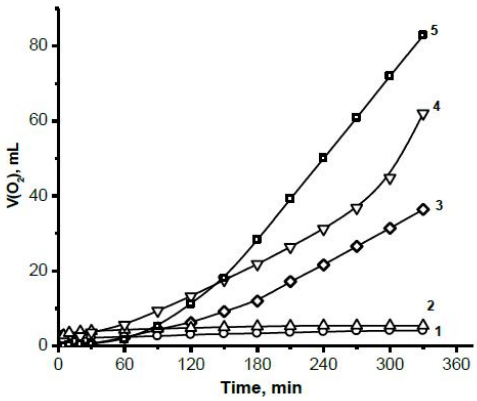

Figure 5. PVP $40 \cdot 10^3$/ Al_2O_3 (1), PVP $40 \cdot 10^3$ (2), PVP $40 \cdot 10^3$/ Al_2O_3/Au (3), PVP $10 \cdot 10^3$/ Al_2O_3/Au (4), PVP $350 \cdot 10^3$/ Al_2O_3/Au (5)

The catalytic activity of AuNPs depends on the size and amount of gold nanoparticles deposited on the surface of Al2O3. We have found that in dependence of the molecular weight of PVP the size distribution of PVP-AuNPs is varied from 10 to 20 nm. The concentration of Au nanoparticles deposited on Al2O3 is very small and equal to 0.06-0.1%. As illustrated in Fig.5, the rate of H2O2 decomposition increases exponentially while Al2O3 itself and PVP supported onto Al2O3 do not show any catalytic activity in decomposition of H2O2.

It should be noted that in the presence of Al2O3/AuNPs-PVP the rate of H2O2 decomposition exhibits an induction period that depends on the molecular weight of PVP and changes in the following order PVP-350 103 > PVP-40 103 > PVP- 10 103. As seen from Fig.5, decomposition of H2O2 in the presence of Al2O3/AuNPs-PVP-350 103 starts after 1 h while the same reaction starts immediately in the presence of Al2O3/AuNPs-PVP-10 103. This is probably explained by less accessibility of gold nanoparticles to substrate due to surrounding of catalytic centers by high molecular weight PVP.

5. Conclusions

Poly(N-vinylpyrrolidone) protected gold nanoparticles were prepared by "one-pot" method and impregnated on the surface of Al2O3. The average size of AuNPs stabilized by PVP is varied from 10 to 20 nm. The amount of deposited onto Al2O3 gold nanoparticles is extremely low and in the range of 0.06-0.1%. The catalytic activity of Al2O3/AuNPs-PVP nanocatalysts increases exponentially with induction period of time in dependence of molecular weight of PVP.

References

[1] I. Motoyuki, K. Hidehiro, *KONA Powder and particle journal,* 2009, 119-129.
[2] Suresh K. Balasubramanian, Liming Yang, Lin-Yue L. Yung, Choon-Nam Ong, Wei-Yi Ong, Liya E. Yu, *Biomaterials,* 2010, 31, 9023-9030.
[3] Jingfang Zhou, John Ralston, Rossen Sedev, David A. Beattie, *J. of Colloid and Interface Sci.,* 331, 251–262, 2009.
[4] M. Haruta, T. Kobayashi, H. Sano, N. Yamada, *Chem. Lett.* 1987, 16, 405-408.
[5] Lu-Cun Wang, Xin-Song Huang, Qian Liu, Yong-Mei Liu, Yong Cao, He-Yong He, Kang-Nian Fan, Ji-Hua Zhuang, *Journal of Catalysis*, 2008, 259, 66–74.

S6-P57
Holographicaly made polymer molds

Miha Devetak (1)*, Irena Drevenšek Olenik (2,3)
(1) CE PoliMaT, Tehnološki park 24, 1000 Ljubljana, Slovenia
(2) University of Ljubljana, Faculty of Mathematics and Physics, Jadranska 19, 1000 Ljubljana, Slovenia
(3) Jožef Stefan Institute, Department of Complex Matter, Jamova 39, 1000 Ljubljana, Slovenia
*miha.devetak@polimat.si

1. Introduction

We investigated the process and properties of 1D and 2D polymer molds. Fabrication of such structures is possible by several variations and approaches. We have successfully created and characterized one dimensional and two dimensional gratings from polymer composites filled with liquid crystals or nanoparticle solutions. The fabrication method was holographic lithography with a UV laser. Polymer molds with or without inserted nanoparticle solutions or with liquid crystals have a variety of possible applications in science and industry [1-5].

2. Theory and experimental results

12-60 micron thick gratings are produced in in-house made liquid crystal cells. Patterning is achieved by interference of 2-4 coherent laser beams emanating from a mirror based or prism based beam splitter. The origin of the laser beam is an Argon laser, operating at the wavelength of 351 nm. The resulting 1D or 2D periodic pattern triggers photo polymerized phase separation of the polymer and liquid crystal or modifies the polymer layer where the intensity is applied. Micrometer sized domains of polymerized structures under 10 micrometer regime were produced with high depth to pitch ratio. Next step in the processing of materials depends on the type of application they are produced for. By containing the liquid crystals they are suitable for switching experiments and liquid crystal characterization by addition of indium thin oxide coating on the encapsulating glass.
Empty molds were produced with removal of unprocessed polymer or removal of liquid crystal filling. Such molds could be used with or without filling.

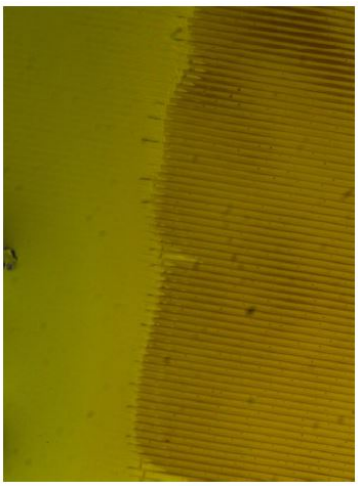

Figure 1. The figure presents the filling progression of polymer mold with a nanoparticle solution. The darker area is filled with the solution of nanoparticles progressing into empty polymer mold region.

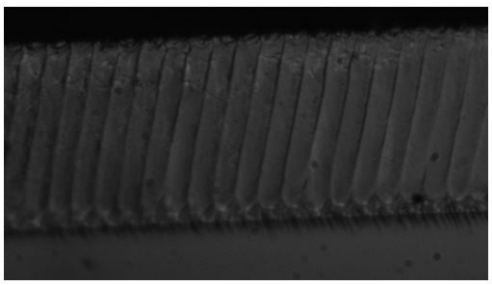

Figure 2. The figure displays the polymer-nanoparticle grating with the thickness about 55 micrometers and grating pitch of 8 micrometers. High depth to pitch ratio is desired for the use in neutron optics. Insertion of certain types of nanoparticles broadens the usability of such materials.

3. Conclusions

We have fabricated periodic molds with high depth to pitch ratio and filled them with liquid crystals and nanoparticle solutions. They will be tested for their diffraction efficiencies and other optical applications. The key is to choose proper parameters of fabrication and the technique itself to pursue the characteristics of the mold required for the targeted application.

Acknowledgements

The authors acknowledge the financial support from the Ministry of Higher Education, Science and Technology of the Republic of Slovenia through the contract No. 3211-10-000057 (Centre of Excellence Polymer Materials and Technologies).

References

[1] J. Milavec, M. Devetak, J. Li, R.A. Rupp, B. Yao, I. Drevenšek Olenik. Effect of structural modifications on the switching voltage of a holographic polymer-dispersed liquid crystal lattice. Journal of optics, 2010, vol. 12, no. 1, p015106-1- p015106-8.
[2] M. Devetak, J. Milavec, R.A. Rupp, B. Yao, I. Drevenšek Olenik. Two-dimensional photonic lattices in polymer-dispersed liquid crystal composites. J. opt. A, Pure appl. opt. (Print), 2009, vol. 11, p024020-1-p02420-8, doi: 10.1088/1464- 4258/11/2/024020.
[3] G. Moad, C. Barner-Kowollik; in Barner-Kowolik, C., (Ed.); Handbook of RAFT Polymerization, Wiley-VCH, Weinheim, 2008, p51.
[4] H. Rauch and S. A. Werner, Neutron Interferometry, Vol.12 of Neutron Scattering in Condensed Matter (Oxford University Press, New York, 2000).
[5] B. J. Gabrys. Applications of polarized neutrons to non-magnetic materials, Physica B, 1999, 267-268, p122-p130.

S6-P58

Preparation and characterization of polyurethane nanocomposites towards enhanced thermal behavior

N. V. Gama*, A. R. Valente, S. Magina, J. Coutinho, A. Barros-Timmons
(1) CICECO and Department of Chemistry, University of Aveiro – Campus Santiago, 3810-193 Aveiro, Portugal
*nuno.gama@ua.pt

1. Introduction

Polyurethanes (PU) are very commonly found in our everyday life due to their applications which range from the car industry to clothing, to building construction namely as thermal insulating material. In that sense, it is of major interest to find ways of improving their thermal behavior. The use of phase change materials (PCM) has been receiving significant attention as additives towards energy management. On the other hand the use of carbon nanotubes has also been receiving attention due to their mechanical, electric and thermal properties. Hence, in view of the low thermal conductivity of PUs the use of carbon nanotubes (CNTs) was explored aiming at enhancing the action of PCMs.

2. Theory

Polyurthane foams can be rigid, flexible or semi-rigid depending on the chemical nature of the polyol and isocyante used. [1] Due to their low thermal conductivity and low cost they are commonly used as thermal insulating materials. Yet the need for energy management requires the development of materials with enhanced thermal properties. For this reason the use of phase change materials (PCMs) has been explored by Sarier et al. [2] However, the full benefit of (PCMs) is compromised by the low thermal conductivity of PU hence, for overcome that limitation the addition of a material which with good thermal conductivity was considered. This could also bring additional benefits such as thermal stability and superior mechanical properties. [3,4]
In this study different formulations have been tested based on glycerol and methylene diphenyl diisocyanate (MDI). Next, the percentage of PCM was adjusted as well as the percentage of multiwall carbon nanotubes. Furthermore, the effect of the aspect ratio on the thermal conductivity of MWCNTs was also assessed. Figure 1 illustrates a typical SEM image of the nanocomposites obtained.

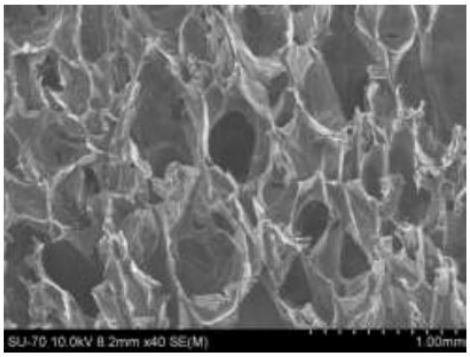

Figure 1. SEM image of PU foam containing 1w% MWCNT and 4% PCM

3. Experimental

Glycerol, TEGOSTAB B 8404 (EVONIK) surfactant, POLYCAT 34 (Air Products) catalyst and blowing agent (Water) were placed in a polypropylene cup together with the PCM material (Micronal DS 5008 X, Tm=24ºC). The mixture was homogenized using an IKA Ost Basic mixer with rotating blades, for about 20 seconds at 700 rpm. In parallel MWCNTs (previously treated with acid) were dispersed in methylene diphenyl diisocyanate (MDI) for 1 h using a Sonics Vibra Cell sonicator. The MWCNT /MDI mixture was added to the polyol mixture and stirred for 20 seconds at 700 rpm. Foams were obtained by free expansion in the mold, at room temperature.

4. Results and discussion

Various formulations were first prepared without any additives in order to adjust the base formulation. Next, formulations were prepared using different percentages of PCM and different percentages of MWCNTs. The best conditions were used to prepare the nanocomposite PU/PCM/MWCNT. In order to check the homogeneity of the materials, samples were taken from different points of along the direction of the foam expansion as illustrated in figure 2. Thermogravimetry was also used to assess the thermal stability of the nanocomposites and FTIR was used to monitor the extension of the reaction as well as the effect of MWCNTs on the kinetics of the polymerization reaction.

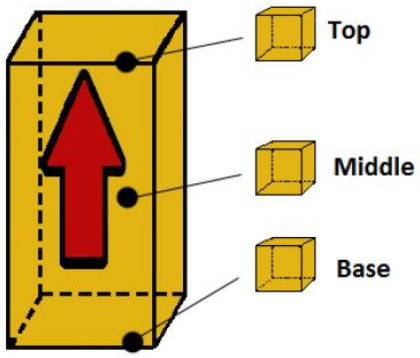

Figure 2. Sketch illustrating the points of sample collection along the foam expansion direction.

5. Conclusions

Formulations have been tested to prepare well distributed PU/PCM/MWCNTs nanocomposites along the direction of the foam expansion. The effect of the aspect ratio of the nanotubes and of its aggregation on the thermal behavior suggests that the use of MWCNTs with higher aspect ratios is required and that more work need to done in order to improve the dispersion of these nanofillers as well as reduce the thermal resistance at the PU/MWCNT interface through further functionalization of the carbon nanotubes.

Acknowledgements

The authors would like to acknowledge Doctors Mónica Oliveira and Alexandra Fonseca from Mechanical Engineering Department of the University of Aveiro for providing the carbon nanotubes and access to the thermal conductivity measurements. Also the authors would like to acknowledge Dow Chemical for kindly supply of the isocyanate. CICECO acknowledges FCT for the Pest-C/CTM/LA0011/2011 project.

References

[1] Szycher, M., Szycher's handbook of polyurethanes. 1999.
[2] Sarier, N. and Onder, E., Thermal characteristics of polyurethane foams incorporated with phase change materials. Thermochimica Acta, 2007. 454(2): p. 90-98.
[3] Han, Z. and Fina, A., Thermal conductivity of carbon nanotubes and their polymer nanocomposites: A review. Progress in Polymer Science, 2011. 36(7): p. 914-944.
[4] Dolomanova, V., Rauhe, J.C.M., Jensen, L.R., Pyrz, R., and Timmons, A.B., Mechanical properties and morphology of nano-reinforced rigid PU foam. Journal of Cellular Plastics, 2011. 47(1): p. 81-93.

S6-P59

Application of epoxy functionalized polypropylene as compatibilizer for PP/EVOH blends

Xiaoyan Meng*, Patrick Knaack, Simone Knaus
Vienna University of Technology, Institute of Applied Synthetic Chemistry, Getreidemarkt 9, 1060 Vienna, Austria
*xiaoyan.meng@ias.tuwien.ac.at

1. Introduction

Polypropylene (PP) is a widely used partially crystalline thermoplastic polymer. For example, PP films are often applied in packaging because of low cost, easy processing and good moisture barrier properties, but these films have the drawback that their barrier properties to oxygen and many organic solvents are poor. A common modification method in industry is to blend a small amount of a barrier material to obtain a low-cost product with enhanced barrier properties. For PP, ethylene-vinyl alcohol copolymer (EVOH) was found to be a good barrier candidate, and, since PP and EVOH have a poor miscibility, a compatibilizer is commonly used in such formulations. [1-4] In previous works a novel "reactive compatibilizer" (i.e. a compatibilizer bearing a functional group capable of forming a covalent bond to blend components) was synthesized by grafting of an epoxy-functional maleimide (Miepo) to PP. [5] The aim of the present work is to study the influence of the novel compatibilizer PP-g-Miepo (Figure 1), on surface tension, morphology, thermal and mechanical properties of PP/EVOH blends.

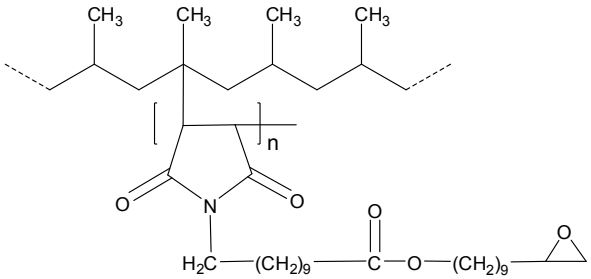

Figure 1. Structure of PP-g-Miepo

2. Experimental

Extrusion grade PP (RB307MO) was supplied by Borealis Company and EVOH with 48 mol% content of ethylene was from Eval Europe (grade: G156B). Prior to processing, EVOH was dried in a vacuum oven at 80°C for 24 h. As compatibilizer PP-g-Miepo with degrees of grafting (DG) from 0.4 to 1 wt% (synthesized in our labs by reactive extrusion) were used. Binary (PP/EVOH) and ternary (PP/EVOH/PP-g-Miepo) blends were prepared using a Haake MiniLab corotating twin-screw extruder. All components were premixed and simultaneously fed into the extruder.

Ternary blends were prepared in weight proportions of (PP+PP-g-Miepo):EVOH of 85:15, and as comparison, binary blend in weight proportions of PP:EVOH of 85:15 was also prepared. For all experiments, the screw speed was 90 rpm, the barrel temperature 230°C, and the residence time 5 minutes.

Films were prepared by hot pressing and surface tension was measured with a Kruess Static contact angle testing instrument. The morphology of the blends was studied by scanning electron microscopy (SEM). The cryofractrued surfaces of specimens were sputter-coated with a thin layer of gold and then examined. Thermal measurements were carried out under helium atmosphere with a differential scanning calorimeter. The tensile measurements were performed at a crosshead speed of 10mm/min and at 23°C using an mechanical testing instrument according to ISO 527-2 standard.The tensile test specimens were moulded by Mini-injection in accordance with ISO 527-2-5a.

3. Results and discussion

As expected, surface tension of the PP/EVOH blends is enhanced by addition of PP-g-Miepo, because of the more polar structure of the graft copolymer compared to unmodified PP. SEM photomicrographs of the blends are shown in Figure 2. After addition of PP-g-Miepo, the size of EVOH particles becomes smaller and the dispersion in the PP matrix more uniform. An increasing content of PP-g-Miepo in ternary blends causes no significant differences in morphology (see Figure 2b, 2c). On the other hand, an increase of DG of PP-g-Miepo results in a further decrease of the size of EVOH particles and the dispersion becomes more homogeneous (see Figure 2c, 2d). These results indicate that PP-g-Miepo acts as a compatibilizer improving the morphological properties of PP/EVOH blends already at low concentrations (5 wt% with respect to the total blend) and that a graft copolymer with higher DG is more effective.

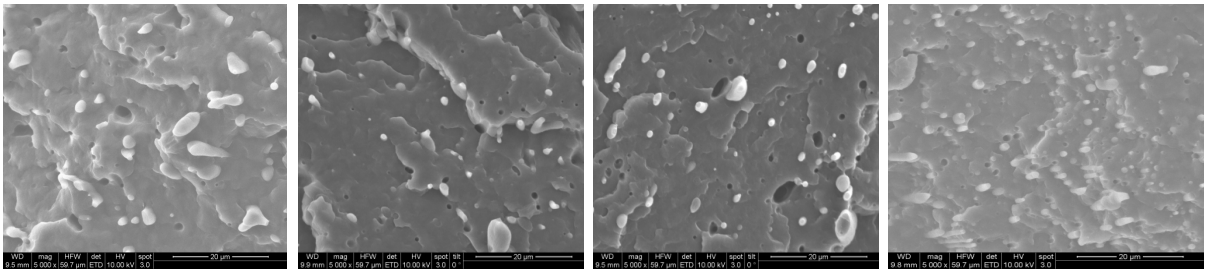

(a) (b) (c) (d)

Figure 2. SEM micrographs of cryofractured blends: (a) PP/EVOH 85/15; (b) PP/EVOH/PP-g-Miepo (DG 0.4 wt%) 80/15/5; (c) PP/EVOH/PP-g-Miepo (DG 0.4 wt%) 70/15/15; (d) PP/EVOH/PP-g-Miepo (DG 1 wt%) 75/15/10.

The thermal and mechanical properties of PP/EVOH and PP/EVOH/PP-g-Miepo blends are listed in Table 1. With increasing content of PP-g-Miepo (5 wt% to 15 wt%) the melting (T_m) and crystallization temperatures (T_c) of PP in ternary blends shift towards higher values compared to the binary blends. The slight shift of T_c indicates that the compatibilizer acts as a nucleating agent in the PP crystallization process. Addition of PP-g-Miepo to PP/EVOH blends results in a decrease of E modulus and an increase of elongation at break, whereas tensile strength at break remains basically constant. An increase of the compatibilizer content does not have a significant influence on mechanical properties. The strong influence of the DG of the graft copolymer observed in SEM images is also shown by the results of thermal analysis and tensile tests. The compatibilizer with a DG of 1 wt% is a more effective nucleating agent in the PP crystallization process, and tensile strength and elongation at break are significantly higher compared to values obtained with a DG of 0.4 wt%.

Table 1. Thermal and mechanical properties of PP/EVOH and PP/EVOH/PP-g-Miepo blends

PP (wt%)	EVOH (wt%)	PP-g-Miepo (wt%)	Degree of grafting of PP-g-Miepo (wt%)	T_m of PP (°C)	T_c of PP (°C)	E Modulus (MPa)	Tensile strength at break (MPa)	Elongtion at break (%)
85	15	-	-	145.3	106.5	1002	33.0	470
80	15	5	0.4	147.4	108.3	632	33.2	658
75	15	10	0.4	148.4	107.3	640	33.3	698
70	15	15	0.4	149.7	109.2	685	32.2	696
75	15	10	0.4	148.4	107.3	640	33.3	698
75	15	10	0.6	144.8	110.4	564	33.4	694
75	15	10	1	148.3	115.0	603	35.2	889

*Neat PP: T_m 146.7°C, T_c 111.2°C

4. Conclusions

In this work, the effects of the novel graft copolymer PP-g-Miepo, applied as compatibilizer in PP/EVOH blends, on the properties of the blends were studied. No evidence for covalent bonding of PP-g-Miepo to EVOH during melt blending was found, but the graft copolymer showed to be an effective compatibilizer for PP/EVOH. The degree of functionalization of PP-g-Miepo was found to have stronger influence on the properties of the blends than the amount of compatibilizer in the system.

Acknowledgements

The author would like to acknowledge the financial support of the China Scholarship Council.

References

[1] J.B. Faisant, A. Aït-Kadi, M. Bousmina, L. Deschênes, *Polymer*, 1998, 39, 533-545.
[2] J.H. Yeo, C.H. Lee, C.S. Park, K.J. Lee, J.D. Nam, S.W. Kim, *Adv. Polym. Tech.* 2001, 20, 191-201.
[3] M.J. Abad, A. Ares, L. Barral, I.J. Eguiazábal, *Polym. Int.* 2005, 54, 673-678.
[4] M. Montoya, M.J. Abad, L. Barral, C. Bernal, *Eur. Polym. J.* 2006, 42, 265-273.
[5] K. Wallisch, Master Thesis (Radikalisches Pfropfen von neuen Epoxy-funktionellen Monomeren auf Polypropylen), Vienna University of Technology, 2010.

S6-P60
Evaluation of tribological performance of some engineering polymer in use in bogies under railway carriages

A. Mimaroglu (1)* and H. Unal (1,2)
(1) University of Sakarya, Faculty of Engineering, Esentepe Kampusu, Adapazari, Turkey.
(2) University of Sakarya, Faculty of Technology, Esentepe Kampusu, Adapazari, Turkey
*mimarog@sakarya.edu.tr

Abstract
Polymer and polymer composites have been increasingly used in various industrial applications such as, aerospace, automotive, railway and chemical industries. This is because of these materials provided high strength/weight ratio in comparison to classic material and self-lubricant conditions. However, applications of classic polymer materials are limited due to their low mechanical, thermal and tribological properties. Therefore reinforcements are used to improve their properties. The used reinforcement and additive materials are glass fiber , $CaCO_3$, kaolin, talc, wollastonite , and mica fillers and MoS_2, graphite, carbon, wax and polytetrafluoroethylene (PTFE) as solid lubricants . Solid lubricants were proved to be generally helpful on developing a continuous transfer film between the two counterparts and accordingly reduce the frictional coefficient PA6 is a high performance engineering plastic used in electrical/electronics, automobile, packaging, textiles and consumer applications because of their excellent mechanical properties, Depending on process route PA6 are known PA6 (extruded) and a more costly Cast PA6.
The friction and wear performance of cast polyamide (Cast PA), 10%wt. graphite filled polyamide 6 (PA 6+%10G), and 10%wt. graphite and 6% wax filled polyamide 6 (PA6+%10G+6%W) sliding against stainless steel under dry sliding conditions were studied by a pin-on-disc wear arrangement. The aim was to evaluate the tribological behavior of the above materials that enable to suggest alternative material for use in bogies under railway carriages than the costly cast PA polymer composite. Tribological tests were done at sliding speed range 0.5- 2.0 m/s and under applied loads range 50- -150N. Optical microscopy utilized to examine worn surfaces of tested materials It was found that the friction coefficient of the tested materials decrease with the increase in applied load and decrease in sliding speed values The lowest wear rate is $2{,}24^{-15}$ m^2/N, for 10%wt.graphite filled PA6 composite. This suggests its use in bogies of railway carriages.

Keywords: cast polyimide; graphite; wax; friction; wear; polymer

S6-P61
Organo-modified layered double hydroxide particles carrying photoactive intercalates

Rainer Puchleitner*, Gisbert Rieß, Wolfgang Kern
Chair of Chemistry of Polymer Materials, Montanuniversität Leoben, Otto Glöckel-Straße 2, A-8700 Leoben, Austria
*rainer.puchleitner@unileoben.ac.at

1. Introduction
A novel mechanism for the production of organo-modified photoreactive LDH (Layered Double Hydroxide) systems was proposed. A silane surface-modified LDH host structure, capable of covalently bonding with a polymer matrix, was intercalated via anion exchange with photoactive azosulfonate ions. The modification steps as well as the photochemical reactions were investigated with Fourier transform infrared spectroscopy (FTIR), ultraviolet-visible spectrophotometry (UV-Vis), nuclear magnetic resonance (NMR) and thermal gravimetric analysis (TGA).

2. Theory
Polymer composites enhanced with inorganic filler systems have been extensively studied over the years. Artificially produced nanoparticles such as LDHs are of special interest due to their numerous advantageous properties such as improved tensile strength [1] thermal stability [2] or barrier properties [3].
However LDHs exhibit poor a compatibility with polymer matrices, based on their hydrophilic properties. Thus the need arises for surface modifications using intercalation agents such as sodium dodecyl sulfate [4] or similar surfactants, resulting in an organo-modified filler system [5]. LDHs exhibit a high number of hydroxyl groups on their external surfaces and edges, allowing modifications with multi-functional silanes[6.] Such modified particles may covalently bond with a polymeric matrix. [7]
Additionally LDHs are known for their capability for ion exchange and are therefore used as drug delivery [8] and controlled release systems [9]. LDHs, generally referred to as anionic clay, are composed of positively charged layers balanced by negative interlayer ions which are prone for ion exchange procedures. The goal of this work is to produce surface active particles capable of covalently bonding with a polymeric matrix, in combination with the ability to introduce a photoactive agent to the polymer residing in the interlayer space of the filler system.

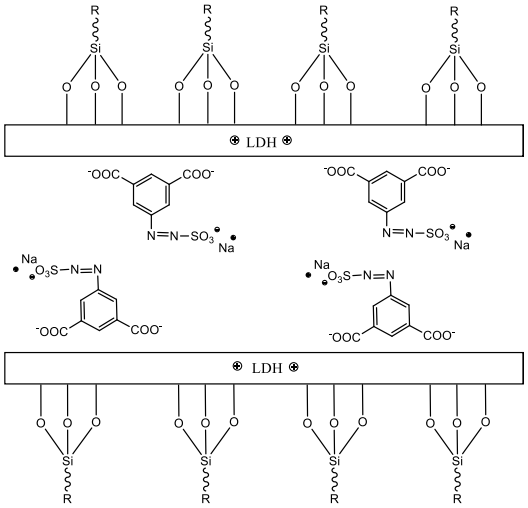

Figure 1: Schematic figure of a LDH host structure bearing a silylated reactive surface, intercalated by photoreactive azosulfonate molecules.

3. Experimental

3.1 Preparation of the photoactive intercalation agent

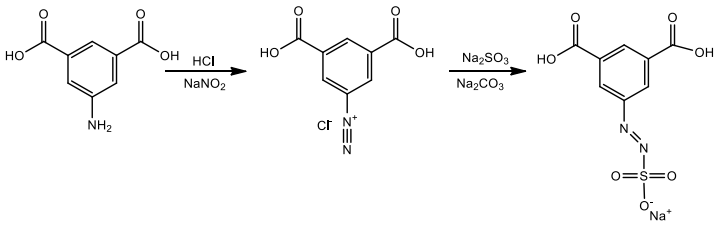

Figure 2: Preparation of the azosulfonate in a two-step process

The photoactive azosulfonate (AZO) was prepared according to the mechanisms shown in figure 2. The LDH host structure was prepared by a coprecipitation of magnesium nitrate hexahydrate ($Mg(NO_3)_3 * 6H_2O$) and aluminum nitrate nonahydrate ($Al(NO_3)_3) * 9H_2O$) in an aqueous solution using KOH to adjust the pH value. In the second step the external surfaces of the LDH were silylated via a deposition process from aqueous solution. Under acidic conditions the silane was allowed to hydrolyze forming reactive silanol groups. The LDH powder was dispersed in the solution resulting in slurry which was vigorously stirred during the silane deposition. The silylated powder was filtered, rinsed with ethanol and cured for a short time at elevated temperature. After another drying step the LDH was again dispersed in deionized water and the photoactive azoszulfonate, amounting to two times the theoretical ion exchange capability of the LDH, was added. This excess was chosen to ensure an optimum anion exchange process. The obtained orange powder was again filtered, rinsed and dried.

4. Results and Conclusion

The proposed chemical structure of the photoactive azosulfonate was confirmed using spectroscopic methods (NMR;FTIR). Additionally UV-Vis kinetics were recorded to monitor the decomposition of the azosulfonate upon irradiation with UV-light.

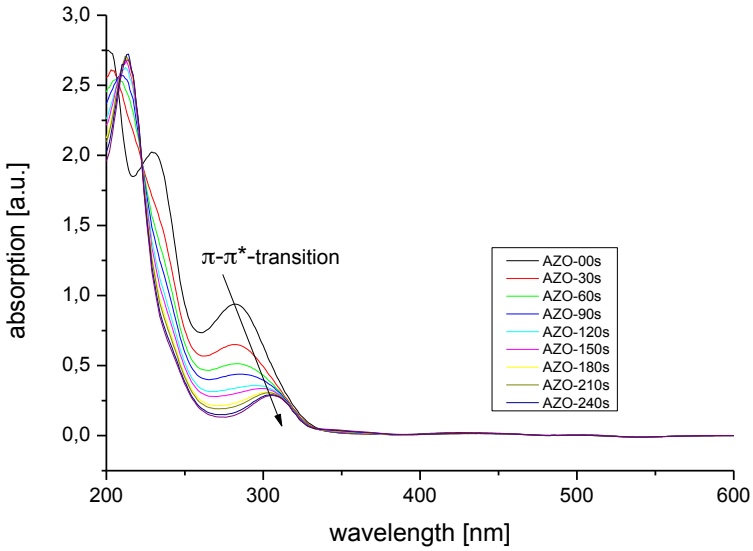

Figure 3: Decrease and shift of the absorption peak at 290 nm upon radiation with UV light due to decomposition of the azosulfonate. (AZO in aqueous solution)

The successful modification with the silane modification agents was confirmed by FTIR-and TGA-analysis. A significant increase in the weight loss of the samples as well as the emerging of bands related to the silane and azosulfonate molecules were detected. These results show, that LDHs can be successful modified to bear a reactive silylated surface for covalently bonding with a polymeric matrix and additionally deliver a photoactive azosulfonate to the composite for purposes such as UV-crosslinking (e.g. polyvinyl alcohol).

References

[1] H.-B. Hsueh, C.-Y. Chen, *Polymer* **2003**, *44*, 1151–1161.
[2] T. Kuila, S. K. Srivastava, A. K. Bhowmick, *J. Appl. Polym. Sci.* **2009**, *111*, 635–641.
[3] A. Leuteritz, B. Kutlu, J. Meinl, D. Wang, A. Das, U. Wagenknecht, G. Heinrich, *Molecular Crystals and Liquid Crystals* **2012**, *556*, 107–113.
[4] a) Y. Yuan, Y. Zhang, W. Shi, *Applied Clay Science* **2011**, *53*, 608–614. b) P. Zhang, G. Qian, Z. P. Xu, H. Shi, X. Ruan, J. Yang, R. L. Frost, *Journal of Colloid and Interface Science* **2012**, *367*, 264–271.
[5] F. Bruna, R. Celis, M. Real, J. Cornejo, *Journal of Hazardous Materials* **2012**, *225–226*, 74–80.
[6] a) Y. Yuan, Y. Zhang, W. Shi, *Applied Clay Science* **2011**, *53*, 608–614. b) Y. Sun, Y. Zhou, Z. Wang, X. Ye, *Applied Surface Science* **2009**, *255*, 4497–4502.
[7] J. Zhu, P. Yuan, H. He, R. Frost, Q. Tao, W. Shen, T. Bostrom, *Journal of Colloid and Interface Science* **2008**, *319*, 498–504.
[8] Z. P. Xu, G. Q. Lu, *Layered double hydroxide nanomaterials as potential cellular drug delivery agents*, **2006**, International Union of Pure and Applied Chemistry,
[9] Z. Xu, Z. Gu, X. Cheng, F. Rasoul, A. Whittaker, G. Lu **2011**, *13*, 1253-1264.

S6-P62
Prediction of the electrospun nanofiber morphology based on the physical characteristics of the polymer solutions

Romana Rošic (1)*, Jan Pelipenko (1), Julijana Kristl (1), Petra Kocbek (1), Marija Bešter-Rogač (2), Saša Baumgartner (1)

(1) University of Ljubljana, Faculty of Pharmacy, Aškerčeva cesta 7, 1000 Ljubljana, Slovenia
(2) University of Ljubljana, Faculty of Chemistry and Chemical Technology, Aškerčeva cesta 5, 1000 Ljubljana, Slovenia
*romana.rosic@ffa.uni-lj.si

1. Introduction

Polymer nanofibers are one of the most modern nanocomposite systems, which have been widely investigated in recent years. Efficient, reproducible, continuous one-step technology for their preparation is electrospinning, which enables the transformation of a polymer solution into solid nanofibers by using a high voltage supply [1, 2]. Since it was already shown that the solution parameters have a huge impact on the nanofiber preparation, the majority of published papers routinely examine viscosity, conductivity and surface tension of the polymer solution, meanwhile other, indeed crucial, physical characteristics are very rarely investigated [3].

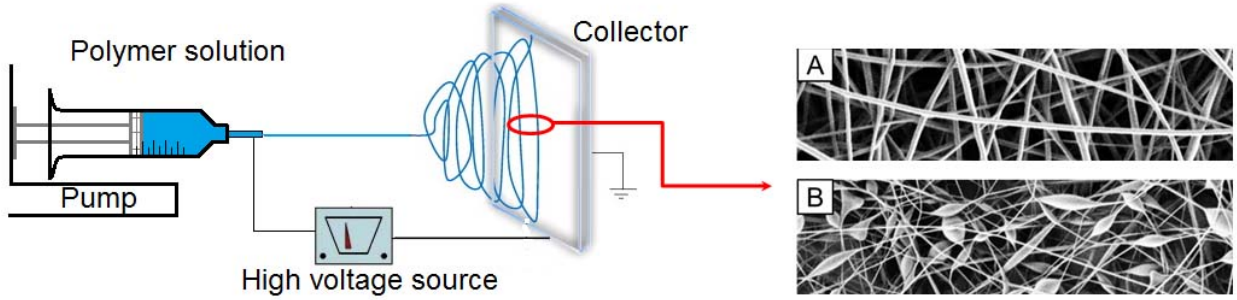

Figure 1. A sheme representing the basic of the electrospinning process and two distinctive morphologies of the obtained products.

This study is an in-depth investigation of the physical parameters carried out using poly (vinyl alcohol) (PVA) solutions in a broad concentration range, as this polymer is one of the first investigated and commonly used for nanofiber formation. Rheological properties in bulk and at the interface as well as surface tension, conductivity and small-angle X-ray scattering (SAXS) of the solutions were determined and nanofibers were produced. The aim of the research was to reveal the correlations between the source material and the obtained electrospun nanofibers plus set guidelines for the prediction of the electrospinning outcome.

2. Experimental

Preparation and physical characterization of PVA solutions: PVA solutions from 2 to 14 % (w/w) were prepared from PVA powder (Mowiol® 20-98, Sigma-Aldrich, Germany) by dissolving the polymer in distilled water at 90°C for 2 hours. The viscosity of the solutions was determined with Ubbelohde microviscometers (Analytics GmbH, Mainz, Germany); surface tension with a tensiometer K10T (Krüss GmbH, Germany) using Wilhelmy's plate method and the conductivity with a conductivity cell InLab®741 (Mettler Toledo). Rheology of the PVA solutions in bulk were measured by a Physica MCR 301 rheometer (Anton Paar, Graz, Austria) using a cone-plate measuring system. For this purpose, rotational and oscillatory test were performed. The interfacial rheological properties were determined using the same rheometer, but with an interfacial bi-cone measuring cell. The SAXS experiments were performed with an evacuated Kratky compact camera system (Anton Paar, Austria) with a block collimating unit, attached to a conventional X-ray generator (Bruker AXS, Germany) equipped with a sealed X-ray tube producing Ni-filtered Cu K_ X-rays with a wavelength of 0.154 nm (operating power was 40 kV×35 mA). All measurements were performed at 25 ± 0.1 °C.
Electrospinning and characterization of nanofibers: All PVA solutions were electrospun under the same process parameters, i.e. applied voltage 15 kV, needle-to-collector distance 15 cm, flow rate 0.707 ml/h, using planar aluminum foil as a collector. Morphology of obtained product was examined with a scanning electron microscope (Carl Zeiss, Germany).

3. Results and discussion

Viscosity, conductivity and surface tension were primarily evaluated and then an added value was given to our research with a detailed study of the bulk and interfacial rheology as well as by SAXS measurements of the polymer solutions. Results revealed that all of the measured solution parameters increased with polymer concentration (Fig. 2). Increased bulk and interfacial rheological parameters are a result of entanglements and rearranging of polymer molecules that enables more inter-polymer interactions leading to firmer structures. To the latter, the results of surface tension can also be attributed, since at lower concentrations PVA solutions behave as a solution of a surface active substance, while at higher concentration molecules have minimal effect on the surface tension and therefore measurements are close to the surface tension of the solvent. An increase in conductivity of PVA solutions despite the fact that PVA is a non-ionic polymer can be ascribed as a consequence of a residual production salts in PVA powder. Additionally, better insight into the internal molecular structure of the PVA solutions was provided by calculating the

radius of gyration (R_g), a parameter indicating dimensions of polymer chain, from the SAXS measurements (Fig. 2). Notably, we are the first one to incorporate the scattering analysis in the investigation of the solutions for electrospinning.

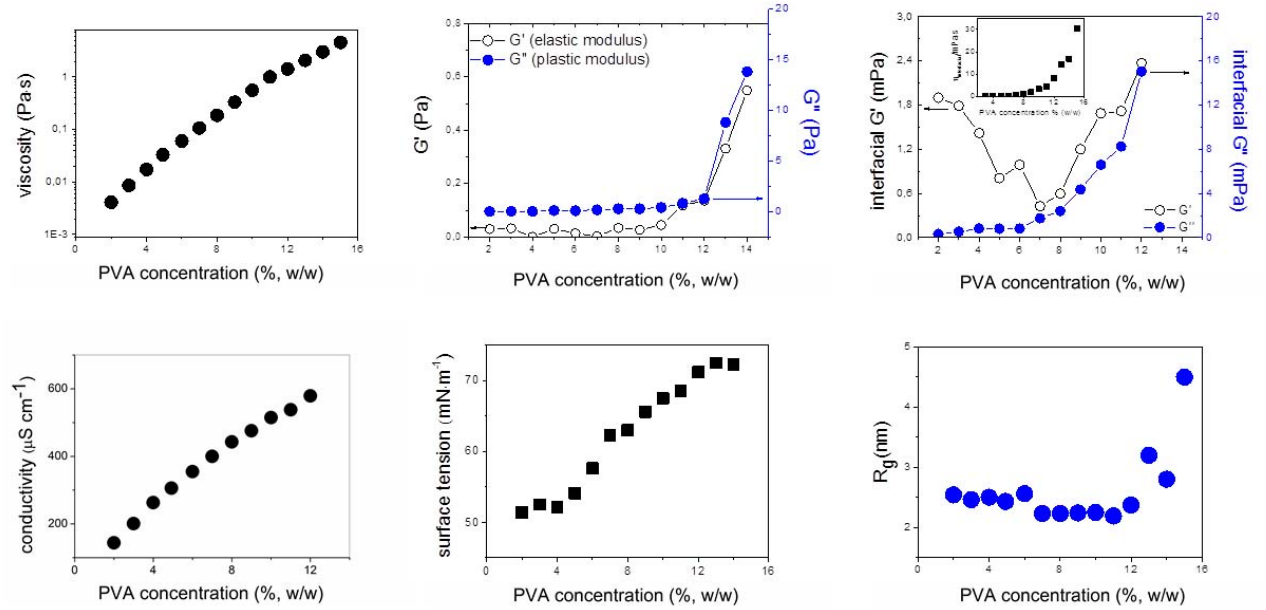

Figure 2: Measured physical parameters as a function of polymer concentration.

A detailed analysis of the combined results revealed a significant finding. The turning points, where the raising behavior of the individual parameter changes, show similar trend regardless the chosen physical property. Our results show that all measured parameters demonstrate the first turning point at a concentration ~5-6 % (w/w) and the second one at ~ 12 % (w/w) respectively, indicating that crucial rearrangements of the molecules occur in the solution at these concentrations. Even more, these turning points are in excellent agreement with the significant variations in the electrospinning process and nanofiber morphology. Our correlation analysis between the physical properties of the polymer solutions and the obtained electrospun product revealed that smooth nanofibers are formed from the PVA solutions in the concentration range from 8 to 12 % (w/w), where solutions exhibit Newtonian behavior, have viscosities in the range from 0.2 to 1.3 Pas, with a strong predominance of bulk and interfacial plasticity over elasticity, a conductivity from 0.45 to 0.6 $mS \cdot cm^{-1}$, a surface tension from 63 to 70 $mN \cdot m^{-1}$ and R_g equal to 2.2 ± 0.1 nm.

5. Conclusions

The experimental data obtained with various methods in the present study correlate well and provide an advanced understanding of the molecular behavior and motion in the PVA solutions, which are fundamental for an explanation of the outcome of the electrospinning process. Importantly, fibrous structures are formed when the polymer is predominantly in the bulk phase, since only properly firm internal polymer structures formed in the solution that are able to be oriented in the direction of an applied electric field, enable complete polymer elongation during electrospinning. Last but not the least, these findings are not advanced exclusively for PVA as a polymer, but other polymer solutions may give similar results.

References

[1] V. Beachley, X. Wen, *Prog. Polym. Sci*. 2010, 35, 868–892.
[2] J. Pelipenko, P. Kocbek, B. Govedarica, R. Rošic, S. Baumgartner, J. Kristl, *Eur. J. Pharm. Biopharm.* 2012; doi:10.1016/j.ejpb.2012.09.009
[3] R. Rošic, J. Pelipenko, P. Kocbek, M. Bešter-Rogač, S. Baumgartner, J. Kristl, *Eur. Polym. J.* 2012, 8, 1374–1384.

S6-P63
Structured polyurethane rigid foams: impact and bullet proof

Z. Safidine (1), A. Lamri (2)
(1) Macromolecular Chemistry Laboratory, Ecole Militaire Polytechnique, BEB 17, 16111 Algiers, Algeria
(2) Centre de recherche et développement, BP 66B Blida, Algeria

ABSTRACT

The field of composite materials in general and matrixes in particulate has been a great development in recent years due to their improved physical and chemical properties as well as the processes facilities. Polymers called cellular regain increasingly the field having regard to significant generated characteristics. Such matrixes reinforced with high modulus organic fibers namely commercial Kevlar®, are the main subject of research works performed at Macromolecular Chemistry Laboratory (MCL)/EMP. This work focuses on the development of composite plates within the polyurethane and/or unsaturated polyester reinforced with Kevlar® fibers. After preparing of resin injection system, adaptable to conventional methods of RTM facility "Resin Transfer Molding" and Va.RTM "Vacuum Resin Transfer Molding", we consider an appropriate technological solutions tested each time in our many trials, that used to refine and optimize our combined system to achieve good impregnation of the Kevlar® fibers with polyurethane foams and perform composite plates suitable for further evaluation. Two main characteristics, respectively the resilience of the composite plates using the Charpy test in order to estimate the impact behavior and the ballistic protection in accordance withNIJ0101.04 Standard were performed.

Keywords: *Polyurethane Foam, Kevlar composite, RTM, SRIM, resilience, ballistic test, NIJ Standard*.

S6-P64
Hybrid conducting polymer-silver composites

Jaroslav Stejskal*, Patrycja Bober, Miroslava Trchová
Institute of Macromolecular Chemistry, Academy of Sciences of the Czech Republic, 162 06 Prague 6, Czech Republic
*stejskal@imc.cas.cz

1. Introduction

The combination of conducting polymers and metals is the promising way in the design of new conducting materials [1]. Polymers are expected to provide the processing and materials properties, metals the high conductivity. Among conducting polymers, polyaniline and polypyrrole, are the most promising candidates [2]. These organic semiconductors have conductivities at the level of units S cm^{-1}. They are easily prepared by the oxidation of respective monomers and they have excellent environmental stability. Silver is the metal with the highest conductivity and cheapest among noble metals. Flexible electronics is the most straightforward application.

The responsivity of conducting polymers belongs to another attractive feature. These polymers are able to respond to external stimuli, such as pH, temperature, humidity, organic vapors, gases, etc., by the change in conductivity or in colour. This is exploited in the design of sensors. The preparation of hybrid composites is illustrated in the present communication on the composites composed of polyaniline and silver. The systems based on polypyrrole are analogous.

2. Strategy

If we abstain from the simple mixing of both components, there are two synthetic approaches to be considered in the preparation of hybrid polyaniline–silver composites. The first is based on the oxidation of aniline with silver salts, such as silver nitrate [1,3] (Fig. 1). The reaction between two non-conducting chemicals thus yield a hybrid composite composed of two conductors. The stoichiometry expect the silver content to be 68.9 wt.%. There are, of course, problems to be solved: slow reaction rate, macroscopic inhomogeneity of samples and rather unpredictable conductivity.

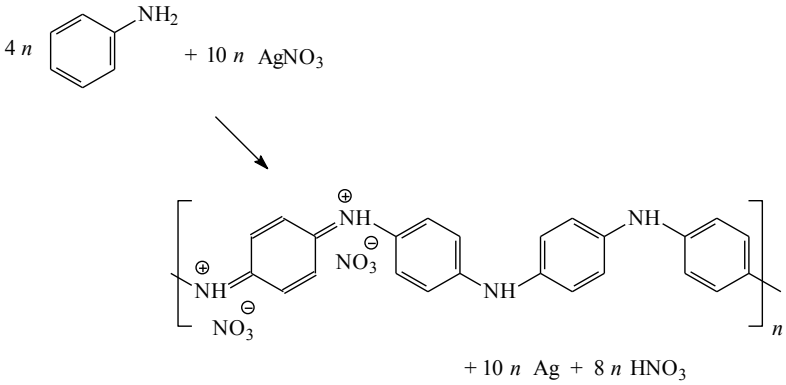

Figure 1. The oxidation of aniline with silver nitrate yields polyaniline–silver composite. Nitric acid is a by-product.

Another approach is based on the reduction of silver salts with polyaniline (Fig. 2). In the latter case, the stoichiometry predicts ≈30 wt.% content of silver.

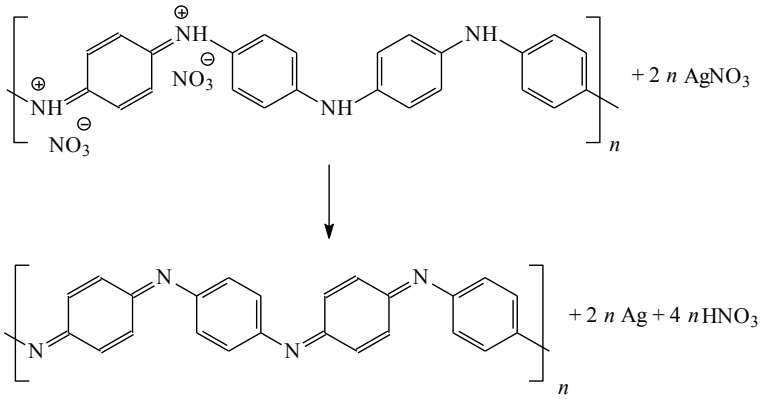

Figure 2. Polyaniline (emeraldine nitrate) is able to reduce silver nitrate to metallic silver. Polyaniline is oxidized from emeraldine to pernigraniline oxidation state at the same time.

3. Results

Not only the content of silver, but rather the morphology of hybrid composites is probably decisive in the conductivity, which varies between 10^{-5} and 10^{3} S cm^{-1}. Polyaniline can be produced as globules, nanotubes or nanorods, and the same applies to silver, which is even richer in the morphology (Fig. 3).

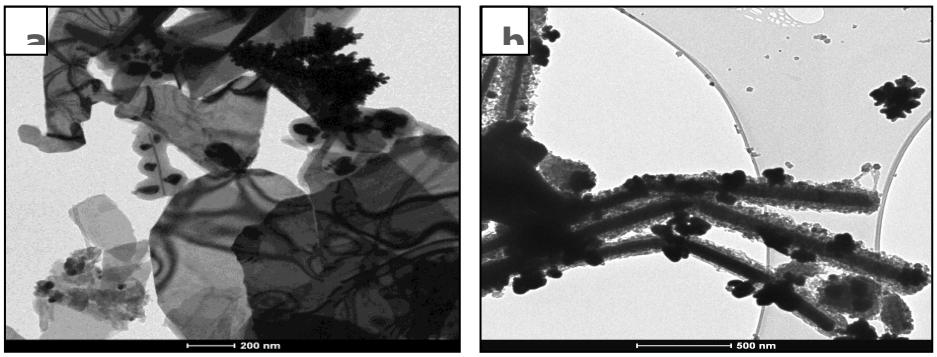

Figure 3. Examples of morphology of polyaniline and silver (dark regions) in the composites prepared by the oxidation of aniline with silver nitrate [3,4].

4. Conclusions

The simple expectation that the introduction of silver will increase the conductivity of composite is logical but turns to be false. Polyaniline–silver composites can be prepared but there are still three open problems:

(1) The control of conductivity, which is promising but, so far, rather unpredictable;

(2) the understanding of particle size and morphology of both polyaniline and silver counterparts; and

(3) the design of composite forms, which include, in addition to powders, also colloidal dispersions and thin films.

Acknowledgements
Authors than the Czech Grant Agency (202/09/1626) and Technology Agency of the Czech Republic (TE1010022) for the financial support.

References
[1] J. Stejskal, *Chem. Pap.* 2013, in press.
[2] J. Stejskal, I. Sapurina, M. Trchová, *Prog. Polym. Sci.* 2010, 25, 1420–1481.
[3] N.V. Blinova, J. Stejskal, M. Trchová, I. Sapurina, G. Ćirić-Marjanović, *Polymer* 2009, 50, 50–56.
[4] P. Bober, J. Stejskal, M. Trchová, J. Hromádková, J. Prokeš, *React. Funct. Polym.* 2010, 70, 656–662.

S6-P65
Mechanical properties of polymer nanocomposites using polycation-modified montmorillonite

Gorazd Šebenik (1)*, Miroslav Huskič (2,3), Majda Žigon (2,3)
(1) Knauf Insulation, d.o.o., Trata 32, 4220 Škofja Loka, Slovenia
(2) National Institute of Chemistry, Hajdrihova 19, 1000 Ljubljana, Slovenia
(3) Center of Excellence PoliMaT, Tehnološki Park 24, 1000 Ljubljana, Slovenia
*gorazd.sebenik@knaufinsulation.com

1. Introduction
Polymer/clay nanocomposites (PCNs) have attracted a great interest from academic and industrial researchers since by adding a small amount of clay (3-5 wt.%) they frequently attain improvement in many properties as compared to the neat polymers, e.g. improved strength, enhanced modulus, decreased thermal expansion coefficient, increased thermal stability, and reduced gas permeability [1,2]. The surface of the clay layers is hydrophilic and therefore has to be modified to ensure good intercalation with mostly hydrophobic conventional polymers. The most common method for clay modification is cation exchange with organic ammonium salts containing different numbers, length and structure of organic chains. Beside cations also polycations have been used for clay modification. Polycation-modified clay minerals have been extensively studied as catalysts or adsorbents for organic pollutants while the possibility of PNC preparation has not been extensively studied. The purpose of this study is therefore to use polyionic polyesters for clay modification and subsequent polymer nanocomposite (PNC) preparation. We assume that protonated parts of the polyester penetrate into the interlayer spaces, while unprotonated parts remain close to the external surfaces in form of loops or free chain ends. This part of macromolecule should be better miscible with polymers, such as unsaturated polyesters (UP) and epoxides (E), than quaternary ammonium salts with long alkyl chains. Better miscibility leads to enhanced intercalation and consequently improved physical and mechanical properties of nanocomposites. The effect of polyester's side-chain length, cation exchange ratio, and amount of organoclays on the morphology, mechanical and thermal properties of nanocomposites were determined.
Novel types of polyesters were synthesized from N-alkyldiethanolamines (alkyl being octyl, ODEA, dodecyl, DDEA, or hexadecyl, HDEA) and succinic acid anhydride [3]. By addition of HCl they were transferred to polyester hydrochlorides and used for montmorillonite (MMT) modification.
Unsaturated polyester (UP) and epoxy (E) nanocomposites with 1 wt.%, 3 wt.% and 5 wt.% of modified MMTs were prepared and characterized by dynamic mechanical analysis (DMA), X-ray diffraction (XRD) and thermogravimetric analysis (TGA) and their properties were compared to pure cured resins. Besides, nanocomposites with commercial modified MMTs were prepared, tested and the properties were compared.

3. Experimental
Reactants molar ratios for MMT modification (calculated from cation exchange capacity of MMT and polyester monomer unit) MMT:P:HCl were 1:3:3 or 1:3:1.5. The amount of 5 g MMT (4.25 mmol cations) and 130 ml of demineralized water were mixed together at 60 °C for 3 hours. Polyester (12,75 mmol nitrogen atoms) was dissolved in 100 ml of HCl 6.38 or 12.75 mmol HCl) at 60°C. PES HCl was added to MMT and mixed by magnetic stirrer for 21 hours at 70°C. Then the product was filtered and washed several times with demineralised water until there was no reaction of $AgNO_3$ with chlorine ions. After drying at 60°C to constant mass the modified MMT was milled to particle size of less than 50 µm. MMT modified by polyesters PH (with HDEA), PD (with DDEA) and PO (ODEA) were designated as M1, M2 and M3 (ratio 1:3:1.5) or M4, M5, and M6 (ratio 1:3:3).
Unsaturated polyester and epoxy resin nanocomposites with 1 wt.%, 3 wt.% and 5 wt.% of modified MMT (M1-M6) were prepared. Samples were cured in glass moulds at 90°C for 20 hours.
Thermogravimetric analysis (TGA) was performed on a Mettler Toledo TGA/DSC1. The samples of 15 mg were heated from 40°C to 1000 °C at a heating rate of 10 °C/min in a nitrogen atmosphere. The XRD experiments were performed on an X-ray powder diffractometer PANalytical X'Pert PRO MPD in 0.33°steps from 1.5° to 15°.

Mechanical properties were measured with a TA Q800 dynamic mechanical analyzer (DMA) at 25°C at 1Hz and a heating rate of 2 K/min.

4. Results and discussion

The XRD diffractograms of modified MMTs showed few Bragg reflections in the low-angle range. The basal spacing of MMT modified with polyesters PO, PD and PH were 1.80, 3.65 and 4.12 nm respectively, and it was independent of cation ratio. After the incorporation of modified MMTs in epoxy and unsaturated polyester resin the position of diffraction did not change significantly. The XRD diffractograms of nanocomposites with UP resin is shown in Figure 1.

The polyester content in modified MMT was determined by TGA. Weight loss increases by increasing the side chain length (Figure 2). The results of TGA analysis showed that the quantity of polyester in modified MMT is also independent of reactants ratio for PD and PH, while difference in weight loss between M3 (34%) and M6 (30%) was observed. This difference might arise from a better solubility of PO-HCl as compared to PD-HCl and PH-HCl, which leads to differences in intercalation.

The storage modulus of all nanocomposites is higher than the storage modulus of pure cured unsaturated polyester and epoxy resin. The modulus increases with increasing MMT content and decreases with increasing side-chain length of modifying polyester (Figure 3). It is evident that the polyester with a long alkyl side-chain acts as a plasticizer.

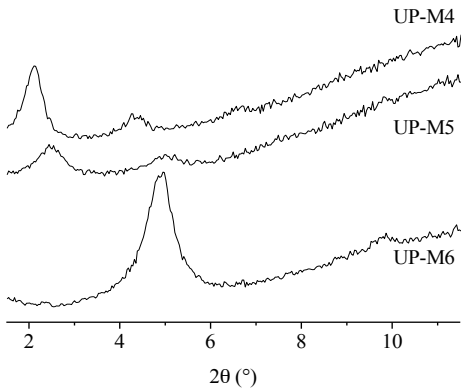

Figure 1: XRD diffractograms of unsaturated polyester resin with 5 wt.% of modified MMTs.

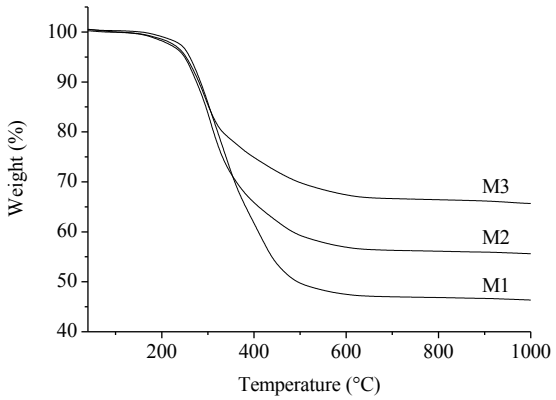

Figure 2: TGA curves of MMT modified with polyester hydrochlorides.

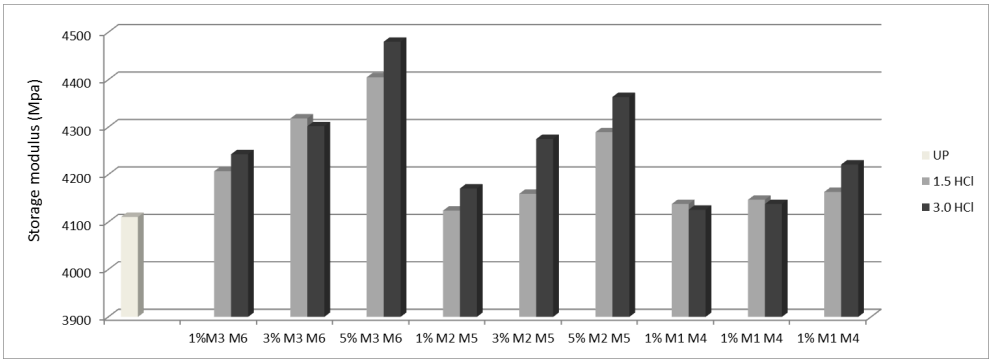

Figure 3: A comparison of storage moduli of pure unsaturated polyester and related nanocomposites in dependence of the type and quantity of modified MMT.

The glass transiton temperature (T_g) of nanocomposites was determined from the loss modulus measurements. The results confirm that the long alkyl side-chain in polyester acts as a plasticizer. Decrease in T_g was more pronounced in unsaturated polyester than in epoxy resin.

5. Conclusions

MMT was successfully modified with polyester hydrochlorides based on N-alkyldiethanolamine. Two reactants ratios were used for modification, but no big differences were observed in terms of basal spacing or quantity of modifier bound to MMT.

Intercalated nanocomposites were prepared with unsaturated polyester and epoxy resin. The storage modulus increases with increasing MMT content and decreases with the length of side-chain length in modifying polyester. The storage moduli of nanocomposites prepared with MMT, modified by polyesters with octyl and dodecyl side-chains, are higher than the moduli of nanocomposites prepared with commercial modified MMT. When polyester with hexadecyl side-chain is used, the values are approximately the same.

Acknowledgements
This study is a part of research Program P2-0145 supported by the Ministry of Higher Education, Science and Technology of Republic of Slovenia and Slovenian Research Agency. The authors are grateful for the support.

References
[1] Alexandre, M., Dubois P., Polymer-layered silicate nanocomposites: preparation, properties and uses of a new class of materials, Mat. Sci. Eng. 28, 2000, 1-63.
[2] Sinha Ray, S., Okamoto, M., 2003. Polymer/layered silicate nanocomposites: a review from preparation to processing. Prog. Polym. Sci. 28, 1539-1641
[3] Šebenik, G., Huskić, M., Žagar, E., Žigon, M., 2012. Ionic polymers with tunable liquid-crystalline properties. Polymer International 61, 451-457.

S6-P66
Nanocomposites for coatings industry application: Compatibility of solvent, copolymer and surface modified nanoparticles

Urban Šegedin (1)*, Franci Malin (1), Klemen Burja (2), Bogdan Znoj (1), Peter Venturini (1)
(1) Central R&D of Helios Group, Helios Domžale d.d., Količevo 2, 1230 Domžale, Slovenia
(2) Centre of Excellence for Polymeric Materials and Technologies, Tehnološki park 24, 1000 Ljubljana, Slovenia
*urban.segedin@helios.si

1. Introduction
Focus of present research was on preparation of nanocomposites based on high solids styrene acrylic copolymer (HS SAC) suitable for coatings industry application. Silica, alumina and montmorillonite nanoparticles with organically modified surfaces were used for improved compatibility with SACs. Extensive investigation of solvents led to improved compatibility of components, improved stability and distribution of nanoparticles throughout the dry SAC matrix.

2. Theory
Nanocomposites based on acrylic copolymers and inorganic nanoparticles have been used in coatings industry for preparation of coatings with improved properties [1-14]. Nanoparticles are defined as particles below 100 nm in size in at least one dimension [1]. Blending or physical mixing and incorporation of nanoparticles into copolymers via covalent bond (through surface modifications) enhance their mechanical, optical and thermal properties [1]. Improved resistance to mar and abrasion, resistance to UV or IR irradiance and enhanced adhesion can be detected. Films of nanocomposites remain transparent, but show enhanced hardness, rheological properties, mechanical and chemical resistance and anticorrosion protection. Insufficient dispersion process results in agglomeration and loss of nanoparticle functionality. This leads to increase in haze values and turbidity of nanocomposites. For better compatibility surface modification of inorganic nanoparticles has been used [1-5]. Several different nanoparticles can be used in same formulations – for example silica and montmorillonite [6]. In recent years *in situ* synthesis of nanoparticles has been used with polymerization and nanoparticle synthesis take place simultaneously [7-9]. So far, a lot of different inorganic materials have been described for preparation of nanocomposites suitable for coatings industry application. ZnO nanoparticles [10], nano-silica [11], montmorillonite [12-13], nano-alumina, nano-titania (in rutile or anatase mineral form), Ag, Cu, Au nanoparticles and carbon nano-rods have been studied as well [1, 14].
Literature data on compatibility of solvents, copolymers and nanoparticles is limited to surface modification of nanoparticles [12, 15] and only a few authors have considered the effect of solvent and/or copolymer [11, 16]. Some authors are misleading with inappropriate terminology when it comes to the compatibility [17, 18]. As our research shows, incorporation of nanoparticles into copolymer through covalent bond (from surface modification) cannot be treated as improved compatibility. This has been displayed as instability of original surface modified nanoparticles in different solvents. Therefore, solvent in which the SAC synthesis is preformed is also of utmost importance.

3. Experimental
Syntheses of HS SACs and nanocomposites with incorporated nanoparticles (INP) were performed on RC1*e*^{TM} reaction calorimeter (Mettler-Toledo). Stainless steel high pressure reactor HP60 was used for syntheses at elevated pressure. Nanocomposites with blended or mixed nanoparticles (MNP) were prepared by blending of HS SACs and nanoparticles post to the syntheses under dissolver stirrer and sonification. MNP were also prepared *in situ* on RC1*e*^{TM} where nanoparticle dispersions were added to the initial solvent. Silica, alumina nanoparticles and montmorillonite were used for nanocomposite preparation.
Compatibility of surface modified nanoparticles with different solvents and SAC was evaluated by the means of UV/VIS spectroscopy and gloss/haze measurements of dry nanocomposite films. Intercalation/exfoliation of montmorillonite, distribution and agglomeration of nanoparticles through the SAC matrix where evaluated by X-ray diffraction and electron microscopy (SEM, TEM). Dry film hardness, rheological and thermal properties where also evaluated. Electrochemical impedance measurements (EIS) confirmed that the flake-like structure of montmorillonite leads to improved barrier effect and superior anticorrosion protection

[19].

4. Results and discussion

Solvent testing showed that the best compatibility between solvent, SAC and surface modified nanoparticles can be reached with methoxypropylacetate as solvent. Inappropriate combination of solvent and nanoparticles resulted in destabilization and intensive agglomeration. This behavior has been observed as sedimentation or confirmed by UV/VIS measurements. MNP alumina nanocomposites show largest turbidity and haze values. These are undesirable for the application of nanocomposite in high gloss - low haze clearcoats. Best results in terms of transparency were achieved with INP silica nanocomposites that were completely transparent (**Figure 1,** right). Example of gloss and haze evaluations for different concentrations of montmorillonite in nanocomposites is also shown on the left hand side of the figure. Distribution of nanoparticles through SAC matrix has been assessed by the means of electron microscopy (SEM, TEM).

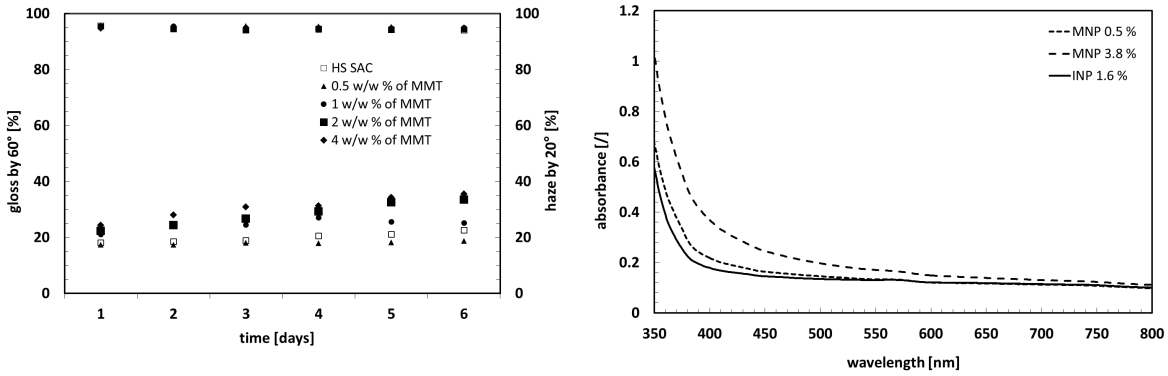

Figure 1. HS SAC – montmorillonite nanocomposites with different montmorillonite content showing high gloss and low haze (left); HS SAC – silica nanocomposites showing high transparency of INP nanocomposite compared to MNP nanocomposites (right).

6. Conclusions

In present study, the focus was on compatibility of solvent, HS SAC and surface modified inorganic nanoparticles. The solvent showing the best compatibility and stability is methoxypropylacetate. Optimal formulations for nanocomposite preparation result in low haze and high gloss of dry films. Further, enhanced stability and nanoparticle distribution, evaluated through UV/VIS measurements and electron microscopy (SEM, TEM), suggests that through proper formulation, high quality clearcoats can be prepared.

Acknowledgements

Operation was part financed by the European Union, European Social Fund. Operation implemented in the framework of the Operational Program for the Human Resources Development for the Period 2007-2013, Priority axis1: Promoting entrepreneurship and adaptability, Main type of activity 1.1.: Experts and researchers for competitive enterprises.

The authors acknowledge the support from CE PoliMaT (financially supported by the Ministry of Education, Science, Culture and Sport of the Republic of Slovenia through the contract No. 3211-10-000057 (Centre of Excellence for Polymer Materials and Technologies)) where syntheses on RC1*e*™ were performed.

References

[1] D. K. Chattopadhyay, K. V. S. N. Raju, *Prog. Polym. Sci.* **2007,** 32, 352-418.
[2] F. Deflorian, M. Fedel, S. Dire, V. Tagliazucca, R. Bongiovanni, L. Vescovo, M. Minelli, M. G. de Angelis, *Prog. Org. Coat.* **2011,** 72, 44-51.
[3] H. C. Huang, T. E. Hsieh, *Ceram. Int.* **2010,** 36, 1245-1251.
[4] D. Li, Q. Liu, L. Yu, X. Li, Z. Zhang, *Appl. Surf. Sci.* **2009,** 255, 7871-7877.
[5] K. Xu, S. Zhou, L. Wu, *Prog. Org. Coat.* **2010,** 67, 302-310.
[6] T. Yu, J. Lin, J. Xu, T. Chen, S. Lin, X. Tin, *Compos. Sci. Technol.* **2007,** 67, 3219-3225.
[7] E. Amerio, P. Fabbri, G. Malucelli, M. Messori, M. Sangermano, R. Taurino, *Prog. Org. Coat.* **2010,** 62, 129-133.
[8] Z. J. Ma, J. Hu, Z. J. Zhang, *Eur. Polym. J.* **2007,** 43, 4169-4177.
[9] W. Tanglumlert, P. Prasassarakich, P. Supaphol, S. Wongkasemjit, *Surf. Coat. Technol.* **2006,** 200, 2784-2790.
[10] A. K. Mishra, R. S. Mishra, R. Narayan, K. V. S. N. Raju, *Prog. Org. Coat.* **2010,** 67, 405-413.
[11] S. Bussell, *Polym. Paint. Col. J.* **2010,** December, 26-28.
[12] B. Essen, *Polym. Paint. Col. J.* **2010,** December, 22-24.
[13] S. Pavlidou, C. D. Papaspyrides, *Prog. Polym. Sci.* **2008,** 33, 1119-1198.
[14] F. Hussain, M. Hojjati, M. Okamoto, M. E. Gorga, *J. Compos. Mat.* **2006,** 40, 1511-1575.
[15] N. Kircher, E. Besten, U. Nolte, M. Berkei, M. Sengotta, *European Coatings Journal* **2010,** 6, 20-24.
[16] M. Huskić, M. Žigon, *Journal of Applied Polymer Science* **2009,** 113, 1182-1187.

[17] M. Azpeitia, P. Perez, I. Garmendia, *Pitture e Vernici – European Coatings* **2010**, 86, 53.
[18] O. Pyrlik, A. Nennemann, *Pitture e Vernici – European Coatings* **2010**, 86, 52.
[19] J. Sander, L. Kirmaier, M. Manea, D. Schukin, E. Skorb; Anticorrosive coatings: fundamentals and new concepts, Vincentz Network, Hanover, **2010**.

S6-P67
Mechanical properties of HDPE polymer composites filled with glass spheres, talc and calcium carbonate

Münir TAŞDEMİR*
Marmara University Technology Faculty, Dep. of Met. and Materials Eng., Istanbul 34722, Turkey
*munir@marmara.edu.tr

ABSTRACT
In the present work, high density polyethylene based composites filled with glass spheres, talc and calcite particles were prepared. Fillers contents in the HDPE were 5, 10, 15, and 20 wt%. HDPE composites filled with glass spheres, talc and calcium carbonate were prepared using extrusion compounding and injection molding. The effects of filler contents on the mechanical, morphological and thermal properties of the polymer composites were studied. The modulus of elasticity, yield and tensile strength, % elongation, Izod notched impact strength and Shore D hardness of the composites were determined.

1. Introduction
Innovations in modern technology have placed ever increased demands on advanced composite materials. Polymeric matrix composites are used in engineering applications as they present low density and high strength. However, they are not used in large scale applications due to their high cost [1]. High-density polyethylene (HDPE) is one of the most common materials because of its excellent flexibility, good process ability, and low cost. However, its use is restricted because of its lower strength, photo degradation, poor compatibility with polar inorganic fillers leads to a decrease in the mechanical properties of the composites and so on [3-6].

2. Experimental
Seventeen different polymer composites were prepared. Compositions of HDPE polymer composites that were formed are given in Table 1. Extrusion and injection conditions are given in Table 2.

Table 1: Composition of the different composite formulations

Groups	HDPE (wt %)	Glass spheres (Hollow) (wt %)	Glass spheres (filled with alumina silicate) (wt %)	Talc (wt %)	Calcium carbonate (wt %)
1	100	-	-	-	-
2	95	5	-	-	-
3	90	10	-	-	-
4	85	15	-	-	-
5	80	20	-	-	-
6	95	-	5	-	-
7	90	-	10	-	-
8	85	-	15	-	-
9	80	-	20	-	-
10	95	-	-	5	-
11	90	-	-	10	-
12	85	-	-	15	-
13	80	-	-	20	-
14	95	-	-	-	5
15	90	-	-	-	10
16	85	-	-	-	15
17	80	-	-	-	20

2. Result and discussion
Mechanical properties of the HDPE polymer composites are given in Figure 1. The relationship between the elasticity modulus and the percentage of the filler of HDPE composites is shown in the Figure 1-A. The elasticity modulus of HDPE/Glass spheres (hollow) composites increases as the filler concentration increases from 0 to 20 wt. On the other hand, the elasticity modulus of HDPE/glass

spheres (filled with alumina silicate) and calcium carbonate composites shows an increment as the filler concentration increases from 0 to 20 wt %. The results showed that the elasticity modulus of composites improved with increasing the fillers concentration. The yield strength of glass spheres (hollow and filled with alumina silicate), talc and calcium carbonate filled composites were measured, as shown in Figure 1-B. The yield strength of the hollow glass spheres, glass spheres filled with alumina silicate and calcium carbonate composites decreased linearly with increasing filler content from 0 to 20 wt %. The relationship between the ratio percentage of the filler and ultimate tensile strength of HDPE composites is shown in the Figure 1-C. Ultimate tensile strength of all composites shows a decrement as the filler concentration increases from 10 to 20 wt %. Above 10 wt % the results were not that good because the particles agglomerated at a higher percentage of talc and calcium carbonate composites. On the other hand, ultimate tensile strength of HDPE/glass spheres and HDPE/glass spheres (filled with alumina silicate) composites shows a decrement as the filler concentration increases from 10 to 20 wt%. The elongation at break of glass spheres (hollow and filled with alumina silicate), talc and calcium carbonate filled composites was measured, as shown in Figure 1-D. With increased loading, the elongation at break of the composites decreased for all. The minimum elongation at break is observed at the 20 wt % talc concentration for HDPE. Figure 1-E illustrates the effect of glass spheres, talc and calcium carbonate on the Izod impact strength (notched) of HDPE composites. The impact strength decreased as the all particles concentration increased from 0 to 20 wt. The relationship between the glass spheres, talc and calcium carbonate content and the hardness of the HDPE composites is shown in Figure 1-F. The hardness of the composites increased (from 0 to 5wt %) linearly with an increase weight percentage of glass spheres, talc and calcium carbonate. This was due to the uniform distribution of filler in the HDPE matrix.

Table 2: Extrusion and injection conditions of the HDPE polymer composites

	Extrusion	Injection
Process		
Temperature (^{o}C)	180–220	180–220
Pressure (bar)	20-30	110–140
Waiting time in mold (s)	-	15
Screw speed (rpm)	25	25
Mould temperature (^{o}C)	-	40

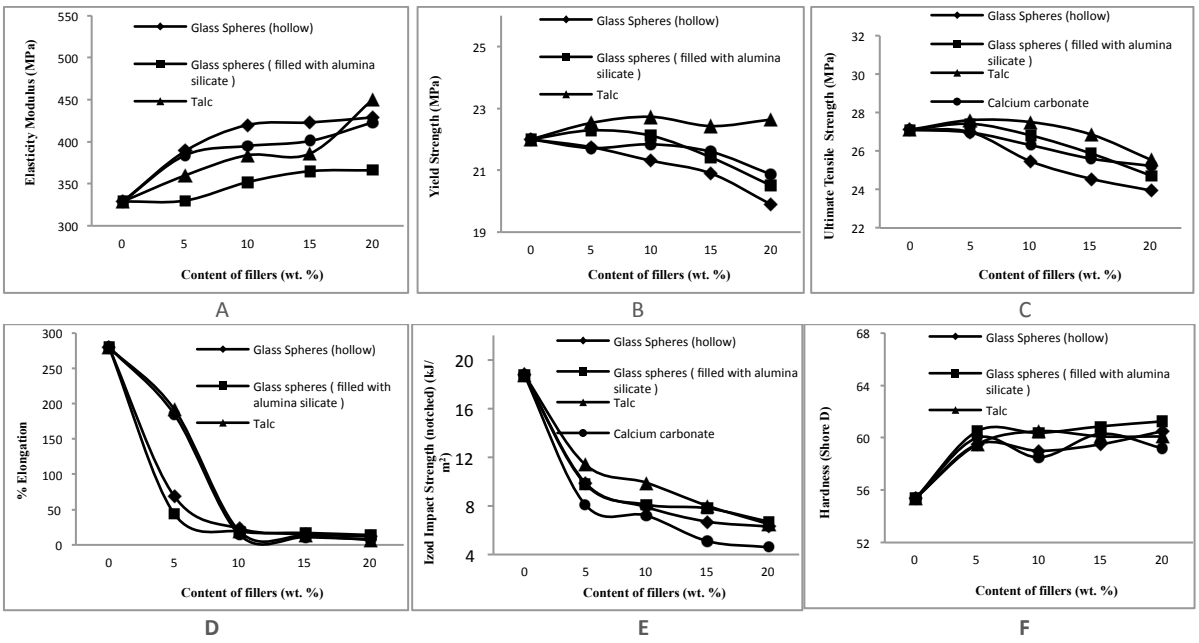

Figure 1: Mechanical properties of the HDPE polymer composites

3. Conclusions

Substantial improvements in the some mechanical properties were obtained by the addition of filler. For example, the results showed that the elasticity modulus of composites improved with increasing the filler content. This was due to the uniform distribution of filler in the HDPE matrix. Also, hardness, Vicat softening temperature and HDT values of composites improved with increasing the filler content. On the other hand, yield and tensile strength, % elongation, MFI values of the composites were decreased.

Acknowledgement

This work has been supported by the Scientific Research Project Program of Marmara University (Project no: FEN-D-130213-0044). The authors are grateful to Marmara University for their financial support and the provision of laboratory facilities.

References
[1]. S. Kalachandra, D.F. Taylor, D.C. DePorter, H.J. Grubbs, J.E. McGrath, Polymer, 1993, 34 (4), 778.
[3] S. Sahebian, S.M. Zebarjad, S.A. Sajjadi, Z. Sherafat, A. Lazzeri J Appl Polym Sci , 2007, 104, 3688.
[4] A. Ammala,A.J. Hill, P. Meakin, S.J. Pas, T.W. Turney, J Nanopart Res, 2002, 4, 167.
[5] S.C. Li, Y.N. Li, Journal of Applied Polymer Science, 2010, 116, 2965.
[6] Q. Wang, H. Chen, Y. Liu, Polym-plast Technol Eng, 2002, 41(2), 215.

S6-P68
Recycled polyamide-6/waste silk & cotton fibre polymer composites: Effect of fibre length

Münir TAŞDEMİR (1)*, Dilara KOÇAK (2), Nigar Merdan (3), Ismail USTA (2), Mehmet AKALIN (2)
(1) Marmara University, Technology Faculty, Dep. of Met. and Materials Eng., 34722, Istanbul, Turkey
(2) Marmara University, Technology Faculty, Dep. of Textile Eng., 34722, Istanbul, Turkey
(3) Istanbul Commerce University, Engineering & Design Faculty, 34378, Istanbul, Turkey
*munir@marmara.edu.tr

Summary
In this study, besides the classic textile applications, a different application area was chosen to evaluate silk and cotton wastes. Silk and cotton waste and recycled PA_6 polymer was mixed and a composite structure was obtained. Silk and cotton wastes were in fibre lengths of 1mm, 2.5 mm and 5mm. The recycled PA_6/Silk and cotton wastes were mixed in the rates of 97% / 3% respectively. The mixture was made by twin screw extruder. The samples were tested in terms of tensile strength, % elongation, yield strength, elasticity module and Izod Impact Strength.

1. Introduction
In the literature, natural fibres are used as a reinforcement material as well as mineral and glass fibres in composite structures. Studies were concentrated especially on: high density polyethylene, polypropylene, polyamide-6 and polyamide-12/wood flour, cellulose flour and cellulose fibres[1], dicumyl peroxide-modified cellulose/LLDPE composites[2], low density polyethylene (LDPE)/cellulose fibers[3], wood fibers as reinforcing fillers for polyolefins[4], polypropylene/wood fiber composites[5], jute fiber reinforced thermoplastic polymers (LDPE, HDPE, PE copolymer, and PP)[6], polypropylene (PP) and high density polyethylene (HDPE) filled with wood and cellulose flour[7]. In this study, 1, 2.5 and 5mm long cotton and silk wastes in 97%(recycled PA_6)/3%(waste fibre) mixture rate with recycled PA_6/ waste silk and recycled PA_6/ waste cotton were mixed and the composite structures produced were examined.

2. Experimental
Recycled PA_6/ waste silk and cotton polymer composites mixture rates and fibre lengths in groups are given in Table 1.

Table 1. Recycled PA_6/ waste silk and cotton polymer composite mixture ratio and fibre length

Groups	PA_6 (%)	Silk (%)	Cotton (%)
1	100	-	-
2	97	3 (Silk length: 1 mm)	3 (Cotton length: 1 mm)
3	97	3 (Silk length: 2.5 mm)	3 (Cotton length: 2.5 mm)
4	97	3 (Silk length: 5 mm)	3 (Cotton length: 5 mm)

3. Result and discussion
Mechanical properties of the PA_6/waste silk and PA_6/waste cotton polymer composites are given in Figure 1. As seen in Figure 1, the addition of 1mm length silk waste to recycled PA_6 increases the elasticity modulus of polymer composites, and increasing the length of silk decreased elasticity modules. Addition of 1mm fibre length silk waste gave the highest elasticity modulus value. The values of yield strength and tensile strength were decreased with in the first group which is 1mm fibre lengths but increased with increasing fibre lengths. With the addition of waste silk, % elongation values were decreased considerably. Hardness values were decreased slightly and Izod impact strength values of the composites were also decreased compared to 100% recycled PA_6 .The

addition of waste cotton to recycled PA_6 increases the elasticity modulus of the polymer composite. However, the increase in fibre length causes a decrease in the elasticity values. The values of yield strength and tensile strength values were decreased with increasing fibre lengths. Considerable decreases were observed on the values of % elongation with the addition of cotton waste to recycled PA_6. However, the increase in fibre lengths causes an increase in elongation values. Hardness values were also decrease with addition of cotton waste to recycled PA_6 after an initial increase in Group 2. The addition of cotton waste to recycled PA_6 to form polymer composite increases the Izod impact strength of the resultant composites with increasing fibre lengths.

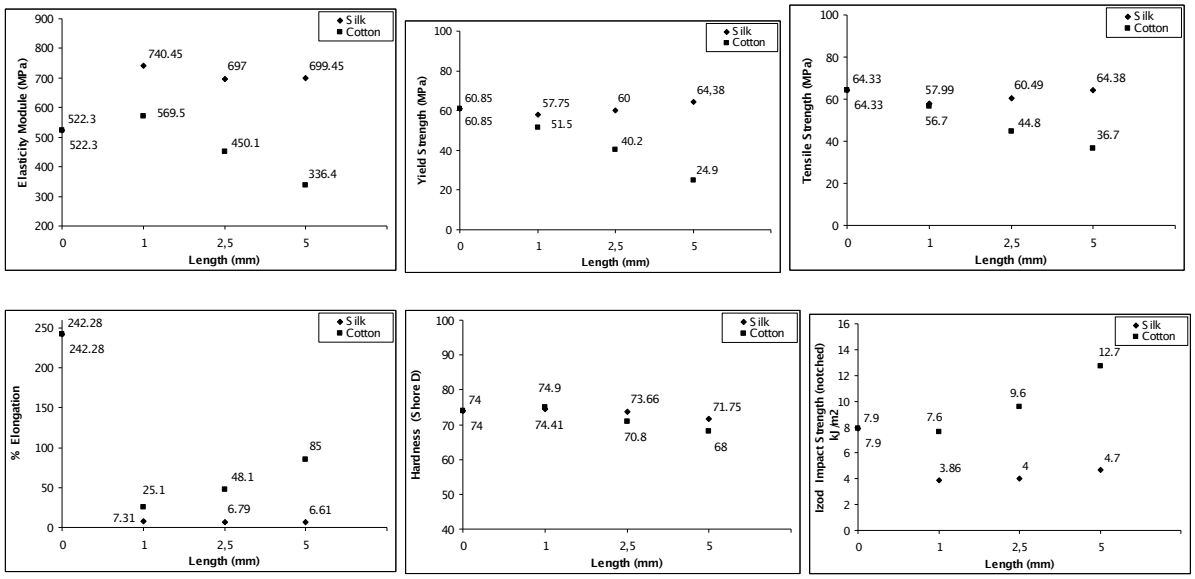

Figure 1. Mechanical properties of the PA_6/waste silk and PA_6/waste cotton polymer composites

4. **Conclusions**

There is an important increase in the elasticity modulus of the composites made up of PA_6 polymer/waste silk fibres. The amount of the increase for the composite made up with the addition of 1mm length waste silk fibres especially can be explained in terms of attachment achieved by the dimensional volume increase. Improvement in elastic modulus of the polymer composite with the addition of waste cotton fibres of 1 mm length was achieved. But, elastic modulus decrease was observed in composites made with the addition of 2.5mm and 5mm waste cotton fibres. This can be explained in relation to the waste cotton fibre dimensional volume. When flow resistance values of the composed composites are considered, because of circular segment of the silk fibre, there is no flow problem, whereas cotton fibre show flow disturbance because of non-circular segment. When tensile strength values are evaluated, there is no strength increase in either fibre added to PA_6 polymer. As silk fibre is stronger than cotton fibre, tensile values were protected as before. Elongation values of the composites seemed to decrease in waste silk and cotton fibres with PA_6 polymer. The reason for that is that polymer structure is weaker than fibres and the waste fibres are in more fragile structure As a result, with the addition of waste cotton fibres to the PA_6 polymer and elasticity modulus values of composite formed with silk fibres increase and the composite formed in both fibres meet the demanded characteristics in themselves.

Acknowledgement: This work has been supported by the Scientific Research Project Program of Marmara University (Project no: FEN-D-130213-0044). The authors are grateful to Marmara University for their financial support and the provision of laboratory facilities.

References

[1] C. Klason, J. Kubát, HE. Strömvall, Int. J. Polym. Mater. 1984, 10,159.
[2] S. Sapieha, P. Allard, YH. Zang, J. Appl. Polym. Sci. 1990, 41,2039.
[3] S. Sapieha, JP. Pupo, HP. Schreiber, J. Appl. Polym. Sci. 1989, 37,233.
[4] RT. Woodhams, G. Thomas, K. Rodgers, Polym. Eng. Sci. 1984, 24,1166.
[5] RG. Raj, BV. Kokta, C. Daneault, Int. J. Polym. Mater. 1989, 12,239.
[6] AC. Karmaker, G. Hinrichsen, Polym. Plast. Technol. Eng. 1991, 30,609.
[7] H. Dalväg, C. Klakson, HE. Strömvall, Int. J. Polym. Mater. 1985, 11,9.

S6-P69

The impact of starch and of aerosil on electrets properties of polyethylene films

Dmitry Temnov*, Elena Fomicheva, Valentin Burda, Valery Stojarov, Yuriy Gorokhovatsky
Herzen State University, nab.reki Moiki, Saint-Petersburg, Russia
*tde@herzen.spb.ru

1. Introduction

World ecology causes a lot of attention today. One of the most important environmental problems is the disposal of waste. From the time of disposal of the polymer to its decomposition are dozens of years. It is possible to reduce the time of polymer degradation adding starch, which is fast degraded and separating the polymer chains into shorter and reducing the decomposition of recycled polymer. At the same time, polymer electrets are widely used in industry, technology, and medicine, therefore ways to increase the stability of the polymer electrets materials are very interesting. Thus addition of fillers, which lead to the improvement of electrets properties of polymer and accelerate its time degradation, is an actual problem of polymer physics.

2. Experimental

Films of polyethylene (PE) with aerosol and starch fillers (thickness of 300 μm) were investigated. Time and temperature stability of the electrets state were investigated by isothermal and thermally stimulated relaxation of potential. The samples were polarized by corona discharge to the potential around 1 kV. There are results of measuring in Figures 1, 2.
Relaxation processes in composite polymers were determined by thermally stimulated depolarization (TSD).

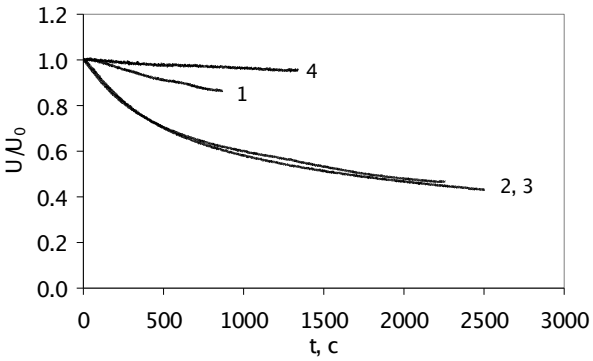

Figure 1. Time dependences of the surface potential of the polarization in the field of a negative corona discharge. T = 70°C. 1 – PE; 2 – PE + 4 vol.% starch; 3 – PE + 6 vol.% starch; 4 – PE + 4 vol.% starch + 1 vol.% aerosil.

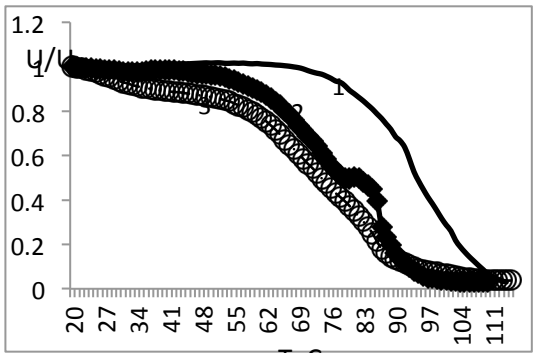

Figure 2. Temperature dependences of the surface potential of the polarization in the field of a negative corona discharge. 1 – PE; 2 – PE + 4 vol.% starch; 3 – PE + 4 vol.% starch + 1 vol.% aerosil.

3. Results and discussion

The addition of starch in polyethylene leads to decrease in its electrets properties as shown in Figure 1. This change can be explained by the fact that in the temperature range from 20 °C to 60 °C is the conversion of starch to glucose with the release of bound water, which is quite a lot of starch. The presence of bound water in the composites with starch can be judged by the presence in the IR spectrum of the band at 1625-1650 cm^{-1} and 3400-3500 cm^{-1} (Figure 3). As we know from [1, 2], water is the catalyst for the conduction in polymers, thus increasing the number of water molecules leads to an increase in conductivity and, therefore, weaken the stability of electrets-density polyethylene.
Adding aerosil increased the stability of the electrets state of polyethylene and starch (Figures 1, 2). Moreover, the stability of electrets material obtained is not just returning to the previous level, but is higher than the stability of pure polyethylene. Studies have shown that the stability of electrets state polyethylene and starch is greatly increased when added to a 1% vol. Aerosil, and a further increase of the volume fraction of aerosil a noticeable change in the material properties of electrets does not.
This result can be explained by the fact that on the surface of silica particles are usually silanol groups, which absorbs water, so that there is a characteristic of a particle around a shell consisting of hydroxyl groups and adsorbed water [3, 4] (Figure 3). Accordingly, the water molecules in the polymer volume become smaller, and its conductivity should then decrease, and the stability of the electrets state increase.
Results of the study of depolarization currents (Figure 4) showed that the composite spectra are identical spectrum source PE, i.e. starch has no effect on the relaxation processes in polyethylene of high pressure. Adding to aerosil composite PE with starch results in a new relaxation process, which corresponds to the peak position of the maximum of about 60° C (Figure 4). The position of the peak does not depend on the volume fraction of aerosil. Changing the amount of silica leads to in a change of the peak height.

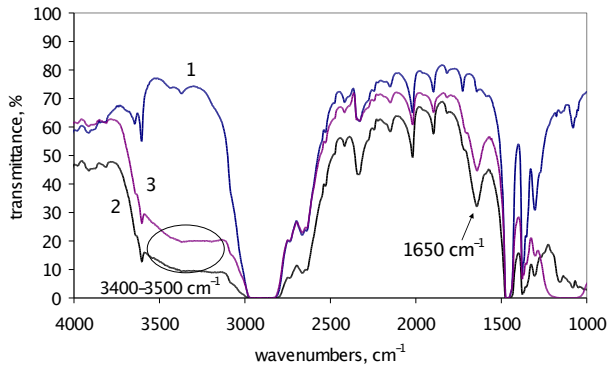

Figure 3. IR spectrums: 1 – PE; 2 – PE + 4 vol.% starch; 3 – PE + 4 vol.% starch + 2 vol.% aerosil. 1650 cm^{-1} и 3400-3500 cm^{-1} – band of the adsorbed water-related silanol groups of hydrogen bond.

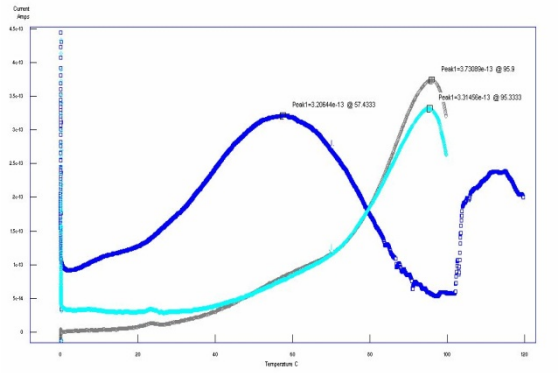

Figure 4. The temperature dependence of the depolarization currents (temperature of polarization - 70°C, heating rate 6°C/min). 1 – PE; 2 – PE + 4 vol.% starch; 3 – PE + 6 vol.% starch; 4 – PE + 6 vol.% starch + 1 vol.% aerosil.

Previous research of the polypropylene with aerosil showed similar results [5]. Adding aerosil in polypropylene led to a similar shape of the peak is also shifted by 40-50° C relative to the peak in the unfilled polymer. Maximum current at the same time also increases with the percentage of aerosil.

Studies of samples by X-ray analysis showed that the adding of the filler did not affect either the size of the crystallites, or the degree of crystallinity of polyethylene. It can be concluded that the change in the characteristics of electrets polyethylene and new relaxation processes not related to the change in the structure of the polymer.

4. Conclusions

Adding of starch in polyethylene to accelerate the decomposition of the polymer was not enough, as this deteriorated electrets properties of the polymer. To increase electrets stability of polyethylene requires adding in polyethylene of aerosil. Studies of samples by TSD showed that the addition of aerosil led to a new relaxation process with a peak at 50-60° C. Introduction into polyethylene starch does not show any changes in the spectrum TSD. Examination of samples by X-ray analysis showed that the change in the properties of polyethylene by adding to it the starch and aerosil is not due to changes in the structure of the original polymer, and, apparently, because of a change in its electrical properties.

Acknowledgements

The work was performed as part of the project to the strategic development of Herzen State Pedagogical University and RFBR grant number 12-02-31432.

References

[1] Gorokhovatsky Yu.A., Aniskina L.B. et al. Manifestation of the spin-orbital interaction in vibrational spectra of polyelectrolytes - fibrous and film of electrets on the basis of polypropylene and polyethylene // Izvestia: Herzen University Journal of Humanities & Sciences. – Spb., 2009, №11(79). P. 47-61.

[2] Aniskina L.B., Victorovich A.S., GAlikhanov M.F., Temnov D.E. Polyelectrolyte model of fibrous on the basis of polyethylene and polypropylene// Izvestia: Herzen University Journal of Humanities & Sciences. – Spb., 2010, № 135. P. 24-36.

[3] Parida S.K., Dash S., Patel S. and Mishra B.K. Adsorption of organic molecules on silica surface // Advances in Colloid and Interface Science, Vol. 121, Issues 1-3, 2006. P. 77-110.

[4] Roy M., Nelson J.K., MacCrone R.K., Schadler L.S., Reed C.W., Keefe R. and Zenger W. Polymer Nanocomposite Dielectrics – The Role of the Interface. // IEEE Transactions on Dielectrics and Electrical Insulation, Vol. 12, № 4, 2005. P. 629-643.

[5] Fomicheva E.E., Temnov D.E., Galikhanov M.F. Relaxation processes in composite films of polypropylene// Vestnik of Kazan technology university, 2010, №10. P. 223-230.

S6-P70
Enhanced thermal stability of multi-wall carbon nanotubes with polyaniline coating

Miroslava Trchová*, Zuzana Morávková, Jaroslav Stejskal
Institute of Macromolecular Chemistry, Academy of Sciences of the Czech Republic, Heyrovsky Sq. 2, 162 06 Prague 6, Czech Republic
*trchova@imc.cas.cz

1. Introduction

Nanocomposites based on carbon nanotubes (CNT) and polyaniline (PANI) are promising materials due to the combination of the properties of both components. CNT modified with PANI have been proposed for applications in sensors [1], supercapacitors [2], or in optical devices [3]. Multi-walled carbon nanotubes (MWCNT) were coated by PANI overlayer *in situ* in water–ethanol mixture during the oxidation of aniline with ammonium peroxydisulfate (Figure 1). Transmission electron microscopy confirmed the coaxial structure of composites. The composite was subsequently carbonized under inert atmosphere at 650 ^{o}C. The coaxial PANI coating of carbon nanotubes converted to nitrogen-containing carbon [4, 5]. Such surface-modified CNT were highly catalytically active [6]. In the present study, the thermal stability is analyzed in detail for commercial multi-wall carbon nanotubes (MWCNT) coated with PANI [5].

One of the important characteristics of the PANI/CNT nanocomposites is the nature of the PANI–CNT interaction, which can be studied by various spectroscopic methods. The Raman and FTIR spectroscopic studies consist of two parts. The first concentrates on the molecular changes connected with the exposure of MWCNT coated with PANI to elevated temperature. The second is devoted to the comparison of PANI alone and when deposited on MWCNT with respect to the possible interaction between both components. The Raman spectra showed that PANI salt interacts with MWCNT *via* the charge-transfer, especially with the phenazine-rich nucleation centers which adsorb on the surface of the MWCNT during the *in-situ* polymerization of aniline. The interaction of MWCNT surface with PANI stabilizes the polaronic structure of the doped polyaniline by π–π interactions [7].

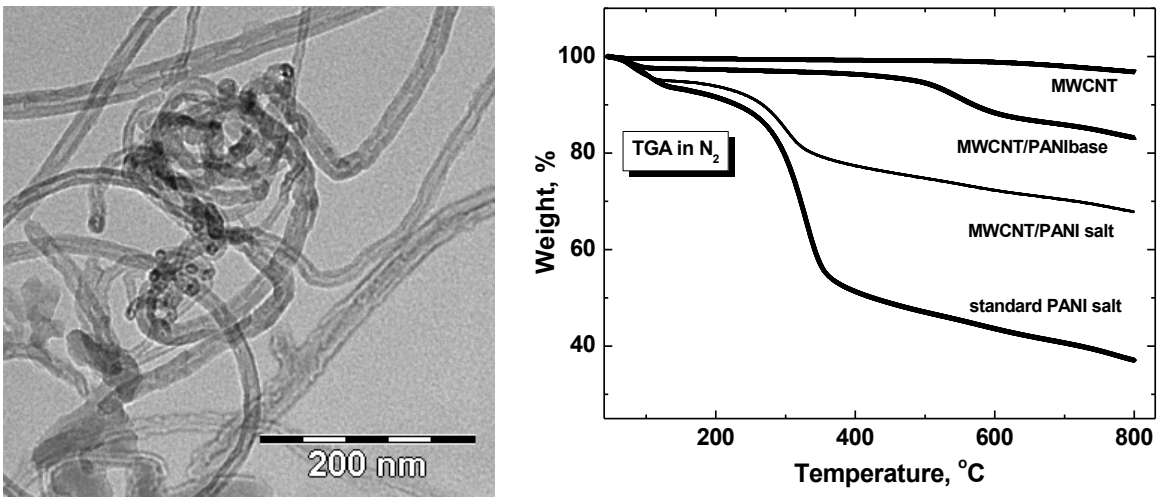

Figure 1. Transmission electron image of MWCNT coated with PANI salt (left). TGA of MWCNT, MWCNT/PANI composites and of standard PANI salt in nitrogen atmosphere (right).

2. Experimental

MWCNT were coated by PANI *in situ* during the oxidation of aniline with ammonium peroxydisulfate in a mixture of ethanol (50 vol. %)–water. PANI alone and PANI-coated MWCNT were subsequently carbonized under nitrogen atmosphere at 650 °C. Transmission electron micrographs were taken with a JEOL JEM 2000FX microscope. Thermogravimetric analysis (TGA) was carried out in air or nitrogen flow, 50 cm^3 min^{-1}, at a heating rate of 10 °C min^{-1} with a Perkin Elmer TGA 7 Thermogravimetric Analyzer.

Structural changes were studied Fourier-transform infrared (FTIR) spectra of potassium bromide pellets in the range 400–4000 cm^{-1} at 64 scans per spectrum at 2 cm^{-1} resolution using a fully-computerized Thermo Nicolet NEXUS 870 FTIR Spectrometer with a DTGS TEC detector. Raman spectra excited with HeNe 633 nm were collected on a Renishaw inVia Reflex Raman microspectrometer. A research-grade Leica DM LM microscope with an objective magnification ×50 was used to focus the laser beam on the sample placed on an X–Y motorized sample stage. The scattered light was analyzed by the spectroscope with holographic gratings 1800 lines mm^{-1}. A Peltier-cooled CCD detector (576×384 pixels) registered the dispersed light.

3. Results and discussion

MWCNT coated with carbonized PANI salt exhibit the Raman spectrum close to that of the pristine MWCNT before heating. On the contrary, the spectra of MWCNT and MWCNT coated with PANI base correspond after exposure to 650 °C to a more disordered carbon-like material according to their Raman spectrum. This means that the coating with PANI salt has a protective effect on the structure of MWCNT when exposed to elevated temperature. During heating, the over layer of PANI salt thermally deprotonates to PANI base at first, and subsequently converts to carbonized PANI coating. The integrity of the coating is not damaged. When the PANI coating was chemically deprotonated to PANI base before heating, the accompanying volume contraction reduced the contact between MWCNT and PANI base coating and introduced defects, such as cracks. The protective effect of PANI coating was then lost. The possible interactions between PANI and MWCNT are discussed on the basis of Raman spectra.

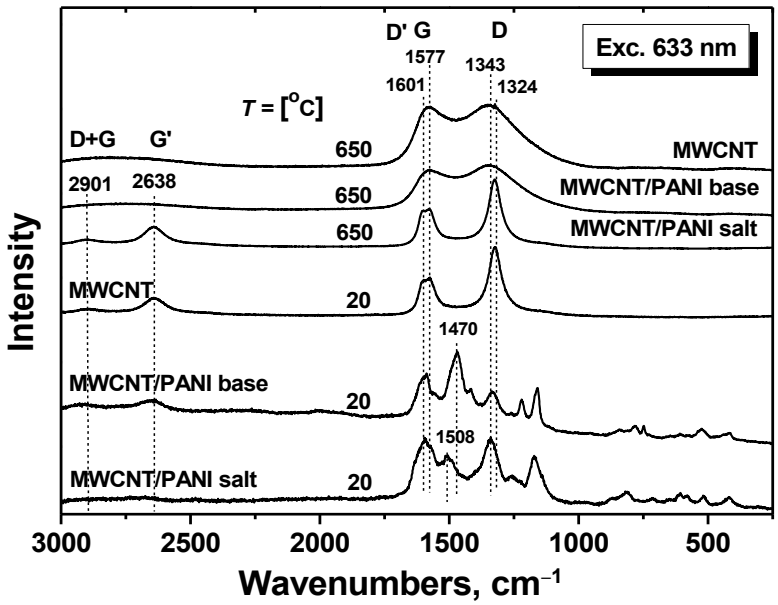

Figure 2. Raman spectra of MWCNT and MWCNT/PANI composites before and after carbonization.

4. Conclusions

MWCNT were coated *in situ* during the oxidation of aniline with a coaxial overlayer of PANI salt in water–ethanol mixture. The deprotonation of MWCNT/PANI salt to MWCNT/PANI base by treating with ammonium hydroxide solution leads to the materials with lower thermal stability at high temperatures than MWCNT/PANI base obtained by thermal deprotonation as it has been shown by TGA. During the chemical deprotonation, the contacts of the MWCNT and PANI-base coating break due to volume contraction. On the contrary, this does not happen during thermal deprotonation at elevated temperature. The interaction between MWCNT and PANI salt further enhances this effect.

Acknowledgements

The authors thank the Czech Grant Agency (205/12/0911, and 202/09/1626) for financial support.

References

[1] S. Srivastava, SS. Sharma, S. Agrawal, S. Kumar, M. Singh, Y.K. Vijay, Synth. Met. 2010, 160, 529–534.
[2] V. Branzoi, F. Branzoi, L. Pilan, Surf. Interface Anal. 2010, 42, 1266–1270.
[3] V. Bavastrello, T.B.C. Terencio, C. Nicolini, Polymer 2011, 52, 46–54.
[4] M. Trchová, E.N. Konyushenko, J. Stejskal, J. Kovářová, G. Ćirić-Marjanović, Polym. Degrad. Stab. 2009, 94, 929–938.
[5] Z. Rozlívková, M. Trchová, M. Exnerová, J. Stejskal, Synth. Met. 2011, 161, 1122–1129.
[6] C Jin, T.C. Nagaiah, W. Xia, B. Spliethoff, S. Wang, M. Bron, W. Schuhmann, M. Muhler, Nanoscale 2010, 2, 981–987.
[7] Z. Morávková, M. Trchová, E. Tomšík, J. Čechvala, J. Stejskal, Polym. Degrad. Stab. 2012, 97, 1405–1414.

S6-P71

Preparation and characterization of novel type I/type II photoinitiators for two-photon submicro-stereolithography

Maximilian Tromayer (1)*, Zhiquan Li (1), Jan Torgersen (2), Aliasghar Ajami (3), Arnulf Rosspeintner (4), Sergej Naumov (5), Juergen Stampfl (2), Robert Liska (1)

(1) Institute of Applied Synthetic Chemistry, Vienna University of Technology, Getreidemarkt 9/163/MC, 1060 Vienna, Austria,
(2) Institute of Materials Science and Technology, Vienna University of Technology, Favoritenstrasse. 9-11, 1040 Vienna, Austria
(3) Institute of Applied Physics, Vienna University of Technology Wiedner Hauptstrasse. 8, 1060 Vienna, Austria
(4) Physical Chemistry Department, University of Geneva, Quai Ernest Ansermet 30, CH-1211 Geneva, Switzerland
(5) Leibniz Institute of Surface Modification (IOM), Permoserstr. 15, D-04318 Leipzig, Germany
*maximilian.tromayer@ias.tuwien.ac.at

1. Introduction

The process of two-photon induced polymerization (TPIP) has attracted considerable interest because it enables free-form stereolithography/rapid prototyping with a resolution in the sub-micrometre range. Parts containing ultra-small features like scaffolds for tissue engineering, photonic crystals, optical waveguides and microelectronic components may thus be produced. The properties of the used photoinitiator (PI) inducing polymerization are crucial for obtaining high quality microstructures as well as achieving high writing speed, broad processing windows and low polymerization threshold, which all are necessary preconditions for the industrial applicability of the TPIP-process. So far, there are no PIs commercially available which would satisfy these conditions.

2. Theory

To achieve high efficiency in TPIP the PIs should possess a large cross section for two-photon absorption (TPA cross section), i.e. the two-photon excitation process has a high probability, which demands a planar π system with long conjugation length and suitable donor and/or acceptor groups. Furthermore, the quantum yield for the generation of the initiating species from the excited triplet state of the PI molecule should be high. Generally there are two distinct mechanisms by which the active initiating species is formed: In Type I PIs, the energy of the triplet state is dissipated by homolytic scission of a weak bond in the molecule, forming two radicals. Type II PIs on the other hand generate radicals by hydrogen transfer from a donor (usually heteroatoms with active hydrogen atoms in the α-position) to an acceptor group (usually a carbonyl group). Thus far PIs suitable for TPIP only employ the bimolecular Type II mechanism where diffusion and back electron transfer limit the photoreactivity, therefore the aim of this study was to also screen for new compounds reacting via Type I mechanism.
The investigated compounds are derivatives of the chromophore 2,6-dibenzylidenecyclohexanone with a general structure outlined in **Figure 1**. Besides fulfilling the conditions leading to a high TPA cross section, the synthesis is facile and can be carried out in as little as one step in many cases.
R^1 and R^3 are usually donor substituents containing the groups responsible for radical formation as well as leading to a redshift and stronger absorption, R^2 is an alkyl chain enhancing the solubility.
R^1 and R^3 are either identical in case of symmetric structures, or different, leading to asymmetric ones.

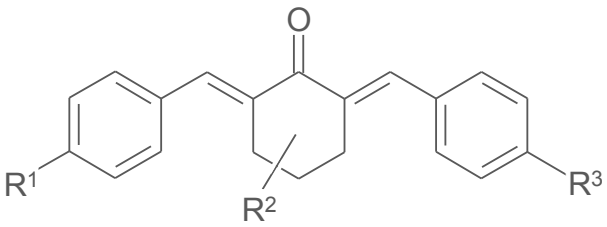

Figure 1. Substituted 2,6-dibenzylidenecyclohexanone, R^1-R^3 being variable substituents

3. Experimental

A typical procedure for symmetric PIs (R^1 = R^3) employs a classical aldol condensation, reacting 2.5 eq. of the R^1-substituted aldehyde with 1 eq. of R^2-substituted cyclohexanone under alkaline conditions in dry ethanol. Depending on the properties of the aldehyde, the reaction is carried out either at room temperature or elevated temperatures. The product either precipitates or is isolated from the reaction mixture by extraction and purified by column chromatography.
For asymmetric PIs the monosubstituted 2-benzylidenecyclohexanone containing R^1 is synthesized in a separate step and then further reacted with the aldehyde carrying the R^3 substitutent.
Structure-activity relationships were investigated both by quantum chemical calculations as well as experimental tests employing z-scan to determine the TPA cross sections, UV-VIS spectroscopy, TPIP structuring tests to evaluate processing windows and overall performance, and finally in some cases cytotoxicity assays.

References
[1] Cumpston, B. H.; Ananthavel, S. P.; Barlow, S., et al. *Nature* 1999, 398, (6722), 51-54.
[2] Wu, J.; Zhao, Y.; Li, X., et al., *New J. Chem*. 2006, 30, (7), 1098-1103.
[3] Li, Z.; Siklos, M.; Pucher, N., et al. *J Polym Sci Part A: Polym Chem.* 2011, 49, (17), 3688-3699.

S6-P72
Analysis of damage mechanisms by acoustic emission (A.E) and digital image correlation (D.I.C.) of a woven composite assembly

Faci Youcef (1)*, T. C. Herbelot (2), A. Imad (3), B. Mostefa (4)
(1) Mechanics Laboratory of Lille, CNRS UMR 8107, Ecole Polytech'Lille, University of Lille, FranceCité Scientifique, Avenue Paul Langevin, 59655 Villeneuve d'Ascq, France
(2) Centre Nationale de Soudage et ContrôleBP, 64 Route Dely Brahim, Cheraga, 16000 Alger, Algerie
*elfaci@yahoo.fr

Abstract;
This work study the damage and fracture evolution of a single lap bolted assembly (fiber / epoxy).Three configurations are studied (0°,45°,0°,45°),(0°,45°,0°,45°)s and (0°,45°,0 °,45,0°)s. All material types were tested under tensile loading .An experimental approach was carried out in order to analyze the sequence of damage mechanisms using acoustic emission (A.E.) and measurement of fields by digital image correlation (D.I.C.) techniques simultaneously. then confirmed by microscopic observations in scanning electron (SEM). The A.E. technique allows the monitoring of the evolution of acoustic activities by taking into account the number of counts, duration, maximum amplitude and energy of the events. The treatment of these four parameters by planar localization allows precise determination of the fracture.Four modes of damage are identified: matrix cracking, fibre-matrix debonding or fibre pull-out, delamination ,Fibre breaking.The DIC techniques and the fracture surfaces observations permit to confirm the damage scenarios.

Keywords: Bolted assembly, Composite, Acoustic emission, Digitale image corrélation, Damage

Session 7: Coatings and adhesives

S7-P73
Synthesis and structure properties of one component urethane adhesives

Ema Fabjan (1)*, Darko Moderc (2), Jerneja Godnjavec (1), Ida Poljanšek (1), Dolores Kukanja (1,2)
(1) CO PoliMaT, Tehnološki park 24, 1000 Ljubljana, Slovenia
(2) Mitol Sežana, Partizanska cesta 78, 6210 Sežana, Slovenia
*ema.fabjan@polimat.si

1. Introduction
Polyurethane adhesives are widely used in different industries. The performance of an adhesive is related to its viscoelastic properties, consequently the relationship between composition and properties is of great importance. The advantages of polyurethane adhesives are improved toughness, water resistance and a broad range of chemical resistance. The relatively low viscosity of polyurethane adhesives allows them to permeate into porous materials.
One-component urethane adhesives (prepolymers) were prepared from difunctional linear polyether polyol and two different isocyanates. The structure of prepolymer was varied by using different stehiometric excess of isocyanate. The amount of free NCO groups was between 5 and 24 %. The simulation of the synthesis was performed using rheological measurements at different temperatures for samples with 15 % of NCO content. The molar masses of the synthesized prepolymers were determined by GPC. For investigation of the synthesized urethane prepolymers thermal properties, the DSC/TGA techniques were used. Also viscosity and adhesion strength of the polyurethane adhesives were tested [1].
Polyurethanes are block copolymers with alternating soft segment - polyether or polyester polyol and hard segments - the urethane linkages blocks [2, 3]. The most common method of preparing polyurethane (–NH–COO–) is condensation reaction of a diisocyanate and a polyol as shown in Fig. 1.

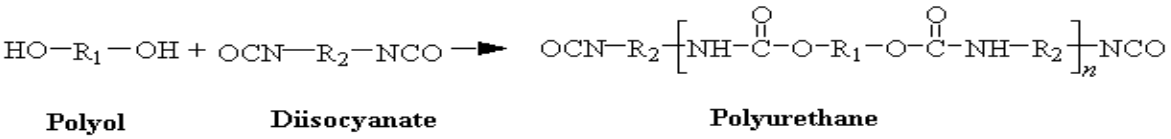

Figure 1: Polyurethane reaction of polyol and diisocyanate

2. Experimental

2.1 Synthesis of NCO-terminated prepolymers

NCO-terminated prepolymers were synthesized by the reaction between a polyol and an excess of isocyanate. The syntheses were carried out in a glass double jacket LabMax reactor (Mettler Toledo), equipped with a stirrer, thermocouple and nitrogen gas inlet system. First, polyol was poured into the reactor. While stirring the 0.1 wt % of concentrated phosphoric acid was added and the reactor vessel was heated up to 80 °C in the period of 1 h under the vacuum of 30-60 mbar. Then, the isocyanate was charged under a nitrogen atmosphere, and the temperature was kept constant at 70 °C, for 2h. Inert atmosphere was used to avoid moisture and subsequent formation of urea linkages. At the end, prepolymer samples were cooled to 50 °C and poured out. The samples were stored under constant conditions at 20 °C and 60 % of relative moisture. NCO-terminated urethane prepolymers were prepared from linear polypropylene ether polyol (PPG 2000) and two different isocyanates:

- a monomeric diphenylmethane diisocyanate with high 2,4'-isomer content (MDI 2,4)
- a mixture of diphenylmethane-4,4' diisocyanate with isomers and higher functional homologues (pMDI 4,4) urethane prepolymer

Samples were prepared with different free NCO content in urethane prepolymers as described in Table 1.

Table 1: Samples of urethane prepolymers prepared from PPG 2000, MDI 2,4; and pMDI 4,4

Samples based on pMDI 4,4	A1	A2	A3	A4	A5
Samples based on MDI 2,4	B1	B2	B3	B4	B5
% NCO in prepolymer	5	10	15	20	24

2.2 Measurements and analyses

The instrinct viscosity of urethane prepolymers was performed at 20 °C by using a Brookfield RV rotational viscometer according to the standard ISO 2555. Wood-to-wood binding strength (N/mm^2) was measured using Zwick 1435 mechanical testing machine. For this purpose three specimens (100mm long, 20mm wide and 3mm thick) with adhering surface of 2 cm^2 were kept under the pressure of 7.5 kg/cm^2 for at least 24h. Tensile shear strength was determined after 24 hours with constant crosshead speed of 50 mm/min, using Zwick 1435 (Modification of the EN 14293:2006 standard method). The number average molecular weight (Mn) and the weight average molecular weight (Mw) of urethane prepolymers were determined by GPC instrument Agilent 1260 Infinity Quaternary LC using polystyrene standards. The samples were dissolved in tetrahydrofuran, which was also used as carrier solvent at a rate of 1 ml/min. Thermogravimetrical analysis (TGA) was performed on Metller Toledo TGA/DSC1 apparatus and differential scanning calorimetry (DSC) measurements were performed on a Metller Toledo DSC1 device. Rheological behaviour was determinated at different temperatures using Rheomether Anton Parr MCR 301. Homogenized mixtures of polyol and isocyanate were put on »peltier« plate which was heated under nitrogen atmosphere to desired temperature for 10 min.

3. Results and discussion

Fig. 2 shows the dependence of Brookfield viscosity on free NCO content in polyurethane prepolymers. At higher percentages of NCO groups viscosity decreases. The unreacted isocyanate lowers the viscosity of the end product. Viscosity and tensile shear strength of prepolymers is higher for samples A, which are prepared from a mixture of isocyanates. The maximum value of tensile shear strength is achieved with 15 wt.% of free NCO content in prepolymer based on pMDI 4,4.

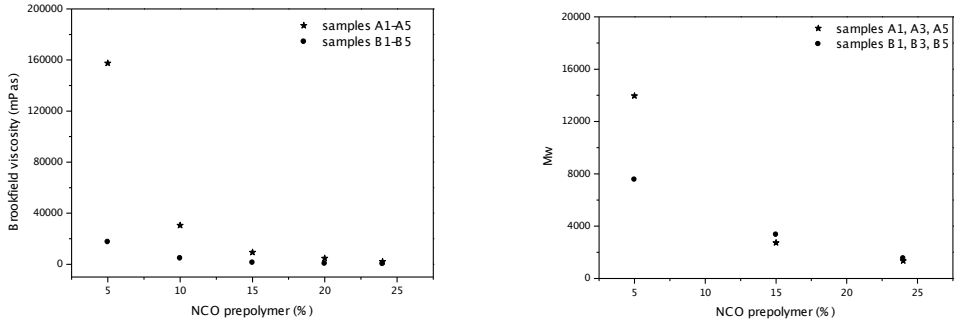

Figure 2: The effect of free NCO content in urethane prepolymers on Brookfield viscosity and average molecular weight

By increasing of free wt. % of NCO in prepolymers the average molecular weights decrease. The peaks, which appear at the highest retention time (more than 10 min), correspond to the component with the lowest molecular weight, therefore, to unreacted MDI monomers. The distribution of molecular weights is very broad. The significant difference in average molecular weight is detected at 5 wt. % of NCO in the end products. Higher molecular weight is observed by using pMDI 4,4. As already mentioned, in order to optimize the reaction process the rheological behavior was observed during the synthesis of the prepolymer at different temperatures. From the experimental results obtained it may be concluded that at higher temperatures the rate of the synthesis is higher and time of reaction decreases.

5. Conclusions

NCO-terminated urethane prepolymers were prepared from difunctional polypropyleneglycol polyols and two types of isocyanate: monomeric diphenylmethane diisocyanate with high 2,4'-isomer content and mixture of diphenylmethane-4,4' diisocyanate with isomers and higher functional homologues. Higher viscosity and tensile shear strength were reached in polyurethane adhesives prepared by using the mixture of isocyanates. The maximum tensile shear strength is achieved in formulation with 15 wt. % of free NCO content in prepolymer. Molecular weight of end products increased with lowering the ratio of NCO/OH. The significant difference in average molecular weight between samples based on pMDI 4,4 and MDI 2,4 was detected at 5 wt. % of NCO in the synthesized prepolymers.

Acknowledgements

The authors wish to gratefully acknowledge the support for the presented work received from the Ministry of Higher Education, Science and Technology of the Republic of Slovenia through the contract No. 3211-10-000057 (Center of Excellence for Polymer Materials and Technologies).

References

[1] D. G. Lay, P. Cranley, Adhes Age 1994; 37(6), 6-9.
[2] Oertel G. Polyurethane handbook. New York: Hanser Publishers; 1985.
[3] U. Šebenik, M. Krajnc, Int J Adhes Adhes 2007, 27 (7), 527-535.

S7-P74
UV-induced 2.5D-patterning of poly[2-(2´-norbornyl)-2-oxazoline]

Martin Fimberger (1,2)*, Verena Schenk (1,2) and Frank Wiesbrock (1,2)
(1) Polymer Competence Center Leoben GmbH, Roseggerstrasse 12, 8700 Leoben, Austria
(2) Graz University of Technology, Institute for Chemistry and Technology of Materials, Stremayrgasse 9, 8010 Graz, Austria
*martin.fimberger@pccl.at

1. Introduction

This work aimed at the extension of a toolbox of basic polymers for tailor-made photoresists by combining the structural motifs of 2-oxazolines and norbornenes in one monomer followed by a cationic ring-opening polymerization (CROP) of the 2-oxazoline function [1]. In order to overcome possible side-reactions of the norbornyl moiety during this cationic polymerization, a macroinitiator needed to be used.

2. Experimental

The synthesis of 2-(2´-norbornyl)-2-oxazoline **NbOx** started from 5-norbornene-2-carbonitrile and ethanol-2-amine using cadmium acetate dihydrate as catalyst in analogy to a literature protocol for the synthesis of 2-phenyl-2-oxazoline [2]. The polymerization of **NbOx** was initiated by oligo(2-ethy-2-oxazoline)-2-ethyl-2-oxazolinium cations. Formulations containing poly[2-(2´-norbornyl)-2-oxazoline] **pNbOx** and 1,4-butanedithiol or 3,4-dimercaptotoluene as well as catalytic amounts of Lucirin TPO-L™ as photoinitiator were cast onto FR4 substrates and illuminated with UV-light through a mask. After development with chloroform, the negative pattern of the illumination mask was reproduced [3].

3. Results and discussion

In this study, the previously unreported 2-norbornyl-2-oxazoline monomer was successfully synthesized and purified. The monomer was subsequently polymerized using a cationic 2-oxazolinium macroinitiator, as the initiator methy tosylate failed to yield a soluble polymer, presumingly due to side-reactions of the highly reactive methyl cation with the olefinic side-chains. A trimodal distribution of molecular weights of **pNbOx** was observed which can be explained by chain-transfer and subsequent chain-coupling reactions during the polymerization [4].

The polymer could be successfully subjected to polymeranalogous transformations such as thiol-ene crosslinking, which was proven using the polymer as base of a photoresist. 1,4-Butanedithiol as crosslinker allowed for very short processing windows only (< 5 min.), while 3,4-dimercaptotoluene as crosslinker paved the way for significantly increased processing times [3]. UV-induced crosslinking could be achieved with catalytic amounts of the photoinitiator Lucirin TPO-L, revealing feature sizes in the 30 µm range.

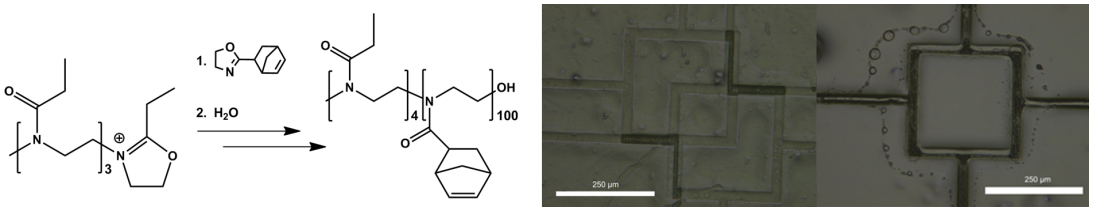

Figure 1. Initiation scheme for the polymerization of **NbOx** with an oxazolinium initiator (left). Microscopic pictures of developed resists either crosslinked by 1,4-butanedithiol or 3,4-dimercaptotoluene. (right).

Acknowledgements
This study was performed at the Institute for Chemistry and Technology of Materials of the Graz University of Technology and the Polymer Competence Center Leoben GmbH (PCCL) within the framework of the Kplus-program of the Austrian Ministry of Traffic, Innovation and Technology. PCCL is funded by the Austrian Government and the State Governments of Styria and Upper Austria.

References
[1] V. Schenk, L. Ellmaier, E. Rossegger, M. Edler, T. Griesser, G. Weidinger, F. Wiesbrock, *Macromol. Rapid Commun.* 2012, 33, 396-400.
[2] T. Bodner, L. Ellmaier, V. Schenk, J. Albering, F. Wiesbrock, *Polym. Int.* 2011, 60, 1173-1179.
[3] M. Fimberger, V. Schenk, E. Rossegger, F. Wiesbrock, *Macromol. Symp*. 2013, submitted.
[4] F. Wiesbrock, R. Hoogenboom, M.A.M. Leenen, S.F.G.M. van Nispen, M. van der Loop, C.H. Abeln, A.M. van den Berg, U.S. Schubert, *Macromolecules* 2005, 38, 7957-7966.

S7-P75
Investigation and properties of new type semi-interpenetrating polymer networks on the base phenoxy-resin

V. Genadiev, I. Iliev, M. Petkov
Research Institute of Building Materials, Sofia, Bulgaria

ABSTRACT
Recently the obtaining of polymer composites on the base of polymer hybrid matrix has been attracting a special scientific interest. Semi-interpenetrating polymer networks (SPIN), are typical examples of this kind of polymer matrix. Semi-interpenetrating polymer networks are obtained on the base of phenoxy – resin, diphenylmethane diisocyanate and liquid epoxy resin (in varying quantities). Obtained polymer materials (SIPN) are characterized by DTA. IR spectroscopy has been identified as the likely mechanism for obtaining SIPN. Also, the studied polymer composites (SPIN), have defined physical and mechanical properties and their field of application.

S7-P76

Enzymatic polymerisation: cross-linking alkyd resins via a new enzymatic approach in order to replace toxic heavy metals

Katrin Greimel (1,2)*, Elke Scholz (1), Karolina Härnvall (1), Veronika Perz (1), Enrique Herrero Acero (1), Georg M. Guebitz (1,2)

(1) ACIB GmbH, Petersgasse 14, 8010 Graz, Austria

(2) University of Natural Resources and Life Sciences, Vienna, Institute of Environmental Biotechnology, Konrad Lorenz Straße 20, 3430 Tulln, Austria

*katrin.greimel@acib.at

1. Introduction

Alkyd resins are polyesters that contain unsaturated fatty acids. They are used as binding agents in different paints and coatings. The drying process of these coatings is based on the oxidative cross-linking of the unsaturated fatty acid moieties. This process is commonly catalysed by cobalt based complexes as they are the most effective ones. However, these cobalt catalysts are suspected to be potentially carcinogenic [1,2] in aerosol and therefore market environmental and health awareness is driving the coating industry towards the replacement of toxic catalysts by environmentally friendlier siccatives.

In this work we present the development of a new environmentally friendly approach for the drying of alkyd resins that is based on an enzyme and is capable of replacing the currently used cobalt system [3]. The potential of a laccase from *Trametes hirsuta* in combination with two different electron mediators (2,2'-azino-bis(3-ethylbenzothiazoline-6-sulphonic acid (ABTS) and 1-hydroxybenzotriazol (HBT)) was evaluated regarding its capability to crosslink the unsaturated fatty acids and consequently harden the resin.

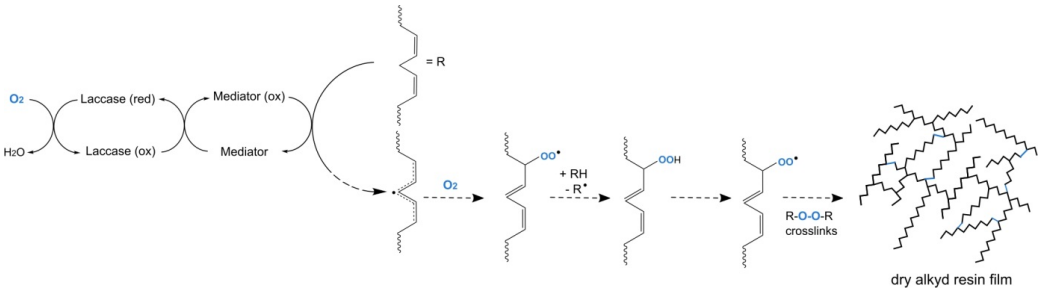

Figure 1. Proposed drying process of alkyd resins with the laccase/mediator system

2. Experimental

The new laccase based siccative system was evaluated regarding its capability to crosslink the unsaturated fatty acids and consequently harden the resin. The oxidation of the alkyd resin by the laccase mediator system was followed by monitoring the oxygen consumption during the crosslinking process with an optical oxygen sensor in two different setups. Additionally, to reveal more mechanistic details on a chemical level of the drying reaction FTIR spectroscopy was used. Finally the drying performance of the laccase mediator system was measured and compared with the cobalt catalyst using the drying time recorder. This method is a standard method widely used and accepted in the coating industry to measure the drying performance of new products or formulation additives.

The distribution of the enzyme within the alkyd resin film was monitored using the confocal laser scanning microscope (CLSM) after labeling the enzyme with a fluorescent dye.

3. Results and discussion

Following the oxidation of the alkyd resin using the oxygen sensor, we could clearly see that oxygen was consumed in a higher extent in the LMS samples compared to the pure alkyd resin emulsion. When comparing the two tested mediators there was a significant difference in terms of oxygen consumption between them. In addition FTIR spectroscopy showed a clear decrease of the band assigned to double bonds (3010 cm^{-1}), which can be correlated to the drying of the alkyd resin.

The measured drying time of the cobalt siccative was 12 hours at the given conditions. The laccase alone did not show a significant effect on the hardening reaction and the alkyd resin itself was not drying at all. By addition of the mediator together with the enzyme, the overall drying time could be significantly shortened to 43 hours.

It could be seen, that the laccase forms aggregates in the alkyd resin. Those aggregates are homogeneously distributed all over the film and are present also in lower layers.

4. Conclusions

We demonstrate a new enzyme based siccative for the drying of alkyd resins. This system can replace toxic heavy metals that are conventionally used in alkyd resins, which will soon become inacceptable in coatings and related products.

Acknowledgements
This study was performed within the Austrian Centre of Industrial Biotechnology ACIB and the COST Action 868. This work has been supported by the Federal Ministry of Economy, Family and Youth (BMWFJ), the Federal Ministry of Traffic, Innovation and Technology (bmvit), the Styrian Business Promotion Agency SFG, the Standortagentur Tirol and ZIT - Technology Agency of the City of Vienna through the COMET-Funding Program managed by the Austrian Research Promotion Agency FFG.

References
[1] J. R. Bucher, J. R. Hailey, J. R. Roycroft, J. K. Haseman, R. C. Sills, S. L. Grumbein, P. W. Mellick and B. J. Chou, Toxicol Sci., 1999, 49, 56-67.
[2] D. Lison, M. De Boeck, V. Verougstraete and M. Kirsch-Volders, Occup Environ Med., 2001, 58, 619-625.
[3] K.J. Greimel, V. Perz, K. Koren, R.Feola, A. Temel, C. Sohar, E. Herrero Acero, I. Klimant, G.M. Guebitz, Green Chem., 2013, 15, 381-388.

S7-P77
Biofunctionalization of cyclic olefin polymers for microarray application

Stefan Höllbacher (1)*, Milijana Roljic (2), Andreas Koller (2), Stefan Köstler (3)*, Michael Wallner (2), Gabriele Gadermaier (2), Sylvia Scheicher (3), Birgit Kirchhofer (4), Maria Kaufmann (4), Werner Balika (4), Georg Bauer (4), Fatima Ferreira-Briza (2), Fritz Aberger (2) and Volker Ribitsch (1)
(1) Institute of Chemistry, Karl-Franzens-University, Graz, Austria,
(2) Department of Molecular Biology, Paris Lodron University of Salzburg, Austria
(3) MATERIALS - Institute of Surface Technologies and Photonics, JOANNEUM RESEARCH, Graz, Austria
(4) Sony DADC Austria AG, BioSciences Business Department, Anif, Austria
*stefan.hoellbacher@uni-graz.at, *stefan.koestler@joanneum.at

1. Introduction
Microarrays are well established and commonly used for biomedical research and diagnostics. Polymer materials are an interesting alternative to glass substrates which currently are mostly used in microarray experiments. Besides their lower production costs, polymer materials easily allow for the integration of further functional structures on these biochips. There is a steadily increasing demand for faster and more reproducible analytical processes using smaller amount of sample. Therefore optimized handling protocols regarding the spotting, the hybridization and the data evaluation are essential. Such workflow optimization can be facilitated by combining microarrays with nanostructures and microfluidic systems. In order to exploit the advantages of polymeric materials in these challenging applications, suitable approaches for effective surface modification and biofunctionalization of these materials are required.
One of the most promising material classes for biochip applications are cyclic olefin polymers (COP). They are especially suited for miniaturized biosensor systems comprising optical detection schemes due to their easy processing by embossing or injection moulding and excellent optical properties (high transparency and low autofluorescence). While a huge number of well developed surface modification techniques is available for many standard materials used in microfluidic technology (such as glass, silicon or PDMS), such methods are rather scarce for polymers like COP[1]. Previously, COP surface modification was reported by methods such as plasma treatment[2], UV-O_3 treatment[3], polyelectrolyte adsorption[4] and recently silane modification[5].
We report on the development of an innovative coating technology starting with the moulding of tailored COP-Chips followed by sputter-coating and the vapour deposition of a functional glycidoxypropyltrimethoxysilane (GOPTS) monolayer (**Figure 1**). The GOPTS coating enables the direct immobilization of biomolecules such as amino-functionalized oligonucleotides and the covalent bonding of different polysaccharide based coatings on polymeric chips (**Figure 1**). This allows application of COP based chips for DNA and protein microarrays, in diagnostics, microfluidic devices and lab-on-chip systems.

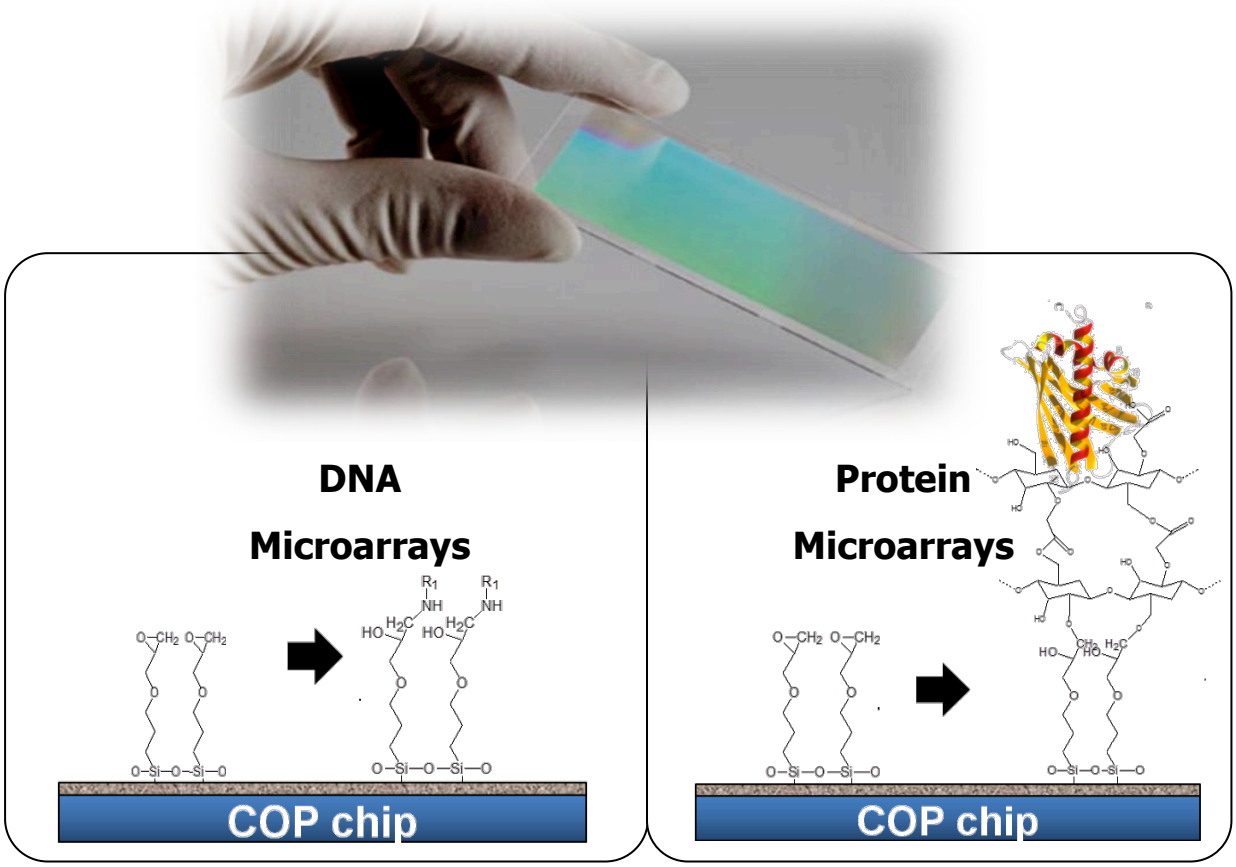

Figure 1. Epoxidesilane modification of COP chips for immobilization of oligonucleotides (Left); immobilization of proteins via functionalization of COP with polysaccharide coatings (Right).

2. Experimental

For the deposition of GOPTS, a sol-gel process (SG), and the formation of self-assembled monolayers from organic solvents (OS) and via vapour phase deposition (VPD) were investigated. The surfaces were characterized by a broad range of surface analytical techniques such as X-ray photoelectron spectroscopy (XPS), attenuated total reflectance infrared spectroscopy (ATR-IR), atomic force microscopy (AFM) and contact angle measurements. Oligonucleotide probes were spotted onto functionalized polymer slides (**Figure 2**) to evaluate the suitability of COP substrates for DNA-microarray applications. The novel GOPTS coated microarray substrates were tested in hybridization experiments with complementary oligonucleotide probes and characterized with respect to background fluorescence, binding capacity, and hybridization efficiency.

Number	Spotted Oligos
2	Cy5-probe-60mer-NH2
3	Cy3-probe-60mer-NH2
4	Cy5-probe-30mer-NH2
5	Cy3-probe-30mer-NH2
6	NH2-probe-30mer
7	NH2-probe-60mer
8	NH2-neg.probe-30mer
9	NH2-neg.probe-60mer

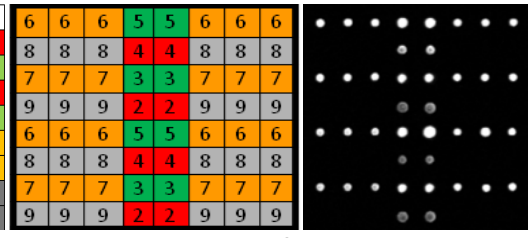

Figure 2. Spotted oligonucleotides on coated COP-Chip surfaces

3. Results and Conclusion

The VPD of a GOPTS monolayer turned out to be the most promising coating method owing to the low process complexity and coating optimization possibilities, which leads to high performance microarrays. Characterization demonstrates the functionalization by silica sputtering and subsequent GOPTS functionalization. Analysis of processed COP microarrays revealed that these polymer slides are suitable for DNA microarray experiments with very high binding capacities (**Figure 3 left**), hybridization efficiencies (**Figure 3 right**) and a low variation coefficient values which are comparable to commercial glass microarray slides. Furthermore, the feasibility of carrying out protein microarray experiments could be shown by polysaccharide based surface functionalization of COP-Chips.

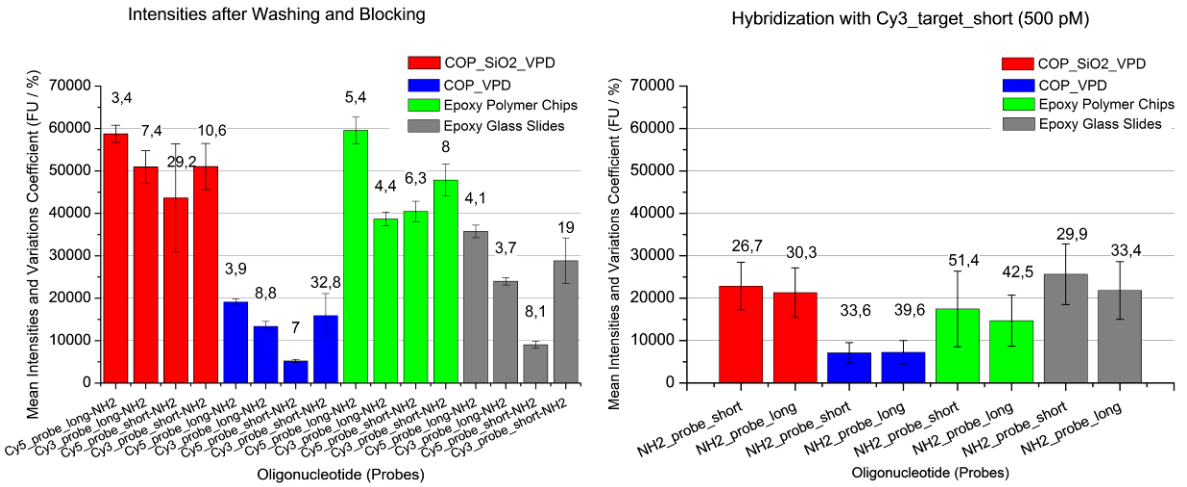

Figure 3. (Left) Scanning intensities of spotted fluorescence labeled and amino-modified oligonucleotides (probes) after blocking GOPTS coated COP-Chips (COP_SiO2_VPD), on GOPTS coated COP-Chips (COP_VPD), on commercial 3D-epoxy polymer chips and epoxy glass slides. (Right) Scanning intensities of Cy3 labeled oligonucleotides (targets) after hybridization on unlabeled and amino-modified oligonucleotides (negative and positive probes) after blocking.

Acknowledgements
Financial support of the Austrian Research Promotion Agency (FFG) via the project “content loading” and of the Austrian ministry for Innovation, Technology and Transport (BMVIT) via the project Biosens is gratefully acknowledged!

References
[1] Goddard JM, Erickson D, Analytical and Bioanalytical Chemistry 2009, 394, 469-479.
[2] Beaulieu I, Geissler M, Mauzeroll J, Langmuir 2009, 25, 7169-7176.
[3] Diaz-Quijada GA, Peytavi R, Nantel A, Roy E, Bergeron MG, Dumoulin MM, Veres T, Lab on a Chip 2007, 7, 856-862.
[4] Laib S, MacCraith BD, Analytical Chemistry 2007, 79, 6264-6270
[5] Raj J, Herzog G, Manning M, Volcke C, MacCraith BD, Ballantyne S, Thompson M, Arrigan DWM, Biosensors Bioelectron. 2009, 24, 2654-2658

S7-P78
Advanced UV-curable resins for adhesion application

Rebecca Kramer (1)*, Ling Yue (2), Rainer Puchleitner (2), Gisbert Riess (2), Wolfgang Kern (2)
(1) Polymer Competence Center Leoben GmbH, Roseggerstraße 12, 8700, Leoben, Austria
(2) Montanuniversität Leoben, Chair of Chemistry of Polymeric Materials, Otto Glöckel-Straße 2, 8700, Leoben, Austria
*rebecca.kramer@pccl.at

1. Introduction
Currently acrylic and epoxy UV-curable resins are used in various industrial applications including car varnishes or dental materials. Due to their excellent mechanical properties and the short reaction time UV-curable materials are often employed as adhesions for numerous polymeric materials [1]. The present study investigates the curing behavior of acrylates as well as epoxides, with regard to factors such as composition, amount of photo initiator, chemical structure, curing mechanism and irradiation time.

2. Theory
A significant difference between acrylic and epoxy resins is their curing mechanism. In addition to the fact that aerial oxygen might inhibit the radical crosslinking reaction of acrylic resins, a complete conversion of the functional groups is necessary [2]. Otherwise the cationic crosslink reaction of epoxy resins is not influenced by oxygen. Another considerable advantage is their behavior after stopping the irradiation: once started, the curing continues without further irradiation with UV-light [3].
Thus a number of resin formulations comprising of an acrylic or epoxy resin as well as a photo initiator were mixed and irradiated with various UV-light intensities using a belt conveyor irradiation device for industrial applications.

3. Experimental
The materials used for the experiments were an epoxy resin as well as an acrylic resin, based on commercial available systems. To evaluate the influence of the photo initiator, different formulations with various amounts of photo initiator were prepared under the exclusion of light, to prevent the decomposition of the photo initiator.

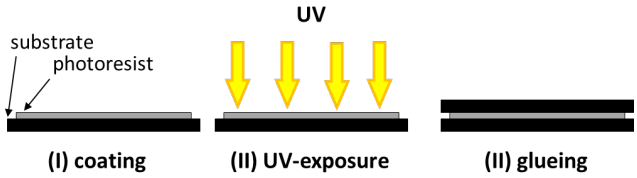

Figure 1. Scheme of UV-curing

4. Results and discussion

The conversion rate of acrylates (C=C double bond at 835 cm^{-1}) as well as epoxides (ring opening of epoxy groups) was determined by FTIR-spectroscopy, using the decrease of the corresponding absorption band as an index for the conversion. Reaction kinetics were recorded by comparison of different formulations with respect to the area of the characteristic absorption bands.

Figure 2 shows the influence of the irradiation dose as well as the influence of the photo initiator. It can be observed that with extended irradiation time the conversion increases. Analogue to this, the same effect can be observed for higher photo initiator concentration. The acrylic resins (see Figure 3) show similar results. With an increase of the irradiation time and the concentration of the photo initiator higher conversions can be observed. Compared to the epoxy resins, the acrylic resins require a higher irradiation dose to reach the maximum conversion.

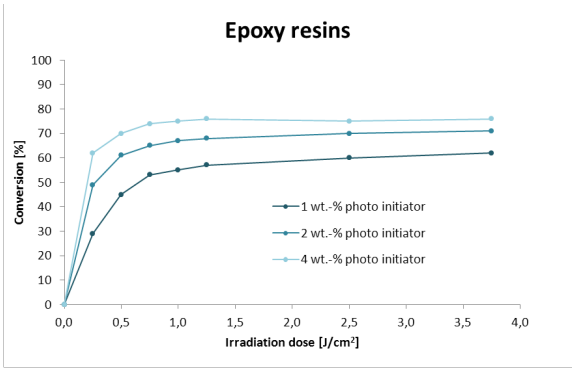

Figure 2. Reaction kinetics of epoxy resins containing different amounts of photo initiator

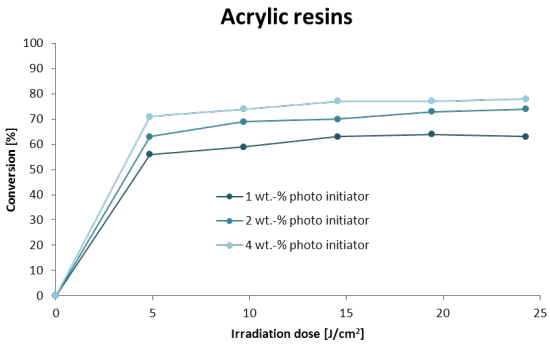

Figure 3. Reaction kinetics of acrylic resins containing different amounts of photo initiator

Due to the fact that the curing of the epoxy resins continues after stopping the UV irradiation dose of approximately 3.7 J/cm^2 is sufficient for a complete curing. In contrast to that the acrylic resins need an irradiation dose of about 25 J/cm^2.

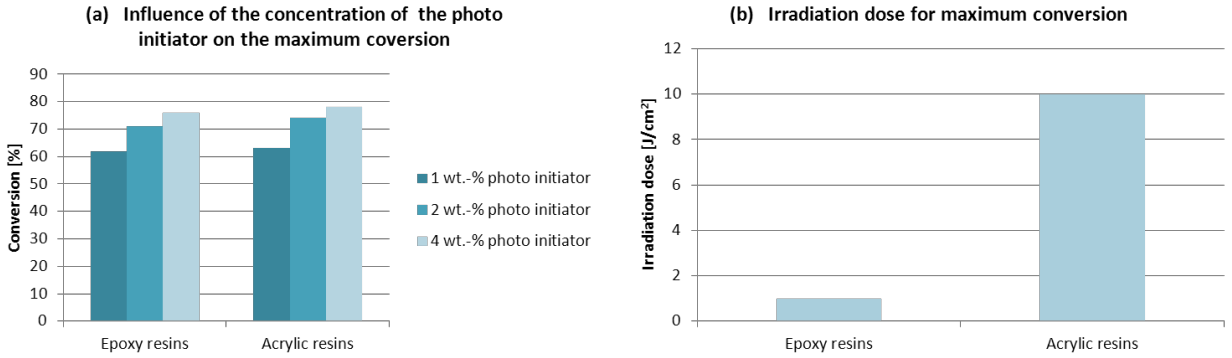

Figure 4. Influence of the concentration of the photo initiator (a) and the irradiation dose (b) on maximum conversion.

5. Conclusions

It is demonstrated that for increasing photo initiator concentrations and irradiation doses, all formulations show a significant tendency towards high conversions. Finally an ideal formulation was found for both systems fitting industrial requirements such as a high conversion and low energy costs. Potential applications for those resins might be glueing, lamination, varnishing, off-set printing or as primer for improved adhesion of varnishes.

Acknowledgements

This study was performed at the Polymer Competence Center Leoben GmbH (PCCL, Austria) with contributions of the Chair of Chemistry of Polymeric Materials (University of Leoben). PCCL is funded by the Austrian Government and the State Governments of Styria and Upper Austria.

References
[1] C. Decker, *Progress in Polymer Science* **1996**, 21, 593-650.
[2] K. Studer, C. Decker, E. Beck, R. Schwalm, *Progress in Organic Coatings* **2003**, 48, 92-100.
[3] C. Decker, T. N. T. Viet, H. P. Thi, *Polymer International* **2001**, 50, 986-997.

S7-P79
Iron based drier in high solid alkyds

B. Pirš*, S. Skale, J. Zabret, B. Znoj, P. Venturini
Central R&D of Helios Group, Helios Domžale d.d., Količevo 2, 1230 Domžale, Slovenia
*Barbara.pirs2@heilios.si

1. Introduction
Alkyd resins represent a class of polymers that are used in decorative surface coating formulations due to their low cost and versatility. One of most important aspect of alkyd coatings application is drying. This ensures proper chemical and physical characteristics of cured coating film. At present, alkyd surface coatings formulations mostly use organic cobalt salts as promoters of oxidative curing. Recent laboratory tests showed potentially carcinogenic properties of cobalt driers. This will, due to REACH legislation, limit or prohibit their use in decorative alkyd coatings [1].
In our work we study iron salts as possible alternative to cobalt driers. Kinetics of oxidation, physical drying and overall cured film performance was evaluated to find optimal iron driers concentrations. Results were compared with established cobalt drier alkyd coatings formulation.

2. Theory
Surface coatings application and performance requirements are usually determined with their binder. Alkyd polyesters are main binder in coating formulations for decorative and industrial applications since middle of 20th century, because they combine low costs and versatility with good esthetics, non-demanding application and proper service performance characteristics.
In past decade, enforcement of new environmental and health EU legislation is driven fast development of new surface coatings, especially in field of alkyd coatings. We were forced to abandon some of anticorrosive pigments, replace solvents containing aromatic fractions and stimulated to introduce alkyd resins with reduced solvents content (low VOC alkyds). At present, main focus of research of alkyd coatings are alternative driers. This could present challenging task, since introduction of new environmental and health friendly materials is often associated with deterioration of applicative and performance properties of surface coatings. In our case, deterioration is showed as poorer drying. This is manifested in prolonged dry to touch times, poor through drying and in consequence lower cured film hardness [2].
Drying of alkyd surface coatings is a combination of physical drying and chemical curing. Physical drying is evaporation of solvent from applied coating film. Chemical curing is free-radical reaction known also as autoxidation, where atmospheric oxygen reacts with double bonds in unsaturated fatty acids that remain in alkyd resin. The reaction is usually catalyzed with combination of organic metal salts, known as driers. In combination with alkyd resin they determine cured coating film performance [2]. Driers are typically classified by function as surface drier, through drier and auxiliary drier [4]. Surface driers possess catalytic effect and promote rapid surface drying. Through driers promote curing beneath the surface of the coating. They form oxygen-metal-oxygen crosslinks between the polymer molecules, which contribute to the through-drying process [5]. Auxiliary driers inhibit phase separation from the coating surface [4]. Effective drying is usually achieved with proper mixture of all three drier's types. This ensures proper chemical and physical properties of cured coating film [5]. Various surface driers demonstrate different catalytic behaviors [6]. The most widely used surface driers in solvent-borne alkyd coatings are cobalt salts (Co salts). Since their possible carcinogenic nature, use of Co salts in coating formulations will be limited, especially in decorative coating for general public use. Determination of effective alternative driers could present demanding problem. Since substitution of driers in an alkyd coating can impact not only the rate of chemical reactions, but also whole curing behavior and the network structure. The properties, which than reflects in modified physical and chemical properties of cured films [7].
Numerous studies were completed on different metal salts with the main focus on manganese and iron salts. The emphasis of the studies were oxidation reactions, especially curing kinetics [9,10]. Research was mainly performed on model substances [8]. Existing studies give us better understanding of curing mechanisms. But they lack applicability for alkyd coatings with lower VOC, which are used in coating industry. In our work, we focused on optimal concentration of iron driers mixtures and their impact on overall performance of cured alkyd with lower VOC.

3. Experimental
Materials: Long oil alkyd resin with low VOC (90 wt. % of solid content based on phthalic acid anhydride, polyol-pentaerythritol and linoleic fatty acids), driers (Cobalt bis(2- ethylhexanoate) with 10 % of Co and Fe-complex Borchy Oxy Coat with 1wt. % of Fe complex in 1,2-propylene glycol), anti-skinning agent (Methyl Ethyl Ketone – MEK) and aromatic free gasoline Shellsol D-40 were used for preparation of alkyd coating samples.

Sample preparation: Samples were prepared by adding individual components to alkyd resin and mixed with propeller stirrer for 10 minutes at room temperature. Tests were carried out after 24 h of sample storage.
Time-resolved FTIR experiments: FTIR spectra were obtained on a Nicolet 6700 spectrometer using the transmission technique (KBr crystal, range 4000-400 cm^{-1}, resolution $4cm^{-1}$). Measured conversion of alkyd double bonds versus time were used for determination and comparison of alkyd curing kinetics catalyzed by Co and Fe based driers.
Drying time: Drying performance of samples with different concentration of Fe and Co-based driers as a part of curing process was determined according to ASTM D5895-03 using BYK drying recorder.
Physical methods: Mechanical properties, elastic (storage module) and plastic (loss module) of cured film was studied with frequency domain oscillatory tests, performed with Anton Paar MCU380 rheometer. Sensor amplitude was selected in elastic deformations range. Rheometer MCU380 was also used for evaluation of coating drying with Tack test. For determination of cured coating hardness we used standard König method.
Electrochemical methods: Electrochemical impedance spectroscopy was used for evaluation of protective performance of coatings. Measurements were performed with Parstat 2273 potenciostat and Tait cell. EIS data were evaluated with proper equivalent circuits.

4. Results and discussion

FTIR method was used for evaluation of the curing kinetics of alkyd coatings with different driers and its concentration by quantitative determination of double bounds concentration in alkyd coating. Curing process of alkyd coating with Fe based drier was slower compared to alkyd coating with Co based drier. The curing process is pseudo-first-order reaction for samples with Fe and Co based driers (Fig. 1). Major difference during curing was observed in the beginning and at the end of the reaction. For the alkyd samples with Fe based driers the induction time was observed and curing of the double bonds was still noticed after 24 hours. On the other hand, the samples with Co based drier did not showed any induction times. The curing process was finished before 10 hours since double bond peak in FTIR diagram diminished. Application and physical properties of cured coating samples were analyzed by evaluation of drying times and by rheological parameters. Drying times for alkyd samples with Fe based and Co based drier are different. That can be also observed in rheological parameters during curing. Cured alkyd films were evaluated by hardness measurements and electrochemical impedance spectroscopy (EIS). Alkyd films cured with iron drier show lower hardness and poorer protective properties in comparison to coatings cured with cobalt drier. Protective underperformance of alkyd coatings cured with iron drier is consequence of higher water uptake and bigger porosity.

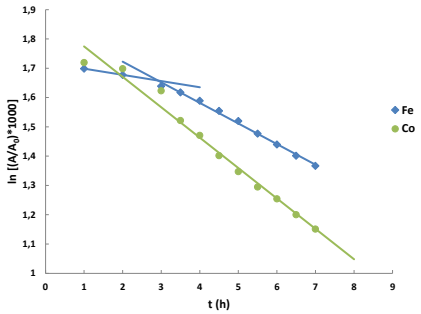

Figure 1: Graph represent the conversion of alkyd double bonds during time for Co and Fe based catalytic driers (assumption of pseudo-first-order rate reaction).

5. Conclusions

Alkyd resins with low VOC with Co and Fe based driers have different kinetic rates during curing. With FTIR method it was observed, that iron drier has lower catalytic ability than cobalt drier. Iron drier show different influence on drying and curing properties of alkyd resin with low VOC, when compared to cobalt drier. IR spectra show, that all double bonds of alkyd resin disappear with Co based drier before 24 hours of curing. While with Fe based drier they can be still observed. Hardness measurements indicate similar behavior. Higher values of hardness are achieved with Co based drier. Different curing process of alkyd coating film with both driers were also confirmed by oscillatory and EIS methods. Results of the present study clearly demonstrate that the iron based drier with the combination of tested low VOC alkyd resin does not give us desired coating performance and further research on drier modifications are needed.

Acknowledgements

»Operation part financed by the European Union, European Social Fund. Operation implemented in the framework of the Operational Programme for Human Resources Development for the Period 2007-2013, Priority axis 1: Promoting entrepreneurship and adaptability, Main type of activity 1.1.: Experts and researchers for competitive enterprises.«

References

[1] Tracton Arthur A. T. 2006. 51 Alkid resines. Coatings technology handbook. Third edition 2006 76-1,76-18.
[2] Hofland A. 2012. Alkyd resines: From down and out to alive and kicking. Progress in Organic Coatings 73. 274-282

[3] Bouwman E., Van Gorkum R. 2007. A study of new manganese complexes as potential driers for alkyd paints. Journual of coating Technology Resrch 4. 491-503.
[4] Soucek M.D., Khattab T., Wu J. 2012. Review of autoxidation and driers. Progres in Organic Coatings 73. 435-454.
[5] Pilemand C., Wallström E., Poulsen P. B. 2005. Substitution of Cobalt Driers and Methyl Ethyl Ketoxime in Oxidative Drying Systems. European oatings2/2005. 7-20.
[6] Oyman O. Z. 2005. Towards Environmentally Friendly Catalysts For Alkyd Coatings. Doktorska dizertacija.Technische Universiteit Eindhoven. Nizozemska. 1-183.
[7] Erich S. J. F., Laven J., Pel L., Huinink P. H., Kopinga K. 2006. NMR depth profiling of drying alkyd coatings with different catalysts. Progress in Organic coatings 55. 105-111.
[8] Warzeska T. S., Zonneveld M., Van Gorkum R., MuizebeltJ.W., Bouwman E., Reedijk J. 2002. Methods for studying the drying of alkyd paint using (EL) as model compound. Progress in Organic Coatings 44. 243-248.
[9] Oyman O.Z., Ming W. Van der Linde R. 2003. Oxidation of model compound emulsions for alkyd paints under the influence of cobalt drier. Progress in Organic Coatings 48. 80-91.
[10] Erich S. J. F., Laven J., Pel L., Huinink P. H., Kopinga K. 2006. Influence of catalyst type on the curing process and network structure of alkyd coatings. Polymer 47. 1141-1149.

S7-P80

Textile-polymer composite barrier materials against UV radiation and microorganisms growth

J. Sójka-Ledakowicz (1)*, J. Olczyk (1), T. Jesionowski (2)
(1) Textile Research Institute, Brzezinska 5/15, 92-103 Lodz, Poland
(2) Poznan University of Technology, Institute of Chemical Technology and Engineering, M. Sklodowskiej-Curie 2, 60-965 Poznan, Poland
* ledakowicz@iw.lodz.pl

1. Introduction

The intensive development of the production of micro and nanostructures, is now a priority direction of textile materials engineering, enabling the elaboration of advanced multifunctional textile-based materials[1,2]. The aim of the research works carried out by a research team was the formation of new textile-polymer composites consisting of substrate material based on polyester fibres and of coatings based on acrylic polymers, containing non-toxic nanostructured ZnO modifiers. The new composite material is to provide for a man protection against the harmful effects of microbes and ultraviolet [UV] radiation.

2. Theory

Zinc oxide preparations, micronized to the micro-and nanometric size, and ZnO- SiO_2 hybrids were used to obtain textile-polymer composites protecting against UV and microbial effect. These formulations were applied onto the surface and into the structure of the textile materials made of polyester fibres by coating or dip-coating method using a paste, based on acrylic polymers.
Adequate preparation of the textile substrate affects the method of modifiers introduction into the structure of selected textile substrates. Alkaline or enzymatic pretreatment of products made of polyester fibres was performed to loosen their structure, to improve wettability and to improve adhesive properties - as compared to materials not subjected to such treatments. Initial modification of textile substrates made of polyester fibres contributes to the increase of functional end groups -COOH, -OH, which in turn improve the hydrophilic and adhesive properties of these fibers.

3. Experimental

Polyester (poly(ethylene terephthalate)) woven fabric was modified. ZnO and ZnO-SiO_2 modifiers were introduced to textile structure. A very important step in this process, before the application of zinc oxides onto textile substrates, is the pre-treatment of these materials. Two methods of surface modification of textile substrates were applied to improve adhesion properties, to loosen the structure and to improve wettability.
Liquid Sorption of fibres - was tested according to the own method developed at Textile Research Institute, by setting indicators on the instrument Sorp-3. Wetting angle - tested according to goniometric method using Goniometer PGX (by FIBRO Systems). Evaluation of the surface microstructure of the modified materials – using scanning electron microscope with the adapter ESD.
Alkaline treatment: the bath contained sodium hydroxide 38°Bé, sodium carbonate, sequestering-wetting agent. Bath ratio 10:1, bath temperature 98°C, time 60 min.
Enzymatic treatment: the bath contained TEXAZYM PES (produced by INOTEX) – the enzyme from the esterases group, temperature 35^0C, process time 30 min., pH-4.2, the bath ratio 10:1.
Preparations of zinc oxide nanoparticles were introduced into the structure of the textile substrate by coating with pastes based on acrylic resins or dip-coating using dispersions based on acrylic polymers.

The resulting new composite materials were evaluated with reference to protective properties against UV (the whole UV range using spectrophotometer according to PN-EN 13758-1:2005) and microbial effect for selected microorganisms (using screening qualitative method).

4. Results and discussion

The use of initial modification of woven fabrics made of polyester fibres contributes significantly to the increased deposition of coating pastes, and above all to the increase of the amount of ZnO, ZnO-SiO_2 nanoparticles attached to the textile surface(tab.1,phot.1).

Modification of textile substrate surface using alkaline and enzymatic treatment improves the fibres hydrophilic and adhesive properties.

Samples coated with ZnO-SiO_2 showed good antibacterial activity against the tested bacteria species *Staphylococcus aureus.*

Table 1.

The results obtained for the polyester woven fabric – alkali or enzyme pre-treated - and then modified by coating with pastes containing micronized ZnO-SiO_2

Sample	UPF – Ultraviolet Protection Factor	**Paste** – deposition degree onto woven fabric [g/m^2]	**Oxide** – deposition degree onto woven fabric [g/m^2]
TPES/0	25	0	0
TPES raw	25	0	0
TPES/ZnO-SiO_2/ unmodified	>50 (56)	15.8	3.20
TPES/ ZnO-SiO_2/modified alkali scouring	>50 (70)	18.75	3.80
TPES/ ZnO-SiO_2/modified enzyme scouring	>50 (52)	17.85	3.75

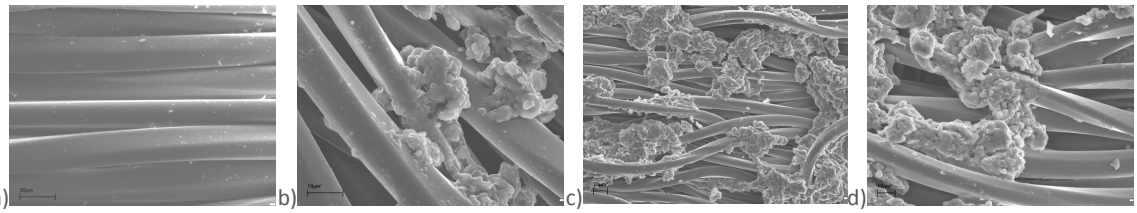

Phot 1. SEM of polyester fabrics: a) raw b)unmodified c) alkali scouring d) enzyme scouring - modified with ZnO-SiO_2

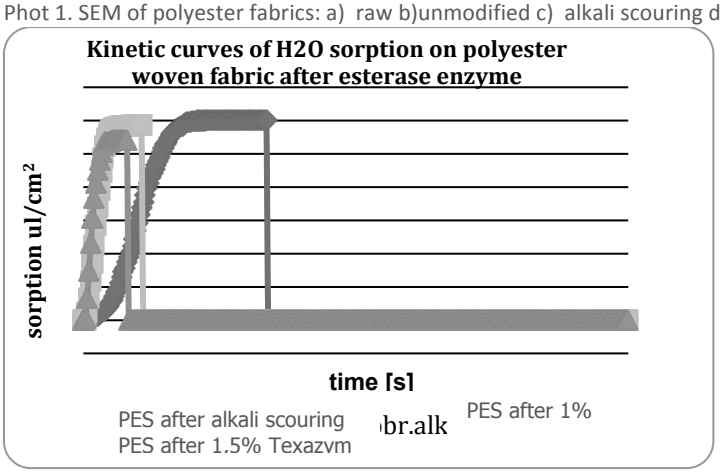

Fig. 1 Water sorption - kinetic curves - for the polyester woven fabrics treated with esterase enzyme.

5. Conclusions

The study justify the initial surface modification (alkaline or enzymatic) of the polyester woven fabrics in order to improve adhesion properties. Such products are characterized by an increased amount of attached ZnO, ZnO-SiO_2 particles to the surface. The resulting textile-polymer composites containing on the surface and in their structure ZnO or ZnO-SiO_2 particles, exhibit good barrier properties against UV radiation (UPF> 40) and the inhibitory effect against selected microorganisms.

References
[1] Sójka-Ledakowicz J., WalawskaA., Olczyk j., Jesionowski T. "Microstructure analysis of the layers containing nanoparticles hybrids ZnO-SiO2, TiO2-SiO2 on textiles fabric" EPF 2011, XII GEP Congress, Granada, Spain
[2] Siwińska-Stefańska K., Przybylska A., Sójka-Ledakowicz J., WalawskaA., Olczyk j., Jesionowski T. : The effect of oxide composite on the barrier properties of textile fabrics" Chemical Review nr 89(12); 2010 s.1189-1195 ISSN 0033-2496

Acknowledgement
The study was realised within the Key-Project POIG no. 01.03.01-00-006/08, acronym ENVIROTEX co-financed by the European Regional Development Fund within Operational Programme Innovative Economy 2007 – 2013 and statutory works of Textile Research institute realised in 2012 and financed by the Ministry of Science and Higher Education.

S7-P81
Adhesive activity AlTiN layers based on forming polymer coatings

Y. Auchynnikau (1)*, N. Chekan (2), E. Esimont (1), I. Akula (2), V.Stuk (3)
(1) Grodno State University, Faculty of engineering innovation, str. Ozeshko 22, 230023 Grodno, Belarus
(2) Physical-Technical Institute, str. Kuprevicha 10, 220141, Minsk, Belarus
(3) JSC Belkard, SMC «Promagromash», str. Schastnogo 38, 230026 Grodno, Belarus
*ovchin_1967@mail.ru

1. Introduction
In terms of market production has been a steady rise in prices for energy, materials, labor, which has a great influence on the prices of the goods and products, and in connection with this priority in the development of modern engineering is to create a resource-saving technologies, the creation of materials with improved performance in the based on the development of nano technology, nano materials, surface engineering.

2. Theory
The great interest in this connection is shown to the coatings produced by plasma-chemical methods based on vacuum technology. It is known that coatings based on diamond-like carbon (DLC), obtained from the plasma of cathodic arc discharge, possess high hardness - up to 60 ÷ 80 GPa, a low coefficient of friction of the order of 0.08-0.1 without the supply of external lubrication in pairs with different materials , high wear resistance, corrosion resistance to most corrosive environments, including exposure to biologically active fluids (blood, synovial fluid, etc.). However, this coating has a number of shortcomings that prevent the full use them in engineering. Diamond-like coatings are characterized, high residual stress, leading to a sharp decrease in the values of the bond coating adhesion to the substrate, the presence of particulate matter in the plasma flow, reducing friction and anti-corrosion properties of the coatings, prevent widespread use of diamond-like carbon coatings (DLC) in the formation of hardened layers on the metal-working surfaces tools, precision friction pairs and tooling used in the casting of plastic products, petrochemical products.

3. Experimental
However, there were some shortcomings constraint of such coatings. For example, a large, from a fraction of a micron to tens of microns, particulate matter (PM) in the plasma flow significantly limits the scope of the DLC coatings produced by cathodic arc method. For products mikroelektromechanikal and precision mechanics, optics, and are not allowed to cover the graphite macroinclusions. The same requirements apply to abrasion by diamond-like coatings that are applied to products superfinishing mechanics and optics. The presence of MCH significantly diminish the protection and anti-corrosion properties of carbon coatings, as they are the source of defects, such as punctures, resulting in the separation of particulates from the cover because of the low particulate adhesive bond to the substrate. Development of technological process of strengthening the foundations of engineering products of structural steels by applying antifriction, corrosion-resistant coatings with low mechanical stress and are characterized by a low density of macroscopic defects is the actual problem, the solution of which will increase your endurance. One of the areas to obtain such protective layers is to obtain combined coatings, including in its membership several chemical elements. So widely used in engineering, aviation coatings based on titanium nitride, titanium carbide, titanium carbonitride, drawbacks of these coatings is insufficient heat resistance located in the 800-873 K

4. Results and discussion
Thin film coating and nitrides of transition metals are widely used in many technical fields, especially where related to use in products of their high hardness, chemical resistance and improved tribological properties. Among these, the most studied thin-film coating systems based on TiN. The main drawback of anti-adhesive layers TiN limited oxidation (~ 450-500 ° C). To increase the heat resistance of these coatings in the formation of layers of introducing more chemical elements such as Al, Cr, Cu that increase generated oxidation coatings. Initially, the work in this direction were made by plasma chemical synthesis coatings chemistry TiAlZrN, because Such systems are used in obtaining electronic equipment industry. On the basis of these coatings have been

proposed formulations TiAlN, that were analogues of TiN, but has a higher temperature characteristics and intended solutions for technical applications.

5. Conclusions

Found that the active aluminum reacts with nitrogen and aluminum oxides are not formed, while the titanium forms as nitrides and oxides. In general, the deposition of coatings obtained from alloyed Ti-Al cathodes using arc evaporation mainly formed titanium nitride and aluminum. Cover AlTiN, formed under high vacuum in the chamber characterized by a large number of inclusions, which are actually the same physical and mechanical properties of the matrix of the coating. The increase in gas pressure in the vacuum chamber causes an increase in the geometric dimensions of the inclusions, increasing their concentration in the matrix of the coating. This distribution of inclusions observed at a bias voltage on the cathode - 50V. The increase in bias voltage on the cathode leads to a change of the distribution of inclusions in a matrix coating with increasing pressure of the reaction gas in the chamber is the dispersion of structural components in the coating AlTiN.

S7-P82
Application of magnetron method to obtain barrier materials on textile background media

Joanna Koprowska, Błażej Wiśniewski
Textile Research Institute, Brzezinska 5/15, 92-103 Lodz, Poland
*koprowska@iw.lodz.pl

1. Introduction

The aim of the research was to obtain barrier materials coated with thin metallic coatings that lower human exposure to electromagnetic fields in a wide range of frequencies and limit interference with electronic devices indoors.

2. Theory

The Earth's natural environment has been disrupted by electromagnetic field, which is primarily generated by such sources as huge amount of radio and television broadcasting stations, satellites, radars, radio navigation, mobile radio communication, including mobile phones. Unit power of these devices is very different and it can reach up to 10 MW or more [1] This has led to the increased interest in barrier materials to protect both a man against external electromagnetic fields, as well as electronic equipment.

3. Experimental

Barrier materials for protection against electromagnetic fields have been obtained at the Textile Research Institute using the special device which applies magnetron sputtering method to deposit thin metallic coatings on various textile media (Figure 1). The materials are in a tape form - 60 cm wide, long from a few to several meters. Coatings can be applied continuously ("roll to roll") in a single layer or in multi-layer systems, on one or both sides of textile media (Figure 2).

Fig. 1 The device to deposit thin metallic coatings onto various textile media

Fig. 2 Barrier materials with different metal alloy coatings - examples

4. Results and discussion

Single metals, such as copper and binary or ternary alloys (Cu / Sn, Ni / Cr, Cu / Zn / Ni, Ni / Cu / Fe) are deposited on textile background material (nonwovens, woven fabrics). On the basis of tests on shielding effectiveness (SE) performed by Electromagnetic Compatibility Laboratory at Wroclaw University of Technology it was found that the value of SEMIN. for newly obtained sputtered materials ranged from 20 to 26 dB. However, for the best samples SE value was in the range 38-52 dB for the frequency of 27.12 MHz. Average surface resistance (tests performed at Textile Research Institute in Lodz) for the above mentioned materials for the best SE results ranged from 1.6 to 5.0 Ω. On this basis, textile background material was selected (polypropylene (PP) nonwoven of 150 g/m2), on which the metallic coating gave the best shielding effectiveness results.

Textile barrier materials against electromagnetic fields can be used to:
- reduce interferences of electronic devices operation in the following sites: computer centres, banks, stock exchange premises, data banks, telephone operation centres, hospitals, offices, consulting rooms,

- reduce human exposure to external electromagnetic field (if the measured values exceed the permissible field strength limits) by the so-called architectural shielding - room shielding.

5. Conclusions

- Magnetron method is an effective technique to obtain materials with metallic coatings on various textile substrates
- The best results of shielding effectiveness were obtained for the following coatings on polypropylene nonwoven: Cu / Sn (44-52 dB), and for Cu / Zn / Ni (32-38 dB) for 27.12 MHz frequency. looking forward to receiving your contributions.

Acknowledgements
The research work was realised within the Key-Project POIG no. 01.03.01-00-006/08, acronym ENVIROTEX co-financed by the European Regional Development Fund within Operational Programme Innovative Economy 2007 – 2013.

References

[1] H. Aniołczyk, Ekspozycja zawodowa i w środowisku komunalnym na pola elektromagnetyczne [Occupational exposure and in municipal environment onto electromagnetic field] Handbook in Polish – ISBN 83-88261-50-9, Instytut Medycyny Pracy im. Prof. J. Nofera, Łódź, 2000

Session 8: Theory, modeling and simulations

S8-P83
Model for the prediction of elegational heating rubber compounds in conical dies

Leonhard Perko (1)*, Michael Fasching (2), Walter Friesenbichler (1)
(1) Montanuniversitat Leoben, Department of Polymer Engineering and Science, Chair of Injection Molding of Polymers, Otto-Gloeckel-Strasse 2, 8700 Leoben, Austria
(2) Polymer Competence Center Leoben, Roseggerstrasse 12, 8700 Leoben, Austria
*leonhard.perko@unileoben.ac.at

1. Introduction

The bulk temperature is a very important parameter for the processing of rubber compounds. Temperature is crucial for many material properties like viscosity, heat conductivity, density, heat capacity and the cross linking behavior. Polymers usually have a low thermal conductivity and show effects like heat dissipation generating an inhomogeneous bulk temperature that is very difficult to measure and even harder to predict by means of simulation. Besides shear heating, which is a well-known phenomenon, elongational heating is neglected by most of the injection molding simulation tools. It occurs whenever there are abrupt changes in the cross section of the flow. Some scientific authors describe the pressure loss according to the elongational flow [1-5], but as far as we know no efforts have been made to calculate and measure the heating effect according to this special kind of flow.

2. Theory

Eq. 1 shows the law of conservation of energy [6] for the cylindrical coordinate system

$$\underbrace{\rho \cdot c_v \cdot \frac{DT}{Dt}}_{\text{witnessed change of energy over time}} = \underbrace{\sigma_{rz} \cdot \frac{\partial v_z}{\partial r}}_{\text{shear heating}} + \underbrace{\sigma_{zz} \cdot \frac{\partial v_z}{\partial z}}_{\text{elongational heating}} \underbrace{- T \cdot \left(\frac{\partial p}{\partial T} \right)_v \cdot \frac{\partial v_z}{\partial z}}_{\text{(de)compression}} \underbrace{- \frac{1}{r} \cdot \frac{\partial (r \cdot q_r)}{\partial r}}_{\text{heat conduction}} + \underbrace{\dot{S}}_{\text{inner sources of energy}} \qquad (1)$$

where z = flow direction; r = radius in m ; ρ = material density in kg/m3; cv = heat capacity in J/(kg*K); T = Temperature in K; t = time in s; σrz = stress in the r-plane into the z-direction in N/m2; vz = flow rate into the z-direction in m/s ; p = pressure in Pa*s; qr = specific heat flow in W/m2 and S = inner heat sources in W/m3.
This equation describes the thermodynamic changes in a fluid that flows through a circular conduit, like it occurs in polymer processing when a thermoplastic polymer melt or a rubber compound is injected through a runner system into a mold. The term on the left side describes the temperature change in the material whereas the terms on the right side describe the different mechanisms of heat creation. Shear heating and elongational heating are the two dissipative terms in the equation of energy where the second is the main topic of this work.

3. Experimental
For the verification of the theoretical calculations experiments on an injection molding machine were made.

4. Results and discussion
The experimental setup as well as the results of this work cannot be shown right now due to a non-disclosure agreement with the industrial partners. A longer version of this abstract has already been written but still has to be cleared by the consortium. It will be sent in within the next three weeks.

References
[1] F.N. Cogswell, *Polymer Engineering and Science* 1972 12, 1, 64-73
[2] D.M. Binding, *Journal of Non-Newtonian Fluid mechanics* 1988 27, 2, 173-189
[3] M.E. Mackay, G. Astarita, *Journal of Non-Newtonian Fluid Mechanics* 1996 70, 3, 219-235
[4] M. Ansari, A. Alabbas, S.G. Hatzikiriakos, E. Mitsoulis, *International Polymer Processing XXV* 2012 4, 287-296
[5] M. Ansari, T. Zisis, S.G. Hatzikiriakos, E. Mitsoulis
[6] R.B. Bird, Transport Phenomena, Jon Wiley & Sons, New York, 2007, p. 333 ff.

S8-P84
Numerical (CFD) simulation of polymer-drug distribution during injection molding using OpenFOAM and SIGMASOFT®

Herwig Juster*, Klaus Straka, Georg Steinbichler
Johannes Kepler University, Institute of Polymer Injection Molding and Process Automation, Altenberger Strasse 69, 4040, Linz, Austria
*herwig.juster@jku.at

1. Introduction
It has been estimated that 40% of all active pharmaceutical ingredients (APIs) can be considered poorly water soluble. Nevertheless, water affinity determines the absorption efficiency of a given API within the human organism. Therefore, new processes and formulations need to be developed to enhance the bioavailability of such substances [1].
Injection Molding (IM) is known to be an effective and cost-efficient method for advanced manufacturing. As a result, this technique was here chosen to fabricate drug dosage forms with enhanced solubility. In other words, a dispersion of polymer material, API and additives is prepared and then injected into the designed tablet mold under high pressure (Figure 1) [2].

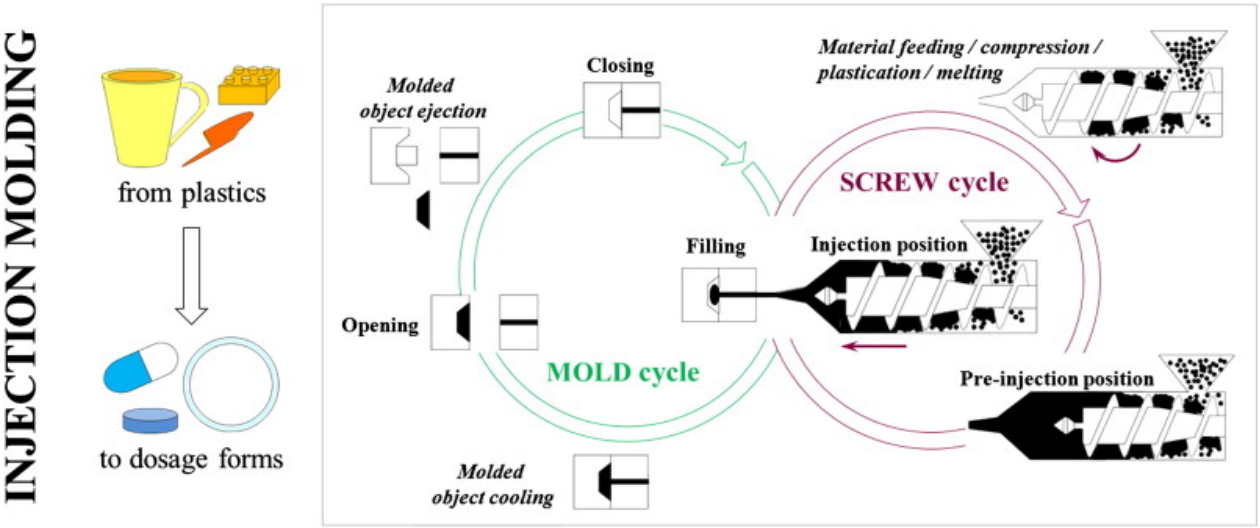

Figure 1. Graphical representation of the injection molding cycle [2]: Using injection molding technique for drug delivery.

2. Theory
In order to enhance the solubility of the API, solid dispersions are here approached. In this case, the solid dispersion consists of a system where the API is dispersed in a polymer matrix.
The solid dispersion is then used to prepare drug dosage forms through injection molding technique, which further allows the preparation of gender targeted dosages by changing the API concentration in the polymer matrix (gender conforming

medications).The distribution homogeneity of the drug within the polymer matrix must be ensured by the end of the injection molding process. This is necessary to provide the same product quality in each pharmaceutical dosage form, regarding drug content.

3. Experimental

In this work, the open source CFD software package OpenFOAM (Open Field Operation and Manipulation) is used to simulate the API distribution in the melt during processing in the plasticizer unit (Figure 2). OpenFOAM comes with a number of predefined solvers for different tasks, which can be modified for each problem [3]. The polymer BASF Soluplus® (Figure 3) is used as the polymer matrix which contains the API (solid dispersion). Soluplus® is a polyvinyl caprolactam-polyvinyl acetate-polyethylene glycol graft co-polymer with a glass transition temperature of approximately 70°C [4]. The simulation results obtained will be validated by performing real injection molding experiments of this solid dispersion.

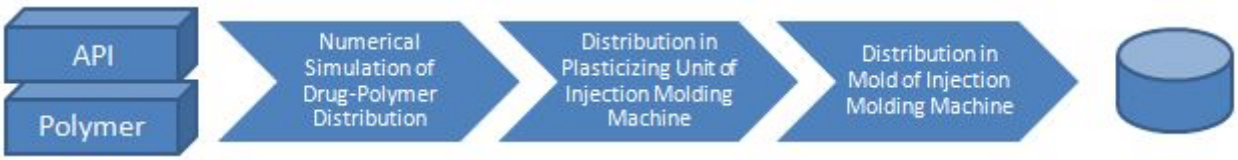

Figure 2. Process Flow Chart

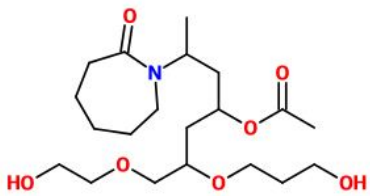

Figure 3. Soluplus®-Monomer: Used as a drug carrier matrix system

Further goals of this project are also the simulation of the API distribution in the individual cavities of the injection mold, as well as the simulation of the pressure and temperature exposure of the melt during the whole process, in order to control undesired degradation of the API. These simulations will be performed using the polymer simulation software SIGMASOFT®. The optimization of the screw design, in terms of mixing performance is also a long-term goal of this project.

5. Conclusions

The processing of drug carrying polymers using injection molding technique along with process simulation play a key role in the improvement of the resulting tablets solubility . This in turn, will certainly contribute for the implementation of more cost-effective production technologies within the pharma industry, allowing yet for the efficient development of gender-targeted medications.

References

[1] C.A Lipinski, Curr Drug Dis. 2001; 4:17-19
[2] L. Zema et.al, Injection Molding and its application to drug delivery, Journal of Controlled Release, Vol. 159, Issue 3, 2012
[3] OpenFOAM, User Guide, Version 2.1.1, 2012
[4] BASF SE, Technical Information, Care Chemicals Division, Pharma Ingredients, 2010

S8-P85
Application of singular systems in polymer science

Nataša A. Kablar
Lola Institute, Kneza Višeslava 70a, 11000 Belgrade, Serbia
Faculty of Computer Science, Knez Mihailova 6/V, 11000 Belgrade, Serbia

Extended Abstract

In this paper we present time varying and time invariant singular systems which include mathematical model, and dynamical analysis and synthesis, with controller design that can be used in modeling materials and dynamical changes in polymer science. Application of this approach can give further dynamical insight in qualitative properties of materials used in material science and new materials in polymers, that can be used in production of comonents for electronics, medical devices, parts for renewable energy components, etc. Also it gives approaches and ways how to mathematically model materials and polymers in material and polymer sciences. Further it gives ways how to examine their dynamical properties of mathematical models of materials and polymer materials. It will also be given ways and insights how to further improve materials that can be used.

Model of Singular Systems

In material and polymer sciences it can be used model techniques and mathematical modelling. In this ppaer we use system and control theory to propose mathematicala modelling techniques and dxynamical analysis results for analysing qualitative proiperties of the system, and controller design techniques for designing controllers and stabilizing techniques or stabilizers for materials in material and polymer sciences.

Applicable models from systems and control theory can be both time varying and time invariant and nonlinear and linear models. Many material characteristics can be modeled using any of these models. In this ppaer we propose how to use time varying and time invariant singular systems models, but in further work we will include singularly impuslive and impulsive dynamical systems theory because of characteristics of materials that can be modeled with this approach or modelling strategies or controller needs that use this mathematical models and approaches.

Time varying singular systems can be used for modelling in many areas ranging from economy and demography, social sciences, electronics and mechanics, biology and chemistry, and other areas. Here we will for the first time propose how to use time varying and time invariant singular systems for mathematical modelling and control theory in material and polymer sciences.

Time varying singular systems is given with

$$E(t)\dot{x}(t) = f(x(t), u(t), d(t), a(t), t)$$

$$y(t) = g(x(t), u(t), d(t), a(t), t)$$

With function f: $\boldsymbol{R}^n \times \boldsymbol{R}^m \times \boldsymbol{R}^d \times \boldsymbol{R} \rightarrow \boldsymbol{R}$, $t > 0$ for every $t \in \boldsymbol{R}$. State variable is $x(t) \in \boldsymbol{R}^n$ where n is dimension of the state space. Control variable is $u(t) \in \boldsymbol{R}^m$. Disturbance $d(t) \in \boldsymbol{R}^d$ represents disturbance of material characteristics of material. $E(t)$ is singular time varying matrix. In special case $E(t)=I$ the model becomes classical time varying model of the system.

In specification to material and polymer sciences we introduce material characteristic as state variable $x(t)$ given above, or function $a(t) = m(a, b(t), t)$, with function m: $\boldsymbol{R} \times \boldsymbol{R} \times \boldsymbol{R} \rightarrow \boldsymbol{R}$, a being the coefficient that represents static characteristics of material, and $b(t)$ being coefficient that represent time varying characteristics of material.

In material and polymer sciences first step is mathematical modeling in form of time varying or time invariant singular or classical system, and further design of controllers and control laws $u(t)$ that will enable controller techniques and stabilizing of material. Specific control techniques and control laws will be given in paper.

Dynamical Analyses and Qualitative Properties

According to mathematical model of the material, it will be given dynamical analyses and it will be shown qualitative properties of materials, that include stability, dissipativity, controllability, observability, stabilizibility and controller design, and robustness of material, and other characteristics of material that are of interest in material and polymer sciences.

Design of Controllers

According to mathematical model of material it will be given controller techniques that can be used in modelling controllers and stabilizers for controlling and stabilizing material properties.

Control of Material Characteristics

According to mathematical model of the material characteristics and material, it wil be chosen specific state variable that corresponds to materia characteristic of interest that has to be analysed and improved. Control techniques that we will propose will be based on systems and control theory and needs in material science for improvement of this material characteristic and material properties.

Proposition of New Control Techniques

According to control theory ways and approaches and needs in materal sciences ot will be proposed control techniques that can be applied in material and polymer science and new control techniques that needs to be applied currentlky in material sceinces based on theory presented.

Proposition of New Materials

According to specific charactersitic of materials and its values over time it can be seen the behavior of material characterized with this characteristic. According to mathematical model and dynamical systems theory and control theory it can be further proposed ways hoe to improve this characteristic and material proiperties. Possibility of stabilization can be improvement of material characteristics or addition of new component acting as stabilizer. It is main focus of paper that starts with classical systems and control theory that can be aplied in materail and polymer science. Furtherways will be mentioned also, but concrete work on them will be base for further work.

Conclusion

In this paper we have presented syngular systems theory and mathematical models. It is shown how to dynamicaly analyse the mathematical models. It is further shown how to make controller designs and how to examine specific cjharacteristic of material of

interest, and how to improve this characteristics properties and ways how to propose new materials or stabilization methods of materials in material and polymer sciences.

Further Research

Further research will explore new mathematical mdels in polymer and material sciences with establishing concrete mathematical models. It will be further used specialzed dynamical systems thgeory to material sciences for exploring dynamical characteristics and modelling of materials in material sciences. Further,m it will be prosposed, according to the dynamical analyses, statistical properies and quantitative results, improvement of materials and new controller techniques, and it will be proposed systematic and general way how to propose new materials and materials building. Further insights will be given how to produce this materials.

Acknowledgement

The author is gratefull to all of those that were suppostive and creative in achieving this results.

References

[1] *Singular Systems*, S. L. Campbell, SIAM Journal, 1980.
[2] *Analysis and Design of Singular Systems*, D. Lj. Debeljković, 1992.
[3] *Robustness Stability of Nonlinear Nonstationary Singular Systems*, N. A. Kablar, Master Thesis, University of Belgrade, Faculty of Mechanical Engineering, Belgrade, 1998.
[4] *Singularly Impulsive Dynamical Systems with Application in Biology*, N. A. Kablar, Doctoral Thesis, University of Belgrade, Faculty of Mechanical Engineering, Belgrade, 2007.
[5] Classical references in material and polymer sciences.

S8-P86

Neuron networks based on macromolecules and an alternative to Darwinist approach to the problem of complex systems evolution

Ibragim Suleimenov (1)*, Dina Shaltykova (1), Sergei Panchenko (1,2)
(1) Almaty University of Power Engineering and Telecommunications, Baitursynov st.126, 050013, Almaty, Kazakhstan
(2) al-Faraby Kazak National University, Physico-Technical Faculty, al-Faraby av. 71, 050014, Almaty, Kazakhstan
*Esenych@yandex.ru

1. Introduction

It has been believed until recently that all evolution scenarios of complex systems within the natural science framework are related to the concept of mutations in one way or another [1-4]. It was supposed that elements forming any complex system, over the course of time may change qualities sporadically as a result of random fluctuations (mutations in biological terminology). Provided that qualities acquired by the elements as a result of mutations improve their adaptability to the environment, they are inherited or otherwise consolidated.

This scenario has been initially employed in the theory of origin of species, and corresponding point of view is often referred to as Darwinist in literature. It has been used to interpret the evolution mechanism of systems of different nature, including socio-economic ones.

However, attempts to explain the evolution mechanism, preceding biological, encounter significant limitations. The most known limitation is the astronomical period of time required for emergence of macromolecules capable of carrying genetic information as a result of random mutations. (Some sources cite that this period exceeds the age of the Galaxy)

This work considers an evolution scenario, that alters from the point of view based on analysis of random fluctuations of complex system elements.

2. Macromolecule as neural network

It is shown that significant number of complex systems of different nature may be considered as analogues of neural network. In particular, method of imitational modeling established that any partially dissociating macromolecule may be considered as an analogue of Hopfield neuroprocessor due to its own properties.

In this case, every functional group of a macromolecule is viewed as an analogue of a neuron; charge state corresponds to logical variable, describing output of the neuron (presence of charge – logical one, its absence – logical zero). Charge state of functional group (e.g. carboxyl) depends on tension of electrostatic field, created in corresponding point by the rest of charges of the system. (One of the mechanisms of impact of electrostatic field on the charge of a separate functional group is related to “relocation” of charge in correspondence to the same mechanism of relocation of “holes” in a semiconductor).

Impact of functional groups’ charges on the state of each one of them within the framework of considered analogy plays the role of reverse connections of Hopfield’s neural network.

Numerical experiments performed in fig. 1 show that macromolecule possesses the main quality of a neuron network – ability to image recognition. Experiments involved introducing different sequences of binary variables to “inputs” of neuron analogues (set

of functional groups of the model macromolecule). Physically it corresponds to treating allotted fragment of a macromolecule with electrostatic fields of different configuration. It is necessary to note that within the theory of neural networks used complexes of logical variables is viewed as "image" which may (or may not) be identified by the corresponding network.
Identification of a specific image is determined by a matrix of weight coefficients of neuron network; in the case of Hopfield's network these weights characterize reverse connections. Simply put, this matrix sets images that are stored in the memory of neural network.
Fig. 1 shows decimalized binary number of sequence, which is being applied to the set of inputs of macromolecular neuron network, on the abscissa. The ordinate contains the frequency of identification of images, each one of them having a number, by the network as a whole. A model fragment of macromolecule containing … functional groups (analogies of neurons) was used in calculations. It is seen that there are indeed images that are identified significantly more often than others. Thus, it can be stated that a macromolecule, as a neuron network analogy, indeed stores a certain complex of images. Significantly, the matrix of weight coefficients in the case of macromolecular neuron network depends on the configuration of polymer chain (since electrostatic potential determining influence of charged groups on each other depends on the distance between them).

3. Evolution scenario

Therefore, change in configuration of the macromolecule creates transformation of images stored in the memory of corresponding neuron network.
This work demonstrates that random interaction between macromolecules, repeated multiple times, may result in the creation of certain stable states, i.e. creates certain relatively stable images that are introduced to the memory of the pair of interacting macromolecules. Experimental and theoretical evidence in support of this conclusion is presented. In particular, it is shown that existence of a number of metastable states in the system based on cross-linked or linear polyacrylic acid and polyvinylcaprolactam allows to implement the case when "consecutive mutual rewriting" of information leads to emergence of some stable state, which may be interpreted as a result of controlled evolutionary process.
Emergence of such stable states, which may be called protocodon sequences allows to interpret the origin of genetic code. However, it has to be noted that this case is in regards to the evolution of neural network in general. It excludes the need to consider random fluctuations, characteristic to separate elements of the system, in order to explain the mechanism behind the appearance of orderly sequences. Somewhat simplifying, in accordance with suggested mechanism, enveloping system appears first, which then implements "tuning" of its elements.

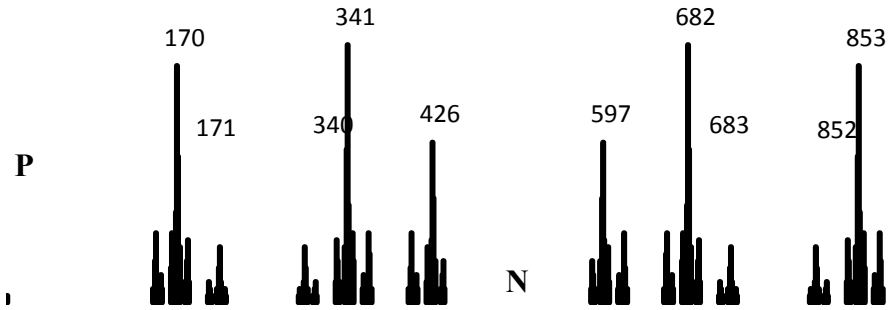

Figure 1. Frequency diagram of image recognition by model macromolecule considering as neural network

Obtained results allow proposing a general scenario of evolution for complex systems of random nature, which may be called neural network evolution. It is realized provided that a particular system may be considered as an analogy to neural network. (It should be noted that a number of complex systems, including those of socio-economic nature, that comply with noted analogy, in particular, a fragment of society may also be considered as analogy to neural network). The proposed scenario consists of the following stages.
On the first stage, an analog of a neuron network as evolves as it is, and parameters of the elements that form the analog of neuron either remain unchanged or change insignificantly. During the second stage, the transformed neural network implements "choice" of elements' characteristics that are most appropriate to the new state of the system as a whole. It can be wittingly predicted that the velocity of "directed" mutations will significantly exceed those of random ones, which form the base of the Darwinist approach.

4. Conclusions

1. "Neuron network" principle of complex systems' evolution allows to overcome serious limitations of Darwinist point of view, attempting to unveil the mechanism of evolution that preceded biological. The mechanism of protobiological evolution, in accordance to the concept developed in this work, is defined by the neuron network properties of macromolecules.
2. Neuron network properties of partially dissociated macromolecules are detected both in numerical and labarotory experiments. One of their manifestations is, in particular, appearance of stabilized states over the course of multiple destruction and reconstruction of the interpolymer complex formed by a certain pair of nonionic and ionogenic polymers.

3. Neuron network properties of partially dissociated macromolecules may form the base for artificial neuron networks of macromolecular level, which, in turn, are the foundation for the development of full-scale neuronanocomputers capable of modeling evolutionary processes in systems of different natures.

References

[1] Avetisov V.A., Kuz'min V.V., and Goldanskii V.I., *Phys. Today*, 1991,44, 33
[2] Delaye L., Lazcano A., Physics of Life Reviews, 2005, 2, 47–64
[3] Bartsev S.I., Mezhevikin V.V., Okhonin V.A., Advances in Space Research, 2001, 28, 607–612
[4] Gaeta F. S., Bencivenga U., Canciglia P., Rossi S., Mita D. G., Cell Biophysics, 1987, 10, 103-125

S8-P87
Deflection of polymer gear tooth under static load using numerical analysis

Boštjan Zafošnik*, Nina Hanžič, Jože Flašker
University of Maribor, Faculty of Mechanical Engineering, Smetanova ulica 17, 2000, Maribor, Slovenija
*bostjan.zafosnik@guest.arnes.si

1. Introduction

Polymer gears have many excellent characteristics regard to metallic gears such as corrosion resistance, self-lubrication, noise reduction. On the other hand they have some important disadvantages such as small load capacity, small wear resistance, big dependence on influence of temperature. It is typically for polymers that stress strain curves are not the same for loading and loading. This is important at frequently change of load where permanent set is not recovered before next loading starts.

Gears are normally subjected to cyclic loading. In case when number of cycles during service life is very small and gear is used only for partial rotation (e. g. application of gear and four bar mechanism for a slow motion of a gear rack) with enough time for strain recovery, permanent set effect of polymer can be neglected.

Basically a stress magnitude at a gear tooth root is independent of Young's modulus. This is especially case for gears made of steel. Opposite to this a deflection of the gear tooth is strongly depended on Young's modulus. Big deflection of the gear tooth can lead to disturbance in gear meshing. For structural steel material Young's modulus (E) is approximately 200 GPa. Young's modulus of polymers can significantly vary with changes in structure of polymer and other parameters. It is usually determined using procedure described in a standard ISO 527-1 [1] from the slope between extensions of 0.05% and 0.25%. Therefore very accurate test results must be developed for its determination. When data for stress strain curve are achieved from a diagram from a literature (Figure 1 [2]), an accuracy of determined Young's modulus can lead to unreliability results. On the other hand thermoplastic polymers (e. g. Polyoxymethylene(POM)) exhibits different stress strain behavior in tension and compression region what can also be important for deflection of the gear tooth and cannot be described only with Young's modulus.

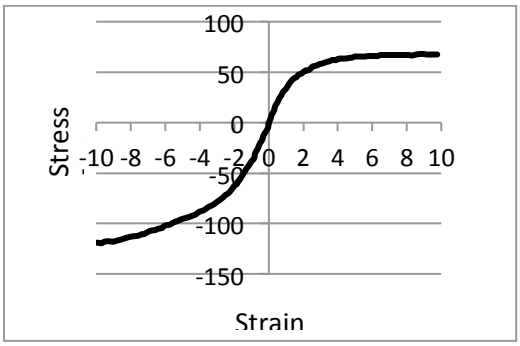

Figure 1. Stress strain behavior of a Polyoxymethylene (POM) [2]

2. Determination of gear tooth deflection

There are many ways how to determine the gear tooth deflection. It can be determined from analytical expression, which considers deflection of a tooth body by bending, shearing and radial component, deflection due to displacement and deformation at the tooth [2]. With this approach a deflection is described using Young's modulus.

On the other hand numerical methods (e. g. finite element methods) can be very helpful for determination of stress strain behavior of analyzed element. Usually linear elastic materials are modeled using Hook's law. Thermoplastic polymers, where permanent sets can be neglected, can be modeled with appropriate hyperelastic constitutive law. In presented work two types of analysis were done. Results done with Hook's law (E = 2600, 2900, 3200, 3500, 3800, 4100, 4400 MPa and Poisson's ratio of n = 0,35) were compared with 3rd order Ogden strain energy potential which describes more precisely stress strain behavior of POM presented in Figure 1. Departure of linear elastic region was identified using offset of elastic region for 2% [3]. Due to symmetry of the gear only one tooth and two half of neighbor's teeth were considered in the analysis.

3. Results and discussion

Influence of Young's modulus on deviation of maximum displacement at addendum circle regard to displacement determined with 3rd order Ogden strain energy potential is presented in Figure 2.

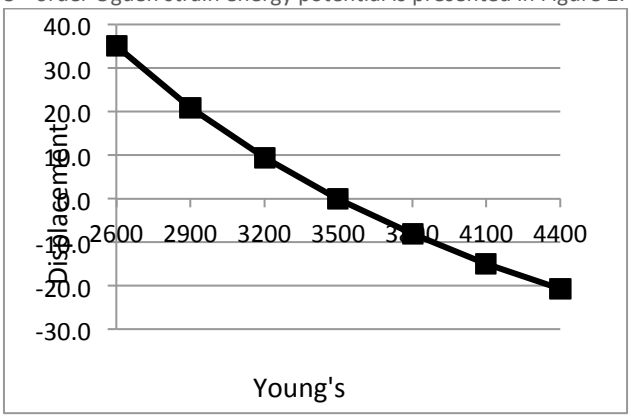

Figure 2. Influence of Young's modulus on deviation of maximum displacement at addendum circle

Results in Figure 1 show that for *E* = 3500 MPa results for deflection of the gear tooth agree with 3rd order Ogden strain energy potential when Hook's law is considered in the analysis. For lower and higher values of Young's modulus from *E* = 3500 MPa results deviate significantly.

A value of *E* = 4177 MPa was determined from Figure 1 using standard ISO 527-1 what leads to 15% lower deflection of the gear tooth.

5. Conclusions

In this work an influence of Young's modulus on deflection of polymer gear tooth with no permanent set was presented. Deflection was determined with finite element method. Results show that it is very important to determine accurate value of Young's modulus. Accurate determination of Young's modulus can be questionable when it is determined using results of stress strain presented in diagram from literature. In this case it is better to use appropriate strain energy potential of hyperelastic constitutive law.

References

[1] SIST EN ISO 527-1:2000, Polimerni materiali – Določevanje nateznih lastnosti - 1. del: Splošna načela (ISO 527-1:1993 vključno s popravkom 1:1994), SIST, Ljubljana, 2000.
[2] L. W. McKeen, The effect of temperature and other factors on plastics and elastomers, 2nd ed., New York, 2008.
[3] R.A. Pethrick, Polymer Science and Tehnology for Enginners and Scientists, Whittles Publishing, Dunbeath, Caithness, 2010, p. 33.
[4] K. Terashima, N. Tsukamoto in J. Shi, Development of Plastic Gears for Power Transmission, Bulletin of JSME, Vol. 27, No. 231, 1984, p. 2062.

Session 9: Polymer degradation and stabilization

S9-P88

The use of elemental sulfur in the synthesis of oligomeric polysulfide stabilizers-modifiers for rubber and the study of the composition's influence on their efficiency

Elena Cherezova*, Julia Karaseva
Kazan National Research Technological University, 68 Karl Marx street, 420015 Kazan, Republic of Tatarstan, Russian Federation,
*cherezove@rambler.ru

One of the most important problems in chemistry and polymer technology is the problem of working properties' stability of polymeric materials. The most common way to solve it is putting stabilizers-antioxidants in polymeric materials [1]. An innovative approach is the antioxidants' creation, which are capable to inhibit the oxidation chain by different mechanisms, for example, the widely used stabilizers which destroy hydro peroxides without radical formation and accept peroxide radicals - the primary products of polymers' oxidation. These polyfunctional stabilizers include phenolic antioxidants, containing the atoms of sulfur (II), phosphorus (III), nitrogen (III) [2].

A perspective approach to the synthesis of additives for polymers is the development of multi-functional structures of agents, which are able to participate in the reactions of stabilization, modification and others. In this paper we propose a methodology of

the synthesis of complex polysulfide additives which contain the oligomer of dicyclopentadiene with sulfur (DCPD-Sx) and bis(3,5-di-*tert*-butyl-4-hydroxyphenyl)polysulfide (sterically hindered phenols with sulfur SHPh-S_y), which can be vulcanizing agent, stabilizer and modifier for rubber:

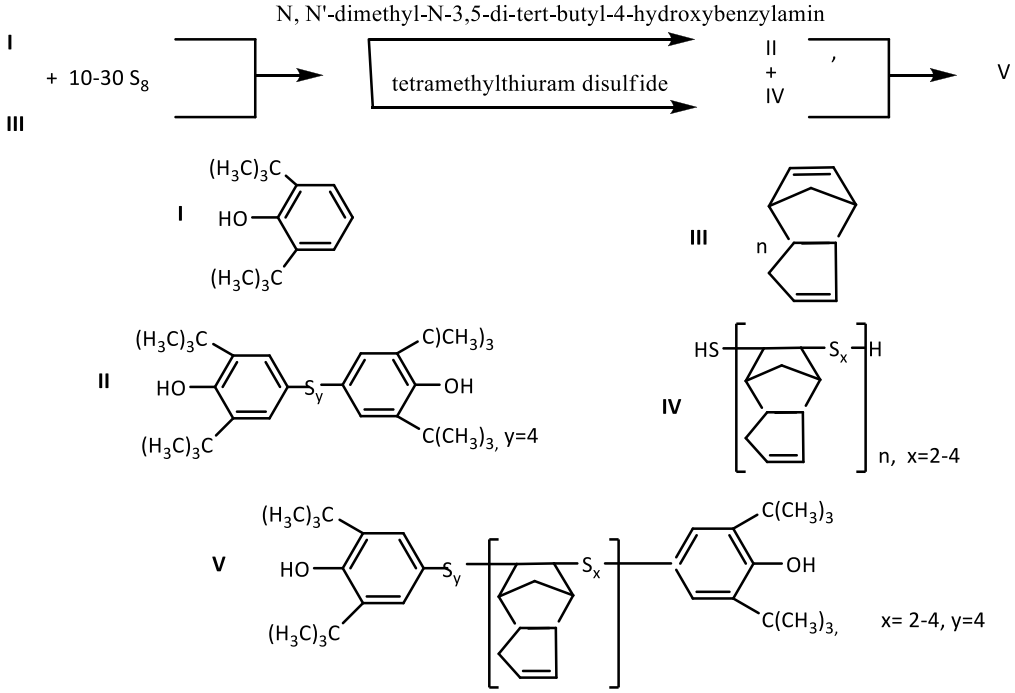

The use in the synthesis the method of copolymerization excludes waste's formation, which is important to improve the environmental performance of the process. The developed method of multifunctional additives synthesis can vary the amount of stabilizing components SHPh-S_y. Target products, containing 10-30 % by weight of SHPh-S_y and 90-70 % by weight of DCPD-S_x respectively, were obtained. An antioxidant effectiveness of the synthesized additives was evaluated by induction period of oxidation of the synthetic isoprene rubber SIR by manometric method at 135-140 °C and a pressure of oxygen PO2 = 250 mm.Hg.[4].

Table 1. The dependence of the induction period before oxidation of the rubber (τ, min) on the concentration (C, parts by weight) of stabilizing additive (PO2 = 250 mm.Hg., T = 135-140 ° C)

№	The type of the additive	The amount of the additive (parts by weight) per 100 parts by weight SIR-3	The amount of SHPh-S_y, parts by weight	The amount of DCPD-S_x, parts by weight	The period before oxidation of the rubber, min
К	-	-	-	-	11,7
1	DCPD-S_4/ SHPh-S_y (90/10)	1,5	0,15	1,35	100,0
2	DCPD-S_4/ SHPh-S_y (90/10)	3,0	0,3	2,7	110,0
3	ДЦПД-S_4/ПЗФ-S_y (90/10)	4,5	0,45	4,05	130,0
4	DCPD-S_4/ SHPh-S_y (80/20)	1,0	0,2	0,8	123,0
5	DCPD-S_4/ SHPh-S_y (80/20)	1,5	0,3	1,2	136,0
6	DCPD-S_4/ SHPh-S_y (80/20)	2,25	0,45	1,8	147,0
7	DCPD-S_4/ SHPh-S_y (70/30)	0,5	0,15	0,35	81,0
8	DCPD-S_4/ SHPh-S_y (70/30)	1,0	0,3	0,7	107,0
9	DCPD-S_4/ SHPh-S_y (70/30)	1,5	0,45	1,05	113,0
10	DCPD-S_4	1,2	-	1,2	40,7
11	SHPh-S_y	0,3	0,3	-	64,0
12	DCPD-S_4 + SHPh-S_y (80+20)	1,0	0,2	0,8	100,0
13	DCPD-S_4 + SHPh-S_y (80+20)	1,5	0,3	1,2	110,0
14	DCPD-S_4 + SHPh-S_y (80+20)	3,0	0,6	2,4	120,0

According to experimental data (Table 1), the largest induction period before the oxidation of SIR has the sample with the additive, containing 20% parts by weight of SHPh-S_y and 80% parts by weight of DCPD-S_4 (Table 1, experiments 4-6). If you change this setting that ratio is reduced (Table 1, experiments 1-3, 7-9). It is shown that the stabilizing ability of the synthesized products DCPD-S_4/SHPh-S_y regardless of the ratio of SHPh-S_y and DCPD-S_4 components is above of mixed compositions of separately obtained DCPD-S_4 and SHPh-S_y (Table 1, experiments 10, 11). It should be noted that the increase in the synthesized products in the rubber SIR leads to an almost linear increase of the time before oxidation of SIR (Table 1).
Thus, the synthesized additives are effective stabilizers for rubber SIR, the best antioxidant properties has a supplement, containing 20% by weight of SHPh-S_y and 80% by weight of DCPD-S_4.
It is revealed that a complete replacement of the sulfur additives in the composition of rubber compounds for pressure hoses based on SIR leads to the formation of the vulcanizing grid with low density, while the physical and mechanical characteristics of the vulcanizates are at the level of control.

References

[1] K.B. Piotrowski, Z.N. Tarasova. Ageing and stabilization of synthetic rubber and vulcanizates, Moscow, 1980, 264 p.
[2] E.N. Cherezova. N-, P-, S-containing polymer stabilizers with sterically hindered phenolic fragments: synthesis, structure relationship with antioxidant properties, Kazan, 2002, 36 p.
[3] J.S. Karaseva, E.N. Cherezova. Two-component multi-functional additive on the basis of elemental sulfur. Reports. IV-th International Youth Conference "Tinchurin readings", Kazan, 2009, P. 84 – 85.
[4] Y.O. Averko-Antonovich. Laboratory workshop on the physics and chemistry of macromolecular compounds, Kazan, 2001, 60 p.

S9-P89

Innovative analytical tools for the evaluation of the ageing behaviour of polymeric wood-coatings

Gabriele Christine Eder*, Lidija Spoljaric-Lukacic, Manuel Weiss and Volker Uhl
OFI, Austrian Research Institute for Chemistry and Technology, Franz Grill Straße 5, 1030 Wien, Austria
*gabriele.eder@ofi.at

1. Introduction

In practical use, the polymeric coating of wooden window frames can gradually show damages like delamination, crack formation, discolouration or embrittlement with increasing life time. The failure modes can be reproduced in long lasting natural weathering tests or specially designed accelerated ageing tests. In the work presented here we aim to find innovative analytical tools which allow recognizing and identifying such damages at a very early state and, thus, reducing the product development time for polymeric wooden coatings significantly.

2. Experimental

Two types of acrylic coatings were chosen for the investigations: (i) a white model system containing inorganic fillers and (ii) a translucent system type. In order to achieve a broad applicability of the results, variations in the binding agent and the additives used were selected for each type of coating- yielding in a total of 4 white and 4 translucent coating systems. For each coating type 5 identical samples were prepared, one was used as reference, the other 4 samples were subjected to accelerated weathering with artificial sunlight in an Atlas Weather-O-meter CI 3000+ according to standard EN ISO 4892-2. Samples were taken after increasing exposure time (275, 1238, 1922 and 3388h) which corresponds to an accumulated radiation of 0.9, 3.0, 5.3 and 10,2 GJ/m^2 in the spectral range 300-2500nm. For comparison, the average annual radiation exposure in Austria is ~4 GJ/m^2.a in the given spectral range.
The analytical tools chosen to detect the ageing induced chemical, physical and mechanical changes of the coatings were surface sensitive vibrational spectroscopy (infrared and Raman microscopy), scanning electron microscopy /energy dispersive X-ray spectroscopy (SEM-EDX), Nanoindentation, Chemiluminesence measurements (CL) and pulse phase thermography (PPT).

3. Results and discussion

It can be shown that the application of a combination of innovative analytical tools allows describing the ageing induced changes occurring on (i) the surface of a polymeric coating material and the (ii) interface of the coating to the wooden carrier material. Spectroscopic techniques such as attenuated total reflection (ATR) Fourier transformed infrared (FT-IR) imaging and Raman microscopy were applied (i) to detect chemical changes e.g. to identify and characterise the formed surface species as well as (ii) to determine changes in the surface composition upon ageing. By combining the spectroscopic information with the elemental information from SEM/EDX measurements, it is possible to deduce models for the damaging mechanisms of the aged surfaces. It can be shown that the surface abundance of the inorganic filler material is increasing upon ageing, while the organic binder is subject to degradation. The extent of this degradation is found to be dependent on the chemical composition of the coating (modification of the binder, additives). The results derived from the molecular spectroscopy could be directly correlated to the results obtained for ageing induced changes in the oxidative stability (Chemiluminesence measurements) of the coatings.
Furthermore, nanoindentation measurements on the various (original and weathered) surfaces revealed that the hardness and elastic modulus of the coating surfaces might be strongly influenced by the ageing process. Thus, we aim to correlate the

spectroscopically derived changes of the surface species with the changes in the mechanical properties of the coatings (e.g. embrittlement).
Information on the adhesion of the coating to the wooden carrier material can be derived from the pulse phase thermography measurements. As all features within the sample laminate, which disturb a homogenous thermal dissipation like e.g. delamination can be visualized with this setup, information on the quality of the adhesion of the coating to the wooden carrier can be obtained.

Acknowledgements
We thank our college Andrea Feldmann for the implementation of the SEM measurements. The work was funded by the State of Lower Austria and the European Regional Development Fund (EFRE) under the project "Optisurf".

S9-P90

Time dependent investigations on the thermal stability of polystyrene and the influence of lubricants

T. J. Hinterberger (1)*, R. F. Haßlacher (2), S. Hild (2), O. Brüggemann (1)
(1) Johannes Kepler University, Institute of Polymer Chemistry, Welser Straße 42, 4060 Leonding, Austria
(2) Johannes Kepler University, Institute of Polymer Science, Altenberger Straße 69, 4040 Linz, Austria
*thomas.hinterberger@jku.at

1. Introduction

The thermal degradation of polymers (e.g. polystyrene) has been studied for decades and is therefore well known [1, 2]. Degradation steps respectively depolymerisation mechanisms of polystyrene caused from thermal stress are well studied and proposed in literature [3, 4]. It is commonly observed that there are different parameters causing decomposition of the polymer chains, particularly in processing machines (e.g. injection moulding) [5]. In this work the time-temperature dependencies of the thermal degradation of polystyrene have been investigated by using various thermal measurement setups.

2. Experimental

In this series four commercially available grades of polystyrene are characterized. Investigations of the time dependent thermal stability are executed by thermal gravimetric analysis in different atmospheres (inert and oxidative) with the cooling rates matching those accomplished in injection moulding machines.
By performing rheological measurements, time-temperature dependencies of the thermo-mechanical stability can be determined. With increasing duration time of the samples in the plate-plate rheometer, sample material streams out of the two plates. This results in a distinction of two sample areas for further analyses. Sample material remaining between the two rheometer-plates is damaged thermo-mechanically (inner region of the sample). On the other hand sample material streaming out of the two plates gets only thermally damaged (outer region). The samples (of the inner and outer region) were characterized using size-exclusion chromatography and differential scanning calorimetry. The influence of lubricants, which are already present in the polymer, was investigated by comparing three commercially available polystyrene-types with a lubricant-free polystyrene.

3. Results and discussion

In performing thermo gravimetric analysis of polystyrene, the influence of the time-dependent degradation with respect to an achieved cooling rate (0.6 °C min^{-1}) of processing machines is demonstrated. In these measurements the important role of inert or oxidative atmospheres in respect to the degradation behaviour can be shown (Figure 1).

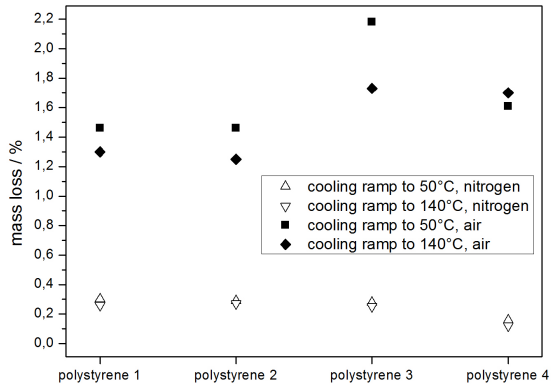

Figure 1. Mass loss of polystyrene measured in different atmospheres after thermally stressing the sample for 180 minutes at 250 °C.

The change in molecular weight is obtained by using the samples after executing the rheological measurements with a plate-plate rheometer where time- and temperature dependent analyses were implemented. The change in molecular weight after a certain degradation time is measured using size-exclusion chromatography (Figure 2). The distinction between the two sample areas shows the influence of the degradation. The thermal degradation results in a higher reduction of molecular weight, compared with the thermo-mechanically stressed samples.

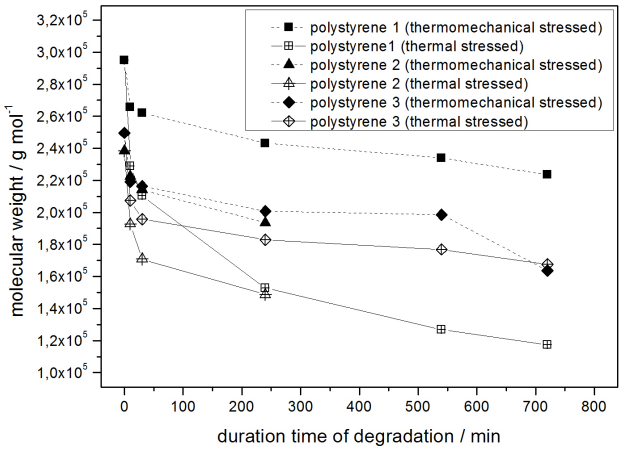

Figure 2. Change in molecular weight as a function of duration time of the polymer degradation in a plate-plate rheometer.

The thermo-analytical measurements demonstrate that the influence of lubricants in polymers is not negligible and have an influence in the melt performance of the polymer in processing machines.

4. Conclusions

In this work, the thermal and thermo-mechanical stability of polystyrene and the influence of lubricants are demonstrated. Furthermore, a correlation of the obtained thermo-analytical and size-exclusion chromatography data is reported.
The achieved data of the performed measurements show, on the one hand, the time-dependency of the polymer degradation which has an important effect for the polymer processing. On the other hand, the change of physical data (e.g. glass transition temperature) can be assigned to the modification of the polystyrene, for example the addition of lubricants.

Acknowledgements

This work was financially supported by FFG.

References

[1] H. H. G. Jellinek, *Journal of Polymer Science*. 1949, 4, 1-12
[2] G. J. Knight, *Journal of Polymer Science, Polymer Letters Edition*. 1967, 5, 855-857
[3] T. Faravelli, M. Pinciroli, F. Pisano, G. Bozzano, M. Dente, E. Zanzi, *Journal of Analytical and Applied Pyrolysis*. 2001, 60, 103-121
[4] T. Sawaguchi, M. Seno, Journal of Polymer Science Part A: Polymer Chemistry. 1998, 36, 209-213
[5] C. Capone, L. Di Landro, F. Inzoli, M. Penco, L. Sartore, *Polymer Engineering and Science*. 2007, 47, 1813-1819

S9-P91

Determination of stabilizers in encapsulation materials for photovoltaic modules

Ingrid Hintersteiner (1)*, Wolfgang Buchberger (1), Gernot Wallner (2)
(1) Johannes Kepler University, Institute of Analytical Chemistry, Altenberger Straße 69, A-4040 Linz, Austria
(2) Johannes Kepler University, Institute of Polymer and Material Testing, Altenberger Straße 69, A-4040 Linz, Austria
*ingrid.hintersteiner@jku.at

1. Introduction

Renewable energies are becoming increasingly important; particularly technologies based on sunlight are very promising. In order to generate electricity using sunlight, photovoltaic (PV) modules are utilized. Due to various advantages, embedding films as well as the front- and back-layers are made from synthetic polymers. To ensure that these materials can fulfil various requirements including UV-resistance, processing- and temperature-stability, the addition of stabilizers is essential. Since the amount of (intact) stabilizers can be an indicator for the durability of the polymeric materials, the current study provides a method for the **determination of stabilizers in commercially relevant encapsulants** for PV modules.

2. Theory

PV modules (Figure 1) typically consist of several layers: a package of connected solar cells represents the core of the module which is embedded in an encapsulant. Front- and back-sheets are the outer layers of the photovoltaic module, whose main purpose is to protect the module from environmental influences such as moisture or mechanical damage. On the other hand, it is also important to insulate the active elements of the photovoltaic module to protect the environment. Due to various advantages, such as lighter weight, easier processing and lower cost compared with inorganic materials [1], embedding films as well as the front- and back-layers made from synthetic polymers are well established.

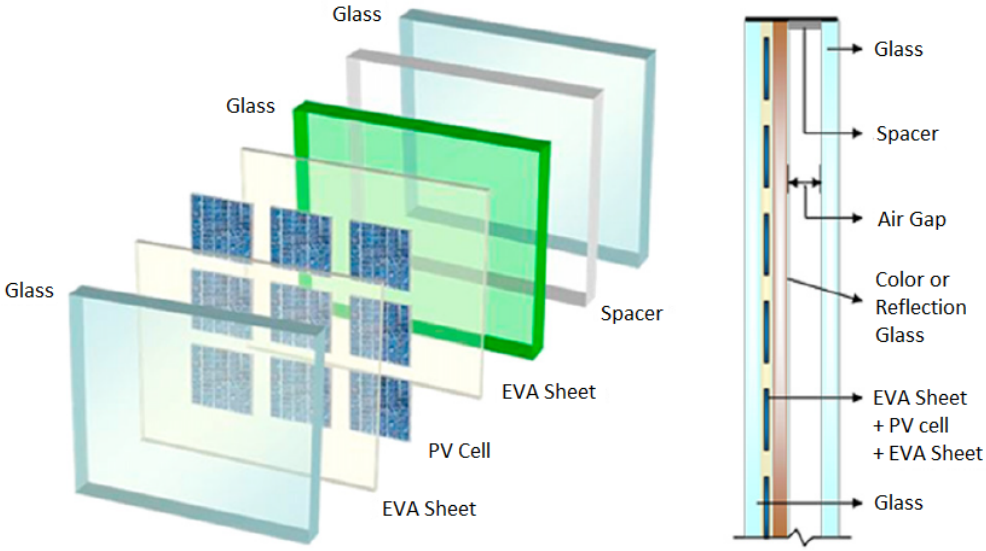

Figure 1. Schematic representation of a photovoltaic module [2]. Instead of glass, polymeric front- and back-sheets are quite common. In this example, EVA is used as the encapsulant, but other polymeric materials such as polyvinylbutyral (PVB) or thermoplastic silicon elastomers (TPSE) can also be used.

Polymers undergo several degradation reactions over time. Environmental influences such as temperature or UV-light can lead to an oxidation of the polymer chains which affects physical properties such as tensile strength, surface appearance or the color of the material. As a result, this might lead to performance losses of the PV modules over time. Oxidation of the polymer can occur in different life stages, for instance during manufacturing or storage of the polymer resin, during processing or at the end use of the plastic article. In order to retard or inhibit degradation processes, stabilizers like antioxidants or UV absorbers are added to the polymeric materials [3].

3. Experimental

Commonly used encapsulation materials, namely ethylene vinylacetate (EVA), polyvinylbutyral (PVB), and a thermoplastic silicon elastomer (TPSE) were investigated. In a first step, the stabilizers were extracted from the matrix. This can be done by either dissolving and precipitating the polymer (where the stabilizers remain in solution) or via an extraction from a grained sample. Depending on the polymeric material, different solvents or combinations of solvents were utilized (e.g. toluene and methanol for

EVA, methanol for PVB and acetonitrile for TPSE).

Following the extraction procedure, quantification was performed using high performance liquid chromatography with UV detection (HPLC/UV). Additives that did not show any UV absorption, as for instance Tinuvin 770 (Figure 2), were quantified using gas chromatography coupled with mass spectrometry (GC/MS).

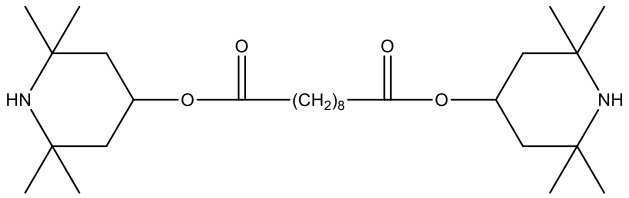

Figure 2. Hindered amine light stabilizer Tinuvin 770

4. Conclusions

For polymeric encapsulation materials the addition of thermal and light stabilizers is crucial for the performance of the PV module. The current study provides methods for the extraction and subsequent quantification of stabilizers in commonly used EVA, PVB, and TPSE encapsulation materials. These methods will be particularly valuable for estimating the reliability and performance losses of the PV modules over time by analyzing samples which have been subject to accelerated aging tests.

Acknowledgements

This research work was performed in work package WP-01 "Performance requirements and test methods for polymeric encapsulation materials for rigid and flexible PV cells" of the cooperative research project SolPol-3 on Solar-electrical Systems based on Polymeric Materials (www.solpol.at). This Project is funded by the Austrian Climate and Energy Fund (KLI.EN) within the program "Neue Energien 2020".

References

[1] A. W. Czanderna, F. J. Pern, *Sol Energ Mat Sol C* (43), 1996, p. 116.
[2] K. E. Park, G. H. Kang, H. I. Kim, J. G. Yu, J. T. Kim, *Energy* 2010, 35 (6), p. 2682.
[3] H. Zweifel, R. D. Maier, M. Schiller, Plastics Additives Handbook, 6th edition, Hanser, München, 2008, p. 1.

S9-P92

Thermal degradation studies of non-woven flax and hemp fiber reinforced green-composites

Arunjunai Raj Mahendran (1,2)*, Nicolai Aust (2), Günter Wuzella (1), Uwe Müller (1)

(1) Wood Carinthian Competence Center, Kompetenzzentrum Holz GmbH, Klagenfurter Straße 87-89, 9300 Sankt Veit an der Glan, Austria

(2) Chair of Chemistry of Polymeric Materials, University of Leoben, Otto Glöckel-Straße 2, 8700 Leoben, Austria

*a.mahendran@kplus-wood.at

1. Introduction

The effective use of natural fibers as reinforcement in composites is in practice for the past two decades due to their low cost and abundance in nature. In many applications the thermal decomposition behavior of composites is important. Thus, for the design of natural fiber composites as construction material the decomposition kinetics have to be known.

Two methods are commonly used to predict the kinetics, where the "model free kinetic method" is more advantageous than the "model fitting method" since it allows the prediction of the thermal decomposition kinetics at arbitrary temperatures without prior knowledge of the decomposition mechanism. The model free kinetic method is also helpful in predicting isothermal values from non-isothermal measurements. In this study, the isoconversional model of the free kinetic method by Vyazovkin was used to investigate the thermal decomposition of natural fiber composites, because all other methods introduce systematic errors when calculating the activation energy [1].

2. Experimental

Flax and hemp fleeces were prepared using a non-woven needle punch carding machine. The fleeces were of 25 cm x 25 cm in size and the grammage of each fleece was around 2000 g/m². The fleeces were impregnated with an acrylic resin dispersion supplied by BASF (viscosity at 23 °C = 300-1500 mPas), which is a mixed product of a modified polycarboxylic acid and a polyhydric alcohol as crosslinking agent. The fiber fleeces were impregnated at two different resin contents basing on the total weight of the composite (15 and 30 wt.-%). The impregnated fiber fleeces were dried for 24 h at room temperature and pressed by a compression molding process at a temperature of 180 °C for 6 min.

Thermal degradation in terms of change in weight loss was observed using the TGA Q500 thermogravimetric analyzer (TA Instruments). The samples were cut into small fragments and distributed in an open sample pan with amounts of 4-6 mg. For the thermal decomposition kinetic analysis, the composites were heated from 50 to 500 °C at four different heating rates, 10, 20, 30, and 40 °C min^{-1}, respectively.

3. Results and discussion

The thermal decomposition of the acrylic binder shows a single stage decomposition with two distinct shoulders, where for the natural fiber reinforced composites a two stage decomposition occurs (Figure 1). The first peak in the differential thermo-gravimetric curves of the composites is caused by the decomposition of cellulose and hemicellulose in the fibers. The second peak results from the decomposition of the acrylic binder and the lignin.

The onset of decomposition of the hemp fiber reinforced composites is earlier than for the flax fiber reinforced composites in the temperature range of 200-400°C due to the higher thermal stability of flax. Due to their higher lignin content, the residues of the flax fiber reinforced composites are also higher.

The apparent activation energy determined from the non-isothermal data using Vyazovkin's method shows an increase and decrease in trend, demonstrating the complexity of the decomposition mechanism in natural fiber reinforced composites.

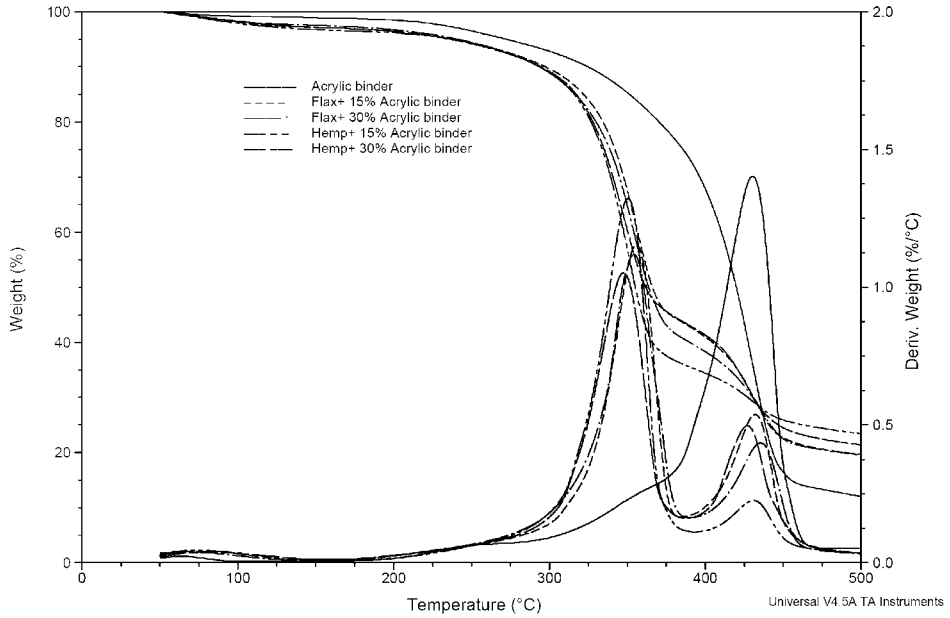

Figure 1. Thermogravimetric and Differential thermogravimetric curves measured at 10 °C/min for the acrylic binder and the fiber reinforced composites.

A slight increase of the activation energy was observed before 20 % of conversion, providing an idication of the occurrence of an accelerated degradation process of the main composition which is approaching balance in the initial stage [2]. After 70 % of conversion, the activation energy values increase and drop again, which is due to the complex multi-step reaction mechanism at this stage. Decomposition of the acrylic binder and lignin occurs in parallel at the final stage.

4. Conclusions

Natural fiber reinforced composites show a distinct degradation of the fibers of cellulose and hemicellulose at the initial stage, and acrylic binder degradation in parallel with lignin decomposition at higher temperatures. A complex multi-step decomposition mechanism occurrs for natural fiber reinforced composite which can be observed by the increase and decrease of the apparent activation energy regime. An increase of the resin content leads to an improve of the thermal stability for both, flax and hemp fiber reinforced composites. The flax fiber reinforced composites show a higher thermal stability compared to the hemp fiber reinforced composites.

References

[1] S. Vyazovkin. J. Comput. Chem. **2001**, 22(2), 178-183.
[2] F. Yao, Q. Wu, Y. Lei, W. Guo, Y. Xu. Polym. Degrad. Stabil. **2008**, 93(1) 90-98.

S9-P93
Additives impact on the photochemical degradation of ethylene vinyl acetate

Cornelia Peike*, Lea Purschke, Karl-Anders Weiß, Michael Köhl
Fraunhofer Institute for Solar Energy Research, Heidenhofstr.2 79110, Freiburg, Germany
*Cornelia.Peike@ise.fhg.de

1. Introduction
This study concerns the investigation of the influence of polymer additives on the photochemical degradation of Ethylene vinyl acetate (EVA). EVA has been the most widely used encapsulation material for photovoltaic modules for the last two decades. Despite, the impact of certain additives on the aging of EVA, i.e. the yellowing, is not fully understood, yet. Therefore, laminates, containing foils with a systematic variation of the most commonly used EVA additives, were produced and subjected to UV aging tests. Afterwards, the chemical aging of the encapsulation was observed by means of Raman spectroscopy, FT-IR/UV/vis spectroscopy and ATR-IR spectroscopy. The occurrence of a severe fluorescence background in the Raman spectra was found. The pattern of the fluorescence appeared to by influences by the additive formulation. Also, the intensity of the fluorescence was strongly dependent on the additive formulation.

2. Theory
EVA has been the most commonly used encapsulation material in photovoltaic modules for the last two decades. Even though the various degradation mechanisms of EVA have been investigated for years, the aging process under the influence of heat, humidity and especially UV radiation is not fully understood yet [1, 2, 3]. The main thermal and photochemical degradation processes of EVA result in the formation of conjugated polyenes and ab-unsaturated carbonyl groups. These chromophoric groups can show strong fluorescence and are supposed to be one reason for the yellowing of EVA. Furthermore, volatile compounds such as acetic acid and hydroperoxides are formed whilst degradation [1]. Those degradation by-products may in turn accelerate cell metallization corrosion [4, 5]. Polyene formation at impurities within the polymeric structure, especially at the vinyl acetate groups, is described to be the major reason for discoloration of EVA. Finally, these processes may leading to dramatic losses in PV module energy output due to a reduced transmission in the UV and vis range and due to poor mechanical properties. The usage of additives such as UV light stabilizers, UV absorbers and antioxidants in EVA sheets for PV application improves EVA stability significantly [6]. At the same time, some of these stabilizing additives but also traces of curing agents or polymerization catalysts are the origin of other aging effects [7]. In which way the EVA degradation is accelerated or retarded by the exact additive formulation was investigated.

3. Experimental

Table 1. Formulations of EVA foils.

Additiv		#1	#2	#3	#4	#5	#6	#7	#8	#9	#10	#11	#12	#13	#14
Function	Name	(g)													
	Elvax 150	100													
Curing agent	TBEC	1,5	1,5	1,5						1,5	1,5		1,5		1,5
Curing agent	Lupersol 101				1,5							1,5		1,5	
antioxidant	Irgafos 168			0,25	0,25				0,25					0,25	0,25
UV absorber	Tinuvin 234		0,3	0,3			0,3			0,3					
UV absorber	Cyasorb 531				0,3			0,3			0,3				
HALS	Tinuvin 123		0,13												
HALS	Tinuvin 770			0,13	0,13	0,13				0,13	0,13	0,13	0,13	0,13	0,13
Adhesion promoter	Dow Corning Z6030		1,2	1,2	1,2					1,2	1,2	1,2	1,2	1,2	1,2

Laminates were manufactured at 145°C for 12 min in a Meier laminator. The laminates consist of a low-iron solar glass as front- and backside material and 14 different EVA foils with a systematically varied additive formulation (tab. 1). Raman Spectroscopic measurements were perfomed using a WiTec Alpha 500 with an excitation wavelength of 532 nm. The UV aging tests were carried out in a climatic cabinet with a fluorescence tube (UV-A: 222 W/m^2, UV-B: 8 W/m^2).

4. Results and discussion
Raman peaks of the different additives were determined in the foils (not shown). The UV aged laminates showed a severe fluorescence background in the Raman spectra, already after short periods of UV aging (fig.1). Furthermore, the fluorescence pattern showed a strong dependency on the formulation and the intensity of the fluorescence was also correlated to the additive formulation (results not shown).

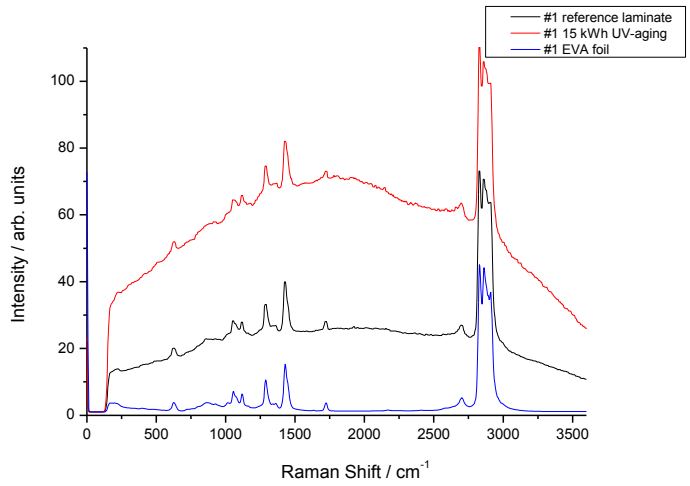

Figure 1. Exemplary Raman spectrum of the pure foil #1 and the laminate #1 before aging and after 15 kWh UV aging.

Acknowledgements
The authors would like to thank Michael Kempe from NREL for the manufacturing of the EVA foils and the support in this project.

References
[1] Allen, N.S., Edge, M., Rodriguez, M., Liauw, C.M., Fontan, E., "Aspects of thermal oxidation, yellowing and stabilization of ethylene vinyl acetate copolymer", Polymer Degradation and Stability, 71, 1-14 (2001).
[2] Pern, F.J. and A.W. Czanderna, EVA degradation mechanisms simulating those in PV modules, Proc. 1lth Photovoltaic AR and D Review Meeting, Denver, CO, May 13-15, 1992 (American Institute of Physics Proc. No. 268, New York, 445-452 (1992).
[3] Pern, F.J., "Ethylene vinyl acetate (EVA) encapsulants for photovoltaic modules: Degradation and discoloration mechanisms and formulation of improved photostability", Die Angewandte Makromolekulare Chemie, 252 (4523) 195-216 (1997).
[4] Czanderna, Encapsulation of PV modules using ethylene vinyl acetate copolymer as a pottant: A critical review, Solar Energy Materials and Solar Cells 43 (2) (1996) 101-181.
[5] M.D. Kempe, G.J. Jorgensen, K.M. Terwilliger, T.J. McMahon,. C.E. Kennedy, T.T. Borek, Acetic Acid Production and Glass Transition Concerns with Ethylene-Vinyl Acetate Used in Photovoltaic Devices. Solar Energy Materials & Solar Cells, 91, 315–329, 2007.
[6] Pern, F.J., "Ethylene vinyl acetate (EVA) encapsulants for photovoltaic modules: Degradation and discoloration mechanisms and formulation of improved photostability", Die Angewandte Makromolekulare Chemie, 252 (4523) 195-216 (1997).
[7] Allen, N.S., Edge, M., [Fundamentals of Polymer Degradation and Stabilisation], Elsevier Science Publishers Ltd., Essex, 22-33 (1994).

S9-P94

Investigation of persistent organic pollutants carried by synthetic polymers in the water environment

Afrim Syla(1)*, Marta Korchemlyuk (2)*
(1) University of Prishtina- Republic of Kosova
(2) Carpathian National Nature Park, 6, Vasyl Stus Str., Yaremche, Ivano-Frankivsk region, Ukraine, 78500
*afrimsyla2002@yahoo.com, kormarta@yahoo.com

Abstract
Plastic materials comprise one of the most persistent macroscopic pollutants in rivers waters and beaches in the world. Thermoplastic resin pellets are melted and formed into an enormous number of inexpensive consumer goods, many of which are discarded after a relatively short period of use, dropped haphazardly onto watersheds and then make their way to the water where some get ingested by water life. In 2011 and 2012 pre-production thermoplastic resin pellets and post-consumer plastic fragments were collected and analyzed for contamination for persistent organic pollutants (POPs). Samples were taken from the different river water, and selected sites in Kosovo and Ukraine . The total concentration of PCBs ranged from 27 to 980 ng/g; DDTs from 22 to 7100 ng/g and PAHs from 39 to 1200 ng/g, and aliphatic hydrocarbons from 1.1 to 8600 ng/g. Analytical methods were developed to extract, concentrate and identify POPs that may have accumulated on plastic fragments and plastic pellets. The results of this study confirm that plastic debris is a trap for POPs.
Keywords: Persistent organic pollutants; Plastic contaminants; PCBs in plastics; DDTs in plastics; PAHs in plastics.

S9-P95

Properties of flexible polyurethane foams modified by the addition of graphite based fillers

Anna Bryskiewicz*, Joanna Ryszkowska
Warsaw University of Technology, Faculty of Materials Science and Engineering, Woloska 141, 02-507, Warsaw, Poland
*awolska@inmat.pw.edu.pl

1. Introduction

Flexible polyurethane foams (FPFs) are polymer materials that have high flammability. For this reason, FPFs are modified by the addition of flame retardants and other fillers. In this work expandable graphite were used to verify its ability to improve thermal stability and fire resistance of FPFs. The prepared foams were characterized by physical and mechanical measurements, thermogravimetric analysis (TGA), dynamic mechanical analysis (DMA), and flammability tests.

2. Theory

Flexible polyurethane foams are widely used in many industries, including the furniture, construction and automotive fields. These materials are also commonly used in mattresses and upholstery foams. FPFs have many advantages, such as a wide range of flexibility and hardness, good cushioning, high durability during use, good thermal and acoustic insulation properties, resistance to chemicals, low price and low density [1–3]. The main disadvantages of FPFs are their high flammability and high degrees of toxic fumes emitted during combustion. These toxic combustion products are mainly carbon monoxide (CO), carbon dioxide (CO_2) and hydrogen cyanide (HCN). CO is dangerous for people at any concentration. In lower concentrations, it causes loss of movement coordination, and in higher concentrations, it may lead to sudden death [4,5]. For this reason, FPF are modified to reduce their flammability and smoke toxicity, while maintaining adequate mechanical properties. There are many types of modifications of FPF. In this work FPFs were modified by the addition of two types of expandable graphite.
Expandable graphite (EG) is a product of natural origin that has specific properties. It is formed through the special physical and chemical treatment of graphite ore. EG is used as an additive causing the increase of fire resistance of insulations, plastics and coatings. The greatest advantage of this material is its low price, which great reduces expenses in industrial production. It was decided to use this filler to verify thermal and mechanical properties of FPFs.

3. Experimental

Foams tested in this study were produced in Zachem S.A. (Ciech Chemical Group), and they were prepared by the one-shot method. Two types of expandable graphite were examined: EG50 (the particle size was approximately 0.15 mm and the expansion was approximately 50) and EG250 (the particle size was approximately 0.18 mm and the expansion was approximately 250). The flexible polyurethane foam (FPF) and the series of FPFs with addition of 2,5%, 5%, 7,5%, 10% and 15% of EG50 and EG250 were examined. Expandable graphite was obtained from Sinograf (Poland).
The apparent density, flexibility, thermogravimetric analysis (TGA), dynamic mechanical analysis (DMA) and linear flammability test has been carried out.

4. Results and discussion

Selected parameters of tested foams obtained in production process, physical, mechanical and thermal measurements are presented in Table 1. The one of the important parameter for assessing the possibility of producing a flexible polyurethane foam is the measure of its the rise time during production. It could be observed that addition of EG50 and EG250 leads to increase of this value. Minor differences were observed to foams modified by the addition of EG250. Addition of EG50 caused more than twice extended in rise time of FPFs, which implies huge difficulties in the production process of FPFs.

Table 1. Selected parameters of FPFs modified by the addition of EG50 and EG250.

	Rise time [s]	Apparent density [kg/m^3]	Flexibility [%]	$T_{5\%mass\ loss}$ [°C]	SM [MPa]
FPF	92	26,6	46,3	237,18	2,323
FPF+2,5%EG50	120	26,0	23,7	242,18	2,541
FPF+5%EG50	147	28,0	33,1	243,89	2,781
FPF+7,5%EG50	190	32,4	38,0	241,25	2,537
FPF+10%EG50	210	35,4	46,7	240,82	5,646
FPF+15%EG50	205	37,3	48,8	240,11	4,421
FPF+2,5%EG250	110	29,8	35,8	241,00	4,526
FPF+5%EG250	106	27,1	43,2	239,58	2,679
FPF+7,5%EG250	126	28,0	41,3	240,29	2,479
FPF+10%EG250	125	28,4	42,8	241,32	3,074
FPF+15%EG250	124	29,9	36,9	242,82	3,199

Results of the apparent density of tested foams showed that addition of tested fillers leads to achieve the higher values of this parameter of FPF. The higher values of apparent density were observed in foams with addition of EG50, wherein these values increased with increasing the filler content. This means that addition of this filler results in worse properties of FPFs. Results of the flexibility measurements showed that addition of tested fillers usually leads to achieve foams with worse flexibility values. Only foams modified with addition of 10% and 15% of EG50 reached higher values of flexibility. In the others foams this value was worse than FPF, wherein the worst value was obtained to foam with addition of 2,5% EG50.The values of flexibility obtained to foams with addition of EG250 were less dependent on amount of this filler. Thermogravimetric analysis gave information about thermal stability of tested materials. The temperature corresponding to 5 % mass loss is considered to be the initial temperature of the sample's decomposition process. The value of 5 % mass loss increased in the foam with the addition of EG50 and EG250 in comparison to the value for FPF without fillers. The values obtained to foams with EG50 and EG250 were similar. The highest value of this temperature were observed in foam with the addition of 5% EG50 and 15% EG250. From DMA there were set SM values of tested materials. Addition of EG50 or EG250 allowed to achieve higher SM values in comparison with unfilled foam. The highest value was achieved to the foam with addition of 10% EG50.

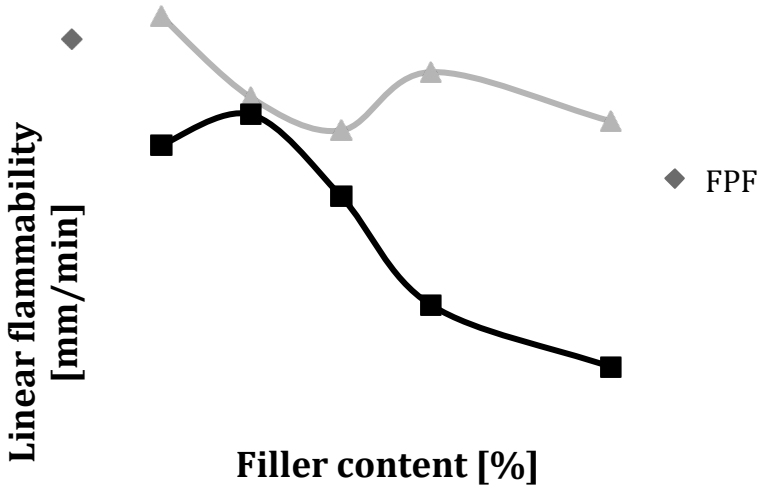

Figure 1. Linear flammability of FPF modified by the addition of EG50 and EG250

Results of the linear flammability of tested foams are presented in figure 1. The values of linear flammability of foams modified by the addition of EG50 and EG250 were lower than unfilled foams. It means that this type of modification could be effective way to improve fire resistance of FPFs. It could be also observed that the addition of EG250 allowed to achieve better results in lowering flammability of FPFs. Foam modified by the addition of 15% EG250 reached more than twice lower value of linear flammability than unfilled foam.

5. Conclusions

Modification of flexible polyurethane foam by the addition of expandable graphite allows to obtain material with lower flammability and higher thermal stability than conventional flexible polyurethane foam. The filler which allows to achieve better results is expandable graphite with bigger expansion (EG250). Increase of the filler content increases the fire resistance and thermal stability of flexible polyurethane foams but also deteriorate the mechanical properties of the foams, which have to be taken into account in the production of FPFs.

Acknowledgements

These studies were the part of the project No NCBiR/ERA-NET-MATERA/06/2011. Special acknowledgements are addressed to Zachem S.A. (Ciech Chemical Group) in Bydgoszcz for help in the realization of these studies.

References

[1] S. Duquesne, R. Delobel, M. Le Bras, G. Camino, Polym. Degrad. Stab. 2002, 77, 333-344.

[2] M. Sultan, H.N. Bhatti, M. Zuber, I.A. Bhatti, M.A. Sheikh, Carbohydr. Polym. 2011, 86, 928-935.
[3] H. Mahfuz, V.K. Rangari, M.S. Islam, S. Jeelani. Compos. 2004, 35, 453-460.
[4] T. Sawicki, Bezp. Pr. 2003, 7-8, 43.
[5] J. Iwko, Mech. 2007, 10.

Session 10: Polymer processing and recycling

S10-P96
RC1 reaction calorimeter – a powerful tool in polymer synthesis, degradation and synthesis of inorganic nanoparticles

Klemen Burja (1)*, Urban Šegedin (2), Matjaž Kunaver (1), Edita Jasiukaityte-Grojzdek (1), Alojz Anžlovar (1), Dolores Kukanja (1,3), Ida Poljanšek (1), Silvester Bolka (1)

(1) Centre of Excellence PoliMaT , Tehnološki park 24, 1000 Ljubljana, Slovenia
(2) Helios Group, Količevo 2, 1230 Domžale, Slovenia
(3) Mitol, Partizanska cesta 78, 6210 Sežana, Slovenia
*klemen.burja@polimat.si

1. Introduction

RC1 Reaction Calorimeter was used to study and optimize formulations of vinyl acetate and ethylene copolymer dispersion, glycolysis processes of wood liquefaction, high-solid hydroxyl acrylic resin, poly (methyl methacrylate) pre-polymer and ZnO nanoparticles preparation in laboratory or industrial 'scale up' research work. The reactor was equipped with calorimeter probe and several thermometers and for calorimetric studies of reactions, heat flow and c_p determination, Attenuated Total Reflectance Fourier Transform Infrared spectroscopy (ATR-FTIR) to trace monomer consumption and product formation, Focused Beam Reflectance Measurement (FBRM) technique for particle size and particle size distribution determination and real time calorimetric measurements with special RTCal reaction vessel. RC1 Reaction Calorimeter proved to be a powerful tool for the glycolysis of wood particles, preparation of polymers and nano fillers.

2. Experimental

RC1 was developed for safety studies of chemical industrial processes. Since equipment is software controlled and fully automatized a lot of industrial processes can be simulated on small scale and knowledge can be directly transferred to larger scale. Highly controlled procedures were supported by *in situ* ATR-FTIR, *in situ* FBRM, gas consumption, torque and calorimetric measurements that helped to optimize processes in studied cases of wood liquefaction, esterification of liquefied wood, preparation of pre-polymer for Plexiglas production, preparation of ZnO nanoparticles dispersion, co-ethylene-vinyl acetate dispersion synthesis and high-solid hydroxyl-acrylic resins. Majority of experiments were made in high-pressure reactor. Some experiments were performed in a special RTCal glass reaction vessel for more accurate calorimetric studies of processes and as a support for other *in situ* analysis.

3. Results and discussion

a) Liquefied wood [1]

The calorimetric, ATR-FTIR and FBRM *in situ* measurements showed that wood liquefaction process performed in much smaller time scale. The process was faster for about 30%. FBRM showed particles of wood sawing got smaller than 10mm already after 3.5 h instead of 5 h, the same time was needed for 99 % of the reaction energy to be absorbed, which was proven by the heat-flow integral of the whole process. Since ATR-FTIR absorbance of characteristic bands are dependent on concentration of soluble components close to the tip of probe in this particular case less accurate results were obtained although they showed similar trends as FBRM and calorimetric analysis.

Calorimetric and *in situ* ATR-FTIR measurements of the esterification reaction of liquefied wood with dibasic organic acids either at atmospheric pressure distillation or at slight vacuum indicated that the same reaction time is required in both cases though much less energy is required for water distillation in slight vacuum conditions. Equilibrium reaction of esterification to product formation is shifted by simultaneous water discharge, which is much faster process than esterification, so reaction speed depends of ester formation.

b) Synthesis of zinc oxide nanoparticles [2]

In the synthesis of ZnO nanoparticles FBRM and FTIR measurements were used to optimize the time of the reaction while having the highest yield of nanoparticles with tailored size and distribution. Despite the limitations of both characterization methods synthesis was monitored via occurrence of intermediates and by-products. The results were used to scale up the preparation process that led to the same product quality but in a five to ten–fold larger quantity.

c) Synthesis of high-solid poly-hydroxyl acrylate

Kinetic studies of synthesis of high-solid (HS) hydroxyl-acrylic resin for polyurethane metal coatings were done by comparing the course of reaction at reflux conditions or at critical conditions (at higher reaction temperature than is the boiling point of the used solvent). The synthesis of HS resin at solvent reflux was performed in monomer starving conditions. According to ATR-FTIR measurements no monomer accumulation was noticed. The heat of reaction measurements were also followed and gave better insight of the process. Nonlinear dependence at reflux conditions indicates slight monomer accumulation. At critical conditions it showed a linear dependence meaning that monomer consumption was immediate with no monomer accumulation.

d) VAE dispersion synthesis [3]

Gas consumption of ethylene was measured for the synthesis of vinyl acetate - ethylene (VAE) dispersion. The experimental parameters such as ethylene pressure during synthesis, initiator concentration, vinyl acetate (VAc) addition and agitation were varied to optimize the copolymerization of ethylene. The quantity of ethylene copolymerized in VAE was calculated from pressure drop. The results matched NMR and DSC analysis.

Table 1. Ethylene content in vinyl acetate-ethylene copolymers determined by DSC, ^{1}H NMR measurements and the measured ethylene consumption [2]

Sample	The amount of ethylene in VAE copolymer (wt %)		
	Flory-Fox equation (from DSC)	^{1}H NMR	Ethylene gas consumption
VAE (ethylene 20 bar, VAc dosing 180 min)	8.5	8.3	9.5
VAE (ethylene 30 bar, VAc dosing 240 min)	14.9	16.3	14.9

e) Poly(methyl methacrylate) pre-polymer optimization

Reaction temperature exposition time in the preparation of pre-polymer for poly(methyl methacrylate), PMMA, production was optimized. Heating and cooling temperature gradient of the pre-polymer synthesis was set exactly as it was in industrial scale and the optimum reaction time was identified by viscosity measurements during process with torque measurements. Good repeatability in pre-polymer preparation is of crucial importance for quality in PMMA production.

5. Conclusions

In situ ATR-FTIR, FBRM, calorimetric measurements, viscosity or gas consumption measurements used in line with a batch computer controlled reactor (?) can be used to scale up polymerization, hydrolysis or other processes. RC1 proved to be a valuable tool for optimization of laboratory and industrial scale up polymerizations and other processes.

Acknowledgements

This work was supported by the Ministry of Education, Science, Culture and Sport of the Republic of Slovenia Grant number 3211-10-000057 (Centre of Excellence for Polymer Materials and Technologies), whose contribution is fully recognized.

References

[1] M. Kunaver, E. Jasiukaityte, N. Čuk, *Bioresour. technol.* 2012, 103, 360-366
[2] A. Anžlovar, K. Kogej, Z.C. Orel, M. Žigon, *e-XPRESS Polym. Lett*. 2011, 5(7), 604-619.
[3] I. Poljanšek, E. Fabjan, K. Burja, D. Kukanja, accepted for publication in *Progress in Organic Coatings*

S10-P97
Melt compounding of PP/clay nanocomposites in vibration force field

Strashimir Djoumaliisky (1)*, Bernd Kretzschmar (2), Regine Boldt (2), Georgi Kotzev (1)
(1) Institute of Mechanics/Bulgarian Academy of Sciences, Acad. G. Bonchev St., 1113 Sofia, Bulgaria
(2) Leibniz-Institut für Polymerforschung Dresden e. V., Hohe Str. 6, 01239 Dresden, Germany
*str_djum@imbm.bas.bg

1. Introduction

It is well known that Introduction of vibrations into the extrusion process is a way for intensification of mixing and dispersion of fillers in the polymer melts. Usually, a low-frequently vibration force field can be introduced into the extrusion process by axial vibration of the screw. Thus solid conveying, melting and metering stages are all under the action of a vibration force field resulting in positive effects on the material transportation and plasticizing as well as a uniform dispersion of filler particles in the extrudates [1,2]. A more efficient melt compounding could be achieved using an extrusion mixing die, in which the molten polymer composite is subjected on continuously changing shear and extensional deformations created by vibrations of a moveable mandrel [3]. Thus, a combination of extensional flow with vibration field during extrusion was expected to achieve break up of the agglomerates of nanofillers and improve the dispersion of nanoparticles in polymer matrix.
This study comprehensively analyzes the influence of the vibrations force field in this mixing device on morphology, and rheological and mechanical properties of clay filled PP composites.

2. Experimental

Polypropylene (HD120MO, Borealis AG, Austria) with a MFI (230/2.16) of 8 g/10 min and organically modified clay with a quaternary ammonium salt (Nanofil 5, Sued Chemie, Germany) were used. PP–g-maleic anhydride (Polybond 3200, Crompton Polybond Corp.) with MFI (230/2.16) = 115 g/10min, and M_w of about 42 000 was used as coupling agent.

PP/clay composites were prepared using an extrusion system consisting of a twin screw extruder (Leistritz Micro27, Germany, D = 27 mm, 36:1 L/D) and a mixer, in which vibration force field is applied. The mixing device consists of series of convergent-divergent zones (c-d zones) whose geometry is described in details in Ref. [3, 4]. The barrel temperature profiles were 180, 200, 200, 200, 200, 200, 200, 200, 200, 200 and 210^0 C from the hopper to the mixer. The screw speed and throughput was kept constant - 150 rpm and 6 kg/h, respectively. The dimensions of c-d zones and frequency could be adjusted independently in the range from 0.40/2.0 to 0.5/1.9 mm and 0 to 10 Hz, respectively. The extrudates were cooled and pelletized immediately and collected for measurements.
PP/clay composites were characterized by rheological properties, optical microscopy, TEM, SAXS and mechanical tests.

3. Results and discussion
The molten polymer composite moving through the flow channel is subjected to continuously changing shear and extensional deformations resulting in melt viscosity reduction. Two kinds of viscosity reduction are inherent in this case. The first of them is real and due to chain scission in the PP molecules. It is established an increase of the MFI with the increase of the oscillations frequency. Another type of viscosity reduction is due to shear thinning induced by vibrations. It is temporary and ceases when vibrations stop. An indirect measure for this fact is a decrease of melt pressure with the increase of the oscillations frequency. At the same time the amplitude decreases with increase of the oscillations frequency (Figure 1).

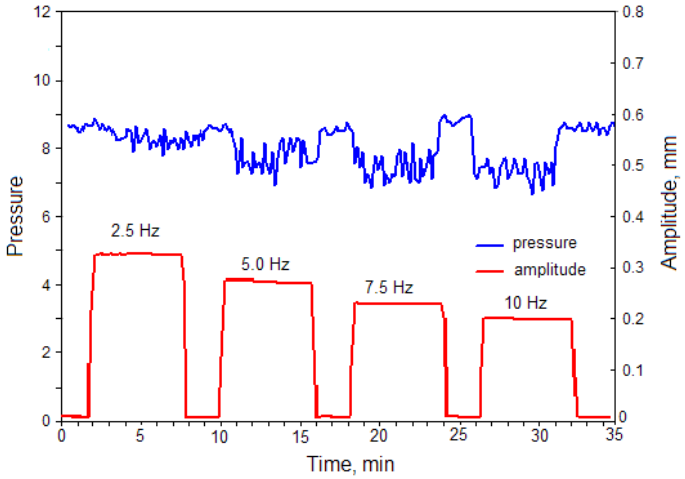

Figure 1: Effect of vibration frequency on amplitude and melt pressure in the flow channel.

The rheometric measurements show that composites prepared in vibration force field have higher viscosities compared to the composites prepared without oscillations. The increase in viscosity with increase of oscillation frequency is due to the better filler distribution and to the exfoliated nanoclay structure formed in PP/clay composites.
The mechanical properties of composites, such as tensile strength at break and Charpy impact strength, in general, depend on applied vibration force field. The increase of oscillation frequency positively affected the mechanical properties only at higher entrance gap, respectively lower outlet values of c-d zones. In other words, tensile strength of composite prepared with vibration shows little increase of about 5% than those prepared without vibration. It is important to note that in this case the increase of impact strength is about of 25 % (Figure 2).
The results obtained are confirmed by microscopic measurements and SAXS.

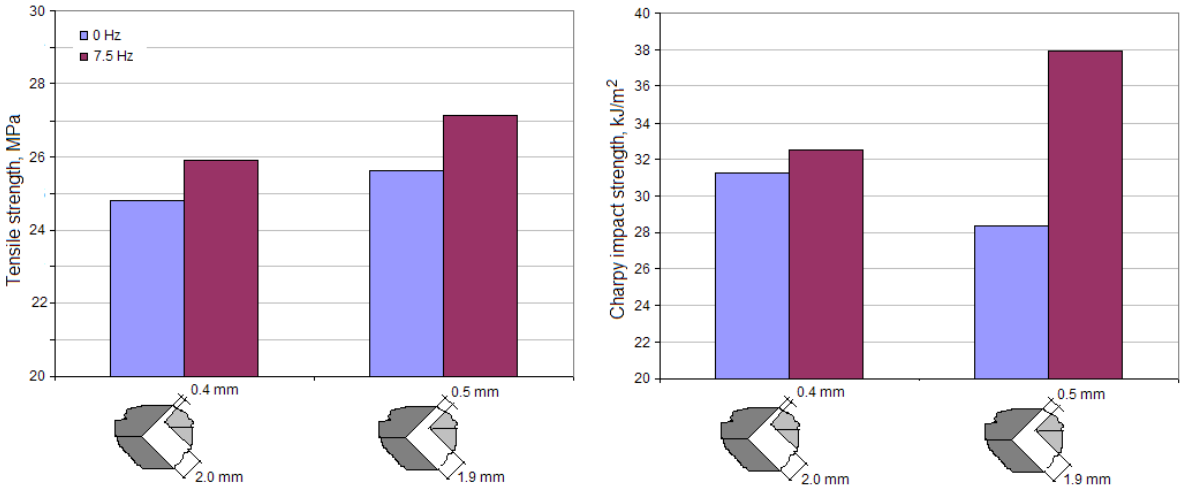

Figure 2: Mechanical properties of PP/clay composites prepared in vibration forced field depending on oscillation frequency and gaps dimensions.

4. Conclusions

PP/clay composites were melt compounded in vibration forced field depending on processing parameters. The efficiency of the mixing device was demonstrated by rheological properties, optical microscopy, TEM, SAXS and mechanical tests. It was established positive effect of vibration forced field on viscosity, filler dispersion and mechanical properties of the composites due to continuously changing shear and extensional deformations in the flowing polymer melt.

Acknowledgements

The authors are grateful for the financial support of the Bulgarian Ministry of Education and Science – National Science Fund (Project No DO 02-202/2008).

References

[1] W. Luo, N. Zhou, Z. Zhang, H. Wu, Polym. Testing, 2006, **25**, 124-129.
[2] Q. Xuemei, Q. Jinping, C. Xianwu, Polymer Bulletin, 2006, **56**, 607-618.
[3] Bulgarian Patent Reg. № 110658.
[4] G. Kotzev, S.Djoumaliisky, M. Natova, R. Benavente, J. Reinf. Plast. Comp., 2012, **31,** 1353–1363.

S10-P98

Preparation, characterisation and application of extrusion foams based on secondary polymers

Strashimir Djoumaliisky (1)*, Irena Borovanska (1), Anton Apostolov (2), Georgi Kotzev (1)
(1) Institute of Mechanics/Bulgarian Academy of Sciences, Acad. G. Bonchev St., 1113 Sofia, Bulgaria
(2) Laboratory on Polymers, Sofia University St. K. Ohridski, J. Bourchier Blvd. 1, 1164 Soifia, Bulgaria
*str_djum@imbm.bas.bg

1. Introduction

The recycling of mixed plastic waste is an up-to-date problem of scientific and practical importance and for its realization it is necessary to make quantitative assessment of the secondary plastics stream, to investigate the conditions of mixing and homogenization with compatibilizers in reactive extrusion, and to search for new technological solutions. Foaming technologies can be used as a perspective way for broadening the range of recyclates application. Recently, several investigations have been conducted on extrusion foaming for HDPE/PP, PP/PS, PET/PP blends [1-4].

The aim of the present study to quantitatively evaluate the plastic packing waste on the base of statistical experiment and to investigate the foaming process of model polymer blends, their morphology and properties. Applications of the foamed blends are discussed, too.

2. Experimental

Three model blends from recycled polymers were investigated: B1 (45 wt.% PET, 12 wt.% LDPE, 15 wt.% HDPE, 12 wt.% PP and 16 wt.% PS), B2 (25 wt.% LDPE, 25 wt.% HDPE, 25 wt.% PP and 25 wt.% PS) and B3 (50 wt.% LDPE and 50 wt.% PP), respectively.

The polymer blends were melt-compounded in Brabender DSE 35/17D twin screw extruder with different compatibilizing agents such as maleic anhydride grafted polypropylene, ethylene vinyl acetate and ethylene propylene dien monomer. The extrusion foaming was conducted in a Brabender single screw extruder (30D/25) equipped with slit die (3x6x12 mm) by adding of 1 wt.% chemical blowing agent azodicarbonamide Genitron AC-4.
The polymer blends were characterized by rheological properties, DSC and SEM. The foams produced were characterized in terms of bulk densities, gas bubble morphology and sound absorption depending on blowing agent concentration, processing temperature and extrusion rate. The bubble morphology (bubble number, bubble size, foaming grade) was determined by image analysis software.

4. Results and discussion

Foaming of polymer blends is a possibility for utilizing mixed plastic waste. It should be pointed out that processing temperature is one of the most important variables in the extrusion foaming process because it affects both the melt viscosity and the amount of gas released upon the thermal decomposition of the chemical blowing agent. The higher melt temperature of the blend B1 (Tm = 260^{o}C) leads to reduction of melt viscosity, degassing of gas-containing polymer melt and coalescence of the gas bubbles. As a result of these phenomena the bulk density of foamed blend B1 is higher with about 30% than that of foamed blend B2 and the bubble morphology is aggravated. Foamed blend B1 has significantly larger gas bubbles, which are non-uniformly distributed through the cross-section of the extrudates.
The lower melt temperature for blend B2 (Tm = 210^{o}C) leads to a finer and more uniform gas bubble distribution. A melt temperature of 210^{o}C appears to be critical for the formation of open bubbles. It is established that the extrusion rate also affects the morphology of the foams. The foaming grade reaches a maximum value as the extrusion speed increases to 60 rpm and a further increase in the speed tends to reduce the foaming grade. At the same time, bubble size decreases with increasing the extrusion speed (Figure 1).

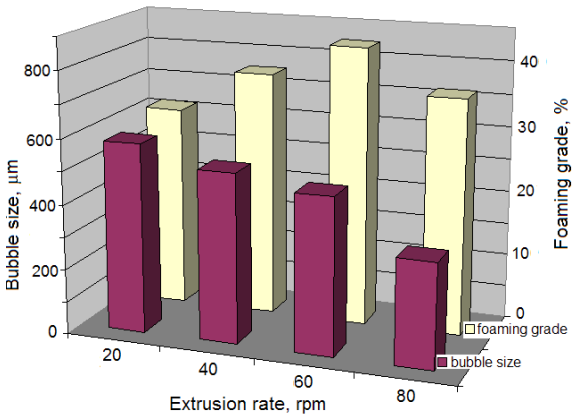

Figure 1: Foaming grade and average bubble size of blend B2 vs. extrusion rate

A correlation between the rheological properties and foam morphology of modified blend B3 is established. The higher amount of EPDM enhances the elastic properties of the blends, which, together with the higher viscosity, promotes more efficient foaming, expressed in greater number of bubbles with finer dimensions and more uniform distribution. The structure obtained determines better sound absorbing properties of modified blend B3 with increasing frequency of the sound wave (Figure 2). The results can be explained according to the sound absorption mechanism.

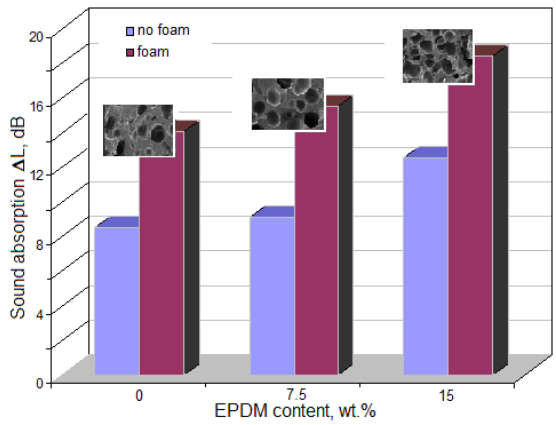

Figure 2: Sound absorption of foamed blend B3 modified with different content of EPDM (frequency 2000 Hz).

Conclusions

In the present study a quantitative evaluation of the plastic packing waste by means of separate collection was made. The model polymer blends were characterized by rheological measurements, DSC and SEM. The foams prepared were characterized in terms of bulk densities and gas bubble morphology. Based on the results profiles with a sandwich-like structure consisting of an external skin built of virgin HDPE and a core of foamed blend B3 were produced. These products could replace wood materials in different applications.

Acknowledgements

The authors are grateful for the financial support of the Bulgarian Ministry of Education and Science – National Science Fund (Project No DTK 02/7-2010).

References

[1] M. Lee, C. Tzoganacis, C.B. Park, Polym. Eng. Sci., 1998, **38**, 1112-1120.
[2] P. Zhang, N.Q. Zhou, Q.F. Wu, M.Y. Wang, X.F. Peng, J. Appl. Polym. Sci., 2007, **104**, 4149-4159.
[3] S.T. Lee, J. Cell. Plast. 2010, **46,** 321-331.
[4] C.Z. Sahagun, R. Gansalez-Nunes, J. Cell. Plast., 2006, **42,** 469-485

S10-P99
Characterization of mechanically recycled, non-sorted plastic waste

Diego Molina*, Gianmarco Griffini, Raffaella Suriano, Gigliola Clerici, Marinella Levi, Stefano Turri

Politecnico di Milano, Dipartimento di Chimica, Materiali e Ingegneria Chimica "G. Natta", Piazza Leonardo da Vinci 32, 20133, Milano, Italy
*diego.molina@chem.polimi.it

1. Introduction

The increasing volume of plastics consumption inevitably leads to the production of large amounts of plastic waste. Plastic recycling process is becoming one of the most interesting topics in order to reduce worldwide environmental pollution. Usually, plastic recycling separates a large quantity of post consumption plastics from common municipal waste into different and homogeneous polymer typologies (such as PET, PE, PP) [1-2]. Those polymer families could easily be reinserted into productive cycle with few properties drawbacks.

Unfortunately a large fraction of the total amount of plastic waste cannot be efficiently selected and sorted into homopolymer classes, mainly due to their uneconomic processing. This fraction is commonly named PLASMIX and it's formed by some fractions of mixed polymers, usually exploited in packaging. The main part of this mix is composed by damaged PP, HDPE, PS and LDPE, and some trace of PET and PVC. Even with the development of advanced material selection and recycling procedures, PLASMIX shows poor mechanical properties and reduced aesthetic qualities that make this mix hardly to be exploited in different low profiled market applications [1-3].

The main reason for these poor properties is the incompatibility of most polymers pairs [3]. A well known technique to improve mechanical properties of immiscible polymer blends is to develop an efficient compatibilization process. Compatibilization of PLASMIX is however a difficult task due to the simultaneous compatibilization issues of different polymers present. Moreover the compatibilizer must be chosen, and the compatibilization process must be developed, with a cheap and simple, i.e. already on market, technology, in order to let the material be renewed with a non expensive investment.

The aim of this contribution is to investigate the potential use of SBS as compatibilizer to induce an increase in the interface properties of the different polymer phases present in PLASMIX. Moreover exploiting co-rotating extrusion processing, with a reduced resident time and degradation of the material, the exploration of the possible synergic contribution of compatibilizer and stabilizers is demonstrated, and the reason for improvement in mechanical properties of compatibilized recycled polymers is discussed.

2. Experimental

The materials considered in this work were kindly provided by ICMA San Giorgio S.p.A. and were obtained by co-rotating twin-screw extrusion of recycled mixed plastic waste (PLASMIX) composed by different proportions of HDPE, PP and PET. As compatibilizing agent, SBS rubber was added to the recycled mixed plastic waste in different proportions. As stabilizing agent, Irganox B225 (Ciba) was added to prevent oxidation during the extrusion process. Other additives such as Talc and $CaCO_3$ were also employed to improve mechanical properties of the extruded product.

In order to characterize the recycled mixed plastic waste, the following techniques were employed. IR spectra were collected in ATR mode on a Nicolet 760-FTIR spectrophotometer controlled by OMNIC software. Samples were collected with 64 scans at a 4 cm^{-1} resolution. Differential Scanning Calorimetry (DSC) was performed on weighted samples (~ 10 mg) with a DSC/823^e Mettler Toledo differential scanning calorimeter. Scan rate was 20 °C/min. Rheological measurements were conducted on a Rheometrics

DSR 200 rheometer in a parallel plate configuration (25 mm diameter plates) at 200-230 °C. Flow curves were collected by performing steady stress experiments on each sample for 5 minutes in the 500 – 6000 Pa range and by recording the viscosity of the sample. The determination of tensile properties of the extruded plastics was performed, according to ISO 527-2:1997, with a Zwick Proline Z010 TH universal testing machine with a crosshead speed of 1mm/min. Test were performed at room temperature and at least five specimens were tested for each samples.

3. Results and discussion

The main aim of this work is to characterize and to optimize the composition and the mechanical properties of recycled mixed plastic waste namely PLASMIX in order to continue exploiting them even at the end of their life cycle. Different PLASMIX samples with various proportions of SBS acting as compatibilizing agent were first investigated by Infrared spectroscopy and IR spectra confirmed the presence of PP, PE, PS, PMMA, PET and SBS in the recycled blends, as expected.

To examine the heterogeneity of these samples, optical microscopy images were acquired and in all the PLASMIX samples many inclusions ranging from 10 µm to 2 mm were observed. The existence of these particles is partly responsible for the poor mechanical properties of the recycled mixed plastics waste, because it reduces the interface properties of different polymer phases present in PLASMIX.

By adding a small amount of compatibilizer, an improvement in the mechanical properties was attainable: as shown in Figure 1, comparing modified to unmodified samples, an increase in strain at break point was achieved after the compatibilization process. A decrease of elastic modulus was also found for modified sample, because SBS rubber also acts as a plasticizing agent.

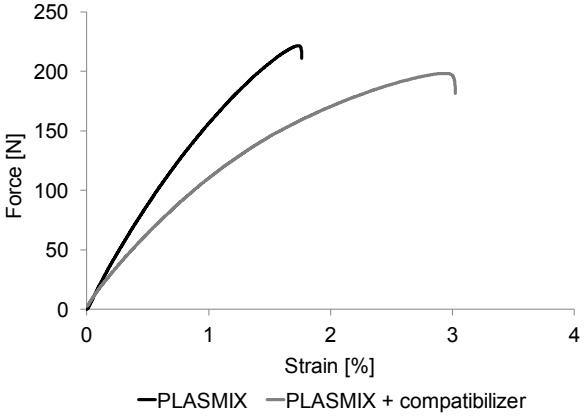

Figure 1. Stress-strain curves of unmodified (black line) and compatibilized (grey line) PLASMIX.

The data in Figure 2 also shows that PLASMIX and compatibilized samples at high temperatures (200-230°C) have approximately the same viscosity in the considered range of shear rates. This Figure means that compatibilizers protect from degradation of modified recycled blends and allow to process them with standard co-rotating extrusion systems.

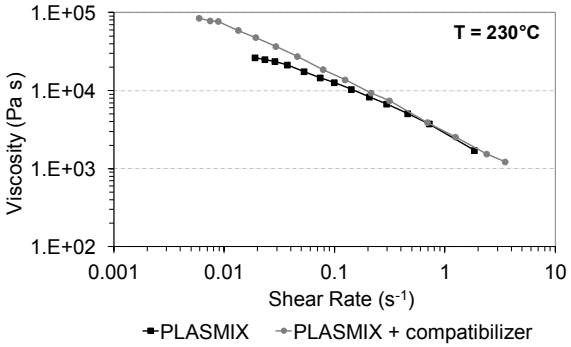

Figure 2. Viscosity curves of unmodified (black line) and compatibilized (grey line) PLASMIX.

4. Conclusions

As a result of this study, the improvement of mechanical properties of compatibilized recycled plastic waste compared to the unmodified one could be achieved. In addition, no modifications to the rheological behavior of the compatibilized systems was found, indicating that a simple and cheap process of compatibilization may allow to processes this otherwise wasted material into technologically valuable components.

Acknowledgements

This work was partially funded by Regione Lombardia ("ECO-IMPATTO Eco progettazione di compositi e manufatti ottenuti da plastiche di scarto post-consumo" project).

References
[1] S.M. Al-Salem, P. Lettieri, J. Baeyens, *Waste Management* **2009**, 29, 2625-2643.
[2] A.S.F. Santos, J.A.M. Agnelli, D. W. Trevisan, S. Manrich, *Polym. Degrad. Stab*. **2002**, 77, 441-447.
[3] S.E. Luzuriaga, J. Kovarova, I. Fortelny, *Polym. Degrad. Stab*. **2011**, 96, 751-755.

S10-P100
Ultrasound-based monitoring of the plasticizing process in injection moulding machines

Bernhard Praher*, Klaus Straka, Jesenka Usanovic, Georg Steinbichler
Johannes Kepler University Linz, Institute of Polymer Injection Moulding and Process Automation,
Altenbergerstrasse 69, 4040 Linz, Austria
*bernhard.praher@jku.at

1. Introduction
In an injection moulding process solid polymer granules are plasticized in a heated barrel containing a rotating screw and stored in the screw ante-chamber. The temperature of the polymer melt stored in the screw ante-chamber after the plasticization should be homogeneous. However, in reality the polymer melt in the screw ante-chamber is not homogeneous due to the complex thermal history of the polymer during the plasticizing in the channel of the screw. We developed two different system based on ultrasound for the non-invasive monitoring of the plasticizing process along the screw and measuring temperature gradients in the screw ante-chamber. The systems can be used for the validation of numerical simulations, to get a better understanding of the plasticizing process and as an input for novel control systems.

2. Theory
Due to the fact the sound velocity in a polymer melt is temperature depending, we developed a tomography system [1] using the measured transit times of ultrasonic pulses along different sound paths for calculating the temperature distribution in radial direction of a polymer melt in the screw-ante chamber of an injection moulding machine. Figure 1 shows the schematic of the developed tomography temperature measurement system.

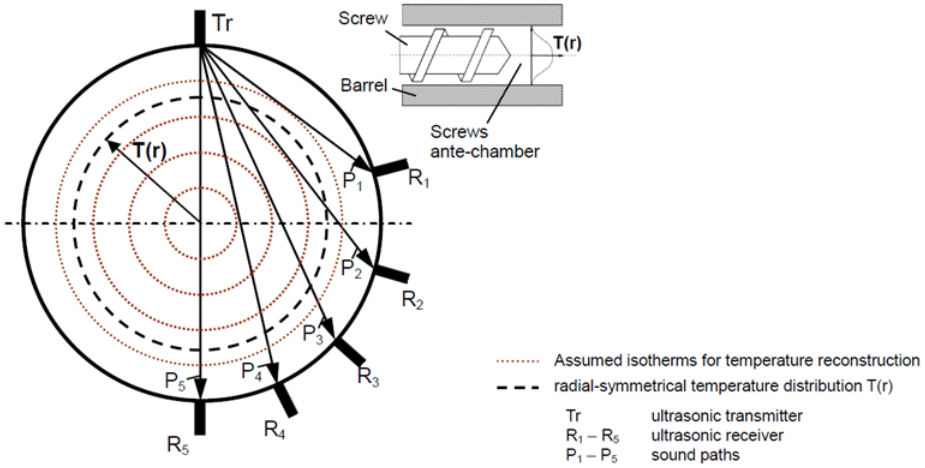

Figure 1. Schematic of the developed tomography temperature measurement system for the estimation of radial temperature distributions in the screw-ante chamber.

For the determination of the solid bed - melt pool ratio in the channel of the plasticizing screw we developed a non-invasive ultrasonic measurement system based on reflection measurements: an ultrasonic pulse is transmitted into the barrel and reflected due to the acoustic boundaries (barrel/polymer/screw flight or screw root) during the plasticizing process. By automated analysis of the reflected pulses - measured at different positions of the screw - it is possible to monitor the melting process online (in opposition to the time-consuming 'screw pulling-out' method).

3. Simulation, experimental and results
For the validation of the developed tomography system we simulated the transit time of ultrasonic pulses along the sound paths P1, P2,.., P5 (Figure 1a) in a polypropylene (PP) melt using available pressure-volume-temperature data. Figure 2a provides the theoretically calculated sound velocity in PP as a function of the temperature and pressure. The simulation result of a temperature

reconstruction of the proposed system is shown in Figure 2b assuming a rotational-symmetrical temperature distribution during the transit time measurements.

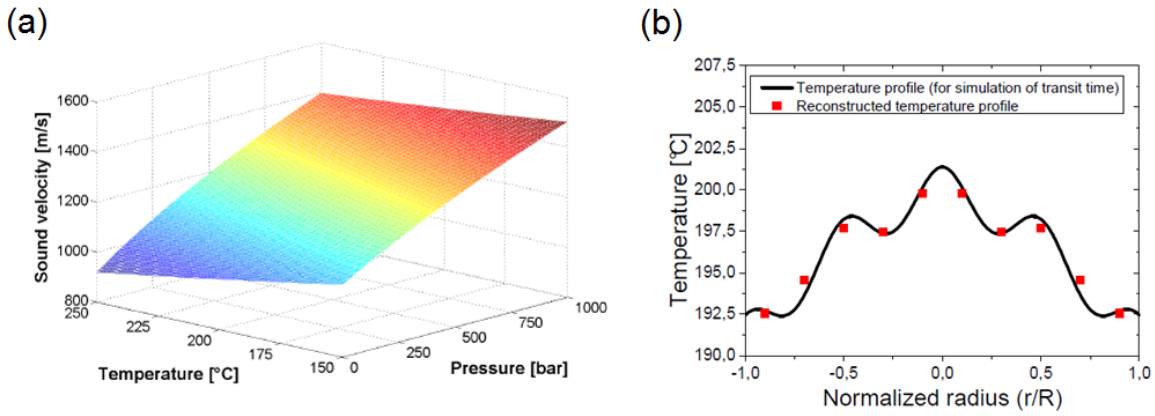

Figure 2. Theoretically calculated sound velocity in PP (a) and simulation results of temperature distribution reconstruction from ultrasonic transit time measurements (b).

In Figure 3a the experimental setup for reflection measurement is shown. Results and interpretation from ultrasound reflection measurements are displayed in Figure 3b.

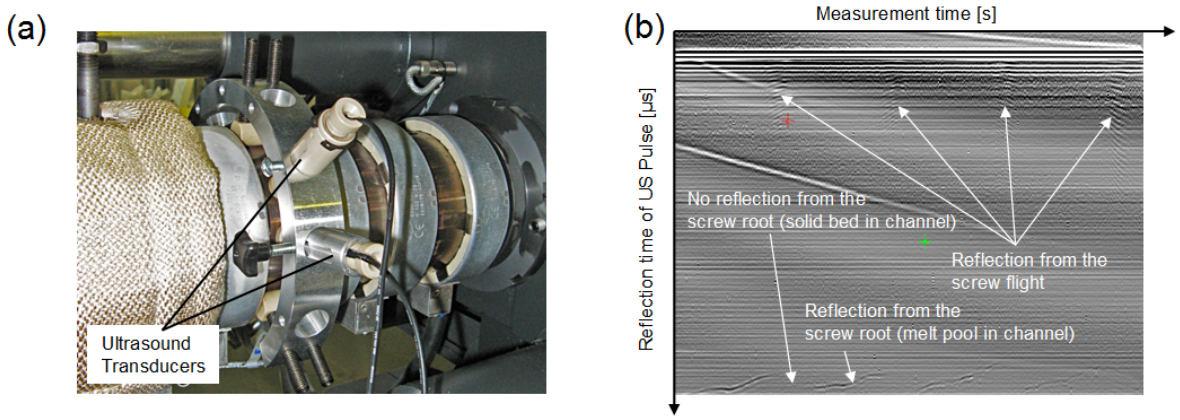

Figure 3. Experimental setup for ultrasonic reflection measurement (a) and received signals (b).

4. Conclusions

Two novel ultrasound-based methods for measuring the two-dimensional temperature distribution of a polymer melt in the screw ante-chamber and monitoring the melting process along the plasticizing screw are proposed. The precision and validity of the systems were evaluated by simulations and preliminary experiments.

Acknowledgements

We would like to thank Michael Hettrich-Keller for his help in constructing the measurement setup. This work was partly funded by the COMET K-Project APMT (FFG project number 825344).

References

[1] B. Praher, K. Straka, G. Steinbichler, "A Novel Ultrasound-Based System for Temperature Distribution Measurements in Injection Moulding" : Proceedings 'The 13th Mechatronics Forum International Conference', Vol. 1/3, Trauner Verlag, Linz/Austria, Seite(n) 213-220, 9-2012, ISBN: 978-3-99033-042-5

S10-P101
Recycling Kerrock

Matej Vovk (1)*, Andrej Beličič (1), Milan Šernek (2)
(1) Kolpa d.d., Rosalnice 5, 8330 Metlika, Slovenia
(2) University of Ljubljana, Biotechnical faculty, Department of wood science and technology, Cesta VIII/34, 1000 Ljubljana, Slovenia
*matej.vovk@kolpa.si

1. Introduction

Kerrock is a solid surface composite material, which is composed of 40 wt. % of polymethylmethacrylate (PMMA) and 60 wt. % of aluminum trihydroxide (ATH) filler with silane as a coupling agent [1]. Because of its composition and form, machining of Kerrock is similar to machining of wood. Additionally, it can also be thermoformed like thermoplastics [2]. Kerrock is widely used for working surfaces and claddings for indoor and outdoor applications. Interfacial morphology, interfacial adhesion between filler and polymer matrix, dispersion of ATH particles and concentration of adhesion promoting agent have the biggest impact on the mechanical characteristics of Kerrock.

During the production process of Kerrock, there are a lot of residues in powder form, made due to the surface processing (grinding). We would like to use this powder to make a new composite. It is possible to chemically recycle Kerrock, however the energy consumption is too high. One possibility to recycle powder particles of Kerrock is to mix it with asphalt [3], another option is to combine the powder in a hot press or with methylmethacrylate (MMA) or polyester resin addition before press [4], [5]. Our idea, however is to use less expensive adhesives that are most commonly used in woodprocessing industry and to combine Kerrock powder with wood. We think it would be interesting to combine such different materials into one composite.

In preliminary research we studied the surface free energy of Kerrock, contact angle between Kerrock and different adhesives and shear strength of the adhesive bond in two-layered test specimens.

2. Experimental

We calculated the surface free energy of Kerrock by measuring the contact angle between the plates of Kerrock and two polar (demineralized water and formamide) and one nonpolar liquid (diiodomethane). We used standard white Kerrock plates (3mm thick, 27 x 27 mm). Measurements were executed at room temperature (22 °C) and relative air humidity of 40 – 50 %. All measurements were made on Kruss Processor Tensiometer K100.

In next step we measured the contact angle of different adhesives with Kerrock. Adhesives used were ureaformaldehyde (UF) Lendur 200 (manufactured by Nafta Lendava, d.o.o.), melamine-urea-formaldehyde (MUF) Meldur H97 (manufactured by Melamin, d.d.) and phenol formaldehyde (PF) Borofen B-407/45 (manufactured by Fenolit, d.d.). Kerrock plates were the same dimensions as before, and so were the conditions and apparatus.

In the last part of the experiment we made two-layered test specimens of Kerrock and wood with different adhesives (UF, MUF and PF) and measured the shear strength of adhesive bond. We used standard white (colour 108) Kerrock boards (12 mm thick, 120 x 500 mm) and wooden boards (5 mm thick, 120 x 500 mm) made out of beech. Adhesives used were the same as before. We put 200 g/m2 of adhesive on each wooden board and covered it with Kerrock board. All together was put in a hot press and left under conditions described in Table 1. Next day we cut the boards into samples according to modified standard SIST-TS CEN/TS 13354:2004 [6] and got samples that were 17 mm thick, 45 wide and 40 mm long. Samples were then put in standard climate conditions for one week. Shear strength of the adhesive bond was measured on Zwick Z100 apparatus according to already mentioned standard.

Table 1. Hot press conditions and duration.

Adhesive	Pressure [bar]	Temperature [°C]	Time [min]
UF	15	120	7
MUF	15	140	9
FF	15	150	12

3. Results and discussion

Differences in contact angles between Kerrock and different liquids are great due to different characteristics of liquids and their surface tension. Highest contact angles were measured between Kerrock and demineralized water (82,2°); contact angle between Kerrock and formamide was 62,6° and between Kerrock and diiodomethane it was 40,7°. These results show that smaller contact angles and better wettability is achieved with nonpolar liquid with low surface tension (Table 2). Calculated surface free energy of Kerrock was 39,7 mJ/m2.

Table 2. Surface tensions and contact angle measurements.

Liquid	Surface tension [mJ/m^2]	Contact angle with Kerrock [°]
Demineralized Water	72,8	82,2
Formamide	58,0	62,6
Diiodomethane	50,8	40,7

MUF and UF adhesives could wet Kerrock, as their contact angle with this material was lower than 90°. This was not the case with PF, as it had a contact angle of 90,6° (Table 4).

Table 4. Adhesive characteristics and their contact angle with Kerrock.

Adhesive	Density [kg/m^3]	Surface tension [mJ/m^2]	Contact angle between Kerrock and adhesive [°]
UF	1268	72,3	86,9
MUF	1271	73,3	79,9
FF	1190	51,2	90,6

The highest average value of shear strength was determined in samples containing MUF (14,7 N/mm2), samples with PF were second (12,9 N/mm2) and the lowest shear strength was determined at samples with UF adhesive (8,1 N/mm2) (Figure 1). This results show that only specimens containing UF adhesive did not reach the shear strength required by the standard (10 N/mm2). It is not coincidental that specimens containing MUF adhesive had highest shear strength, as the contact angle between Kerrock and this adhesive was also the lowest. Though PF had highest contact angle, it also had high shear strength, which is a consequence of its characteristics as it is solid and rigid as it cures.

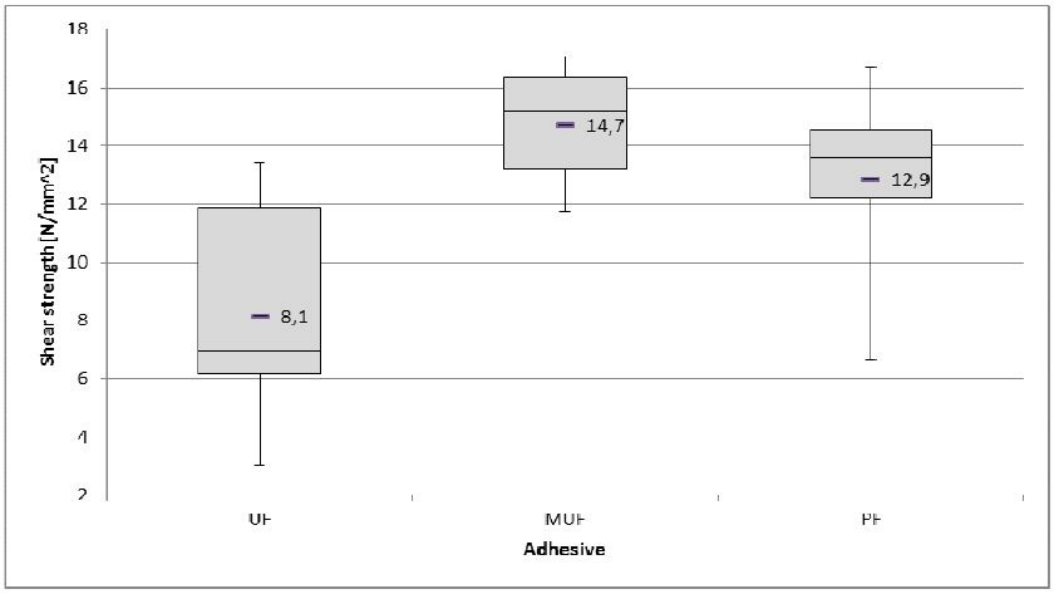

Figure 1. Shear strength of different adhesive bonds in two-layered test specimens containing Kerrock and wooden boards.

4. Conclusions

We find these results very useful to continue our research combining Kerrock solid surface material residues with wood. MUF showed very good shear strengths of the adhesive bond as its contact angle with Kerrock was the lowest, although still high enough. Based on these results we think it is possible to recycle Kerrock residues by combining them with wood.

Acknowledgements

This work was done under a project KROP Kolpa d.d. – 000477, which is financed under Ministry of economic development and technology, EU and Kolpa, production and processing of plastics, d.d.

References

[1] Duggins R. B., Ford C., Miller H. C. Filled polymethyl methacrylate article and a process for its manufacture. United states patent US 3 827 933. 1974, p. 5.

[2] Peters C. R., Young J. E. Process for making bowls comprising acrylic plastic filled with alumina trihydrate. United states patent US 6 554 944 b1. 2003, p. 17.
[3] Tušar M., Beličič A., Prešeren M. Asfalt z dodanim PMMA/ATH: Patentna prijava: P-201100092. Ljubljana, Urad republike Slovenije za intelektualno lastnino. 2011, p. 6.
[4] Kočevar G., Beličič A. Postopek za izdelavo stisnjene plošče iz prahu kompozita polimetilmetakrilata in aluminijevega hidroksida. Patent SI 22995. 2009, p. 10.
[5] Kočevar G., Beličič A.. Integrirana kompozitna plošča s stisnjeno ploščo iz prahu kompozita polimetilmetakrilata in aluminijevega hidroksida. Patent SI 22996 A. 2009, p 4.

S10-P102

An investigation on effects of soya oil on properties of polymer modified bitumen
The modification and study of bitumen with a α-Olefin Copolymer –soya oil

Farhad Zafari (1)*, Mohamad Rahi (2), Hossein Nazockdast (3), Nazanin Moshtagh (4)
(1) Research assistant , Polymer Engineering Department, Amirkabir University of Technology, Hafez St 158754413 Tehran, Iran
(2) Reasercher of R&D department of Pasargad Company , Mirdamad Blvd, 193954598Tehran, Iran
(3) Professor , Polymer Engineering Department, Amirkabir University of Technology, Hafez St, 158754413, Tehran, Iran
(4) Research assistant , Polymer Engineering Department, Amirkabir University of Technology, Hafez St 158754413 Tehran, Iran
*zafarifarhad@yahoo.com

1. Introduction
The pavement with polymer modified bitumen (PMB) exhibits higher resistance to rutting and thermal cracking, lower fatigue damage, stripping, aging and temperature susceptibility[1-5]. α-Olefin copolymers, due to their excellent elasticity, toughness, low brittleness temperature, good chemical resistance and superior heat resistance

2. Theory
Adding polymers to bitumen improves some properties of bitumen such as elasticity and thermal resistance. However, the immiscibility and density difference of α-Olefin copolymers and bitumen cause phase separation and migration of polymer to the surface of binders. The bitumen consists of two phases: asphaltene and maltene. One reason of phase separation is due to absorption of maltene to polymer and incompatibility of bitumen phases .To solve this problem, different percentages of soya oil added to bitumen- polymer binders to Compensation deficiency of maltene which is in equilibrium with asphaltene phase.

3. Experimental
The polymer modified bitumen (PMB) samples consisting of a60/70 penetration grade bitumen with a constant weight percentage of poly α-olefin copolymer and different percentages of Soya oil as modifiers, are prepared by using a stator-rotor mixer at 190°C. Table1 shows the formulations examined for specification compliance. The morphology of samples were studied by using optical microscopy and the rheological properties of binders are perused over a wide range of temperature and frequency in the linear viscoelastic regime with dynamic shear rheometer (DSR) and the storage stability of all samples were measured.

Sample	***modifier trade name***[†]	***Formulation***
TafMAH1[1]/4P	Tafmer® MH7010	Bitumen/ 4wt% MH7010
TafMAH1[1]/4P/2O	Tafmer® MH7010	Bitumen/ 4wt% MH7010+2wt% Soya oil
TafMAH1[1]/4P/4O	Tafmer® MH7010	Bitumen/4wt%MH7010+ 4% wtSoya oil

Table1. Formulation of prepared samples and base bitumen specifications

4. Results and discussion
Figure1 shows the optical photomicrographs of the PMB samples. A distinction can be made between the PMB samples whose continuous phase is a bitumen matrix with dispersed polymer particles in TafMAH1 /4P sample. As it can clearly be seen in Figure1 (b), addition of 2%wt Soya oil has made swollen polymer particles very smaller and addition of 4%wt caused uniform distribution of polymer in bitumen and disappearance of particles.

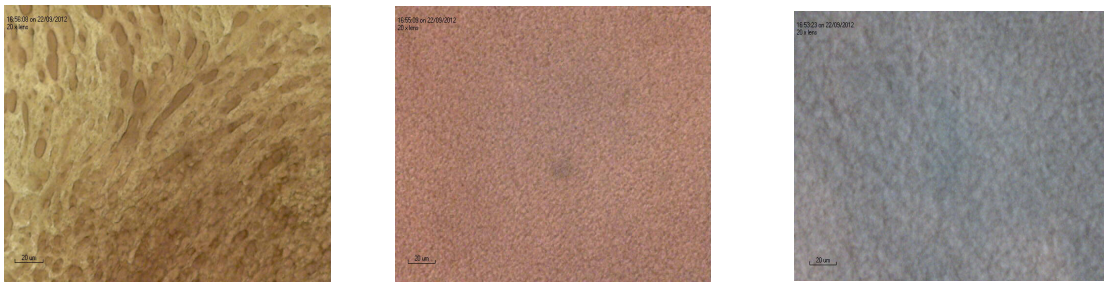

(a) (b) (c)

Figure1. Optical photomicrographs of PMB samples:
(a) TafMAH1 /4P, (b) TafMAH1 /4P/2O, (c) TafMAH1 /4P/4O

The complex modulus, storage modulus, loss modulus, rutting factor (*G*/sinδ)*, fatigue factor (*G*.sinδ)*, tan*δ* and complex viscosity of versus temperature at 10*Hz were plotted* . Temperature sweep tests showed that a pronounced enhancement in elastic response. And all of above factors were drawn against frequency at 50°C also. Elastic modulus plateau and viscosity up-turn from frequency at lower frequencies and very slightly increase in damping factor (plateau region in high frequencies)clearly prove the existence of an elastic network created by swollen polymeric phase in all PMB samples.
In storage stability test, the increase in softening point of both top and bottom of PMB samples in comparison with base bitumen is the evidence of significant interaction between binders components.

5. Conclusions
By using rheological techniques, it was demonstrated that commercially available α-Olefin copolymer and soya oil are able to appreciably modify the properties of bituminous materials. Adding soya oil improves the fatigue resistance in intermediate and low temperature and facilitate the bitumen processing in high temperatures.

Acknowledgements
The study carried out in Research and Development deportment of Pasargad Oil company and Amirkabir university of technology. The copolymer and soya oil used in the study was supplied by Danabaspar company.

References
[1] Hossain M, Swartz S, Hoque E. Fracture and tensile characteristics of asphalt–rubber concrete. J Mater Civil Eng 1999;11(4):287.
[2] Airey GD, Singleton TM, Collop J. Properties of polymer modified bitumen after rubber–bitumen interaction. J Mater Civil Eng 2002;14(4):344.
[4] Mull MA, Stuart K, Yehia A. Fracture resistance characterization of chemically modified crumb rubber asphalt pavement. J Mater Sci 2002;37(3):557.
[5] Lu XH, Isacsson U. Rheological characterization of styrene–butadiene styrene copolymer modified bitumens. Construct Build Mater 1997;11(1):23–32.
[6]. Mark JE, Polymer Data Handbook, 'Olefin Copolymers', Oxford University Press, 1999, On-line version

S10-P103
Properties of LDPE exposed to extensive mechanical recycling simulated by extrusion

Huiying Jin (1), Joamin Gonzalez-Gutierrez (1), Pavel Oblak (1), Barbara Zupančič (1)*, Igor Emri (1,2)
(1) University of Ljubljana, Faculty of Mechanical Engineering, Centre for Experimental Mechanics, Pot za Brdom 104, 1000 Ljubljana, Slovenia
(2) Institute for Sustainable Innovative Technologies, Pot za Brdom 104, 1000 Ljubljana, Slovenia
*barbara.zupancic@fs.uni-lj.si

1. Introduction
In 2011, total plastic production in Europe was 58 million tons, and post-consumer waste was 25.1 million tons of which 10.3 million tons (41%) were disposed of in landfills [1]. According to EU directives (DIRECTIVE 2008/98/EC) Member States should support the use of recyclates, in line with the waste hierarchy and with the aim of a recycling society, and should not support the landfilling or incineration of such recyclates whenever possible.
There are mainly three options for plastics recovery: mechanical recycling, feedstock recycling and energy recovery [2]. Mechanical recycling is the most widely practiced of these methods as it is relatively easy and economic. However, properties of mechanically recycled polymers do not remain the same because of degradation from heat, mechanical stress, oxidation and ultraviolet radiation

during reprocessing and lifetime [3]. In polymeric materials thermo-mechanical and thermo-oxidative degradation occurs mainly due to chain scission, branching and crosslinking reactions. For one of the most widely used plastics – LDPE, it is a commonly accepted fact that degradation mechanism is the simultaneous occurrence of both chain scission and crosslinking, although it shows a higher tendency to crosslink or chain branching [4].
Several research groups have investigated the effects of mechanical recycling of a variety of polyolefins, including LDPE [5], but the effect of extensive mechanical recycling has not been reported.
Within our investigation we analyzed several physical properties of recycled LDPE that affect, on one hand, processability of the material, and on the other hand, long-term stability (durability) of LDPE. Results within this paper are limited to the presentation of the effect of mechanical recycling on the melt flow index (MFI), and creep properties of LDPE recyclates. Other results are available in the paper that we published recently [6].

2. Experimental

Low Density Polyethylene (LDPE) OKITEN® 245S produced by DIOKI (Croatia) with a density of 0.924 g/cm^3 and melting point of 114 °C was used for the purposes of this investigation. The manufacturer indicated the presence of a slip agent and a thermal stabilizer in the material, but no antiblocking agent.
Process of extensive mechanical recycling was simulated by repeated cycles of extrusion. We used a Haake Polylab PTW 16/40 OS twin screw extruder produced by Thermo Scientific (Germany), and perform one hundred extrusion cycles. LDPE was extruded at screw rotation of 150 min^{-1}, a processing temperature of 240 °C and with a throughput between 1200 and 1300 g/h. Samples of cylindrical shape were taken for the first ten extrusions, and thereafter from every next tenth extrusion cycle. The remaining extruded material was cooled in a water tank and then pelletized using a Thermo Haake pelletizer (type 557-2685) before being submitted to a new extrusion cycle.
Melt flow index (MFI) measurements were performed according to standards ASTM D1238 and ISO 1133. For this purpose, an Extrusion Plastometer of the Italian producer ATS Faar S.p.a., was used. The melt flow properties were measured at the temperature of 190 °C by applying pressure via prescribed gravimetric mass of 2.16 kg.
Creep measurements were performed in the Shear Creep Torsiometer which has been developed at the Centre for Experimental Mechanics of the Faculty of Mechanical Engineering, University of Ljubljana. For the purpose of shear creep measurements we used LDPE cylindrical sample of 5.70 ± 0.05 mm in diameter and 40.0 ± 1.0 mm in length, taken during the process of extrusion. Measurements of shear creep compliance, J(t), were performed within the temperature range between 30 °C to 80 °C. The stresses applied to each specimen were selected as to remain in the linear viscoelastic region for all materials, and ranged from t_0 = 6.7 × 10^4 Pa at 30 °C to 2.7 × 10^4 at 80 °C. Other details on the creep measurements procedure are described in [6].

3. Results and discussion

Figure 1 presents the results of the melt flow index (MFI) measurements. Decrease in MFI with consecutive extrusions indicates a decrease in the ability of molten LDPE to flow under pressure. This suggests reduction in the mobility of polymeric chains, which can be attributed to crosslinking or molecular enlargement. However, results presented below indicate that crosslinking is probably the dominating mechanism; this was also confirmed by solubility studies described and analyzed in [6].

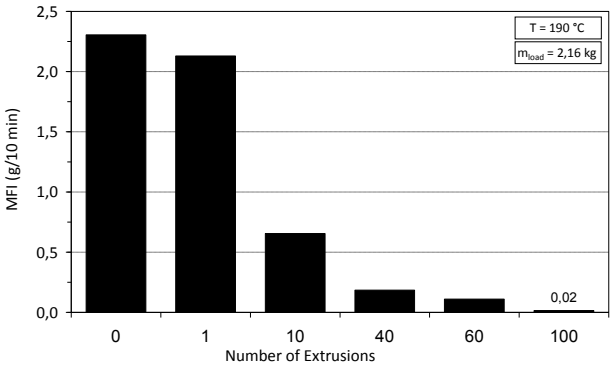

Figure 1. MFI of LDPE recyclates exposed to certain number of extrusion cycles

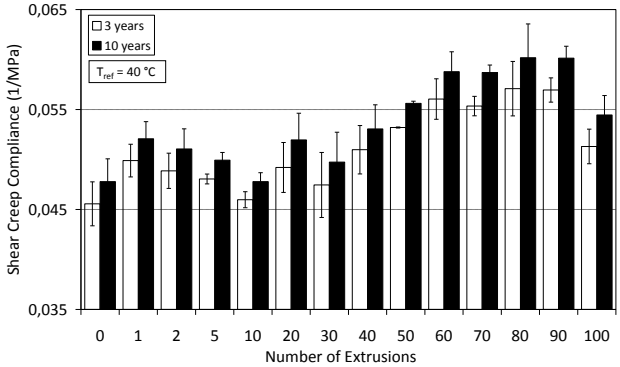

Figure 2. Shear creep compliance after 3 and 10 years for LDPE recyclates exposed to certain number of extrusion cycles

Comparison of creep compliance values after 3 and 10 year are presented in Figure 2 for virgin and recycled LDPE materials at the reference temperature of 40 °C in order to study the effect of mechanical recycling on long-term stability of polymeric products [6]. It can be seen that the maximum differences in creep compliance between virgin LDPE and recycled ones is less than 10 % until the 40th extrusion cycle at 3 and 10 years, while after the 40th extrusion cycle, the maximum differences are approximately 25 % and 26 % at 3 years and 10 years, respectively. In addition, the increase/decrease of creep compliance in comparison to the creep compliance of virgin LDPE reflects the changes in mobility of molecular chains caused by crosslinking leading to a decrease in crystallinity of the solid LDPE [6]

4. Conclusions

Change in the melt flow index (MFI) shows that molten behavior of LDPE is significantly affected by mechanical recycling of polymer suggesting reduced chain mobility due to crosslinking. This indicates that the technological parameters should be modified when processing recycled LDPE.

Changes in polymer chain mobility also lead to the increase of creep compliance after 40th extrusion cycle on, which means that long-term behaviour of solid LDPE deteriorated only after 40th recycling cycles.

Obtained results are promising and benefitial information for the industry, which should according to the EU directives (DIRECTIVE 2008/98/EC) ensure proper waste management, as well as take measures to promote high quality recycling.

References

[1] Plastics-the facts 2012. An analysis of European plastics production, demand and recovery for 2011. Plastics Europe 2012.
[2] V. Goodship, *Introduction to plastics recycling* (2nd edition), Smithers-Rapra Technology Limited, 2007.
[3] F.P. La Mantia, *Basic concepts on the recycling of homogeneous and heterogeneous plastics*. In: La Mantia FP, editor. Recycling of PVC and mixed plastic waste, Chem Tec Publishing, 63-76, 1996.
[4] M. Chanda,S.K. Roy, *Plastics technology handbook* (4th edition), CRC Press, 2006.
[5] A. Choudhury, M. Mukherjee, B. Adhikari, *Thermochim. Acta*. **2005**, 430, 87-94.
[6] H. Jin, J. Gonzalez-Gutierrez, P. Oblak, B. Zupančič, I. Emri, *Polym. degrad. stab.* [Print ed.], **2012**, 97(11), 2262-2272.

Session 11: Advances in polymer analysis, characterization and testing

S11-P104
Tailoring of sol-gel hybrid materials for analytical applications

Merima Čajlaković (1)*, Michael Suppan (1), Volker Ribitsch (2)
(1) Institute for Surface Technologies and Photonics, Steyrergasse 17, 8010, Graz, Austria
(2) University of Graz, Institute of Chemistry, Colloid & Polymers, Heinrichstrasse 28, 8010, Graz, Austria
*merima.cajlakovic@joanneum.at

1. Introduction

Critical care is one of the most challenging areas of medicine, e.g., while giving the treatment to the patient, careful diagnosis and other disease-causing agent in the biological fluids is a deciding factor. Furthermore, fast breath analysis is attractive and permits non-invasive monitoring of a patient's state of health. The use of breath gas analyzers is typically restricted to a laboratory environment due to the expensive, cumbersome nature of most breath analysis systems. Therefore is the development of a portable, low-cost system attractive as such a system would be compatible with home healthcare and advanced athletic performance monitoring applications. A key requirement for such a breath monitoring device is a disposable sensor element, capable of operating at a range of breath rates in high humidity, which is incorporated into a lightweight, compact sensing module. Luminescence-based oxygen sensors have been expanded researched in last years due to their advantages over the Clark electrode [1]. These sensors combine the intrinsic sensitivity of the luminescence process with the wide availability of low-cost optoelectronic unit, thereby enabling a range of sensor configurations and facilitating design features such as miniaturization and disposability. Sol-gel polymer materials offer an interesting sensor matrix, due to their ease of fabrication and the versatility of the process. This paper addresses some key issues that include response time, influence of humidity and enhanced sensitivity in the range of interest for breath sensing, which can be modified by use of a range of Organically Modified SILicate (ORMOSIL) materials.

2. Theory

The polymer matrix in this work is produced *via* the sol-gel process. Using this technology the direct immobilization of sensitive indicator dyes by physical entrapment is possible due to its simplicity of preparation, low-temperature encapsulation, chemical inertness, tunable porosity, optical transparency, mechanical stability and negligible swelling behavior [2-4]. Other advantages of silica supports include biocompatibility and resistance to microbial attack. In general, the sol-gel process involves hydrolysis of alkoxide precursors under acidic or basic conditions, followed by condensation and polycondensation of the hydroxylated units, which leads to the formation of a porous gel. Materials prepared by sol-gel gel route can range from simple inorganic glasses (e.g. tetraethoxysilane, TEOS, tetramethoxysilane, MEOS) to more complex hybrid materials called ORMOSILs [5, 6]. These materials facilitate the development of a broad range of innovative materials and are of general form $R_{4-x}Si(OR')_x$, where R represents an organic group such as $–CH_3$, $-C_2H_5$, $-C_6H_5$, $(-CH_2)nNH_2$. R is not hydrolysable and these silanes are used as network modifiers and network formers. They can combine the advantages of the organic and inorganic constituents within the same matrix and the physico-chemical properties can be tailored through choice of water/precursor molar ratio, R. Therefore, the fabrication of materials with desired hydrophobicity, flexibility and stability can be achieved. The organoslilicon precursors selected for use here have the effect of reducing the response time, increasing the hydrophobicity of the surface of resulting polymer material as well as reducing the connectivity of its microstructure. Furthermore the increased hydrophobicity reduces cross-sensitivity to humidity sensitivity, what is of particular relevance when selecting a material for use in a breath monitoring applications, due to the high

level of humidity in breath.

3. Experimental

All sol-gel based sensitive films were prepared by mixing the relevant precursor (TEOS, ethyltriethoxysilane ETEOS, n-propyltriethoxysilane PTEOS, phenyltriethoxysilane PhTEOS, 3,3,3,-trifluoropropyltrimethoxysilane TFP-TMOS) with ethanol as co-solvent, followed by dropwise addition of aqueous HCl at pH 1. After stirring an ethanolic solution of $RuCl_3.3\ H_2O$, (4,7-diphenyl-1,10-phenathroline) was subsequently added to the sol. The volume ratio between sol-gel precursors was verified as well as the molar ratio R. The sol-gel synthesis was performed at room temperature and aged for various times before formation of sensor films by dip-coating, depending on the precursor used. After deposition onto microscope slides which were pretreated in concentrated HNO_3 for 24 hours, the sensor films were dried at 110 °C for 12 hours.

4. Results and discussion

Response time

Rapid response time is an important consideration in designing a device for breath-by-breath monitoring. In order to measure the intrinsic response time of the sensor films and not that of the gas handling system (i.e. the time taken to fill the gas cell and lines), the gas exchange times must be minimized. This was achieved by realizing a measurement equipment that allowed fast measurement interval less than 86 ms. The response time has been defined as t_{90}, the time taken to achieve 90 % of the optical signal change, when switching from o to 100 % of O_2 (rise time) and in opposite direction (fall time). As it can be seen from Table 1, the shortest response time was found for ETEOS and PTEOS-based sensor films.

Table 1: Rise time t_{r90} and fall time t_{f90} experimentally determined for 10 sensitive sensor films

Sensitive Membrane	*Rise time t_{r90} [ms]*	*Fall time t_{f90} [ms]*
OR7	650	2270
OR8	320	1050
OR11	30	350
OR17	980	1720
OR18	270	1320
OR19	170	610
OR20	50	320

Influence of relative humidity

Humidity interference can affect the response of oxygen-sensitive film when used in gas sensing applications such as breath measurement. Figure 1 shows the influence of humidity response of the fluorinated films compared to ETEOS-PTEOS-derived films. It is clear that fluorinated films are completely humidity insensitive, while the other shows a negligible effect.

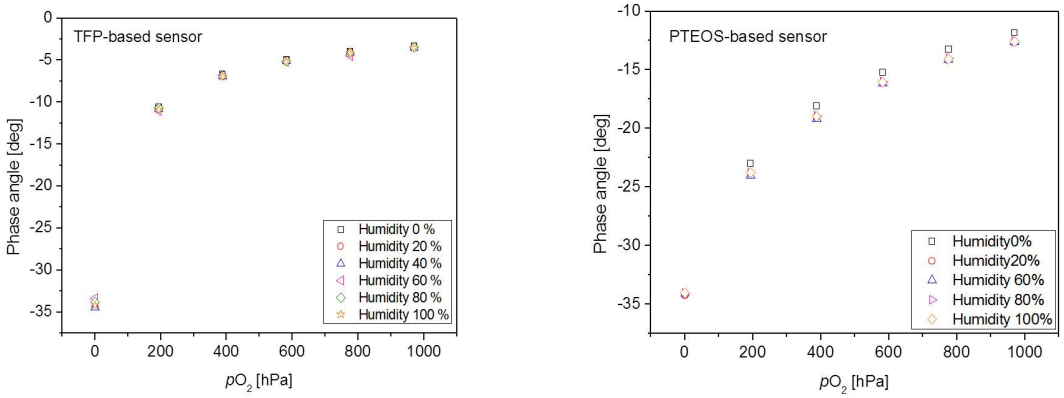

Figure 1: Influence of humidity on the sensor response

5. Conclusions

The sol-gel technology has proven itself as a powerful method for designing new luminescent materials. They possess a number of interesting features including: (a) sol-gels can be manufactured at low temperatures and physiological pHs: (b) their microstructure can be tailored to some extent; (c) they are optically transparent from the UV to NIR; (d) the index of refraction can be varied to some extent; (e) they provide a certain permeation selectivity; (f) they are mechanically and chemically stable; and (g) the fabrication procedure enables any desired geometric shape to be tailored. The presented work shows how increased hydrophobicity can eliminates the influence of humidity and the fast sensor films can be produced. Optical oxygen sensors presented here indicate the potential of low-cost and high-performance sensor systems for use in industrial, clinical and environmental applications. It highlights the fact that sensor performance is enhanced by the unique combination of the luminophore and the sol-gel-based matrix.

References
[1] O. S. Wolfbeis, *Fiber Optic Chemical Sensors and Biosensors*, CRC Press, Boca Raton, FL, 1991, vol.1.
[2] C. J. Brinker, G. W. Scherer, in Sol-gel Science*:* The Physics and Chemistry of Sol-Gel Processing, Academic Press, Boston, MA, 1990**.**
[3] I. Gill, *Chemistry of Materials*, 13, **2001**, 3404.
[4] G. Carturan, R. D. toso, S. Boninsegna, R. d. Monte, Journal of Materials Chemistry, 14, **2004**, 2087.
[5] O. Lev, M. Tsionsky, L. Rabinovich, V. Glezer, S. Sampath, I. Pankratov, J. Gun, Anal. Chem., 67, **1995**, 22A.
[5] P. Lavin, C. M. McDonagh, B. D. MacCraith, *J. Sol-Gel Sci. Technol*., 13, **1998**, 641.

S11-P105
Deformation of short fibre reinforced polypropylene: correlation between acoustic emission and X-ray computed tomography

Thomas Koch (1)*, Dietmar Salaberger (2), Martin Palmstingl (1), Marcus Schoßig (3)
(1) Institute of Materials Science and Technology, Vienna University of Technology, Vienna, Austria
(2) Upper Austrian University of Applied Sciences, Wels, Austria
(3) University of Applied Sciences Merseburg, Merseburg, Germany
*thomas.koch@tuwien.ac.at

1. Abstract
The presented work deals with the investigation of fracture and damage during the deformation of notched short fibre reinforced polypropylene materials. With the help of X-ray tomography the events detected by acoustic emission can be related to processes occurring in the fracture process zone and the damaged region in the direct vicinity of the cracks.

2. Introduction
Acoustic emission (AE) is a suitable method to detect micro deformation processes occurring during loading of short fibre reinforced polymers. In principle, characteristic effects like fibre fracture, debonding and matrix deformation can be detected and distinguished. Nevertheless there is some uncertainty in interpreting the results and giving direct correlation to the different sources of acoustic signals. Some approaches were done by insitu scanning electron microscopy coupled with acoustic emission [1]. But it should be kept in mind that in that case only a relative small part on the surface could be observed. The most part of the acoustic signals develop in the whole damaged region around the crack-tip. X-ray computed tomography with µm resolution gives the possibility to characterize the debonding (void generation) and fibre fracture. Examples of application of X-ray computed tomography for the characterization of short-fiber reinforced polymers are given in [2-5]. The combination of these two non-destructive testing methods should have a big potential in the field of describing damage processes of polymer composites.

3. Experimental
Different polypropylene (PP) composites, containing 10, 20 or 30 % short glass fibres, were investigated. Specimen (80 mm x 10 mm x 4 mm) were manufactured from compression moulded plates and subsequently notched (radius 0.25 mm).
A standard tensile machine was used to apply tensile loads. To freeze different loading states in the specimen the machine was stopped at interesting points of the load-elongation curve and the notch was filled with epoxy resin. With this the visco-elastic recovery of the specimen could be prevented. Of course only one loading state can be investigated for every specimen.
The AE measurements were realised with the 3-channel measuring system AMSY-4 (Vallen-Systeme, Icking, Germany) including the preamplifier AEP-3 and a broadband sensor AE204A. The bandwidth of the preamplifier and the AE sensor were 95 – 1000 kHz and 150 – 650 kHz (calibration certificate), respectively. The AE acquisition settings used throughout were as follow: threshold = 40.0 dB, rearm time = 0.4 ms, duration discrimination time = 200 µs and total gain = 40 dB. For a suitable coupling of the broadband sensor to the specimen surface, beeswax was used.
For the generation of X-ray tomography data a sub-µm CT nanotom (Phoenix-xray, Wunstorf, Germany) was used. The Nanofocus® tube was operated at 50 kV and a focal spot size of about 2 µm. A Hamamatsu detector with 2300 x 2300 pixels was used. The resolution was set to 2 or 3 µm per voxel to be able to extract single fibres. Every specimen was characterized by tomography before the mechanical loading and after the fixation.

4. Results
Typical examples of X-ray tomography of loaded samples are shown in Figure 1. Different features can be determined from the tomograms: size and shape of the crack, fibre fracture, debonding, pull-out and by comparing the initial state and the loaded state also the movement of fibres due to deformations of the matrix.
Analysing the AE signals by wavelet transformation can give information about the origin of the different events (Figure 2).

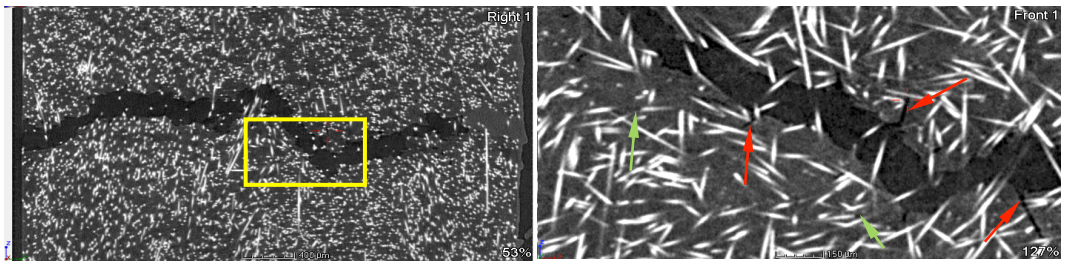

Figure 1. X-ray tomographed pictures of a specimen containing 30 wt.-% glass fibres in the loaded state showing a crack. The red arrows on the right picture indicate long holes after pull-out, the green arrows indicate debonding.

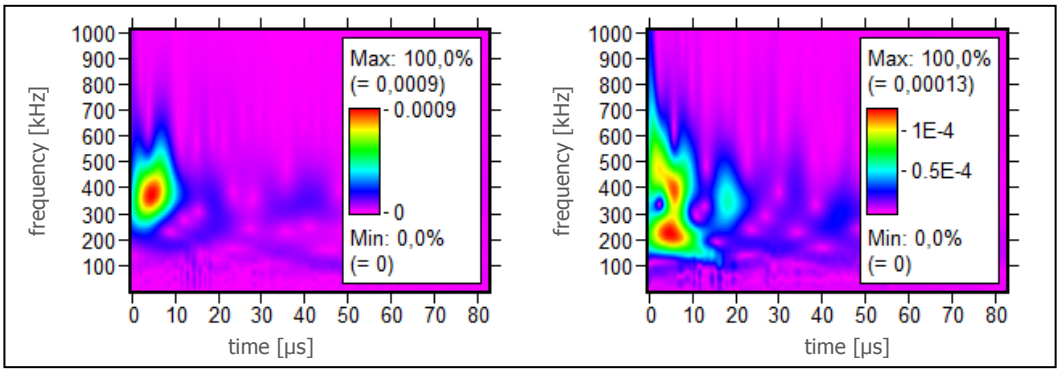

Figure 2. Examples of wavelet transformed AE signals showing debonding (frequency range from 300 to 500 kHz) and fibre fracture (frequency range between 150 and 280 kHz)

5. Conclusions

X-ray computed tomography with µm resolution gives the possibility to characterize the fracture and damage behavior during deformation of fibre-reinforced polymers including crack growth, debonding (void generation), pull-out and fibre fracture. By quantitative analysis of the amount of events detected by tomography a good correlation with the number, size and frequency characteristics of the AE signals can be shown.

The next steps will comprise insitu testing. For that a small sized tensile device will be installed inside the tomography device and the AE signals will be recorded online.

Acknowledgements

This work is part of the K-Project "Non-Destructive Testing and Tomography" supported by the COMET Programme of the Austrian Research Promotion Agency (FFG) and the Province of Upper Austria (LOÖ).

References

[1] M. Schoßig, A. Zankel, C. Bierögel, P. Pölt, W. Grellmann, *Compos. Sci. Techn.* **2010**, 71, 257–265.
[2] D. Salaberger, K. Kannappan, J. Kastner, J. Reussner, T. Auinger, *Int. Polym. Process.* **2011**, 3 , 283-291.
[3] F. Cosmi, A. Bernasconi, N. Sodini, *Compos. Sci. Techn.* **2011**, 71, 23-30.
[4] H.B. Shen, S. Nutt, D. Hull, *Compos. Sci. Techn.* **2004**, 64, 2113-2120.
[5] T. Koch, D. Salaberger, A. Zankel, H. Reingruber, A. Steiger-Thirsfeld, Y. Voronko, S. Seidler, *Macromol. Symp*. **2012**, 315, 115-124.

S11-P106
Thermal conductivity measurements on solid and liquid polymers including resins using the laser flash technique

André Lindemann*, Jürgen Blumm
NETZSCH-Gerätebau GmbH, Wittelsbacherstr. 42, 95100 Selb, Germany
*andre.lindemann@netzsch.com

The laser flash method [1] has been well-known for characterizing thermophysical properties such as the thermal diffusivity of solid materials. Fast measurement times, easy sample preparation and high accuracy are only some of the advantages of this non-contact, non-destructive measurement technique. In a laser flash test, the front side of a plane-parallel sample disk is heated by a short laser pulse. The resulting temperature rise on the rear side of the sample is measured versus time using an infrared detector (fig. 1).

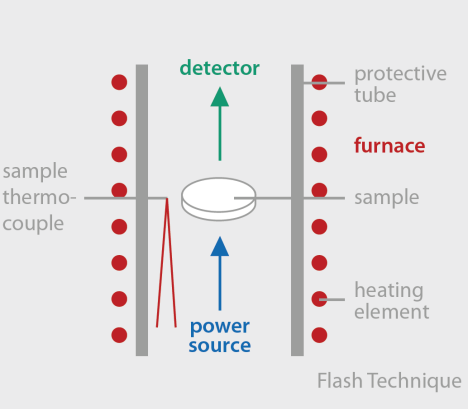

Figure 1: Principle of the flash technique.

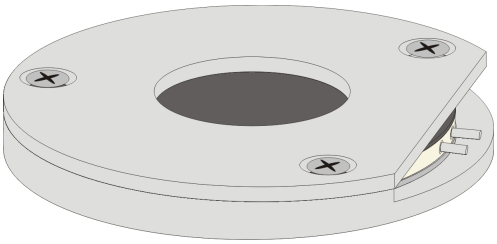

Figure 2: New sample holder for low-viscosity liquids, pastes and resins.

Nowadays, characterization of liquids, pastes and resins is becoming increasingly important for industrial applications. Special container systems are required for samples such as water-based fluids, oils, molten polymers [2], liquid metals [3] and resins. In the past, however, measurements on polymer melts and resins during curing were mostly expensive since the sample holder could only be used for one measurement, e.g. during a cross-linking reaction or due to the deformation during cooling, from the liquid to the solid state. In order to overcome this, a new sample holder for low-viscosity liquids such as water, oils and resins (e.g. during curing) was developed (fig. 2). The special design with parts from stainless steel and a PEEK ring allows time- and cost-reduced measurements with a high precision. The stainless steel plates and the PEEK ring can be easily exchanged after the measurements on melts or resins (one-way parts).
Presented in this work are technical details of the new container and various application examples on liquids and resins. Reliability tests (on water) show the comparison with literature. Furthermore, application examples with different sample holders for liquids and solids are shown and the influence of different filling materials on the thermal conductivity will be discussed.

References

[1] Parker W J, Jenkins R J, Butler C P and Abbott G L, *J. Appl. Phys.*, **32,** (1961) 1679-1684.
[2] Blumm J, Lindemann A, Characterization of the thermophysical properties of molten polymers and liquids using the laser flash technique, *High Temperatures – High Pressures*, **35/36**, (2007), 627-632.
[3] Kaschnitz E., Küblböck M., *High Temperatures – High Pressures*, **37**, (2008) 221–230.

S11-P107

The study of interaction of natural silk protein with polyacrylonitrile fiber

Nabiyeva Iroda, Khasanova M., Sadriddinov B., Rafikov A.
Department of Chemical Technology and Design of Fibrous Materials and Paper
Tashkent Institute of Textile and Light Industry, Shokh-Jahon Str. 5, 100100, Tashkent, Uzbekistan

1. Introduction

Methods of chemical fibers modification for improving their functional characteristics with the aim to enhance consumer properties of fiber materials and goods are widely using now. In this article the polyacrylonitrile (PAN) fiber-nitron modification process by proteins of natural silk investigation results are presented. The amino acid composition of natural silk solutions before and after fiber modification, and quantitative determination of protein on fiber were studied.

2. Theory

Row materials of natural silk basically are cocoons silkworm. Silkworm rearing by sheets of mulberry and after it will be saturated, rearing stops, silkworm will begin weave of a filament in the form of cocoons. The cocoon consists of a fibrous capsule, inside of which dolly of silkworm is remains. Depending on grain type of silkworm, technology of its cultivation silk-bearing of cocoons changes in a wide range (45.23-49.75 %). Technology's various of getting cocoons and their preparation to unwinding, directed on the greatest possible increase of an output a filament from cocoons are developed.

The filaments are unwinding from the assembled cocoons in automatic cocoon-reeling machine. For getting a filament of natural silk, in automatic cocoon-reeling machine the cocoons process in the heated bath and from 7-8 cocoons the elementary filaments are unite in one filament, which is accepted in reel of the automatic device. Further filament is twist and is accepted in textile chucks. From this filament receive thin fabrics of wide assortment, both household and technical function.

Modification methods are different and realizing in different stages of manufacturing process. For example, method of introducing of metal salts in spinning solution; method of inclusion of metal salts into fresh-formed gel-fiber and others. These methods are used for giving fibers electro conducting, ion- exchanging, sorption and other specific properties. By heat and γ-radiation of qualified fiber is reached increasing its heat resistance and sorption abilities of metal ions and dyestuffs from solution.

Our vision is that modification of nitron fiber by metal salts together with natural silk solution is perspective method. Effectiveness of this method revealed by follow:

- Interaction of polymer, that contain certain functional groups of protein-carrier of necessary properties with metal cations lead to formation of complex compounds, as result of donor-acceptor bounds;
- Possibility of giving to fiber necessary characteristic due to combination initial characteristic of the metal cations and protein.

The presence in protein macromolecule of side substituents of alkaline and acidic character stipulate for improving of modified by protein polyacrylonitrile fibers dyeability.

3. Experimental

Natural silk wastage protein fixedly sit on fiber surface with subsequent increasing it moisture sorption and dyeability by anion dyes and decrease electrization in contrast with initial fiber [1-4].

The absence of experimental data related to interaction character of natural silk protein with PAN fiber make difficult forecast it textile-technological properties.

In this work amino acid composition of natural silk solutions before and after modification of nitron fiber have been studied, as well defermined quantity of protein on fiber.

For modification of fiber were used vastages of natural silk (VNS), solved in different solvents compositions presented below:

I. Sodium thiocyanate +acetic acid.
II. Calcium chloride+ethyl alcohol
III. Sodium thiocyanate + ethyl alcohol
IV. Calcium chloride +glycerin

The concentration of protein in solutions before and after fiber modification, as well in washing water after processing was determined by Kaar-Kal spectral photometric method. Obtained experimental data are presented in tab.1.

Table 1. Dependence of protein quantity on fibers from solvent VNS composition.

Composition of natural silk vastages solvent		Quantity of protein, mg/ml			
		In solution before fiber processing	In solution after fiber processing	In washing water	In fiber, in % from quantity in solution before fiber processing
I	Sodium thiocyanate + acetic acid.	4,254	3,402	0,142	16,69
II	Calcium hloride + ethyl alcohol	4,870	2,216	0,142	54,96
III	Sodium thiocyanate + ethyl alcohol	4,453	2,343	0,179	43,36
IV	Calcium chloride + glycerin	5,062	2,340	0,175	50,31

It is identifyed that solvents II and IV are more effective. Solvents Calcium hloride+ethyl alcohol and Sodium thiocyanate + ethyl alcohol contribute to more safety of protein. Experiments have showed, that protein obtained from solvents contained Calcium chloride more hold on fiber, compared with protein, that obtained from solvents contained Sodium thiocyanate. Evidently it may be explained by forming of chemical bounds, between functional groups of fiber Nitron (-COON), protein (-COON-OH-NH_2), -S-S-, -NH- and others), glycerin (-OH) and cations of polyvalent metal (Ca^{+2}).

Sorption and fixation of protein on fibers take place in all solutions of natural silk and absence of protein in washing waters of modificated fiber is evidence of it.

It may be concluded, that all four solutions of VNS can be used for modification of fiber-nitron. But the contain of protein in gel fiber more at using of solvent- Calcium hloride+ethyl alcohol or Calcium chloride +glycerin compared with other solvents.

For determination of intermolecular interaction type the analysis of amino acid composition of protein in all four solvents have been made, as before, so after processing of gel fiber Nitron. Results of amino acid analysis presented in table 2. According these data (including amino acids in total), protein keeped most firmly at processing gel fiber by solution containing Calcium chloride.

It is known, that glutamine and asparagine remains in polypeptide chain are neutral, but last amides are high polar and at interaction of theirs with similar groups form hydrogen bounds. Composition of these amino acids (for solution II, IV) before and after processing is essentually different. Therefore intermolecular interaction of fibroin with synthetic fiber nitron is the result of hydrogen bounds. Abundance of amid groups leads to formation multitude of such bounds.

Cysteine takes part in forming of intramolecular and intermolecular covalent bounds. SH-groups of it are easy oxidized and form disulfide bridges –S-S-of cysteine. In our case cystein is not revealed in “after processing” solution. On the element analysis picture (fig.1) one can distinctly see, that in modified fiber even after extraction sulfur and oxygen atoms (molecules) are present. This indicate to the effect that intrapeptide and interpeptide links (in particular covalent bonds) are take place. Original fiber (fig.2) contains only carbogen atoms.

For establish of gel fiber Nitron modification rational regime it was processing in bath of different composition.

It was established [5], that maximum sorption of VNS by gel fiber in modification bath take place at t = 70 ^{0}C during 2-5 sec. The further extension of processing period to no purpose. Therefore regime of modification processing of gel fiber Nitron was following: processing time 1-5 s, t - 70 ^{0}C, module of bath 1:50.

Results of study have showed, that increase of VNS and Calcium chloride content in modification bath lead to increase of protein content in modificated fiber.

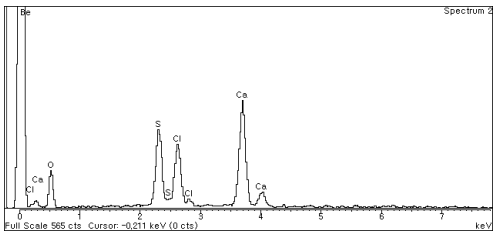

Figure 1. Elements composition of modified polyacrylonitrile Nitron fiber

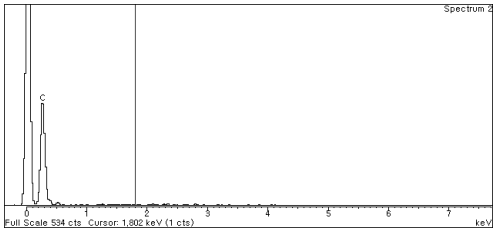

Figure 2. Elements composition of original polyacrylonitrile fiber – nitron

4. Conclusions

The results of quantitative determination of protein, as well the results of determination of element composition of VNS solution have showed, that between synthetic fiber and proteins of natural silk take place formation of physical and chemical bound. Besides it may be concluded, that fibroin connects with surface of gel fiber Nitron not only by hydrogen bonds but it connected by disulfide bridges. As solvent VNS we recommend solution composed of Calcium chloride and glycerin (or ethyl alcohol).

References

1. Nabieva I.A., Ergashev K.E. (2005). Improvement of hygienic properties of fiber- nitron by modification it with natural silk solutions, Textile University, Collection of scientific works, pp. 251-255, Russian, Moscow.
2. Nabieva I.A. Khamraev A.J., Ikramova I.A. (1997), The study of modified by fibroin fiber- nitron dyeing with azo dyes, Silk, № 4, 17-20.
3. Nabieva I. A., Alimova J.M., Khamzaeva J., Ergashev K.E. (1997), The study of dyeing kinetics of fiber- nitron modified by natural silk, Silk, №1, p.21-25.
4. Nabieva I. A., Bobozhonov Kh.Kh., Khamzaev A.L. (1999), The study of modified by fibroin fiber- nitron dyeing with vat dyes, Silk, №1, p.30-33.
5. Nabiev I.A., Sadriddinov B.B., Ergashev K.E. Printing of Blend Fabric with Active dyes (2003), Waters International GPC 2003 and ISPAC-16. Symposium, June 7-12, USA

S11-P108
Advances approach to the polymer of environmental capacity of surface water

Qendresa Rexha
Str. Cajupi Tophane III/4, 10000 Prishtine- Kosovo
* ddesarexha@gmail.com

Abstract

The increase of anthropogenic impact on water resources causes increase of adverse natural phenomena and processes. Actually, the human activities that generated global climate change is the cause of the current effects - significant reduction in water content for certain periods of the year, the loss of small streams, reducing the degree of dilution of reused waters that are discharged into water bodies, and as a result – declining of their self-cleaning ability.

This paper presents comparative characteristics of integrated performance assessment of water quality of the Sitnica River in the Republic of Kosovo .

Water quality monitoring of the River Sitnica is necessary to assess environmentally balanced condition. The paper presents comparative characteristics of the complex criteria such as Index of Water Pollution (IWP), Environmental Index of Water Quality (EIWQ) and Hydro-ecological Potential (HEP).

Assessment of environmental safety is the likelihood of natural and man-made hydro-ecosystem to maintain resistance under the influence of anthropogenic factors (to maintain positive value of hydro-ecological potential).

In 2010 and 2012 pre-production thermoplastic resin pellets and post-consumer plastic fragments were collected and analyzed for contamination for persistent organic pollutants (POPs). Samples were taken from the different river water, and selected sites in Kosovo. The total concentration of PCBs ranged from 27 to 886 ng/g; DDTs from 21 to 6130 ng/g and PAHs from 23 to 964 ng/g.

S11-P109
Evidence for microgel formation in aqueous solutions of atactic poly(methacrylic acid). A light scattering study

Simona Sitar (1)*, Petra Metul (1), Vladimir Aseyev (2) and Ksenija Kogej (1)
(1) University of Ljubljana, Faculty of Chemistry and Chemical Technology, Aškerčeva 5, 1000 Ljubljana, Slovenia
(2) University of Helsinki, Department of Chemistry, Laboratory of Polymer Chemistry, FIN-00014 HY, Helsinki, Finland
*simona.sitar@fkkt.uni-lj.si

1. Introduction

Poly(methacrylic acid), PMA, is one of the most extensively investigated synthetic polyelectrolytes, mainly due to the conformational transition, which occurs in aqueous solutions when the carboxyl groups on the PMA chain are ionized [1]. In aqueous solutions, PMA chain can either be in a compact or in an unfolded form/extended conformation, depending on the solution pH, i.e. on the degree of ionization of the carboxyl groups on PMA, and also on the ionic strength. PMA can be prepared in three isomer forms: as atactic PMA (a-PMA), syndiotactic PMA (s-PMA) or isotactic PMA (i-PMA). Recent studies on PMA have been focused on the atactic form. The conformational change of a-PMA in dilute aqueous solution has intensively been studied using

potentiometry [1], fluorimetry [2], light scattering [3,4], etc. The opinion on what forces stabilize the compact structure of a-PMA at low degree of ionization, α, are quite divided, but mostly agree with the interpretation that the compact conformation of a-PMA at $\alpha = 0$ is stabilized by short range interactions and/or by hydrogen bonds between COOH groups.
In the present work the dynamic and static light scattering measurements were performed on aqueous solutions of atactic poly(methacrylic acid). Our aim was to study the effect of the degree of neutralization, α_N, polymer concentration, c_p, and salt concentration, c_s, on polymer size. We determined the radius of gyration, R_g, the hydrodynamic radius, R_h, and the shape parameter, $\rho = R_g/R_h$, from which the shape of particles can be estimated. The polymer concentration was kept constant at 2 g/l. The concentration of salt, NaCl, was varied from 0.01 to 0.5 M. The degree of neutralization of carboxyl groups was α_N = 0, 0.25, 0.50, 0.75, and 1.

2. Results and discussion

For α_N=0 all correlation functions were bi-exponential and resulted in bimodal distribution of relaxation times, Γ. The fast and slow diffusing particles were determined from the slope of corresponding Γ_f or Γ_s versus q^2 dependencies and were associated with individual aPMA chains (small particles) and intermolecular associates (large particles). Hydrodynamic radii for small particles were $R_{h,1}$=(11-13) nm; no angular dependency of scattered light was obtained in this case. Hydrodynamic radii were considerably higher for large particles. $R_{h,2}$ values were extrapolated to zero angle and found to be in the range from 100 nm to more than 300 nm, depending on the salt concentration. The $R_{g,2}$ values were obtained for the large particles from the angular dependencies of the scattered light intensity. The shape parameter, ρ, was calculated for the large particles from the $R_{h,2}$ and $R_{g,2}$ values by using the Debye-Bueche particle scattering function [5]. The ρ values were between 0.6 and 0.8 and are characteristic for microgels [6] and suggest structures with rather high packing density.
Correlation functions for $\alpha_N > 0$ were single exponential or bi-exponential, depending on the salt concentration. Given that at $\alpha_N > 0$ some carboxyl groups on the aPMA chain are neutralized and intermolecular association is suppressed, we believe that the reason for bimodal distribution in this region of α_N values is so called polyelectrolyte effect [7]. This is believed to be the reason for the observance of the slow decay process in polyelectrolyte solutions at low salt concentrations. For α_N = 0.25 we observed the above mentioned effect at NaCl concentration $c_s \leq 0.05$ M, for α_N = 0.5 and 0.75 at $c_s \leq 0.07$ M NaCl and for α_N = 1 at $c_s \leq 0.1$ M NaCl. For high enough salt concentrations (for α_N = 0.25 at $c_s > 0.05$M, for α_N = 0.5 and 0.75 at $c_s > 0.07$ and for α_N = 1 at $c_s > 0.1$ M) only one particle size was observed, which can be attributed to single aPMA chains. The size of single aPMA chains increases from around 13 nm at α_N = 0 to around (17-20) nm for $\alpha_N \geq 0.5$. Somewhat higher R_h values are consistent with chain expansion for $\alpha_N > 0$. A weak angular dependency was obtained of the light scattering intensity for $\alpha_N > 0$, which made possible determination of R_g and ρ in dependence on α_N.

Acknowledgements

This work was financially supported by the Slovenian Research Agency, ARRS, through the Physical Chemistry program P1-0201. In addition, a great part of the experimental work has become possible thanks to the established bilateral agreement between the Academy of Finland (Grants no. 132404 and 134581) and the ARRS.

References

[1] Katchalsky, A.; Spitnik, P. ''Potentiometric Titrations of Poly(methacrylic acid)'', *J. Polym. Sci.* **1947**, *2*, 432-446.
[2] Olea, A. F.; Thomas, J. K. ''Fluorescence Studies of the Conformational Changes of Poly(methacrylic acid) with pH'', *Macromolecules* **1989**, *22*, 1165-1169.
[3] Kogej, K.; Cerkovnik, J.; Bergmans, H.; Paoletti, S. ''Light Scattering of Aqueous Solutions of Poly(methacrylic acid) and Poly(sodium methacrylate)'', *Acta Chim. Slov.* **2001**, *48*, 395-406.
[4] Kogej, K.; Berghmans, H.; Reynaers, H.; Paoletti, S. ''Unusual Behavior of Atactic Poly(methacrylic acid) in Aqueous Solutions Monitored by Wide-Angle Light Scattering'', *J. Phys. Chem*. **2004**, *108*, 18164-18173.
[5] Burchard, W. “Angular Dependence of Scattered Light from Hyperbranched Structures in a Good Solvent. A Fractal Approach” *Macromolecules* **2004**, *37*, 3841-3849.
[6] Savin, G.; Burchard, W. “Uncommon Solution Behavior of Poly(N-vinylimidazole). Angular Dependence of Scattered Light from Aggregates in Ethanol” *Macromolecules* **2004**, *37*, 3005-3017.
[7] Cong, R.; Temyanko, E.; Russo, P. S.; Edwin, N.; Uppu, R. M. ''Dynamics of Poly(styrenesulfonate) Sodium Salt in Aqueous Solution'', *Macromolecules* **2006**, *39*, 731-739.

S11-P110

The analysis of polyactic acid using solvent enhanced light scattering gel permeation chromatography

John D. Stenson (1)*, Bassem Sabagh (1)
(1) Malvern Instruments Ltd., Worcestershire, UK
* John.Stenson@Malvern.com

1. Introduction

Biodegradable polymer derivatives are being used to replace traditional polyesters and polystyrene in a wide range of commercial and biomedical applications. One of the most popular biopolymers is polylactic acid (PLA) which is derived from renewable sources such as corn or sugar cane. PLA has several different polymerisation routes and many copolymer derivatives. As a consequence it is a very versatile product but this can cause great problems during analysis by Gel Permeation Chromatography (GPC).
This work demonstrates the use of Solvent Enhanced Light Scattering (SELS) Triple Detection GPC for the analysis of PLA using the Malvern Instruments Viscotek 305 GPC system. The absolute molecular weight and structure of three PLAs has been studied and differences between them observed.

2. Theory

Triple detection GPC is the most accurate method for measuring the absolute molecular weight, size and structure of a material. Traditionally, in GPC the solvent used to dissolve the sample and the eluent used for chromatography are the same. However, it is also important to consider the Refractive Index Increment (dn/dc) of the sample in the eluent and ensure it is sufficiently high to produce good signals in both the Refractive Index (RI) and Light Scattering detectors. This is not the case for PLA which is known to dissolve well in Chloroform but generally poorly in Tetrahydrofuran (THF) and Acetone. This is because most low RI solvents are weak solvents for mid-to-low polarity polymers. Importantly, the mobile phase of choice does not need to dissolve the sample, it only needs to support or maintain the materials solubility during analysis. This means it is possible to dissolve the sample in a stronger solvent, such as chloroform, and then use a low RI solvent, such as acetone, for the eluent during GPC analysis.

3. Experimental

Three polylactic acid samples were selected for analysis, D-Lactide (PDLA), L-Lactide (PLLA) and a meso-Lactide (PDLLA). These samples were analysed using the Malvern Instruments Viscotek 305 GPC system. Two different methodologies were followed, Triple detection and Universal calibration. In both cases three proprietary Viscotek I-series columns were connected in series and the sample eluted at 1mL/min over 50 minutes. The column and detectors (Refractive Index (RI), Right-Angle Light Scattering (RALS), Low Angle Light Scattering (LALS) and Viscometer) were kept at a constant temperature of 35°C throughout the experiment. For Triple detection, the sample was dissolved in chloroform and eluted from the columns using Acetone. The instrument constants were obtained using a known polystyrene standard with a narrow molecular weight distribution. For universal calibration the samples were eluted from the columns using THF. The following polystyrene standards were used to create a calibration line; PS1000, PS2800, PS6000, PS13k, PS30k, PS65k, PS170k, PS400k, and PS2000k. The results produced by this calibration method will act as a check for the results produced by SELS GPC.

4. Results and Discussion

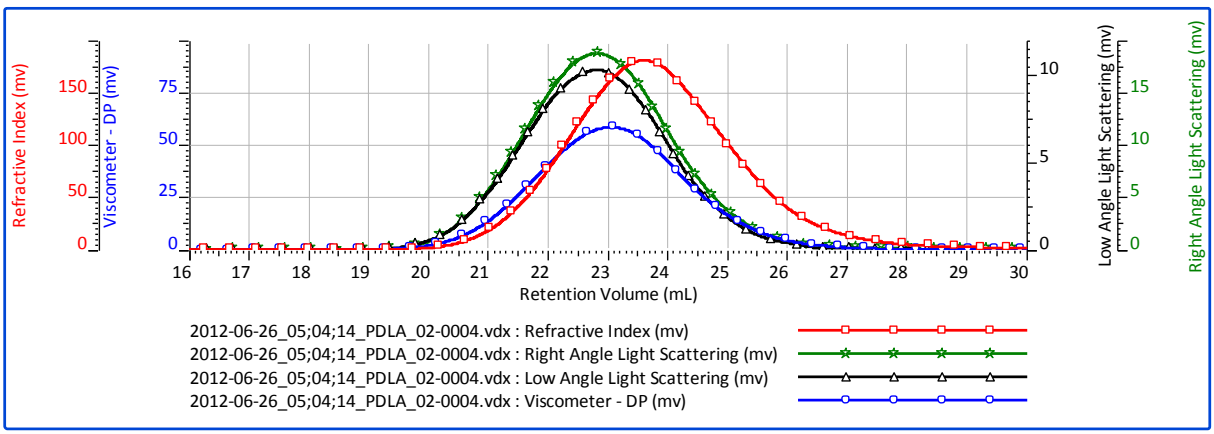

Figure 1: Example triple detection chromatogram for PLA by Solvent Enhanced Light Scattering GPC

Figure 1 shows a representative triple detection chromatogram for PLA produced by SELS GPC. A strong positive response can be seen in all of the detectors. The responses recorded by the Refractive index and Light scattering detectors are only possible due to the increased dn/dc of the PLA in Acetone. This result is only possible when following the SELS methodology.

Triple detection - Acetone

Sample Id	Mw (kDa)	Mn (kDa)	Mw/Mn	IV (dl/g)	Rh (nm)	dn/dc (mL/g)
PDLA	92	48	1.91	0.72	9.70	0.09
PLLA	81	45	1.78	0.65	8.99	0.09
PDLLA	79	47	1.71	0.61	8.75	0.09

Universal calibration - THF

Sample Id	Mw (kDa)	Mn (kDa)	Mw/Mn	IV (dl/g)	Rh (nm)	dn/dc (mL/g)
PDLA	93	39	2.47	1.09	10.88	0.05
PLLA	80	42	1.90	0.98	10.13	0.05
PDLLA	84	47	1.85	0.87	9.96	0.05

Table 1. Quantitative parameters produced by Triple detection and Universal calibration. **Mw**= Weight average Molecular weight (kDa), **Mn**= Number average Molecular weight (kDa), **Mw/Mn**= Polydispersity, **IV**= Intrinsic viscosity (dL/g), **Rh**= Hydrodynamic radius (nm), **dn/dc**= refractive index increment (mL/g).

Samples were analysed using both triple detection and universal calibration, the results of which are shown in Table 1. The Mw and Mn data obtained were very similar for both methods. Importantly, this confirms that the SELS process has not altered the sample material properties. The effect of using a mobile phase with a low refractive index can be seen in the dn/dc data where acetone gives a value of 0.09 mL/g, almost double that of the same samples in THF. The different eluents also had an effect on the conformation of the samples as shown by the large change in the IV and Rh parameters measured.

Figure 2 shows the Mark-Houwink plot for the three polylactic acid samples produced by Triple detection. The Mark-Houwink relationship is used to describe structural differences as a function of molecular weight. The y-axis is the intrinsic viscosity on a log scale measured directly from the differential viscometer for each slice of elution volume. The x-axis is the absolute molecular weight measured by the light scattering detector.

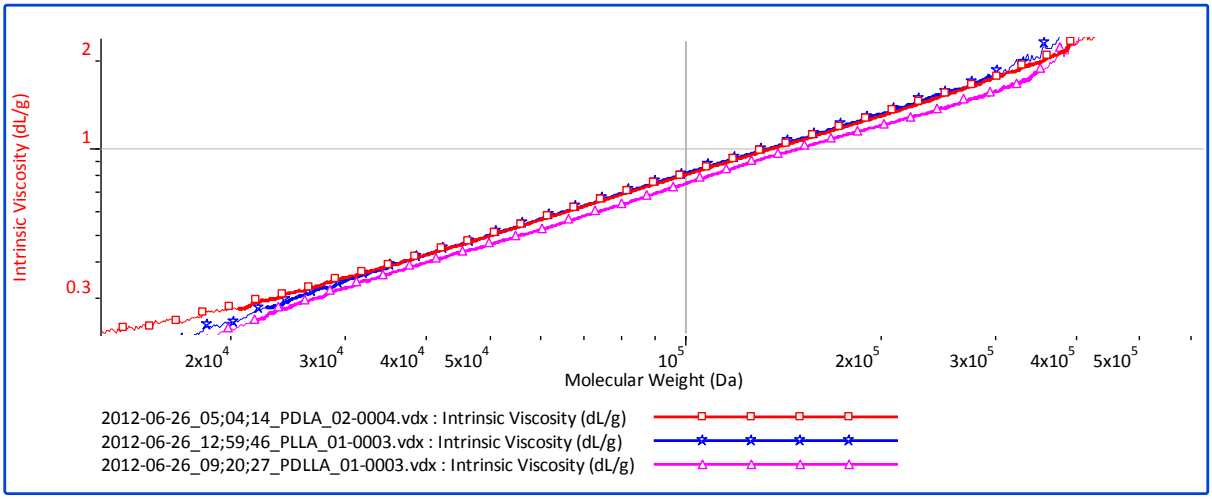

Figure 2: Mark-Houwink relationship for three polylactic acids produced by Triple detection.

PLLA and PDLA produce very similar relationships suggesting the structures of these materials are the same. PDLLA runs parallel to these samples but at a lower IV throughout the molecular weight range. The IV is known to be inversely proportional to the density of the material. This result is indicative of PDLLA having a more dense structure than either PLLA or PDLA throughout the molecular weight range. It is possible that this increase in density is due to structural differences between the samples caused by the different monomer subunits.

5. Conclusions

The technique of Solvent Enhanced Light Scattering (SELS) triple detection GPC provided insight into the polymer's structure. By using SELS quantitative data could be determined using the refractive index, light scattering and viscometry detectors. The direct determination of the absolute molecular weight by light scattering in SELS eliminates the uncertainty in the measurement due to chromatographic factors. By employing the viscometer and light scattering detectors differences in the Mark-Houwink plots were observed. This result suggests that PDLLA has a denser structure than PDLA or PLLA at the same molecular weight.

PRESENTING AUTHORS INDEX